

Advances

in Clinical and Experimental Medicine

MONTHLY ISSN 1899-5276 (PRINT) ISSN 2451-2680 (ONLINE)

advances.umw.edu.pl

2025, Vol. 34, No. 7 (July)

Impact Factor (IF) – 1.9
Ministry of Science and Higher Education – 70 pts
Index Copernicus (ICV) – 171.00 pts



WROCLAW
MEDICAL UNIVERSITY

Advances
in Clinical and Experimental
Medicine



Advances in Clinical and Experimental Medicine

ISSN 1899-5276 (PRINT)

ISSN 2451-2680 (ONLINE)

advances.umw.edu.pl

MONTHLY 2025

Vol. 34, No. 7

(July)

Advances in Clinical and Experimental Medicine (*Adv Clin Exp Med*) publishes high-quality original articles, research-in-progress, research letters and systematic reviews and meta-analyses of recognized scientists that deal with all clinical and experimental medicine.

Editorial Office

ul. Marcinkowskiego 2–6
50-368 Wrocław, Poland
Tel.: +48 71 784 12 05
E-mail: redakcja@umw.edu.pl

Editor-in-Chief

Prof. Donata Kurpas

Deputy Editor

Prof. Robert Śmigiół

Managing Editor

Marek Misiak, MA

Statistical Editors

Wojciech Bombała, MSc
Anna Kopszak, MSc
Dr. Krzysztof Kujawa
Jakub Wronowicz, MSc
Maciej Wuczyński, MSc

Manuscript editing

Marek Misiak, MA
Paulina Piątkowska, MA

Publisher

Wrocław Medical University
Wybrzeże L. Pasteura 1
50-367 Wrocław, Poland

Online edition is the original version
of the journal

Scientific Committee

Prof. Sandra Maria Barbalho
Prof. Antonio Cano
Prof. Chong Chen
Prof. Breno Diniz
Prof. Erwan Donal
Prof. Chris Fox
Prof. Yuko Hakamata
Prof. Carol Holland
Prof. Sabine Bährer-Köhler

Prof. Markku Kurkinen
Prof. Christopher S. Lee
Prof. Christos Lionis
Prof. Leszek Lisowski
Prof. Raimundo Mateos
Prof. Zbigniew W. Raś
Prof. Dorota Religa
Prof. Jerzy W. Rozenblit
Prof. Silvina Santana

Prof. Sajee Sattayut
Prof. Barbara Schneider
Prof. James Sharman
Prof. Jamil Shibli
Prof. Luca Testarelli
Prof. Michał J. Toborek
Prof. László Vécsei
Prof. Cristiana Vitale
Prof. Ming Yi
Prof. Hao Zhang

Section Editors

Basic Sciences

Prof. Iwona Bil-Lula
Prof. Dorota Danuta Diakowska
Prof. Paweł Andrzej Karpiński
Prof. Bartosz Kempisty
Dr. Wiesława Kranc
Dr. Anna Lebedeva
Dr. Piotr Chmielewski
Dr. Phuc Van Pham
Dr. Sławomir Woźniak

Bioinformatics and Genetics

Assoc. Prof. Izabela Łączmańska
Prof. Łukasz Łączmański

Clinical Anatomy, Legal Medicine, Innovative Technologies

Prof. Rafael Boscolo-Berto

Dentistry

Prof. Marzena Dominiak
Prof. Tomasz Gedrange
Prof. Jamil Shibli
Prof. Luca Testarelli

Laser Dentistry

Prof. Kinga Grzech-Leśniak

Dermatology

Prof. Jacek Szepietowski
Assoc. Prof. Marek Konop

Emergency Medicine, Innovative Technologies

Prof. Jacek Smereka

Evidence-Based Healthcare

Assoc. Prof. Aleksandra Królikowska
Dr. Robert Prill

Gynecology and Obstetrics

Assoc. Prof. Tomasz Fuchs
Dr. Christopher Kobierzycki
Dr. Jakub Staniczek

Histology and Embryology

Dr. Mateusz Olbromski

Internal Medicine

Angiology

Dr. Angelika Chachaj

Cardiology

Dr. Daniel Morris
Assoc. Prof. Joanna Popiołek-Kalisz
Prof. Pierre François Sabouret

Endocrinology

Prof. Marek Bolanowski

Gastroenterology

Assoc. Prof. Katarzyna Neubauer

Hematology

Prof. Andrzej Deptała

Prof. Dariusz Wołowicz

Nephrology and Transplantology

Prof. Mirosław Banasik

Prof. Krzysztof Letachowicz

Assoc. Prof. Tomasz Gołębiowski

Rheumatology

Assoc. Prof. Agata Sebastian

Dr. Sylwia Szafraniec-Buryło

Lifestyle Medicine, Nutrition and Health Promotion

Assoc. Prof. Michał Czaplą

Prof. Raúl Juárez-Vela

Dr. Anthony Dissen

Microbiology

Assoc. Prof. Adam Junka

Molecular Biology

Dr. Monika Bielecka

Prof. Dorota Danuta Diakowska

Dr. Phuc Van Pham

Neurology

Assoc. Prof. Magdalena Koszewicz

Dr. Nasrollah Moradikör

Assoc. Prof. Anna Pokryszko-Dragan

Dr. Masaru Tanaka

Neuroscience

Dr. Simone Battaglia

Dr. Francesco Di Gregorio

Dr. Nasrollah Moradikör

Omics

Prof. Mariusz Fleszar

Prof. Paweł Andrzej Karpiński

Oncology

Prof. Andrzej Deptała

Prof. Adam Maciejczyk

Prof. Hao Zhang

Gynecological Oncology

Dr. Marcin Jędryka

Ophthalmology

Dr. Małgorzata Gajdzis

Prof. Marta Misiuk-Hojło

Orthopedics

Prof. Paweł Reichert

Otolaryngology

Prof. Tomasz Zatoński

Pediatrics

Pediatrics, Metabolic Pediatrics, Clinical
Genetics, Neonatology, Rare Disorders

Prof. Robert Śmigiel

Pediatric Nephrology

Prof. Katarzyna Kiliś-Pstrusińska

Pediatric Oncology and Hematology

Assoc. Prof. Marek Ussowicz

Pharmaceutical Sciences

Assoc. Prof. Marta Kepinska

Prof. Adam Matkowski

Pharmacoeconomics

Dr. Sylwia Szafraniec-Buryło

Psychiatry

Dr. Melike Küçükkarapınar

Prof. Jerzy Leszek

Assoc. Prof. Bartłomiej Stańczykiewicz

Public Health

Prof. Monika Sawhney

Prof. Izabella Uchmanowicz

Pulmonology

Prof. Anna Brzecka

Qualitative Studies, Quality of Care

Prof. Ludmiła Marcinowicz

Assoc. Prof. Anna Rozensztrauch

Radiology

Prof. Paweł Gać

Rehabilitation

Assoc. Prof. Aleksandra Królikowska

Dr. Robert Prill

Surgery

Assoc. Prof. Mariusz Chabowski

Telemedicine, Geriatrics, Multimorbidity

Assoc. Prof. Maria Magdalena

Bujnowska-Fedak

Prof. Ferdinando Petrazzuoli

Editorial Policy

Advances in Clinical and Experimental Medicine (Adv Clin Exp Med) is an independent multidisciplinary forum for exchange of scientific and clinical information, publishing original research and news encompassing all aspects of medicine, including molecular biology, biochemistry, genetics, biotechnology and other areas. During the review process, the Editorial Board conforms to the "Uniform Requirements for Manuscripts Submitted to Biomedical Journals: Writing and Editing for Biomedical Publication" approved by the International Committee of Medical Journal Editors (www.ICMJE.org). The journal publishes (in English only) original papers and reviews. Short works considered original, novel and significant are given priority. Experimental studies must include a statement that the experimental protocol and informed consent procedure were in compliance with the Helsinki Convention and were approved by an ethics committee.

For all subscription-related queries please contact our Editorial Office: redakcja@umw.edu.pl

For more information visit the journal's website: advances.umw.edu.pl

Pursuant to the ordinance of the Rector of Wrocław Medical University No. 37/XVI R/2024, from March 1, 2024, authors are required to pay a fee for each manuscript accepted for publication in the journal Advances in Clinical and Experimental Medicine. The fee amounts to 1600 EUR for all types of papers.

Indexed in: MEDLINE, Science Citation Index Expanded, Journal Citation Reports/Science Edition, Scopus, EMBASE/Excerpta Medica, Ulrich's™ International Periodicals Directory, Index Copernicus

Typographic design: Piotr Gil, Monika Kołęda

DTP: Wydawnictwo UMW

Cover: Monika Kołęda

Printing and binding: Drukarnia I-BiS Bierórscy Sp.k.

Contents

Editorials

- 1069 Gustavo Vicentis de Oliveira Fernandes, Grace Mosley, Ana Cristina Cañizares, Juliana Campos Hasse Fernandes, Romana Muller
Standardizing clinical evaluations of periodontal condition to guide assessments and diagnoses using the Periodontal Assessment Protocol (GF-PAPro)
- 1079 Barbara Schneider, Lars Meiländer, Tilman Wetterling
Suicidal behavior and substance dependence
- 1085 Krzysztof Kujawa, Wojciech Bombała, Anna Kopszak, Jakub Wronowicz, Maciej Wuczyński, Łukasz Lewandowski, Michał Czapla
New statistical guidelines for manuscripts submitted to *Advances in Clinical and Experimental Medicine*

Meta-analysis

- 1091 Shuang Qi, Meng Zhao, Yinyao Sun, Sunaina Boro, Bhawna Arora, Sanjay Rastogi
Impact of vitamin D supplementation on symptom severity and quality of life in patients with irritable bowel syndrome: A meta-analysis

Original papers

- 1105 Adomas Janulionis, Viktorija Sutova, Vita Langiene, Ernestas Virsilas, Violeta Drejeriene, Arunas Liubsys, Arunas Valiulis
Electrical impedance tomography confirmed the impact of the method of delivery of term neonates on early lung aeration
- 1113 Turkan Dubus, Gokce Cangel, Fatih Kesmezacar, Aziz Ari
Surgical approach to pulmonary metastases and its impact on prognosis
- 1123 Yi Ma, Xuebin Geng
Prognostic value of the systemic inflammation response index on 3-year outcomes of elderly patients with acute coronary syndrome after stent implantation
- 1131 Huaqian Xu, Xue Li, Yue Zhuo, Chunyan Li, Chengzhi Bai, Jie Chen, Shanhong Tang
Prognostic value of inflammation-related model in hepatitis B acute-on-chronic liver failure
- 1139 Dawei Yang, Qian Yang, Yixing Wang, Fengxia Liu, Zhi Xing, Shitong Li, Jianyou Zhang
Impact of intravenous infusion of lidocaine on intrapulmonary shunt and postoperative cognitive function in patients undergoing one-lung ventilation
- 1145 Bohui Zhou, Junfang Lian, Yanping Wang, Yanling Yang, Hua Bai, Suhui Wu
Development and validation of a model to preoperatively predict the risk of placenta accreta spectrum in women with placenta previa
- 1155 Maciej Polak, Grzegorz J. Nowicki, Maja Chrzanowska-Wąsik, Barbara J. Ślusarska
Do sociodemographic and health predictors affect the non-insulin-based insulin resistance index? A cross-sectional study
- 1165 Joanna Małecka, Magdalena Goliwąg, Katarzyna Adamczewska, Jacek Lewandowski, Dawid Łochyński
The translation into Polish, cultural adaptation, and initial validation of the Action Research Arm Test in subacute stroke patients
- 1175 Cihat Öztürk, Rukiye Akyol, Sadık Küçükğünay, Elif Sevim
Investigation of integron gene cassettes in trimethoprim-sulfamethoxazole-resistant *Acinetobacter baumannii* isolates
- 1183 Chia-Chia Lu, Yi-Chin Yang, Yi-Wen Hung, Yen-Chun Peng
Esomeprazole inhibits liver inflammation and carcinogenesis by suppressing farnesoid X receptors and NF-κB signaling

Research-in-progress

- 1191 Ponnusamy Subramaniam, Preyaangka Thillainathan, Anthony Angwin, Shobha Sharma
Unfolding memories: Crafting digital life storybooks for dementia care via telehealth

Reviews

- 1201 Aneta Nowicka, Lidia Gil
Microbial metabolomics in acute myeloid leukemia: From pathogenesis to treatment
- 1213 Daniel Wolny, Mateusz Stojko, Alicja Zajdel
Novel strategies of glutathione depletion in photodynamic and chemodynamic therapy: A review
- 1223 Klaudia Szymanek, Karolina Tądel, Iwona Bil-Lula
Acute kidney injury during transplantation and the role of inflammasomes: A brief review

Standardizing clinical evaluations of periodontal condition to guide assessments and diagnoses using the Periodontal Assessment Protocol (GF-PAPro)

Gustavo Vicentis de Oliveira Fernandes^{1,A–F}, Grace Mosley^{1,C–F},
Ana Cristina Cañizares^{1,B–F}, Juliana Campos Hasse Fernandes^{2,A–F}, Romana Muller^{1,B–F}

¹ A.T. Still University – Missouri School of Dentistry & Oral Health, St. Louis, USA

² private researcher, St. Louis, USA

A – research concept and design; B – collection and/or assembly of data; C – data analysis and interpretation;
D – writing the article; E – critical revision of the article; F – final approval of the article

Advances in Clinical and Experimental Medicine, ISSN 1899–5276 (print), ISSN 2451–2680 (online)

Adv Clin Exp Med. 2025;34(7):1069–1077

Address for correspondence

Gustavo Vicentis de Oliveira Fernandes
E-mail: gustfernandes@gmail.com

Funding sources

None declared

Conflict of interest

None declared

Received on May 30, 2025

Reviewed on June 21, 2025

Accepted on June 24, 2025

Published online on July 23, 2025

Abstract

In a highly evolved and developed world, where professionals seek greater knowledge and understanding of advanced surgeries and high technologies, basic concepts have become distant, posing challenges in achieving an accurate periodontal diagnosis. Therefore, utilizing a step-by-step clinical and radiographic periodontal assessment protocol can facilitate precise diagnosis. This editorial introduces the Periodontal Assessment Protocol (GF-PAPro), developed based on the most substantial scientific literature, to guide clinicians and experts in standardized clinical periodontal assessments.

Key words: assessment, periodontitis, protocol, classification, gingivitis

Cite as

de Oliveira Fernandes GV, Mosley G, Cañizares AC, Hasse Fernandes JC, Muller R. Standardizing clinical evaluations of periodontal condition to guide assessments and diagnoses using the Periodontal Assessment Protocol (GF-PAPro). *Adv Clin Exp Med.* 2025;34(7):1069–1077.
doi:10.17219/acem/207502

DOI

10.17219/acem/207502

Copyright

Copyright by Author(s)

This is an article distributed under the terms of the Creative Commons Attribution 3.0 Unported (CC BY 3.0) (<https://creativecommons.org/licenses/by/3.0/>)

Highlights

- This editorial outlines the essential clinical steps for patient assessment, providing a practical and accessible reference for both clinicians and specialists.
- A novel protocol – the Periodontal Assessment Protocol (GF-PAPro) – was developed and introduced to simplify and standardize clinical periodontal assessments, offering clear guidance for practitioners.
- A practical diagnostic guide was provided to support the clinical identification of periodontitis and gingivitis.

Background

According to the World Health Organization (WHO), severe periodontal disease, characterized by 6-mm pockets and significant alveolar bone loss, is on the rise. With more than 1 billion cases reported worldwide, periodontal disease is considered a public health concern.¹ This trend is attributed to an aging population and increased longevity, along with socioeconomic factors. The global disease burden is expected to continue rising.¹ Periodontal disease manifests in various forms, from gingivitis to severe chronic periodontal disease. Early diagnosis and treatment are essential for the successful management of periodontal disease and for slowing its progression.

Thus, periodontal assessment is a cornerstone of comprehensive dental care, serving as the primary means of detecting, diagnosing and monitoring periodontal diseases. Given the high prevalence of periodontal diseases around the world, severe periodontitis is estimated to affect 5–15% of adults; routine periodontal evaluations are essential.^{2,3} These assessments typically involve a combination of visual examinations, probing measurements and radiographic assessment to evaluate the periodontal status. Tools such as Periodontal Screening and Recording (PSR),⁴ Basic Periodontal Examination (BPE)⁵ and GF-Periodontal Diagnosis and Risk Assessment (GF-PeDRA)⁶ are widely recommended for screenings, enabling clinicians to identify patients who require more comprehensive periodontal charting and intervention.

Beyond initial detection, periodontal assessments play a critical role in informing treatment planning and long-term maintenance strategies. Accurate diagnosis, incorporating clinical signs such as bleeding on probing (BoP), pocket depths, clinical attachment loss (CAL), and radiographic bone loss (RBL),⁷ is fundamental to effective patient care. Furthermore, understanding patient-specific risk factors, such as smoking and diabetes, enhances the ability to predict disease progression and tailor interventions accordingly. As periodontal research continues to evolve, integrating evidence-based guidelines and standardized assessment protocols remains crucial for improving patient outcomes and advancing oral healthcare practices.⁸

In a highly evolved and developed world, where professionals seek greater knowledge and understanding of advanced surgeries and high technologies, basic concepts

have become distant, posing challenges in achieving an accurate periodontal diagnosis. Therefore, utilizing a step-by-step clinical and radiographic periodontal assessment protocol can facilitate precise diagnosis. Thus, this editorial introduces the Periodontal Assessment Protocol (GF-PAPro), developed based on the most substantial scientific literature, to guide clinicians and experts in standardized clinical periodontal assessments.

Step-by-step clinical periodontal examination

Medical and dental history

The patient should be regularly evaluated, paying attention to both systemic and oral conditions. Systemic and behavioral factors significantly influence disease progression and treatment outcomes. Next, document the systemic conditions (e.g., diabetes, cardiovascular diseases, smoking), note any medications that may affect the periodontium (e.g., phenytoin), consider smoking history and psychosocial factors, and provide a history of periodontal treatment and maintenance.^{9,10}

Extraoral examination

It is recommended to assess the lymph nodes, temporomandibular joint and trigeminal nerve outlets (including the supraorbital, infraorbital and mental foramina) for any tenderness, asymmetry or abnormal sensitivity. A thorough evaluation of the lips and cheeks should include inspection and palpation of both the cutaneous (external skin) and vermillion (red) zones of the lips, noting color, texture, hydration, presence of fissures, ulcers, or lesions. The cheek mucosa should be examined bilaterally for signs of trauma, leukoplakia, pigmentation, ulceration, or other mucosal abnormalities.

Intraoral examination

Inspect and palpate the tongue (dorsal, ventral and lateral surfaces) and other intraoral structures for any mucosal lesions, swellings or deviations that may indicate systemic

or local pathology. Periodontal symptoms can overlap or mimic other conditions. A comprehensive intraoral exam helps prevent misdiagnosis. If applicable, scaling of plaque and calculus (debridement) before probing is strongly recommended. Then, 14 parameters are presented to achieve a precise and accurate clinical evaluation.¹¹ The number of remnant teeth should be analyzed and registered, excluding periodontally hopeless teeth (extraction recommended).

Plaque and calculus detection

Use a disclosing agent to stain plaque or conduct a visual inspection and score the plaque index (e.g., Silness and Løe or O'Leary). This fact is significant because bacterial biofilm is the primary etiologic factor in periodontal and peri-implant diseases. Its presence and distribution inform oral hygiene instructions and risk assessment. Bacterial plaque is the main etiological factor of periodontal diseases (plaque-induced disease). Therefore, an accurate appraisal should link certain gingival inflammations to other conditions affecting the periodontium, resulting in a non-plaque-induced disease.

The most recommended exam is the O'Leary Plaque Control Record (PCR),¹² which measures the presence or absence of plaque on tooth surfaces. It should record the presence (1) or absence (0) of plaque on four surfaces per tooth (buccal, lingual, mesial, distal) and must evaluate all teeth. Then, calculate: $PCR (\%) = (\text{number of surfaces with plaque} [\text{max } 4] / \text{total number of surfaces examined}) \times 100$.

Gingival assessment

Evaluate the color (healthy pink vs erythematous), contour (knife-edged vs rolled), consistency (firm vs edematous), and BoP (6 surfaces). Bleeding on probing is recognized as a crucial clinical indicator for assessing periodontal health and predicting disease progression, highlighting its importance in monitoring patients' post-treatment outcomes.^{13,14} It serves as a sign of inflammation in the periodontal tissues and is a valuable prognostic tool during the maintenance phase of periodontal therapy.¹⁵ Bleeding on probing is an early sign of gingival inflammation and correlates with disease activity; its persistence may be associated with future CAL. After probing the sulcus or periodontal pocket, it is recommended to observe the site for 5–10 s to determine if any bleeding occurs. It is essential to apply light, even pressure, ideally 15–25 g (0.15–0.25 N·cm),¹⁶ to prevent patient discomfort and ensure accurate readings.

Probing pocket depth or probing depth measurement

As described by Fernandes and Muller,² periodontal probing should be performed with precise technique: The probe must be gently inserted to the base of the sulcus

at the correct angulation, and advanced using the walking-stroke method. Six sites per tooth – mesiobuccal, mid-buccal, distobuccal, mesiolingual (or palatal), mid-lingual (or palatal), and distolingual (or palatal) – should be measured with a calibrated periodontal probe (e.g., UNC-15). Remember to apply slight pressure. Additionally, it is important to record pocket depths to the nearest millimeter: measurements of 4.1–4.4 mm are rounded down to 4 mm (with clinical discretion to round up at exactly 4.5 mm), whereas readings of 4.6–4.9 mm should be rounded up to 5 mm, always selecting the closest probe mark.^{2,17} Probing depth (PD) provides insight into the depth of periodontal pockets as well as the degree of inflammation and detachment. It is crucial to assess gingival swelling or inflammation – conditions that can mimic a pseudopocket – and to confirm these findings with radiographic evaluation.¹⁷ Probing dental implants must be conducted carefully to prevent damage to the peri-implant tissues. Utilize a light probing force with a plastic or titanium peri-implant probe. Probing depths around dental implants should likewise be measured at 6 sites per implant. Unlike natural teeth, peri-implant soft tissues do not possess a periodontal ligament; consequently, PDs of 4–5 mm may fall within normal limits, particularly around tissue-level implants.

However, a progressive increase in PDs over time – particularly when accompanied by BoP, suppuration or radiographic evidence of bone loss – may signal peri-implant disease, such as peri-implant mucositis or peri-implantitis.^{18–20}

Clinical attachment level

The CAL is the single most critical parameter in periodontal assessment, reflecting the position of the gingival margin (GM) relative to the cemento-enamel junction (CEJ); under normal conditions, the GM lies approx. 1 mm coronal to the CEJ (though it may occasionally be 2 mm or more above).

For greater accuracy, the position of the GM must be clinically measured by detecting the CEJ and the actual position of the GM ([+] when above CEJ; [–] when below CEJ). As described by Fernandes and Fernandes,⁷ clinical attachment level (CAL) is calculated as the difference between PD and the position of the GM:

$$CAL = PD - GM.$$

When there is no gingival recession, the GM is assumed to lie 3 mm coronal to the CEJ, so CAL may be estimated as PD minus 3 mm. It is important to recognize that a GM positioned at the CEJ (0) often reflects minimal recession. Clinically, PDs up to 3 mm are considered normal – occasionally extending to 4 mm – and facilitate effective oral hygiene and thorough debridement. Consequently, a 3 mm PD threshold is recommended as the pedagogical and technical standard. In cases of gingival overgrowth (pseudopockets), however, PD readings may be artificially

increased.⁷ Therefore, according to the 018 Classification, periodontitis requires the confirmation of interdental CAL at ≥ 2 non-adjacent teeth or buccal/facial CAL ≥ 3 mm with pocketing > 3 mm on ≥ 2 teeth, while excluding non-periodontal causes (e.g., caries, trauma). Staging reflects the severity and complexity, ranging from stage I to stage IV, based on CAL, RBL, tooth loss, and other parameters described below. Grading reflects the rate of progression, where grade A indicates slow progression and grade C indicates rapid progression, based on risk factors and evidence of progression determined.

Bone loss pattern

The bone loss pattern is classified as horizontal (uniform reduction in bone height in the arch) and vertical (angular, oblique bone defects adjacent to the tooth). Horizontal bone loss is the most common form, while vertical bone loss is more complex and can lead to periodontal pockets or infrabony defects. Precise evaluation of these diagnostic patterns is essential to guide the selection, timing and design of periodontal regenerative therapies.

Gingival recession

Gingival recession (Rec) is associated with root sensitivity, aesthetic problems, and CAL. It is measured from the CEJ to the GM. However, if the GM position is equal to the CEJ (CAL = 0), a small Rec should be considered. The most widely adopted recession classification systems are those proposed by Miller²¹ and by Cairo et al.²²

Miller's classification is divided into 4 classes: class I – marginal tissue recession does not extend to the mucogingival junction (MGJ); there is no loss of interproximal bone or soft tissue, and it has an excellent prognosis for root coverage; class II – recession extends to or beyond the MGJ, but still with no loss of interproximal bone or soft tissue, resulting in an excellent prognosis for treatment; class III – recession extends beyond the MGJ with some loss of interproximal bone or soft tissue, or malpositioning of teeth, resulting in expected partial root coverage; and class IV – recession extends beyond the MGJ with severe loss of interproximal bone or soft tissue, or severe tooth malposition, presenting a poor prognosis with no possible root coverage.

The classification by Cairo et al. was developed to address some of Miller's limitations, making it more applicable to both single and multiple recession-type defects. It is divided into 3 types: recession type 1 (RT1) involves recession with no interproximal CAL; the interproximal CEJ is clinically not detectable at both the mesial and distal aspects of the tooth, presenting facial CAL only. Within Cairo's 2011 classification, Recession type 2 (RT2) is defined by the presence of gingival recession accompanied by interproximal CAL that is less than or equal to the buccal attachment loss (interproximal CAL \leq buccal CAL).²²

In contrast, recession type 3 (RT3) is characterized by interproximal attachment loss that exceeds the buccal attachment loss (interproximal CAL $>$ buccal CAL).²²

Furcation involvement

Furcation involvement indicates whether the case involves advanced periodontal destruction, significantly impacting prognosis and treatment. As detailed by Romana and Fernandes,²³ furcation involvement may be assessed horizontally with a Nabers probe – using Glickman's²⁴ or Hamp, Nyman and Lindhe's²⁵ classification systems – or evaluated vertically according to Tarnow and Fletcher's criteria.²⁶ Glickman's classification presents 4 different grades: grade I: Furcation is felt with the probe, but the tip does not enter the furcation more than 1 mm; grade II: Probe tip penetrates the furcation more than 1 mm, extending to $\frac{1}{3}$ of the buccal to lingual width, but does not entirely go through to the other side; grade III: Furcation is not clinically visible, but the probe completely passes between the roots to the other side on mandibular molars and the maxillary first premolar (through-and-through). The probe passes between the roots and touches the palatal root on the maxillary molars; and grade IV: Same as Grade III, except that the furcation is clinically visible. Hamp, Nyman and Lindhe's classification identifies 3 grades of furcation involvement: grade I: The probe penetrates horizontally into the furcation up to 3 mm; grade II: Probe penetration into the furcation is more than 3 mm but does not go through to the other side; and grade III: Penetration from one side to the other, through-and-through.

Essentially, the steps for furcation assessment involve: 1) inserting the probe beneath the margin and rotating the instrument's tip into the furcation; 2) observing the horizontal extent of interradicular bone loss; 3) verifying the vertical bone loss with a periodontal probe; and 4) using the number of millimeters of bone loss (both horizontally and vertically) to determine the furcation involvement grade based on our recommendation (above).

Tooth mobility

Tooth mobility reflects periodontal support and occlusal trauma, influencing the decision to retain or extract a tooth. For evaluation, it is recommended to use the ends of 2 instrument handles to push the tooth in a buccolingual direction gently, or to use the index finger along with 1 end of an instrument handle. Always compare the mobility of a tooth with that of the adjacent or contralateral teeth. In addition to manual evaluation, Periotest or electronic devices can also be utilized.

Mobility can be assessed using either static or dynamic methods. Static mobility refers to the horizontal or vertical displacement of a tooth when gentle pressure is applied, typically using the ends of 2 instrument handles or a combination of an index finger and an instrument

handle. The tooth is moved in a buccolingual direction, and its mobility is compared to adjacent or contralateral teeth. This traditional method provides a qualitative, momentary evaluation of looseness. Dynamic mobility, on the other hand, evaluates the tooth's response to a rapid, low-impact force, typically using electronic devices such as the Periotest or the Tooth Mobility Measuring Device (TMD). These devices measure the damping characteristics of the periodontium and provide quantitative values that can be tracked over time, allowing for more objective and reproducible monitoring of changes in mobility, especially in cases involving splinted teeth, trauma or implants.

Miller's Mobility Index (MMI) categorizes tooth mobility into 4 grades. Grade 0 – physiologic mobility – is defined as horizontal movement under 0.2 mm. Grade I denotes slight horizontal mobility in the buccolingual direction between 0.2 mm and 1 mm. Grade II reflects moderate horizontal mobility of 1 mm or more without vertical (axial) displacement. Grade III combines severe horizontal movement exceeding 1 mm with vertical depressibility of the tooth into its socket.²⁷

Radiographs

Diagnostic radiographs are indispensable for accurate periodontitis diagnosis. A series of full-mouth X-rays (FMX) of 18 films – 14 periapical images using the paralleling technique for precise bone-level assessment and 4 bitewings – provides comprehensive detail. Bitewing radiographs offer high-resolution views of crestal bone, whereas panoramic images serve as an adjunctive overview but lack the detail necessary for definitive diagnosis. In select cases, cone beam computed tomography (CBCT) may be employed to evaluate furcation involvement, implant planning or complex osseous defects. These imaging modalities allow clinicians to confirm furcation lesions (evidenced by radiolucency in molar furcations), assess crestal bone morphology (noting irregular contours, triangulation, or “fuzziness”), identify periapical pathology (to rule out endo-periodontal lesions), visualize interproximal calculus deposits (as radiopaque spurs), and examine root anatomy (including concavities, root length, and divergence).^{28,29}

The most recent guidelines emphasize the role of radiographic images in the visual assessment of interproximal alveolar bone levels and the determination of RBL. While periapical radiographs are commonly used to evaluate the periodontium around the roots and RBL, this type of image can present undesirable angulations and distortions. Bitewing X-rays, on the other hand, offer better diagnostic quality for determining the percentage of RBL relative to root length, while also allowing for assessment of the level and pattern of proximal bone loss.

When assessing radiographic bone levels, measure the distance from the CEJ to the alveolar bone crest. Given that the biological width (supracrestal tissue attachment) typically averages around 2.0 mm (with some individual

variation), any CEJ–bone distance up to 2 mm should be considered within normal limits and not classified as RBL.

While variations can happen, it is essential to have a standard measure for guidance and sound clinical judgment. Thus, the calculation for the worst site with bone loss is: $RBL (\%) = ((\text{distance from CEJ to bone}) - 2.0 \text{ mm}) \times 10\%$ (indicating that for each millimeter found in the result, it is considered 10%). This CEJ–bone crest measurement is essential for periodontal diagnosis: Values up to 2 mm (within the supracrestal tissue attachment) indicate no RBL whereas any distance exceeding 2 mm denotes the presence of RBL. Given the emphasis on the quality of radiographs (the best possible) for accurate periodontal diagnosis, clinicians must employ meticulous techniques when exposing radiographs, positioning the receptor to capture the desired teeth and supporting structures in the image. In order to develop diagnostically acceptable radiographs, students and professionals should recall the correct placement of the receptor, such as a digital sensor or radiographic film. The guidelines for proper film placement are summarized in Table 1 below.

To reduce distortion in the image of the teeth, the dental professional has to be skilled in a radiographic technique to produce the most accurate presentation of the dentition.³⁰ It is noteworthy that current radiation safety guidelines for the use of lead aprons and collars have undergone changes. According to the American Dental Association (ADA), lead shields are no longer required for exposure to digital radiographs; however, clinicians must still follow the “as low as reasonably achievable” (ALARA) principle.^{31,32}

Extension and distribution

The extension and distribution of periodontitis refer to the extent to which the condition is present in the mouth. Proper classification is crucial for accurate diagnosis, prognosis and treatment planning in both gingivitis and periodontitis. In gingivitis cases, it is necessary to observe the number of sites with BoP; the condition will be localized if there is involvement of up to 30% of the sites, whereas a generalized condition involves more than 30% of the sites. When classifying periodontitis, it is considered localized if up to 30% of teeth are affected and generalized when more than 30% of teeth are involved. It is also necessary to consider the molar–incisor pattern, as well as former aggressive and juvenile periodontitis, which primarily affect the first molars and incisors, resulting in a significant vertical bone loss pattern.¹¹

Occlusal analysis

Traumatic occlusion can exacerbate periodontal breakdown in the presence of inflammation. Identifying signs of occlusal trauma (wear facets, fremitus and mobility) is highly relevant; use articulating paper and clinical judgment to assess these signs.

Table 1. Guide to film placement for areas of interest and minimal requirements for a diagnostic image

Area of interest	Type of image	Placement	Must cover	Acceptable distortion	XCP RINN instrument setup
Maxillary and mandibular molars	periapical	Behind molars with mesial edge of receptor at midline on second premolar. Set the bite block on the occlusal edge of the teeth. Adjust the position of the receptor to parallel as the patient closes	Distal half of the second premolar and back. At least 2 mm of periapical bone	Less than 50% of proximal overlap. Any more than that, the contact must be open on another periapical in the FMX series	"L-shaped" rod, yellow ring and yellow holder. Once assembled, the receptor should be centered in the yellow ring
Maxillary and mandibular premolars	periapical	Behind premolars with mesial edge of receptor at midline on canine. Set the bite block on the occlusal edge of the teeth. Adjust the position of the receptor to parallel as the patient closes	Distal half of the canine and back. At least 2 mm of periapical bone	Less than 50% of proximal overlap. Any more than that, the contact must be open on another periapical in the FMX series	"L-shaped" rod, yellow ring and yellow holder. Once assembled, the receptor should be centered in the yellow ring
Maxillary and mandibular canines	periapical	Behind the canine with canine centered. Set the bite block on the occlusal edge of the teeth. Adjust the position of the receptor to parallel as the patient closes	Distal half of the lateral incisor and mesial half of the first premolar. At least 2 mm of periapical bone	Less than 50% of proximal overlap. Any more than that, the contact must be open on another periapical in the FMX series	"Chair-shaped" rod, blue ring and blue holder. Once assembled, the receptor should be centered in the yellow ring
Maxillary and mandibular central incisors	periapical	Behind the central incisors with central incisors centered. Set the bite block on the occlusal edge of the teeth. Adjust the position of the receptor to parallel as the patient closes	Entire central incisors and mesial half of lateral incisors. At least 2 mm of periapical bone	Less than 50% of proximal overlap. Any more than that, the contact must be open on another periapical in the FMX series	"Chair-shaped" rod, blue ring and blue holder. Once assembled, the receptor should be centered in the yellow ring
Molar bitewing	bitewing	Behind molars with mesial edge of receptor at midline on second premolar. Hold the bite block centered between maxilla and mandible as the patient closes to distribute mandibular and maxillary teeth evenly	Distal half of the second premolar and back. At least 2 mm of periapical bone	Less than 50% of proximal overlap. Any more than that, the contact must be open on another periapical in the FMX series	"L-shaped" rod, red ring and red holder. Once assembled, the receptor should be centered in the red ring
Maxillary and mandibular premolars	bitewing	Behind premolars with mesial edge of receptor at midline of the canine. Hold the bite block centered between maxilla and mandible as the patient closes. Hold the bite block centered between maxilla and mandible as the patient closes to distribute mandibular and maxillary teeth evenly	Distal half of the canine and back. At least 2 mm of periapical bone	Less than 50% of proximal overlap. Any more than that, the contact must be open on another periapical in the FMX series	"L-shaped" rod, red ring and red holder. Once assembled, the receptor should be centered in the red ring

Receptor – X-ray film, digital sensor or phosphor plate; FMX – full-mouth X-rays; XCP – Extension Cone Paralleling system.

Peri-implant condition

Assessing the condition of peri-implants is critical for classifying the health or disease status of dental implants, ensuring accurate diagnosis and guiding treatment planning for preventive maintenance or therapeutic interventions. The health condition of peri-implant tissues presents an absence of inflammation – no BoP or suppuration – with stable, shallow PDs (generally ≤ 4 mm, occasionally up to 5 mm) and no evidence of progressive bone loss beyond normal physiologic remodeling. For peri-implant mucositis, the clinical conditions include inflammation of the soft tissues surrounding the implant, with the presence of BoP and/or suppuration, increased PDs (which may be due to swelling), but with no bone loss beyond initial remodeling. In the case of peri-implantitis, there is inflammation of the peri-implant mucosa accompanied

by progressive bone loss, with BoP and/or suppuration present, increased PDs compared to previous exams, and RBL beyond initial remodeling. In summary, implant assessment should include evaluation of PDs, BoP and suppuration, RBL relative to baseline, and KMW (ideally ≥ 2 mm), as well as consideration of occlusal loading and prosthetic design aspects.¹⁹

Need for complex rehabilitation

Need for complex rehabilitation is crucial for distinguishing between stage III and stage IV periodontitis, which are typically associated with significant periodontal destruction, tooth loss and impaired function. In these stages, patients often require complex interdisciplinary treatment to restore occlusal stability, esthetics and masticatory function. It may involve advanced

surgical and prosthetic procedures, such as bone regeneration, guided tissue regeneration (GTR) and the use of dental implants to replace missing teeth. Stage IV periodontitis, in particular, indicates a high level of complexity in rehabilitation, as it involves severe alveolar bone loss, bite collapse, tooth migration (flaring and drifting), secondary occlusal trauma, and fewer than 10 opposing tooth pairs, necessitating not only periodontal treatment but also complex restorative approaches. Treatment planning in such cases involves careful occlusal analysis, evaluation of remaining periodontal support, and management of both natural dentition and implant-supported prostheses.¹¹

How to use the GF-PAPRo checklist

The GF-PAPRo checklist streamlines the intraoral periodontal examination by providing a structured framework to assess key clinical parameters. Using this tool, clinicians can systematically evaluate periodontal health and accurately classify patients as periodontally healthy, presenting with gingivitis or exhibiting periodontitis. In periodontitis cases, it aids in staging and grading. Each row corresponds to a specific clinical or diagnostic parameter (e.g., BoP, CAL, RBL), and the rightmost column (“Sequence for Periodontal Dx”) provides numbered steps aligned with the diagnostic flow. Red numbers indicate sequential steps used to diagnose gingivitis, whereas black numbers indicate steps used to diagnose periodontitis.

To use the step-by-step (the rightmost column in Table 2), it is necessary to complete the checklist row by row (sequentially from 1 to 20) for each patient. As you document findings, follow the sequence numbers in the right column, which correspond to the proposed diagnostic decision tree from Fernandes and Fernandes.⁷ After assessing each parameter, note its coded numeral: if it is a red number, incorporate the finding into your gingivitis diagnostic reasoning; if it is a black number, follow the periodontitis algorithm, including staging and grading modifiers. Examples of application (right column – diagnosis):

1. Step 1 (red and black): Measure interdental CAL. If CAL is present on at least 2 non-adjacent teeth, periodontitis is suspected.

2. Step 2 (red and black): Calculate percentage bone loss relative to patient age (RBL/age). Values above expected norms support a diagnosis of periodontitis.

3. Step 3 (red and black): Count teeth lost to periodontitis (including those deemed hopeless and planned for extraction).

4. Step 4:

- Black pathway: Re-measure PD to further characterize periodontitis.
- Red pathway: If BoP exceeds 10% of sites without any CAL or RBL, diagnose gingivitis; if BoP is ≤10%, consider the periodontium healthy.

5. Step 5:

- Red pathway: Note gingival phenotype (redness, edema, recession) to complete the gingivitis assessment or refine periodontitis staging.
- Black pathway: Review the pattern of bone loss (horizontal vs vertical) for periodontitis staging.

6. Step 6:

- Red pathway: Record the plaque index to contextualize gingival inflammation.
- Black pathway: Examine furcation involvement as part of periodontitis grading.

7. Step 7:

- Red pathway: Determine the extent and distribution of BoP: ≤10% excludes gingivitis, 10–30% indicates localized gingivitis, while >30% indicates generalized gingivitis.
- Black pathway: Assess tooth mobility to inform periodontitis severity.

8. Steps 8, 9, 11–13 (black only): Apply the staging (I–IV) and grading (A–C) criteria for periodontitis based on cumulative findings.

9. Step 10 (black only): Define distribution of disease – localized, generalized or molar–incisor pattern – to complete the periodontitis diagnosis.

By following these red- and black-coded steps in sequence, clinicians can rapidly differentiate gingivitis from periodontitis, stage and grade disease, and ensure a standardized, evidence-based diagnosis.

In summary, the red-coded steps rapidly identify gingivitis – relying on BoP in the absence of attachment loss or bone loss – while the black-coded steps provide a systematic pathway for diagnosing, staging and grading periodontitis. By adhering to this structured sequence, GF-PAPRo ensures consistent, evidence-based diagnoses, enhances teaching and training, standardizes clinical documentation, and supports clear interdisciplinary communication.

Final considerations

Table 2 provides a summary checklist and sequence of assessments, detailing the clinical steps for periodontal evaluation and a recommended order for achieving a periodontal diagnosis. They can be used daily and make it easier to remember each clinical step. Furthermore, GF-PAPRo is presented for the first time in the literature, allowing for the establishment of periodontal/peri-implant diagnosis, classifying the disease by severity, complexity, extent, and distribution (stage and grade), and analyzing all parameters recommended by the latest periodontal guidelines (2018), which include both clinical and radiographic parameters.¹¹

Table 2. Checklist for GF-PAPro – Intraoral examination, presenting the logical sequence for clinical assessment and periodontal diagnosis (Dx)

GF-Periodontal Assessment Protocol (GF-PAPro)				
Pt id:		Pt age:		
Sequence for clinical assessment	Parameters	Guide	Check	Sequence for Periodontal Dx* Periodontitis (black) / Gingivitis (red)
1	Number of remnant teeth (exclude periodontally hopeless tooth – extraction recommended)	n = _____	<input type="checkbox"/>	–
2	Tooth loss including periodontally hopeless teeth planned for extraction	() No one () None due to periodontitis () Loss of up to 4 teeth due to periodontitis () Loss of ≥ 5 teeth due to periodontitis	<input type="checkbox"/>	3/3
3	Diabetes	() No diabetic () HbA1C >5.6% and <7.0% () HbA1C > 7.0%	<input type="checkbox"/>	12 (modifier for Grade)
4	Smoker (cigarettes)	() Non-smoker () < 10 cigarettes/day () ≥ 10 cigarettes/day	<input type="checkbox"/>	13 (modifier for Grade)
5	Any other systemic condition (besides diabetes)	() No () 1 or 2, but controlled () > 2, but controlled () 1 or 2, but not controlled () > 2, but not controlled	<input type="checkbox"/>	–
6	Plaque index (4 surfaces)	PCR (%) = (n surfaces with plaque / n surfaces) × 100	<input type="checkbox"/>	6
7	Gingival assessment	() Healthy gingiva (firm and resilient, coral pink, stippled, uniform color, Knife-edged margins, scalloped appearance following the CEJ, firm and adapted) () Inflamed gingiva (erythematous [red], possibly bluish-red or cyanotic in chronic inflammation, enlargement, soft, spongy, loss of stippling/ smooth, shiny, pits easily under gentle pressure, rounded or rolled margins, loss of scalloping (verify drug-induced hyperplasia) () Melanin pigmentation (physiological pigmentation in darker-skinned individuals [brown-black patches]) () with Rec (typical) () V-shaped Rec defects Clefts (Stillman's cleft) () Cratering of interdental papillae: necrotizing ulcerative () Desquamation or ulceration: desquamative gingivitis	<input type="checkbox"/>	5
8	BoP (6 surfaces)	BoP (%) = (n sites bleeding / (n teeth × 6)) × 100	<input type="checkbox"/>	4
9	PD (the worst site)	_____mm	<input type="checkbox"/>	4
10	CAL (the greatest interdental)	_____mm	<input type="checkbox"/>	1/1
11	Bone loss pattern	() N/A () horizontal () vertical	<input type="checkbox"/>	5
12	Rec (the greatest Rec)	() No () Facial/Lingual () Interdental _____mm	<input type="checkbox"/>	–
13	Furcation involvement	() Class I () Class II () Class III () Class IV	<input type="checkbox"/>	6
14	Tooth mobility	() Grade 0 () Grade I () Grade II () Grade III	<input type="checkbox"/>	7
15	Radiographic Periodontal Assessment (RBL) (bitewing – the worst site)	RBL (%) = ((CEJ to bone) – 2.0 mm [STA/BW]) × 100 Periapical – Observe periodontal structure around the root and in the cervical area () N/A or () Yes. _____%	<input type="checkbox"/>	2/2 and 11 (use [%RBL/ age] to Grade)
16	Extension and distribution	() N/A () Localized (up to 30%) () Generalized (> 30%) () Molar-Incisor Localized (up to 30%) () Molar-Incisor Generalized (> 30%)	<input type="checkbox"/>	10/7
17	Occlusal analysis	() No trauma () With trauma/without periodontitis () With trauma and periodontitis	<input type="checkbox"/>	8
18	Peri-implant condition	() Mucositis () Peri-implantitis up to 50% of the implant () Peri-implantitis over 50% of the implant	<input type="checkbox"/>	–
20	Need for complex rehabilitation	() N/A () < 10 opposing pairs () Masticatory dysfunction () Bite collapse, drifting, or flaring () Secondary occlusal trauma (mobility > II)	<input type="checkbox"/>	9

* Fernandes GVdO, Fernandes JCH. Revisiting and rethinking on staging (severity and complexity) periodontitis from the new classification system: A critical review with suggestions for adjustments and a proposal of a new flowchart. Dent Med Probl. 2025;62(2):371–391. doi:10.17219/dmp/192121. BoP – bleeding on probing; BW – biological width; CEJ – cement-enamel junction; mm – millimeters; N/A – not applied; PD – probing depth; RBL – radiographic bone loss; STA – supracrestal tissue attachment.

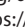
Use of AI and AI-assisted technologies


Not applicable.

ORCID iDs

Gustavo Vicentis de Oliveira Fernandes


 <https://orcid.org/0000-0003-3022-4390>

Grace Mosley  <https://orcid.org/0009-0000-9618-4323>

Ana Cristina Cañizares  <https://orcid.org/0009-0003-3844-2509>

Juliana Campos Hasse Fernandes

 <https://orcid.org/0000-0001-7603-3544>

Romana Muller  <https://orcid.org/0000-0002-0476-1136>

References

- World Health Organization (WHO). *Global Oral Health Status Report: Towards Universal Health Coverage for Oral Health By 2030*. Geneva, Switzerland: World Health Organization (WHO); 2022. ISBN:978-92-4-006148-4.
- Fernandes GVO, Mueller R. Back to the basics: Mastering probing techniques for comprehensive periodontal assessment. *J Basic Clin Dent*. 2024;1(1):1–8. <https://j-bcd.com/index.php/j-bcd/article/view/18/6>. Accessed March 15, 2025.
- Preshaw PM. Detection and diagnosis of periodontal conditions amenable to prevention. *BMC Oral Health*. 2015;15(Suppl 1):S5. doi:10.1186/1472-6831-15-S1-S5
- Khocht A, Zohn H, Deasy M, Chang KM. Assessment of periodontal status with PSR and traditional clinical periodontal examination. *J Am Dent Assoc*. 1995;126(12):1658–1665. doi:10.14219/jada.archive.1995.0115
- Dale CLT, Smorthit K, Storey M, Srinivasan V. The importance of the Basic Periodontal Examination for paediatric orthodontic patients. *Br Dent J*. 2021;231(3):163–168. doi:10.1038/s41415-021-3292-5
- Fernandes GVO, Fernandes JCH. A new algorithm/tool used to achieve the periodontal risk assessment, diagnosis and prognosis (GF-PeDRA): A clinical study with 221 patients. *Dent Med Probl*. 2025 [in press].
- Fernandes GVDO, Fernandes JCH. Revisiting and rethinking on staging (severity and complexity) periodontitis from the new classification system: A critical review with suggestions for adjustments and a proposal of a new flowchart. *Dent Med Probl*. 2025;(2):371–391. doi:10.17219/dmp/192121
- Salvi GE, Rocuzzo A, Imber J, Stähli A, Klinge B, Lang NP. Clinical periodontal diagnosis [published online as ahead of print on July 14, 2023]. *Periodontol 2000*. 2023. doi:10.1111/prd.12487
- Isola G, Santonocito S, Lupi SM, et al. Periodontal health and disease in the context of systemic diseases. *Mediators Inflamm*. 2023; 2023:9720947. doi:10.1155/2023/9720947
- Tavares LTR, Saavedra-Silva M, López-Marcos JF, Veiga NJ, Castilho R de M, Fernandes GV de O. Blood and salivary inflammatory biomarkers profile in patients with chronic kidney disease and periodontal disease: A systematic review. *Diseases*. 2022;10(1):12. doi:10.3390/diseases10010012
- Caton JG, Armitage G, Berglundh T, et al. A new classification scheme for periodontal and peri-implant diseases and conditions: Introduction and key changes from the 1999 classification. *J Clin Periodontol*. 2018;45(Suppl 20):S1–S8. doi:10.1111/jcpe.12935
- O’Leary TJ, Drake RB, Naylor JE. The Plaque Control Record. *J Periodontol*. 1972;43(1):38. doi:10.1902/jop.1972.43.1.38
- Lang NP, Joss A, Orsanic T, Gusberti FA, Siegrist BE. Bleeding on probing: A predictor for the progression of periodontal disease? *J Clin Periodontol*. 1986;13(6):590–596. doi:10.1111/j.1600-051X.1986.tb00852.x
- Badersten A, Nilvéus R, Egelberg J. Scores of plaque, bleeding, sup-puration and probing depth to predict probing attachment loss 5 years of observation following nonsurgical periodontal therapy. *J Clin Periodontol*. 1990;17(2):102–107. doi:10.1111/j.1600-051X.1990.tb01070.x
- Joss A, Adler R, Lang NP. Bleeding on probing: A parameter for monitoring periodontal conditions in clinical practice. *J Clin Periodontol*. 1994;21(6):402–408. doi:10.1111/j.1600-051X.1994.tb00737.x
- Seki K, Nakabayashi S, Tanabe N, Kamimoto A, Hagiwara Y. Correlations between clinical parameters in implant maintenance patients: Analysis among healthy and history-of-periodontitis groups. *Int J Implant Dent*. 2017;3(1):45. doi:10.1186/s40729-017-0108-0
- Heitz-Mayfield LJA. Conventional diagnostic criteria for periodontal diseases (plaque-induced gingivitis and periodontitis). *Periodontol 2000*. 2024;95(1):10–19. doi:10.1111/prd.12579
- Fernandes GVO, Mosley GA, Ross W, Dagher A, Martins BGDS, Fernandes JCH. Revisiting Socransky’s complexes: A review suggesting updated new bacterial clusters (GF-MoR complexes) for periodontal and peri-implant diseases and conditions. *Microorganisms*. 2024;12(11):2214. doi:10.3390/microorganisms12112214
- Fernandes GVDO, Martins BGDS, Fraile JF. Revisiting peri-implant diseases in order to rethink the future of compromised dental implants: Considerations, perspectives, treatment, and prognosis. *Dent Med Probl*. 2024;61(5):637–640. doi:10.17219/dmp/187215
- Fernandes GVO, Fernandes JCH. Call to review how staging periodontitis using the 2017 Classification of Periodontal and Peri-Implant Diseases and Conditions: Suggestions for modifications and improvements to help clinicians in the decision-making diagnosis. *Env Dent J*. 2024;6(1):[no pages given]. <https://dentaljournal.org/volVolumeno1/call-to-review-how-staging-periodontitis-using-the-2017-classification-of-periodontal-and-peri-implant-diseases-and-conditions-suggestions-for-modifications-and-improvements-to-help-clinicians-in-the-decision-making-diagnosis>. Accessed March 15, 2025.
- Miller PD. A classification of marginal tissue recession. *Int J Periodontics Restorative Dent*. 1985;5(2):8–13. PMID:3858267.
- Cairo F, Nieri M, Cincinelli S, Mervelt J, Pagliaro U. The interproximal clinical attachment level to classify gingival recessions and predict root coverage outcomes: An explorative and reliability study. *J Clin Periodontol*. 2011;38(7):661–666. doi:10.1111/j.1600-051X.2011.01732.x
- Mueller R, Fernandes GVO. Navigating furcation: A guide for an accurate assessment. *J Basic Clin Dent*. 2025;2(1):1–11. <https://j-bcd.com/index.php/j-bcd/article/view/23/10>. Accessed March 15, 2025.
- Glickman I. *Clinical Periodontology: Prevention, Diagnosis, and Treatment of Periodontal Disease in the Practice of General Dentistry*. 4th ed. Philadelphia, USA: Saunders; 1972. ISBN:978-0-7216-4137-9.
- Hamp S, Nyman S, Lindhe J. Periodontal treatment of multi rooted teeth: Results after 5 years. *J Clin Periodontol*. 1975;2(3):126–135. doi:10.1111/j.1600-051X.1975.tb01734.x
- Tarnow D, Fletcher P. Classification of the vertical component of furcation involvement. *J Periodontol*. 1984;55(5):283–284. doi:10.1902/jop.1984.55.5.283
- Wu CP, Tu YK, Lu SL, Chang JH, Lu HK. Quantitative analysis of Miller mobility index for the diagnosis of moderate to severe periodontitis: A cross-sectional study. *J Dent Sci*. 2018;13(1):43–47. doi:10.1016/j.jds.2017.11.001
- Alasqah M, Alotaibi FD, Gufran K. The radiographic assessment of furcation area in maxillary and mandibular first molars while considering the new classification of periodontal disease. *Healthcare (Basel)*. 2022;10(8):1464. doi:10.3390/healthcare10081464
- Kurt-Bayrakdar S, Bayrakdar İŞ, Yavuz MB, et al. Detection of periodontal bone loss patterns and furcation defects from panoramic radiographs using deep learning algorithm: A retrospective study. *BMC Oral Health*. 2024;24(1):155. doi:10.1186/s12903-024-03896-5
- Yen M, Yeung AWK. The performance of paralleling technique and bisecting angle technique for taking periapical radiographs: A systematic review. *Dent J*. 2023;11(7):155. doi:10.3390/dj11070155
- American Dental Association (ADA). ADA Releases Updated Recommendations to Enhance Radiography Safety in Dentistry (published February 1, 2024). Chicago, USA: American Dental Association (ADA); 2024. <https://www.ada.org/about/press-releases/ada-releases-updated-recommendations-to-enhance-radiography-safety-in-dentistry>. Accessed March 15, 2025.
- Benavides E, Krecioch JR, Connolly RT, et al. Optimizing radiation safety in dentistry: Clinical recommendations and regulatory considerations. *J Am Dent Assoc*. 2024;155(4):280–293.e4. doi:10.1016/j.adaj.2023.12.002

Suicidal behavior and substance dependence

Barbara Schneider^{1,2,A,D,F}, Lars Meiländer^{1,A,E–F}, Tilman Wetterling^{3,D–F}

¹ LVR Clinic Cologne Merheim, Germany

² Department of Psychiatry, Psychosomatic Medicine and Psychotherapy, Goethe-University of Frankfurt, Germany

³ Department of Psychiatry and Neurosciences, Charité – Universitätsmedizin Berlin, Germany

A – research concept and design; B – collection and/or assembly of data; C – data analysis and interpretation;

D – writing the article; E – critical revision of the article; F – final approval of the article

Advances in Clinical and Experimental Medicine, ISSN 1899–5276 (print), ISSN 2451–2680 (online)

Adv Clin Exp Med. 2025;34(7):1079–1084

Address for correspondence

Barbara Schneider

E-mail: Barbara.Schneider@lvr.de

Funding sources

None declared

Conflict of interest

None declared

Abstract

Suicidal behavior is a common psychiatric emergency and poses a significant challenge in mental health care. Substance use disorders are among the most frequently observed mental health conditions in individuals who die by suicide.

Key words: suicide, alcoholism, substance-related disorders

Received on February 11, 2025

Reviewed on June 16, 2025

Accepted on June 18, 2025

Published online on July 25, 2025

Cite as

Schneider B, Meiländer L, Wetterling T. Suicidal behavior and substance dependence. *Adv Clin Exp Med.* 2025;34(7):1079–1084. doi:10.17219/acem/207291

DOI

10.17219/acem/207291

Copyright

Copyright by Author(s)

This is an article distributed under the terms of the Creative Commons Attribution 3.0 Unported (CC BY 3.0) (<https://creativecommons.org/licenses/by/3.0/>)

Highlights

- Substance use disorders are strongly linked to suicide risk: Psychological autopsy studies reveal that 19–63% of suicide cases involve substance dependence, with alcohol-related disorders contributing significantly to suicide mortality.
- Alcohol and drug addiction elevate suicide risk across populations: Suicide rates are alarmingly high among those with substance dependence – 8 in 100 alcoholics die by suicide, and risks rise with cannabis, heroin and nicotine use.
- Comorbid depression and addictions sharpen suicide vulnerability: The presence of both substance use disorders and depression drastically increases suicide risk, demanding integrated mental health and addiction treatment strategies.
- Comprehensive care is essential for suicide prevention in addicted individuals: Effective suicide prevention must target acute suicidal behavior and address underlying substance use and co-occurring psychiatric disorders for long-term outcomes.

Introduction: Substance use disorder and suicide

Substance use disorders (SUDs) and suicidal behavior are both of great importance in medical and psychosocial care.^{1,2} In Western countries, the majority of suicides are linked to mental disorders, with alcohol use disorders accounting for approx. 22% of all suicide cases.^{3–6} Considering important association between suicide and SUDs, the following narrative review aims to provide a comprehensive overview of the current scientific knowledge covering the most important studies in this field. We conducted a literature search across multiple databases (PubMed, Embase, Web of Science, and PubPsych). Psychological autopsy studies indicate that nearly 1/3 of male suicides and approx. 15% of female suicides involved SUDs. Meta-analyses of cohort studies, primarily involving inpatient populations, and controlled studies using the psychological autopsy method have demonstrated that SUDs are associated with a substantially increased risk of suicide.^{7–10} Substance dependence has been shown to elevate suicide risk by a factor of 3 to 17.^{9,11}

Among individuals with addiction who died by suicide, women were significantly more likely than men to have experienced sexual abuse, to be dependent on prescription drugs and to have a history of previous suicide attempts. Addicted women were also generally younger, more likely to be intoxicated at the time of death, and tended to use less violent methods compared to non-addicted women.^{12,13}

Different psychotropic drugs and suicide risk

The following list details the suicide risks associated with different psychotropic substances.

– Between 15% and 61% of all suicides were alcohol-related.⁷ The lifetime risk of suicide for alcohol-dependent people is around 8% and remains constant over lifetime.^{14,15} Alcoholism has repeatedly been identified as a significant risk

factor for all forms of suicidal behavior, despite differences in diagnostic systems, age groups and proportion of men.^{7,8,16} The risk of suicide in alcoholism is particularly high in middle age^{17–19}; between the ages of 20 and 50, the risk rose sharply, especially in the presence of a depressive disorder.²⁰ Worldwide, the prevalence of alcohol use disorders is higher among men than among women.^{21,22} However, women with alcohol use disorders have a higher risk of suicide than men (up to 10 times higher in men and up to 16 times higher in women than in the general population).¹⁶

– The following risk factors for suicide in alcoholism have been identified⁷:

- heavy drinking (equivalent to at least 70 g alcohol/day);
- nicotine consumption of more than 20 cigarettes per day;
- suicide “threats”;
- living alone;
- little social support;
- relationship problems and breakups;
- little schooling, previous suicide attempts;
- comorbidity with affective disorders.

After adjustment for other mental disorders, the risk of suicide associated with alcohol dependence decreases.²³ The risk of suicide attempts was 27 times higher in alcoholics than in the general population after 25 years.²⁴

– Smoking is associated with an about twofold increased risk of suicide in both, men and women, even after adjustment (i.e., statistical correction) for mental illness and other, mostly sociodemographic factors.^{7,25} The risk of suicide increased by an additional 24% for every 10 cigarettes smoked.²⁶ In contrast to current smokers, former smokers do not have an increased risk of suicide.²⁶ Nicotine dependence increased the risk of attempted suicide by almost a factor of 1, even after adjustment for sociodemographic characteristics and other mental and physical illnesses.²⁷

– Young men with cannabis use disorder had a 2.56-fold higher risk of suicide compared to the general population.²⁸ After 30 years of follow-up, risk of suicide was not increased after adjustment for confounding variables, including psychiatric diagnosis, social relationships, parental

use of psychotropic medication, alcohol consumption, cigarette smoking, and use of other drugs.²⁹ Chronic or heavy cannabis use can increase the risk of suicidal ideation (odds ratio (OR) = 2.5) and suicide attempts (OR = 3.2).²⁸

- Opioid and opiate use were associated with a 14-fold increase in the risk of suicide compared to the general population.⁸ Heroin users in a methadone substitution program, although methadone reduces suicidal behavior (compared to heroin users who are not in a substitution program),³⁰ had an 18.4 times higher risk of suicide than the general population.³¹ Particularly high risk was observed for female users (standardized mortality ratio (SMR) = 27.0).³¹ Female gender and psychopathology (depressed mood, inadequate behavior, suicidal intent, fear of psychological disintegration, insight into the psychopathology, high self-expectations) were associated with suicide among heroin users.³²

- Among all acute illicit drug use, cocaine use is most frequently associated with suicide.³³ Mixed drug use is associated with a 16- to 20-fold increase in suicide risk.⁸ The concurrent use of alcohol with illicit drugs further elevates this risk.³⁴ Furthermore, the data indicates that among individuals who use drugs, 21.9% have attempted suicide, a figure that rises to 42.2% for those who use heroin.³⁵

Comorbidity

Comorbidities of addictive disorders with other mental disorders and with physical illnesses are very common. It has been found that drug use increases the risk of suicide among people with schizophrenia.³⁶ The comorbidity of psychotropic use disorders and affective disorders has been associated with a particularly high risk of suicide, even in adolescents.^{37,38} Conner et al.³⁹ found that the comorbidity of depressive disorders and alcohol dependence increased the risk of suicide by a factor of 4.5 in 20-year-olds and by a factor of 83 in those over 50.

Potential mechanisms linking SUDs and suicidal behavior

Suicidal behavior is thought to be triggered by an interplay between genetic, psychological and environmental factors.⁴⁰ All psychotropic substances affect the body's neurotransmitter systems, and current evidence suggests that neurobiological factors are likely to lead to suicidal behavior, in particular, deficits in serotonin.⁴¹ There are only a few models that have been developed to explain the association between SUDs and suicidal behavior.^{1,42–44} These models include predisposing and triggering factors, such as impulsiveness, hopelessness, lack of social support, aggressivity, low self-worth, interpersonal conflicts, and the experience of being offended. Sometimes, people use psychotropic substances when feeling helpless and

aggressive. However, substance use can increase aggression and impair cognitive abilities, resulting in a lack of alternative coping strategies.⁴²

Therapeutic interventions

Treatment of suicidal behavior must include the treatment of SUDs and that of comorbid mental disorders. Use of medications for maintaining abstinence in alcohol dependence and opioid dependence (naltrexone, acamprosate, buprenorphine, and methadone) should be offered. A significant reduction of suicidal behavior has only been found in the treatment with the opioid agonist methadone in opioid dependent patients compared to patients without opioid agonist treatment (hazard ratio (HR) = 0.60).³⁰ Comorbidity of schizophrenia and affective disorders must also be treated: Clozapine was found to significantly reduce suicides and suicide attempts in patients with schizophrenia (OR = 0.23).⁴⁵ Long-term lithium treatment, when compared to a placebo or other drugs, was associated with a reduction in death by suicide and suicide attempts, particularly in individuals with bipolar disorder.^{46,47} There is currently no evidence that other psychotropic drugs, such as serotonin reuptake inhibitors and other antidepressants, reduce suicidal behavior.⁴⁸ Preliminary evidence for the short-term efficacy of ketamine in suicidal behavior was noted by the majority of reviews; however, long-term effects remained unknown and also effects in addicted subjects must be reconsidered. Due to the low quality of many studies and the limitations of core studies, further research, in particular in SUDs, is required.⁴⁹

Inpatient treatment, if necessary, under protected conditions, is indicated for acute suicidal behavior. Accepting suicidal behavior as a distress signal, understanding the meaning and subjective necessity of this signal, and dealing with failed coping attempts are the basic prerequisites for treatment in a suicidal crisis.⁵⁰ The most important prerequisite for effective crisis intervention is the development of a trusting and sustainable relationship that allows patients to talk openly about their current complaints and the situation that triggers suicidal behavior.⁵⁰ Particular attention must be paid to the increasing narrowing of personal options and the loss of interpersonal relationships in the case of suicidal behavior of substance abusers.

Special challenges in the treatment of suicidal substance users

Special challenges arise due to the affective symptoms that frequently occur during detoxification and withdrawal treatment: These are particularly depression, cognitive impairment, increased aggression, and impulsivity, which

are often associated with suicidal behavior.⁴² A variety of difficulties can occur throughout the whole treatment of suicidal addicts.⁵¹ The quality of the relationship between patient and therapist significantly impacts the recognition of suicidality, but it is often difficult to establish a stable, trusting relationship. Overcoming a crisis takes time. However, addicts often “flee” back into substance use quickly and often use psychotropic substances as a form of self-medication, in particular in comorbid mental health conditions. Further medical treatment is frequently inseparable from psychiatric treatment, including treatment of suicidal behavior. Suicides of people with dependence disorders often occur outside the system of medical and psychosocial care. As a consequence of the circumstances of abuse (e.g., intoxication),⁵² unstable living conditions and a lack of social integration, suicidal addicts often cannot be reached (in time) by the suicide prevention support system. Further research on pharmacological and psychosocial interventions is necessary.⁵³

Limitations

However, there are several limitations to epidemiological research into the relationship between SUDs and suicidal behavior. Although there is already extensive research on SUDs and suicide in general, recent and high-quality studies on this topic are lacking, especially in Europe. There is a lack of standardized measurement of suicidality across studies, as well as a potential publication bias in suicide research. Moreover, suicide risks for SUDs are estimated in various study designs, in different countries with different age structures and different socioeconomic conditions. The studies reported adjusted risk ratios (often adjusted for age and gender) and unadjusted risk ratios, especially in studies that only calculated SMRs. Furthermore, relying on self-reported data on substance use may result in consumption levels being underestimated. Despite all these limitations, there is a high level of evidence of risk factors associated with suicide risk in SUDs. However, research on potential protective factors for suicide, such as social support, access to mental health services and harm reduction programs in SUDs is lacking. Furthermore, the impact of different diagnostic systems or changes in patterns of psychotropic substance use, in particular of multiple substance use, on suicide risk estimates is still unclear.

Conclusions

Early recognition and, most importantly, effective treatment of addiction could significantly reduce suicide rates worldwide. In addition to targeted interventions for suicidal behavior and SUDs, general suicide prevention strategies – such as restricting access to common means of suicide (e.g., firearms) – play a crucial role in reducing suicidal behavior.

Numerous research questions remain open for future investigation, including how suicide risk varies across age groups in relation to specific psychotropic substances used, gender identities and socioeconomic backgrounds. Additionally, there is a need to examine how established theoretical models of suicidality – such as:

- Joiner’s Interpersonal Theory of Suicide⁵⁴;
- the Cry of Pain Model⁵⁵;
- O’Connor’s Integrated Motivational–Volitional Model⁵⁶;
- the Fluid Vulnerability Theory of Suicide⁵⁷;
- and the Cubic Model of Suicide,⁵⁸

relate to the link between suicidal behavior and substance use. To date, these models have not adequately addressed the impact of psychotropic substances on suicidality. This gap highlights the need for new theoretical considerations and integrations.


Although there is a broad array of literature for suicide prevention measures,^{40,59–62} previous preventive measures should be supplemented by innovative approaches. Artificial intelligence (AI) could play a role in this regard. It promises new ways to reduce the effects of SUDs, refine treatment standards and minimize the risk of relapse through tailored treatment plans.⁶³ Machine learning models show promise in suicide prevention. However, challenges like data limitations, bias and interpretability issues need addressing. Integrating AI in clinical workflows, particularly in risk assessment and early intervention, continued research and ethical scrutiny are crucial to fully realize AI’s potential in suicide prevention.^{64,65}


Use of AI and AI-assisted technologies

Not applicable.

ORCID iDs

Barbara Schneider  <https://orcid.org/0000-0003-4864-7084>

Lars Meiländer  <https://orcid.org/0009-0002-7820-5738>

Tilman Wetterling  <https://orcid.org/0000-0002-6807-4060>

References

1. Schneider B, Wetterling T. *Sucht und Suizidalität*. Stuttgart, Germany: Verlag W. Kohlhammer; 2016. ISBN: 978-3-17-023360-7, 978-3-17-028798-3, 978-3-17-028799-0, 978-3-17-028800-3.
2. World Health Organization (WHO). Suicide prevention (SUPRE). Geneva, Switzerland: World Health Organization (WHO); 2024. https://www.who.int/health-topics/suicide#tab=tab_1. Accessed June 22, 2024.
3. Sluga W, Grünberger J. Self-inflicted injury and self-mutilation in prisoners [in German]. *Wien Med Wochenschr*. 1969;119(24):453–459. PMID:5801632.
4. Carrasco-Barrios MT, Huertas P, Martín P, et al. Determinants of suicidality in the European general population: A systematic review and meta-analysis. *Int J Environ Res Public Health*. 2020;17(11):4115. doi:10.3390/ijerph17114115
5. Schneider B. *Risikofaktoren für Suizid*. Regensburg, Germany: Roderer; 2003. ISBN: 978-3-89783-372-2.
6. Fu XL, Qian Y, Jin XH, et al. Suicide rates among people with serious mental illness: A systematic review and meta-analysis. *Psychol Med*. 2021;52(2):351–361. doi:10.1017/S0033291721001549
7. Schneider B. Substance use disorders and risk for completed suicide. *Arch Suicide Res*. 2009;13(4):303–316. doi:10.1080/13811110903263191

8. Wilcox HC, Conner KR, Caine ED. Association of alcohol and drug use disorders and completed suicide: An empirical review of cohort studies. *Drug Alcohol Depend.* 2004;76 Suppl:S11–S19. doi:10.1016/j.drugalcdep.2004.08.003
9. Yuodelis-Flores C, Ries RK. Addiction and suicide: A review. *Focus (Am Psychiatr Publ).* 2019;17(2):193–199. doi:10.1176/appi.focus.17203
10. Too LS, Spittal MJ, Bugeja L, Reifels L, Butterworth P, Pirkis J. The association between mental disorders and suicide: A systematic review and meta-analysis of record linkage studies. *J Affect Disord.* 2019;259:302–313. doi:10.1016/j.jad.2019.08.054
11. Schneider B, Georgi K, Weber B, Schnabel A, Ackermann H, Wetterling T. Risk factors for suicide in substance-related disorders [in German]. *Psychiatr Prax.* 2006;33(2):81–87. doi:10.1055/s-2005-866858
12. Pirkola S. Alcohol and other substance misuse in suicide [doctoral thesis]. Helsinki, Finland: Department of Mental Health and Alcohol Research, National Public Health Institute and Department of Psychiatry, University of Helsinki; 1999. <https://citeseerx.ist.psu.edu/document?repid=rep1&type=pdf&doi=afdf3012f16e7e7520465c97333568084218b36f>.
13. Pirkola S, Isometsä E, Heikkinen M, Lönnqvist J. Employment status influences the weekly patterns of suicide among alcohol misusers. *Alcohol Clin Exp Res.* 1997;21(9):1704–1706. PMID:9438533.
14. Inskip HM, Harris EC, Barraclough B. Lifetime risk of suicide for affective disorder, alcoholism and schizophrenia. *Br J Psychiatry.* 1998;172:35–37. doi:10.1192/bjp.172.1.35
15. Nordentoft M. Absolute risk of suicide after first hospital contact in mental disorder. *Arch Gen Psychiatry.* 2011;68(10):1058. doi:10.1001/archgenpsychiatry.2011.113
16. Hiroeh U, Appleby L, Mortensen PB, Dunn G. Death by homicide, suicide, and other unnatural causes in people with mental illness: A population-based study. *Lancet.* 2001;358(9299):2110–2112. doi:10.1016/S0140-6736(01)07216-6
17. Kölves K, Värnik A, Toeding LM, Wasserman D. The role of alcohol in suicide: A case-control psychological autopsy study. *Psychol Med.* 2006;36(7):923. doi:10.1017/S0033291706007707
18. Schneider B, Kölves K, Blettner M, Wetterling T, Schnabel A, Värnik A. Substance use disorders as risk factors for suicide in an Eastern and a Central European city (Tallinn and Frankfurt/Main). *Psychiatry Res.* 2009;165(3):263–272. doi:10.1016/j.psychres.2008.03.022
19. Lupi M, Chiappini S, Mosca A, et al. Alcohol use disorders and suicidal behaviour: A narrative review. *Actas Esp Psiquiatr.* 2025;53(1):165–180. doi:10.62641/aep.v53i1.1772
20. Conner KR, Beautrais AL, Conwell Y. Risk factors for suicide and medically serious suicide attempts among alcoholics: Analyses of Canterbury Suicide Project data. *J Stud Alcohol.* 2003;64(4):551–554. doi:10.15288/jsa.2003.64.551
21. Glantz MD, Bharat C, Degenhardt L, et al. Corrigendum to “The epidemiology of alcohol use disorders cross-nationally: Findings from the World Mental Health Surveys” [Addict Behav. 2020;102:106128]. *Addict Behav.* 2020;106:106381. doi:10.1016/j.addbeh.2020.106381
22. Glantz MD, Bharat C, Degenhardt L, et al. The epidemiology of alcohol use disorders cross-nationally: Findings from the World Mental Health Surveys. *Addict Behav.* 2020;102:106128. doi:10.1016/j.addbeh.2019.106128
23. Flensborg-Madsen T, Knop J, Mortensen EL, Becker U, Sher L, Grønbaek M. Alcohol use disorders increase the risk of completed suicide, irrespective of other psychiatric disorders: A longitudinal cohort study. *Psychiatry Res.* 2009;167(1–2):123–130. doi:10.1016/j.psychres.2008.01.008
24. Rossow I, Romelsjö A, Leifman H. Alcohol abuse and suicidal behaviour in young and middle aged men: Differentiating between attempted and completed suicide. *Addiction.* 1999;94(8):1199–1207. doi:10.1046/j.1360-0443.1999.948119910.x
25. Schneider B, Wetterling T, Georgi K, Bartusch B, Schnabel A, Blettner M. Smoking differently modifies suicide risk of affective disorders, substance use disorders, and social factors. *J Affect Disord.* 2009;112(1–3):165–173. doi:10.1016/j.jad.2008.04.018
26. Li D, Yang X, Ge Z, et al. Cigarette smoking and risk of completed suicide: A meta-analysis of prospective cohort studies. *J Psychiatry Res.* 2012;46(10):1257–1266. doi:10.1016/j.jpsychires.2012.03.013
27. Yaworski D, Robinson J, Sareen J, Bolton JM. The relation between nicotine dependence and suicide attempts in the general population. *Can J Psychiatry.* 2011;56(3):161–170. doi:10.1177/070674371105600306
28. Borges G, Bagge CL, Orozco R. A literature review and meta-analyses of cannabis use and suicidality. *J Affect Disord.* 2016;195:63–74. doi:10.1016/j.jad.2016.02.007
29. Price C, Hemmingsson T, Lewis G, Zammit S, Allebeck P. Cannabis and suicide: Longitudinal study. *Br J Psychiatry.* 2009;195(6):492–497. doi:10.1192/bjp.bp.109.065227
30. Molero Y, Zetterqvist J, Binswanger IA, Hellner C, Larsson H, Fazel S. Medications for alcohol and opioid use disorders and risk of suicidal behavior, accidental overdoses, and crime. *Am J Psychiatry.* 2018;175(10):970–978. doi:10.1176/appi.ajp.2018.17101112
31. Lee CTC, Chen VCH, Tan HKL, et al. Suicide and other-cause mortality among heroin users in Taiwan: A prospective study. *Addict Behav.* 2013;38(10):2619–2623. doi:10.1016/j.addbeh.2013.03.003
32. Darke S, Ross J. Suicide among heroin users: Rates, risk factors and methods. *Addiction.* 2002;97(11):1383–1394. doi:10.1046/j.1360-0443.2002.00214.x
33. Petit A, Reynaud M, Lejoyeux M, Coscas S, Karila L. Addiction to cocaine: A risk factor for suicide? [in French]. *Presse Med.* 2012;41(7–8):702–712. doi:10.1016/j.lpm.2011.12.006
34. Kittirattanapaiboon P, Suttajit S, Junsirimongkol B, Likhitsathian S, Srisurapanont M. Suicide risk among Thai illicit drug users with and without mental/alcohol use disorders. *Neuropsychiatr Dis Treat.* 2014;10:453–458. doi:10.2147/NDT.S56441
35. Darke S, Slade T, Ross J, Marel C, Mills KL, Tesson M. Patterns and correlates of alcohol use amongst heroin users: 11-year follow-up of the Australian Treatment Outcome Study cohort. *Addict Behav.* 2015;50:78–83. doi:10.1016/j.addbeh.2015.06.030
36. Popovic D, Benabarre A, Crespo JM, et al. Risk factors for suicide in schizophrenia: Systematic review and clinical recommendations. *Acta Psychiatr Scand.* 2014;130(6):418–426. doi:10.1111/acps.12332
37. Brent DA, Perper JA, Moritz G, et al. Psychiatric risk factors for adolescent suicide: A case-control study. *J Am Acad Child Adolesc Psychiatry.* 1993;32(3):521–529. doi:10.1097/00004583-199305000-00006
38. Cheng AT. Mental illness and suicide. A case-control study in east Taiwan. *Arch Gen Psychiatry.* 1995;52(7):594–603. doi:10.1001/archpsyc.1995.03950190076011
39. Conner KR, Beautrais AL, Conwell Y. Moderators of the relationship between alcohol dependence and suicide and medically serious suicide attempts: Analyses of Canterbury Suicide Project data. *Alcohol Clin Exp Res.* 2003;27(7):1156–1161. doi:10.1097/01.ALC.0000075820.65197.FD
40. World Health Organization (WHO). *Preventing Suicide: A Global Imperative.* Geneva, Switzerland: World Health Organization (WHO); 2014. ISBN:978-92-4-156477-9.
41. Wisłowska-Stanek A, Kołosowska K, Maciejak P. Neurobiological basis of increased risk for suicidal behaviour. *Cells.* 2021;10(10):2519. doi:10.3390/cells10102519
42. Hufford MR. Alcohol and suicidal behavior. *Clin Psychol Rev.* 2001;21(5):797–811. doi:10.1016/s0272-7358(00)00070-2
43. Lamis DA, Malone PS. Alcohol use and suicidal behaviors among adults: A synthesis and theoretical model. *Suicidol Online.* 2012;3:4–23. PMID:23243500. PMCID:PMC3519287.
44. Conner KR, Duberstein PR. Predisposing and precipitating factors for suicide among alcoholics: Empirical review and conceptual integration. *Alcohol Clin Exp Res.* 2004;28(5 Suppl):65–175. doi:10.1097/01.alc.0000127410.84505.2a
45. Forte A, Pompili M, Imbustaro B, et al. Effects on suicidal risk: Comparison of clozapine to other newer medicines indicated to treat schizophrenia or bipolar disorder. *J Psychopharmacol.* 2021;35(9):1074–1080. doi:10.1177/02698811211029738
46. Cipriani A, Hawton K, Stockton S, Geddes JR. Lithium in the prevention of suicide in mood disorders: Updated systematic review and meta-analysis. *BMJ.* 2013;346:f3646. doi:10.1136/bmj.f3646
47. Del Matto L, Muscas M, Murru A, et al. Lithium and suicide prevention in mood disorders and in the general population: A systematic review. *Neurosci Biobehav Rev.* 2020;116:142–153. doi:10.1016/j.neubiorev.2020.06.017
48. Braun C, Bschor T, Franklin J, Baethge C. Suicides and suicide attempts during long-term treatment with antidepressants: A meta-analysis of 29 placebo-controlled studies including 6,934 patients with major depressive disorder. *Psychother Psychosom.* 2016;85(3):171–179. doi:10.1159/000442293

49. Shamabadi A, Ahmadzade A, Hasanzadeh A. Ketamine for suicidality: An umbrella review. *Br J Clin Pharmacol*. 2022;88(9):3990–4018. doi:10.1111/bcp.15360
50. Sonneck G, Goll H, eds. *Krisenintervention Und Suizidverhütung: Ein Leitfaden Für Den Umgang Mit Menschen in Krisen*. Wien, Austria: Facultas; 1985. ISBN:978-3-85076-171-0.
51. Schneider B, Meiländer L, Pallenbach E. Suizidalität und Suchterkrankung. In: Yousefi HR, ed. *Sucht – Jahrbuch Psychotherapie: Heft 4 – 2024/4. Jahrgang – Internationale Zeitschrift für PsychoPraxis*. Nordhausen, Germany: Traugott Bautz Verlag; 2023:71–84. ISBN:978-3-95948-630-9.
52. Zador D, Sunjic S, Darke S. Heroin-related deaths in New South Wales, 1992: Toxicological findings and circumstances. *Med J Aust*. 1996; 164(4):204–207. doi:10.5694/j.1326-5377.1996.tb94136.x
53. Rizk MM, Herzog S, Dugad S, Stanley B. Suicide risk and addiction: The impact of alcohol and opioid use disorders. *Curr Addict Rep*. 2021; 8(2):194–207. doi:10.1007/s40429-021-00361-z
54. Joiner T. *Why People Die by Suicide*. Cambridge, USA: Harvard University Press; 2009. ISBN:978-0-674-02549-3.
55. Williams JMG. *Cry of Pain: Understanding Suicide and Self-Harm*. London, UK: Penguin Books; 1997. ISBN:978-0-14-025072-5.
56. O'Connor RC. The integrated motivational-volitional model of suicidal behavior. *Crisis*. 2011;32(6):295–298. doi:10.1027/0227-5910/a000120
57. Rudd MD. Fluid vulnerability theory: A cognitive approach to understanding the process of acute and chronic suicide risk. In: Ellis TE, ed. *Cognition and Suicide: Theory, Research, and Therapy*. Washington, D.C, USA: American Psychological Association; 2006:355–368. doi:10.1037/11377-016
58. Shneidman ES. Overview: A multidimensional approach to suicide. In: Jacobs D, Brown HN, eds. *Suicide: Understanding and Responding*. Madison, USA: International Universities Press; 1989:1–30. ISBN:978-0-8236-6695-9.
59. Nordentoft M. Crucial elements in suicide prevention strategies. *Prog Neuropsychopharmacol Biol Psychiatry*. 2011;35(4):848–853. doi:10.1016/j.pnpbp.2010.11.038
60. Zalsman G, Hawton K, Wasserman D, et al. Suicide prevention strategies revisited: 10-year systematic review. *Lancet Psychiatry*. 2016; 3(7):646–659. doi:10.1016/S2215-0366(16)30030-X
61. Fiedler G, Schneider B, Giegling I, et al. *Suizidprävention Deutschland: Aktueller Stand und Perspektiven*. Kassel, Germany: Universität Kassel; 2021. doi:10.17170/kobra-202107014195
62. World Health Organization (WHO). *Live Life: An Implementation Guide for Suicide Prevention in Countries*. Geneva, Switzerland: World Health Organization (WHO); 2021. ISBN:978-92-4-002662-9.
63. Tassinari DL, Pozzolo Pedro MO, Pozzolo Pedro M, et al. Artificial intelligence-driven and technological innovations in the diagnosis and management of substance use disorders. *Int Rev Psychiatry*. 2025; 37(1):52–58. doi:10.1080/09540261.2024.2432369
64. Abdelmoteleb S, Ghallab M, IsHak WW. Evaluating the ability of artificial intelligence to predict suicide: A systematic review of reviews. *J Affect Disord*. 2025;382:525–539. doi:10.1016/j.jad.2025.04.078
65. Yildiz E. Machine learning and artificial intelligence in suicide prevention: A bibliometric analysis of emerging trends and implications for nursing [published online as ahead of print on May 28, 2025]. *Issues Ment Health Nurs*. 2025. doi:10.1080/01612840.2025.2505904

New statistical guidelines for manuscripts submitted to *Advances in Clinical and Experimental Medicine*

Krzysztof Kujawa^{1,D–F}, Wojciech Bombała^{1,D–F}, Anna Kopszak^{1,D–F}, Jakub Wronowicz^{1,D–F},
Maciej Wuczyński^{1,D–F}, Łukasz Lewandowski^{2,D–F}, Michał Czapla^{3,4,E,F}

¹ Statistical Analysis Centre, Wrocław Medical University, Poland

² Department of Biochemistry and Immunochemistry, Faculty of Medicine, Wrocław Medical University, Poland

³ Department of Emergency Medical Service, Faculty of Nursing and Midwifery, Wrocław Medical University, Poland

⁴ Group of Research in Care and Health (GRUPAC), Faculty of Health Sciences, University of La Rioja, Spain

A – research concept and design; B – collection and/or assembly of data; C – data analysis and interpretation;

D – writing the article; E – critical revision of the article; F – final approval of the article

Advances in Clinical and Experimental Medicine, ISSN 1899–5276 (print), ISSN 2451–2680 (online)

Adv Clin Exp Med. 2025;34(7):1085–1090

Address for correspondence

Krzysztof Kujawa

E-mail: krzysztof.kujawa@umw.edu.pl

Funding sources

None declared

Conflict of interest

None declared

Abstract

The updated statistical reporting guidelines for *Advances in Clinical and Experimental Medicine* (ACEM) streamline the way in which authors describe their statistical analyses and results. In response to the rising popularity of advanced techniques – such as Bayesian statistics and machine learning – the revisions balance methodological rigor with article readability.

Key words: statistical analysis guidelines, test assumptions, machine learning, Bayesian statistics

Received on June 6, 2025

Accepted on June 6, 2025

Published online on June 25, 2025

Cite as

Kujawa K, Bombała W, Kopszak A, et al. New statistical guidelines for manuscripts submitted to *Advances in Clinical and Experimental Medicine*. *Adv Clin Exp Med.* 2025;34(7):1085–1090. doi:10.17219/acem/206009

DOI

10.17219/acem/206009

Copyright

Copyright by Author(s)

This is an article distributed under the terms of the Creative Commons Attribution 3.0 Unported (CC BY 3.0) (<https://creativecommons.org/licenses/by/3.0/>)

Highlights

- *Advances in Clinical and Experimental Medicine* (ACEM) has introduced new statistical reporting guidelines to enhance clarity, transparency and methodological rigor in scientific articles.
- Authors are no longer required to include certain statistical test details (e.g., test statistics, degrees of freedom), unless they are critical for interpretation.
- For selected methods, authors may be asked to submit raw statistical output (e.g., auto-generated software reports) to support peer review accuracy – these will not appear in the published article.
- The updated guidelines now include clear instructions for using Bayesian analysis and machine learning methods in research publications.
- These changes aim to improve the quality of statistical analysis in academic publishing while maintaining reader-friendly formatting.

Introduction

With the growth of data in medical and other sciences and the development of techniques for their analysis (e.g. nonparametric tests and models, machine learning and methods used in bioinformatics), the importance of the correctness of statistical analysis of collected data and the appropriateness of its description and obtained results is also growing. Unfortunately, many studies show numerous errors and deficiencies in this area.^{1,2} Therefore, various efforts are made with the ultimate goal of achieving a sufficiently high level of description of the statistical analysis methods used and the presentation of their results. A sufficiently high level means meeting 2 basic requirements: enabling each reader to verify the truthfulness of the findings and to repeat the research in an identical manner. Among the above-mentioned activities are:

- publishing articles evaluating scientific articles in terms of the statistical analyses used therein,^{2–4}
- publishing general recommendations and guides on statistical analysis addressed to all interested parties, including authors, reviewers and editors of journals,^{5–8}
- formulating guidelines by individual editorial offices for authors who intend to publish articles,^{9,10}
- integrating interested parties into organizations aimed at coordinating activities in the field of setting standards for the use of statistical analyses in scientific publications, e.g., the World Association of Medical Editors (WAME) (<https://wame.org/index.php>) and International Committee of Medical Journal Editors (ICMJE) (<https://www.icmje.org>).

The *Advances in Clinical and Experimental Medicine* (ACEM) statistical guidelines provide a set of clear instructions, supported by examples, to ensure the journal's requirements are as understandable as possible and aligned with the recommendations outlined in the above sources. Among other things, emphasis is placed on the presentation of the results of verification of test or model assumptions, which is the basis for assessing the reliability of the results obtained using them. However, sometimes

a need for changes is noticed, resulting from the development of data analysis methods, as well as from critical opinions regarding these requirements, including from authors of publications and members of the editorial board. This article presents new, slightly modified guidelines for statistical analyses in articles published in ACEM.

The primary objective of the statistical analysis guidelines is to help authors prepare manuscripts that use appropriate methods for the given research problem. The changes to the guidelines were made to make it easier for authors to prepare manuscripts correctly in terms of statistical analysis, and to enable editors to prepare the final version of articles more quickly.

The primary objective of the statistical analysis guidelines is to assist authors in preparing articles that employ suitable methods for the specific research issue. Therefore, the requirement to publish test values has been removed. In certain cases, rather than requiring the inclusion of 'technical' details of a given analysis, authors may be asked to submit unedited, raw reports that are automatically generated by statistical analysis software. These reports will not be included in the publication but will allow statistical reviewers to assess the accuracy of the relevant part of the statistical analysis.

The guidelines have also been supplemented with requirements for the use of Bayesian statistics and machine learning.

List of ACEM's requirements concerning statistical analyses

Statistical analysis description

Introductory remarks

- All of the information regarding statistical analyses should be collected in the "Statistical analyses" section and enable a reader to repeat the analyses in exactly the same way.

- b) A set of the essential statistical analysis results (see Statistical analysis description and Introductory remarks for details) should be presented in the main paper body.
- c) The authors may be requested to provide additional detailed results of the analyses to assess the correctness of the analysis. In such cases, raw reports from the statistical software are acceptable, as they are not intended for publication.
- d) Results of checking test or model assumptions must also be included in the form of simplified supplementary materials (point I.3), which should present only essential information, such as a list of variables that meet the given assumption and those that do not, along with p-values or small-sized graphs (e.g., histograms, scatter-plots, etc.). Other details may be requested by reviewers, if necessary, solely for the purpose of verifying the appropriateness of a given test, etc.

Providing a list of statistical analysis tools and explaining how a given tool was used, e.g.:

- a) χ^2 test: specify which test type was used: a test of independence or consistency, Pearson's χ^2 test or maximum likelihood, and whether Yates's correction was used.
- b) Analysis of variance (ANOVA): explain which type was used (e.g., one-way, two-way, repeated measures, nested) and which correction was applied when the assumption of sphericity/homogeneity of variance was not met.
- c) Student's t-test: Determine whether the test was used for matched pairs or for independent groups and whether the correction for heterogeneity of variances (e.g., Welch's) was applied.
- d) Multivariate regression: Explain whether and how any predictor selection was made, including the procedure and threshold values used. If a selection mode was applied, also provide the initial set of predictors.
- e) Meta-analysis should include the following items:
 - a table with selected publications along with effects size or other measures;
 - the type of the model used (fixed or random) with the criteria for making a choice (prior analysis);
 - the summary of the effect size integration (forest plots);
 - heterogeneity analysis;
 - sensitivity analysis;
 - paper quality evaluation;
 - publication bias assessment using funnel plots (in each case), standard Begg's and Mazumdar's test or Egger's test (when $n > 10$, in both cases).
- f) Statistical analysis tools available in programming languages such as Python and R:
 - provide complete list of the packages along with their version number;
 - provide a key part of the script in a supplementary file or list values of the given function's parameters, when a given analysis may be run in many ways.
- g) Bayesian statistics:
 - Clearly state the Bayesian approach – explicitly mention that Bayesian inference was used and justify why Bayesian methods were chosen over frequentist alternatives. Explain whether a full or empirical Bayes approach was used.
 - Define the prior distributions (gaussian/beta/gamma/Dirichlet/Laplace etc.), declaring the type of priors (informative/weakly-informative/non-informative) for each parameter, referring to the literature/domain knowledge based on which the a priori distribution was assumed – in case of using informative or weakly-informative priors. State whether the results of the analysis changed under different prior assumptions; the Statistical Editor can demand results from sensitivity analysis.
 - Specify the likelihood function used to generate data.
 - Feature whole posterior distributions instead of showing only point estimates. Use credible intervals instead of confidence intervals (CIs).
 - Show key Bayesian metrics (posterior mean, median or mode etc.). Use statements such as “the probability of effect being >0 is X%” or “with probability of p, the parameter is between X1 and X2”. Abstain from using frequentist language (“statistical significance”, etc.).
 - Perform model diagnostics. Perform posterior predictive checks. Simulate new data from posterior and compare it with observed data. Check for model fit with use of posterior predictive plots. In case of Markov Chain Monte Carlo (MCMC) methods, declare the used software (Stan/JAGS/PyMC3 etc.), number of chains, iterations, burn-in period. Report R-hat (convergence), and effective sample size,
 - For visualization, use appropriate types of plots (density plots, histograms, ridge plots, violin plots, trace plots).
 - Compare the different models and select the most suitable one for further description in the manuscript (e.g., Bayes factor, Watanabe–Akaike information criterion, leave-one-out cross-validation).
 - Discuss the clinical implications of the model, referring to real-life situations
- h) Machine learning methods:
 - Explicitly state the purpose of the model. Was it used for visualization, prediction, feature engineering, modelling of some phenomena? For methods used solely for visualization or exploratory purposes (e.g., t-distributed stochastic neighbor embedding (t-SNE) and similar techniques), the same level of methodological rigor and detailed reporting is not required as for predictive or inferential models. However, the purpose of the method must be explicitly stated, and overinterpretation of visualizations should be avoided.
 - Explain the rationale for choosing a particular machine learning model. In case of using the less-explainable (“black box”) models, use techniques to interpret the results, such as Shapley (SHAP) values.

If multiple models are available for the task, the optimal one should be selected for further interpretation based on the goodness of fit or performance metrics (depending on the aim of the study).

- Describe how was the data used: How was it split into training/validation/test sets? Was stratification or other kind of sampling used?
- Specify the data transformations leading to the creation of the input vector. Provide information on how each variable was scaled.
- Check for potential data leakage or the “perfect separation” problem, and address these issues if they arise.
- Provide a list of hyperparameters for the models and a rationale for setting them on the chosen levels. Describe calibration procedures if they were performed.
- Each model presented in the manuscript should be evaluated using the appropriate performance metrics: R-squared or mean absolute percentage error (MAPE) for regression models; a confusion matrix for classification models; and mutual information or the Calinski–Harabasz (C–H) index for clustering models. Additionally, the receiver operating characteristic (ROC) curve should be used to describe the performance of binary classifiers.
- When presenting multiple models, compare them using a common metric. Ideally, this metric should be clinically relevant.
- Upload the final model as a set of weights or as a supplementary file. Alternatively, especially when comparing multiple models, provide the code (including the random seed used) that was used to train the models. If neither of these solutions is possible, please provide an explanation.
- Where possible (e.g., for decision trees, regression trees and simple artificial neural networks), provide a visualisation of the model architecture.
- We do not accept manuscripts regarding automated data mining, natural language processing, complex agent systems or generative artificial intelligence.

Checking the assumptions of the models or statistical tests used

The results of the tests used to verify whether assumptions are met should be included in the supplementary materials. The list of test examples provided below contains only the most commonly used methods and should be expanded as appropriate to reflect any additional tests employed.

- Testing the normality of distributions: The choice of test should be related to the sample size (N) (Table 1).
- Student's t-test, parametric ANOVA: Data normal distribution and variance homogeneity.
- ANOVA (parametric) for repeated measurements: Data normal distribution, between-group variance and in-group variance (sphericity).

Table 1. Recommended method for testing the normality of a data distribution according to sample size

N	Recommended way to test the normality of distribution
<10	Testing the normality of the distribution is uncertain because of low power of tests. In further analyses, use a non-parametric one or justify its normality based on appropriate publications
10–50	Shapiro–Wilk test
>50	Any other methods (Lilliefors test, skewness, histogram, box plot, quantile-quantile (Q–Q) plot)

d) Pearson correlation: Normal data distribution, linear relationships between the variables.

e) Linear regression:

- linear relationship between predictors and the response variable (small-sized scatter plots);
- no multicollinearity, e.g., using variance inflation factor (VIF);
- homoscedasticity, i.e., the residual constant variance (Breusch–Pagan test);
- normal distribution of model residuals.

f) Logistic regression:

- a linear relationship between predictors and the logit of the response variable (Box–Tidwell test or visual assessment based on an appropriate plot);
- no multicollinearity among explanatory variables e.g., using VIF or generalized variance inflation factor (GVIF);
- no extreme outliers.

g) Cox regression:

- proportional hazard assumption;
- linearity: the log-hazard function is linearly related to all predictors;
- no multicollinearity among the predictors.

Family of hypotheses

When applicable, apply the appropriate correction to the p-values.

Data presentation in tables or graphs

For a normal distribution, the correct measures of central tendency are the mean and standard deviation (SD). Otherwise, the median and the first and third quartiles (Q1 and Q3) should be used. If n is greater than 8, use the quartiles; otherwise, use the min–max range.

Presentation of statistical analysis results

General rules

a) Presentation of a given test result should include (excluding post hoc test – see below):

- test name,
- degrees of freedom (df) or sample/group sizes (n) when df is not applicable,

- statistical significance (p) with an accuracy of 3 decimal places; however, if p is less than 0.001, we use the expression “ $p < 0.001$ ”, and when p is greater than 0.999, we use the expression “ $p > 0.999$ ”.
- b) Post hoc test results:
- only p -values are required;
 - present all p -values as 3 decimal places, both below and above the alpha level;
 - when the table is large or the number of tables with post hoc results is large, they can be included as supplementary materials.
- c) Include effect size measures, always with their CIs, such as odds ratio (OR), hazard ratio (HR), beta coefficients, etc. If applicable, explain the method of CI calculation.
- d) Avoid using unreliable methods, such as stepwise regression, selecting predictors for multiple regression based on the results of univariate regressions, and post hoc least significant difference (LSD) tests (which are too liberal). The use of such methods requires justification.

The test results should be reported following the examples below:

- a) For Student's t -test: “ t -test: $df = 26$; $p = 0.004$ ”;
- b) For analysis of variance test: “ANOVA: $df = (2, 150)$; $p = 0.076$ ”;
- c) For Mann–Whitney test (Wilcoxon rank sum test): “M–W test: $n = (12, 15)$; $p = 0.010$ ”;
- d) For Kruskal–Wallis test: “K–W test: $n = (14, 15, 18)$, $p = 0.211$ ”;
- e) For χ^2 test: “ χ^2 test: $df = 1$, $p = 0.032$ ”;
- f) For Pearson's correlation: “ $r = 0.62$, $n = 45$, $p = 0.004$ ”;
- g) For multivariate regression models:
- Coefficients (B) and/or standardized coefficient (β), their CIs, and p -values, e.g.: Table 2
 - Overall model statistics, including the model name and specification, the p -value, and an appropriate goodness-of-fit measure (e.g., adjusted R^2 , Nagelkerke R^2 , Concordance Index, etc.) An example: $p = 0.005$, $\text{adj-}R^2 = 0.23$.

Tables concerning statistical analysis in the published supplementary materials

- a) In accordance with general guidelines, they should contain only necessary content (i.e., variable names, df or n , and p).

- b) Raw reports produced automatically by statistical programs are unacceptable because they contain many unnecessary elements.

Rules for preparing figures (graphs)

Figures should be titled and explained (preferably in the footer) so that they are understandable without referring to other parts of the publication

Detailed rules

- a) Each axis label should contain the units when applicable.
- b) Bar plots can only be used to present frequency or count data.
- c) If a sample size is less than 10, all data should be presented as dots along with the measure of central tendency appropriate for a given test (usually median).
- d) A line representing the relationship should be presented alongside the CI.
- e) If statistical significance is indicated in the chart by symbols (e.g., * for $p < 0.05$), the tables containing all the elements required for a given statistical analysis must be referenced.

Conclusions

As data analysis methods continue to evolve, so too do the expectations for precision – both in the description of methods used and in the presentation of results. The updated guidelines, informed by past experience with submitted manuscripts, aim to strike a sensible balance. The goal is to reconcile the demand for methodological rigor with the need for clarity and readability – essential for a fair and effective peer review process. This balance involves limiting the scope of results presented in the main text, while allowing draft versions of full results to be submitted to the editors at the reviewers' request – without requiring them to be fully polished for publication.

ORCID iDs

Krzysztof Kujawa  <https://orcid.org/0000-0003-2812-4702>
 Wojciech Bombała  <https://orcid.org/0009-0001-9989-8337>
 Anna Kopszak  <https://orcid.org/0009-0007-7674-7863>
 Jakub Wronowicz  <https://orcid.org/0000-0002-1454-2068>
 Maciej Wuczyński  <https://orcid.org/0000-0001-7376-1933>
 Łukasz Lewandowski  <https://orcid.org/0000-0002-7624-631X>
 Michał Czapla  <https://orcid.org/0000-0002-4245-5420>

Table 2. An example of how to present the results of a multivariate regression model

Variable	B	95% CI (B)	β	95% CI (β)	p-value
Intercept	75.19	35.19; 115.19	–	–	<0.001
Var1	–0.30	–1.25; 0.66	–0.04	–0.15; 0.08	0.544
Var2	–0.53	–0.94; –0.12	–0.16	–0.29; –0.04	0.012
Var3	0.57	0.25; 0.90	0.21	0.09; 0.33	0.001

B – coefficient; β – standardized coefficient; Var1, Var2, Var3 – predictors; 95% CI – 95% confidence interval.

References

1. Ordak M. Implementation of SAMPL guidelines: Recommendations for improving statistical reporting in biomedical journals. *Clin Med (Lond)*. 2025;25(3):100304. doi:10.1016/j.clinme.2025.100304
2. Thiese MS, Ronna B, Robbins RB. Misuse of statistics in surgical literature. *J Thorac Dis*. 2016;8(8):E726–E730. doi:10.21037/jtd.2016.06.46
3. Abubakar B, Uthman YA, Jatau AI, Danbatta A, Nuhu HN, Mustapha M. Misuse of analysis of variance in African biomedical journals: A call for more vigilance. *Bull Natl Res Cent*. 2022;46(1):232. doi:10.1186/s42269-022-00924-8
4. Wolkewitz M, Lambert J, Von Cube M, et al. Statistical analysis of clinical COVID-19 data: A concise overview of lessons learned, common errors and how to avoid them. *Clin Epidemiol*. 2020;12:925–928. doi:10.2147/CLEP.S256735
5. Panos GD, Boeckler FM. Statistical analysis in clinical and experimental medical research: Simplified guidance for authors and reviewers. *Drug Des Dev Ther*. 2023;17:1959–1961. doi:10.2147/DDDT.S427470
6. Renard C. 5 key practices for data presentation in research. Amsterdam, the Netherlands–New York, USA: Elsevier; 2025. <https://www.elsevier.com/connect/5-key-practices-for-data-presentation-in-research>. Accessed June 6, 2025.
7. Wasserstein RL, Schirm AL, Lazar NA. Moving to a world beyond “ $p < 0.05$.” *Amer Statist*. 2019;73(Suppl 1):1–19. doi:10.1080/00031305.2019.1583913
8. Lang TA, Altman DG. Basic statistical reporting for articles published in biomedical journals: The “Statistical Analyses and Methods in the Published Literature” or the SAMPL Guidelines. *Int J Nurs Stud*. 2015;52(1):5–9. doi:10.1016/j.ijnurstu.2014.09.006
9. Alfonso F, Torp-Pedersen C, Carter RE, Crea F. European Heart Journal quality standards. *Eur Heart J*. 2021;42(28):2729–2736. doi:10.1093/eurheartj/ehab324
10. New England Journal of Medicine (NEJM). New manuscripts. Waltham, USA: Massachusetts Medical Society (MMS); 2025. <https://www.nejm.org/author-center/new-manuscripts>. Accessed June 6, 2025.

Impact of vitamin D supplementation on symptom severity and quality of life in patients with irritable bowel syndrome: A meta-analysis

Shuang Qi^{1,A,D}, Meng Zhao^{2,B,D}, YINUO Sun^{2,C,D}, Sunaina Boro^{3,E}, Bhawna Arora^{4,E}, Sanjay Rastogi^{5,F}

¹ Department of Pediatrics, Heilongjiang Academy of Chinese Medicine Sciences, Harbin, China

² Department of Surgery, First Affiliated Hospital, Heilongjiang University of Chinese Medicine, Harbin, China

³ Department of Periodontics and Oral Implantology, Regional Dental College, Guwahati, India

⁴ Department of Pedodontics, Adesh University, Bathinda, India

⁵ specialist, Oral and Maxillofacial Surgery, Guwahati, India

A – research concept and design; B – collection and/or assembly of data; C – data analysis and interpretation;

D – writing the article; E – critical revision of the article; F – final approval of the article

Advances in Clinical and Experimental Medicine, ISSN 1899–5276 (print), ISSN 2451–2680 (online)

Adv Clin Exp Med. 2025;34(7):1091–1104

Address for correspondence

Shuang Qi

E-mail: qs19890906qs@outlook.com

Funding sources

None declared

Conflict of interest

None declared

Received on April 2, 2024

Reviewed on May 5, 2024

Accepted on July 22, 2024

Published online on January 24, 2025

Abstract

Background. Vitamin D supplementation could offer irritable bowel syndrome (IBS) patients significant improvements in terms of symptom severity and overall quality of life (QoL). Yet, the potential benefits and risks associated with vitamin D supplementation still require additional investigation.

Objectives. We aimed to evaluate the impact of vitamin D supplementation on IBS using a systematic review and meta-analysis.

Materials and methods. A comprehensive search was carried out utilizing 4 electronic databases (PubMed, Embase, Scopus, and Cochrane Library) to identify articles published in English-language peer-reviewed journals. The odds ratios (ORs), risk ratios (RRs) and mean differences (MDs), along with their respective 95% confidence intervals (95% CIs), were computed. Heterogeneity was evaluated using the appropriate p-value and Cochrane Q and I² statistics. For the analysis, RevMan 5.3 was utilized.

Results. Nine randomized controlled trials involving a total of 780 participants were included in this study. Vitamin D supplementation, in adolescents and young adults with IBS, improves the IBS symptoms severity score, QoL and serum 25(OH)D levels compared to controls. We obtained an OR of 2.34 (95% CI: 1.56–3.50) for change in the IBS severity scoring system (IBS-SSS), OR = 2.51 (95% CI: 1.71–3.70) for change in QoL, low risk of any adverse events (RR 0.49 (95% CI: 0.35–0.69)), and substantial changes in serum 25(OH)D level (MD = 11.29 (95% CI: 7.13–15.45)). Results were statistically significant (p < 0.05).

Conclusions. Vitamin D supplementation could lead to better IBS management with a low risk of adverse events.

Key words: irritable bowel syndrome, vitamin-D supplementation, IBS-specific QoL questionnaires, IBS symptom severity, IBS severity score system

Cite as

Qi S, Zhao M, Sun Y, Boro S, Rastogi S, Arora B. Impact of vitamin D supplementation on symptom severity and quality of life in patients with irritable bowel syndrome: A meta-analysis. *Adv Clin Exp Med.* 2025;34(7):1091–1104. doi:10.17219/acem/191463

DOI

10.17219/acem/191463

Copyright

Copyright by Author(s)

This is an article distributed under the terms of the Creative Commons Attribution 3.0 Unported (CC BY 3.0) (<https://creativecommons.org/licenses/by/3.0/>)

Introduction

Irritable bowel syndrome (IBS) is a widespread and intricate gastrointestinal illness characterized by persistent abdominal pain and variations in bowel movements.¹ It has a global prevalence of approx. 11%. Approximately 30% of those who exhibit symptoms of IBS suffer from increased levels of stress and a diminished quality of life (QoL).² Individuals afflicted with IBS may have increased absenteeism, with the degree of work impairment directly correlated to the severity of symptoms.³ Multiple primary and secondary treatments for IBS have been established.^{4,5}

The majority of current medications target the most prevalent symptoms. Nevertheless, an individualized and meticulous approach to treating IBS should prioritize addressing the fundamental pathophysiological mechanisms rather than the prevailing symptoms. Hence, it is imperative to develop innovative approaches that specifically target the underlying mechanisms of IBS while mitigating any potential adverse effects. Multiple observational studies have indicated that individuals with IBS exhibit a greater occurrence of vitamin D deficiencies compared to control groups.^{6–8} Consequently, vitamin D deficiency is believed to have a significant impact on the development of IBS, as well as the severity of symptoms and overall QoL.^{9,10} The involvement of vitamin D in the pathogenesis of IBS may be elucidated by its crucial role in the production of antimicrobial peptides, anti-inflammatory agents, immune cell trafficking and differentiation, gut barrier function, and the balance of calcium and phosphate levels.^{11,12} Moreover, there is empirical evidence suggesting that vitamin D exerts a substantial beneficial influence on gastrointestinal well-being and augments the composition of the gut microbiota. The presence of vitamin D receptors (VDR) in the gut has been found to have an impact on gut function, motility and the symptoms associated with IBS.¹³

Numerous interventional studies have demonstrated the efficacy of vitamin D administration in mitigating the symptoms associated with depression and anxiety, which are frequently observed as psychological comorbidities in individuals suffering from IBS.^{14,15} However, whether vitamin D supplementation helps with IBS is still debatable in randomized controlled trials (RCTs), and its significance in the management of IBS is still an open problem.

Objectives

Given the ongoing debate surrounding the efficacy of vitamin D supplementation in the treatment of IBS, this study performed a systematic review and meta-analysis to determine its impact on the severity of symptoms, change in the irritable bowel syndrome severity score (IBS-SSS) and QoL in individuals with IBS using 9 RCTs selected using pre-specified inclusion-exclusion criteria.^{16–24}

Materials and methods

This research was carried out in accordance with the recommendations provided by Preferred Reporting Items for Systematic reviews and Meta-Analyses (PRISMA)²⁵ and Assessing the Methodological Quality of Systematic Reviews (AMSTAR).²⁶

Eligibility criteria

The current investigation encompassed articles showing data on the efficacy and safety of the impact of vitamin D supplementation on the severity of symptoms and QoL in individuals with IBS. Studies that satisfied the following inclusion criteria were incorporated: 1) patients with IBS; 2) adolescents and adult individuals ranging in age from 15 to 50 years; 3) evaluating the comparative efficacy and safety of either vitamin D supplementation on the severity of symptoms or QoL in individuals with IBS; 4) implementation of a RCT as the chosen study design. The study selection spanned from 2000 to 2023. We selected studies that contained full text and offered adequate data for the creation of 2×2 table. This meta-analysis included the following quantifiable outcomes as primary measures: improvement in IBS-SSSs, serum 25(OH)D levels and QoL in individuals of both the intervention and control groups. Excluded from consideration were studies that were obsolete, anecdotal or relied exclusively on expert assessments. Additionally, studies based on animal experiments or trials, as well as those where the original data and crucial information from the authors were unavailable, were also excluded. In addition, studies that encompassed patients with IBS alongside HIV, cancer and other systemic diseases, non-research publications, qualitative studies, and articles not published in English were also excluded.

Information sources

The current investigation was carried out after an exhaustive search was conducted in 4 databases: Embase, PubMed, Scopus, and the Cochrane Library. The search encompassed the years 2000–2023, and it made use of particular key words, such as “irritable bowel syndrome”, “IBS”, “vitamin D”, “vitamin D supplementation”, “IBS-specific QoL questionnaires”, “quality of life”, “QoL”, “gastrointestinal tract disorder”, “symbiotic”, “vitamin D deficiency”, “bloating”, “diarrhea”, “IBS symptom severity”, “IBS severity score system”, “IBS-SSS”, “placebo”, “meta-analysis”, “RCT”, and “randomized controlled trial”. The key words were identified and verified for consistency in both Embase and MEDLINE databases, in accordance with the PICOS framework.²⁷ (Table 1^{16–24}).

Search strategy

The aforementioned key words were entered into the Title (ti)-Abstract (abs)-Keyword (key) field in the Scopus

Table 1. Database search strategy

Database	Search strategy
Scopus	#1 "irritable bowel syndrome," OR "IBS," OR "vitamin-D," OR "vitamin-D supplementation," OR "IBS-specific QoL questionnaires," OR "quality of life," OR "QoL" OR "gastrointestinal tract disorder," OR "vitamin-D deficiency," OR "bloating," OR "diarrhea" #2 "IBS symptom severity," OR "IBS severity score system," OR "IBS-SSS," OR "placebo," OR "meta-analysis," OR "RCT," OR "randomized controlled trial" #3 #1 AND #2
PubMed	#1 "irritable bowel syndrome" OR "IBS" OR "Vitamin-D" [MeSH terms] OR "vitamin-D supplementation" OR "IBS-specific QoL questionnaires" OR "Quality of life" OR "QoL" [all fields] OR "Gastrointestinal tract disorder" OR "vitamin-D deficiency" OR "bloating" [all fields] OR "diarrhea" [all fields] #2 "IBS symptom severity," OR "IBS severity score system," [MeSH terms] OR "IBS-SSS," OR "placebo," OR "meta-analysis," OR "RCT" [all fields] OR "randomized controlled trial" #3 #1 AND #2
Embase	#1 "irritable bowel syndrome"/exp ⁵ OR "IBS"/exp OR "vitamin-D"/exp OR "vitamin-D supplementation"/exp OR "IBS-specific QoL questionnaires"/exp OR "quality of life"/OR "QoL"/exp OR "gastrointestinal tract disorder"/exp OR "vitamin-D deficiency"/exp OR "bloating"/exp OR "diarrhea"/exp #2 "IBS symptom severity"/exp OR "IBS severity score system"/exp OR "IBS-SSS"/exp OR "Placebo"/exp OR "meta-analysis"/exp OR "RCT"/exp OR "randomized controlled trial"/exp #3 #1 AND #2
Cochrane Library	#1 (irritable bowel syndrome): ti, ab, kw [@] OR (IBS): ti, ab, kw OR (vitamin D): ti, ab, kw OR (vitamin-D supplementation): ti, ab, kw OR (IBS-specific QoL questionnaires): ti, ab, kw OR (quality of life) OR (QoL): ti, ab, kw OR (Gastrointestinal tract disorder): ti, ab, kw OR (vitamin-D deficiency): ti, ab, kw OR (Bloating): ti, ab, kw OR (diarrhea) (word variations have been searched) #2 (IBS symptom severity): ti, ab, kw OR (IBS severity score system): ti, ab, kw OR (IBS-SSS): ti, ab, kw or (placebo): ti, ab, kw or (meta-analysis): ti, ab, kw or (RCT): ti, ab, kw or (randomized controlled trial): ti, ab, kw (word variations have been searched) #3 #1 AND #2

MeSH terms – Medical Subject Headings; \$ exp – explosion in Emtree (searching) of selected subject terms and related subjects); @ ti, ab, kw – either title or abstract or keyword fields.

search. Cochrane search terms included "irritable bowel syndrome" and "vitamin D supplementation." The PICO structure was used for establishing the specific criteria for selection. "P" in this context represented patients diagnosed with irritable bowel syndrome; "I" denoted the supplementation of vitamin D; "C" represented a control; and "O" comprised the enhancement of clinical outcomes, specifically the change in IBS-SSSs, serum 25(OH)D levels, QoL, and risk of adverse events. The research design incorporated in this study was limited to the implementation of RCTs.

Selection process

Relevant studies were identified through an independent, comprehensive evaluation of the pertinent literature by 2 researchers who independently collected the demographic profiles of the patients and event data containing relevant components from the studies that were included.

Assessment of risk of bias

To assess the possibility of bias in the research examined, a well-established and standardized questionnaire was utilized. The evaluation of bias was performed utilizing a method from the Cochrane Collaboration as detailed in the Cochrane Handbook (version 5.3).²⁸ Randomization-induced bias, bias arising from variations from intended interventions, bias due to missing outcome data, bias in outcome assessments, and bias in the selection of reported outcomes were the 5 components taken into consideration in this instrument.

Data collection process and data items

The evaluation of potential bias was carried out independently by 2 reviewers. An additional reviewer acted as an arbitrator to settle any outstanding disputes. In the end, the potential bias was evaluated and classified as either "high risk", "low risk" or "unclear risk." The existence of publication bias was evaluated by the utilization of a funnel plot,²⁹ while the statistical significance of this bias was determined by conducting Begg's test³⁰ using MedCalc (MedCalc Software, Ostend, Belgium).³¹

Statistical analyses

The effect of multiple dichotomous and continuous outcomes was assessed and analyzed using the software application Review Manager (RevMan) 5.3 (The Nordic Cochrane Centre, The Cochrane Collaboration, Copenhagen, Denmark).³² The integration of RevMan software has facilitated the optimization of the procedure for arranging, retrieving and removing superfluous references. The researchers used forest plots³³ to assess the impact of outcome factors across all the investigations. The DerSimonian and Laird approach was utilized to determine the odds ratio (OR), risk ratio (RR) and mean difference (MD). This was accomplished by adopting a 2×2 table³⁴ that was constructed using event data. The binary outcomes were evaluated using the OR³⁵ along with a 95% confidence interval (95% CI). Statistical approaches, including the χ^2 test with a corresponding p-value and the I^2 test,³⁶ were employed to evaluate heterogeneity. Given the varying settings under which the investigations were performed, a random effect model³⁷ was used.

Results

Literature search results

Electronic scanning techniques were employed to conduct an extensive search in Embase, PubMed, Scopus, and the Cochrane Library, yielding a total of 164 papers that satisfied the inclusion criteria specified by the PICOS framework. However, 154 papers were eliminated owing to being duplicates, and 42 papers were omitted because their titles and abstracts were erroneous. Subsequently, a total of 112 records were subjected to further screening, resulting in the exclusion of 37 records owing to unrelated fields. The remaining 75 records were then evaluated to determine their eligibility. Nevertheless, following the application of the inclusion-exclusion criteria, cumulative counts of 66 studies were determined to be ineligible and thus excluded. The main issues that led to the exclusion of studies were a lack of enough data for the construction of 2×2 tables and the absence of essential outcome measures. This meta-analysis employed a total of 9 RCTs that matched the planned inclusion criteria

and covered the time period from 2000 to 2023, as seen in Fig. 1.

The analysis includes a total of 780 adolescents and young adults from different age groups. The demographic features of the studies included in this meta-analysis are presented in Table 2. The text presents a comprehensive account of the authors' identification, publication year, journal of publication, country of publication, intervention, study design, total participant count, participant age, number of individuals in the intervention and control groups, supplement dosages, study duration, and primary outcomes assessed. Afterwards, the previously indicated event data was used to carry out the meta-analysis.

Assessment of the risk of bias

Risk of bias evaluation results for the included studies, as evaluated with the preset questionnaire, are presented in Table 3. The graph depicting the risk of bias and the description of the risk of bias in Fig. 2 indicates that the present meta-analysis exhibits a minimum risk of bias. Among the 9 RCTs used in the analysis, it was

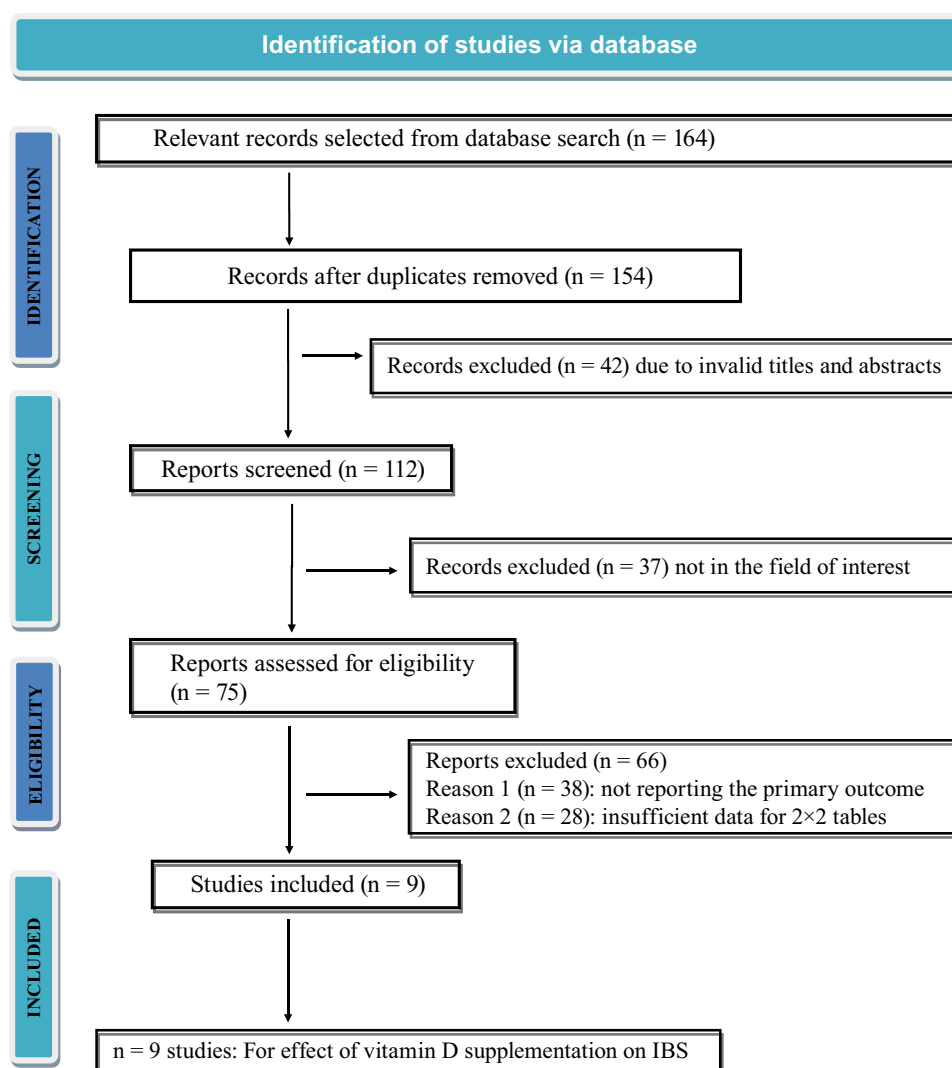


Fig. 1. Preferred Reporting Items for Systematic reviews and Meta-Analyses (PRISMA) study flow diagram

Table 2. Characteristics of the included randomized clinical trials (RCTs)

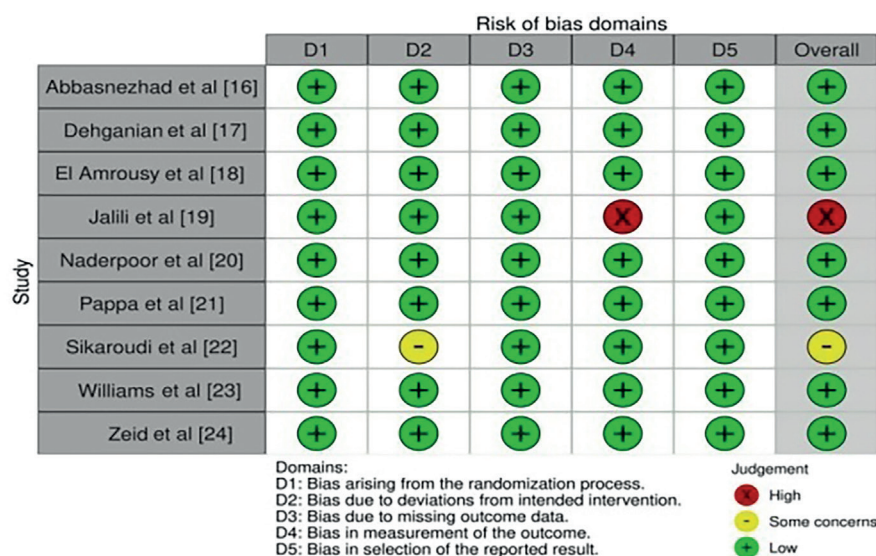
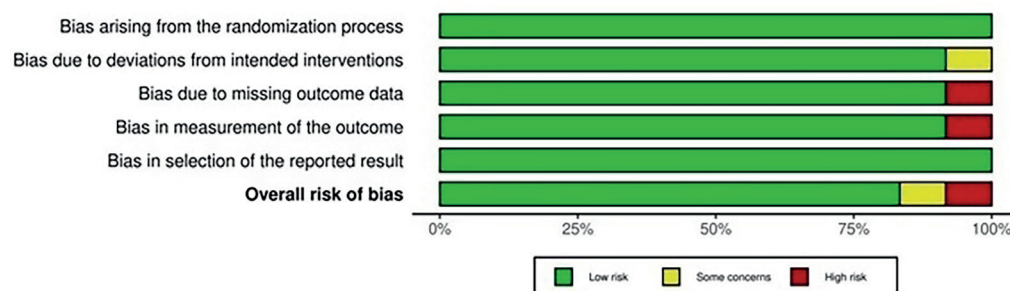
Study ID	Year of publication	Journal title	Country of study	Intervention	Total number of participants	Age of participants [years], mean \pm SD	Participants in intervention group	Participants in control group	Dose of vitamin D	Duration of study	Primary outcome
Abbasnezhad et al. ¹⁶	2016	<i>Neurogastroenterology and Motility</i>	Iran	Effect of vitamin D on gastrointestinal symptoms and health-related quality of life in irritable bowel syndrome patients	90	41.3 \pm 15	45	45	50,000 IU fortnightly	6 months	IBS severity score system (IBS-SSS) and IBS-specific QoL questionnaires
El Amrousy et al. ¹⁷	2018	<i>Saudi Journal of Gastroenterology</i>	Egypt	Vitamin D supplementation in adolescents with irritable bowel syndrome	112	16.4 \pm 1.5	56	56	2000 IU daily	6 months	IBS symptoms severity scores (SSSs) and disease-specific QoL
Dehghanian et al. ¹⁸	2016	<i>Iranian Journal of Nutrition Sciences and Food Technology</i>	Iran	Effects of vitamin D3 supplementation on clinical symptoms in patients with irritable bowel syndrome	66	37 \pm 9	36	30	50,000 IU weekly	1.5 months	IBS symptoms severity scores (SSSs) and disease-specific QoL
Jalili et al. ¹⁹	2019	<i>International Journal of Preventive Medicine</i>	Iran	Effects of vitamin D supplementation in patients with irritable bowel syndrome	116	42.24 \pm 12.26	58	58	50,000 IU weekly	1.5 months	IBS symptoms severity scores (SSSs) and disease-specific QoL
Naderpoor et al. ²⁰	2019	<i>Nutrients</i>	Australia	Effect of vitamin D supplementation on fecal microbiota	32	32.7 \pm 10.3	14	12	10000 IU weekly	4 months	IBS symptoms severity scores (SSSs) and disease-specific QoL
Pappa et al. ²¹	2014	<i>Journal of Clinical Endocrinology and Metabolism</i>	USA	Maintenance of optimal vitamin D status in children and adolescents with inflammatory bowel disease	63	14.8 \pm 3.1	32	31	1000 IU daily	12 months	IBS symptoms severity scores (SSSs) and disease-specific QoL
Khalighi Sikaroudi et al. ²²	2020	<i>Complementary Medicine Research</i>	Iran	Vitamin D3 supplementation in diarrhea-predominant irritable bowel syndrome patients	88	35.07 \pm 11.73	44	44	50,000 IU weekly	2 months	IBS symptoms severity scores (SSSs) and disease-specific QoL
Williams et al. ²³	2022	<i>European Journal of Nutrition</i>	UK	Effect of vitamin D supplementation on people with IBS	135	30.01 \pm 10.46	68	67	50,000 IU weekly	3 months	change in IBS symptom severity; change in IBS-related quality of life.
Zeid et al. ²⁴	2020	<i>Family Medicine</i>	Egypt	Effect of vitamin D3 (cholecalciferol) supplementation on gastrointestinal symptoms in patients with irritable bowel syndrome	78	37.64 \pm 11.13	39	39	4000 IU daily	3 months	IBS severity score system (IBS-SSS) and IBS-specific QoL questionnaires

SD – standard deviation; IBS – irritable bowel syndrome; QoL – quality of life.

Table 3. Risk of bias assessment of the included studies

Study ID and year	Abbasnezhad et al. ¹⁶	El Amrousy et al. ¹⁷	Dehghanian et al. ¹⁸	Jalili et al. ¹⁹	Naderpoor et al. ²⁰	Pappa et al. ²¹	Khalighi Sikaroudi et al. ²²	Williams et al. ²³	Zeid et al. ²⁴
Was a consecutive or random sample of patients enrolled?	Y	N	Y	Y	Y	Y	Y	Y	Y
Did the study avoid inappropriate exclusions?	Y	N	Y	Y	Y	Y	Y	Y	Y
Did all patients receive the same reference standard?	Y	N	Y	Y	Y	Y	Y	Y	Y
Were all patients included in the analysis?	Y	N	Y	Y	Y	Y	Y	Y	Y
Was the sample frame appropriate to address the target population?	Y	N	Y	Y	Y	Y	Y	Y	Y
Were study participants sampled in an appropriate way?	Y	N	Y	Y	Y	Y	Y	Y	Y
Were the study subjects and the setting described in detail?	Y	N	Y	Y	Y	Y	Y	Y	Y
Were valid methods used for the identification of the condition?	Y	N	Y	Y	Y	Y	Y	Y	Y
Was the condition measured in a standard, reliable way for all participants?	Y	N	Y	Y	Y	Y	Y	Y	Y
Was there appropriate statistical analysis?	Y	N	Y	Y	Y	Y	Y	Y	Y

Y – yes; N – no.

**Fig. 2.** Risk of bias assessment of the included studies

observed that 7 studies had a low risk of bias, whilst 1 paper showed a moderate risk of bias. The bias resulting from the divergence from the targeted intervention

was identified as the cause of the moderate risk. Nevertheless, our research demonstrated a notably elevated risk as a result of bias in the assessment of the outcome.

Statistical findings

Change in irritable bowel syndrome symptoms severity score

To investigate the likelihood of a change in IBS-SSSs in adolescents and young adults with IBS using vitamin D supplementation, the OR was calculated from the event data extracted from the included studies, as depicted in Fig. 3. It was found that vitamin D supplementation has a higher likelihood of improving IBS-SSS scores than control, with an OR of 2.34 (95% CI: 1.56–3.50) and a Tau^2 value of 0.220, $\chi^2 = 20.331$, degrees of freedom (df) = 8, $Z = 4.14$, $I^2 = 61\%$, and $p < 0.001$. Furthermore, the funnel plots shown in Fig. 3 exhibit a symmetrical structure, suggesting a low likelihood of publication bias. Additionally, the p-value of Begg's test ($p = 0.182$) was statistically insignificant, above the specified significance level of 0.05.

Change in quality-of-life in individuals with IBS

To determine the possible impact of vitamin D supplementation on the QoL of adolescents and young adults with IBS, we calculated the OR using event data from the included trials, as shown in Fig. 4. The findings suggest that vitamin D supplementation is more likely to improve QoL compared to the control group. The OR was 2.51 (95% CI: 1.71–3.70; $\text{Tau}^2 = 0.191$, $\chi^2 = 18.77$, df = 8, $Z = 4.67$, $I^2 = 57\%$, $p < 0.001$). Furthermore, the symmetrical configuration of the funnel diagrams depicted in Fig. 4, along with a statistically negligible p-value on Begg's test ($p = 0.314$), above the specified significance level of 0.05, clearly suggest a minimal likelihood of publication bias.

Risk of adverse events

To assess the risk of any adverse events in adolescents and young adults with IBS using a vitamin D supplement, the RR was calculated from the event data extracted from

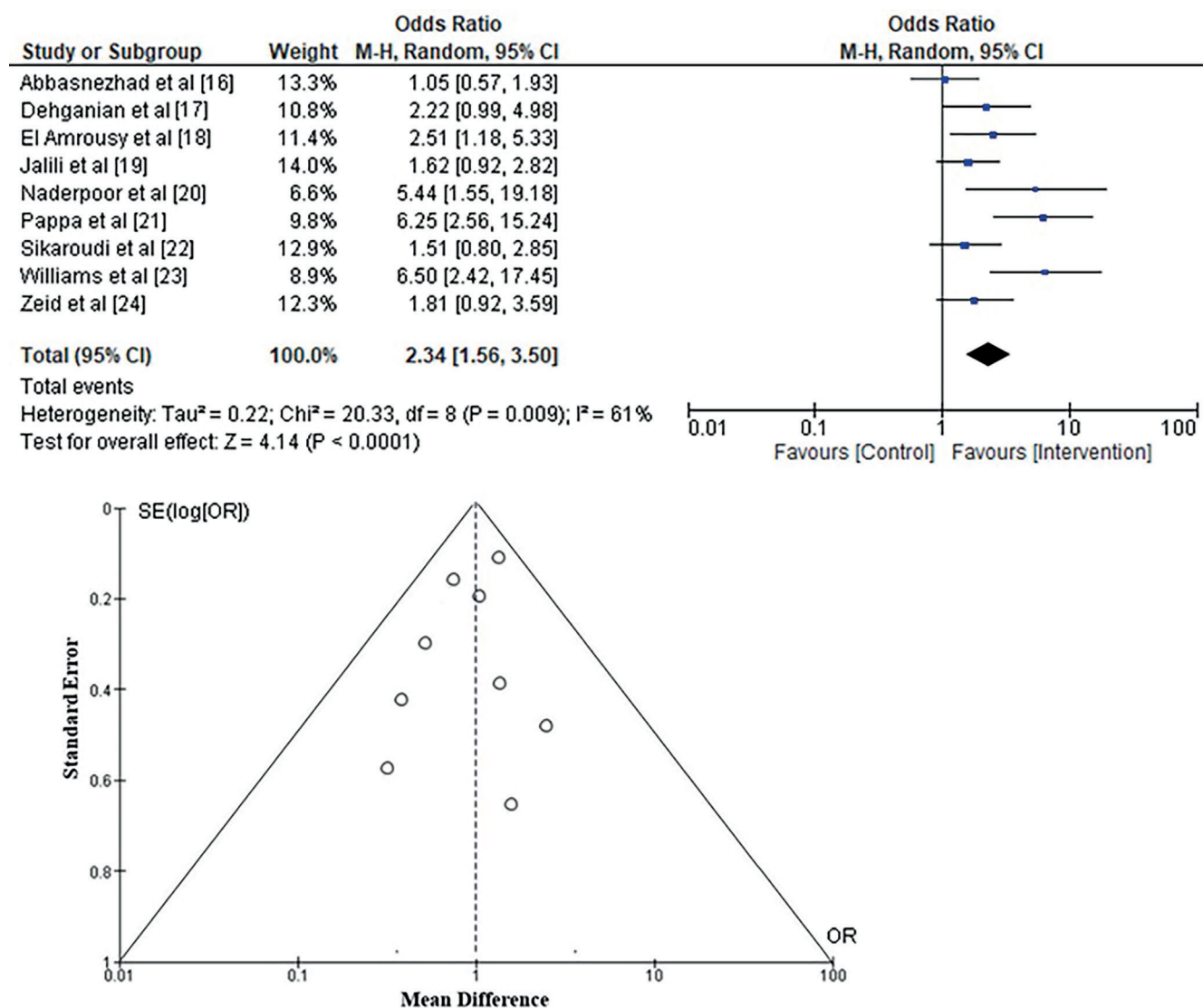


Fig. 3. Forest plot for changes in irritable bowel syndrome severity scores (IBS-SSS)

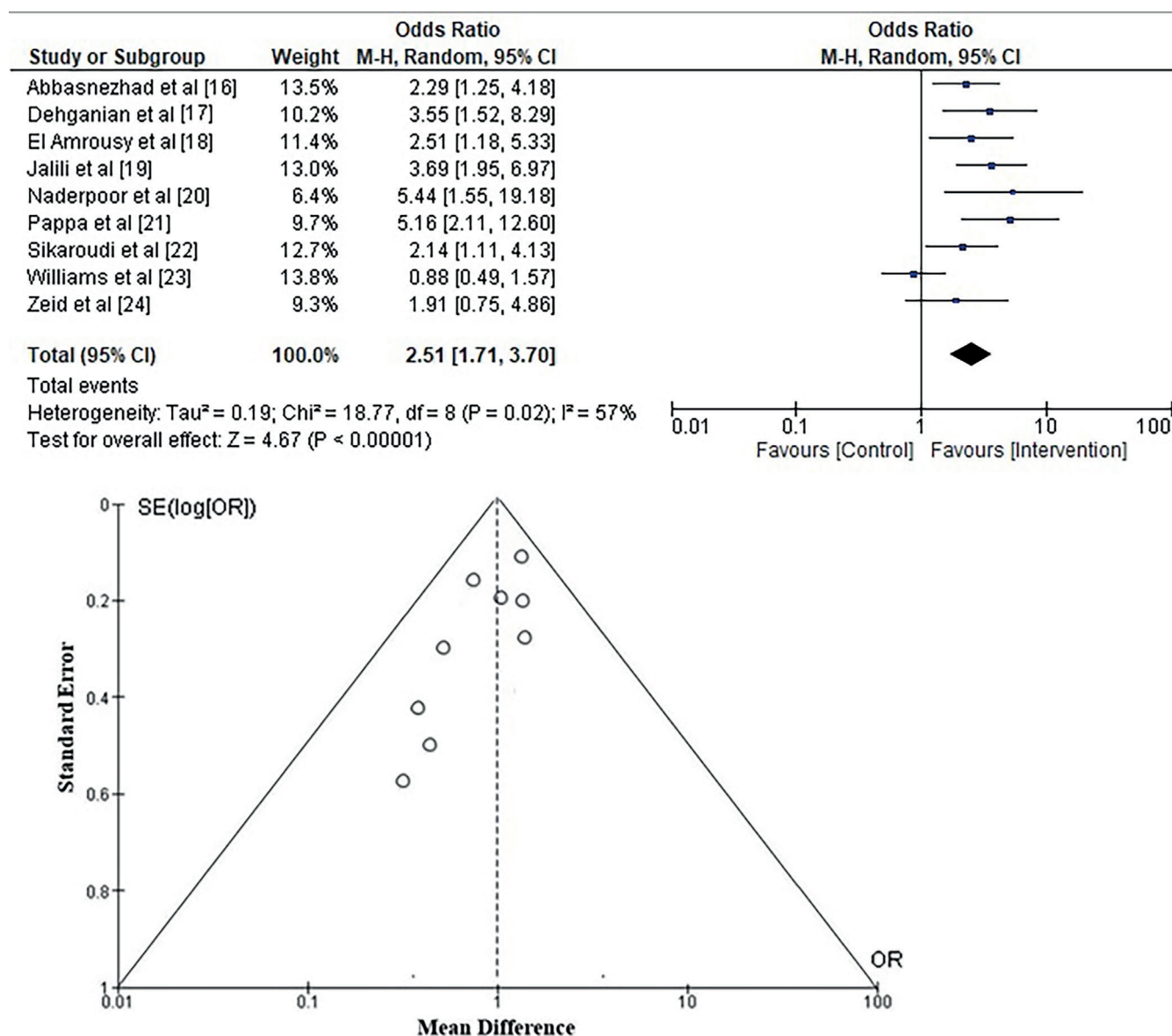


Fig. 4. Forest plot for changes in quality of life (QoL)

the included studies, as depicted in Fig. 5. It was found that vitamin D supplementation has a low risk of adverse events, with an RR of 0.49 (95% CI: 0.35–0.69) and a τ^2 value of 0.16, $\chi^2 = 25.62$, $df = 8$, $Z = 4.11$, $I^2 = 69\%$, and $p < 0.001$. The symmetrical structure of the funnel plots in Fig. 5 and the insignificant statistical p -value of 0.284 for the Begg's test – which is higher than the preset significance level of 0.05 – also suggest that there is little chance of publication bias.

Change in serum 25-hydroxy vitamin D levels

To assess the effect of vitamin D supplementation on the fluctuation of serum 25(OH)D levels in adolescents and young adults with IBS, the MD was calculated using the data collected from the studies included, as shown in Fig. 6. The study found a significant increase in serum 25(OH)D levels with vitamin D supplementation.

The statistical analysis showed a MD = 11.29 (95% CI: 7.13–15.45; $\tau^2 = 37.60$, $\chi^2 = 170.29$, $df = 8$, $Z = 5.32$, $I^2 = 64\%$, and $p < 0.001$). Similarly, the symmetrical configuration of the funnel plots depicted in Fig. 6 and the statistically insignificant p -value of Begg's test ($p = 0.244$), surpassing the predetermined significance level of 0.05, provide more evidence for the unlikelihood of publication bias.

Discussion

Irritable bowel syndrome is a prevalent and persistent illness that impacts the gastrointestinal tract. Common symptoms include cramping, stomach pain, bloating, excessive gas, and alternating episodes of diarrhea and constipation.³⁸ Irritable bowel syndrome can manifest at any age and may arise from either a bacterial or parasitic infection of the intestines or as a result of stress.^{39,40} Several effective

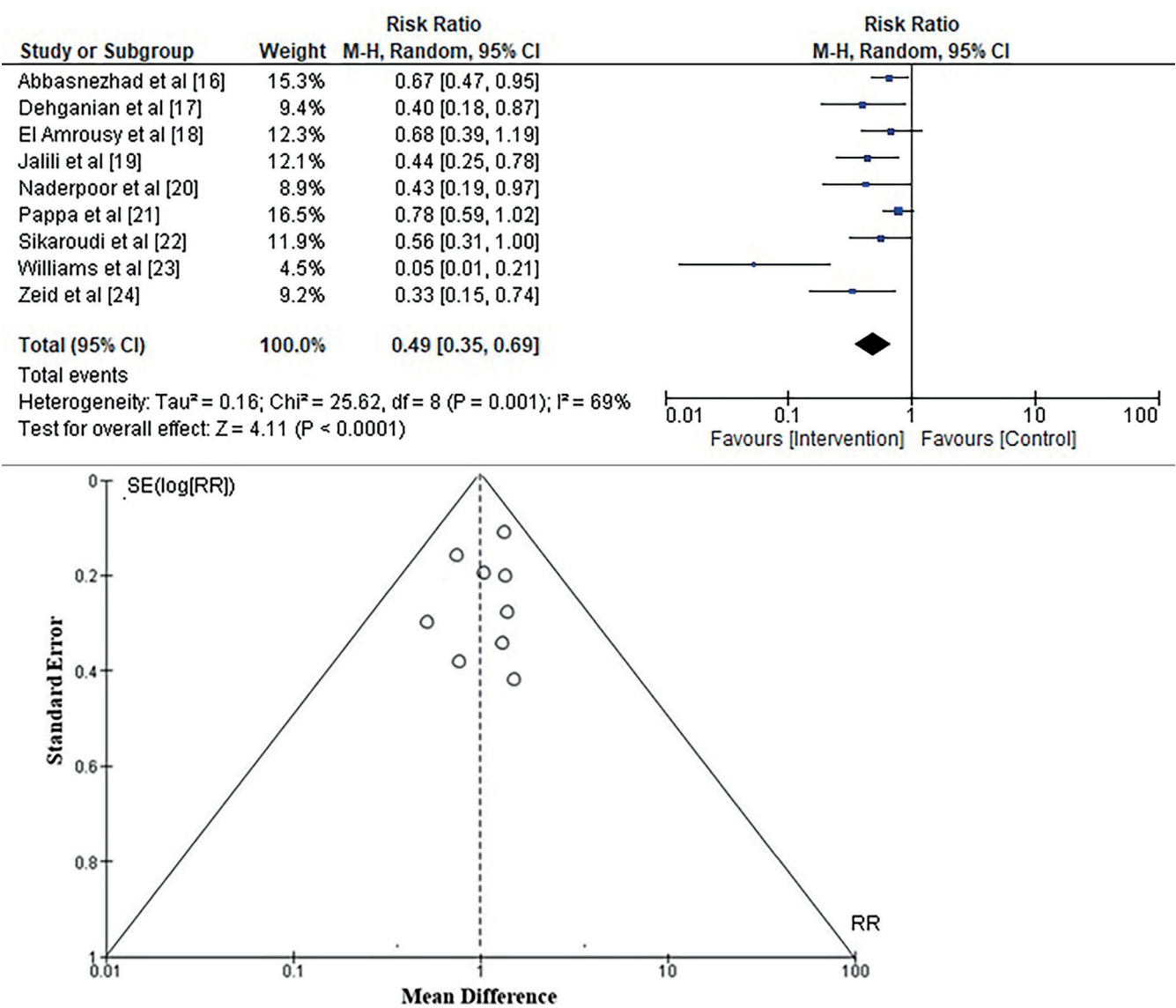


Fig. 5. Forest plot for risk of adverse events

treatments for IBS, targeting the most common symptoms, have been developed. They include dietary changes, medication supplementation and psychological therapies.^{41,42} These emergent treatments have demonstrated favorable outcomes in many studies with regard to enhanced QoL and IBS-SSS scores. The IBS-SSS scores were determined using 5 visual analogue scales (VAS): pain severity, pain duration, stomach bloating, bowel satisfaction, and interruption with daily activities. The severity scores of IBS were measured on a scale ranging from 0 (indicating the least severe) to 500 (indicating the most severe).^{43,44}

Several studies found that people with IBS experienced less severe symptoms and an overall better QoL after supplementing with fiber, microbiota and vitamin D since deficiency of these factors is often linked to IBS.^{45–47} For example, Huang et al.⁴⁸ reported in their study that vitamin D supplementation was superior to placebo for IBS treatment with greater improvement in IBS-SSS scores (weighted mean difference (WMD): –84.21, 95% CI: –111.38 to –57.05).

Similarly, in a study conducted by Chong et al.,⁴⁹ the impact of the addition of vitamin D on IBS was examined. Their study included a total of 685 patients from 8 different studies. The findings of this analysis revealed a significant improvement in IBS-SSS scores as a result of vitamin D addition. They reported a significant effect size (standardized mean difference (SMD)) of –0.77 (95% CI: –1.47 to –0.07, $p = 0.04$, $I^2 = 91\%$). Nevertheless, it was noticed that there were improvements in IBS-QoL ratings, but these improvements were not statistically significant (SMD: 0.54; 95% CI: –0.34 to 1.41, $p = 0.15$, $I^2 = 87\%$). There are, however, a lot of studies on different IBS treatment plans. In the same vein, Abuelzam et al.⁵⁰ concluded that vitamin D was ineffectual in alleviating gastrointestinal symptoms in IBS, whereas Yan et al.⁵¹ found that vitamin D supplementation may be linked to a decrease in IBS-SSS scores but not an increase in IBS-QoL scores. However, there is still debate about the number of patients who may benefit from vitamin D supplementation and whether or not there are any adverse effects.

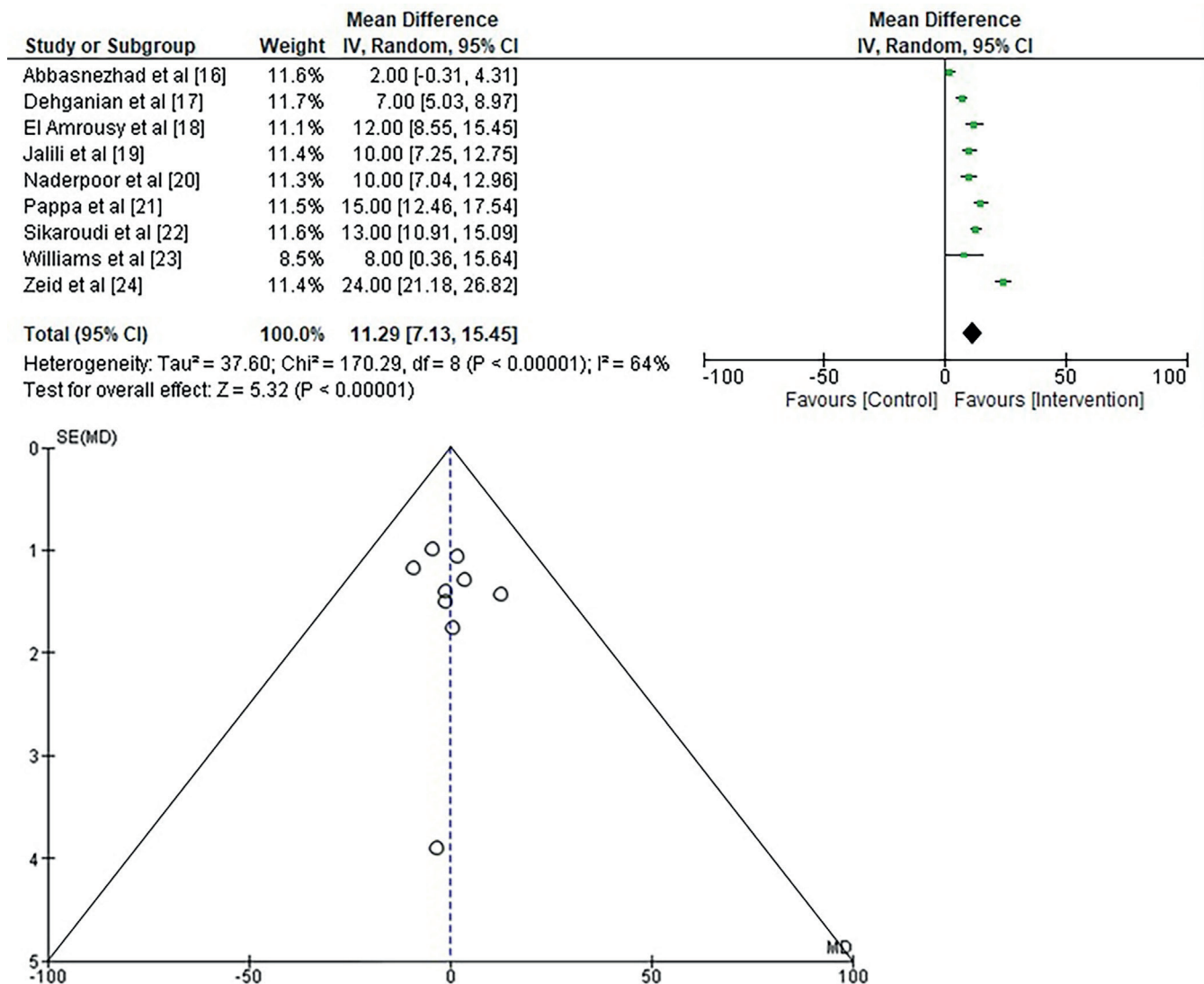


Fig. 6. Forest plot for changes in serum 25 (OH)D levels

Consequently, the purpose of this study was to assess the efficacy of vitamin D supplementation regimens for IBS in terms of their influence on QoL and the degree to which they improved the IBS-SSS score in patients who suffer from IBS. The study included 10 RCTs with a total of 831 participants. The primary findings of the included RCTs are as follows:

The study conducted by Abbasnezhad et al.¹⁶ employed a randomized, double-blind clinical design to investigate the effects of vitamin D on gastric and intestinal symptoms and health-related QoL in a sample of 90 persons diagnosed with IBS. The research entailed the random allocation of individuals who were designated to acquire either 50,000 IU of vitamin D3 or a placebo at biweekly intervals over 6 months. The IBS-SSS and IBS-specific QoL questionnaires were used for baseline and after-intervention assessments. During the 6-month intervention period, the patients who were administered vitamin D demonstrated a notable enhancement in symptoms associated with IBS, such as pain in the abdomen and distention, bloating,

trembling, and overall symptoms of the gastrointestinal tract (excluding discontentment with bowel habits), in comparison to the placebo group. Following the intervention, the vitamin D group demonstrated notable enhancements in both the IBS-SSS and IBS-QoL scores in comparison to the placebo group. The average alterations in IBS-SSS scores were -53.82 ± 23.3 and -16.85 ± 25.01 , respectively ($p < 0.001$). In a similar vein, the average change in IBS-QoL scores was 14.26 ± 3 compared to 11 ± 2.34 , respectively ($p < 0.001$). The researchers have concluded that vitamin D is a feasible and reliable option for improving the QoL and mitigating symptoms associated with IBS.

El Amrousy et al.¹⁷ performed a RCT to examine the effectiveness of vitamin D supplementation in a group of 112 adolescents diagnosed with IBS and vitamin D deficiency. The individuals were allocated randomly to 2 groups that were properly matched based on age and gender. One cohort received oral vitamin D3 at a daily dosage of 2,000 IU for 6 months, whilst the 2nd cohort received a placebo for the same period. Prior to and 6 months after

the intervention, the study evaluated the levels of vitamin D and results of assessment using different IBS scoring systems (IBS-SSS, IBS-QoL and total scores). The administration of vitamin D supplements to individuals diagnosed with IBS over 6 months resulted in significant improvements in IBS-SSS ($p < 0.001$), IBS-QoL ($p < 0.001$) and overall scores ($p = 0.02$) compared to the control group receiving a placebo for IBS. A notable elevation in serum vitamin D levels was observed in persons with IBS following the injection of vitamin D, with a twofold increase from 17.2 ± 1.3 to 39 ± 3.3 ng/mL ($p < 0.001$). No significant change in serum vitamin D levels was seen in the placebo group ($p = 0.66$). No adverse effects were observed over the trial period, suggesting that vitamin D was tolerated well. The efficacy of vitamin D supplementation in controlling IBS and vitamin D insufficiency in teenagers was determined by those researchers.¹⁷

Dehghanian et al.¹⁸ conducted a clinical experiment with 66 patients to investigate the effects of vitamin D3 supplementation on the clinical signs in individuals with IBS and lack of vitamin D. The study revealed that the administration of vitamin D supplements to patients with IBS led to a considerable elevation in serum 25(OH)D levels (with a MD of less than 14 at the conclusion of the study: $-23/24 \pm 14$). Additionally, there was a noteworthy reduction in the intensity of clinical manifestations ($p < 0.05$). The efficacy of the vitamin D dosage used in this trial (50,000 IU per week) in alleviating symptoms of IBS was determined by those researchers.¹⁸

Jalili et al.¹⁹ conducted a study to examine the impact of vitamin D supplementation on individuals diagnosed with IBS. The study employed a randomized, double-blind, placebo-controlled clinical trial design to examine the impact of weekly administration of 50,000 IU of vitamin D or a placebo comprising medium chain triglycerides on a cohort of 116 patients diagnosed with IBS for 6 weeks. The research findings indicated a significant increase in the serum levels of 25-hydroxy vitamin D, with values ranging from 21.10 ± 5.23 to 36.43 ± 12.34 in the group receiving vitamin D ($p < 0.001$). Nevertheless, the placebo group did not exhibit any notable disparity in serum levels prior to and following the experiment. At weeks 0 and 6, the severity scores of symptoms related to IBS, the disease-specific QoL and the total score were evaluated. The group administered vitamin D showed significantly larger improvements in IBS-SSS, IBS-QoL and overall ratings compared to the group receiving a placebo ($p < 0.05$). The results of this study indicate that the administration of vitamin D can potentially improve the severity of symptoms and overall QoL in patients diagnosed with IBS.

Naderpoor et al.²⁰ conducted a randomized controlled study to investigate the effects of vitamin D supplementation on intestinal microbiota. This research was comprised of a sample of 26 individuals who exhibited either vitamin D deficiency (together with a 25-hydroxyvitamin D (25(OH)D) level below 50 nmol/L), overweight or obesity

(with a body mass index (BMI) above 25 kg/m²), and were otherwise in a state of physical wellbeing. The participants provided fecal samples initially and after being administered a loading dosage of 100,000 IU of cholecalciferol, which was followed by a daily dose of 4,000 IU or a placebo for 16 weeks. The analysis of the fecal microbiota was conducted using 16S rRNA sequencing, with a specific focus on the V6–8 region. There were no significant differences observed in the microbiome diversity between the groups treated with vitamin D or placebo at both the initial and final stages of the research (all $p > 0.05$). Additionally, no clustering was seen concerning the administration of vitamin D throughout the time of follow-up ($p = 0.3$). However, a significant association was seen between the composition of the community and the genus-level with the supplementation of vitamin D ($p = 0.04$). According to a linear discriminatory analysis with a threshold of 3.0, the vitamin D group showed a higher occurrence of the genera *Lachnospira* and a lower occurrence of the genus *Blautia*. Additionally, it was noted that individuals with a 25(OH)D level exceeding 75 nmol/L exhibited a higher percentage of the *Coprococcus* genus and a lower percentage of the *Ruminococcus* species, as compared to those with a 25(OH)D level below 50 nmol/L. The findings of their research demonstrate that the intake of vitamin D supplements has significant effects on the type of fecal bacteria.

Pappa et al.²¹ undertook a randomized clinical trial to compare 2 regimens designed to maintain sufficient levels of vitamin D in children and adolescents with a diagnosis of IBS. The study comprised a cohort of 63 participants, ranging in age from 8 to 18 years, who were diagnosed with IBS and had a baseline 25(OH)D level over 20 ng/mL. Among the participants, 48 individuals successfully concluded the trial, but 1 participant withdrew from the study due to experiencing unfavorable effects. A daily dosage of 400 IU of oral vitamin D2 was supplied to the intervention Group A, consisting of 32 participants. A daily dosage of 1000 IU was delivered to Group B during the summer/fall period and 2,000 IU throughout the winter/spring season ($n = 31$). The key outcome was the probability of consistently achieving a 25(OH)D level of 32 ng/mL or higher during all regular checkups every 3 months over 12 months. Three participants in Group A (9.4%) and 3 individuals in Group B (9.7%) achieved the main outcome ($p = 0.97$). No significant disparities were seen in the incidence of adverse reactions, all of which were of a minor magnitude. Participants in Group A exhibited a greater percentage of individuals with a C-reactive protein (CRP) level of 1 mg/dL or above (31% vs 10%, $p = 0.04$) and interleukin 6 (IL-6) levels exceeding 3 pg/mL (54% vs 27%, $p = 0.05$). The researchers reached the determination that daily oral administrations of vitamin D2 up to 2,000 IU were inadequate for the maintenance of normal 25 (OH) D levels, notwithstanding their demonstrated tolerability.

The efficacy of vitamin D3 supplementation on symptom improvement, corticotrophin-releasing hormone

levels in serum and IL-6 levels in a cohort of 88 patients with diarrhea-predominant IBS (IBS-D) who exhibited vitamin D deficiencies was investigated in a RCT conducted by Khalighi Sikaroudi et al.²² Participants were randomly allocated to 2 groups. In the experimental group, a weekly dosage of 50,000 IU of vitamin D3 was administered, whereas the control group received a placebo for 9 weeks. Furthermore, all patients received mebeverine at a dosage of 135 mg twice a day, in addition to receiving supplementation. The IBS-SSS, blood 25(OH)D3, serum corticotrophin-releasing hormone (CRH) levels and IL-6 levels were assessed before and during treatments. A total of 74 patients participated in the completion of this study. The experimental group demonstrated a statistically significant reduction in the severity of symptoms associated with IBS ($p < 0.01$) and IL-6 levels ($p = 0.02$) compared to the control group. Nevertheless, no statistically significant disparities were detected in the serum concentration of CRH. In addition, it was observed that the therapy group demonstrated a significant reduction in IBS-SSS scores and IL-6 levels at the end of the study compared to initial measurements ($p < 0.01$ and $p < 0.03$, respectively). The findings of their research indicate that the ingestion of vitamin D3 has the ability to modulate the concentrations of CRH and IL-6 in the circulatory system, hence potentially ameliorating symptoms in individuals diagnosed with IBS-D. Patients with IBS-D who have deficiencies in vitamin D should consider taking vitamin D3 supplements.

The study by Tazzyman et al.²⁸ employed a randomized, double-blind, three-arm parallel strategy to examine the effects of vitamin D on the QoL of persons diagnosed with IBS. The study conducted a comparative analysis of the impacts of vitamin D, placebo and a combination with probiotics. Furthermore, the subjects were classified according to their level of vitamin D, namely, whether levels were deficient or sufficient. The assessment of vitamin D levels was performed using blood tests administered at both the initial and final stages. The evaluation of IBS symptoms was conducted utilizing a validated questionnaire. Furthermore, the assessment of dietary intake was conducted by utilizing a food frequency questionnaire. Insufficient recruitment of individuals from the replete stratum was seen among a significant portion of the population affected by IBS due to a deficit in vitamin D. A significant association was identified in the initial dataset between the concentration of vitamin D in the circulatory system and general wellbeing. The prevalence of vitamin D deficiency among individuals diagnosed with IBS was significant, indicating the need for screening and possibly supplementation to address this issue.

In a study conducted by Williams et al.,²³ a randomized clinical trial was carried out. The trial included 135 volunteers who were randomly assigned to receive either vitamin D (3,000 IU per day) or a placebo for 12 weeks. The study revealed that the administration of vitamin D

did not exert any influence on the severity of symptoms and the overall wellbeing of persons suffering from IBS. The primary variable of interest was the change in the severity of symptoms related to IBS, whereas the secondary variables comprised alterations in QoL associated with IBS. An intent-to-treat strategy was employed to analyze individuals. In the initial stages of the investigation, it was observed that 60% of the participants exhibited a shortage or inadequacy of vitamin D. In comparison to the placebo group, the intervention group exhibited a statistically significant elevation in vitamin D levels (45.1 ± 32.88 nmol/L vs 3.1 ± 26.15 nmol/L; $p < 0.001$). There was no significant difference in IBS severity of symptoms over time between the active and placebo trial arms (-62.5 ± 91.57 vs -75.2 ± 84.35 , $p = 0.426$). The trial arms did not exhibit a statistically significant distinction in QoL changes (-7.7 ± 25.36 vs -11.31 ± 25.02 , $p = 0.427$). There was a lack of evidence to substantiate the efficacy of vitamin D in the management of symptoms associated with IBS. Nevertheless, the prevalence of vitamin D deficiency suggests that it is necessary to implement frequent screening and supplementation in this population to achieve comprehensive health advantages.

The efficacy of vitamin D3 (cholecalciferol) supplementation on gastrointestinal symptoms in adults with IBS was investigated by Zeid et al.²⁴ through a randomized clinical trial including 80 patients at El-Mahsama Family Practice Center in Ismailia, Egypt. The study participants were randomly allocated to 2 separate groups: An intervention group and a control group. An oral dose of 4,000 IU of vitamin D3 was administered to the experimental group, whereas the control group received a placebo made up of edible paraffin. The approved treatment was delivered to both groups daily for 12 weeks. The IBS-SSSs were assessed at the start of the trial and again after 12 weeks. After 12 weeks, the intervention group showed a notable decrease in IBS-SSS scores (114.36 ± 67.36) compared to the control group (292.13 ± 74.77 , $p < 0.001$). The study found that there was a significant difference in IBS-SSS ratings between persons receiving vitamin D (-164.72 ± 67.77) and those receiving the placebo (-12.13 ± 50.78 , $p < 0.001$). The researchers concluded that individuals suffering from IBS reported improved overall health and relief of their gastrointestinal symptoms after receiving vitamin D3 therapy.

According to the findings of our meta-analysis, the administration of vitamin D supplements resulted in a significant improvement in QoL and IBS-SSS scores in comparison to the utilization of a placebo. The results were supported by ORs more than 1 (OR = 2.34; 95% CI: 1.56–3.50) for changes in IBS-SSS scores, (OR = 2.51, 95% CI: 1.71–3.70) for changes in QoL, and statistically significant p -values below 0.05. Furthermore, results have indicated that the administration of vitamin D supplements is linked to a decreased occurrence of negative outcomes (RR: 0.49; 95% CI: 0.35–0.69) and a notable alteration in serum 25(OH)D concentrations (MD = 11.29; 95% CI: 7.13–15.45).

Limitations

One notable component of this research is the utilization of extensive search phrases that encompass the investigation of “irritable bowel syndrome” and “vitamin D supplementation” across many databases. Nevertheless, it is important to elucidate specific constraints. This study excluded research in languages other than English. Second, it is essential to recognize the potential presence of selection bias in this research, as a significant number of the studies were purposefully omitted. Third, it was not possible to establish a correlation between the outcomes and factors such as age, ethnic background and gender. Fourth, the small sample size of participants in each subgroup and the limited number of studies resulted in substantial levels of heterogeneity and variation. Fifth, it is unfeasible to conduct a sensitivity analysis to identify the source of this variation. Lastly, since the follow-up period of the trials was short, the long-term effects of vitamin D on IBS remain unclear.

Conclusions


This is a comprehensive review of RCTs evaluating both the safety and efficacy of vitamin D supplementation within adolescents and young adults diagnosed with IBS. This study revealed that the administration of vitamin D supplements yields notable improvements in both IBS-SSS scores and QoL assessments among IBS patients, compared to the control group. Given their cost-effectiveness and safety, vitamin D supplementation is a favorable and practical approach to addressing IBS. However, because there is a limited number of investigations included, along with a significant variation and a wide range of ages, further studies are necessary to obtain a more thorough knowledge of the effects of supplementation with vitamin D.


ORCID iDs


Shuang Qi  <https://orcid.org/0009-0001-5646-4379>

Meng Zhao  <https://orcid.org/0009-0007-1859-6366>

Yinuo Sun  <https://orcid.org/0009-0005-6807-9143>

Sunaina Boro  <https://orcid.org/0009-0001-9892-787X>

Sanjay Rastogi  <https://orcid.org/0000-0001-8573-3075>

Bhawna Arora  <https://orcid.org/0009-0003-6853-5378>

References

1. Ford AC, Sperber AD, Corsetti M, Camilleri M. Irritable bowel syndrome. *Lancet*. 2020;396(10263):1675–1688. doi:10.1016/S0140-6736(20)31548-8
2. Huang KY, Wang FY, Lv M, Ma XX, Tang XD, Lv L. Irritable bowel syndrome: Epidemiology, overlap disorders, pathophysiology and treatment. *World J Gastroenterol*. 2023;29(26):4120–4135. doi:10.3748/wjg.v29.i26.4120
3. Buono JL, Carson RT, Flores NM. Health-related quality of life, work productivity, and indirect costs among patients with irritable bowel syndrome with diarrhea. *Health Qual Life Outcomes*. 2017;15(1):35. doi:10.1186/s12955-017-0611-2
4. Voß U, Lewerenz A, Nieber K. Treatment of irritable bowel syndrome: Sex and gender specific aspects. *Handb Exp Pharmacol*. 2013;214:473–497. doi:10.1007/978-3-642-30726-3_21
5. Lacy BE, Weiser K, De Lee R. Review: The treatment of irritable bowel syndrome. *Ther Adv Gastroenterol*. 2009;2(4):221–238. doi:10.1177/1756283X09104794
6. Bin Y, Kang L, Lili Y. Vitamin D status in irritable bowel syndrome and the impact of supplementation on symptoms: A systematic review and meta-analysis. *Nutr Hosp*. 2022;39(5):1144–1152. doi:10.20960/nh.04044
7. Rebelos E, Tentolouris N, Jude E. The role of vitamin D in health and disease: A narrative review on the mechanisms linking vitamin D with disease and the effects of supplementation. *Drugs*. 2023;83(8):665–685. doi:10.1007/s40265-023-01875-8
8. Yu XL, Li CP, He LP. Vitamin D may alleviate irritable bowel syndrome by modulating serotonin synthesis: A hypothesis based on recent literature. *Front Physiol*. 2023;14:1152958. doi:10.3389/fphys.2023.1152958
9. Lea R, Whorwell PJ. Quality of life in irritable bowel syndrome. *Pharmacoeconomics*. 2001;19(6):643–653. doi:10.2165/00019053-200119060-00003
10. Abboud M, Haidar S, Mahboub N, Papandreou D, Al Anouti F, Rizk R. Association between serum vitamin D and irritable bowel syndrome symptoms in a sample of adults. *Nutrients*. 2022;14(19):4157. doi:10.3390/nu14194157
11. Barbara G, Barbaro MR, Fuschi D, et al. Inflammatory and microbiota-related regulation of the intestinal epithelial barrier. *Front Nutr*. 2021;8:718356. doi:10.3389/fnut.2021.718356
12. Lin L, Zhang J. Role of intestinal microbiota and metabolites on gut homeostasis and human diseases. *BMC Immunol*. 2017;18(1):2. doi:10.1186/s12865-016-0187-3
13. Xiao L, Liu Q, Luo M, Xiong L. Gut microbiota-derived metabolites in irritable bowel syndrome. *Front Cell Infect Microbiol*. 2021;11:729346. doi:10.3389/fcimb.2021.729346
14. Menon V, Kar SK, Suthar N, Nebhinani N. Vitamin D and depression: A critical appraisal of the evidence and future directions. *Indian J Psychol Med*. 2020;42(1):11–21. doi:10.4103/IJPSYM.IJPSYM_160_19
15. Głąbska D, Kołota A, Lachowicz K, Skolmowska D, Stachoń M, Guzek D. Vitamin D supplementation and mental health in inflammatory bowel diseases and irritable bowel syndrome patients: A systematic review. *Nutrients*. 2021;13(10):3662. doi:10.3390/nu13103662
16. Abbasnezhad A, Amani R, Hajiani E, Alavinejad P, Cheraghian B, Ghadiri A. Effect of vitamin D on gastrointestinal symptoms and health-related quality of life in irritable bowel syndrome patients: A randomized double-blind clinical trial. *Neurogastroenterol Motil*. 2016;28(10):1533–1544. doi:10.1111/nmo.12851
17. El Amrousy D, Hassan S, El Ashry H, Yousef M, Hodeib H. Vitamin D supplementation in adolescents with irritable bowel syndrome: Is it useful? A randomized controlled trial. *Saudi J Gastroenterol*. 2018;24(2):109. doi:10.4103/sjg.SJG_438_17
18. Dehghanian L, Rustee A, Hekmatdoost A. Effects of vitamin D3 supplementation on clinical symptoms in patients with irritable bowel syndrome and vitamin D deficiency: Clinical trials. *Iranian J Nutr Sci Food Technol*. 2016;11(1):11–18. <https://nsft.sbm.ac.ir/article-1-1899-en.html>. Accessed August 15, 2024.
19. Jalili M, Vahedi H, Poustchi H, Hekmatdoost A. Effects of vitamin D supplementation in patients with irritable bowel syndrome: A randomized, double-blind, placebo-controlled clinical trial. *Int J Prev Med*. 2019;10(1):16. doi:10.4103/ijpvm.IJPVM_512_17
20. Naderpoor N, Mousa A, Fernanda Gomez Arango L, Barrett HL, Dekker Nitert M, De Courten B. Effect of vitamin D supplementation on faecal microbiota: A randomised clinical trial. *Nutrients*. 2019;11(12):2888. doi:10.3390/nu11122888
21. Pappa HM, Mitchell PD, Jiang H, et al. Maintenance of optimal vitamin D status in children and adolescents with inflammatory bowel disease: A randomized clinical trial comparing two regimens. *J Clin Endocrinol Metab*. 2014;99(9):3408–3417. doi:10.1210/jc.2013-4218
22. Khalighi Sikaroudi M, Mokhtare M, Shidfar F, et al. Effects of vitamin D3 supplementation on clinical symptoms, quality of life, serum serotonin (5-hydroxytryptamine), 5-hydroxy-indole acetic acid, and ratio of 5-HIAA/5-HT in patients with diarrhea-predominant irritable bowel syndrome: A randomized clinical trial. *EXCLI J*. 2020;19:652–667. doi:10.17179/EXCLI2020-2247
23. Williams CE, Williams EA, Corfe BM. Vitamin D supplementation in people with IBS has no effect on symptom severity and quality of life: Results of a randomised controlled trial. *Eur J Nutr*. 2022;61(1):299–308. doi:10.1007/s00394-021-02633-w

24. Zeid W, Ezzeldeen E, Khattab M, Ahmed S, Abdo M. Effect of vitamin D3 (cholecalciferol) supplementation on gastrointestinal symptoms in patients with irritable bowel syndrome attending El-Mahsama Family Practice Center, Ismailia, Egypt: A randomized clinical trial. *Al-Azhar Int Med J*. 2020;1(7):37–42. doi:10.21608/aimj.2020.32333.1254
25. Liberati A, Altman DG, Tetzlaff J, et al. The PRISMA statement for reporting systematic reviews and meta-analyses of studies that evaluate healthcare interventions: Explanation and elaboration. *BMJ*. 2009;339:b2700. doi:10.1136/bmj.b2700
26. Shea BJ, Reeves BC, Wells G, et al. AMSTAR 2: A critical appraisal tool for systematic reviews that include randomised or non-randomised studies of healthcare interventions, or both. *BMJ*. 2017;358:j4008. doi:10.1136/bmj.j4008
27. Cumpston MS, McKenzie JE, Thomas J, Brennan SE. The use of 'PICO for synthesis' and methods for synthesis without meta-analysis: Protocol for a survey of current practice in systematic reviews of health interventions. *F1000Res*. 2021;9:678. doi:10.12688/f1000research.24469.2
28. Higgins JPT, Altman DG, Gotzsche PC, et al. The Cochrane Collaboration's tool for assessing risk of bias in randomised trials. *BMJ*. 2011;343:d5928. doi:10.1136/bmj.d5928
29. Sterne JAC, Egger M. Funnel plots for detecting bias in meta-analysis. *J Clin Epidemiol*. 2001;54(10):1046–1055. doi:10.1016/S0895-4356(01)00377-8
30. Begg CB, Mazumdar M. Operating characteristics of a rank correlation test for publication bias. *Biometrics*. 1994;50(4):1088–1101. PMID:7786990.
31. Elovic A, Pourmand A. MDCalc Medical Calculator app review. *J Digit Imaging*. 2019;32(5):682–684. doi:10.1007/s10278-019-00218-y
32. Schmidt L, Shokraneh F, Steinhausen K, Adams CE. Introducing RAPTOR: RevMan Parsing Tool for Reviewers. *Syst Rev*. 2019;8(1):151. doi:10.1186/s13643-019-1070-0
33. Dettori JR, Norvell DC, Chapman JR. Seeing the forest by looking at the trees: How to interpret a meta-analysis forest plot. *Global Spine J*. 2021;11(4):614–616. doi:10.1177/21925682211003889
34. George BJ, Aban IB. An application of meta-analysis based on DerSimonian and Laird method. *J Nucl Cardiol*. 2016;23(4):690–692. doi:10.1007/s12350-015-0249-6
35. Szumilas M. Explaining odds ratios [Erratum in: *J Can Acad Child Adolesc Psychiatry*. 2015;24(1):58]. *J Can Acad Child Adolesc Psychiatry*. 2010;19(3):227–229. PMID:20842279. PMCID:PMC2938757.
36. Melsen WG, Bootsma MCJ, Rovers MM, Bonten MJM. The effects of clinical and statistical heterogeneity on the predictive values of results from meta-analyses. *Clin Microbiol Infect*. 2014;20(2):123–129. doi:10.1111/1469-0691.12494
37. Barili F, Parolari A, Kappetein PA, Freemantle N. Statistical primer: Heterogeneity, random- or fixed-effects model analyses? *Interact Cardiovasc Thorac Surg*. 2018;27(3):317–321. doi:10.1093/icvts/ivy163
38. Tazzyman S, Richards N, Trueman AR, et al. Vitamin D associates with improved quality of life in participants with irritable bowel syndrome: outcomes from a pilot trial. *BMJ Open Gastroenterol*. 2015;2(1):e000052. doi:10.1136/bmjgast-2015-000052
39. Enck P, Aziz Q, Barbara G, et al. Irritable bowel syndrome. *Nat Rev Dis Primers*. 2016;2(1):16014. doi:10.1038/nrdp.2016.14
40. Radovanovic-Dinic B, Tesic-Rajkovic S, Grgov S, Petrovic G, Zivkovic V. Irritable bowel syndrome: From etiopathogenesis to therapy. *Biomed Pap Med Fac Univ Palacky Olomouc Czech Repub*. 2018;162(1):1–9. doi:10.5507/bp.2017.057
41. Black CJ, Ford AC. Best management of irritable bowel syndrome. *Frontline Gastroenterol*. 2021;12(4):303–315. doi:10.1136/flgastro-2019-101298
42. Alammam N, Stein E. Irritable bowel syndrome. *Med Clin North Am*. 2019;103(1):137–152. doi:10.1016/j.mcna.2018.08.006
43. Francis CY, Morris J, Whorwell PJ. The irritable bowel severity scoring system: A simple method of monitoring irritable bowel syndrome and its progress. *Aliment Pharmacol Ther*. 1997;11(2):395–402. doi:10.1046/j.1365-2036.1997.142318000.x
44. Betz C, Mannsdörfer K, Bischoff S. Validation of the IBS-SSS [in German]. *Z Gastroenterol*. 2013;51(10):1171–1176. doi:10.1055/s-0033-1335260
45. Linsalata M, Riezzo G, Orlando A, et al. The relationship between low serum vitamin D levels and altered intestinal barrier function in patients with IBS diarrhoea undergoing a long-term low-FODMAP diet: Novel observations from a clinical trial. *Nutrients*. 2021;13(3):1011. doi:10.3390/nu13031011
46. Radziszewska M, Smarkusz-Zarzecka J, Ostrowska L. Nutrition, physical activity and supplementation in irritable bowel syndrome. *Nutrients*. 2023;15(16):3662. doi:10.3390/nu15163662
47. Wyon MA, Wolman R, Nevill AM, et al. Acute effects of vitamin D3 supplementation on muscle strength in judoka athletes: A randomized placebo-controlled, double-blind trial. *Clin J Sport Med*. 2016;26(4):279–284. doi:10.1097/JSM.0000000000000264
48. Huang H, Lu L, Chen Y, Zeng Y, Xu C. The efficacy of vitamin D supplementation for irritable bowel syndrome: A systematic review with meta-analysis. *Nutr J*. 2022;21(1):24. doi:10.1186/s12937-022-00777-x
49. Chong RH, Yaow CYL, Loh CYL, et al. Vitamin D supplementation for irritable bowel syndrome: A systematic review and meta-analysis. *J Gastroenterol Hepatol*. 2022;37(6):993–1003. doi:10.1111/jgh.15852
50. Abuelazm M, Muhammad S, Gamal M, et al. The effect of vitamin D supplementation on the severity of symptoms and the quality of life in irritable bowel syndrome patients: A systematic review and meta-analysis of randomized controlled trials. *Nutrients*. 2022;14(13):2618. doi:10.3390/nu14132618
51. Yan C, Hu C, Chen X, et al. Vitamin D improves irritable bowel syndrome symptoms: A meta-analysis. *Heliyon*. 2023;9(6):e16437. doi:10.1016/j.heliyon.2023.e16437

Electrical impedance tomography confirmed the impact of the method of delivery of term neonates on early lung aeration

Adomas Janulionis^{1,B–D}, Viktorija Sutova^{1,C,D}, Vita Langiene^{2,B,C}, Ernestas Virsilas^{1,3,E}, Violeta Drejeriene^{2,B,E}, Arunas Liubsys^{1,3,A,C,E}, Arunas Valiulis^{1,A,C,E,F}

¹ Clinic of Children's Diseases, Institute of Clinical Medicine, Faculty of Medicine, Vilnius University, Lithuania

² Obstetrics and Gynecology Clinic, Vilnius City Clinical Hospital, Lithuania

³ Centre of Neonatology, Vilnius University Hospital Santaros Clinics, Lithuania

A – research concept and design; B – collection and/or assembly of data; C – data analysis and interpretation;

D – writing the article; E – critical revision of the article; F – final approval of the article

Advances in Clinical and Experimental Medicine, ISSN 1899–5276 (print), ISSN 2451–2680 (online)

Adv Clin Exp Med. 2025;34(7):1105–1112

Address for correspondence

Arunas Valiulis

E-mail: arunas.valiulis@mf.vu.lt

Funding sources

The survey was funded by the Vilnius University within PhD study program of Adomas Janulionis.

Conflict of interest

None declared

Acknowledgements

We are very grateful to the newborns and their families for participating in our survey, as well as to the staff of the Obstetrics and Gynecology Clinic of Vilnius City Clinical Hospital for technical support.

Received on December 22, 2023

Reviewed on April 30, 2024

Accepted on July 2, 2024

Published online on January 27, 2025

Cite as

Janulionis A, Sutova V, Langiene V, et al. Electrical impedance tomography confirmed the impact of the method of delivery of term neonates on early lung aeration. *Adv Clin Exp Med.* 2025;34(7):1105–1112. doi:10.17219/acem/190742

DOI

10.17219/acem/190742

Copyright

Copyright by Author(s)

This is an article distributed under the terms of the Creative Commons Attribution 3.0 Unported (CC BY 3.0) (<https://creativecommons.org/licenses/by/3.0/>)

Abstract

Background. The number of infants born via cesarean section (CS) is increasing globally due to medical and cultural reasons.

Objectives. This study aimed to determine the effect of the mode of delivery on early lung aeration in newborns using electrical impedance tomography (EIT).

Materials and methods. The case-control study was conducted from December 2020 to April 2021. It included 32 term neonates delivered by CS and 20 term neonates delivered by normal vaginal delivery (NVD) as controls. Electrical impedance tomography examinations were performed with a Swisstom BB2 device with NEO SensorBelt and 32 integrated electrodes at 47.68 Hz. Three data recordings were conducted within 30, 60 and 90 min (mean times: 13, 62 and 93 min, respectively) after the birth.

Results. Cesarean section neonates, compared to those delivered by NVD, had greater non-aerated areas in gravity-dependent lung regions at the 2nd recording ($p = 0.04$). The CS group showed lower changes in lung stretch at the 2nd and 3rd recording compared to the NVD group ($p = 0.022$ and $p = 0.032$, respectively). In the study group, lung regions with the lowest stretch (10–20%, 20–30% and 30–40%) corresponded with increased total lung capacities 1 h after birth compared to the control group ($p = 0.024$, $p = 0.004$ and $p = 0.044$, respectively). Measurements from the 1st and 3rd EIT recording showed a greater distribution of tidal volume (TV) in the right lung toward the central regions among CS neonates compared to NVD neonates, whereas NVD neonates showed increased distribution of TV toward the central-ventral regions of the right lung immediately after birth.

Conclusions. The mode of delivery significantly affects early postnatal lung aeration in term neonates assessed using EIT. Caesarean section neonates were characterized by poorer aeration in gravity-dependent lung regions, whereas NVD neonates demonstrated greater changes in lung stretch and more intense tissue expansion, potentially leading to better postnatal adaptation.

Key words: cesarean section, normal vaginal delivery, electrical impedance tomography, lung aeration, term neonates

Background

The transition from the intrauterine to the extrauterine environment poses significant challenges for neonates, primarily due to fundamental changes in their breathing and circulation. Fetal lungs are known to be filled with fluid, and thus, the aeration of the lungs with air is one of the most important physiological changes that occur immediately after birth. However, it remains unclear exactly how and when the fluid is completely removed from the lungs. Several key mechanisms and stages of fluid clearance from the lungs have been identified, starting during fetal development and continuing through labor and the first hours after birth.¹ It is also known that both gestational age and the method of birth influence lung fluid clearance and aeration.^{1,2} However, it is uncertain whether all lung regions achieve uniform aeration and synchronization post-birth, or if differences in lung aeration exist depending on the mode of delivery and other factors.

A variety of methods and techniques are available for assessing lung aeration in neonates after birth. These methods have been summarized in a recently published systematic review.³ However, some methods are indirect (such as respiratory monitoring and capnography), while others involve ionizing radiation (such as chest radiography), and static, one-dimensional lung imaging. Additionally, lung ultrasonography reflects the overall fluid–air ratio in the lung rather than providing clear identification of the aeration of individual lung segments. In recent years, noninvasive techniques such as respiratory inductive plethysmography or electrical impedance tomography (EIT) have been increasingly used to assess the dynamic changes in lung aeration in neonates.⁴ Earlier studies from Lithuania have highlighted the utility of EIT in both pre-term and term neonates.^{5–8}

Objectives

The study aimed to assess the characteristics of lung aeration in term neonates born via NVD and cesarean section (CS) using EIT.

Materials and methods

Study participants

Our case-control study included 52 spontaneously breathing term neonates born at the Department of Obstetrics and Gynecology of the Vilnius City Clinical Hospital (Lithuania), between December 2020 and April 2021. Among these, 20 were born via NVD (control group) and 32 infants (38 weeks ± 0.5) were delivered by CS (study group). This included 28 elective CS and 4 emergency surgeries. All emergency CS were conducted due to abnormal fetal heart rate patterns. None of the infants required assistance for adaptation in the delivery room. Neonates meeting the inclusion criteria were randomly selected.

The study was approved by the Vilnius Regional Biomedical Research Ethics Committee (approval No. 1287 issued on November 24, 2021), and written informed consent was obtained from the parents of all newborns. The main characteristics of the newborns are presented in Table 1.

Data collection utilized the Electrical Impedance Tomography device (Swisstom AG, Landquart, Switzerland). A NEO SensorBelt equipped with integrated 32 electrodes was positioned circumferentially around the thorax at the nipple level, operating at a sample rate of 47.68 Hz.

Three data recording sessions were conducted on the day of birth for each neonate. Data were collected at 3 intervals: immediately after birth (0 min), 60 min after birth and 90 min after birth. All recordings were conducted with the infants in the supine position. For breastfeeding sessions, measurements were delayed to avoid disrupting mother–infant bonding. Similarly, for any procedures such as blood draws, heel pricks or routine nursing care, measurements were postponed from the scheduled time frames unless the delay exceeded 30 min beyond the designated time frame. Each EIT recording session lasted a minimum of 5 min. All studied infants were spontaneously breathing. Figure 1 shows the process of data recording.

Data analysis was conducted using Ibox 1.4 software (https://www.sentec.com/fileadmin/documents/_EIT_documents/ibeX_Product_Information.pdf). The impedance signal was processed using a respiratory rate filtering

Table 1. Characteristics of spontaneously breathing term neonates included in the study

Mode of delivery		Natural vaginal delivery (n = 20)		Cesarean delivery (n = 32)	
Characteristic		mean	\pm SD	mean	\pm SD
Gestational age (weeks + days)		39 +5	1 +2	38 +4	0 +5
Maturity index (New Ballard Score)		26.9	1.59	26.7	1.26
Weight [g]		3,502	313	3,439	380
Cord blood pH		7.3	0.10	7.3	0.04
Apgar scores	1 min	8.9	1.3	9	1.15
	5 min	9.1	0.94	9.3	0.68

SD - standard deviation.



Fig. 1. Electrical impedance tomography data recording process

function. The following EIT parameters were compared between the 2 groups of study participants:

1. Center of ventilation (CoV), indicating the best-ventilated lung areas;
2. Silent spaces, representing lung areas with minimal or no ventilation (impedance changes $<10\%$);
3. Relative stretch, reflecting the potential of the lungs to expand during inspiration;
4. Relative tidal volume, expressed as a fraction of total ventilated lung area;
5. Distribution of tidal volume between the right and left lungs separately, referring to the sum of tidal volumes per lung and the regional distribution (ventral, dorsal, central-ventral, and central-dorsal segments).

Statistical analyses

The results were analyzed using IBM SPSS Statistics v. 22 (IBM Corp., Armonk, USA). The Mann–Whitney test was used to compare results between groups. Data from 3 episodes were compared using the Friedman test, with the Wilcoxon rank-sum test used for paired data when the Friedman's test indicated significant differences between groups. Statistical significance was determined at $p < 0.05$. During analysis, 2 neonates were excluded in episode I, 1 neonate in episode II and 5 neonates in episode III due to discontinuation of EIT recording or recording errors, which precluded comparison across all 3 episodes.

Results

The 1st data recording was performed as soon as possible after birth, depending on the condition of the newborn, but no later than within 30 min (average 13 min). The 2nd recording occurred at an average of 62 min, and the 3rd one at 1.5 h (average 93 min) after birth.

Silent spaces

Statistically significant changes related to this parameter were observed only in the lung's dependent regions (portions most influenced by gravity). Neonates born via CS had more silent spaces in these regions at 1 h after birth compared to those born via NVD (Table 2). The median silent space in dependent lung regions was 0 and did not differ between groups or over time, indicating that 50% of neonates had no unventilated areas in these regions (Fig. 2).

Relative stretch of lung tissue

A statistically significant difference between neonates born via NVD and those born via CS was observed at 1 h and 1.5 h after birth. In the NVD group, greater

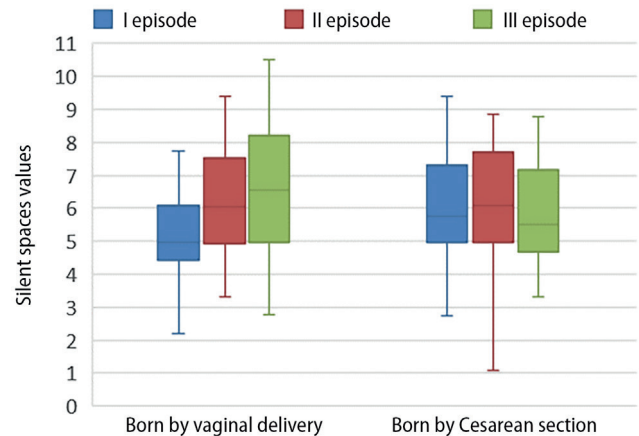


Fig. 2. Silent spaces in dependent lung regions. Comparison of 3 episodes CS – cesarean section; NVD – normal vaginal delivery.

stretch-related changes were observed, particularly in the least ventilated spaces, corresponding to the 25% quartile (the lowest stretch, also referred to as 'grey spaces'). There was little to no difference in median relative stretch across episodes between neonatal groups. Lung tissue stretch induced by the same tidal volume (25%, 50%

Table 2. Episode II: silent spaces

Parameter	Group	N	Q1	Median	Q3	Minimum value	Maximum value	Mann–Whitney average ranks	Z	p-value
Non-dependent lung regions [%]	CS	30	4.97	5.52	7.69	1.10	18.23	25.84	-0.329	0.742
	NVD	19	4.67	6.08	7.92	3.31	17.68	24.47		
Dependent lung regions [%]	CS	30	0.00	0.00	0.55	0.00	2.76	28.71	-2.055	0.040
	NVD	19	0.00	0.00	0.00	0.00	11.60	22.65		

Asterisks indicate true outliers and circles indicate conditional outliers. CS – cesarean section; NVD – normal vaginal delivery.

Table 3. Episodes II and III: relative stretch

Quartile	Group	N	Q1	Median	Q3	Minimum value	Maximum value	Mann–Whitney average ranks	Z	p-value
Episode II										
Quartile –	CS	30	0.42	0.45	0.46	0.35	0.54	19.11	–2.298	0.022
	NVD	19	0.44	0.48	0.51	0.33	0.56	28.73		
Median	CS	30	0.58	0.62	0.66	0.53	0.73	21.89	–1.211	0.226
	NVD	19	0.60	0.65	0.71	0.51	0.74	26.97		
Quartile +	CS	30	0.79	0.81	0.83	0.56	0.88	25.26	–0.103	0.918
	NVD	19	0.78	0.81	0.83	0.69	0.88	24.83		
Episode III										
Quartile –	CS	29	0.43	0.46	0.48	0.35	0.53	16.73	–2.142	0.032
	NVD	15	0.46	0.48	0.50	0.40	0.56	25.48		
Median	CS	29	0.58	0.61	0.68	0.53	0.70	17.93	–1.696	0.090
	NVD	15	0.61	0.66	0.69	0.59	0.74	24.86		
Quartile +	CS	29	0.79	0.80	0.83	0.65	0.86	19.87	–0.978	0.328
	NVD	15	0.80	0.82	0.84	0.65	0.87	23.86		

CS – cesarean section; NVD – normal vaginal delivery.

Table 4. Episode II: relative stretch categories and relative tidal volume

Relative stretch category	Group	N	Q1	Median	Q3	Minimum value	Maximum value	Mann–Whitney average ranks	Z	p-value
0.2	CS	30	2.16	3.15	3.60	1.65	5.10	30.79	–2.257	0.024
	NVD	19	1.62	1.97	3.10	1.15	5.54	21.33		
0.3	CS	30	4.43	6.21	8.08	1.97	11.97	32.32	–2.852	0.004
	NVD	19	3.31	4.05	6.02	2.45	8.08	20.37		
0.4	CS	30	8.05	10.29	11.45	2.76	12.61	30.16	–2.011	0.044
	NVD	19	7.13	8.98	10.15	4.02	14.83	21.73		

CS – cesarean section; NVD – normal vaginal delivery.

and 75%, respectively) decreased insignificantly over time in the study group and slightly increased during the last episode in the control group (Table 3).

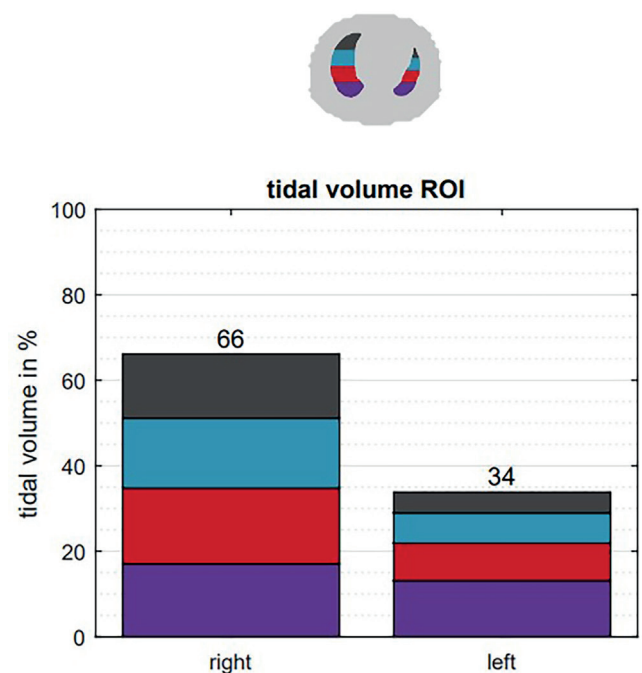
Relative lung stretch categories of 10–20%, 20–30% and 30–40% correlated more with greater lung capacities in the study group of neonates compared to the control group (i.e., smaller changes in stretch – grey spaces occupied a larger proportion of the lung image in the study group). These changes were statistically significant at 1 h after birth (episode II) (Table 4).

Center of ventilation

The results showed no statistically significant shift in the center of ventilation between or within groups. In the study group, more neonates had a CoV value not exceeding the mean at 90 min after birth (right-to-left shift). In the ventral-dorsal projection, the variation of the center of ventilation in the study group was similar at 1 h and 1.5 h after birth.

Distribution of tidal volume

There was no significant temporal variation in the distribution of tidal volume between the left and right lung in the study and control cohorts. However, a greater dis-



20210429160724.zri - EA_2023-02-01 16h35m.pdf

Fig. 3. Example electrical impedance tomography (EIT) image of tidal volume distribution between regions of interest (ROI) of the left and right lungs of a spontaneously breathing term neonate. Graphical results are ensemble averaged

Table 5. Regions of interest: episodes I and III

Side	Region	Group	N	Q1	Median	Q3	Minimum value	Maximum value	Mann–Whitney average ranks	Z	p-value
Episode I											
Right lung	central dorsal [%]	CS	30	17.88	18.12	25.27	17.76	34.94	30.60	−2.020	0.043
		NVD	20	17.80	17.89	18.15	17.59	30.94	22.10		
	dorsal [%]	CS	30	16.63	16.69	19.74	16.38	25.43	28.00	−0.990	0.322
		NVD	20	16.57	16.65	16.97	16.40	24.99	23.83		
Episode III											
Right lung	central ventral [%]	CS	29	16.59	16.73	18.67	12.89	29.98	28.67	−2.290	0.022
		NVD	15	16.40	16.55	16.68	14.70	19.91	19.31		
	central dorsal [%]	CS	29	18.02	18.10	26.82	17.74	36.67	28.20	−2.117	0.034
		NVD	15	17.79	17.90	20.30	17.65	28.55	19.55		

CS – cesarean section; NVD – normal vaginal delivery.

Table 6. Regions of interest: comparison of 3 episodes

Region	Group	Episodes	Friedman average ranks	p-value
Central ventral areas of the right lung [%]	CS	I	1.80	0.627
		II	2.07	
		III	2.13	
	NVD	I	2.47	0.003
		II	1.97	
		III	1.57	
Central ventral areas of the left lung [%]	CS	I	2.07	0.247
		II	2.27	
		III	1.67	
	NVD	I	1.95	0.791
		II	2.10	
		III	1.95	

CS – cesarean section; NVD – normal vaginal delivery.

tribution of tidal volume toward the central regions was observed in the right lung of the study group immediately after birth and at the end of the recording (Table 5). Neonates born via NVD had a greater volume distribution toward the central-ventral regions of the right lung immediately after birth (Table 6). Fig. 3 illustrates the distribution of tidal volume between the left and right lung of a spontaneously breathing term neonate.

Discussion

There are few studies on respiratory adaptation in neonates immediately after birth, primarily due to the lack of appropriate instruments or techniques for noninvasive assessment of lung aeration in real time. Our study intended to fill this gap.

Our analysis revealed differences between the 2 study groups in several EIT parameters: silent spaces, relative stretch, relative tidal volume, and distribution of lung aeration. The most pronounced differences in aeration were observed at 1 h after birth rather than immediately post-birth. Neonates born via NVD had significantly fewer unventilated (or poorly ventilated) spaces in the dependent lung regions. This aligns with prior research indicating that in healthy neonates without mechanical ventilation, dependent lung regions (those most affected by gravity) exhibit better aeration compared to independent lung regions (those least influenced by gravity).⁹ Conversely, a higher distribution of aeration to independent lung regions was generally found in intensive care unit (ICU) patients and was associated with worse respiratory status.¹⁰ However, Schinckel et al. concluded that gravity plays a limited role in stable, spontaneously breathing neonates, and that ventilation patterns are more anatomically determined.¹¹ Larger silent spaces in neonates born by CS may be due to retained pulmonary fluid or alveolar collapse caused

by a lack of surfactant. According to a study by Blank et al., comparing lung adaptation between identical groups of neonates using ultrasound, complete lung fluid clearance after birth can take several hours, and differences between groups may persist beyond 1.5 h.¹² We observed statistically significant differences in ventilation in several EIT parameters in episode II, but these differences persisted only in 1 parameter – relative stretch – in episode III. In episode II, neonates born by elective CS showed the highest percentage of relative tidal volume in both lungs (grey spaces on EIT images), primarily in areas with the lowest stretch (10–20%, 20–30% and 30–40%). These spaces correspond to areas with reduced aeration, although they receive slightly more air than silent spaces, where impedance changes are below 10%. Lung tissue expansion depends on the proportion of tidal volume entering the lung, and is, therefore, the highest in well-ventilated areas. Finally, changes in the distribution of aeration were identified only in neonates born by normal vaginal delivery, and these changes varied over time. This suggests that central ventral lung areas received the most air immediately after birth, with ventilation becoming more homogeneous by the end of the study.

Previous studies have associated CS births with higher rates of respiratory distress syndrome, transient tachypnea of the newborn and persistent pulmonary hypertension of the newborn.^{13–15} In normal vaginal deliveries, maternal catecholamines are believed to determine the regulation of surfactant production and sodium ion transport across epithelial cells, facilitating lung fluid resorption. During the transition period, the increase in pulmonary perfusion must be consistent with an increase in aeration; otherwise, the normal adaptation of the newborn is impaired. However, because neonates born by CS have slower lung fluid clearance and greater amounts of residual lung fluid, optimal gas exchange is achieved over a longer period. In addition, there is less surfactant produced to cover the alveolar surface.¹⁶ If CS is performed before spontaneous labor onset, neonatal lungs are significantly less mature than in the case of post-labor CS.^{17–19}

Post-CS respiratory changes during the early adaptation period have been described in animal studies using contrast-enhanced lung X-ray imaging. However, the invasiveness and radiation risks limit its clinical utility.²⁰ A 2018 study using lung ultrasound compared neonates born by different modes of delivery but found significant differences only at baseline, which disappeared within 2 h after birth. Regardless of delivery mode, all neonates achieved lung aeration and partial fluid resorption within 20 min after birth, with complete fluid clearance occurring within several hours.¹²

To date, numerous publications have focused on short- and long-term respiratory morbidity associated with the mode of delivery.^{21–25} However, there are few publications describing differences in lung adaptation among term neonates in the first hours after birth. In 2017, Bhargava

et al. analyzed differences in oxygen saturation between term neonates delivered vaginally and via CS and found significantly lower saturation levels in the CS group during the initial 30 min after birth. Neonates typically take 12–14 min to reach a saturation rate of 95%. These findings are consistent with our observation that adaptation to extrauterine life is slower in the CS group.²⁶

The first breaths after birth establish the lung functional residual capacity (FRC), increase pulmonary circulation and facilitate carbon dioxide (CO₂) removal. Expired CO₂ levels (ECO₂) correlate with lung aeration and indicate airway patency and pulmonary gas exchange. However, measurements of ECO₂, respiratory rate and tidal volume in neonates delivered vaginally vs by CS did not reveal significant differences in lung adaptation during the transition period. These measurements were performed during the first 30 min of life.²⁷ In contrast, Finn et al. reported a delay in the establishment of FRC in the CS group. This is consistent with our study and with previous plethysmography findings,²⁸ suggesting that larger amounts of fluid in the lung interstitium may delay the time for gas exchange to become optimal in neonatal lungs.²⁹ However, in the study by Finn et al.,²⁸ this delay was most notable in the initial minutes of life, whereas in our EIT study, it became apparent at the end of the first hour of life.

Blank et al. used lung ultrasound to monitor changes in lung aeration in healthy neonates and found that partial lung fluid resorption occurred within the first 20 min after birth, with full FRC achieved within 4 h. Neonates born by different modes of delivery were compared using a validated scoring system: higher scores indicated better lung aeration and fluid clearance. Neonates delivered by elective CS had significantly lower lung aeration at 1–10 min and 11–20 min after birth compared to those born vaginally and those delivered by emergency CS. According to Blank et al., neonates born by elective CS had insignificantly lower lung aeration at 1 h after birth compared to other groups, whereas our EIT study recorded the most significant difference between the study and control groups at 1 h after birth. Lung ultrasound showed no difference between the NVD and CS groups. Significantly better aeration was observed via echocardiography in neonates delivered by emergency CS compared to those in the elective CS group (up to 1 h after birth).³⁰ In term pregnancies, such surgeries are usually performed due to intrauterine hypoxia or failed vaginal delivery, often after the onset of labor and subsequent lung fluid clearance. Thus, it poses less risk for respiratory adaptation compared to elective CS performed before the onset of spontaneous labor when there is incomplete lung maturation and surfactant deficiency. A more detailed EIT study is needed in the future to compare these CS groups separately.

Martelius et al. used ultrasound to study postnatal lungs in term infants. They observed a significant decrease in the abundance of B-lines, indicative of lung fluid migration, during the first 24 h in both groups of infants

born by normal vaginal delivery and elective CS. At 1 h after delivery, there was no significant difference between the groups, but by 3 h after birth, CS was associated with significantly higher lung fluid content than normal vaginal delivery. However, this difference disappeared at 24 h after birth.^{31,32} Compared with lung ultrasound, EIT identified delayed fluid clearance and poorer aeration earlier in neonates born by elective CS.

Limitations

The limitations of our study include the fact that neonates were only examined in the supine position; they were not placed in the prone position. Another limitation is that the study was conducted at a single center.

Conclusions

No statistically significant differences in lung aeration immediately after birth were found between neonates born by normal vaginal delivery and neonates born by CS. At 1 h after birth, poorer ventilation was observed in the CS group, particularly in dependent lung regions and in both lungs combined. After 1.5 h, more pronounced changes related to lung tissue stretch persisted in the NVD group. In this group, the tidal volume distribution steadily increased throughout the 1.5-h observation period. Electrical impedance tomography is a suitable method for assessing lung aeration in term neonates during early adaptation.

Data availability

The datasets generated and/or analyzed during the current study are available from the corresponding author on reasonable request.

Consent for publication

Not applicable.

ORCID iDs

Adomas Janulionis  <https://orcid.org/0009-0000-1912-1062>
 Viktorija Sutova  <https://orcid.org/0009-0007-8496-4323>
 Ernestas Virsilas  <https://orcid.org/0000-0001-6135-0993>
 Arunas Valiulis  <https://orcid.org/0000-0002-0287-9915>

References

1. Tefera M, Assefa N, Mengistie B, Abrham A, Teji K, Worku T. Elective cesarean section on term pregnancies has a high risk for neonatal respiratory morbidity in developed countries: A systematic review and meta-analysis. *Front Pediatr*. 2020;8:286. doi:10.3389/fped.2020.00286
2. Engle WA. A recommendation for the definition of "late preterm" (near-term) and the birth weight-gestational age classification system. *Semin Perinatol*. 2006;30(1):2–7. doi:10.1053/j.semperi.2006.01.007
3. Masner A, Blasina F, Simini F. Electrical impedance tomography for neonatal ventilation assessment: A narrative review. *J Phys Conf Ser*. 2019;1272(1):012008. doi:10.1088/1742-6596/1272/1/012008

4. Lobo B, Hermosa C, Abella A, Gordo F. Electrical impedance tomography. *Ann Transl Med*. 2018;6(2):26–26. doi:10.21037/atm.2017.12.06
5. Viršilas E, Liubšys A, Janulionis A, Valiulis A. Electrical impedance tomography in pulmonary edema and hemorrhage. *Pediatr Neonatol*. 2022;63(4):424–425. doi:10.1016/j.pedneo.2021.12.003
6. Viršilas E, Liubšys A, Janulionis A, Valiulis A. Noninvasive respiratory support effects on sighs in preterm infants by electrical impedance tomography. *Indian J Pediatr*. 2023;90(7):665–670. doi:10.1007/s12098-022-04413-8
7. Šutova V, Janulionis A, Drejerienė V, et al. Application of electrical impedance tomography in the assessment of pulmonary ventilation in spontaneously breathing preterm and term neonates [in Lithuanian]. *Health Sci East Eur*. 2020;30(3):44–48. doi:10.35988/sm-hs.2020.067
8. Viršilas E, Janulionis A, Liubšys A, Valiulis A. Functional lung imaging using electrical impedance tomography: Clinical applications [in Lithuanian]. *Health Sci East Eur*. 2020;30(1):44–48. doi:10.35988/sm-hs.2020.032
9. Frerichs I, Schiffmann H, Oehler R, et al. Distribution of lung ventilation in spontaneously breathing neonates lying in different body positions. *Intensive Care Med*. 2003;29(5):787–794. doi:10.1007/s00134-003-1726-y
10. Schibler A, Yuill M, Parsley C, Pham T, Gilshenan K, Dakin C. Regional ventilation distribution in non-sedated spontaneously breathing newborns and adults is not different. *Pediatr Pulmonol*. 2009;44(9):851–858. doi:10.1002/ppul.21000
11. Schinckel NF, Hickey L, Perkins EJ, et al. Skin-to-skin care alters regional ventilation in stable neonates. *Arch Dis Child Fetal Neonatal Ed*. 2021;106(1):76–80. doi:10.1136/archdischild-2020-319136
12. Blank DA, Kamlin COF, Rogerson SR, et al. Lung ultrasound immediately after birth to describe normal neonatal transition: An observational study. *Arch Dis Child Fetal Neonatal Ed*. 2018;103(2):F157–F162. doi:10.1136/archdischild-2017-312818
13. Hunter T, Shah J, Synnes A, et al. Neonatal outcomes of preterm twins according to mode of birth and presentation. *J Matern Fetal Neonatal Med*. 2018;31(5):682–688. doi:10.1080/14767058.2017.1295441
14. Anadkat JS, Kuzniewicz MW, Chaudhari BP, Cole FS, Hamvas A. Increased risk for respiratory distress among white, male, late preterm and term infants. *J Perinatol*. 2012;32(10):780–785. doi:10.1038/jp.2011.191
15. Blue N, Van Winden K, Pathak B, et al. Neonatal outcomes by mode of delivery in preterm birth. *Am J Perinatol*. 2015;32(14):1292–1297. doi:10.1055/s-0035-1562931
16. Tribe RM, Taylor PD, Kelly NM, Rees D, Sandall J, Kennedy HP. Parturition and the perinatal period: Can mode of delivery impact on the future health of the neonate? *J Physiol*. 2018;596(23):5709–5722. doi:10.1113/JP275429
17. Karlström A, Lindgren H, Hildingsson I. Maternal and infant outcome after caesarean section without recorded medical indication: Findings from a Swedish case–control study. *BJOG*. 2013;120(4):479–486. doi:10.1111/1471-0528.12129
18. Hansen AK, Wisborg K, Uldbjerg N, Henriksen TB. Elective caesarean section and respiratory morbidity in the term and near-term neonate. *Acta Obstet Gynecol Scand*. 2007;86(4):389–394. doi:10.1080/00016340601159256
19. Ramachandrapa A, Jain L. Elective cesarean section: Its impact on neonatal respiratory outcome. *Clin Perinatol*. 2008;35(2):373–393. doi:10.1016/j.clp.2008.03.006
20. Hooper SB, Kitchen MJ, Siew ML, et al. Imaging lung aeration and lung liquid clearance at birth using phase contrast X-ray imaging. *Clin Exp Pharmacol Physiol*. 2009;36(1):117–125. doi:10.1111/j.1440-1681.2008.05109.x
21. Bulut O, Buyukkayhan D. Early term delivery is associated with increased neonatal respiratory morbidity. *Pediatr Int*. 2021;63(1):60–64. doi:10.1111/ped.14437
22. Ahimbisibwe A, Coughlin K, Eastabrook G. Respiratory morbidity in late preterm and term babies born by elective cesarean section. *J Obstet Gynaecol Can*. 2019;41(8):1144–1149. doi:10.1016/j.jogc.2018.11.002
23. Edwards MO, Kotecha SJ, Kotecha S. Respiratory distress of the term newborn infant. *Pediatr Respir Rev*. 2013;14(1):29–37. doi:10.1016/j.prrv.2012.02.002
24. Condò V, Cipriani S, Colnaghi M, et al. Neonatal respiratory distress syndrome: Are risk factors the same in preterm and term infants? *J Matern Fetal Neonatal Med*. 2017;30(11):1267–1272. doi:10.1080/14767058.2016.1210597
25. Gondwe T, Betha K, Kusneniwar GN, et al. Mode of delivery and short-term infant health outcomes: A prospective cohort study in a peri-urban Indian population. *BMC Pediatr*. 2018;18(1):346. doi:10.1186/s12887-018-1324-3
26. Bhargava R, Mathur M, Patodia J. Oxygen saturation trends in normal healthy term newborns: Normal vaginal delivery vs. elective cesarean section. *J Perinat Med*. 2018;46(2):191–195. doi:10.1515/jpm-2016-0373
27. Blank DA, Gaertner VD, Kamlin COF, et al. Respiratory changes in term infants immediately after birth. *Resuscitation*. 2018;130:105–110. doi:10.1016/j.resuscitation.2018.07.008
28. Lee S, Hassan A, Ingram D, Milner AD. Effects of different modes of delivery on lung volumes of newborn infants. *Pediatr Pulmonol*. 1999;27(5):318–321. doi:10.1002/(SICI)1099-0496(199905)27:5<318::AID-PPUL4>3.0.CO;2-E
29. Finn D, De Meulemeester J, Dann L, et al. Respiratory adaptation in term infants following elective caesarean section. *Arch Dis Child Fetal Neonatal Ed*. 2018;103(5):F417–F421. doi:10.1136/archdischild-2017-312908
30. Blank DA, Rogerson SR, Kamlin COF, et al. Lung ultrasound during the initiation of breathing in healthy term and late preterm infants immediately after birth: A prospective, observational study. *Resuscitation*. 2017;114:59–65. doi:10.1016/j.resuscitation.2017.02.017
31. Martelius L, Janér C, Süvari L, et al. Delayed lung liquid absorption after cesarean section at term. *Neonatology*. 2013;104(2):133–136. doi:10.1159/000351290
32. Martelius L, Süvari L, Janér C, et al. Lung ultrasound and static lung compliance during postnatal adaptation in healthy term infants. *Neonatology*. 2015;108(4):287–292. doi:10.1159/000438453

Surgical approach to pulmonary metastases and its impact on prognosis

Turkan Dubus^{1,A–F}, Gokce Cangel^{2,B,C}, Fatih Kesmezacar^{3,C}, Aziz Ari^{4,B}

¹ Basaksehir Cam and Sakura City Hospital, Department of Thoracic Surgery, University of Health Sciences, Istanbul, Turkey

² Department of Thoracic Surgery, Haseki Training and Research Hospital, University of Health Sciences, Istanbul, Turkey

³ Vocational School of Health Services, Istanbul University-Cerrahpasa, Imaging Program, Turkey

⁴ Department of General Surgery, Istanbul Training and Research Hospital, University of Health Sciences, Istanbul, Turkey

A – research concept and design; B – collection and/or assembly of data; C – data analysis and interpretation;

D – writing the article; E – critical revision of the article; F – final approval of the article

Advances in Clinical and Experimental Medicine, ISSN 1899–5276 (print), ISSN 2451–2680 (online)

Adv Clin Exp Med. 2025;34(7):1113–1121

Address for correspondence

Turkan Dubus

E-mail: drturkandbs@yahoo.com

Funding sources

None declared

Conflict of interest

None declared

Received on September 21, 2023

Reviewed on November 13, 2023

Accepted on July 24, 2024

Published online on December 6, 2024

Abstract

Background. Pulmonary metastasectomy (PM) is an important procedure for the treatment of metastatic nodules in the lung. The choice of surgical approach, whether thoracotomy or video-assisted thoracoscopic surgery (VATS), remains controversial in terms of the impact on patient prognosis.

Objectives. This study aimed to evaluate the outcomes and impact on survival of patients undergoing PM with VATS compared to thoracotomy.

Materials and methods. A retrospective evaluation of 136 patients who underwent PM between September 2012 and July 2020 was performed. Data on the demographics, primary tumor histopathology, metastatic features, surgical approach, surgical outcomes, and survival status were analyzed. Statistical analyses included descriptive statistics, survival analysis and Cox regression models.

Results. Of the participants, 84 underwent thoracotomy and 52 underwent VATS. The median survival time of thoracotomized patients was 86.6 months, while it was 99.6 months for VATS patients. A gender-specific analysis revealed a significantly longer survival time for female VATS patients compared to thoracotomy. Multivariate analysis showed significant independent effects of specific tumor types and the number of nodes removed on survival. Overall, no significant difference in survival was found between the 2 surgical methods.

Conclusions. Both VATS and thoracotomy are effective and safe options for PM. Video-assisted thoracoscopic surgery may offer advantages, particularly in certain patient groups and tumor types, potentially prolonging survival. Gender-specific analyses suggest a survival benefit of VATS, particularly in women. Further studies are needed to validate these results and optimize surgical decision-making in PM.

Key words: survival, pulmonary metastases, surgical approach, metastasectomy

Cite as

Dubus T, Cangel G, Kesmezacar F, Ari A. Surgical approach to pulmonary metastases and its impact on prognosis.

Adv Clin Exp Med. 2025;34(7):1113–1121.

doi:10.17219/acem/191597

DOI

10.17219/acem/191597

Copyright

Copyright by Author(s)

This is an article distributed under the terms of the Creative Commons Attribution 3.0 Unported (CC BY 3.0) (<https://creativecommons.org/licenses/by/3.0/>)

Background

Pulmonary metastasectomy (PM) is a procedure to surgically remove metastatic nodules in the lungs. Before this procedure can be performed, several important criteria must be met. A candidate for PM must first have the primary tumor under control. This may mean surgical removal of the primary tumor or its control through other treatments. A patient who is eligible for PM should have no extrathoracic metastases. This means that the metastases should be confined to the lungs. The patient must be a suitable candidate for surgery. For this purpose, the general state of health, lung function and ability to tolerate surgery are assessed. The decision is made after weighing the surgical risks and benefits.^{1,2}

There are several surgical approaches for metastasectomy in PM: Video-assisted thoracoscopic surgery (VATS) is a minimally invasive approach that reduces surgical trauma and postoperative pain while preserving lung function. This results in advantages such as a shorter hospital stay, fewer complications and a reduced need for intensive care. Thoracotomy involves making a larger incision in the chest to allow manual examination and exploration of the lung tissue.³

The surgical approach used depends on the patient's specific disease, the size and location of the metastases, the patient's overall health, and the experience of the surgical team. Each approach has its advantages and disadvantages and should be chosen based on the patient's individual needs.⁴

Objectives

In the present study, the treatment outcomes and effects on survival of patients undergoing PM with VATS and thoracotomy were evaluated.

Materials and methods

A total of 136 patients who underwent PM between September 2012 and July 2020 were retrospectively evaluated at the Department of Thoracic Surgery, Istanbul Training and Research Hospital, University of Health Sciences (Istanbul, Turkey). A total of 84 patients underwent thoracotomy and 52 patients underwent VATS.

All patients were evaluated according to age, sex, histopathology of the primary tumor, location and number of radiologically and surgically detected metastatic nodules, type of surgery, type of resection, number of operations, disease-free survival, surgical morbidity and mortality, survival status, and time after the first metastasectomy. Patients for whom follow-up was no longer possible were contacted by telephone. The death data of patients who died were recorded.

In all patients, the primary tumor was surgically controlled, and it was confirmed that there were no metastases

in organs other than the lungs. Preoperative investigations included a physical examination, a chest X-ray and an electrocardiogram (ECG). Respiratory function tests were performed to determine whether patients had sufficient lung capacity for possible anatomical resections. Most patients also underwent positron emission tomography (PET-CT) and magnetic resonance imaging (MRI) of the brain.

Video-assisted thoracoscopic surgery, or thoracotomy, was used as the surgical approach in the patients. Surgical reports were evaluated according to the resection procedure used, and pathology reports were assessed for tumor histology, resection status (R0, R1, R2, and RX) and distance between the staple line and the tumor in patients undergoing VATS.

This study was conducted in accordance with the Declaration of Helsinki. It was reviewed and approved by the Ethics Committee of the Istanbul Training and Research Hospital (approval No. 2020/1488).

Surgical approach

In the thoracotomy group, patients generally underwent a lateral thoracotomy through the 5th intercostal space. For pulmonary nodules <3 cm in diameter and in peripheral locations, wedge resection was preferred to preserve lung tissue, especially in those with respiratory distress or comorbidities, as well as in the elderly. Lobectomy was reserved for nodules >3 cm, for nodes in the hilar region that were unsuitable for wedge resection, or for multiple nodules >3 cm in 1 lobe. Additional nodules that were not detected using CT were palpated manually after resection. Lymph node dissection was performed for nodules with suspected lymph node metastases (cN1/2), especially those of gastrointestinal origin.

In VATS metastectomy, which was usually performed with 2–3 ports using a uniportal or biportal-triportal wedge resection, systematic manual palpation of the lung was not possible.

Statistical analyses

The collected data were summarized using descriptive statistics. To this end, continuous variables were tabulated using means \pm standard deviations (\pm SD) or medians with minimum and maximum values depending on their normal distribution characteristics, whereas categorical variables were expressed as counts and percentages. The normality of numerical variables was assessed using the Shapiro–Wilk, Kolmogorov–Smirnov and Anderson–Darling tests.

In comparing the differences in categorical variables between the groups, Pearson's χ^2 test was used for 2×2 tables with expected cells of 5 or more, Fisher's exact test for 2×2 tables with expected cells of less than 5, and a Fisher–Freeman–Halton test for R×C tables. Additionally, in comparing the differences in numerical variables

regarding surgical and survival outcomes between 2 independent groups, the independent sample t-tests were used for numerical variables determined to conform to normal distribution, and the Mann–Whitney U test was used for numerical variables determined not to conform to normal distribution. After the assumption of homogeneity of variances was confirmed in all t-test analyses, the results were reported.

Given the number of comparisons across various subgroups, we used the Benjamini–Hochberg correction procedure to control the false discovery rate. We analyzed the survival times and influencing factors with Cox proportional hazards regression models using the R-project 4.3.3 (R Foundation for Statistical Computing, Vienna, Austria; <https://www.R-project.org>) software package and its associated packages, namely “survival,” “survminer,” “haven,” “gridExtra,” and “readxl.” The assumptions underlying the Cox regression models were evaluated using Schoenfeld’s global test featuring a variable-based and global examination of whether the proportionality of hazards assumption was violated, with all p-values found to exceed 0.05.

Based on these results, we proceeded to the model selection phase. To this end, we developed 5 distinct Cox proportional hazard models, using different sets of independent variables or data subgroups in each model. Notably, the 4th and 5th models were specifically tailored based on gender to thoroughly examine the effects of various malignancies on mortality risks within the sample. Gender-specific differences were observed among the malignancies studied. Accordingly, while some cancers, i.e., breast and endometrial cancers, were exclusive to women, others, i.e., testicular cancer, were exclusive to men. To more accurately assess the impact of these gender-specific malignancies, we stratified the sample by gender and constructed separate Cox regression models for each group.

We assessed the appropriateness and complexity of the models using Akaike’s Information Criterion (AIC) and Bayesian Information Criterion (BIC). Additionally, we tested the validity of the proportionality of the hazards assumption for each model using the “cox.zph” function and Schoenfeld residuals, which allowed us to determine the most viable models. We evaluated the impact of surgical methods on survival by gender using the Breslow (generalized Wilcoxon) and Tarone–Ware tests. The log-rank test, which assumes that hazard ratios (HRs) between compared groups remained constant over time, was deemed inappropriate if survival curves crossed, indicating that HRs changed over time and were disproportionate.

In contrast, the Breslow test, which gives more weight to early events, provided more consistent results with crossing curves, better detecting the differences observed in the early period. On the other hand, the Tarone–Ware test, which provides a balanced weighting of early and late events, evaluates HRs over a broader time spectrum and thus offers a more flexible alternative for general use. Because of the foregoing, we used both tests.⁵

We conducted the statistical analyses using the Jamovi project 2.3.28 (Jamovi, v. 2.3.28.0, <https://www.jamovi.org>) and JASP 0.17.3 (Jeffreys’ Amazing Statistics Program, v. 0.17.3, <https://jasp-stats.org>) software packages, setting the significance level (p-value) at 0.05.

Results

Of the patients, 80 were male (58.8%) and 56 female (41.2%). The mean age was 57.42 ± 12.93 years (min: 25, max: 76). The origin of the primary tumor was as follows: 36 patients (26.5%) had colorectal carcinoma, 17 (12.5%) had renal cell carcinoma, 26 (19.1%) had breast carcinoma, 21 (15.4%) had osteosarcoma, 10 (7.4%) had soft tissue sarcomas, 12 (8.8%) had endometrial carcinoma, and 14 (10.3%) had testicular carcinoma.

The thoracotomy group exhibited significantly higher values than the VATS group in age, length of hospitalization, number of metastatic nodules removed during surgery, and mortality rate ($p < 0.05$ for each case). Regarding the types of malignancy, colorectal carcinoma and endometrial carcinoma were found to be significantly more prevalent in the thoracotomy group ($p = 0.035$ and $p = 0.029$, respectively), whereas osteosarcoma and testicular carcinoma were found to be significantly more prevalent in the VATS group ($p = 0.002$ and $p < 0.001$, respectively). There was no significant difference between the thoracotomy and VATS groups in gender, follow-up duration, number of metastatic nodules detected with thoracic CT, recurrence of metastasis, and the presence of renal cell carcinoma, breast carcinoma and soft tissue sarcoma ($p > 0.05$ for each case, Table 1).

Survivors had significantly longer follow-up periods ($p < 0.001$), a significantly lower age ($p = 0.034$) and pulmonary nodule size ($p = 0.019$), and shorter hospitalization ($p = 0.007$) compared to the deceased. Survival rates of patients with breast carcinoma were significantly higher than those with other types of malignancies ($p = 0.005$). Conversely, mortality rates of patients with endometrial and soft tissue sarcomas were significantly higher than those with other malignancies ($p = 0.004$ and $p = 0.001$, respectively). There was no significant difference between the survivors and the deceased regarding gender, number of metastatic nodules removed during surgery, number of metastatic nodules detected with thoracic CT, recurrence of metastasis during postoperative follow-up, and the presence of colorectal carcinoma, renal cell carcinoma, osteosarcoma, and testicular carcinoma ($p > 0.05$ for each case, Table 2).

The univariate analysis, including only female patients, revealed that breast carcinoma was associated with a 93% decrease in the mortality risk (95% confidence interval (95% CI): 0.01–0.57, $p = 0.012$), whereas soft tissue sarcomas had a 68.28-fold increase (95% CI: 6.01–775.58, $p = 0.001$) and each 1-year increase in age had a 10%

Table 1. Comparative analysis of surgical methods (thoracotomy compared to video-assisted thoracoscopic surgery (VATS)) and demographic and clinical outcomes

Variables		Surgical methods		p-values
		Thoracotomy (n = 84)	VATS (n = 52)	
Gender †	female	38 (45.2)	18 (34.6)	0.297***
	male	46 (54.8)	34 (65.4)	–
Age [years]		62.9 ± 10.5	48.6 ± 11.7	<0.001*
Survival status‡	alive	55 (65.5) ^a	43 (82.7) ^b	0.048***
	exitus	29 (34.5) ^a	9 (17.3) ^b	–
Follow-up period [months]		63.2 ± 26.6	65.1 ± 23.5	0.661*
Pulmonary nodule size [cm]		3.0 [0.7–5.0]	2.0 [0.8–3.0]	<0.001**
Number of metastatic nodules removed at surgery		2.0 [1.0–9.0]	2.0 [1.0–4.0]	0.025**
Length of hospitalization [days]		4.0 [2.0–12.0]	2.0 [1.0–6.0]	<0.001**
Number of metastatic nodules detected with thorax CT		2.0 [1.0–6.0]	2.0 [1.0–4.0]	0.143**
Recurrent metastasis at postoperative follow-up, yes†		16 (19.0)	9 (17.3)	0.979***
Primary focus ‡	colorectal carcinoma, present	28 (33.3) ^a	8 (15.4) ^b	0.035***
	renal cell carcinoma, present	12 (14.3)	5 (9.6)	0.594***
	breast carcinoma, present	16 (19.0)	10 (19.2)	0.999***
	osteosarcoma, present	6 (7.1) ^a	15 (28.8) ^b	0.002***
	soft tissue sarcoma, present	9 (10.7)	1 (1.9)	0.088***
	endometrium carcinoma, present	11 (13.1) ^a	1 (1.9) ^b	0.029***
	testicular carcinoma, present	2 (2.4) ^a	12 (23.1) ^b	<0.001***

CT – computed tomography. † mean ± standard deviation (±SD) for continuous variables; ‡ count and percentage (n (%)) for categorical variables; [§] median and range [min–max] for non-normally distributed variables. Statistical significance is tested using: *independent samples t-test for comparing means between 2 independent groups when data distribution is assumed to be normal; **Mann–Whitney U test for comparing median values between 2 samples without the assumption of normal distribution; ***Pearson's χ^2 , Fisher's exact or Fisher–Freeman–Halton tests for assessing differences in categorical variables between groups.

Table 2. Survival status outcomes by demographic and clinical variables with statistical significance

Variables		Survival status		p-values
		Alive (n = 98)	Exitus (n = 38)	
Gender †	female	43 (43.9)	13 (34.2)	0.404**
	male	55 (56.1)	25 (65.8)	
Age [years]		58.5 [25.0–75.0]	66.0 [29.0–76.0]	0.034*
Follow-up period [month]		74.5 [35.0–116.0]	37.5 [16.0–105.0]	<0.001*
Pulmonary nodule size [cm]		3.0 [0.7–5.0]	3.0 [1.5–5.0]	0.019*
Number of metastatic nodules removed at surgery		2.0 [1.0–7.0]	3.0 [1.0–9.0]	0.301*
Length of hospitalization [days]		3.0 [1.0–12.0]	4.0 [2.0–9.0]	0.007*
Number of metastatic nodules detected with thorax CT		2.0 [1.0–6.0]	2.0 [1.0–6.0]	0.347*
Recurrent metastasis at postoperative follow-up, yes†		15 (15.3)	10 (26.3)	0.215**
Primary focus ‡	colorectal carcinoma, present	26 (26.5)	10 (26.3)	0.999**
	renal cell carcinoma, present	15 (15.3)	2 (5.3)	0.152**
	breast carcinoma, present	25 (25.5) ^a	1 (2.6) ^b	0.005**
	osteosarcoma, present	13 (13.3)	8 (21.1)	0.388**
	soft tissue sarcoma, present	2 (2.0) ^a	8 (21.1) ^b	0.001**
	endometrium carcinoma, present	4 (4.1) ^a	8 (21.1) ^b	0.004**
testicular carcinoma, present		13 (13.3)	1 (2.6)	0.112**

CT – computed tomography. The † symbol indicates the number and percentage of subjects (n (%)) for categorical data; [§] median values with the range [min–max]. Statistical significances are denoted by p-values with symbols indicating the test used: *Mann–Whitney U test for non-normally distributed data to compare medians between 2 independent samples; **Pearson's χ^2 , Fisher's exact or Fisher–Freeman–Halton tests to determine the significance of differences in categorical data.

Table 3. Impact of surgical methods and clinical factors on survival rates by gender analyzed using Cox proportional hazards models

Clinical factors	Model 1 (only female patients)		Model 2 (only male patients)	
	HR (univariable)	HR (multivariable)	HR (univariable)	HR (multivariable)
Surgical method, VATS vs thoracotomy	0.15 (0.02–1.16 p = 0.070)	1.33 (0.24–7.25 p = 0.742)	0.67 (0.28–1.62 p = 0.376)	7.49 (1.08–51.98 p = 0.042)
Post-surgical follow-up recurrent metastasis, present vs absent	0.75 (0.17–3.41 p = 0.714)	2.80 (0.42–18.48 p = 0.285)	2.95 (1.26–6.92 p = 0.013)	3.33 (1.25–8.89 p = 0.016)
Colorectal carcinoma, present vs absent	–	–	0.85 (0.37–1.92 p = 0.688)	3.00 (0.20–44.70 p = 0.425)
Renal cell carcinoma, present vs absent	0.51 (0.07–3.90 p = 0.513)	0.25 (0.03–1.84 p = 0.175)	0.19 (0.02–1.39 p = 0.101)	0.27 (0.01–6.08 p = 0.411)
Breast carcinoma, present vs absent	0.07 (0.01–0.57 p = 0.012)	0.09 (0.01–0.66 p = 0.018)	–	–
Osteosarcoma, present vs absent	1.20 (0.15–9.37 p = 0.862)	9.12 (1.31–63.50 p = 0.026)	3.11 (1.12–8.63 p = 0.029)	29.24 (2.38–358.96 p = 0.008)
Soft tissue sarcoma, present vs absent	68.28 (6.01–775.58 p = 0.001)	520.48 (41.06–6597.76 p < 0.001)	8.04 (2.98–21.68 p < 0.001)	88.53 (4.88–1606.17 p = 0.002)
Age	1.10 (1.02–1.19 p = 0.017)	1.17 (1.09–1.26 p < 0.001)	1.01 (0.97–1.04 p = 0.677)	1.04 (0.99–1.09 p = 0.121)
Pulmonary nodule size [cm]	1.62 (0.93–2.83 p = 0.090)	1.28 (0.69–2.39 p = 0.433)	1.44 (0.97–2.14 p = 0.073)	2.47 (1.24–4.89 p = 0.010)
Number of metastatic nodules removed during surgery	1.07 (0.78–1.47 p = 0.690)	1.21 (0.90–1.64 p = 0.209)	1.32 (1.10–1.59 p = 0.003)	1.40 (1.08–1.82 p = 0.010)

Hazard ratios (HR) for various factors by gender, calculated using univariable and multivariable Cox proportional hazards models. Hazard ratios are provided with 95% confidence intervals (95% CIs) and associated p-values, indicating the statistical significance of the observed differences. The HRs compare the impact of surgical methods, presence of specific cancer types and other clinical factors on survival rates. A p-value less than 0.05 is considered statistically significant, highlighting potentially meaningful differences between groups based on the studied variables.

increase in mortality risks (95% CI: 1.02–1.19, $p = 0.017$). There was no significant correlation between mortality risk and the surgical method, presence of metastasis, renal cell carcinoma or osteosarcoma, pulmonary nodule size, and number of metastatic nodules removed during surgery ($p > 0.05$ for each case).

Multivariate analysis revealed that breast carcinoma was associated with a 91% decrease in the mortality risk (95% CI: 0.01–0.66, $p = 0.018$), whereas osteosarcoma with a 9.12-fold increase (95% CI: 1.31–63.50, $p = 0.026$), soft tissue sarcomas had a 520.48-fold increase (95% CI: 41.06–6597.76, $p < 0.001$), and each 1-year increase in age was related to a 17% increase in the mortality risk (95% CI: 1.09–1.26, $p < 0.001$). There was no significant correlation between the mortality risk and surgical method, presence of metastasis or renal cell carcinoma, pulmonary nodule size, or number of metastatic nodules removed ($p > 0.05$ for each case).

The univariate analysis, including only male patients, revealed that recurrent metastases during the post-surgical period were associated with a 2.95-fold increase in mortality risk (95% CI: 1.26–6.92, $p = 0.013$), osteosarcoma had a 3.11-fold increase (95% CI: 1.12–8.63, $p = 0.029$) and soft tissue sarcomas had a 8.04-fold increase (95% CI: 2.98–21.68, $p < 0.001$). Each additional metastatic nodule removed during surgery was associated with a 32% increase in the mortality risk (95% CI: 1.10–1.59, $p = 0.003$). There was no significant correlation between the mortality risk and surgical approach, presence of colorectal cancer or

renal cell carcinoma, age, and number of pulmonary nodules ($p > 0.05$ for each case).

Multivariate analysis revealed that undergoing VATS was associated with a 7.49-fold increase in the mortality risk (95% CI: 1.08–51.98, $p = 0.042$), osteosarcoma had a 29.24-fold increase (95% CI: 2.38–358.96, $p = 0.008$) and soft tissue sarcomas had a 88.53-fold increase (95% CI: 4.88–1606.17, $p = 0.002$). Each unit increase in pulmonary nodule size was associated with a 2.47-fold increase in the mortality risk (95% CI: 1.24–4.89, $p = 0.010$) and each additional metastatic nodule removed with a 1.40-fold increase (95% CI: 1.08–1.82, $p = 0.010$). There was no significant correlation between mortality risk and colorectal cancer, renal cell carcinoma and age ($p > 0.05$ for each case, Table 3).

The mean survival time of female patients was 96.45 months, and the survival time of female patients who underwent VATS was significantly longer than those who underwent thoracotomy ($p = 0.047$). The mean survival time of male patients was 87.5 months. There was no significant difference between the male patients who underwent VATS and those who underwent thoracotomy in survival time ($p = 0.297$). The survival analysis of the overall sample revealed a mean survival time of 91.80 months, 86.60 months for those who underwent thoracotomy, and 99.57 months for those who underwent VATS. There was a significant difference between the survival time of patients who underwent VATS and those who underwent thoracotomy ($p = 0.043$, Table 4, Fig. 1).

Table 4. Gender and surgical method impact on survival rates with 95% CIs and test results

Gender	Surgical methods	Estimate	SE	95% CI	p-values	
					Breslow (generalized Wilcoxon)	Tarone–Ware
Female	thoracotomy	88.55	6.32	76.17–100.94	0.047	0.041
	VATS	111.89	3.99	104.06–119.72		
	overall	96.45	4.77	87.10–105.79		
Male	thoracotomy	84.52	5.80	73.15–95.89	0.297	0.299
	VATS	88.66	5.83	77.23–100.08		
	overall	87.50	4.41	78.85–96.15		
All sample	thoracotomy	86.60	–	78.25–94.95	0.043	0.041
	VATS	99.57	–	90.17–109.00		
	overall	91.80	–	85.34–98.26		

VATS – video-assisted thoracoscopic surgery. The impact of gender and surgical methods on survival rates, employing statistical tests such as Breslow (generalized Wilcoxon) and Tarone–Ware to analyze the differences based on surgical methods. The estimates provided are complemented by standard errors (SEs) and 95% confidence intervals (95% CIs). The p-values indicate the significance of the results: lower values suggest stronger statistical evidence against the null hypothesis that there is no difference based on surgical methods.

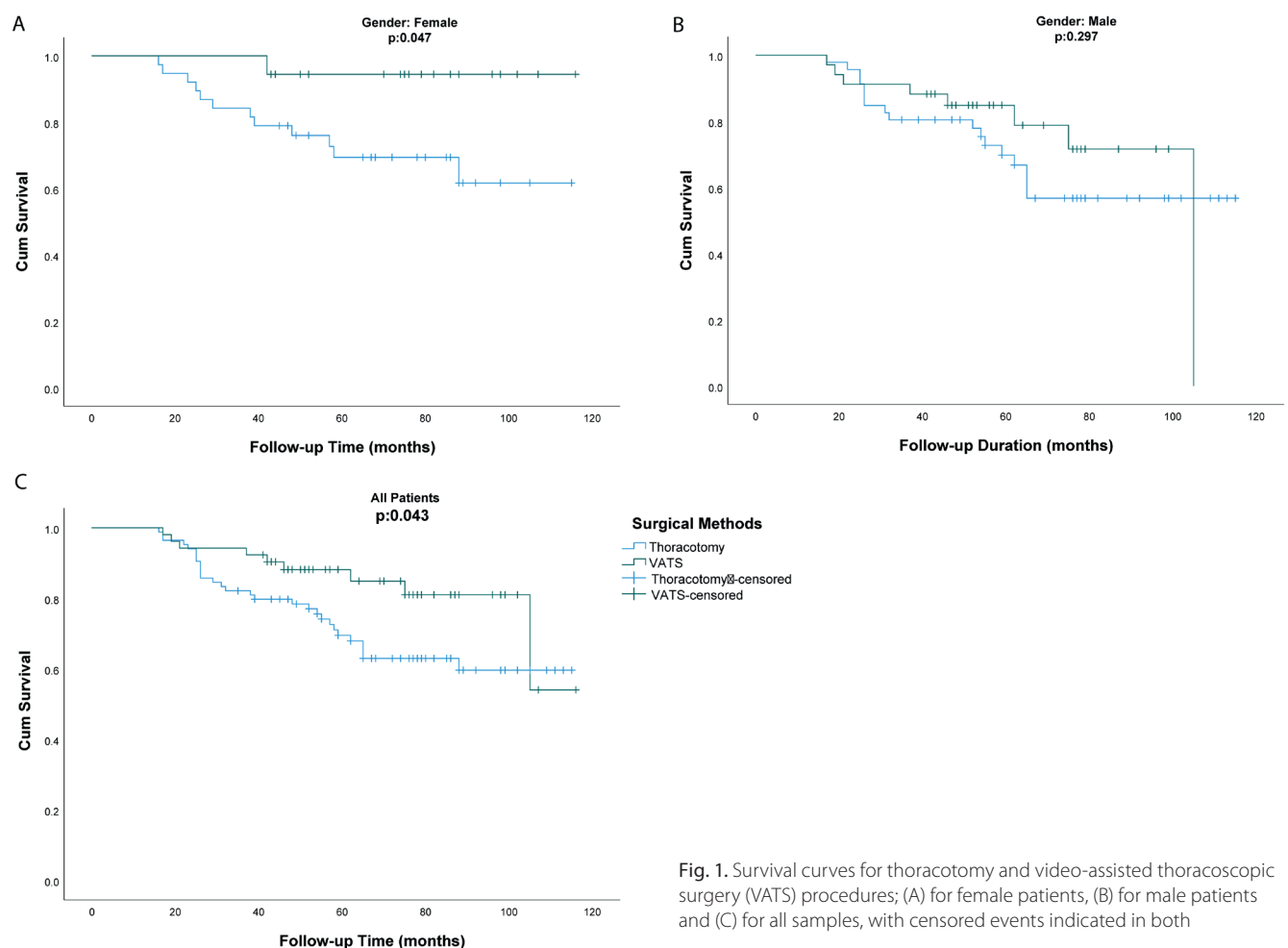


Fig. 1. Survival curves for thoracotomy and video-assisted thoracoscopic surgery (VATS) procedures; (A) for female patients, (B) for male patients and (C) for all samples, with censored events indicated in both

Discussion

Around 30% of cancer patients develop lung metastases. The primary tumors that are most likely to spread to the lungs include colorectal carcinomas, bone and soft tissue sarcomas, malignant melanomas, head and neck

tumors, germ cell tumors, breast cancer, and renal cell carcinomas.^{4,6}

Patient selection, imaging, characteristics of the nodule, and surgeon experience are critical to PM. Thoracotomy offers a comprehensive view, while VATS is less invasive and better suited for remetastectomy.^{7–9}

With VATS, some lesions can only be detected to a limited extent, while CT can reveal small nodules and those that were not palpated during surgery. However, thoracotomy is more effective for certain procedures.^{10–12} In our study, some patients underwent multiportal (2 or 3) VATS surgery with incisions for manual palpation of nodules. However, more additional PMs were performed by thoracotomy than by VATS, suggesting that thoracotomy is still more effective for PMs.

Morbidity depends on the patient's condition, the surgical method and the extent of the resection. Postoperative complications such as atelectasis, pneumonia, cardiac arrhythmias, and bronchopleural fistulas occur in 10–15% of patients after PM.^{13,14} In our study, postoperative morbidity was observed in 11.7% of patients, with the most common complications being dyspnea, pneumonia, cardiac arrhythmias, and persistent air leaks.

In the literature, recurrence is reported in more than 50% of patients after PM. Recurrence after PM can occur particularly in primary sarcomas and melanomas.¹⁵ In our study, however, recurrence was observed in only 18.4% of patients (carcinomas: 15, sarcomas: 10). These results indicate that the recurrence rate in our study was lower compared to the overall recurrence rates reported in the literature.

Markowiak et al.¹⁶ recommend VATS for metastasectomy, especially in patients with a single metastasis. They achieved an R0 resection rate of 90.5 with VATS, similar to thoracotomy, and found no advantage in terms of survival or surgical outcomes over open surgery. In our study, similar results were obtained, with only 3 patients undergoing an R1 resection, while the remaining patients underwent an R0 resection. These results show that VATS is an effective option for metastasectomy and provides similar results compared to open surgical procedures.

Nakajima et al.¹⁷ and Nakas et al.¹⁸ reported no significant differences in survival between VATS and thoracotomy patients. However, Gossot et al.¹⁹ found that VATS resulted in better overall survival rates at 1, 3 and 5 years postoperatively compared with thoracotomy (VATS: 87.4%, 70.9%, and 52.5%, respectively; thoracotomy: 82.3%, 63.6% and 34%, respectively). Similarly, Nakajima et al.²⁰ and Carballo et al.²¹ found that the 5-year survival was better in VATS patients compared with thoracotomy patients (Nakajima et al.: 49.3% vs 39.5%; Carballo et al.: 69.6% vs 58.8%). Chao et al.²² also reported that VATS had no additional negative impact on patient survival compared with thoracotomy (5-year survival of 51% vs 43%).

In our study, the median survival was 86.6 months for thoracotomy patients and 99.6 months for VATS patients. Female patients who underwent VATS had a significantly longer survival compared to those who underwent thoracotomy, suggesting that VATS provides a better survival benefit in PM, especially for women. Further studies are needed to confirm these results, particularly concerning gender differences.

Rusidanmu et al.²³ found that VATS in PM has similar survival rates to thoracotomy but offers better perioperative outcomes, suggesting that VATS is a viable surgical alternative. Survival studies comparing thoracotomy and VATS provide conflicting results, with some favoring thoracotomy and others showing no significant difference. Overall survival and disease-free survival appear to be comparable for the different types of primary tumors.²⁴

The complete removal of all lung metastases is associated with a longer survival. Over 62% of patients who undergo surgical resection survive for more than 5 years. The number of nodules removed during surgery influences the prognosis, with better results observed when only 1 nodule is removed.^{25,26}

In our study, we found that survival was longer in the VATS group than in the thoracotomy group. Video-assisted thoracoscopic surgery prolonged survival and reduced the risk of death, especially in female patients with breast cancer, but tumors such as soft tissue sarcomas and osteosarcomas were associated with a higher risk of death. This suggests that VATS has the potential to improve the efficacy of breast cancer treatment and the quality of life of patients.

We can say that more aggressive tumors, such as sarcomas, require more careful follow-up and treatment planning after surgical treatment. It is possible to increase the reliability and generalizability of the results by conducting such studies with larger sample groups and prospective designs.

In Fig. 1B, the sharp decline in the Kaplan–Meier survival curve for the male VATS group does not mean that all patients died. This decline is largely due to censored cases and the end of the observation period. Censored cases include patients who withdrew from the study or were still alive at the end of the observation period and were not counted as events (such as death) in the survival calculations.²⁷ In the group of male VATS patients, the rapid decline in the survival curve reflects the lack of follow-up data after the last recorded death, which marks the end of the observation period and the censoring of surviving patients. Our analysis shows that 8 male patients in the VATS group died, while 26 are still alive. Therefore, it would be wrong to conclude from the observed decline in the curve that all patients died; rather, it illustrates the impact of the censored cases and the end of the observation period.

The intersection of the survival curves observed in Fig. 1C indicates that the risk of events fluctuates over time. Consequently, at different time points, 1 group may exhibit higher risk, while at another point, the same group may show lower risk. This phenomenon has been described as a “delayed treatment effect”.²⁸

The early intersection of survival curves in thoracotomy and VATS patients indicates that the impact of these techniques on mortality in the initial postoperative period may be comparable. However, in the long term, VATS shows

a reduction in the risk of mortality. Literature indicates that VATS is associated with a lower mortality risk compared to thoracotomy in non-small cell lung cancers (NSCLC). Video-assisted thoracoscopic surgery, a minimally invasive procedure, is linked to reduced complications, faster recovery and lower surgical trauma in the early postoperative period, which aids in quicker immune system recovery and lower infection risk. Studies report lower rates of postoperative pneumonia and arrhythmia, shorter hospital stays and higher 5-year overall survival rates for VATS (e.g., 75.5% vs 56.1%). Lymph node dissection performed employing VATS may positively impact cancer recurrence rates.^{29–31}

However, the early intersection of survival curves may influence the power of statistical tests sensitive to early differences, such as the Gehan–Breslow–Wilcoxon method. This potential limitation in our analysis must be considered when interpreting our results.

Limitations

The limited sample size of our study, heterogeneous distribution of the patient's primary tumor, the presence of other treatment factors such as re-metastastomies, and biases in the choice of surgical method may influence the results.

Conclusions

It can be assumed that VATS is a more effective option for PM compared to thoracotomy and can prolong patient survival. Gender-specific analyses show that VATS significantly prolongs survival in women compared to thoracotomy. In contrast, these differences were not found to be significant in men. These results illustrate the influence of the surgical method and the type of disease on patient survival. Our results support the choice of VATS for PM and an improvement in patient survival.

Supplementary data

The Supplementary materials are available at <https://doi.org/10.5281/zenodo.12548526>. The package includes the following files:

Supplementary Table 1. Assessment of proportional hazards assumption using global Schoenfeld tests across different models.

Supplementary Table 2. Comparative analysis of surgical outcomes by type and associated variables in PM.

Supplementary Table 3. Comparative analysis of surgical outcomes by type and associated variables in PM.

Supplementary Table 4. Analysis of survival status relative to post-surgical recurrent metastasis and primary cancer focus.

Supplementary Table 5. Distribution of survival outcomes by cancer type and presence.

Supplementary Fig. 1. Graphical representation of Schoenfeld residuals for individual variables and global model assessment in Cox proportional hazards analysis – Model 1.

Supplementary Fig. 2. Graphical representation of Schoenfeld residuals for individual variables and global model assessment in Cox proportional hazards analysis – Model 2.

Supplementary Fig. 3. Graphical representation of Schoenfeld residuals for individual variables and global model assessment in Cox proportional hazards analysis – Model 3.

Supplementary Fig. 4. Graphical representation of Schoenfeld residuals for individual variables and global model assessment in Cox proportional hazards analysis – Model 4.

Supplementary Fig. 5. Graphical representation of Schoenfeld residuals for individual variables and global model assessment in Cox proportional hazards analysis – Model 5.

Data availability


The datasets generated and/or analyzed during the current study are available from the corresponding author on reasonable request.


Consent for publication

Not applicable.

ORCID iDs

Turkan Dubus  <https://orcid.org/0000-0002-7222-7998>

Gokce Cangel  <https://orcid.org/0000-0002-7635-760X>

Fatih Kesmezacar  <https://orcid.org/0000-0001-5110-1184>

Aziz Ari  <https://orcid.org/0000-0002-7806-2354>

References

- Cheung F, Alam N, Wright G. Pulmonary metastasectomy: Analysis of survival and prognostic factors in 243 patients. *ANZ J Surg.* 2018;88(12):1316–1321. doi:10.1111/ans.14811
- Treasure T, Farewell V, Macbeth F, et al; PulMiCC Trial Group. Pulmonary Metastasectomy versus Continued Active Monitoring in Colorectal Cancer (PulMiCC): A multicentre randomised clinical trial. *Trials.* 2019;20(1):718. doi:10.1186/s13063-019-3837-y
- Patrini D, Panagiotopoulos N, Lawrence D, Scarci M. Surgical management of lung metastases. *Br J Hosp Med.* 2017;78(4):192–198. doi:10.12968/hmed.2017.78.4.192
- Gonzalez M, Zellweger M, Nardini M, Migliore M. Precision surgery in lung metastasectomy. *Future Oncol.* 2020;16(Suppl 16):7–13. doi:10.2217/fon-2018-0713
- Hu S, Zhang W, Guo Q, et al. Prognosis and survival analysis of 922,317 lung cancer patients from the US-based on the most recent data from the SEER Database (April 15, 2021). *Int J Gen Med.* 2021;14:9567–9588. doi:10.2147/IJGM.S338250
- Cheung FPY, Alam NZ, Wright GM. The past, present and future of pulmonary metastasectomy: A review article. *Ann Thorac Cardiovasc Surg.* 2019;25(3):129–141. doi:10.5761/atcs.ra.18-00229
- Fiorentino F, Treasure T. Is survival really better after repeated lung metastasectomy? *Clin Exp Metastasis.* 2021;38(1):73–75. doi:10.1007/s10585-020-10061-z
- Downey RJ, Bains MS. Open surgical approaches for pulmonary metastasectomy. *Thorac Surg Clin.* 2016;26(1):13–18. doi:10.1016/j.thorsurg.2015.09.003
- Lautz TB, Farooqui Z, Jenkins T, et al. Thoracoscopy vs thoracotomy for the management of metastatic osteosarcoma: A Pediatric Surgical Oncology Research Collaborative Study. *Int J Cancer.* 2021;148(5):1164–1171. doi:10.1002/ijc.33264

10. Sudarshan M, Murthy SC. Current indications for pulmonary metastasectomy. *Surg Oncol Clin North Am*. 2020;29(4):673–683. doi:10.1016/j.soc.2020.06.007
11. Claramunt NP, Cypel M. Video-assisted thoracic surgery as the future of pulmonary metastasectomy. *Ann Thorac Surg*. 2020;110(3):1096–1097. doi:10.1016/j.athoracsur.2020.05.112
12. Mangiameli G, Cioffi U, Alloisio M, Testori A. Lung metastases: Current surgical indications and new perspectives. *Front Surg*. 2022;9:884915. doi:10.3389/fsurg.2022.884915
13. Baldes N, Eberlein M, Bölükbas S. Multimodal and palliative treatment of patients with pulmonary metastases. *J Thorac Dis*. 2021;13(4):2686–2691. doi:10.21037/jtd-2019-pm-09
14. Eisenberg M, Deboever N, Antonoff MB. Pulmonary metastasectomy. *Thorac Surg Clin*. 2023;33(2):149–158. doi:10.1016/j.thorsurg.2023.01.004
15. Sponholz S, Schirren J. Pulmonary metastasectomy: The discussion continues. *Eur J Cardiothorac Surg*. 2022;62(5):ezac315. doi:10.1093/ejcts/ezac315
16. Markowiak T, Dakkak B, Loch E, et al. Video-assisted pulmonary metastectomy is equivalent to thoracotomy regarding resection status and survival. *J Cardiothorac Surg*. 2021;16(1):84. doi:10.1186/s13019-021-01460-8
17. Nakajima J, Takamoto S, Tanaka M, Takeuchi E, Murakawa T, Fukami T. Thoracoscopic surgery and conventional open thoracotomy in metastatic lung cancer: A comparative clinical analysis of surgical outcomes. *Surg Endosc*. 2001;15(8):849–853. doi:10.1007/s004640090005
18. Nakas A, Klimatsidas MN, Entwisle J, Martin-Ucar AE, Waller DA. Video-assisted versus open pulmonary metastasectomy: The surgeon's finger or the radiologist's eye? *Eur J Cardiothorac Surg*. 2009;36(3):469–474. doi:10.1016/j.ejcts.2009.03.050
19. Gossot D, Radu C, Girard P, et al. Resection of pulmonary metastases from sarcoma: Can some patients benefit from a less invasive approach? *Ann Thorac Surg*. 2009;87(1):238–243. doi:10.1016/j.athoracsur.2008.09.036
20. Nakajima J, Murakawa T, Fukami T, Takamoto S. Is thoracoscopic surgery justified to treat pulmonary metastasis from colorectal cancer? *Interact Cardiovasc Thorac Surg*. 2007;7(2):212–217. doi:10.1510/icvts.2007.167239
21. Carballo M, Maish MS, Jaroszewski DE, Holmes CE. Video-assisted thoracic surgery (VATS) as a safe alternative for the resection of pulmonary metastases: A retrospective cohort study. *J Cardiothorac Surg*. 2009;4(1):13. doi:10.1186/1749-8090-4-13
22. Chao YK, Chang HC, Wu YC, et al. Management of lung metastases from colorectal cancer: Video-assisted thoracoscopic surgery versus thoracotomy. A case-matched study. *Thorac Cardiovasc Surg*. 2012;60(6):398–404. doi:10.1055/s-0031-1295574
23. Rusidanmu A, Chin W, Xu J, et al. Does a thoracoscopic approach provide better outcomes for pulmonary metastases? *J Thorac Dis*. 2021;13(4):2692–2697. doi:10.21037/jtd-19-3958
24. Guerrini GP, Lo Faso F, Vagliasindi A, et al. The role of minimally invasive surgery in the treatment of lung metastases. *J Invest Surg*. 2017;30(2):110–115. doi:10.1080/08941939.2016.1230246
25. Forster C, Ojanguren A, Perentes JY, et al. Is repeated pulmonary metastasectomy justified? *Clin Exp Metastasis*. 2020;37(6):675–682. doi:10.1007/s10585-020-10056-w
26. Religioni J, Orłowski T. Surgical treatment of metastatic diseases to the lung. *Pol J Cardiothorac Surg*. 2020;17(2):52–60. doi:10.5114/kitp.2020.97254
27. Kleinbaum DG, Klein M. *Survival Analysis: A Self-Learning Text*. New York, USA: Springer New York; 2012. doi:10.1007/978-1-4419-6646-9
28. Ananthakrishnan R, Green S, Previtali A, Liu R, Li D, LaValley M. Critical review of oncology clinical trial design under non-proportional hazards. *Crit Rev Oncol Hematol*. 2021;162:103350. doi:10.1016/j.critrevonc.2021.103350
29. Batihan G, Ceylan KC, Usluer O, Kaya ŞÖ. Video-assisted thoracoscopic surgery vs thoracotomy for non-small cell lung cancer greater than 5 cm: Is VATS a feasible approach for large tumors? *J Cardiothorac Surg*. 2020;15(1):261. doi:10.1186/s13019-020-01305-w
30. Higuchi M, Yaginuma H, Yonechi A, et al. Long-term outcomes after video-assisted thoracic surgery (VATS) lobectomy versus lobectomy via open thoracotomy for clinical stage IA non-small cell lung cancer. *J Cardiothorac Surg*. 2014;9(1):88. doi:10.1186/1749-8090-9-88
31. Niskakangas A, Mustonen O, Puro I, Karjula T, Helminen O, Yannopoulos F. Results of video-assisted thoracoscopic surgery versus thoracotomy for lung cancer in a mixed practice medium-volume hospital: A propensity-matched study. *Interdiscip Cardiovasc Thorac Surg*. 2023;37(6):ivad189. doi:10.1093/icvts/ivad189

Prognostic value of the systemic inflammation response index on 3-year outcomes of elderly patients with acute coronary syndrome after stent implantation

Yi Ma^{A–F}, Xuebin Geng^{A–E}

Department of Cardiovascular Medicine, Tangshan Gongren Hospital, China

A – research concept and design; B – collection and/or assembly of data; C – data analysis and interpretation;
D – writing the article; E – critical revision of the article; F – final approval of the article

Advances in Clinical and Experimental Medicine, ISSN 1899–5276 (print), ISSN 2451–2680 (online)

Adv Clin Exp Med. 2025;34(7):1123–1130

Address for correspondence

Yi Ma
E-mail: 13831524425@163.com

Funding sources

None declared

Conflict of interest

None declared

Yi Ma and Xuebin Geng contributed equally to the work.

Received on April 8, 2024

Reviewed on May 30, 2024

Accepted on July 2, 2024

Published online on December 6, 2024

Abstract

Background. Few studies have focused on the relationship between the systemic inflammation response index (SIRI) and the prognosis of elderly patients with acute coronary syndrome (ACS).

Objectives. This study aimed to evaluate the predictive value of the SIRI for predicting 3-year outcomes in patients >60 years old after stent implantation and to assess variables associated with SIRI.

Materials and methods. A total of 1,758 patients with ACS who underwent percutaneous coronary intervention (PCI) were enrolled and divided into an older group (n = 960) and a younger group (n = 798) using a cutoff of >60 years. Major adverse cardiac events (MACEs) including all-cause death, nonfatal acute myocardial infarction (AMI) and nonfatal stroke were recorded.

Results. During follow-up, 165 patients experienced 1 or more MACEs. Patients in the older group had a greater incidence of recurrent MACEs and mortality than those in the younger group. The SIRIs were significantly greater in the older group. Multiple linear regression analysis revealed that the level of the SIRI was significantly associated with age, hypertension, diagnosis of AMI, number of diseased vessels, and platelet count. The SIRI was an independent predictive risk factor for MACEs in patients >60 years old. Similar relationships between the SIRI and MACEs were also observed in ACS patients with and without AMI.

Conclusions. The SIRI was an independent predictive risk factor for MACEs in patients aged >60 years with ACS and ACS with or without AMI after stent implantation during 3 years of follow-up. The SIRI can be used as an indicator for identifying high-risk patients for intensive therapy to further reduce MACEs in the PCI era.

Key words: acute coronary syndrome, acute myocardial infarction, major adverse cardiac event, systemic inflammation response index, elderly patients

Cite as

Ma Y, Geng X. Prognostic value of the systemic inflammation response index on 3-year outcomes of elderly patients with acute coronary syndrome after stent implantation. *Adv Clin Exp Med.* 2025;34(7):1123–1130. doi:10.17219/acem/190739

DOI

10.17219/acem/190739

Copyright

Copyright by Author(s)

This is an article distributed under the terms of the Creative Commons Attribution 3.0 Unported (CC BY 3.0) (<https://creativecommons.org/licenses/by/3.0/>)

Background

Coronary artery disease (CAD) is one of the leading causes of cardiovascular death in developing and developed countries. Acute coronary syndrome (ACS) is a critical type of coronary artery disease that includes unstable angina and ST-segment elevation and non-ST-segment elevation myocardial infarctions. It is commonly caused by the rupture of vulnerable atherosclerotic plaques and thrombus formation, leading to the reduction or cessation of coronary blood flow.^{1–3} Due to improved drug therapy and early revascularization, the mortality rates for ACS patients have decreased significantly over the past decades.⁴ However, patients who survive ACS still have worse outcomes and a higher risk for recurrent major adverse cardiac events (MACEs).^{5,6} Elderly patients often seem more likely to experience increased rates of MACEs.⁷ These patients are consequently more fragile and have a greater incidence of comorbidities.⁸ The prognosis may improve through accurate risk stratification and intensive therapy for elderly patients.

It is well known that ischemic heart disease caused by CAD is an inflammatory disease of the arteries.⁹ The immune-inflammatory system is involved in every step of artery wall injury, lipid accumulation, fibrous cap formation, plaque rupture, and clot formation in ACSs.^{3,10,11} As markers of inflammation, white blood cell (WBC) counts, such as neutrophil, lymphocyte and monocyte counts, and their derived indicators are often used to predict the risk of poor outcomes in patients with CAD.^{12,13} Recently, the systemic inflammation response index (SIRI) has emerged in several clinical practices as novel indicator of the balance between inflammation and the immune response.^{14,15} The SIRI, which employs 3 blood cell subtypes (neutrophils, monocytes and lymphocytes), is related to a heightened risk of myocardial infarction (MI), stroke and all-cause death in the general population,¹⁶ and atrial fibrillation in patients with ischemic stroke.¹⁷ The SIRI was significantly greater in patients with ACSs than in those without ACSs and was associated with the severity of CAD.¹⁵ However, few studies have focused on the association between the SIRI and the prognosis of elderly patients surviving an ACS. The present study hypothesized that the SIRI is an independent risk factor for MACEs in elderly patients with ACS after percutaneous coronary intervention (PCI).

Objectives

This study aimed to explore the predictive value of the SIRI on the 3-year outcomes of patients older than 60 years after stent implantation and to evaluate variables associated with the SIRI. Further subgroup analyses were performed to detect associations between the SIRI and MACEs in ACS patients with and without AMI.

Materials and methods

Patients

This retrospective study was conducted at Tangshan Gongren Hospital, China. From November 2018 to October 2019, 1,758 patients with ACS (unstable angina or ST-segment elevation or non-ST-segment elevation MI) who were consecutively admitted to the Department of Cardiovascular Medicine and who underwent primary or selective PCI (primary PCI for patients with acute myocardial infarction (AMI) or selective PCI for ACS patients without AMI) were enrolled in the study. The diagnosis of unstable angina followed the 2015 ESC guidelines for the management of ACSs in patients presenting without persistent ST-segment elevation.¹⁸ The participants were divided into younger ($n = 798$) and older ($n = 960$) groups according to age (≤ 60 years or > 60 years). The exclusion criteria were as follows: 1) severe renal or liver disease; 2) a history of malignancy; 3) pneumonia, periodic fever, rheumatic disease, inflammatory bowel disease, rheumatoid arthritis, systemic lupus erythematosus, myeloma, or any disease affecting WBC counts; and 4) lack of follow-up.

Clinical data

The traditional risk factors included age, sex, height, weight, smoking status, history of previous MIs, diabetes, primary hypertension, and dyslipidemia. The medications included oral aspirin, clopidogrel/ticagrelor, statins, β -receptor blockers, and angiotensin-converting enzyme inhibitors/angiotensin receptor blockers (ACEIs/ARBs). Other factors included heart rate, systolic blood pressure (SBP), diastolic blood pressure (DBP), and left ventricular ejection fraction (LVEF) on admission. Venous blood samples were also obtained on admission to measure WBC subtypes, and platelet counts were measured with an autoanalyzer DxH 900 (Beckman Coulter K.K., Tokyo, Japan). The SIRI was calculated as (neutrophils \times monocytes)/lymphocytes. The levels of cholesterol, triglycerides and lipoprotein were measured after overnight fasting using routine automated laboratory analyzers (AU5800; Beckman Coulter; Brea, USA). All participants provided written informed consent, which was approved by the Ethics Committee of Tangshan Gongren Hospital (approval No. GRY-Y-LL-KJ2022-101). This study was conducted in accordance with the Declaration of Helsinki.

Coronary angiography

All patients received coronary angiography to determine the number of diseased coronary arteries and culprit vessels. Percutaneous coronary intervention procedures were performed by an experienced team at a high-volume center with a 24-h invasive service. A successful procedure was defined as target vessel residual stenosis $< 30\%$ and thrombolysis in MI grade 3 flow. Aspirin, clopidogrel/ticagrelor, statins, ACEIs/ARBs, and β -receptor blockers were used according to guidelines.

Follow-up and outcomes

Patients underwent regular follow-ups at 1 month after stent implantation and every 6 months thereafter. Data were obtained from medical records and/or telephone calls with family members of patients made by independent reviewers. The MACEs were defined as nonfatal AMI, nonfatal stroke and all-cause death. Stroke was defined as a combination of ischemic and hemorrhagic strokes.

Statistical analyses

Numerical variables are presented as the mean \pm standard deviation (\pm SD) and were compared using a Student's t-test. The enumeration data were compared using the χ^2 test. Multiple linear regression analysis was used to determine the significance of the relationships between the SIRI and age, sex, smoking status, body mass index (BMI), history of previous MI, diabetes mellitus, primary hypertension, dyslipidemia, diagnosis of AMI, number of diseased vessels, and platelet count. A curve-fitting method was applied to explore the relationship between the SIRI and MACEs in the older group. Univariate and multivariate Cox proportional hazard models were used to evaluate the hazard ratios of MACEs after adjusting for all variables in the older group, AMI subgroup and non-AMI subgroup. Statistical analysis was performed using the IBM SPSS v. 22.0 software package (IBM Corp., Armonk, USA). The p-value was set at 0.05 to indicate a statistically significant difference and was two-tailed.

Results

Clinical endpoints

The median follow-up duration was 38 months (7–44 months). Among the 1,758 patients, 729 (76%) were men, and the average age was 60 ± 11 years. There were 165 patients who experienced 1 or more adverse clinical events. The details of the MACEs in the 2 groups are listed in Table 1. Patients in the older group had an increased incidence of recurrent MACEs (11.2% compared to 7.1%, $p < 0.001$). Furthermore, mortality was significantly lower in the younger group than in the older group.

Table 1. Major adverse cardiac events in younger and older groups

Variables	Younger (n = 798)	Older (n = 960)	p-value
MACE, n (%)	57 (7.1)	108 (11.2)	0.000
AMI, n (%)	21 (2.6)	18 (1.9)	0.284
Stroke, n (%)	15 (1.9)	21 (2.2)	0.650
All cause death, n (%)	21 (2.6)	69 (7.2)	0.000

MACE – major adverse cardiac events; AMI – acute myocardial infarction.

Characteristics of elderly patients

The comparisons of characteristics between the 2 groups are listed in Table 2. Older patients were more likely to have

Table 2. Comparison of baseline characteristics in younger and older groups

Variables	Younger (n = 798)	Older (n = 960)	p-value
Risk factors			
Age [years]	51 \pm 7	68 \pm 5	0.000
Male, n (%)	687 (86.1)	649 (67.6)	0.000
Diabetes, n (%)	228 (28.6)	235 (24.5)	0.052
Hypertension, n (%)	385 (48.3)	525 (54.7)	0.007
Dyslipidemia, n (%)	87 (10.9)	54 (5.6)	0.000
Smoking, n (%)	333 (41.7)	265 (21.9)	0.000
BMI [kg/m ²]	26.3 \pm 2.4	25.0 \pm 2.5	0.000
Pervious MI, n (%)	49 (6.1)	88 (9.2)	0.018
LVEF (%)	60 \pm 9	60 \pm 8	0.499
Physical examination			
SBP [mm Hg]	129 \pm 16	128 \pm 16	0.125
DBP [mm Hg]	79 \pm 10	77 \pm 10	0.000
Heart rate [bpm]	77 \pm 14	76 \pm 15	0.098
Laboratory finding			
WBC [10 ⁹ /L]	9.07 \pm 3.06	8.52 \pm 3.14	0.000
Neutrophil count [10 ⁹ /L]	6.72 \pm 3.02	6.48 \pm 3.05	0.100
Lymphocyte count [10 ⁹ /L]	1.74 \pm 0.68	1.48 \pm 0.67	0.000
Monocyte count [10 ⁹ /L]	0.50 \pm 0.22	0.47 \pm 0.23	0.001
Platelet count [10 ⁹ /L]	233.08 \pm 57.43	220.73 \pm 58.06	0.000
SIII	1054 \pm 760	1195 \pm 968	0.001
SIRI	2.22 \pm 1.66	2.54 \pm 1.52	0.001
TC [mmol/L]	4.72 \pm 1.08	4.42 \pm 0.95	0.000
TG [mmol/L]	2.15 \pm 1.45	1.68 \pm 0.98	0.000
HDL [mmol/L]	1.14 \pm 0.30	1.15 \pm 0.27	0.329
LDL [mmol/L]	2.70 \pm 0.79	2.47 \pm 0.67	0.000
Coronary angiographic finding			
1 vessel, n (%)	335 (42.01)	330 (34.4)	0.001
2 vessels, n (%)	274 (34.3)	388 (40.4)	0.009
3 vessels, n (%)	189 (23.7)	242 (25.2)	0.460
Diagnosis of AMI, n (%)	528 (66.17)	530 (55.21)	0.000
Medication			
Asprin, n (%)	793 (99.4)	954 (99.4)	0.997
Clopidogrel/tricagrelor, n (%)	798 (100.0)	957 (99.7)	0.317
Statins, n (%)	717 (89.9)	874 (91.0)	0.396
β -blockers, n (%)	375 (47.0)	369 (38.4)	0.000
ACEIs/ARBs, n (%)	246 (30.8)	249 (25.9)	0.023

MACE – major adverse cardiac events; BMI – body mass index; MI – myocardial infarction; LVEF – left ventricular ejection fraction; SBP – systolic blood pressure; DBP – diastolic blood pressure; SIII – systemic immune inflammation index; SIRI – systemic inflammation response index; TG – triglycerides; HDL – high-density lipoprotein; LDL – low-density lipoprotein; AMI – acute myocardial infarction; ACEIs/ARBs – angiotensin-converting enzyme inhibitors/angiotensin receptor blockers; WBC – white blood cells count.

lower BMI and blood lipid levels and were less likely to use ACEIs/ARBs and β -blockers as medications ($p < 0.05$). Female sex, hypertension and previous myocardial infarctions were more prevalent in the older group ($p < 0.005$). Smoking status, dyslipidemia and a diagnosis of AMIs were more common in the younger group ($p < 0.05$). No significant differences were found in the LVEF or percentage of patients with 3-vessel coronary disease ($p > 0.05$). Remarkably, compared with those in the younger group, the SIRIs were significantly greater despite the absolute counts of leukocytes, neutrophils, lymphocytes, and monocytes being significantly lower in the older group ($p < 0.05$).

SIRI-related factors

Multiple linear regression analysis was employed to detect potential factors affecting the SIRI. Multiple linear regression (analysis of variance (ANOVA) $F = 41.985$; $p < 0.001$; $R^2 = 0.209$) revealed that the SIRI was significantly associated with age, hypertension, diagnosis of AMI, number of diseased vessels, and platelet count (Table 3).

SIRI and MACE

The curve-fitting method was used to explore the relationship between the SIRI and MACEs in the older group (Fig. 1). The SIRI was positively associated with MACEs ($p < 0.001$). Univariate and multivariate Cox proportional hazards model analyses revealed that the SIRI (hazard ratio (HR): 1.209, 95% confidence interval (95% CI): 1.147–1.274, $p < 0.001$) was an independent predictive risk factor for MACEs in the >60 -year-old group. Additionally, age (HR: 1.080, 95% CI: 1.048–1.114, $p < 0.001$), hypertension (HR: 2.108, 95% CI: 1.364–3.258, $p = 0.001$), diagnosis of AMI (HR: 1.648, 95% CI: 1.023–2.657, $p = 0.040$), and heart rate (HR: 1.020, 95% CI: 1.007–1.032, $p < 0.001$) were associated with MACEs in patients aged >60 years (Table 4).

Further subgroup analyses for associations of the SIRI with MACEs were performed for the AMI and non-AMI subgroups. In the entire ACS group, 1,056 patients were diagnosed with AMI on admission (AMI group) and 702 were not (non-AMI group). During the observation period, a total of 126 (11.9%) MACEs were recorded in the AMI subgroup (nonfatal AMI: 28 cases; nonfatal stroke: 17 cases; all-cause death: 81 cases) and 39 (5.6%) MACEs were recorded in the non-AMI subgroup (nonfatal AMI: 13 cases;

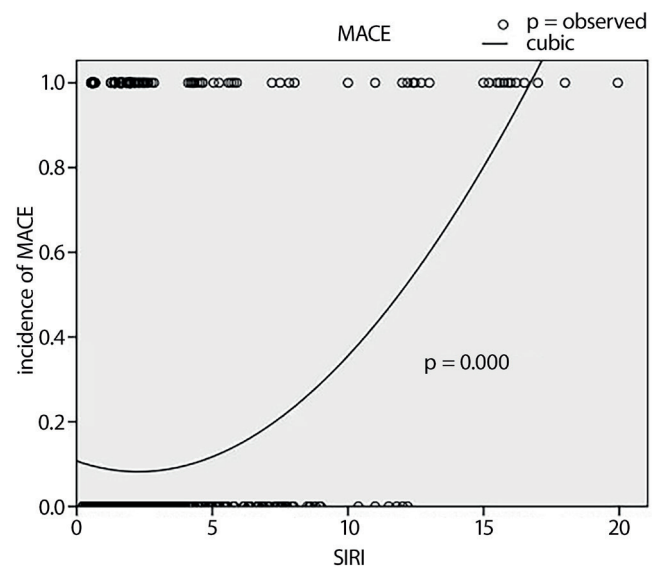


Fig. 1. Curve fitting of systemic inflammation response index (SIRI) levels and major adverse cardiac events (MACEs) in patients >60 years of age after percutaneous coronary intervention (PCI)

nonfatal stroke: 14 cases; all-cause death: 12 cases). The incidence of MACEs was significantly greater in the AMI subgroup (11.9% compared to 5.6%, $p < 0.001$). Patients with an AMI had significantly greater SIRIs than those without an AMI (3.1 ± 2.4 compared to 1.3 ± 0.9 , $p < 0.001$). According to the univariate and multivariate Cox model analyses, the SIRI was found to independently predict the occurrence of MACEs in both the AMI subgroup (HR: 1.213, 95% CI: 1.155–1.274, $p < 0.001$) and the non-AMI subgroup (HR: 1.469, 95% CI: 1.192–1.812, $p < 0.001$). (Table 5,6)

Discussion

The present study revealed that the incidence of recurrent MACEs and the SIRI were significantly greater in the older group than in the younger group. The SIRI was positively associated with MACEs and was an independent predictive risk factor for MACEs in patients aged >60 years with ACS after coronary angioplasty. The SIRI was significantly associated with age, hypertension, AMI, number of diseased vessels, and platelet count in all ACS patients. Similar relationships between the SIRI and MACEs were also observed in ACS patients with and without AMI.

Table 3. Predictive variables of SIRI in multiple linear regression analyses

Variable	Age (1 year)	Hypertension	Diagnosis of AMI	Number of vessels	Platelet count ($1 \times 10^9/L$)	Constant
B	0.032	0.242	1.946	0.140	0.004	-3.234
β	0.151	0.055	0.432	0.050	0.104	-
p-value	0.000	0.013	0.000	0.023	0.000	0.000
95% CI for B	0.022–0.041	0.052–0.433	1.747–2.145	0.019–0.261	0.002–0.006	-4.679–-1.788

SIRI – systemic inflammation response index; AMI – acute myocardial infarction; 95% CI – 95% confidence interval.

Table 4. Univariate and multivariate predictors of MACE in older group

Variable	Univariate		Multivariate	
	HR (95% CI)	p-value	HR (95% CI)	p-value
Age (1 year)	1.100 (1.067–1.133)	0.000	1.080 (1.048–1.114)	0.000
Female	0.904 (0.600–1.361)	0.628	–	–
Diabetes	0.926 (0.544–1.574)	0.775	–	–
Hypertension	2.243 (1.472–3.417)	0.000	2.108 (1.364–3.258)	0.001
Dyslipidemia	1.583 (0.800–3.133)	0.187	–	–
Smoking	1.332 (0.892–1.987)	0.161	–	–
BMI (1 kg/m ²)	0.951 (0.884–1.023)	0.175	–	–
Pervious MI	1.655 (0.959–2.856)	0.070	–	–
LVEF (1%)	0.964 (0.945–0.982)	0.000	–	–
SBP (1 mm Hg)	0.986 (0.974–0.998)	0.024	–	–
DBP (1 mm Hg)	0.976 (0.957–0.996)	0.017	–	–
Heart rate (1 bpm)	1.028 (1.017–1.040)	0.000	1.020 (1.007–1.032)	0.002
WBC (1×10 ⁹ /L)	1.198 (1.136–1.264)	0.000	–	–
Neutrophil count (1×10 ⁹ /L)	1.213 (1.147–1.283)	0.000	–	–
Lymphocyte count (1×10 ⁹ /L)	0.716 (0.516–0.992)	0.045	–	–
Monocyte count (1×10 ⁹ /L)	4.775 (2.456–9.285)	0.000	–	–
Platelet count (1×10 ⁹ /L)	1.004 (1.004–1.006)	0.019	–	–
SIII (1×10)	1.005 (1.003–1.006)	0.000	–	–
SIRI (1)	1.305 (1.245–1.368)	0.000	1.209 (1.147–1.274)	0.000
TC (1 mmol/L)	0.893 (0.730–1.091)	0.269	–	–
TG (1 mmol/L)	0.944 (0.770–1.159)	0.584	–	–
HDL (1 mmol/L)	0.541 (0.259–1.130)	0.102	–	–
LDL (1 mmol/L)	0.775 (0.576–1.042)	0.092	–	–
Number of vessels	1.231 (0.964–1.573)	0.096	–	–
Diagnosis of AMI	2.626 (1.699–4.059)	0.000	1.648 (1.023–2.657)	0.040
β-blockers	1.010 (0.686–1.487)	0.961	–	–
ACEIs/ARBs	0.663 (0.412–1.068)	0.091	–	–

MACE – major adverse cardiac events; BMI – body mass index; MI – myocardial infarction; LVEF – left ventricular ejection fraction; SBP – systolic blood pressure; DBP – diastolic blood pressure; SIII – systemic immune inflammation index; SIRI – systemic inflammation response index; TG – triglycerides; HDL – high-density lipoprotein; LDL – low-density lipoprotein; AMI – acute myocardial infarction; ACEIs/ARBs – angiotensin-converting enzyme inhibitors/angiotensin receptor blockers; WBC – white blood cells count; 95% CI – 95% confidence interval; HR – hazard ratio.

Immune and inflammatory responses play crucial roles in the progression of atherosclerosis^{19,20} and are related to the recurrence of cardiovascular events in ACS patients.^{21,22} White blood cell subtypes have been found to aggressively participate in immune and inflammatory responses and CAD.²³ Neutrophils not only infiltrate the ischemic myocardium and cause a destructive inflammatory reaction but also secrete inflammatory mediators, chemotactic substances and anaerobic free radicals to cause endothelial cell damage and subsequent tissue ischemia.²⁰ The neutrophil count is associated with plaque rupture and thrombosis formation by exacerbating vessel wall inflammation and cell apoptosis.^{24,25} Conversely, lymphocytes are involved in the regulatory pathway of the immune system and inflammation through lymphocyte apoptosis²⁶ and thus play an antiatherosclerotic role. Lymphopenia is correlated with MACEs and a poor prognosis in ACS

patients.^{27,28} Monocytes promote atherosclerosis progression by adhering to the vascular endothelium and transforming into macrophages, activating pro-inflammatory cytokine and reactive oxygen species (ROS) release, stimulating platelets, and being involved in thrombosis and blockage of blood vessels.^{29,30} The elevation of monocytes was independently associated with the risk of cardiovascular events.^{31,32} The SIRI, which integrates 3 leukocyte subtypes, could better reflect the status of inflammation and the immune system in the body and is more sensitive than the components alone. An increase in the SIRI implies an increase in the number of neutrophils and/or monocytes and/or a decrease in the number of lymphocytes. Several studies have shown that the SIRI is related to the prognosis of the general population and cardiovascular patients. A study involving 42,875 adults revealed that the SIRI was closely associated with cardiovascular death and all-cause

Table 5. Univariate predictors of MACE in AMI and non-AMI group

Variables	AMI group		non-AMI group	
	HR (95% CI)	p-value	HR (95% CI)	p-value
Age (1 year)	1.042 (1.024–1.060)	0.000	1.206 (0.989–1.065)	0.169
Female	1.358 (0.871–2.119)	0.177	0.720 (0.365–1.420)	0.343
Diabetes	1.085 (0.737–1.596)	0.775	0.880 (0.418–1.853)	0.736
Hypertension	2.70 (1.438–2.980)	0.000	1.152 (0.604–2.196)	0.667
Dyslipidemia	1.537 (0.896–2.635)	0.118	0.044 (0.561–2.199)	0.233
Smoking	1.702 (1.130–2.565)	0.011	2.311 (1.231–4.337)	0.009
BMI (1 kg/m ²)	0.950 (0.880–1.027)	0.196	0.980 (0.883–1.088)	0.707
Previous MI	0.825 (0.363–1.873)	0.646	2.598 (0.1234–5.473)	0.012
LVEF (1%)	1.011 (0.989–1.033)	0.315	0.937 (0.917–0.958)	0.000
SBP (1 mm Hg)	0.985 (0.974–0.996)	0.007	1.018 (0.995–1.042)	0.122
DBP (1 mm Hg)	0.966 (0.949–0.983)	0.000	1.017 (0.979–1.057)	0.389
Heart rate (1 beat/min)	1.012 (1.002–1.023)	0.019	1.007 (0.976–1.038)	0.674
WBC (1×10 ⁹ /L)	1.137 (1.075–1.202)	0.000	1.113 (0.953–1.299)	0.175
Neutrophil count (1×10 ⁹ /L)	1.156 (1.088–1.228)	0.000	1.219 (1.037–1.433)	0.016
Lymphocyte count (1×10 ⁹ /L)	0.739 (0.554–0.987)	0.040	0.363 (0.199–0.661)	0.001
Monocyte count (1×10 ⁹ /L)	3.189 (1.717–5.922)	0.000	1.505 (0.212–10.680)	0.682
Platelet count (1×10 ⁹ /L)	1.005 (1.002–1.008)	0.001	1.000 (0.995–1.005)	0.967
SIII (1×10)	1.004 (1.003–1.005)	0.000	1.008 (1.004–1.012)	0.000
SIRI (1)	1.273 (1.214–1.334)	0.000	1.509 (1.274–1.787)	0.000
TC (1 mmol/L)	0.812 (0.674–0.978)	0.028	0.659 (0.471–0.923)	0.015
TG (1 mmol/L)	0.979 (0.829–1.157)	0.807	0.914 (0.689–1.212)	0.533
HDL (1 mmol/L)	0.604 (0.310–1.177)	0.138	0.128 (0.030–0.549)	0.006
LDL (1 mmol/L)	0.794 (0.624–1.011)	0.061	0.517 (0.298–0.897)	0.019
Number of vessels	1.280 (1.024–1.600)	0.030	1.200 (0.804–1.792)	0.372
β-blockers	0.622 (0.432–0.895)	0.011	0.484 (0.258–0.909)	0.024
ACEIs/ARBs	1.128 (0.779–1.634)	0.524	0.542 (0.227–1.293)	0.167

MACE – major adverse cardiac events; BMI – body mass index; MI – myocardial infarction; LVEF – left ventricular ejection fraction; SBP – systolic blood pressure; DBP – diastolic blood pressure; SIII – systemic immune inflammation index; SIRI – systemic inflammation response index; TG – triglycerides; HDL – high-density lipoprotein; LDL – low-density lipoprotein; AMI – acute myocardial infarction; ACEIs/ARBs – angiotensin-converting enzyme inhibitors/angiotensin receptor blockers; WBC – white blood cells count; 95% CI – 95% confidence interval; HR – hazard ratio.

Table 6. Multivariate predictors of MACE in AMI and non-AMI group

Variable	AMI group		non-AMI group	
	HR (95% CI)	p-value	HR (95% CI)	p-value
Age (1 year)	1.027 (1.010–1.045)	0.002	–	–
Hypertension	1.947 (1.340–2.830)	0.000	–	–
Number of vessels	1.280 (1.024–1.600)	0.030	–	–
Platelet count (1×10 ⁹ /L)	1.005 (1.002–1.008)	0.000	–	–
SIRI (1)	1.213 (1.155–1.274)	0.000	1.469 (1.192–1.812)	0.000
β-blockers	0.674 (0.462–0.982)	0.040	0.392 (0.196–0.781)	0.008
Smoking	–	–	2.925 (1.483–5.771)	0.002
LVEF (1%)	–	–	0.932 (0.909–0.956)	0.000
Lymphocyte (1×10 ⁹ /L)	–	–	0.562 (0.326–0.966)	0.037

MACE – major adverse cardiac events; AMI – acute myocardial infarction; LVEF – left ventricular ejection fraction; SIII – systemic immune inflammation index; SIRI – systemic inflammation response index; 95% CI – 95% confidence interval; HR – hazard ratio.

mortality in the general population and individuals older than 60 years.³³ Another study from the Kailuan cohort demonstrated that an elevated SIRI increased the risk of stroke and all deaths and was associated with the incidence of MI.¹⁶ Dziedzic et al. confirmed that the SIRI was related to the severity of CAD and the diagnosis of ACS or stable CAD.¹⁵ Lin et al. showed that the SIRI was independently associated with the presence of atrial fibrillation in patients with ischemic stroke.¹⁷ An association between SIRI and MACEs was also suggested for patients with ischemic heart failure who underwent PCI.^{34,35} The mechanisms underlying the relationship between SIRI and MACE may include elevated SIRI levels reflecting an imbalance between proatherogenic and antiatherogenic immune networks, which may promote plaque vulnerability, endothelial dysfunction and thrombotic events, consequently contributing to the occurrence of acute coronary events.²⁰ The present study focused on patients older than 60 years with ACS after PCI. The SIRI was greater in elderly patients, and the incidence of MACEs was positively correlated with the SIRI. The SIRI was demonstrated to be an independent predictive risk factor for MACEs in patients aged >60 years with ACS. This may be explained in part by the following reasons: older patients commonly have more than 1 chronic disease. Inflammation is linked to aging and chronic disease.³⁶ Additionally, senescent cells that accumulate in elderly patients have a unique senescence-associated secretory profile that includes many pro-inflammatory cytokines.³⁷ Moreover, immune function declines during aging, and many immune cell types senesce with aging, resulting in a senescence-associated secretory phenotype. Together, these factors lead to more aggressive immune and inflammatory processes in elderly patients,^{38,39} which can lead to poorer outcomes. Similar analyses were conducted for the AMI and non-AMI subgroups at the same time. In the ACS group, patients with AMI had a greater SIRI than did patients without AMI. This may be due to the higher grade of immune and inflammatory responses to more serious myocardial damage, microvascular obstruction and activation of the immune system in AMI than in unstable angina. Cox regression analysis revealed that the SIRI independently predicted the occurrence of MACEs in both the AMI and non-AMI subgroups, as well as in the elderly subgroup. The exploration of potential factors affecting the SIRI revealed that the SIRI was significantly associated with age, hypertension, diagnosis of AMI, number of diseased vessels, and platelet count. All of these results may indicate that immune-inflammatory responses play pivotal roles in the occurrence of MACEs. It is more effective in elderly patients, AMI patients and patients with hypertension or multi-vessel disease. Targeted anti-inflammatory therapy is potentially beneficial for reducing the incidence of cardiovascular events and improving patient outcomes. Additionally, the SIRI could be used as an indicator for identifying high-risk patients for intensive therapy to further reduce MACEs.

Limitations

There are several limitations to the study that should be considered. First, the data came from 1 medical center and included a relatively small number of participants. Thus, a large multicenter study with a longer follow-up time is necessary to confirm the results. Second, not enough confounding factors were taken into account. For example, pro-inflammatory and/or inflammatory cytokines were not evaluated as part of a multivariable Cox regression analysis, which may affect the clinical prognosis. The results from the present study should be extended in further research.

Conclusions

The present study revealed that the SIRI was an independent predictive risk factor for MACEs in patients >60 years of age with ACS and ACS with or without an AMI after stent implantation over 3 years of follow-up. The SIRI can be used as an indicator for identifying high-risk patients for intensive therapy to further reduce MACE in the era of PCI.

ORCID iDs

Yi Ma  <https://orcid.org/0000-0003-4710-7393>

Xuebin Geng  <https://orcid.org/0000-0001-8478-8920>

References

- Otsuka F, Joner M, Prati F, Virmani R, Narula J. Clinical classification of plaque morphology in coronary disease. *Nat Rev Cardiol*. 2014;11(7):379–389. doi:10.1038/nrcardio.2014.62
- Bentzon JF, Otsuka F, Virmani R, Falk E. Mechanisms of plaque formation and rupture. *Circ Res*. 2014;114(12):1852–1866. doi:10.1161/CIRCRESAHA.114.302721
- Libby P, Pasterkamp G, Crea F, Jang IK. Reassessing the mechanisms of acute coronary syndromes: The “vulnerable plaque” and superficial erosion. *Circ Res*. 2019;124(1):150–160. doi:10.1161/CIRCRESAHA.118.311098
- Puymirat E, Simon T, Cayla G, et al. Acute myocardial infarction: Changes in patient characteristics, management, and 6-month outcomes over a period of 20 years in the FAST-MI Program (French Registry of Acute ST-Elevation or Non-ST-Elevation Myocardial Infarction) 1995 to 2015. *Circulation*. 2017;136(20):1908–1919. doi:10.1161/CIRCULATIONAHA.117.030798
- Jernberg T, Hasvold P, Henriksson M, Hjelm H, Thuresson M, Janzon M. Cardiovascular risk in post-myocardial infarction patients: Nationwide real world data demonstrate the importance of a long-term perspective. *Eur Heart J*. 2015;36(19):1163–1170. doi:10.1093/eurheartj/ehu505
- Okkonen M, Havulinna AS, Ukkola O, et al. Risk factors for major adverse cardiovascular events after the first acute coronary syndrome. *Ann Med*. 2021;53(1):817–823. doi:10.1080/07853890.2021.1924395
- Kochar A, Chen AY, Sharma PP, et al. Long-term mortality of older patients with acute myocardial infarction treated in US clinical practice. *J Am Heart Assoc*. 2018;7(13):e007230. doi:10.1161/JAHA.117.007230
- Salive ME. Multimorbidity in older adults. *Epidemiol Rev*. 2013;35(1):75–83. doi:10.1093/epirev/mxs009
- Björkegren JLM, Lusis AJ. Atherosclerosis: Recent developments. *Cell*. 2022;185(10):1630–1645. doi:10.1016/j.cell.2022.04.004
- Crea F, Libby P. Acute coronary syndromes: The way forward from mechanisms to precision treatment. *Circulation*. 2017;136(12):1155–1166. doi:10.1161/CIRCULATIONAHA.117.029870

11. Libby P, Hansson GK. From focal lipid storage to systemic inflammation. *J Am Coll Cardiol.* 2019;74(12):1594–1607. doi:10.1016/j.jacc.2019.07.061
12. Shiyovich A, Gilutz H, Plakht Y. White blood cell subtypes are associated with a greater long-term risk of death after acute myocardial infarction. *Tex Heart Inst J.* 2017;44(3):176–188. doi:10.14503/THIJ-16-5768
13. Turcato G, Sanchis-Gomar F, Cervellin G, et al. Evaluation of neutrophil-lymphocyte and platelet-lymphocyte ratios as predictors of 30-day mortality in patients hospitalized for an episode of acute decompensated heart failure. *J Med Biochem.* 2019;38(4):452–460. doi:10.2478/jomb-2018-0044
14. Huang J, Zhang Q, Wang R, et al. Systemic immune-inflammatory index predicts clinical outcomes for elderly patients with acute myocardial infarction receiving percutaneous coronary intervention. *Med Sci Monit.* 2019;25:9690–9701. doi:10.12659/MSM.919802
15. Dziedzic EA, Gąsior JS, Tuzimek A, et al. Investigation of the associations of novel inflammatory biomarkers – systemic inflammatory index (SII) and systemic inflammatory response index (SIRI) – with the severity of coronary artery disease and acute coronary syndrome occurrence. *Int J Mol Sci.* 2022;23(17):9553. doi:10.3390/ijms23179553
16. Jin Z, Wu Q, Chen S, et al. The associations of two novel inflammation indexes, SII and SIRI with the risks for cardiovascular diseases and all-cause mortality: A ten-year follow-up study in 85,154 individuals. *J Inflamm Res.* 2021;14:131–140. doi:10.2147/JIR.S283835
17. Lin KB, Fan FH, Cai MQ, et al. Systemic immune inflammation index and system inflammation response index are potential biomarkers of atrial fibrillation among the patients presenting with ischemic stroke. *Eur J Med Res.* 2022;27(1):106. doi:10.1186/s40001-022-00733-9
18. Roffi M, Patrono C, Collet JP, et al. 2015 ESC Guidelines for the management of acute coronary syndromes in patients presenting without persistent ST-segment elevation: Task Force for the Management of Acute Coronary Syndromes in Patients Presenting without Persistent ST-Segment Elevation of the European Society of Cardiology (ESC). *Eur Heart J.* 2016;37(3):267–315. doi:10.1093/eurheartj/ehv320
19. Chistiakov DA, Kashirskikh DA, Khotina VA, Grechko AV, Orekhov AN. Immune-inflammatory responses in atherosclerosis: The role of myeloid cells. *J Clin Med.* 2019;8(11):1798. doi:10.3390/jcm8111798
20. Wang H, Liu Z, Shao J, et al. Immune and inflammation in acute coronary syndrome: Molecular mechanisms and therapeutic implications. *J Immunol Res.* 2020;2020:4904217. doi:10.1155/2020/4904217
21. Akrami M, Izadpanah P, Bazrafshan M, et al. Effects of colchicine on major adverse cardiac events in next 6-month period after acute coronary syndrome occurrence: A randomized placebo-control trial. *BMC Cardiovasc Disord.* 2021;21(1):583. doi:10.1186/s12872-021-02393-9
22. Niu Y, Bai N, Ma Y, Zhong PY, Shang YS, Wang ZL. Safety and efficacy of anti-inflammatory therapy in patients with coronary artery disease: A systematic review and meta-analysis. *BMC Cardiovasc Disord.* 2022;22(1):84. doi:10.1186/s12872-022-02525-9
23. Kounis NG, Soufras GD, Tsigas G, Hahalis G. White blood cell counts, leukocyte ratios, and eosinophils as inflammatory markers in patients with coronary artery disease. *Clin Appl Thromb Hemost.* 2015;21(2):139–143. doi:10.1177/1076029614531449
24. Fernández-Ruiz I. Neutrophil-driven SMC death destabilizes atherosclerotic plaques. *Nat Rev Cardiol.* 2019;16(8):455–455. doi:10.1038/s41569-019-0214-1
25. Shah AD, Denaxas S, Nicholas O, Hingorani AD, Hemingway H. Neutrophil counts and initial presentation of 12 cardiovascular diseases. *J Am Coll Cardiol.* 2017;69(9):1160–1169. doi:10.1016/j.jacc.2016.12.022
26. Weber C, Zernecke A, Libby P. The multifaceted contributions of leukocyte subsets to atherosclerosis: Lessons from mouse models. *Nat Rev Immunol.* 2008;8(10):802–815. doi:10.1038/nri2415
27. Ommen SR, Gibbons RJ, Hodge DO, Thomson SP. Usefulness of the lymphocyte concentration as a prognostic marker in coronary artery disease. *J Am Coll Cardiol.* 1997;79(6):812–814. doi:10.1016/S0002-9149(96)00878-8
28. Núñez J, Núñez E, Bodí V, et al. Low lymphocyte count in acute phase of ST-segment elevation myocardial infarction predicts long-term recurrent myocardial infarction. *Coron Artery Dis.* 2010;21(1):1–7. doi:10.1097/MCA.0b013e328332ee15
29. Gratchev A, Sobenin I, Orekhov A, Kzhyskowska J. Monocytes as a diagnostic marker of cardiovascular diseases. *Immunobiology.* 2012;217(5):476–482. doi:10.1016/j.imbio.2012.01.008
30. Wu MY, Li CJ, Hou MF, Chu PY. New insights into the role of inflammation in the pathogenesis of atherosclerosis. *Int J Mol Sci.* 2017;18(10):2034. doi:10.3390/ijms18102034
31. Berg KE, Ljungcrantz I, Andersson L, et al. Elevated CD14⁺⁺ CD16⁻ monocytes predict cardiovascular events. *Circ Cardiovasc Genet.* 2012;5(1):122–131. doi:10.1161/CIRCGENETICS.111.960385
32. Rogacev KS, Seiler S, Zawada AM, et al. CD14⁺⁺CD16⁺ monocytes and cardiovascular outcome in patients with chronic kidney disease. *Eur Heart J.* 2011;32(1):84–92. doi:10.1093/eurheartj/ehq371
33. Xia Y, Xia C, Wu L, Li Z, Li H, Zhang J. Systemic immune inflammation index (SII), system inflammation response index (SIRI) and risk of all-cause mortality and cardiovascular mortality: A 20-year follow-up cohort study of 42,875 US adults. *J Clin Med.* 2023;12(3):1128. doi:10.3390/jcm12031128
34. Li Q, Ma X, Shao Q, et al. Prognostic impact of multiple lymphocyte-based inflammatory indices in acute coronary syndrome patients. *Front Cardiovasc Med.* 2022;9:811790. doi:10.3389/fcvm.2022.811790
35. Ma M, Wu K, Sun T, et al. Impacts of systemic inflammation response index on the prognosis of patients with ischemic heart failure after percutaneous coronary intervention. *Front Immunol.* 2024;15:1324890. doi:10.3389/fimmu.2024.1324890
36. Salvioli S, Monti D, Lanzarini C, et al. Immune system, cell senescence, aging and longevity: Inflamm-aging reappraised. *Curr Pharm Des.* 2013;19(9):1675–1679. PMID:23589904.
37. Coppé JP, Patil CK, Rodier F, et al. Senescence-associated secretory phenotypes reveal cell-nonautonomous functions of oncogenic RAS and the p53 tumor suppressor. *PLoS Biol.* 2008;6(12):e301. doi:10.1371/journal.pbio.0060301
38. Vicente R, Mausset-Bonnefont AL, Jorgensen C, Louis-Plence P, Brondello JM. Cellular senescence impact on immune cell fate and function. *Aging Cell.* 2016;15(3):400–406. doi:10.1111/acel.12455
39. Pinti M, Appay V, Campisi J, et al. Aging of the immune system: Focus on inflammation and vaccination. *Eur J Immunol.* 2016;46(10):2286–2301. doi:10.1002/eji.201546178

Prognostic value of inflammation-related model in hepatitis B acute-on-chronic liver failure

Huaqian Xu^{A–D}, Xue Li^{B,E}, Yue Zhuo^{B,C}, Chunyan Li^{B,C}, Chengzhi Bai^{C,E}, Jie Chen^{B,C}, Shanhong Tang^{E,F}

Department of Gastroenterology, The General Hospital of Western Theater Command, Chengdu, China

A – research concept and design; B – collection and/or assembly of data; C – data analysis and interpretation;

D – writing the article; E – critical revision of the article; F – final approval of the article

Advances in Clinical and Experimental Medicine, ISSN 1899–5276 (print), ISSN 2451–2680 (online)

Adv Clin Exp Med. 2025;34(7):1131–1138

Address for correspondence

Shanhong Tang

E-mail: shanhongtang@163.com

Funding sources

None declared

Conflict of interest

None declared

Received on September 17, 2023

Reviewed on March 30, 2024

Accepted on August 26, 2024

Published online on November 18, 2024

Abstract

Background. Acute-on-chronic liver failure (ACLF) is characterized by rapid onset, rapid development and a high short-term mortality rate. Systemic inflammation exerts an effect on the disease progression of ACLF.

Objectives. The purposes of this study were to explore the clinical significance that the inflammatory response has on the disease process of hepatitis B virus acute-on-chronic liver failure (HBV-ACLF) patients, to further compare the values of different inflammation-related biomarkers in the prognosis evaluation of HBV-ACLF patients, and to combine inflammatory-related markers to establish a new prediction model.

Materials and methods. Baseline admission data and 90-day outcomes were collected from 247 patients who met the inclusion criteria. According to the 90-day survival situation, they were divided into a survival group and a death group. The differences in baseline data and inflammation levels between the 2 groups were compared. A regression model was used to analyze the risk factors for 90-day mortality and establish a new model.

Results. The study found that the differences between the survival group and the death group were statistically significant in terms of age, total bilirubin (Tbil), prothrombin time (PT), international standardized ratio (INR), inflammation level, and model for end-stage liver disease (MELD) series scores ($p < 0.05$). The monocyte-to-lymphocyte ratio (MLR)-integrated iMELD model (MLR-iMELD) can effectively predict the 90-day survival rate of HBV-ACLF patients. The area under the receiver operating characteristic (ROC) curve (AUROC) of the new model was 0.792, and the best cutoff for predicting the prognosis of 90 days for patients was -0.33 (sensitivity 0.577 and specificity 0.898).

Conclusions. The higher the level of inflammation in patients with HBV-ACLF, the greater the risk of 90-day death. Compared with other inflammation-related markers, the MLR-iMELD model can better predict the 90-day survival rate of HBV-ACLF patients.

Key words: inflammation, prognosis, hepatitis B virus, HBV-ACLF

Cite as

Xu H, Li X, Zhuo Y, Li C, Bai C, Chen J, Tang S. Prognostic value of inflammation-related model in hepatitis B acute-on-chronic liver failure. *Adv Clin Exp Med.* 2025;34(7):1131–1138. doi:10.17219/acem/192624

DOI

10.17219/acem/192624

Copyright

Copyright by Author(s)

This is an article distributed under the terms of the Creative Commons Attribution 3.0 Unported (CC BY 3.0) (<https://creativecommons.org/licenses/by/3.0/>)

Background

Acute-on-chronic liver failure (ACLF) has gained increasing recognition due to its high short-term mortality rate.¹ The Asian Pacific Association for the Study of the Liver (APASL) defines ACLF as an acute liver injury that occurs as a result of chronic liver disease and is triggered by acute factors. Among them, acute liver damage induced by hepatitis B virus (HBV) reactivation, alcohol consumption and infection are the most common. Acute-on-chronic liver failure is characterized by jaundice and coagulation dysfunction, and it is prone to clinical ascites and/or hepatic encephalopathy.² Although there is still no consensus for the definition of ACLF, the poor clinical prognosis in patients with ACLF is undeniable. With changes in the epidemiological profile of ACLF in the Asia-Pacific region, the proportion of acute liver injury caused by alcohol has increased gradually, but acute liver injury caused by HBV reactivation is still the main reason.³ The progression from compensated to decompensated and ACLF after HBV infection is characterized by complications related to cirrhosis and extrahepatic organ tissue damage.⁴

The strong inflammatory reaction caused by immune activation or inhibition during the progression of ACLF is crucial for the prognosis of patients.⁵ Indeed, some studies have confirmed that certain inflammation-related blood laboratory indicators, such as neutrophil-to-lymphocyte ratio (NLR), monocyte-to-lymphocyte ratio (MLR), platelet-to-leukocyte ratio (PWR), and platelet-to-lymphocyte ratio (PLR), among others, can better reflect the baseline inflammatory response and immune status of patients with ACLF or non-ACLF patients.^{6–10} In addition, some inflammatory combination indicators, such as the systemic immune–inflammation index (SII) and the prognostic nutritional index (PNI), have certain clinical value in non-ACLF diseases, but the above indicators are rarely reported in HBV-ACLF.^{11–13} Given the high short-term mortality of HBV-ACLF, early identification and evaluation of the severity of the disease are critical for subsequent treatment and improved patient outcomes. Various prognostic models, including the model for end-stage liver disease (MELD), COSSH-ACLF score and CLIF-C ACLF score, are considered suitable for predicting the prognosis of patients with HBV-ACLF.^{14–18} Among the above models, the MELD serial scoring model (MELD, MELD-Na, iMELD) does not consider the influence of infection and inflammation. Although neutrophils are included in the COSSH-ACLF score, there is a certain subjective bias due to the inclusion of the hepatic encephalopathy score in the model. For the CLIF-C score, which includes white blood cell count (WBC), its clinical application also has certain limitations because white blood cells are easily affected by hypersplenism.

Objectives

Therefore, this study will further explore the influence of the inflammatory response on HBV-ACLF and compare

the clinical value of single inflammation-related indicators for prognostic evaluation. It will suggest a new model with better evaluation efficiency combined with inflammation-related indicators.

Materials and methods

Patients

This is a retrospective observational study. In view of the high incidence of HBV in the Asia-Pacific region, we enrolled patients with HBV-ACLF who met the definition of the APASL: “ACLF is an acute hepatic insult manifesting as jaundice (serum bilirubin ≥ 5 mg/dL or 85 micromol/L) and coagulopathy (international standardized ratio (INR) ≥ 1.5 or prothrombin activity $<40\%$) complicated within 4 weeks by clinical ascites and/or encephalopathy in a patient with previously diagnosed or undiagnosed chronic liver disease/cirrhosis and is associated with a high 28-day mortality”.² We collected the records of HBV-ACLF patients from 2015 to 2020 at the People's Liberation Army The General Hospital of Western Theater Command (Chengdu, China). The study included a total of 271 patients; 24 patients were excluded according to the exclusion criteria, leaving 247 patients who were ultimately included in the study group. All patients were followed up for 90 days, mainly through the hospital medical record system and telephone communication. The study endpoint was the patient's survival at 90 days, and the secondary endpoint was death or liver transplantation. The exclusion criteria were: 1) patients under 18 and over 80 years of age; 2) viral infections other than HBV; 3) combined with other types of chronic liver disease; 4) patients with severe cardiopulmonary disease or chronic kidney disease (CKD); 5) suspected or confirmed malignancy; 6) pregnant or breastfeeding; 7) received a liver transplant; 8) no recent history of hormone or antibiotic use; and 9) incomplete data (Fig. 1).

Clinical data collection

Baseline data and 90-day survival were collected. All clinical data were collected through the hospital health system, and 90-day survival was followed up by telephone by the investigators. Clinical data mainly included routine blood tests (platelets, neutrophils, lymphocytes, monocytes, and leukocytes) and blood biochemical indexes (albumin, prealbumin, alanine aminotransferase (ALT), aspartate aminotransferase (AST), total bilirubin (Tbil), and coagulation parameters (prothrombin time (PT) and INR)). Upon admission, patients underwent calculation of their MELD serial scores. Baseline inflammation-related measures were calculated as follows: $NLR = \text{neutrophil} (\times 10^9/L) / \text{lymphocyte} (\times 10^9/L)$, $MLR = \text{monocyte} (\times 10^9/L) / \text{lymphocyte} (\times 10^9/L)$, $SII = \text{platelet} (\times 10^9/L) * NLR$,

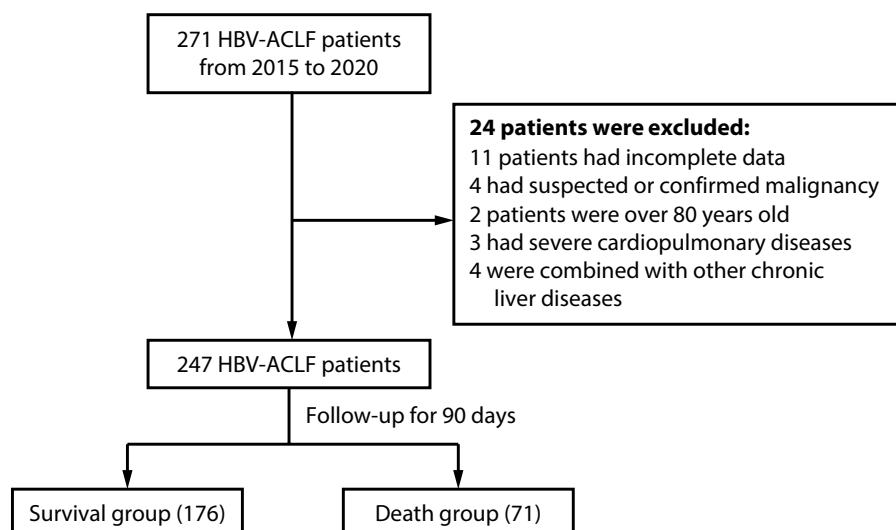


Fig. 1. Study flowchart

PLR = platelet ($\times 10^9/L$)/lymphocyte ($\times 10^9/L$), PWR = platelet ($\times 10^9/L$)/leukocyte ($\times 10^9/L$), and PNI = albumin (g/L) + 5 * lymphocyte ($\times 10^9/L$).

Statistical analyses

Statistical analyses were performed with the use of SPSS v. 27.0 (IBM Corp., Armonk, USA). The Kolmogorov–Smirnov test was used to test the normality of quantitative data. Continuous variables conforming to the normal distribution were expressed as mean \pm standard deviation (\pm SD); if not normally distributed, they were expressed as median (Q1–Q3). Pearson's correlation analysis was used to test the correlation between MELD score and other clinical characteristics of patients. Non-parametric tests were used to determine the indicators with statistical differences between the 2 groups. Multivariate regression models were used to determine the risk factors for 90-day mortality based on the results of multivariate logistic regression to construct a new prediction model. A receiver operating characteristic (ROC) curve was used to further analyze the performance of the model, and the cumulative survival rate of the HBV-ACLF patients at 90 days was plotted using a Kaplan–Meier curve. For all statistical analyses, p-values were two-sided, and $p \leq 0.1$ was considered to indicate statistical significance.

Results

Patient characteristics

A total of 247 HBV-ACLF patients were included in this study. The characteristics of the patients and their laboratory data are shown in Table 1. Among the 247 participants, 176 were in the survival group and 71 were in the death group, with a 90-day survival rate of 71.26%. By comparing the 2 groups, it was found that the levels of platelets,

lymphocytes, albumin, ALT, and PWR were significantly higher in the survival group than in the non-survival patients. The age of the patients in the survival group and their PT, INR, AST, serum creatinine, TBil, neutrophils, monocytes, NLR, MLR, MELD, MELD-na, and iMELD score were significantly lower than those in the death group ($p < 0.05$).

Correlation between inflammatory biomarkers and MELD score

To further understand the correlation between inflammation and the disease status of patients, we used Pearson's correlation analysis to confirm our conjecture. The results showed that there was a certain correlation between inflammation-related markers and MELD score in HBV-ACLF patients, among which NLR, MLR, SII, PNI, leukocyte count, neutrophil count, and monocyte count were positively correlated with MELD score (r-values of 0.254, 0.496, 0.133, 0.145, 0.319, 0.214, and 0.423, respectively). Conversely, PWR and lymphocyte count were negatively correlated with MELD score (r-values of -0.425 and -0.188 , respectively) ($p < 0.05$) (Table 2).

Comparing the predictive value of inflammatory biomarkers and establishing a new predictive model

We compared 90-day survival rates in the 247 hepatitis B virus acute-on-chronic liver failure (HBV-ACLF) patients, among which there were 176 (71.26%) survivors and 71 (28.74%) deceased. Multivariate binary logistic regression was used to screen the variables (Table 3). We found that MLR and iMELD were independent predictors of patient outcomes at 90 days ($p < 0.1$). Therefore, we developed a new prognostic model (MLR-iMELD score) for patients with HBV-ACLF. The mathematical formula was as follows: MLR-iMELD score = $0.855 \times \text{MLR} + 0.125 \times \text{iMELD} - 6.768$. To further evaluate the predictive value of the new

Table 1. Clinical characteristics and outcomes of HBV-ACLF patients

Variable	HBV-ACLF (n = 247)		Z value	p-value
	Survival group (n = 176)	Death group (n = 71)		
Age [years]	48 (37–56)	52 (47–61)	–3.68	<0.001
Platelet [$\times 10^9/L$]	105.00 (76.25–138.00)	80.00 (60.00–128.00)	–2.88	0.004
Neutrophil [$\times 10^9/L$]	4.07 (2.77–5.61)	5.06 (3.50–7.23)	–2.98	0.003
Lymphocyte [$\times 10^9/L$]	1.07 (0.81–1.52)	0.89 (0.71–1.12)	–3.18	0.001
Monocyte [$\times 10^9/L$]	0.46 (0.36–0.67)	0.64 (0.41–0.86)	–2.93	0.003
Leukocyte [$\times 10^9/L$]	5.66 (4.42–7.72)	6.74 (4.93–9.13)	–2.31	0.057
Albumin [g/L]	33.40 (30.79–37.50)	31.50 (28.30–34.80)	–3.44	0.003
Prealbumin [mg/L]	58.50 (37.25–71.00)	43.00 (30.59–57.00)	–3.39	0.001
Tbil [$\mu\text{mol/L}$]	233.80 (160.65–354.50)	344.60 (226.00–481.73)	–4.03	<0.001
ALT [$\mu\text{mol/L}$]	482.65 (162.45–1048.27)	258.30 (97.40–881.80)	–2.28	0.026
AST [$\mu\text{mol/L}$]	365.50 (145.42–815.25)	274.90 (118.70–713.90)	–1.16	0.244
PT [s]	16.80 (14.42–19.50)	21.30 (18.40–25.60)	–6.20	<0.001
Scr [$\mu\text{mol/L}$]	72.00 (61.00–85.75)	75.00 (65.00–93.00)	–2.11	0.035
INR	1.48 (1.29–1.72)	1.90 (1.63–2.29)	–6.16	<0.001
NLR	3.87 (2.59–5.04)	5.82 (3.38–8.41)	–4.54	<0.001
MLR	0.45 (0.33–0.61)	0.68 (0.45–1.02)	–5.18	<0.001
PLR	96.67 (66.11–145.86)	100.00 (67.07–138.77)	–0.30	0.976
PWR	17.93 (12.91–23.99)	13.40 (8.57–19.30)	–3.84	0.004
SII	387.02 (226.42–653.31)	435.15 (257.21–752.97)	–1.50	0.321
PNI	39.35 (36.21–44.02)	38.30 (35.85–45.50)	–3.84	0.213
MELD	18.72 (15.54–22.04)	23.75 (20.62–27.84)	–6.36	<0.001
MELD-Na	19.55 (16.15–24.78)	26.34 (22.80–33.22)	–6.91	<0.001
iMELD	38.42 (32.75–43.53)	47.05 (41.46–52.51)	–6.43	<0.001

PT – prothrombin time; INR – international normalized ratio; ALT – alanine aminotransferase; AST – aspartate aminotransferase; TBil – total bilirubin; Scr – serum creatinine; NLR – neutrophil-to-lymphocyte ratio; MLR – monocyte-to-lymphocyte ratio; SII – systemic immune inflammatory index; PLR – platelet-to-lymphocyte ratio; PWR – platelet-to-leukocyte ratio; PNI – prognostic nutritional index; MELD – a model for end-stage liver disease; MELD-Na – MELD-sodium; iMELD – integrated MELD.

Table 2. Pearson's correlation analysis between inflammation markers and MELD score

Inflammatory markers	MELD		
	r-value	t-value	p-value
Leukocyte	0.319	5.276	<0.001
Neutrophil	0.214	3.425	<0.001
Lymphocyte	–0.188	–2.994	0.003
Monocyte	0.423	7.301	<0.001
NLR	0.254	4.109	<0.001
MLR	0.496	8.947	<0.001
SII	0.133	2.093	0.037
PLR	0.014	0.217	0.828
PWR	–0.425	–7.353	<0.001
PNI	0.145	2.289	0.023

MLR – monocyte-to-lymphocyte ratio; SII – systemic immune inflammatory index; PLR – platelet-to-lymphocyte ratio; PWR – platelet-to-leukocyte ratio; PNI – prognostic nutritional index; MELD – a model for end-stage liver disease.

model, we compared the clinical values of NLR, MLR, PWR, PLR, PNI, MELD, MELD-Na, iMELD, and MLR-iMELD scores by analyzing the area under the ROC curve (AUROC) (Fig. 2). Except for PLR and PNI, all other indicators showed statistical significance. The sensitivity and specificity were 0.606 and 0.767 for NLR, 0.549 and 0.767 for MLR, 0.577 and 0.670 for PWR, 0.803 and 0.597 for MELD score, 0.831 and 0.619 for MELD-Na score, 0.831 and 0.619 for iMELD score, and 0.577 and 0.898 for MLR-iMELD score, respectively (Table 4). The AUROC curves were 0.684 (0.611–0.758) for NLR, 0.711 (0.641–0.780) for MLR, 0.656 (0.579–0.733) for PWR, 0.510 (0.424–0.596) for PNI, 0.758 (0.692–0.825) for MELD score, 0.761 (0.695–0.827) for MELD-Na score, 0.781 (0.715–0.847) for iMELD score, and 0.792 (0.727–0.857) for MLR-iMELD score (Table 4).

Performance of the MLR-iMELD model

By comparing the new model with other inflammation ratios and models, we found that the new model had better

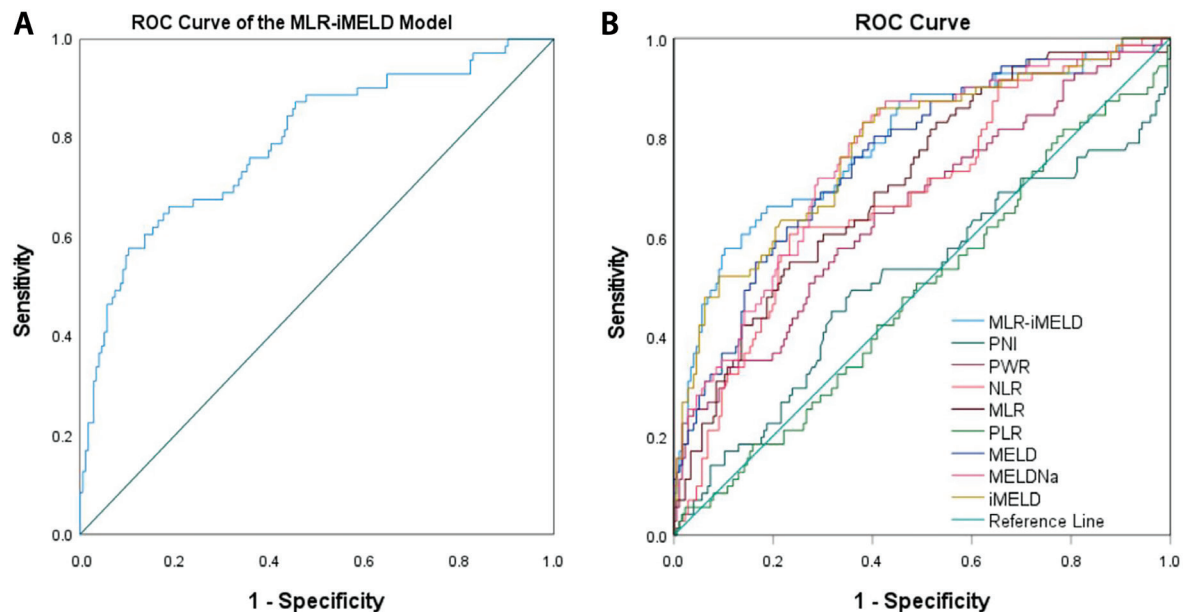


Fig. 2. A. Receiver operating characteristic (ROC) curves of MLR-iMELD for predicting 90-day mortality in hepatitis B virus acute-on-chronic liver failure (HBV-ACLF). The area under the curve (AUROC) was 0.792, the sensitivity and specificity were 0.577 and 0.898, respectively. B. ROC curves analysis for NLR, MLR, PWR, PLR, PNI, MELD, MELD-Na, iMELD, and the new model (MLR-iMELD) for predicting mortality in patients with HBV-ACLF

NLR – neutrophil-to-lymphocyte ratio; MLR – monocyte-to-lymphocyte ratio; PWR – platelet-to-leukocyte ratio; PLR – platelet-to-lymphocyte ratio; PNI – prognostic nutritional index; MELD – a model for end-stage liver disease; MELD-Na – MELD-sodium; iMELD – integrated MELD; MLR-iMELD – MLR-integrated iMELD.

Table 3. Multivariate binary logistic analysis to predict 90-day progression in hepatitis B virus acute-on-chronic liver failure (HBV-ACLF) patients

Variables	β	SE	Wald	OR (95%CI)	p-value
Age [years]	–0.001	0.017	0.002	0.999 (0.966–1.033)	0.960
Leukocyte [$\times 10^9/L$]	–0.078	0.100	0.602	0.925 (0.760–1.126)	0.438
Platelet [$\times 10^9/L$]	–0.003	0.004	0.619	0.997 (0.989–1.005)	0.431
Neutrophil [$\times 10^9/L$]	0.051	0.090	0.319	1.052 (0.883–1.254)	0.572
Albumin [g/L]	–0.025	0.028	0.845	0.975 (0.923–1.029)	0.358
ALT [$\mu\text{mol/L}$]	0.000	0.000	0.073	1.000 (0.999–1.001)	0.786
AST [$\mu\text{mol/L}$]	0.000	0.001	0.011	1.000 (0.999–1.001)	0.917
MLR	0.855	0.509	3.121	2.460 (0.906–6.677)	0.077*
iMELD	0.125	0.029	17.864	1.103 (1.060–1.146)	<0.001*

In multivariate binary logistic regression analysis, MLR and iMELD were independent predictors of 90-day outcomes in HBV-ACLF patients; MLR – monocyte-to-lymphocyte ratio; iMELD – integrated MELD; 95% CI – 95% confidence interval; OR – odds ratio; SE – standard error.

Table 4. Area under curve and cut-off values of the prognostic variables

ROC	AUC	95% CI	Sensitivity	Specificity	Youden's index	Cutoff value	p-value
NLR	0.684	0.611–0.758	0.606	0.767	0.373	5.12	<0.001
MLR	0.711	0.641–0.780	0.549	0.767	0.316	0.63	<0.001
PWR	0.656	0.579–0.733	0.577	0.670	0.247	15.17	<0.001
PLR	0.488	0.407–0.568	0.817	0.216	0.033	59.17	0.761
PNI	0.510	0.424–0.596	0.493	0.642	0.135	37.92	0.801
MELD	0.758	0.692–0.825	0.803	0.597	0.400	20.21	<0.001
MELD-Na	0.761	0.695–0.827	0.831	0.619	0.450	21.66	<0.001
iMELD	0.781	0.715–0.847	0.831	0.619	0.450	40.50	<0.001
MLR-iMELD	0.792	0.727–0.857	0.577	0.898	0.475	–0.33	<0.001

NLR – neutrophil-to-lymphocyte ratio; MLR – monocyte-to-lymphocyte ratio; PWR – platelet-to-leukocyte ratio; PNI – prognostic nutritional index; MELD – a model for end-stage liver disease; MELD-Na – MELD-sodium; iMELD – integrated MELD; MLR-iMELD – MLR-integrated iMELD; 95% CI – 95% confidence interval; AUC – area under the curve.

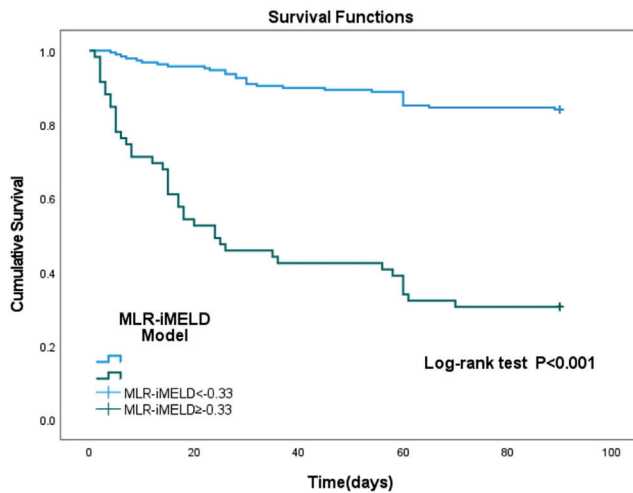


Fig. 3. Kaplan–Meier curve of the MLR-iMELD score ≥ -0.33 , MLR-iMELD score < -0.33 , and Log-rank test $p < 0.001$.

MLR – monocyte-to-lymphocyte ratio; MELD – a model for end-stage liver disease; MLR-iMELD – MLR-integrated iMELD.

clinical value than the MELD series score and the single inflammation index. Based on the AUROC results, the best cutoff value (Youden's index) for identifying MLR-iMELD was -0.33 (sensitivity: 0.577; specificity: 0.898). Patients were divided into 2 groups (MLR-iMELD ≥ -0.33 and MLR-iMELD < -0.33) according to the preselected cutoff points. In order to verify the effectiveness of the model, we further compared the 90-day survival rates of the 2 groups of patients. The Kaplan–Meier curves found that patients with MLR-iMELD scores higher than the cutoff value of -0.33 had a greater risk of poor prognosis (Fig. 3).

Discussion

It is well known that ACLF is a clinical syndrome with acute onset, rapid progression and poor prognosis. The prognosis and treatment of ACLF according to various causes of chronic liver disease are different. Due to the high rate of HBV infection in the Asia–Pacific region, there is also a high incidence of HBV-ACLF in this region.¹⁹ With the proposed systemic inflammation hypothesis, systemic inflammation is considered to be related to the disease progression and prognosis of ACLF. Systemic inflammation caused by pathogen-associated molecular patterns (PAMPs) and damage-associated molecular patterns (DAMPs) induced by certain events (such as infection, viral reactivation, alcohol consumption, etc.) is an important factor, and it can act indirectly through changes in circulatory function and metabolism, as well as directly induce tissue damage.²⁰ In patients with chronic HBV infection, acute exacerbation or recurrence of HBV is the main factor causing acute liver deterioration.²¹ The reactivation of HBV

or superposition with other liver diseases will aggravate hepatocyte necrosis, which leads to the release of circulating DAMPs and promotes an inflammatory response. At the same time, during the process of chronic liver disease progression, the body gradually shows cirrhosis-associated immune dysfunction (CAID), which will create opportunities for HBV reactivation and bacterial infection, so some HBV-ACLF patients may simultaneously have multiple causes that synergistically promote the development of ACLF.^{22,23} Among the 420 patients with ACLF in the PREDICT study, 65% had obvious systemic inflammatory triggers, such as bacterial infection and gastrointestinal bleeding, while 35% had no obvious triggers. However, the patients without obvious triggers still had features of systemic inflammation.²⁴ Meanwhile, the PREDICT study showed that inflammation occurs in the progression of acute decompensated cirrhosis to ACLF.^{25,26} Evidence from a prospective study also indicates that inflammation severity is the most important predictor of ACLF and gastrointestinal bleeding in acute decompensated patients.²⁷ Wu et al. found that NLR and MLR were associated with the risk of death in patients with acute exacerbations of chronic HBV, where NLR was an independent predictor of progression to ACLF.²⁸ However, the impact of inflammation on HBV-ACLF disease development remains to be further explored.

First of all, for this study, statistical differences were found in age, platelets, lymphocytes, neutrophils, monocytes, albumin, prealbumin, ALT, AST, TBil, serum creatinine, PT, INR, PWR, NLR, MLR, and MELD serial scores between the 2 groups (Table 1). Among them, the patients in the death group were older and had lower protein levels, more severe coagulopathy and higher inflammation levels. Platelet levels were higher in the survival group; meanwhile, our previous study found that platelets can effectively predict the survival of HBV-ACLF patients 180 days after plasma exchange.²⁹ The reason may be that platelets are related to liver regeneration, infection, systemic inflammatory response, and immune diseases.^{30,31} In addition, serum ALT levels were higher in the survival group, and we speculated that ALT is a protein with enzyme activity synthesized by liver cells. The higher the ALT level, the more sensitive the liver synthesis function will be, which has a certain predictive effect on the liver function of HBV-ACLF patients.

In analyzing the correlation between inflammatory markers and MELD scores, we found that NLR, MLR, SII, PNI, leukocyte count, neutrophil count, and monocyte count were positively correlated with MELD scores, while PWR and lymphocyte count were negatively correlated with MELD scores. This also proves that as the MELD score increases, inflammatory indicator levels also increase, but indicators related to immune function and nutritional synthesis function will continue to decrease.

Next, considering the progress made in the field of predicting ACLF prognosis with inflammatory markers,^{30,32}

we compared the widely used markers at present. Our findings indicated that NLR, MLR, MELD score, MELD-Na score, and iMELD score were significantly higher in the death group. This validated the results of previous studies.^{25–28} In our study, MLR had better statistical significance than NLR, both in relation to MELD score and in the analysis of 90-day mortality factors. Therefore, we further carried out a multivariate analysis of MLR and established a new MLR-iMELD model. The MLR is the ratio of monocytes to lymphocytes. Liver resident macrophages account for more than 80% of the total number of macrophages in the body, and they make a difference in liver fibrosis and inflammatory immune response.³² Macrophages can be activated by various stimuli, such as bacteria, viruses or necrotic tissue. The inflammatory response of the body can trigger the release of monocytes from the bone marrow to the peripheral blood so that monocytes in the blood can differentiate into tissue macrophages to play an immune role.^{32–34} Just recently, Niehaus et al. described a subpopulation of lymphocytes, mucosal-associated invariant T (MAIT) cells, that were markedly reduced in cirrhotic patients, and the number of MAIT cells decreased with declining liver function.³⁵ For patients with ACLF, liver cell necrosis can cause the release of a large number of inflammatory factors, thereby activating the immune inflammatory response in the body and inducing a large number of granulocytes to migrate from the bone marrow to the peripheral blood, giving rise to a significant decrease in the number of peripheral blood lymphocytes.³⁶ Therefore, changes in monocytes and lymphocytes have certain value in evaluating the prognosis of HBV-ACLF patients. The MLR-iMELD model outperformed the MELD series scores in predicting patients' 90-day survival. Furthermore, patients with high MLR-iMELD scores (≥ -0.33) had a poorer 90-day prognosis.

Limitations

First, this was a single-center observational retrospective study with a relatively small sample size. Second, we included only the baseline data of patients for analysis, so the dynamics of patients were not observed. Third, the assessment of inflammation in our study was based on routine blood tests, so whether other inflammatory biomarkers can better predict prognosis needs to be further explored.

Conclusions

Higher inflammation levels predicted a higher 90-day mortality risk in HBV-ACLF patients. The MLR-iMELD model can better predict the 90-day survival of HBV-ACLF patients than other composite inflammatory indicators.

The clinical value of evaluating inflammation-related indicators may provide a valuable supplement for the assessment of disease status in HBV-ACLF patients.

Supplementary data

The Supplementary materials are available at <https://doi.org/10.5281/zenodo.13627516>. The package includes the following files:

Supplementary Table 1. The original data of this study.

Supplementary Table 2. Normality test of baseline data in survival and death groups. Through normality test, it was found that the statistical value of normality test in the baseline data of the 2 groups of patients was < 0.05 , so they did not conform to the normal distribution.

Supplementary Fig. 1. Test the extreme outliers in the logistic regression hypothesis. We found that there were 8 observations where the studentized residuals were greater than 2 times the SD, but we kept them in the analysis.

Supplementary Fig. 2. Multicollinearity among explanatory variables. Through collinearity diagnosis, we found that all independent variables VIF were less than 5, and the degree of collinearity between independent variables was small.

Supplementary Fig. 3. Box–Tidwell test on variables. A total of 19 items were included in the model analysis in this study, including 9 independent variables: age, MLR, WBC, neutrophil, PLT, albumin, ALT, AST, and iMELD; 9 interaction terms: age*lnage, lnMLR*MLR, lnWBC*WBC, ln neutrophil*neutrophil, lnPLT*PLT, ln albumin*albumin, lnALT*ALT, lnAST*AST, and ln iMELD*iMELD; and intercept term (Constant). Therefore, in this study, it is recommended that the significance level should be $\alpha = 0.00263$ (0.05/19). Based on this significance level, the p-value of all interaction terms in this study is higher than 0.00263, so there is a linear relationship between all continuous independent variables and the logit conversion value of the dependent variable.

Data availability


The datasets generated and/or analyzed during the current study are available from the corresponding author on reasonable request.


Consent for publication


Not applicable.


ORCID iDs

Huaqian Xu  <https://orcid.org/0009-0007-0404-1407>


Xue Li  <https://orcid.org/0000-0002-0952-2687>

Yue Zhuo  <https://orcid.org/0009-0004-6863-3741>

Chunyan Li  <https://orcid.org/0009-0000-1701-6517>

Chengzhi Bai  <https://orcid.org/0000-0001-5785-3002>

Jie Chen  <https://orcid.org/0009-0001-5445-2972>

Shanhong Tang  <https://orcid.org/0000-0001-6652-2942>

References

- Arroyo V, Moreau R, Jalan R. Acute-on-chronic liver failure. *N Engl J Med*. 2020;382(22):2137–2145. doi:10.1056/NEJMr1914900
- Sarin SK, Choudhury A, Sharma MK, et al; APASL ACLF Research Consortium (AARC) for APASL ACLF working Party. Acute-on-chronic liver failure. Consensus recommendations of the Asian Pacific association for the study of the liver (APASL): An update. *Hepatol Int*. 2019;13(4):353–390. doi:10.1007/s12072-019-09946-3
- Wong MCS, Huang JLW, George J, et al. The changing epidemiology of liver diseases in the Asia-Pacific region. *Nat Rev Gastroenterol Hepatol*. 2019;16(1):57–73. doi:10.1038/s41575-018-0055-0
- Wang X, Sun M, Yang X, et al. Value of liver regeneration in predicting short-term prognosis for patients with hepatitis B-related acute-on-chronic liver failure. *Biomed Res Int*. 2020;2020:5062873. doi:10.1155/2020/5062873
- Zaccherini G, Weiss E, Moreau R. Acute-on-chronic liver failure: Definitions, pathophysiology and principles of treatment. *JHEP Rep*. 2021;3(1):100176. doi:10.1016/j.jhepr.2020.100176
- Zhang J, Qiu Y, He X, Mao W, Han Z. Platelet-to-white blood cell ratio: A novel and promising prognostic marker for HBV-associated decompensated cirrhosis. *Clin Lab Anal*. 2020;34(12):e23556. doi:10.1002/jcla.23556
- Sun J, Guo H, Yu X, et al. A neutrophil-to-lymphocyte ratio-based prognostic model to predict mortality in patients with HBV-related acute-on-chronic liver failure. *BMC Gastroenterol*. 2021;21(1):422. doi:10.1186/s12876-021-02007-w
- Ding L, Deng X, Wang K, et al. Preoperative systemic inflammatory markers as a significant prognostic factor after TURBT in patients with non-muscle-invasive bladder cancer. *J Inflamm Res*. 2023;16:283–296. doi:10.2147/JIR.S393511
- Cai J, Wang K, Han T, Jiang H. Evaluation of prognostic values of inflammation-based makers in patients with HBV-related acute-on-chronic liver failure. *Medicine (Baltimore)*. 2018;97(46):e13324. doi:10.1097/MD.00000000000013324
- Bernsmeier C, Cavazza A, Fatourou EM, et al. Leucocyte ratios are biomarkers of mortality in patients with acute decompensation of cirrhosis and acute-on-chronic liver failure. *Aliment Pharmacol Ther*. 2020;52(5):855–865. doi:10.1111/apt.15932
- Zhou YX, Li WC, Xia SH, et al. Predictive value of the Systemic Immune Inflammation Index for adverse outcomes in patients with acute ischemic stroke. *Front Neurol*. 2022;13:836595. doi:10.3389/fneur.2022.836595
- Zhu S, Cheng Z, Hu Y, et al. Prognostic value of the Systemic Immune-Inflammation Index and Prognostic Nutritional Index in patients with medulloblastoma undergoing surgical resection. *Front Nutr*. 2021;8:754958. doi:10.3389/fnut.2021.754958
- Wang D, Hu X, Xiao L, et al. Prognostic Nutritional Index and Systemic Immune-Inflammation Index predict the prognosis of patients with HCC. *J Gastrointest Surg*. 2021;25(2):421–427. doi:10.1007/s11605-019-04492-7
- Peng Y, Qi X, Tang S, et al. Child–Pugh, MELD, and ALBI scores for predicting the in-hospital mortality in cirrhotic patients with acute-on-chronic liver failure. *Exp Rev Gastroenterol Hepatol*. 2016;10(8):971–980. doi:10.1080/17474124.2016.1177788
- Krishnan A, Woreta TA, Vaidya D, et al. MELD or MELD-Na as a predictive model for mortality following transjugular intrahepatic portosystemic shunt placement. *J Clin Transl Hepatol*. 2022;11(1):38–44. doi:10.14218/JCTH.2021.00513
- Perdigoto DN, Figueiredo P, Tomé L. The role of the CLIF-C OF and the 2016 MELD in prognosis of cirrhosis with and without acute-on-chronic liver failure. *Ann Hepatol*. 2019;18(1):48–57. doi:10.5604/01.3001.0012.7862
- Li J, Liang X, You S, et al. Development and validation of a new prognostic score for hepatitis B virus-related acute-on-chronic liver failure. *J Hepatol*. 2021;75(5):1104–1115. doi:10.1016/j.jhep.2021.05.026
- Hernaez R, Solà E, Moreau R, Ginès P. Acute-on-chronic liver failure: An update. *Gut*. 2017;66(3):541–553. doi:10.1136/gutjnl-2016-312670
- Tang X, Li H, Deng G, et al. New algorithm rules out acute-on-chronic liver failure development within 28 days from acute decompensation of cirrhosis. *J Clin Transl Hepatol*. 2022;11(3):550–559. doi:10.14218/JCTH.2022.00196
- Engelmann C, Clària J, Szabo G, Bosch J, Bernardi M. Pathophysiology of decompensated cirrhosis: Portal hypertension, circulatory dysfunction, inflammation, metabolism and mitochondrial dysfunction. *J Hepatol*. 2021;75(Suppl 1):S49–S66. doi:10.1016/j.jhep.2021.01.002
- Lei JH, Peng F, Chen Z, Xiao XQ. Is HBV viral load at admission associated with development of acute-on-chronic liver failure in patients with acute decompensation of chronic hepatitis B related cirrhosis? *BMC Infect Dis*. 2019;19(1):363. doi:10.1186/s12879-019-3988-1
- Piano S, Mahmud N, Caraceni P, Tonon M, Mookerjee RP. Mechanisms and treatment approaches for ACLF [Published online as ahead of print on September 16, 2023]. *Liver Int*. 2023. doi:10.1111/liv.15733
- Granito A, Muratori P, Muratori L. Acute-on-chronic liver failure: A complex clinical entity in patients with autoimmune hepatitis. *J Hepatol*. 2021;75(6):1503–1505. doi:10.1016/j.jhep.2021.06.035
- Trebicka J, Fernandez J, Papp M, et al. PREDICT identifies precipitating events associated with the clinical course of acutely decompensated cirrhosis. *J Hepatol*. 2021;74(5):1097–1108. doi:10.1016/j.jhep.2020.11.019
- Trebicka J, Fernandez J, Papp M, et al. The PREDICT study uncovers three clinical courses of acutely decompensated cirrhosis that have distinct pathophysiology. *J Hepatol*. 2020;73(4):842–854. doi:10.1016/j.jhep.2020.06.013
- Arroyo V, Angeli P, Moreau R, et al. The systemic inflammation hypothesis: Towards a new paradigm of acute decompensation and multi-organ failure in cirrhosis. *J Hepatol*. 2021;74(3):670–685. doi:10.1016/j.jhep.2020.11.048
- Zanetto A, Pelizzaro F, Campello E, et al. Severity of systemic inflammation is the main predictor of ACLF and bleeding in individuals with acutely decompensated cirrhosis. *J Hepatol*. 2023;78(2):301–311. doi:10.1016/j.jhep.2022.09.005
- Wu W, Yan H, Zhao H, et al. Characteristics of systemic inflammation in hepatitis B-precipitated ACLF: Differentiate it from No-ACLF. *Liver Int*. 2018;38(2):248–257. doi:10.1111/liv.13504
- Li X, Li H, Zhu Y, Xu H, Tang S. PLT counts as a predictive marker after plasma exchange in patients with hepatitis B virus-related acute-on-chronic liver failure. *J Clin Med*. 2023;12(3):851. doi:10.3390/jcm12030851
- Greco E, Lupia E, Bosco O, Vizio B, Montrucchio G. Platelets and multi-organ failure in sepsis. *Int J Mol Sci*. 2017;18(10):2200. doi:10.3390/ijms18102200
- Li X, Zhang L, Pu C, Tang S. Liver transplantation in acute-on-chronic liver failure: Timing of transplantation and selection of patient population. *Front Med (Lausanne)*. 2022;9:1030336. doi:10.3389/fmed.2022.1030336
- Grønbaek H, Rødgaard-Hansen S, Aagaard NK, et al. Macrophage activation markers predict mortality in patients with liver cirrhosis without or with acute-on-chronic liver failure (ACLF). *J Hepatol*. 2016;64(4):813–822. doi:10.1016/j.jhep.2015.11.021
- Kratofil RM, Kubes P, Deniset JF. Monocyte conversion during inflammation and injury. *Arterioscler Thromb Vasc Biol*. 2017;37(1):35–42. doi:10.1161/ATVBAHA.116.308198
- Triantafyllou E, Woollard KJ, McPhail MJW, Antoniadis CG, Possamai LA. The role of monocytes and macrophages in acute and acute-on-chronic liver failure. *Front Immunol*. 2018;9:2948. doi:10.3389/fimmu.2018.02948
- Niehaus CE, Strunz B, Cornillet M, et al. MAIT cells are enriched and highly functional in ascites of patients with decompensated liver cirrhosis. *Hepatology*. 2020;72(4):1378–1393. doi:10.1002/hep.31153
- Schwabe RF, Luedde T. Apoptosis and necroptosis in the liver: A matter of life and death. *Nat Rev Gastroenterol Hepatol*. 2018;15(12):738–752. doi:10.1038/s41575-018-0065-y

Impact of intravenous infusion of lidocaine on intrapulmonary shunt and postoperative cognitive function in patients undergoing one-lung ventilation

Dawei Yang^{1,A,B,D}, Qian Yang^{1,A,C}, Yixing Wang^{1,B,C}, Fengxia Liu^{1,C,E}, Zhi Xing^{1,B,C}, Shitong Li^{2,E,F}, Jianyou Zhang^{1,A,B,D–F}

¹ Department of Anesthesiology, Affiliated Hospital of Yangzhou University, China

² Department of Anesthesiology, First People's Hospital Affiliated to Shanghai Jiaotong University, China

A – research concept and design; B – collection and/or assembly of data; C – data analysis and interpretation;

D – writing the article; E – critical revision of the article; F – final approval of the article

Advances in Clinical and Experimental Medicine, ISSN 1899–5276 (print), ISSN 2451–2680 (online)

Adv Clin Exp Med. 2025;34(7):1139–1144

Address for correspondence

Dawei Yang

E-mail: yangdawei307@163.com

Funding sources

None declared

Conflict of interest

None declared

Received on November 14, 2022

Reviewed on August 20, 2024

Accepted on September 2, 2024

Published online on November 6, 2024

Abstract

Background. Intravenous infusion of lidocaine as an anesthesia adjuvant can improve patient outcomes, but its impact on intrapulmonary shunt during one-lung ventilation (OLV) has not been clarified.

Objectives. To determine the effect of intravenous lidocaine infusion on intrapulmonary shunt during OLV and postoperative cognitive function in video-assisted thoracoscopic surgery (VATS).

Materials and methods. Sixty patients who underwent OLV for thoracic surgery were randomized to receive intravenous infusion of lidocaine (lidocaine group, $n = 30$) or normal saline (control group, $n = 30$) for anesthesia induction. Arterial and venous blood gases were measured during two-lung ventilation and at 15 and 30 min after OLV (OLV + 15 and OLV + 30). The Mini-Mental State Examination was administered before the surgery and at postoperative 12 months to assess patient cognitive function.

Results. No significant difference was found in intrapulmonary shunt fraction (Q_s/Q_t) between the lidocaine group and the control group at OLV + 15 ($p = 0.493$) and OLV + 30 ($p = 0.754$). The lidocaine group used significantly lower doses of propofol and remifentanyl compared to the control group (both $p < 0.001$). Furthermore, no significant difference was observed in the incidence of postoperative cognitive dysfunction between the lidocaine group and the control group at 1 year post-operation (3.3% vs 6.7%, $p = 0.554$).

Conclusions. Intravenous lidocaine administered in VATS had no significant impact on intrapulmonary shunt during OLV or postoperative cognitive function. However, it significantly reduced the doses of anesthetics used during the surgery.

Key words: cognitive function, lidocaine, one-lung ventilation, intrapulmonary shunt

Cite as

Yang D, Yang Q, Wang Y, et al. Impact of intravenous infusion of lidocaine on intrapulmonary shunt and postoperative cognitive function in patients undergoing one-lung ventilation. *Adv Clin Exp Med.* 2025;34(7):1139–1144. doi:10.17219/acem/192879

DOI

10.17219/acem/192879

Copyright

Copyright by Author(s)

This is an article distributed under the terms of the Creative Commons Attribution 3.0 Unported (CC BY 3.0) (<https://creativecommons.org/licenses/by/3.0/>)

Background

One-lung ventilation (OLV) is necessary for improved visualization in video-assisted thoracoscopic surgery (VATS). However, it can increase intrapulmonary shunt, leading to postoperative pulmonary complications.^{1,2} An intrapulmonary shunt is defined as the mixing of unoxygenated blood flow with oxygenated blood within the lungs. This phenomenon has the potential to reduce oxygenation levels and, consequently, may result in the development of hypoxemia. Hypoxic pulmonary vasoconstriction is an intrinsic homeostasis mechanism of the pulmonary vasculature. Pulmonary arteries contract due to alveolar hypoxia and transfer blood to the pulmonary segments with higher oxygenation, thereby optimizing ventilation-perfusion matching. In thoracoscopic surgery, hypoxic pulmonary vasoconstriction is an important mechanism of reducing intrapulmonary shunt and maintaining oxygenation in OLV.

Lidocaine is a promising agent used for enhanced recovery after surgery, showing benefits across various surgical procedures. Intravenous lidocaine is noninferior to thoracic epidural analgesia for acute postoperative pain control in major abdominal surgery at 24 h postoperatively.³ It can also reduce the use of opioids in the perioperative period and alleviate postoperative nausea and vomiting in thoracic surgery.⁴ However, the impact of lidocaine on hypoxic pulmonary vasoconstriction and intrapulmonary shunt in patients undergoing OLV is still unknown.

Our study aimed to investigate the impact of intravenous lidocaine on intrapulmonary shunt and cognitive function during OLV in VATS.

Materials and methods

Patients

This is a randomized, double-blind, placebo-controlled clinical trial evaluating the impact of intravenous infusion of lidocaine compared to normal saline on intrapulmonary shunt and postoperative cognitive function in patients undergoing OLV. This study complied with the Declaration of Helsinki and was approved by the ethics committee of Affiliated Hospital of Yangzhou University, China (approval No. 2018-YKL012-01). Informed consent was obtained from each participant. The inclusion criteria consisted of: 1) scheduled video-assisted thoracoscopic resection of pulmonary tumors under general anesthesia; 2) American Society of Anesthesiologists (ASA) physical status classification grades I–II; 3) age between 20 and 70 years; and 4) body mass index (BMI) between 18 and 25 kg/m². Patients were excluded for: 1) preoperative comorbidities involving vital organs (such as diabetes and severe liver and kidney diseases); 2) moderate or more severe anemia; and 3) the forced expiratory volume in the 1st 2nd/forced vital capacity ratio <65%.

Recruitment and randomization

Patients who underwent treatment for pulmonary tumors at our hospital between August 2018 and March 2020 were approached for recruitment. Each patient was randomly allocated in a 1:1 ratio to the lidocaine group or the normal saline group through a computer-generated randomization sequence. Normal saline and lidocaine were preprepared by an assistant and stored in indistinguishable vials. The assistant was not involved in matters other than drug preparation.

Anesthesia protocol

Patients were attached to a standard ASA monitor. Under ultrasound guidance, the radial artery and right internal jugular vein were accessed. The right internal jugular vein catheter measured 18 cm in length, with the catheter tip positioned in the right atrium confirmed with transthoracic echocardiography. Invasively measured mean arterial pressure (MAP), heart rate, oxygen saturation measured with pulse oximetry (SpO₂), and central venous pressure were monitored. The Narcotrend index (NI) was monitored using a Narcotrend® monitor (MT MonitorTechnik GmbH & Co. KG, Hannover, Germany).

For anesthesia induction, a bolus of 1.5 mg/kg lidocaine was administered in the lidocaine group, followed by continuous infusion of 1.5 mg/kg/h lidocaine combined with 0.05 mg/kg midazolam, 1.5–2 mg/kg propofol, 0.3 µg/kg sufentanil, and 0.15 mg/kg cisatracurium. Normal saline instead of lidocaine was administered in the control group, with the doses of other anesthetic agents unchanged.

Intubation was performed with a double-lumen endobronchial tube. Patients were mechanically ventilated with a tidal volume of 8 mL/kg, an inhaled oxygen concentration (FiO₂) of 100%, a respiratory ratio of 1:2, and a respiratory rate of 10–12 breaths/min. During OLV, the non-ventilated branch of the double-lumen tube was open to the atmosphere. The respiratory rate was adjusted to 14–16 breaths/min, while other respiratory parameters remained unchanged, and the partial pressure of end-tidal carbon dioxide (PETCO₂) was maintained at 35–45 mm Hg.

Propofol, remifentanyl and cisatracurium (0.1 mg/kg/h) were used for the maintenance of anesthesia. The doses of propofol and remifentanyl were tuned to keep the NI between 26 and 46 and the MAP within ±20% of the baseline blood pressure. The central venous pressure was maintained at 5–12 cm H₂O with intravenous rehydration (crystalline : colloidal = 2 : 1). Cisatracurium was stopped approx. 30 min before the end of surgery, and other anesthetics were discontinued upon completion of the procedure.

Blood gas analysis

Blood samples were collected from the radial artery and internal jugular vein while the patient was in a lateral

position with two-lung ventilation (TLV), after 15 min of OLV (OLV + 15) and after 30 min of OLV (OLV + 30). Blood gas analysis was performed using a GEM 3500 blood gas analyzer (Instrumentation Laboratory Company, Bedford, USA). The total doses of propofol and remifentanyl (TLV to OLV + 30) and the post-anesthesia recovery time (the time from drug withdrawal to extubation) were recorded. The extubation criteria were: patients had regained consciousness; spontaneous breathing frequency >12 breaths/min; PETCO₂ ≤ 45 mm Hg; SpO₂ > 95%; tidal volume >6 mL/kg; patients could elevate their head for a min of 5 s.

Outcome measures

Intrapulmonary shunt

The intrapulmonary shunt fraction (Qs/Qt) was calculated as $Qs/Qt = (CcO_2 - CaO_2)/(CcO_2 - CvO_2) \times 100\%$, where CcO₂ is the pulmonary capillary oxygen content, CaO₂ is the arterial oxygen content and CvO₂ is the mixed venous oxygen content (replaced with the oxygen content in the right atrium):

$$CcO_2 = 1.36 \times Hb \times SaO_2 + PaO_2 \times 0.0031$$

$$CaO_2 = 1.36 \times Hb \times SaO_2 + PaO_2 \times 0.0031$$

$$CvO_2 = 1.36 \times Hb \times SvO_2 + PvO_2 \times 0.0031$$

In these formulas, 1.36 is the oxygen-carrying capacity of hemoglobin (mL/g); SaO₂ is the alveolar capillary oxygen saturation, which was approximated by the arterial oxygen saturation; PaO₂ is the alveolar oxygen partial pressure, which was calculated by using the formula,

$$PaO_2 = FiO_2 \times (Pb - PH_2O) - (PaCO_2/R) + [PaCO_2 \times FiO_2 \times (1 - R)/R],$$

where Pb is the atmospheric pressure (760 mmHg), PH₂O is the water vapor pressure at 37°C (47 mm Hg), R is the respiratory quotient (0.8), and PaO₂ = 713 - PaCO₂ when FiO₂ = 100%; SaO₂ is the arterial oxygen saturation; SvO₂ is the mixed venous oxygen saturation, which was equal to the saturation of the blood sample extracted from the right atrial (SvcO₂); PvO₂ is the mixed venous oxygen partial pressure, which was equal to the partial pressure of oxygen in the right atrium (PvcO₂).

Cognitive assessment

All patients were evaluated for cognitive function using a validated Chinese version of the Mini-Mental State Examination before the surgery and at 12 months postoperatively. A reduction of ≥2 points from the baseline cognitive score was regarded as postoperative cognitive dysfunction. The cognitive assessment was performed by a single anesthesiologist who was blinded to patient assignment.

Sample size

The primary outcome was intrapulmonary shunt fraction (Qs/Qt), which was 13.24 ± 5.48% in the lidocaine group and 22.36 ± 5.35% in the control group in a previous study.⁴ With a bilateral α of 0.05 and a power of 90%, the sample size was calculated as N1 = N2 = 14 for each group. Our study finally included a total of 60 patients.

Statistical analyses

Measurement data were expressed as mean and standard deviation (SD), or median and interquartile range (IQR). Categorical data were expressed as percentage. Comparisons between the lidocaine and control groups were made using the Mann–Whitney U test, 2 independent-samples Student's t-test or χ² test. Homoscedasticity was verified using Levene's test. Continuous variables were checked for normal distribution with the Shapiro–Wilk test due to the small sample size. Non-normally distributed data (p < 0.05) were analyzed with the Mann–Whitney U test, whereas normally distributed variables were compared using the 2 independent-samples t-test. All statistical analyses were performed using SPSS v. 23.0 (IBM Corp., Armonk, USA). A p < 0.05 indicated a statistically significant difference.

Results

The final analysis included 60 patients with 30 in each group. The flowchart of participant inclusion is shown in Fig. 1. No patients died or were lost to follow-up during the study. No significant difference was found in the basic characteristics between the control group and the lidocaine group (Table 1). The homoscedasticity test results are shown in Supplementary Table 1 (doi.org/10.5281/zenodo.13683171).

The blood gas analysis parameters of PaO₂ and Qs/Qt (intrapulmonary shunt fraction) in the lidocaine group and

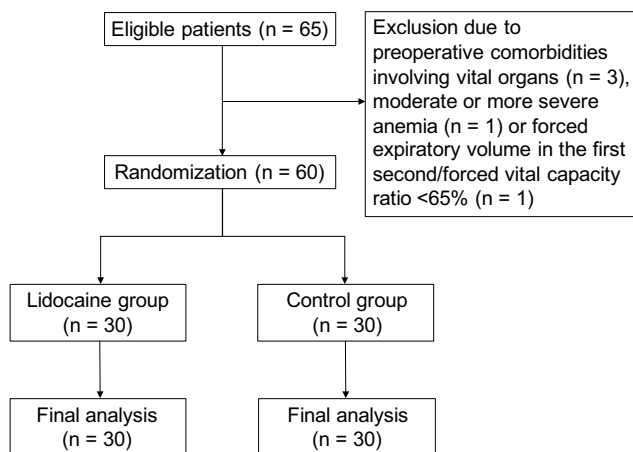


Fig. 1. Flowchart of participant inclusion

Table 1. Characteristics of the patients

Item	Control (n = 30)	Lidocaine (n = 30)	U/t	df	p-value
Age [years], median (IQR)*	48 (38, 54.8)	54.5 (40.3, 59.5)	349	/	0.135
Male/female (n) [†]	15/15	14/16	0.067	1	0.796
BMI [kg/m ²], median (IQR)*	23.7 (22.1, 24.3)	23.05 (21.1, 23.9)	367.5	/	0.222
FEV1 (% predicted), median (IQR)*	91 (87.3, 98.8)	94.5 (89, 101.8)	369.5	/	0.233
FVC (% predicted), mean \pm SD (95% CI) [#]	116.7 \pm 10.7 (112.7, 120.7)	121.6 \pm 9.5 (118.1, 125.2)	-1.88	58	0.065
FEV1/FVC (%), mean \pm SD (95% CI) [#]	80.0 \pm 4.9 (78.2, 81.9)	78.7 \pm 4.7 (77.0, 80.5)	1.51	58	0.298
Right/left lung operation (n) [†]	13/17	14/16	0.600	1	0.439
OLV time [min], mean \pm SD (95% CI) [#]	59.5 \pm 17.2 (53.1, 65.9)	57.8 \pm 17.2 (51.4, 64.3)	0.38	58	0.703
Bleeding volume [mL], median (IQR)*	80 (66.25, 90.75)	70 (61.25, 83.75)	351.5	/	0.144
Intraoperative fluid [mL], mean \pm SD (95% CI) [#]	921.0 \pm 232.6 (834.1, 1007.9)	896.0 \pm 211.9 (816.9, 975.1)	0.435	58	0.665

df – degrees of freedom; IQR – interquartile range; SD – standard deviation; 95% CI – 95% confidence interval; BMI – body mass index; FEV1 – forced expiratory volume in 1 s; FVC – forced vital capacity; OLV – one-lung ventilation; *Mann–Whitney U test; [#]two-sample t-test; [†]Pearson's χ^2 test of independence.

Table 2. Comparisons of hemodynamics between the lidocaine group and the control group

Variable	Control (n = 30)	Lidocaine (n = 30)	U/t	df	p-value
PaO ₂ [mm Hg] median (IQR)*					
OLV + 15	196.5 (140.8, 300.5)	210.0 (125.8, 280.8)	442.5	/	0.912
OLV + 30	198.5 (103.8, 269.5)	198.0 (102.8, 264.8)	426	/	0.723
Qs/Qt (%), mean \pm SD (95% CI) [#]					
OLV + 15	25.8 \pm 6.1 (23.6, 28.1)	24.7 \pm 6.4 (22.3, 27.1)	0.689	58	0.493
OLV + 30	26.6 \pm 8.6 (23.4, 29.8)	26.0 \pm 6.9 (23.4, 28.6)	0.315	58	0.754

*Mann–Whitney U test; [#]two-sample t-test; df – degrees of freedom; OLV – one-lung ventilation; IQR – interquartile range; SD – standard deviation; 95% CI – 95% confidence interval.

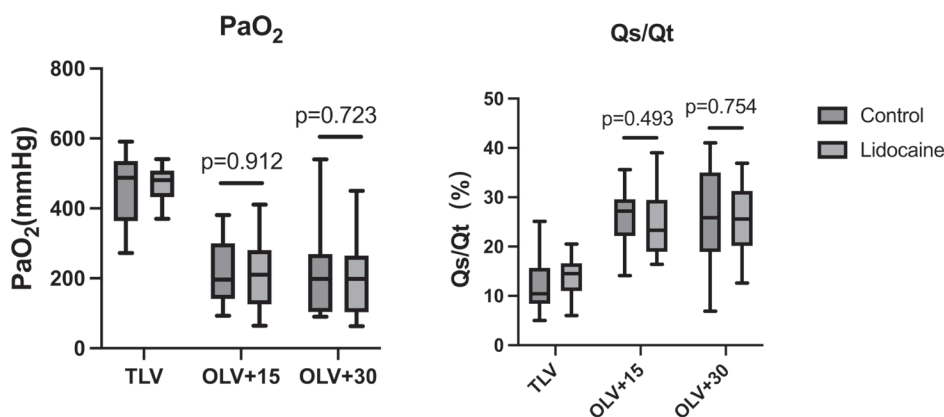


Fig. 2. Comparisons of hemodynamics between the control group and the lidocaine group during video-assisted thoracoscopic resection of pulmonary tumors

PaO₂ – alveolar oxygen partial pressure;
Qs/Qt – intrapulmonary shunt fraction.

the control group are shown in Fig. 2. During OLV, there was no significant difference between the lidocaine group and the control group in the levels of PaO₂ and Qs/Qt (Table 2).

Compared to the control group, the lidocaine group had significantly higher doses of propofol (Mann–Whitney U test, $U = 28.5$, $p < 0.001$) and remifentanyl (Mann–Whitney U test, $U = 63.0$, $p < 0.001$) infused from TLV to OLV + 30. The post-anesthesia recovery time did not differ significantly between the 2 groups (2-sample t-test, $t = -0.635$, $p = 0.528$) (Table 3). Also, the 1-year incidence of postoperative cognitive dysfunction was not significantly different between the lidocaine group

and the control group (1/30, 3.3% vs 2/30, 6.7%; χ^2 test of independence with Yates's correction, $\chi^2 = 0$, $df = 1$, $p = 1.0$).

Discussion

Our study showed that the use of intravenous lidocaine did not significantly increase intrapulmonary shunt during OLV in VATS. Previous animal studies showed that intravenous infusion of lidocaine enhanced the effect of hypoxic pulmonary vasoconstriction and affected intrapulmonary

Table 3. Doses of propofol and remifentanyl and post-anesthesia recovery time

Item	Control (n = 30)	Lidocaine (n = 30)	U/t	df	p-value
Propofol [mg], median (IQR) [#]	194.9 (171.7, 212.9)	121.2 (104.1, 129.1)	28.5	/	<0.001
Remifentanyl [μg], median (IQR) [#]	283.4 (256.8, 319.7)	129.8 (102.2, 173.1)	63	/	<0.001
Post-anesthesia recovery time [min], mean ±SD (95% CI) [*]	9.9 ±2.4 (9.0, 10.8)	10.3 ±2.8 (9.3, 11.4)	0.635	58.0	0.528

df – degrees of freedom; IQR – interquartile range; SD – standard deviation; 95% CI – 95% confidence interval; [#]Mann–Whitney U test; ^{*}two-sample t-test.

shunt.^{5,6} However, there are conflicting opinions regarding the appropriate doses of lidocaine needed to enhance the effects of hypoxic pulmonary vasoconstriction. Also, further investigation has revealed that amide anesthetics, such as lidocaine, are vasoconstrictive at low concentrations and vasodilative at high concentrations.^{7,8} This biphasic effect of lidocaine has also been observed in swine pulmonary arteries, where concentrations of 1 μg/mL led to vasoconstriction, and concentrations of 10–100 μg/mL resulted in vasodilation.⁹ Our study found that intravenous lidocaine did not have a significant impact on intrapulmonary shunt during OLV. This lack of effect may be attributed to the relatively low dose of lidocaine used in our study.

We found that lidocaine significantly reduced the doses of propofol and remifentanyl during video-assisted thoracoscopic resection of pulmonary tumors, likely due to its sedative effect. When administered intravenously to healthy individuals, lidocaine can provide a certain level of analgesia and induce dizziness in over half of the study participants once its plasma concentration reaches 1.5 μg/mL.¹⁰ These results indicate that lidocaine, at clinically relevant concentrations, can induce sedation, leading to a deepening of anesthesia. Forster et al.¹¹ has also suggested that intravenous lidocaine can reduce propofol doses by half during painless colonoscopy, which is consistent with the results of our study. Additionally, we found that intravenous lidocaine did not prolong post-anesthesia recovery time, consistent with previous research.¹²

Animal studies have demonstrated that the intravenous infusion of lidocaine, in combination with adenosine and magnesium, significantly reduces cerebral oxygen consumption.¹³ Additionally, in research focusing on cerebroprotection using an in vitro cerebral ischemia model, lidocaine was found to decrease neuronal damage during cerebral ischemia.¹⁴ Despite the neuroprotective properties of lidocaine, the impact of continuous intravenous lidocaine infusion on postoperative cognitive function in patients remains a topic of debate. Wang et al.¹⁵ conducted a study where patients received a continuous intravenous infusion of lidocaine at a rate of 2 mg/kg/h during laparoscopic colorectal cancer surgery until the conclusion of the procedure. Their findings revealed a significant reduction in the occurrence of cognitive dysfunction within 7 days post-surgery. However, in a multicenter trial involving lidocaine administration in cardiac surgery, where study participants were given 1 mg/kg of lidocaine after

tracheal intubation followed by a continuous infusion, researchers discovered that the use of intravenous lidocaine during and after cardiac surgery did not diminish postoperative cognitive decline at 6 weeks.¹⁶ Similarly, our study on continuous lidocaine infusion during pulmonary surgery found no impact on postoperative cognitive function within a year.

A meta-analysis summarized the dose ranges for intraoperative intravenous lidocaine, indicating a continuous infusion at a rate of 1.5–3.0 mg/kg/h after a bolus injection of 0–2.0 mg/kg.¹⁷ It was found that the plasma concentrations of lidocaine were much lower than the toxic level of 5 μg/mL despite continuous infusion during surgeries.^{18,19} Our study used the same dose of lidocaine and found no obvious adverse effects.

Limitations

There are some limitations to our study. First, our patients were relatively young because older patients are reluctant to participate in clinical trials. This may have compromised the generalizability of our findings. Second, the single-center design and small sample size are additional limitations that should be considered when interpreting the results. Third, the statistical analysis in this study is exploratory and does not incorporate multiple comparisons correction. Hence, the interpretation of the results should be exercised with caution due to the potential for uncontrolled type I error probability, which could also impact the validity of any future meta-analyses. This exploratory analysis provides a foundation for future research in this field.

Conclusions

Our study found that intravenous lidocaine had no significant impact on intrapulmonary shunt during OLV in VATS. However, it significantly reduced the doses of propofol and remifentanyl required. Furthermore, the supplementary use of lidocaine in our patients did not lead to a decline in cognitive function at 1 year post-operation.

Supplementary data

The Supplementary materials are available at <https://doi.org/10.5281/zenodo.13683171>. The package includes the following file:

Supplementary Table 1. Tests of homogeneity of variances (based on mean).

Data availability

The datasets generated and/or analyzed during the current study are available from the corresponding author on reasonable request.

Consent for publication

Not applicable.

ORCID iDs

Dawei Yang  <https://orcid.org/0000-0002-8462-8385>
 Qian Yang  <https://orcid.org/0009-0003-4946-5781>
 Yixing Wang  <https://orcid.org/0000-0002-5165-865X>
 Fengxia Liu  <https://orcid.org/0009-0003-1000-4638>
 Zhi Xing  <https://orcid.org/0000-0002-7606-2094>
 Shitong Li  <https://orcid.org/0009-0001-2143-2596>
 Jianyou Zhang  <https://orcid.org/0000-0002-5570-7885>

References

- Campos JH, Feider A. Hypoxia during one-lung ventilation: A review and update. *J Cardiothorac Vasc Anesth*. 2018;32(5):2330–2338. doi:10.1053/j.jvca.2017.12.026
- Lederman D, Easwar J, Feldman J, Shapiro V. Anesthetic considerations for lung resection: Preoperative assessment, intraoperative challenges and postoperative analgesia. *Ann Transl Med*. 2019;7(15):356–356. doi:10.21037/atm.2019.03.67
- Casas-Arroyave FD, Osorno-Upegui SC, Zamudio-Burbano MA. Therapeutic efficacy of intravenous lidocaine infusion compared with thoracic epidural analgesia in major abdominal surgery: A noninferiority randomised clinical trial. *Br J Anaesth*. 2023;131(5):947–954. doi:10.1016/j.bja.2023.07.032
- Xie Y, Han L, Zhao Y, et al. Effect of ultrasound-guided stellate ganglion block on lung protection for patients undergoing one-lung ventilation. *Am J Transl Res*. 2024;16(3):794–808. doi:10.62347/UFZF5671
- Bindeslev L, Cannon D, Sykes MK. Reversal of nitrous oxide-induced depression of hypoxic pulmonary vasoconstriction by lignocaine hydrochloride during collapse and ventilation hypoxia of the left lower lobe. *Br J Anaesth*. 1986;58(4):451–456. doi:10.1093/bja/58.4.451
- Yukioka H, Hayashi M, Tatekawa S, Fujimori M. Effects of lidocaine on pulmonary circulation during hyperoxia and hypoxia in the dog. *Reg Anesth*. 1996;21(4):327–337. PMID:8837191.
- Konrad C, Schuepfer G, Neuburger M, Schley M, Schmelz M, Schmeck J. Reduction of pulmonary edema by short-acting local anesthetics. *Ren Anesth Pain Med*. 2006;31(3):254–259. doi:10.1016/j.rapm.2006.01.003
- Yu J, Tokinaga Y, Kuriyama T, Uematsu N, Mizumoto K, Hatano Y. Involvement of Ca^{2+} sensitization in ropivacaine-induced contraction of rat aortic smooth muscle. *Anesthesiology*. 2005;103(3):548–555. doi:10.1097/00000542-200509000-00018
- Satoh K, Kamada S, Kumagai M, Sato M, Kuji A, Joh S. Effect of lidocaine on swine lingual and pulmonary arteries. *J Anesth*. 2015;29(4):529–534. doi:10.1007/s00540-014-1965-9
- Wallace MS, Dyck BJ, Rossi SS, Yaksh TL. Computer-controlled lidocaine infusion for the evaluation of neuropathic pain after peripheral nerve injury. *Pain*. 1996;66(1):69–77. doi:10.1016/0304-3959(96)02980-6
- Forster C, Vanhaudenhuyse A, Gast P, et al. Intravenous infusion of lidocaine significantly reduces propofol dose for colonoscopy: A randomised placebo-controlled study. *Br J Anaesth*. 2018;121(5):1059–1064. doi:10.1016/j.bja.2018.06.019
- George S, Singh G, Mathew B, Fleming D, Korula G. Comparison of the effect of lignocaine instilled through the endotracheal tube and intravenous lignocaine on the extubation response in patients undergoing craniotomy with skull pins: A randomized double blind clinical trial. *J Anaesthesiol Clin Pharmacol*. 2013;29(2):168. doi:10.4103/0970-9185.111668
- Letson HL, Granfeldt A, Jensen TH, Mattson TH, Dobson GP. Adenosine, lidocaine, and magnesium support a high flow, hypotensive, vasodilatory state with improved oxygen delivery and cerebral protection in a pig model of noncompressible hemorrhage. *J Surg Res*. 2020;253:127–138. doi:10.1016/j.jss.2020.03.048
- Cao H, Kass IS, Cottrell JE, Bergold PJ. Pre- or postinsult administration of lidocaine or thiopental attenuates cell death in rat hippocampal slice cultures caused by oxygen-glucose deprivation. *Anesth Analg*. 2005;101(4):1163–1169. doi:10.1213/01.ane.0000167268.61051.41
- Wang XX, Dai J, Wang Q, et al. Intravenous lidocaine improves postoperative cognition in patients undergoing laparoscopic colorectal surgery: A randomized, double-blind, controlled study. *BMC Anesthesiol*. 2023;23(1):243. doi:10.1186/s12871-023-02210-0
- Klinger RY, Cooter M, Bisanar T, et al. Intravenous lidocaine does not improve neurologic outcomes after cardiac surgery. *Anesthesiology*. 2019;130(6):958–970. doi:10.1097/ALN.0000000000002668
- Dunn LK, Durieux ME. Perioperative use of intravenous lidocaine. *Anesthesiology*. 2017;126(4):729–737. doi:10.1097/ALN.0000000000001527
- Feldman HS, Arthur GR, Covino BG. Comparative systemic toxicity of convulsant and supraconvulsant doses of intravenous ropivacaine, bupivacaine, and lidocaine in the conscious dog. *Anesth Analg*. 1989;69(6):794–801. PMID:2511782.
- Kaba A, Laurent SR, Detroz BJ, et al. Intravenous lidocaine infusion facilitates acute rehabilitation after laparoscopic colectomy. *Anesthesiology*. 2007;106(1):11–18. doi:10.1097/00000542-200701000-00007

Development and validation of a model to preoperatively predict the risk of placenta accreta spectrum in women with placenta previa

Bohui Zhou^{A,D}, Junfang Lian^B, Yanping Wang^C, Yanling Yang^D, Hua Bai^E, Suhui Wu^F

Third Hospital of Shanxi Medical University, Shanxi Bethune Hospital, Shanxi Academy of Medical Sciences, Tongji Shanxi Hospital, Taiyuan, China

A – research concept and design; B – collection and/or assembly of data; C – data analysis and interpretation;

D – writing the article; E – critical revision of the article; F – final approval of the article

Advances in Clinical and Experimental Medicine, ISSN 1899–5276 (print), ISSN 2451–2680 (online)

Adv Clin Exp Med. 2025;34(7):1145–1153

Address for correspondence

Suhui Wu

E-mail: shwu1215@163.com

Funding sources

This study was supported by Shanxi Provincial Higher Education Science and Technology Innovation Program (grant No. 2022L158) and Fundamental Research Program of Shanxi Province (grant No. 202203021212101).

Conflict of interest

None declared

Received on January 29, 2024

Reviewed on March 24, 2024

Accepted on July 30, 2024

Published online on December 13, 2024

Abstract

Background. Placenta previa, occurring when the placenta covers the cervical opening after 28 weeks, can lead to severe postpartum bleeding, especially when coupled with placenta accreta spectrum (PAS), posing risks of organ damage and necessitating hysterectomy. Accurate preoperative diagnosis of PAS in women with placenta previa is crucial to reduce adverse outcomes.

Objectives. This study aimed to develop a risk prediction model for PAS in women with placenta previa.

Materials and methods. A total of 437 patients with placenta previa, delivering babies between January 2012 and December 2018, were included. Data collected encompassed clinical records, neutrophil-to-lymphocyte ratio (NLR) and sonographic findings. Utilizing univariate and multivariate logistic regression analyses, the study identified key factors correlated with PAS in expectant mothers with placenta previa. A risk prediction model was formulated and evaluated through receiver operating characteristic (ROC) analysis. External validation was performed using additional patients diagnosed with placenta previa.

Results. Independent risk factors for PAS in placenta previa included NLR, timing of cesarean section and miscarriage, placenta previa type, presence of placental lacunae, and uterovesical hypervascularity. The predictive model was established using specific coefficients. The ROC curve indicated an area under the curve (AUC) of 0.821, with a sensitivity of 80.6% and specificity of 68.9%. External validation demonstrated a diagnosis coincidence rate of 75%, and the model exhibited good calibration according to the Hosmer–Lemeshow test ($p = 0.3742, >0.05$).

Conclusions. The developed model showed effective potential in predicting PAS among women with placenta previa. Its application could significantly contribute to the early detection and subsequent management of PAS.

Key words: prenatal diagnosis, NLR, placenta accreta, prediction, placenta previa

Cite as

Zhou B, Lian J, Wang Y, Yang Y, Bai H, Wu S. Development and validation of a model to preoperatively predict the risk of placenta accreta spectrum (PAS) in women with placenta previa. *Adv Clin Exp Med.* 2025;34(7):1145–1153. doi:10.17219/acem/191828

DOI

10.17219/acem/191828

Copyright

Copyright by Author(s)

This is an article distributed under the terms of the Creative Commons Attribution 3.0 Unported (CC BY 3.0) (<https://creativecommons.org/licenses/by/3.0/>)

Background

Placenta previa, defined as the partial or complete coverage of the cervical opening by the placenta after 28 weeks of pregnancy, affects between 0.24% and 1.57% of pregnancies and is a leading cause of postpartum hemorrhage.¹ When placenta previa coexists with placenta accreta spectrum (PAS), the risk of severe postpartum bleeding and damage to adjacent organs significantly increases. In severe cases, hysterectomy may become necessary, posing serious health risks to both mothers and babies.^{2,3}

Placenta accreta spectrum encompasses a spectrum of disorders characterized by trophoblast tissue invading or adhering to the myometrium, with potential extension into the uterine serosa.^{1,4,5} This spectrum includes placenta accreta, placenta increta and placenta percreta, with the incidence steadily rising due to factors such as maternal age advancement and increasing rates of cesarean deliveries.^{5,6} Accurate preoperative diagnosis and risk assessment of PAS in women with placenta previa are crucial to mitigate adverse outcomes and mortality risk.

While ultrasound is the primary method for prenatal PAS diagnosis and risk assessment, its efficacy varies widely, and interpretation depends on operator expertise.⁷ In cases where specific ultrasound features suggest abnormal placental implantation, magnetic resonance imaging (MRI) is often used for further evaluation.⁸ However, the efficacy of ultrasound relies on the operator's skill, and not all sonographers possess the expertise to interpret PAS-related ultrasound characteristics. Additionally, the location of the placenta, especially in cases of posterior placentation associated with placenta previa, can hinder accurate assessment. Although MRI provides a more comprehensive evaluation, it is not universally available, particularly in rural areas.⁸

In response to the need for reliable predictive biomarkers for PAS, the exploration of serological molecular markers has gained recognition.⁹ The neutrophil-to-lymphocyte ratio (NLR), commonly used to assess systemic inflammation, has shown independent prognostic significance in various cancers.¹⁰ Considering the similarities between excessive trophoblast invasion in PAS and tumor cell invasion and metastasis, NLR emerges as a promising candidate for predicting PAS risk in women with placenta previa.^{11,12}

By incorporating NLR as a potential biomarker, our study aims to develop and validate a predictive model for preoperatively assessing the risk of PAS in women with placenta previa. This approach may enhance risk stratification and inform clinical decision-making, ultimately improving maternal and neonatal outcomes.

Objectives

Considering the parallels between trophoblasts and tumor cells, and the predictive value of NLR in tumors, this study aimed to explore the effectiveness of NLR

as a preoperative assessment tool for PAS in individuals with placenta previa. A 2nd objective was to construct and externally validate a predictive model that integrates clinical, ultrasound and NLR data to identify high-risk individuals.

Materials and methods

Participants

This retrospective analysis included 549 patients with placenta previa who delivered at our hospital from January 2012 to October 2021 (437 patients in the development group, who delivered from January 2012 to December 2018, and 112 patients in the validation group, who delivered from January 2019 to October 2021). Inclusion criteria comprised single pregnancies, live births and gestational weeks ranging from 28 to 42. Exclusion criteria involved neoplastic or infectious diseases, preeclampsia, gestational diabetes mellitus, multiple pregnancies, assisted reproduction, or incomplete data. The research protocol received approval from the Institutional Review Board (approval No. YXLL-KY-2021-018).

The study participants were divided into PAS and non-PAS groups based on intraoperative placental implantation outcomes. The patient inclusion and grouping process are detailed in Fig. 1.

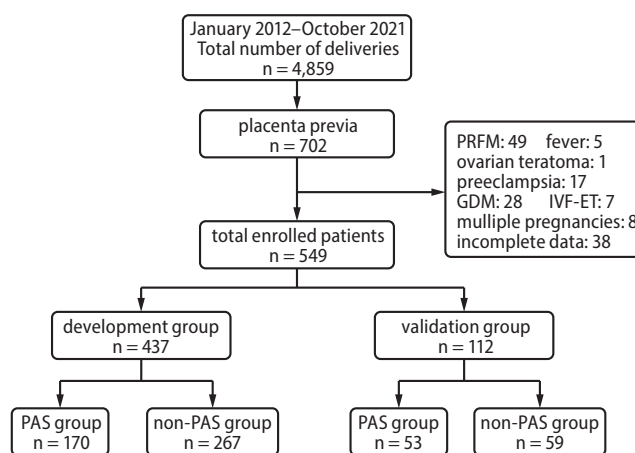


Fig. 1. Flowchart of the recruiting process of patients with placenta previa

GDM – gestational diabetes mellitus; IVF-ET – assisted reproduction; PAS – placenta accreta spectrum; PRFM – premature rupture of fetal membranes.

Study design and setting

Collection of information

Maternal clinical data encompassed various factors: maternal age, place of residence, gestational age, gravidity, parity, history of previous cesarean sections, number of prior abortions, and any previous uterine surgeries, e.g.,

laparoscopic or open myomectomy, hysteroscopy, etc. Additionally, perioperative outcomes were examined, including the mode of delivery, post-delivery blood loss within 24 h and infant birth weight.

We collected complete blood counts (CBCs) taken within 1 week before delivery, preceding the administration of dexamethasone for promoting fetal lung maturation. The NLR was derived by dividing the absolute neutrophil count (ANC) by the absolute lymphocyte count (ALC). Similarly, the platelet-to-lymphocyte ratio (PLR) was calculated by dividing the absolute platelet count by the ALC.

Experienced sonographers with over 10 years of practice in ultrasound diagnostics and holding the qualification of Deputy Chief Physician, following guidelines established by the Society for Maternal–Fetal Medicine (SMFM) in 2021, validated the ultrasound diagnosis within 1–2 weeks before delivery.⁷ The selection of specific ultrasound parameters, including placental lacunae and uterovesical hypervascularity, was based on their documented association with PAS diagnosis and prognosis. Placental lacunae, defined as 3 or more large-sized, irregular, hypoechoic spaces containing vascular flow within the placenta, have been identified as a hallmark feature of PAS on ultrasound imaging. Similarly, uterovesical hypervascularity, characterized by increased flow with the visualization of more than 10 small vessels and/or several main vessels, has been shown to correlate with abnormal placental implantation and increased risk of PAS. By assessing these ultrasound parameters, our study aimed to utilize established criteria to enhance the accuracy and reliability of preoperative PAS risk prediction in women with placenta previa.

Placental data collected included placenta type (classified based on the relationship between the placenta and the cervical opening, categorized as marginal placenta, partial placenta or complete placenta) and placental location, referring to the primary area of the placenta. Placenta accreta spectrum diagnosis was confirmed in all patients, either through intraoperative observations or histopathological examination.

Statistical analyses

For statistical analyses, we utilized IBM SPSS v. 25.0 (IBM Corp., Armonk, USA) and R software v. 4.0 (R Foundation for Statistical Computing, Vienna, Austria). Descriptive statistics were performed to summarize both continuous variables (utilizing mean and standard deviation (SD) or median and interquartile range (IQR), depending on distribution normality) and categorical variables (presented as frequency and proportions). The Shapiro–Wilk test, chosen for its suitability with smaller datasets and sensitivity to deviations from normality, was used to assess the normality of distribution. A significance level below 0.05 typically indicates non-normality.

To develop and validate the regression model predicting the outcome, our study followed a rigorous approach.

Initially, the dataset was randomly split into a training set (80%) and a test set (20%) to ensure unbiased model evaluation, preventing temporal biases from influencing results.

For predictor selection, least absolute shrinkage and selection operator (LASSO) regression was employed, especially suitable for models with potentially numerous predictors compared to observations. Such regression aids in coefficient shrinkage and enhances model interpretability by performing variable selection within the regularization process. The tuning parameter (λ) for LASSO was determined through 10-fold cross-validation on the training set to minimize prediction error and avoid overfitting.

Multivariate logistic regression analysis was conducted to identify independent influencing factors and formulate the PAS prediction model. The assumption of linearity between the logit of the outcome and each continuous predictor was assessed with Stata v. 17 (Stata Corp., College Station, USA) using Component Plus Residual (CPR) plots rather than the Box–Tidwell procedure due to the software's limitations with handling the Box–Tidwell test for models with multiple continuous predictors, which could lead to computational issues or convergence problems.

The CPR plots visually inspected the relationship, ensuring adherence to the linear logit assumption.

To detect multicollinearity among predictors, the variance inflation factor (VIF) was calculated for each variable. The VIF values greater than 10 indicated significant multicollinearity, prompting model review and potential modification for stable estimates.

Influential observations were identified using leverage and Cook's distance measures, helping to detect points disproportionately affecting model fit. Observations with high leverage or Cook's distance significantly exceeding typical thresholds were considered potential outliers or possessing high influence.

Model specification correctness was evaluated using Stata linktest, detecting omitted variables and functional form misspecification through the significant χ^2 term (χ^2), suggesting potential model adjustments.

Overall model performance was assessed via a receiver operating characteristic (ROC) curve and the Hosmer–Lemeshow test, with statistical significance defined as $p < 0.05$. Additionally, the Brier score and likelihood-based measures such as the Akaike information criterion (AIC) and Bayesian information criterion (BIC) were applied to assess model calibration and refinement.

Results

A total of 547 pregnant women meeting the inclusion criteria were enrolled in our study. Based on intraoperative clinical assessments and pathological findings, 223 women (40.7%) were diagnosed with PAS. The distribution of placenta accreta, increta and percreta cases was 123 (22.5%),

Table 1. Basic demographic characteristics and perioperative outcomes in the training and test set

Basic demographic characteristics		Training set		Test set	
		non-PAS (n = 267)	PAS (n = 170)	non-PAS (n = 59)	PAS (n = 53)
Maternal age [years], n (%)	<35	218 (81.6)	135 (79.4)	39 (66.1)	43 (81.1)
	≥35	49 (18.4)	35 (20.6)	20 (33.9)	10 (18.9)
Marital status, n (%)	unmarried	2 (0.7)	0 (0.0)	0 (0.0)	1 (1.9)
	married	265 (99.3)	170 (100)	59 (100)	52 (98.1)
	divorced/separated	0 (0.0)	0 (0.0)	0 (0.0)	0 (0.0)
Place of residence, n (%)	town	159 (59.6)	100 (58.8)	42 (71.2)	28 (52.8)
	rural area	108 (40.4)	70 (41.2)	17 (28.8)	25 (47.2)
Birthweight [g], n (%)	<2,500	66 (24.7)	50 (29.4)	18 (30.5)	21 (39.6)
	2,500–4,000	196 (73.4)	117 (68.8)	40 (67.8)	31 (58.5)
	≥4,000	5 (1.9)	3 (1.8)	1 (1.7)	1 (1.9)
Blood loss within 24 h [mL], n (%)		560 (140)	870 (943)	550 (100)	760 (500)
Hysterectomy, n (%)		4 (1.5)	11 (6.5)	0 (0)	2 (3.8)

PAS – placenta accreta spectrum.

75 (13.8%) and 25 (4.6%), respectively. Notably, only 2 patients in the PAS group had a history of hysteroscopic electrotomy, precluding a comparison regarding previous uterine surgeries between the groups. Hysterectomy was performed in 13 patients (2.4%). No fatalities occurred during the study period. Comprehensive demographic characteristics and perioperative outcomes for both the training and test sets are detailed in Table 1, and all test assumptions are provided in the Supplementary tables.

Variable selection and model development

In the training set, we employed LASSO regression to optimize the selection of predictive variables from clinical characteristics, CBCs and ultrasound findings. This approach was chosen to ensure a rigorous, data-driven selection process, minimizing potential overfitting and enhancing the model's predictive accuracy. The LASSO regression was particularly effective in handling the high dimensionality of our dataset and identified 6 variables that exhibited the strongest associations with the outcome of interest.

The variables selected using LASSO regression included:

- time of caesarean section;
- time of miscarriage;
- NLR;
- type of placenta previa;
- presence of placental lacunae;
- uterovesical hypervascularity.

These variables were then further analysed using multivariate logistic regression to determine their independent effects on the risk of PAS.

A risk model to predict PAS

Following the variable selection, multivariate logistic regression was conducted, which confirmed that the 6 variables identified by LASSO regression (time of caesarean section, time of miscarriage, NLR, type of placenta previa, presence of placental lacunae, and uterovesical hypervascularity) were significant predictors of PAS (Table 2). The logistic risk prediction model was formulated as follows: $P = \exp(w) / [1 + \exp(w)]$, where $W = -3.942 + 0.393 \times \text{time of miscarriage} + 0.482 \times \text{time of caesarean}$

Table 2. Multivariate analysis of factors associated with PAS in the training set

Variable	β	SE	Wald's test	p-value	OR (95% CI)
Previous caesarean section	0.482	0.251	3.698	0.054	1.619 (0.991–2.646)
Time of miscarriage	0.393	0.111	12.540	<0.001	1.529 (1.232–1.896)
Placenta previa classification, n (%)					
Partial placenta previa	1.546	0.453	11.636	0.001	4.695 (1.931–11.416)
Complete placenta previa	1.755	0.307	32.680	<0.001	1.482 (1.192–1.842)
NLR	0.296	0.079	14.042	<0.001	1.344 (1.152–1.569)
Uterovesical hypervascularity	0.871	0.501	3.027	0.082	2.390 (0.896–6.379)
Placental lacunae	1.488	0.642	5.365	0.021	4.427 (1.257–15.592)

95% CI – 95% confidence interval; NLR – neutrophil-to-lymphocyte ratio; OR – odds ratio; PAS – placenta accreta spectrum; SE – standard error.

section + 0.296 × NLR + 1.546 × partial placenta (1 for yes, 0 for no) + 1.755 × complete placenta (1 for yes, 0 for no) + 0.871 × uterovesical hypervascularity (1 for yes, 0 for no) + 1.488 × placental lacunae (1 for yes, 0 for no).

Our evaluation of linearity between predictors and the log odds of the outcome confirmed that the relationship is appropriately linear. The plots showed no systematic deviations from a straight line, suggesting that the linear assumption necessary for logistic regression holds true across all continuous variables.

The VIF analysis revealed that all predictors had VIF values well below the threshold of 10, with the highest being 3.2. This indicates that our model does not suffer from multicollinearity, affirming that the coefficient estimates are stable and reliable. Investigation into influential outliers through leverage and Cook’s distance identified no observations, with leverage exceeding twice the average or Cook’s distance greater than the commonly used cutoff of 4/(N-k-1). This outcome suggests that our model is not unduly influenced by outliers, and the results are robust across the sample.

The linktest used for assessing model specification indicated no signs of misspecification. The significance of the $\hat{\mu}$ term ($p < 0.001$) and the nonsignificance of the $\hat{\mu}^2$ term ($p = 0.995$) confirm that the functional form of the model is correct and that there are no omitted variable biases influencing our results.

Effectiveness of the logistic risk prediction model

The performance of our predictive model in the training set, with an AUC of 0.821 (Fig. 2), indicates a strong ability to distinguish between the outcomes of interest, suggesting that the model is highly effective in capturing

the essential predictors. The Youden index optimal cutoff value of 0.344, which maximizes the sum of sensitivity and specificity, highlights a well-balanced trade-off between both measures, leading to an overall accuracy of 73.5%. These metrics underscore the robustness of the model in the training phase.

Upon external validation in the test set, the model maintained a robust performance with an AUC of 0.775. This slight decrease compared to the training set is typical, as models often perform slightly better on the data on which they were trained. However, the high specificity of 84.7% in the test set indicates that the model is particularly effective at identifying true negatives, which is crucial for clinical settings where false positives can lead to unnecessary interventions.

The sensitivity in the test set was 64.2%, which, while lower than in the training set, still represents substantial predictive power, especially when considered alongside the high specificity. The accuracy of 75.0% in the test set further validates the model’s utility in external populations and reinforces its generalizability (Fig. 3, Table 3).

Additionally, the Hosmer–Lemeshow test result ($p = 0.3742$) confirms good calibration of the model

Table 3. The prediction outcome of PAS using prediction model and actual PAS outcome in the test set

Actual outcome	Predict outcome		Total
	non-PAS	PAS	
Non-PAS	50	9	59
PAS	19	34	53
Total	69	43	112

PAS – placenta accreta spectrum.

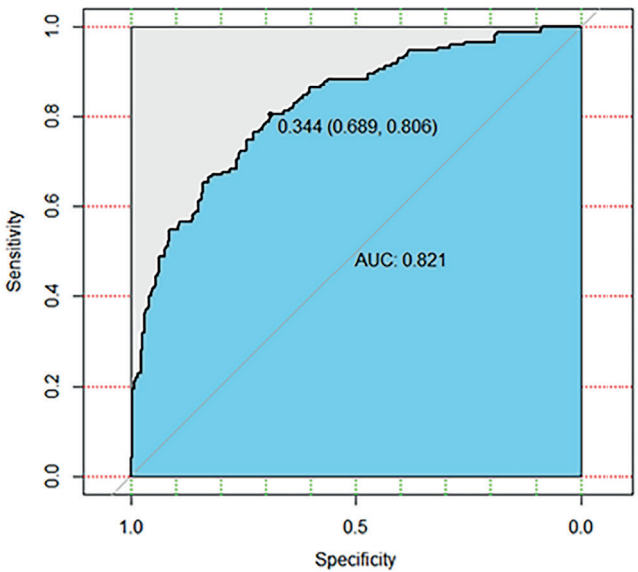


Fig. 2. Receiver operator curves (ROC) for prediction of placenta accreta spectrum (PAS) in the training set

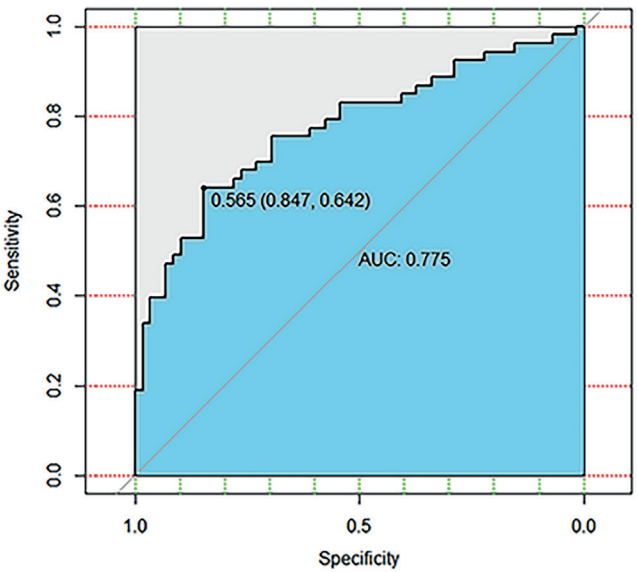


Fig. 3. Receiver operator curves (ROC) for prediction of placenta accreta spectrum (PAS) in the test set

across different subgroups within the dataset, indicating that the predicted probabilities of outcomes are consistent with the observed probabilities. This aspect of model performance is crucial for clinical applicability, ensuring that the model's predictions are not only accurate but also calibrated to the realities of clinical practice. The Brier score, which measures the mean squared difference between the predicted probabilities and the actual outcomes, was 0.18, indicating a good level of predictive accuracy. Furthermore, the AIC and BIC were employed to evaluate model complexity and fit, ensuring that the final model avoids overfitting while maintaining predictive robustness.

Discussion

This study aimed to create a model to identify individuals with placenta previa at high risk for developing PAS by integrating clinical risk factors, NLR and ultrasound findings. The developed risk prediction model was externally validated based on these clinical variables, exhibiting superior predictive accuracy compared to clinical diagnosis alone. This study marks the initial exploration of the potential role of NLR as a predictive biomarker for PAS.

Literature on risk assessment and prediction models for PAS in placenta previa remains limited. Prior studies^{13–15} have explored scoring systems diagnosing PAS using clinical characteristics and ultrasound findings, while Delli Pizzi et al.¹⁴ employed an MRI-based predictive model. These models achieved AUC values ranging from 0.833 to 0.925, sensitivities between 83.3% and 100%, and specificities ranging from 77% to 85.7%. In our study, the prediction model assessing PAS yielded an AUC of 0.821, a sensitivity of 80.6% and a specificity of 68.9%. While our diagnostic efficacy may not surpass that of other studies, the factors included in our prediction model are simple, cost-effective and easily applicable in clinical settings.

The NLR is recognized as a potential biomarker for predicting survival outcomes in various diseases, including cancer and coronary artery disease (CAD).¹¹ Elevated NLR in association with PAS is believed to involve multifactorial mechanisms.

Studies indicate that women with prior cesarean sections exhibit increased uterine artery resistance and a reduced proportion of uterine blood flow in comparison to those with a history of vaginal delivery.¹⁶ This discrepancy in oxygen supply to placental tissue may trigger a local inflammatory response, resulting in the production of cytokines, particularly vascular endothelial growth factor (VEGF). Research has demonstrated common occurrences of local fibrous tissue increase and inflammatory cell infiltration around the scar site.^{4,17} Immunohistochemistry findings have revealed heightened VEGF and phosphotyrosine in extravillous trophoblast cells, potentially promoting

trophoblast infiltration and vascular remodeling among PAS cases compared to normal controls.^{4,18}

Lymphocytes play essential roles in cytotoxic cell death and cytokine production, impacting immune response inhibition. Pregnant women with placental implantation complications have notably decreased natural killer cells (NK cells), which release cytokines to regulate invasion.¹⁹ Recent work by Shainker et al.²⁰ employing a novel proteomics platform unveiled differential plasma protein expression between PAS and control groups. Pathway analyses implicated these differentially expressed proteins in closely regulating inflammation, coagulation, angiogenesis, and invasion in PAS cases. Furthermore, secondary disruptions in the endometrium–myometrial interface might contribute to microenvironmental changes within the uterine scar, leading to immune balance disruptions.

The escalating prevalence of PAS disorders is closely linked to the rising rates of cesarean sections, substantiated by robust epidemiological evidence.^{5,21–25} Notably, a study conducted in Hong Kong observed a surge in PAS incidence among women with prior cesarean deliveries compared to those with unscarred uteruses.²⁴ Correspondingly, as cesarean section rates increased, so did the incidence of PAS disorders. A meta-analysis highlighted an escalating odds ratio (OR) for PAS, rising from 8.6 to 17.4 with 1–2 previous cesarean sections, and soaring to 55.9 following 3 or more prior cesarean deliveries.^{5,25} Another comprehensive systematic review revealed an increase in PAS rates from 0.3% after a single prior cesarean section to 6.7% after 6 previous cesareans.²⁶

The underlying mechanism contributing to the surge in PAS may involve uterine scarring, impairing the decidua interface at the implantation site. This scarring potentially diminishes the integrity of the decidua, fostering increased trophoblast adhesion or infiltration. Consequently, placental implantation into the myometrium may occur in subsequent pregnancies. Surgeries leading to endometrial integrity compromise, such as uterine curettage, postpartum endometritis, hysteroscopic surgery, endometrial ablation, and uterine artery embolization, have also been associated with PAS disorders in subsequent pregnancies. Additionally, our study established abortion as an independent risk factor for PAS.

The primary method for diagnosing PAS is transvaginal ultrasound (TVS). Classical ultrasound signs indicative of PAS encompass features such as placental lacunae, loss of the clear zone, interruption of the bladder wall, uterovesical hypervascularity, placental bulge, and myometrial thinning.²⁷ These ultrasound observations are correlated with the pathophysiology of PAS.^{1,4} Among these signs, placental lacunae have notably been linked to PAS, with studies emphasizing its association with cesarean hysterectomy and maternal complications.^{7,28,30} Conversely, in patients with placenta previa and prior cesarean sections, the absence of lacunae demonstrated a high negative predictive value (NPV) ranging from 88% to 100% for PAS.^{7,29,30}

Alterations in the uterovesical interface present compelling specificity (97.5–99.8%), albeit with lower sensitivity (49.6%).^{1,31,32} Markers observed at the uterus and bladder interface include bridging vessels, hypervascularity between these organs, and interruption of the bladder wall. Color Doppler imaging has proven effective in detecting neovascularity in most PAS cases⁷; however, some of the ultrasound signs mentioned are not exclusive to PAS. For instance, myometrial thinning may result from a prior cesarean scar.^{1,7} Thus, our study specifically selected 2 easily identifiable signs – placental lacunae and uterovesical hypervascularity – which were found to be significantly valuable in distinguishing between the PAS and non-PAS groups.

Despite the pivotal role of ultrasound in the prenatal diagnosis of PAS, the American College of Obstetricians and Gynecologists/The Society for Maternal-Fetal Medicine (ACOG/SMFM) underscores that a negative ultrasound cannot entirely exclude the possibility of PAS. They emphasize the significance of clinical risk factors, highlighting their equal importance to ultrasound findings in predicting PAS (grade 1A).^{33,34} Moreover, the Society of Obstetricians and Gynecologists of Canada (SOGC) highlights that the efficacy of ultrasound in diagnosing PAS is contingent on various factors, including knowledge of clinical risk factors, imaging quality, operator expertise, gestational age, imaging techniques, and adequate bladder filling.³⁵ These considerations further underscore the relevance and importance of our composite scoring model.

As anticipated, the type of placenta played a significant role in the risk of placental implantation disorders. Specifically, complete placenta previa demonstrated a higher likelihood of association with PAS. The absence of endometrial re-epithelialization in the scar region, coupled with inadequate blood supply, potentially facilitated wider and deeper invasion by trophoblast and villous tissue.

While the location of placental attachment showed minimal significance, prior studies have indicated that maternal age above 35 years could elevate the odds of PAS disorders.^{36,37} However, according to the 2018 International Federation of Gynecology and Obstetrics (FIGO) guidelines on the prenatal diagnosis and screening of PAS,⁵ this association might be influenced by confounding factors such as multiparity and previous uterine surgeries, rather than solely by advanced maternal age itself. Our present study did not establish a significant association between age and PAS.

The notable strength of our study lies in its pioneering approach incorporating serum markers into the construction of a predictive model. This strategy facilitated a quantifiable prenatal assessment, specifically aimed at identifying cases of placenta previa at high risk for PAS. We rigorously validated this predictive model and confirmed its accuracy using independent samples. By integrating NLR into our predictive model, we not only improved predictive

accuracy but also gained valuable insights into the pathophysiological mechanisms driving PAS development. This holistic approach, encompassing both clinical and inflammatory markers, enhances the robustness of our predictive model and provides clinicians with a more comprehensive tool for risk assessment in placenta previa patients.

Limitations

This study was conducted at a single center, and both model development and validation were retrospective. Notably, the enrolled participants had placenta previa, raising uncertainties about the model's applicability to PAS patients without placenta previa. In future investigations, we intend to prospectively verify our findings and extend the prediction model to encompass all PAS patients, particularly focusing on the 1st and 2nd trimester. This approach is crucial, considering that current studies predominantly concentrate on high-risk pregnancies in the 3rd trimester. Ultimately, such efforts aim to enhance pregnancy outcomes through improved predictive strategies.

Conclusions

The integration of clinical characteristics, NLR and ultrasound findings in a preoperative prediction model holds significant promise for improving patient care and maternal outcomes in cases of PAS among women with placenta previa.

By leveraging our prediction model, clinicians can effectively stratify patients into high-risk categories, enabling the formulation of tailored delivery plans and timings. This approach facilitates early identification of high-risk cases, allowing for closer monitoring and timely interventions when necessary. As a result, unnecessary interventions can be minimized, while optimal management strategies can be implemented to mitigate the risk of maternal morbidity and mortality associated with PAS.

The implementation of our prediction model is anticipated to not only enhance patient care by ensuring appropriate management strategies but also improve maternal outcomes by reducing the incidence of complications associated with PAS.

Supplementary data

The Supplementary materials are available at <https://doi.org/10.5281/zenodo.12694596>. The package includes the following files:

Supplementary Table 1. Variance inflation factor for all the variables in the final prediction model.

Supplementary Table 2. Cook's distance for all the variables in the final prediction model.

Supplementary Table 3. Verification of test assumptions in the final prediction model.

Data availability

The datasets generated and/or analyzed during the current study are available from the corresponding author on reasonable request.

Consent for publication

Not applicable.

ORCID iDs

Bohui Zhou  <https://orcid.org/0000-0002-8949-462X>
 Junfang Lian  <https://orcid.org/0009-0007-4788-552X>
 Yanping Wang  <https://orcid.org/0009-0007-0489-1735>
 Yanling Yang  <https://orcid.org/0009-0002-1797-9537>
 Hua Bai  <https://orcid.org/0000-0003-1979-3760>
 Suhui Wu  <https://orcid.org/0000-0002-2707-0362>

References

1. Yu FNY, Leung KY. Antenatal diagnosis of placenta accreta spectrum (PAS) disorders. *Best Pract Res Clin Obstet Gynaecol.* 2021;72:13–24. doi:10.1016/j.bpobgyn.2020.06.010
2. O'Brien JM, Barton JR, Donaldson ES. The management of placenta percreta: Conservative and operative strategies. *Am J Obstet Gynecol.* 1996;175(6):1632–1638. doi:10.1016/S0002-9378(96)70117-5
3. Silver RM, Landon MB, Rouse DJ, et al. Maternal morbidity associated with multiple repeat cesarean deliveries. *Obstet Gynecol.* 2006;107(6):1226–1232. doi:10.1097/01.AOG.0000219750.79480.84
4. Jauniaux E, Collins S, Burton GJ. Placenta accreta spectrum: Pathophysiology and evidence-based anatomy for prenatal ultrasound imaging. *Am J Obstet Gynecol.* 2018;218(1):75–87. doi:10.1016/j.ajog.2017.05.067
5. Jauniaux E, Chantraine F, Silver RM, Langhoff-Roos J; for the FIGO Placenta Accreta Diagnosis and Management Expert Consensus Panel. FIGO consensus guidelines on placenta accreta spectrum disorders: Epidemiology. *Int J Gynaecol Obstet.* 2018;140(3):265–273. doi:10.1002/ijgo.12407
6. Morlando M, Collins S. Placenta accreta spectrum disorders: Challenges, risks, and management strategies. *Int J Womens Health.* 2020;12:1033–1045. doi:10.2147/IJWH.S224191
7. Shainker SA, Coleman B, Timor-Tritsch IE, et al. Special Report of the Society for Maternal-Fetal Medicine Placenta Accreta Spectrum Ultrasound Marker Task Force: Consensus on definition of markers and approach to the ultrasound examination in pregnancies at risk for placenta accreta spectrum. *Am J Obstet Gynecol.* 2021;224(1):B2–B14. doi:10.1016/j.ajog.2020.09.001
8. Einerson BD, Rodriguez CE, Kennedy AM, Woodward PJ, Donnelly MA, Silver RM. Magnetic resonance imaging is often misleading when used as an adjunct to ultrasound in the management of placenta accreta spectrum disorders. *Am J Obstet Gynecol.* 2018;218(6):618.e1–618.e7. doi:10.1016/j.ajog.2018.03.013
9. Maurea S, Verde F, Romeo V, et al. Prediction of placenta accreta spectrum in patients with placenta previa using a clinical, US and MRI combined model: A retrospective study with external validation. *Eur J Radiol.* 2023;168:111116. doi:10.1016/j.ejrad.2023.111116
10. Liu Q, Zhou W, Yan Z, et al. Development and validation of MRI-based scoring models for predicting placental invasiveness in high-risk women for placenta accreta spectrum. *Eur Radiol.* 2023;34(2):957–969. doi:10.1007/s00330-023-10058-8
11. Mouchli M, Reddy S, Gerrard M, Boardman L, Rubio M. Usefulness of neutrophil-to-lymphocyte ratio (NLR) as a prognostic predictor after treatment of hepatocellular carcinoma: Review article. *Ann Hepatol.* 2021;22:100249. doi:10.1016/j.aohp.2020.08.067
12. Bartlett EK, Flynn JR, Panageas KS, et al. High neutrophil-to-lymphocyte ratio (NLR) is associated with treatment failure and death in patients who have melanoma treated with PD-1 inhibitor monotherapy. *Cancer.* 2020;126(1):76–85. doi:10.1002/cncr.32506
13. Luo L, Sun Q, Ying D, et al. Scoring system for the prediction of the severity of placenta accreta spectrum in women with placenta previa: A prospective observational study. *Arch Gynecol Obstet.* 2019;300(3):783–791. doi:10.1007/s00404-019-05217-6
14. Delli Pizzi A, Tavoletta A, Narciso R, et al. Prenatal planning of placenta previa: Diagnostic accuracy of a novel MRI-based prediction model for placenta accreta spectrum (PAS) and clinical outcome. *Abdom Radiol.* 2019;44(5):1873–1882. doi:10.1007/s00261-018-1882-8
15. Gao Y, Gao X, Cai J, et al. Prediction of placenta accreta spectrum by a scoring system based on maternal characteristics combined with ultrasonographic features. *Taiwan J Obstet Gynecol.* 2021;60(6):1011–1017. doi:10.1016/j.tjog.2021.09.011
16. Flo K, Widnes C, Værtun Å, Acharya G. Blood flow to the scarred gravid uterus at 22–24 weeks of gestation. *BJOG.* 2014;121(2):210–215. doi:10.1111/1471-0528.12441
17. Donovan BM, Shainker SA. Placenta accreta spectrum. *Neoreviews.* 2021;22(11):e722–e733. doi:10.1542/neo.22-11-e722
18. Wehrum MJ, Buhimschi IA, Salafia C, et al. Accreta complicating complete placenta previa is characterized by reduced systemic levels of vascular endothelial growth factor and by epithelial-to-mesenchymal transition of the invasive trophoblast. *Am J Obstet Gynecol.* 2011;204(5):411.e1–411.e11. doi:10.1016/j.ajog.2010.12.027
19. Laban M, Ibrahim EAS, Elsafty MSE, Hassanin AS. Placenta accreta is associated with decreased decidual natural killer (dNK) cells population: A comparative pilot study. *Eur J Obstet Gynecol Reprod Biol.* 2014;181:284–288. doi:10.1016/j.ejogrb.2014.08.015
20. Shainker SA, Silver RM, Modest AM, et al. Placenta accreta spectrum: Biomarker discovery using plasma proteomics. *Am J Obstet Gynecol.* 2020;223(3):433.e1–433.e14. doi:10.1016/j.ajog.2020.03.019
21. Fitzpatrick KE, Sellers S, Spark P, Kurinczuk JJ, Brocklehurst P, Knight M. Incidence and risk factors for placenta accreta/increta/percreta in the UK: A national case-control study. *PLoS One.* 2012;7(12):e52893. doi:10.1371/journal.pone.0052893
22. Eshkoli T, Weintraub AY, Sergienko R, Sheiner E. Placenta accreta: Risk factors, perinatal outcomes, and consequences for subsequent births. *Am J Obstet Gynecol.* 2013;208(3):219.e1–219.e7. doi:10.1016/j.ajog.2012.12.037
23. Creanga AA, Bateman BT, Butwick AJ, et al. Morbidity associated with cesarean delivery in the United States: Is placenta accreta an increasingly important contributor? *Am J Obstet Gynecol.* 2015;213(3):384.e1–384.e11. doi:10.1016/j.ajog.2015.05.002
24. Cheng KK, Lee MM. Rising incidence of morbidly adherent placenta and its association with previous caesarean section: A 15-year analysis in a tertiary hospital in Hong Kong. *Hong Kong Med J.* 2015;21(6):511–517. doi:10.12809/hkmj154599
25. Sentilhes L, Merlot B, Madar H, Sztark F, Brun S, Deneux-Tharaux C. Postpartum haemorrhage: Prevention and treatment. *Exp Rev Hematol.* 2016;9(11):1043–1061. doi:10.1080/17474086.2016.1245135
26. Marshall NE, Fu R, Guise JM. Impact of multiple cesarean deliveries on maternal morbidity: A systematic review. *Am J Obstet Gynecol.* 2011;205(3):262.e1–262.e8. doi:10.1016/j.ajog.2011.06.035
27. Cali G, Forlani F, Lees C, et al. Prenatal ultrasound staging system for placenta accreta spectrum disorders. *Ultrasound Obstet Gynecol.* 2019;53(6):752–760. doi:10.1002/uog.20246
28. Comstock CH, Love JJ, Bronsteen RA, et al. Sonographic detection of placenta accreta in the second and third trimesters of pregnancy. *Am J Obstet Gynecol.* 2004;190(4):1135–1140. doi:10.1016/j.ajog.2003.11.024
29. Yang JI, Lim YK, Kim HS, Chang KH, Lee JP, Ryu HS. Sonographic findings of placental lacunae and the prediction of adherent placenta in women with placenta previa totalis and prior cesarean section. *Ultrasound Obstet Gynecol.* 2006;28(2):178–182. doi:10.1002/uog.2797
30. Bhide A, Sebire N, Abuhamad A, Acharya G, Silver R. Morbidly adherent placenta: The need for standardization. *Ultrasound Obstet Gynecol.* 2017;49(5):559–563. doi:10.1002/uog.17417
31. Pagani G, Cali G, Acharya G, et al. Diagnostic accuracy of ultrasound in detecting the severity of abnormally invasive placentation: A systematic review and meta-analysis. *Acta Obstet Gynecol Scand.* 2018;97(1):25–37. doi:10.1111/aogs.13238
32. D'Antonio F, Iacovella C, Bhide A. Prenatal identification of invasive placentation using ultrasound: Systematic review and meta-analysis. *Ultrasound Obstet Gynecol.* 2013;42(5):509–517. doi:10.1002/uog.13194

33. Silver RM, Branch DW. Placenta accreta spectrum. *N Engl J Med*. 2018; 378(16):1529–1536. doi:10.1056/NEJMcp1709324
34. Jauniaux E, Kingdom JC, Silver RM. A comparison of recent guidelines in the diagnosis and management of placenta accreta spectrum disorders. *Best Pract Res Clin Obstet Gynaecol*. 2021;72:102–116. doi:10.1016/j.bpobgyn.2020.06.007
35. Hobson SR, Kingdom JC, Murji A, et al. No. 383-Screening, Diagnosis, and Management of Placenta Accreta Spectrum Disorders. *J Obstet Gynaecol Can*. 2019;41(7):1035–1049. doi:10.1016/j.jogc.2018.12.004
36. Thurn L, Lindqvist P, Jakobsson M, et al. Abnormally invasive placenta: Prevalence, risk factors and antenatal suspicion. Results from a large population-based pregnancy cohort study in the Nordic countries. *BJOG*. 2016;123(8):1348–1355. doi:10.1111/1471-0528.13547
37. Kamara M, Henderson J, Doherty D, Dickinson J, Pennell C. The risk of placenta accreta following primary elective caesarean delivery: A case-control study. *BJOG*. 2013;120(7):879–886. doi:10.1111/1471-0528.12148

Do sociodemographic and health predictors affect the non-insulin-based insulin resistance index? A cross-sectional study

Maciej Polak^{1,A–F}, Grzegorz J. Nowicki^{2,A–F}, Maja Chrzanowska-Wąsik^{3,E,F}, Barbara J. Ślusarska^{2,E,F}

¹ Department of Epidemiology and Population Studies, Jagiellonian University Medical College, Cracow, Poland

² Department of Family and Geriatric Nursing, Faculty of Health Sciences, Medical University of Lublin, Poland

³ Clinical Emergency Department, Independent Clinical Hospital No. 4, Lublin, Poland

A – research concept and design; B – collection and/or assembly of data; C – data analysis and interpretation;
D – writing the article; E – critical revision of the article; F – final approval of the article

Advances in Clinical and Experimental Medicine, ISSN 1899–5276 (print), ISSN 2451–2680 (online)

Adv Clin Exp Med. 2025;34(7):1155–1163

Address for correspondence

Grzegorz J. Nowicki

E-mail: gnowicki84@gmail.com

Funding sources

The research was performed as part of the project entitled “Follow Your Hear—prevention and health promotion program for cardiovascular diseases in the Janów district” financed by the Norwegian Financial Mechanism 2009–2014 under the PL Program 13 “Limiting social inequities in health” and the state budget.

Conflict of interest

None declared

Received on November 18, 2023

Reviewed on December 28, 2023

Accepted on July 15, 2024

Published online on November 12, 2024

Cite as

Polak M, Nowicki G, Chrzanowska-Wąsik M, Ślusarska B. Do sociodemographic and health predictors affect the non-insulin-based insulin resistance index? A cross-sectional study. *Adv Clin Exp Med.* 2025;34(7):1155–1163. doi:10.17219/acem/191200

DOI

10.17219/acem/191200

Copyright

Copyright by Author(s)

This is an article distributed under the terms of the Creative Commons Attribution 3.0 Unported (CC BY 3.0) (<https://creativecommons.org/licenses/by/3.0/>)

Abstract

Background. Insulin resistance (IR) is considered a risk factor for cardiovascular diseases (CVD). Therefore, early diagnosis of IR is clinically significant for primary and secondary CVD prevention initiatives. In addition, non-insulin metabolic indices may be useful for diagnosing IR.

Objectives. The first objective was to estimate the triglyceride and glucose (TyG) index and the metabolic score for insulin resistance (METS-IR) index values in a local community with high social deprivation and increased cardiovascular risk according to the Systematic Coronary Risk Evaluation scale. The second objective was to identify significant sociodemographic and health predictors for the TyG index and METS-IR index.

Materials and methods. This cross-sectional study was conducted in the local community of Janów district in eastern Poland and consisted of 2 stages. The 1st stage involved basic research ($n = 4,040$), while the 2nd stage involved enhanced diagnostics ($n = 2,657$). Data from the 2nd stage was used for the analyses. Anthropometric and physiological measurements were taken, blood was drawn for laboratory tests, selected sociodemographic and health variables were evaluated, and the TyG index and METS-IR index were calculated.

Results. The mean TyG index score in the study group was $8.65 (\pm 0.58)$, and the mean METS-IR index score was $41.45 (\pm 9.02)$. Both indices were significantly associated with age, male sex, smoking, and systolic blood pressure (SBP) in a multivariable model. In addition, alcohol consumption and body mass index (BMI) were significantly correlated with the TyG index, whereas education was significantly associated with the METS-IR index.

Conclusions. Our results show the association between IR and sociodemographic and health variables in a group with a high social deprivation rate and increased cardiovascular risk. Early detection of cardio-metabolic risk is important for both primary and secondary CVD prevention. In primary healthcare, this can be accomplished through surrogate markers of IR.

Keywords: insulin resistance, cardiovascular disease, local community, triglyceride and glucose (TyG), metabolic score for insulin resistance (METS-IR)

Background

As one of the leading causes of morbidity and mortality worldwide, cardiovascular diseases (CVD) have a substantial financial impact on healthcare systems and significantly worse wellbeing.¹ Patients with CVD, especially those with multiple risk factors, continue to have a high risk of cardiovascular complications and recurrence despite the development and implementation of several secondary prevention strategies, such as pharmacotherapy, revascularization and rehabilitation.² Therefore, identifying and addressing risk factors in groups at high risk of CVD becomes critical for primary CVD prevention. Glucose and lipid metabolism disorders are a major cause of CVD. Studies indicate that insulin resistance (IR), hyperglycemia and dyslipidemia increase cardiovascular morbidity and mortality.³ Thus, investigating a correlation between primary CVD prevention and both modifiable and non-modifiable risk factors and glycolipid metabolism may help to reduce the worldwide burden of CVD.

Insulin resistance, defined as decreased insulin responsiveness in tissues, is a crucial mechanism in glycolipid metabolism.⁴ Research shows that IR increases the risk of diabetes, hypertension and other illnesses, and may be a primary cause of CVD.^{4–6} In addition, IR is the primary risk factor for coronary artery disease (CAD) in young adults and can cause up to 40% of myocardial infarctions.⁷ The gold standard for assessing IR is the euglycemic insulin clamp technique,⁸ but its use in screening is limited because it is an invasive, expensive and challenging method to use in large cohort studies.⁹ Consequently, IR indices, which do not include insulin levels in their calculation algorithm, have been developed. These methods are easier to use and more cost-effective, particularly in primary healthcare and epidemiological studies.

The triglyceride and glucose (TyG) index, which combines serum triglyceride and fasting plasma glucose levels, is a surrogate marker of IR. Wen et al.¹⁰ found that the TyG index is strongly associated with the incidence of prediabetes compared to other IR indices in the Chinese population. Other research suggests it is more accurate than the homeostatic model assessment index (HOMA-IR) in predicting the incidence and prognosis of hypertension, diabetes, stroke, and other CVD.^{11–13} It should be noted that IR is not only related to glucose and lipid metabolism but also to nutritional status and fat distribution. Unfortunately, the TyG index does not account for these 2 factors, which is undoubtedly its weakness. Therefore, Bello-Chavolla et al.¹⁴ developed a novel metabolic score for IR (METS-IR) index using biochemical and anthropometric variables easily obtained in primary healthcare, and which demonstrate good diagnostic performance for assessing insulin sensitivity. The METS-IR is also a relevant marker for evaluating cardiometabolic risk in both healthy and at-risk study participants, and may be a useful tool for screening insulin sensitivity.¹² Available data indicate that both the TyG index

and METS-IR index are associated with several CVD risk factors, including diabetes, metabolic syndrome, arterial stiffness, CAD, and subsequent cardiovascular events.^{11,15,16}

Sociodemographic, environmental and psychosocial factors significantly impact health, contribute to the development of CVD risk factors, and influence CVD morbidity and mortality.¹⁷ Numerous studies have shown a strong association between socioeconomic status (SES), which includes education, income and occupation, and the prevalence of CVD risk factors.¹⁸ De Mestral et al.¹⁹ emphasize the importance of examining how the SES–CVD relationship varies regionally within countries, particularly in middle-income countries where it may be influenced by place of residence (rural vs urban areas). An example is the Janów district in eastern Poland, a local community characterized by low SES and ranked among the 20% most deprived districts in Lublin Province.²⁰ Comparative analysis of socioeconomic characteristics preceding the study revealed significantly unfavorable differences compared to nationwide indicators: a higher percentage of residents with primary education (23.2% vs 27.55% nationally),²¹ a 15.6% unemployment rate among working-age individuals vs the national average of 14%,²² and 14.6% of the Janów district population receiving social benefits compared to 9.4% across Lublin Province.²³ Low SES is one of several frequently overlooked risk factors for IR. In Europe's multinational, multicultural and socioeconomically diverse regions, a holistic approach that considers both traditional and socioeconomic factors is increasingly important for implementing multidimensional public health programs and integrated social interventions to effectively prevent IR-related diseases. Therefore, understanding the regional relationship between SES and IR is crucial.

Objectives

The 1st objective of the study was to estimate the TyG index and METS-IR index in Janów district, a location characterized by high social deprivation and increased cardiovascular risk according to the Systematic Coronary Risk Evaluation (SCORE) scale. The 2nd objective was to identify significant sociodemographic and health predictors for the TyG index and METS-IR index.

Materials and methods

Study design and participants

The “Take your health to heart” (“Weź sobie zdrowie do serca”) prevention and health promotion program was conducted in the Janów district of eastern Poland from June 14 to March 20, 2016. The initiative was funded by the state budget and the Norwegian Financial Mechanism 2009–2014's Operational Program PL 13 – “Reduction of Social

Inequalities in Health.” Under the PL 13 Program, funding was provided for health promotion and prevention initiatives in local communities with high standardized mortality ratios (SMRs) between 2009 and 2011 in the following categories: malignant neoplasms, CVD, respiratory diseases, digestive diseases, external causes, and total mortality. Out of 38 districts with the highest standardized cardiovascular mortality ratios in Poland, Janów district was ranked 3rd (SMR = 1.357).²⁴

The day before the study, Janów district had a population of 47,500 residents. An epidemiological analysis of CVD incidence among Janów district residents identified a sharp rise in risk between ages 35 and 64. Because the majority of CVD patients are over 65 and healthcare for this group primarily focuses on symptom management, people aged 35–64 were invited to participate in the study, with 18,827 people of this category living in Janów district.

Participants meeting the study criteria were contacted by phone and received invitations from district and municipal authorities, as well as cooperating institutions (religious associations, workplaces, and public utility associations and institutions). The study consisted of 2 stages. Stage 1, the basic study, aimed to identify individuals with a SCORE cardiovascular risk of 5% or higher.²⁵ After a visit by the patient to the doctor, stage 1 ended with the doctor deciding whether to enroll the patient in an educational program for lifestyle improvement or refer them to stage 2. Inclusion criteria for stage 1 were: 1) age 35–64 years; 2) no history of cardiovascular incidents; 3) no CAD diagnosis; (4) informed consent to participate in the study. Exclusion criteria were: 1) history of cardiovascular incidents (heart attack or stroke); 2) CAD diagnosis; 3) pregnancy; 4) inability to provide informed consent to participate in the study; 5) bedridden status; 6) residing in a nursing home or prison. A total of 4,040 participants, 21.45% of the eligible population, participated in stage 1.

Stage 2, involving enhanced diagnostics, was intended for participants scoring 5% or higher on the SCORE scale. This stage was carried out at the Independent Public Complex of Healthcare Facilities in Janów Lubelski. During stage 2, participants underwent a 2nd medical visit, where further testing could be recommended based on enhanced laboratory diagnostics. The aim of this stage included diagnosing the patient, discussing test results with the participant, and referring them for specialized treatment or to a health promotion specialist for better lifestyle management. Of the 3,046 study participants, 168 with diabetes and 221 with a history of cardiovascular events (heart attack or stroke) were excluded. Ultimately, 2,657 respondents were included in the analysis. For the purpose of this study, respondents' results obtained in stage 2 were analyzed.

The study was approved by the Bioethics Committee of the Medical University of Lublin (decision No. KE-0254/112/2014) and conducted in accordance with the Declaration of Helsinki. All participants provided written informed consent.

Anthropometric measurements

Anthropometric measurements of body weight and height were obtained for all respondents. Height was measured using an altimeter to the nearest 0.1 cm, and body weight – without shoes or outer clothing – was measured using a platform scale to the nearest 0.1 kg. Body mass index (BMI) was calculated for each participant by dividing body weight in kilograms (kg) by height in meters squared (kg/m²).²⁶

Blood sampling and laboratory tests

At the blood sample collection point of the Independent Public Complex of Health Care Facility in Janów Lubelski, participants had their blood drawn from the ulnar vein after an overnight fast between 7:00 AM and 9:00 AM. The blood samples were immediately sent to the laboratory for analysis. Serum samples were collected in serum separator tubes (granules) containing a clot activator. Plasma was obtained by centrifugation at 3,000 rpm for 10 min. The serum was used for lipid profile analysis (total cholesterol, triglycerides (TG) and high-density lipoprotein cholesterol (HDL-C)), and serum glucose (FBG) using standard laboratory methods. Cholesterol was calculated using the Friedewald equation when TG levels were <400 mg/dL.²⁷

Physiological measurements

Participants' systolic (SBP) and diastolic (DBP) blood pressure were measured twice. Blood pressure was measured on the left arm using a digital blood pressure monitor. The 1st measurement was taken after a rest period of at least 5 min, and the 2nd measurement was taken 15 min after the first. The mean value of these 2 measurements was used for analysis. An additional measurement was taken after another 15 min if the first 2 measurements differed by more than 5 mm Hg. The mean value of these three measurements was then used for data analysis.²⁸

TyG index and METS-IR index

The anthropometric measurements and biochemical results were used to calculate the METS-IR index and the TyG index for the respondents. The TyG index was calculated using

$$\text{Ln} [\text{TG (mg/dL)} \times \text{FBG (mg/dL)} / 2],^{24}$$

and the METS-IR index was calculated using

$$\frac{\text{Ln} [2 \times \text{FBG (mg/dL)} + \text{TG (mg/dL)}] \times \text{BMI (kg/m}^2\text{)}}{\text{Ln} [\text{HDL-C (mg/dL)}]}.^{14,29}$$

Other variables

A standard questionnaire was used to collect information on age, gender, place of residence, marital status, education, smoking status, frequency of alcohol consumption, and household maintenance.

Two categories of smoking status were identified: non-smoker (those who had never smoked or had stopped smoking at least 1 month before the study) and smoker (those who smoked at least 1 cigarette per day or had smoked a cigarette within the previous month).

Participants were also asked about their alcohol consumption in the year prior to the study. They were also asked how frequently they consumed 1–2 standard doses of alcohol, with 1 dose equivalent to 10 g of pure ethyl alcohol. The respondent could select from the following options: I do not drink alcohol (no alcohol consumption), less than once a month, once a month to once a week, and more than once a week.

Statistical analyses

Numerical variables were presented as mean with standard deviation (SD) and median with interquartile range (Q1–Q3). The distribution of TyG and METS-IR between groups was compared using the Mann–Whitney test or Kruskal–Wallis test. Categorical variables were described by percentages, and the relationship between numerical variables was assessed with Pearson's correlation. In addition, multivariable linear regression with backward elimination ($p < 0.1$) was used to identify significant predictors of TyG and METS-IR. Due to the strong relationship between SBP and DBP, only SBP was included in the multivariable analysis. The results of linear regression were presented as a coefficient (b) with standard error (SE). The coefficient of determination (R^2) was used to describe the goodness-of-fit of the linear regression models. Furthermore, the assumptions of linear regression were checked through plots (linearity (residuals vs fitted), normality of residuals (Q–Q plot), and homogeneity of variance (scale location plot)), whereas the absence of influential observations was confirmed using Cook's distance and the absence of multicollinearity was confirmed with variance inflation factor (VIF). Statistical analyses were performed using IBM SPSS Statistics for Windows, v. 27.0 (IBM Corp., Armonk, USA) and R language (R Core Team (2021); R Foundation for Statistical Computing, Vienna, Austria). P-values < 0.05 were considered statistically significant.

Results

General characteristics of participants

Table 1 shows the characteristics of the study group ($n = 2,657$). The mean age of the study group was 52.7 (± 7.99) years. The majority of participants were women (58.4%, $n = 1,553$), residing in rural areas (66.7%, $n = 1,772$), with vocational education (38.1%, $n = 1,012$), and married (88.1%, $n = 2,343$). The mean TyG index score in the study group was 8.65 (± 0.58) and the mean METS-IR index score was 41.45 (± 9.02).

Relationship between sociodemographic and health variables and levels of the TyG index and METS-IR index

Table 2 shows the relationship between selected sociodemographic and health variables and the TyG index and METS-IR index levels. The TyG index level was positively associated with age ($r = 0.114$, $p < 0.001$), BMI ($r = 0.331$, $p < 0.001$) and blood pressure: SBP ($r = 0.221$, $p < 0.001$), DBP ($r = 0.222$, $p < 0.001$). In addition, a significant increase in the TyG index was observed

Table 1. Baseline demographics and clinical characteristics

Variable		Study group
Demographic and social data		
Age [years] ^b		52.7 \pm 7.99
Sex ^a	female	1,553 (58.4)
	male	1,104 (41.6)
Place of residence ^a	rural	1,772 (66.7)
	urban	885 (33.3)
Education ^a	primary	292 (11)
	vocational	1,012 (38.1)
	secondary	868 (32.7)
	university	485 (18.3)
Marital status	married	2,343 (88.1)
	single	185 (7)
	widow/widower	129 (4.9)
Living alone	no	2,530 (95.2)
	yes	127 (4.8)
Health data		
Smoking status ^a	smoker	413 (15.5)
	former-smoker	558 (21)
	never-smoker	1,686 (63.5)
Alcohol consumption ^a	no or less than once a month	2,374 (89.3)
	between once a month and once a week	157 (5.9)
	more than once a week	126 (4.7)
Clinical data		
BMI [kg/m ²] ^b		28.9 \pm 4.84
Total cholesterol [mg/dL] ^b		223.6 \pm 54.03
LDL-C [mg/dL] ^b		128.3 \pm 59.8
HDL-C [mg/dL] ^b		60.7 \pm 21.17
Triglyceride [mg/dL] ^c		114.7 (80.4–165.5)
Glucose [mg/dL] ^c		94 (87–106)
Blood pressure	SBP [mm Hg] ^b	140 \pm 19.08
	DBP [mm Hg] ^b	85.7 \pm 11.39
TyG ^b		8.65 \pm 0.58
METS-IR ^b		41.45 \pm 9.02

Data are presented as: ^an (%); ^bmean \pm SD; ^cmedian (Q1–Q3); BMI – body mass index; LDL-C – low-density lipoprotein; HDL-C – high-density lipoprotein; SBP – systolic blood pressure; DBP – diastolic blood pressure; TyG – triglyceride-glucose index; METS-IR – metabolic score for insulin resistance index; SD – standard deviation.

in men, participants with primary and vocational education compared to those with higher education ($p \leq 0.01$), as well as in smokers or former smokers compared to never-smokers ($p < 0.001$). Similarly, higher values of the TyG index were associated with more frequent alcohol consumption ($p < 0.001$).

The METS-IR index level was positively associated with age ($r = 0.158$, $p < 0.001$) and blood pressure: SBP ($r = 0.256$, $p < 0.001$), DBP ($r = 0.234$, $p < 0.001$). Men had significantly higher values of the METS-IR index, and as educational level increased, the value of this index decreased. Former smokers had significantly higher values of the METS-IR index compared to smokers or never-smokers ($p < 0.01$, for

comparisons). In addition, respondents who reported consuming 1–2 standard doses of alcohol between once a week or once a month had higher METS-IR values compared to those who reported consuming this amount of alcohol less frequently or not at all ($p = 0.008$).

Multivariable association between Tyg index, METS-IR index, and socioeconomic and health factors

Table 3 shows the significant predictors of the TyG index and METS-IR obtained by linear regression. Age, male

Table 2. Relation between selected sociodemographic and health variables and the TyG index and METS-IR index levels

Variable		TyG	p-value	METS-IR	p-value
Demographic and social data					
Sex	female (n = 1,553)	8.54 ±0.52 8.52 (8.16–8.90)	<0.001 ^a	40.45 ±9.06 39.42 (33.49–43.12)	<0.001 ^a
	male (n = 1,104)	8.8 ±0.64 8.8 (8.34–9.20)		42.87 ±8.79 42.46 (36.46–47.99)	
Place of residence	rural (n = 1,772)	8.65 ±0.6 8.60 (2.88–9.04)	0.675 ^a	41.84 ±9.05 41.30 (35.26–47.41)	<0.001 ^a
	urban (n = 885)	8.65 ±0.56 8.64 (8.25–9.00)		40.67 ±8.92 39.50 (24.36–45.85)	
Education	primary (n = 292)	8.72 ±0.58 8.75 (8.29–9.07)	0.01 ^b	43.5 ±9.06 43.08 (37.28–49.36)	<0.001 ^b
	vocational (n = 1,012)	8.68 ±0.6 8.84 (8.24–9.06)		41.82 ±8.88 41.33 (35.29–47.14)	
	secondary (n = 868)	8.64 ±0.57 8.60 (8.23–9.01)		41.52 ±9.13 40.98 (34.92–47.11)	
	university (n = 485)	8.57 ±0.56 8.53 (8.19–8.93)		39.32 ±8.71 38.04 (32.85–44.52)	
Marital status	married (n = 243)	8.65 ±0.58 8.62 (8.24–9.03)	0.182 ^b	41.55 ±8.92 41.00 (35.15–47.03)	0.100 ^b
	single (n = 185)	8.69 ±0.68 8.66 (8.17–9.11)		40.56 ±10.51 39.53 (31.95–48.50)	
	widow/widower (n = 129)	8.56 ±0.47 8.53 (8.23–8.82)		40.96 ±8.53 39.86 (34.99–46.01)	
Living alone	no (n = 2,530)	8.65 ±0.58 8.62 (8.23–9.02)	0.589 ^a	41.42 ±8.97 40.71 (34.93–46.92)	0.409 ^a
	yes (n = 127)	8.68 ±0.61 8.63 (8.23–9.06)		42.16 ±10.04 41.60 (34.58– 48.63)	
Health data					
Smoking status	smoker (n = 413)	8.8 ±0.66 8.76 (8.30–9.17)	<0.001 ^b	40.81 ±10.2 40.27 (32.97–47.08)	0.001 ^b
	former-smoker (n = 558)	8.73 ±0.59 8.73 (8.31–9.1)		42.59 ±8.78 41.77 (36.31–47.93)	
	never-smoker (n = 1,686)	8.59 ±0.55 8.55 (8.19–8.95)		41.23 ±8.76 40.43 (34.94–46.76)	
Alcohol consumption	no or less than once a month (n = 2,374)	8.62 ±0.57 8.58 (8.21–8.99)	<0.001 ^b	41.33 ±9.05 40.46 (34.82–46.89)	0.008 ^b
	between once a month and once a week (n = 157)	8.89 ±0.63 8.84 (4.46–9.24)		43.37 ±9.00 43.54 (37.25–49.01)	
	more than once a week (n = 126)	8.91 ±0.64 8.89 (8.36–9.40)		41.37 ±8.21 41.79 (34.94–46.72)	

TyG – triglyceride-glucose index; METS-IR – metabolic score for insulin resistance index; BMI – body mass index; data are presented as mean with standard deviation (SD) and median with interquartile range (Q1–Q3). Statistical significance tested with: ^a Mann-Whitney test, ^b Kruskal-Wallis test.

gender, smoking status, and SBP were significantly associated with both TyG and METS-IR. Age and SBP showed a positive relationship with surrogate markers of IR. Moreover, men had higher mean values of both the TyG index and METS-IR index compared to women. Former smokers and never-smokers had lower TyG index values compared to current smokers. However, for METS-IR, participants who were former smokers had higher values than current smokers.

In addition, participants who reported being non-drinkers or consuming alcohol less than once a month had lower TyG index values compared to those who drank alcohol more than once a week. There was also a positive association between BMI and the TyG index. Finally, participants with a university education had lower METS-IR values compared to those with only a primary education level. Based on plots, Cook's distance, and the VIF index, there were no violations of the assumptions of the linear regression model (Supplementary Fig. 1, Supplementary Fig. 2 and Supplementary Table 1).

Discussion

The TyG index and METS-IR index were found to be dependent on sociodemographic and health factors in the local community under study, which is characterized by high social deprivation and increased cardiovascular risk as measured using the SCORE scale. According

to our results, the mean TyG index value among residents of the Janów district in eastern Poland was 8.65 (± 0.58), whereas the mean METS-IR index value was 41.45 (± 9.02). A similar TyG index value was obtained by Mirr et al.³⁰ in a group without diabetes and increased fasting glycaemia, whereas the METS-IR index in their study group was lower (38.2 ± 8.6) than in our study. Li et al.³¹ described slightly different mean TyG index and METS-IR index values in a study conducted in rural areas of China, which were 6.91 and 40.18, respectively. Variations in surrogate markers of IR between our results and earlier studies can be explained by the distinctive characteristics of the Polish population, particularly the high cardiovascular risk determined with SCORE in our study group. This is supported by the findings of Wang et al.,³² who observed that an increase in the METS-IR index level was independently associated with a higher prevalence of coronary artery calcification (CAC). Insulin resistance is strongly related to lifestyle factors such as smoking, alcohol consumption, a high-calorie diet, and physical inactivity. In turn, lifestyle and health-related attitudes are determined by and are related to social, economic and demographic factors. Consequently, the search for associations between IR and sociodemographic variables may contribute to better disease prevention planning, particularly for CVD.

Insulin resistance and aging are closely associated due to factors such as loss of lean body mass, increase in visceral adipose tissue and decline in sex hormone levels.³³

Table 3. Significant predictors of the TyG index and METS-IR index levels

Variable		b	SE	p-value	R ²
TyG					
Demographic and social data	age	0.003	0.001	0.01	0.19
Sex (reference category: female)	male	0.17	0.023	<0.001	
Health and clinical data					
Smoking status (reference category: smoker)	former-smoker	−0.12	0.034	<0.001	
	never-smoker	−0.210	0.03	<0.001	
Alcohol consumption (reference category: more than once a week)	between once a month and once a week	−0.025	0.063	0.70	
	no or less than once a month	−0.16	0.05	0.002	
SBP		0.003	0.009	<0.001	
BMI		0.037	0.002	<0.001	
METS-IR					
Demographic and social data	age	0.102	0.022	<0.001	0.10
Sex (reference category: female)	male	1.488	0.365	<0.001	
Education (reference category: primary)	vocational	−0.929	0.585	0.11	
	secondary	−0.728	0.595	0.22	
	university	−1.877	0.674	0.005	
Health and clinical data					
Smoking status (reference category: smoker)	former-smoker	1.708	0.563	0.003	
	never-smoker	0.625	0.486	0.199	
SBP		0.099	0.009	<0.001	

TyG – triglyceride-glucose index; METS-IR – metabolic score for insulin resistance index; SBP – systolic blood pressure; BMI – body mass index; b – regression coefficients; SE – standard error; R² – coefficient of determination.

Higher METS-IR index values in older adults were observed in the South Korean population studied by Wang et al.,³² whereas higher TyG index values were observed in the American population study by Sun et al.³⁴

In our sample, men had significantly higher IR values than women. This is consistent with findings from a Chinese cohort³⁵ and a Japanese cohort,³⁶ where women showed lower TyG index values and METS-IR index values, respectively. The protective role of estrogen in the development of IR may account for these differences in surrogate markers of IR between men and women.³⁷ However, it must be noted that Nakagomi et al.³⁸ hypothesized that changes in sex hormone levels and body composition related to menopause may diminish the predictive ability of female sex, making it similar to that of male sex, but this hypothesis needs confirmation.

In our study, lower education levels were associated with higher levels of METS-IR index and TyG index in univariate models, although this relationship was observed only for METS-IR in the multivariable analysis. Similar results to ours were obtained by Bukhari³⁹ and Almubark et al.⁴⁰ The correlation between education and IR and diabetes risk was also validated in an extensive European study.⁴¹

Both the TyG index and METS-IR index were found to be related to smoking. Former smokers and never-smokers had lower TyG index values than smokers, and former smokers had higher METS-IR index values than smokers. Similar results were obtained by Ferreira et al.⁴² and Li et al.⁴³ Experimental research indicates that smoking can induce and worsen IR through mechanisms involving catecholamines and other anti-insulin hormones, thus disrupting glucose and lipid metabolism and exacerbating vascular endothelial cell dysfunction.⁴⁴ Smokers also exhibit relatively low insulin sensitivity compared to non-smokers. It should be noted that insulin sensitivity improves within 1–2 weeks after quitting smoking, although it never returns to normal values.⁴⁵ Observations were similar regarding alcohol consumption. Surrogate markers of IR were higher in those who drank alcohol more frequently, although this trend was seen only for the TyG index in the multivariable analysis. The relationship between IR and alcohol consumption was also observed by Bermudez et al.⁴⁶ However, in a meta-analysis of 47 studies, Bendtsen et al.⁴⁷ found that beer intake >500 mL/day is positively associated with abdominal obesity, which plays a key role in the development of IR.

A significant correlation has been observed in certain prospective and cross-sectional studies between the TyG index and BMI⁴⁸ and the METS-IR index and the TyG index and the risk of hypertension.^{49,50} Our study revealed the same relationship. The mechanism explaining the correlation between surrogate markers of IR and hypertension could be attributed to overstimulation of the sympathetic nervous system, which increases cardiac output and peripheral vascular resistance, thereby raising blood pressure.⁵¹ In addition, IR stimulates the activity of the renin–angiotensin–aldosterone

system by increasing tubular Na⁺ reabsorption,⁵² which can cause a rapid rise in blood pressure. In contrast, a higher BMI indicates the presence of excess body fat and is associated with elevated levels of free fatty acids and inflammatory mediators such as interleukin 6 (IL-6) and tumor necrosis factor alpha (TNF- α), which are closely related to IR because they impair lipid homeostasis and lead to inflammation.⁵³

Limitations

The study had several limitations. First, the cross-sectional study design did not allow us to address the causality of the observed relationships. Second, because the respondents had an increased cardiovascular risk, presumably due to risk factors such as poor diet and lack of physical activity being more prevalent in our study group, the TyG index and METS-IR index values may be overestimated compared to the general population. Third, we used surrogate markers of IR instead of including HOMA-IR, which has been more widely used in previous studies. However, previous studies comparing multiple indices to assess IR levels have found similar effects when using HOMA-IR, TyG, and METS-IR indices.^{14,54} Lastly, because every study participant was Polish, it is unclear whether our findings apply to other ethnic groups. Future research examining the relationship between SES and IR should use a nationally representative sample and clarify the mechanisms linking low SES to IR when behavioral-health variables are considered. Nonetheless, our research undoubtedly contributes to understanding the relationship between sociodemographic and health factors and IR in a local community with increased cardiovascular risk and high deprivation. These findings may be useful in the development of primary and secondary CVD prevention strategies.

From a practical standpoint, this work has implications for healthcare professionals and future researchers. The study results may be of key importance for healthcare professionals such as physicians, nurses, dieticians, and others working with low-income, undereducated or at-risk patients for diabetes and CVD. Healthcare workers, particularly those in primary care, can monitor patients undergoing treatment or seeking to adopt a healthier lifestyle over time by using surrogate IR markers to quickly and affordably determine the patient's risk of IR. Such assessments should be routine, especially in communities with low SES. If significant screening deviations occur, the patient may be referred for more expensive, in-depth diagnostic procedures.

Conclusions

The study results show a significant relationship between surrogate markers of IR and sociodemographic and health-related variables. The TyG index and METS-IR index values were found to increase with age and SBP. In addition, these

indices showed higher values in men, people with lower education levels, current or former smokers, and those who consume alcohol more frequently. Furthermore, the TyG index was positively associated with BMI. Low-cost surrogate markers of IR, such as the TyG index or METS-IR index, may find use in primary healthcare for assessing IR, potentially facilitating early prevention of CVD.

Supplementary data

The Supplementary materials are available at <https://doi.org/10.5281/zenodo.12664545>. The package includes the following files:

Supplementary Table 1. The values of VIF for independent predictors for TyG and METS-IR.

Supplementary Fig. 1. Testing the assumption of multivariable linear model for independent predictors for TyG index.

Supplementary Fig. 2. Testing the assumption of multivariable linear model for independent predictors for METS-IR index.

Data availability


The datasets generated and/or analyzed during the current study are available from the corresponding author on reasonable request.


Consent for publication


All authors have read and approved the published version of the manuscript.

ORCID iDs

Maciej Polak  <https://orcid.org/0000-0003-1290-8692>

Grzegorz J. Nowicki  <https://orcid.org/0000-0002-0503-8847>

Maja Chrzanowska-Wąsik  <https://orcid.org/0000-0002-5589-2021>

Barbara J. Ślusarska  <https://orcid.org/0000-0003-0101-9216>

References

- Virani SS, Alonso A, Benjamin EJ, et al. Heart disease and stroke statistics: 2020 update. A report from the American Heart Association. *Circulation*. 2020;141(9):e139–e596. doi:10.1161/CIR.0000000000000757
- Jernberg T, Hasvold P, Henriksson M, Hjelm H, Thuresson M, Janzon M. Cardiovascular risk in post-myocardial infarction patients: Nationwide real world data demonstrate the importance of a long-term perspective. *Eur Heart J*. 2015;36(19):1163–1170. doi:10.1093/eurheartj/ehu505
- Koliaki C, Liatis S, Kokkinos A. Obesity and cardiovascular disease: Revisiting an old relationship. *Metabolism*. 2019;92:98–107. doi:10.1016/j.metabol.2018.10.011
- Ormazabal V, Nair S, Elfeky O, Aguayo C, Salomon C, Zuñiga FA. Association between insulin resistance and the development of cardiovascular disease. *Cardiovasc Diabetol*. 2018;17(1):122. doi:10.1186/s12933-018-0762-4
- Laakso M, Kuusisto J. Insulin resistance and hyperglycaemia in cardiovascular disease development. *Nat Rev Endocrinol*. 2014;10(5):293–302. doi:10.1038/nrendo.2014.29
- Bornfeldt KE, Tabas I. Insulin resistance, hyperglycemia, and atherosclerosis. *Cell Metab*. 2011;14(5):575–585. doi:10.1016/j.cmet.2011.07.015
- Liu A, Abbasi F, Reaven GM. Adiposity indices in the prediction of metabolic abnormalities associated with cardiovascular disease in non-diabetic adults. *Nutr Metab Cardiovasc Dis*. 2011;21(8):553–560. doi:10.1016/j.numecd.2009.12.009
- Muniyappa R, Lee S, Chen H, Quon MJ. Current approaches for assessing insulin sensitivity and resistance in vivo: Advantages, limitations, and appropriate usage. *Am J Physiol Endocrinol Metab*. 2008;294(1):E15–E26. doi:10.1152/ajpendo.00645.2007
- Seifi N, Nosrati M, Koochackpoor G, et al. The association between hyperuricemia and insulin resistance surrogates, dietary- and life-style insulin resistance indices in an Iranian population: MASHAD cohort study. *Nutr J*. 2024;23(1):5. doi:10.1186/s12937-023-00904-2
- Wen J, Wang A, Liu G, et al. Elevated triglyceride-glucose (TyG) index predicts incidence of prediabetes: A prospective cohort study in China. *Lipids Health Dis*. 2020;19(1):226. doi:10.1186/s12944-020-01401-9
- Ding X, Wang X, Wu J, Zhang M, Cui M. Triglyceride-glucose index and the incidence of atherosclerotic cardiovascular diseases: A meta-analysis of cohort studies. *Cardiovasc Diabetol*. 2021;20(1):76. doi:10.1186/s12933-021-01268-9
- Pranata R, Huang I, Irvan, Lim MA, Vania R. The association between triglyceride-glucose index and the incidence of type 2 diabetes mellitus: A systematic review and dose-response meta-analysis of cohort studies. *Endocrine*. 2021;74(2):254–262. doi:10.1007/s12020-021-02780-4
- Guo W, Zhao L, Mo F, et al. The prognostic value of the triglyceride glucose index in patients with chronic heart failure and type 2 diabetes: A retrospective cohort study. *Diabetes Res Clin Pract*. 2021;177:108786. doi:10.1016/j.diabres.2021.108786
- Bello-Chavolla OY, Almeda-Valdes P, Gomez-Velasco D, et al. METS-IR, a novel score to evaluate insulin sensitivity, is predictive of visceral adiposity and incident type 2 diabetes. *Eur J Endocrinol*. 2018;178(5):533–544. doi:10.1530/EJE-17-0883
- Tao LC, Xu JN, Wang TT, Hua F, Li JJ. Triglyceride-glucose index as a marker in cardiovascular diseases: Landscape and limitations. *Cardiovasc Diabetol*. 2022;21(1):68. doi:10.1186/s12933-022-01511-x
- Song Y, Cui K, Yang M, et al. High triglyceride-glucose index and stress hyperglycemia ratio as predictors of adverse cardiac events in patients with coronary chronic total occlusion: A large-scale prospective cohort study. *Cardiovasc Diabetol*. 2023;22(1):180. doi:10.1186/s12933-023-01883-8
- Powell-Wiley TM, Baumer Y, Baah FO, et al. Social determinants of cardiovascular disease. *Circ Res*. 2022;130(5):782–799. doi:10.1161/CIRCRESAHA.121.319811
- Kinge JM, Modalsli JH, Øverland S, et al. Association of household income with life expectancy and cause-specific mortality in Norway, 2005–2015. *JAMA*. 2019;321(19):1916. doi:10.1001/jama.2019.4329
- De Mestral C, Stringhini S. Socioeconomic status and cardiovascular disease: An update. *Curr Cardiol Rep*. 2017;19(11):115. doi:10.1007/s11886-017-0917-z
- Smetkowski M, Gorzelak G, Ploszaj A, Rok J. Poviats threatened by deprivation: State, trends and prospects. Warsaw, Poland: Centre for European Regional and Local Studies EUROREG, University of Warsaw; 2015. doi:10.13140/RG.2.2.22835.84004
- Statistics Poland. *Report on Results: National Census of Population and Apartments 2011* [in Polish]. Warsaw, Poland: Statistics Poland; 2012. https://stat.gov.pl/cps/rde/xbcr/gus/lud_raport_z_wynikow_NSP2011.pdf.
- Provincial Labor Office in Lublin. The situation on the labor market in the Lublin Voivodeship: February 2015. Lublin, Poland: Provincial Labor Office in Lublin; 2015. <https://wuplublin.praca.gov.pl/-/1355901-sytuacja-na-rynku-pracy-w-województwie-lubelskim-luty-2015>.
- Statistics Poland. *Beneficiaries of Social Assistance and Family Benefits in 2012* [in Polish]. Warsaw, Poland: Statistics Poland; 2013. https://stat.gov.pl/files/gfx/portalinformacyjny/pl/defaultaktualnosci/5487/6/3/5/beneficjenci_pomocy_spolecznej_i_swadczen_rodziny_2012.pdf.
- Ministry of Health of the Republic of Poland. Program PL 13. Publication of mortality rates for selected districts [in Polish]. Warsaw, Poland: Ministry of Health of the Republic of Poland; 2014. http://archiwum.zdrowie.gov.pl/aktualnosc-27-2136-Program_PL_13_publicacja_wskaznikow_umieralnosci_dla_wybranych_powiatow.html.

25. Piepoli MF, Hoes AW, Agewall S, et al. 2016 European Guidelines on cardiovascular disease prevention in clinical practice [in Polish]. *Kardiol Pol.* 2016;74(9):821–936. doi:10.5603/KP.2016.0120
26. World Health Organization (WHO). *Physical Status: The Use and Interpretation of Anthropometry. Report of a WHO Expert Committee.* Vol. 854. Geneva, Switzerland: World Health Organization (WHO); 1995. https://iris.who.int/bitstream/handle/10665/37003/WHO_TRS_854.pdf?sequence=1.
27. Boekholdt SM, Arsenault BJ, Mora S, et al. Association of LDL cholesterol, non-HDL cholesterol, and apolipoprotein B levels with risk of cardiovascular events among patients treated with statins: A meta-analysis. *JAMA.* 2012;307(12):1302. doi:10.1001/jama.2012.366
28. Liu Y, Chi HJ, Cui LF, et al. The ideal cardiovascular health metrics associated inversely with mortality from all causes and from cardiovascular diseases among adults in a northern Chinese industrial city. *PLoS One.* 2014;9(2):e89161. doi:10.1371/journal.pone.0089161
29. Simental-Mendía LE, Rodríguez-Morán M, Guerrero-Romero F. The product of fasting glucose and triglycerides as surrogate for identifying insulin resistance in apparently healthy subjects. *Metab Syndr Relat Disord.* 2008;6(4):299–304. doi:10.1089/met.2008.0034
30. Mirr M, Skrypnik D, Bogdański P, Owecki M. Newly proposed insulin resistance indexes called TyG-NC and TyG-NHtR show efficacy in diagnosing the metabolic syndrome. *J Endocrinol Invest.* 2021;44(12):2831–2843. doi:10.1007/s40618-021-01608-2
31. Li X, Xue Y, Dang Y, et al. Association of non-insulin-based insulin resistance indices with risk of incident prediabetes and diabetes in a Chinese rural population: A 12-year prospective study. *Diabetes Metab Syndr Obes.* 2022;15:3809–3819. doi:10.2147/DMSO.S385906
32. Wang Z, Hui X, Huang X, Li J, Liu N. Relationship between a novel non-insulin-based metabolic score for insulin resistance (METS-IR) and coronary artery calcification. *BMC Endocr Disord.* 2022;22(1):274. doi:10.1186/s12902-022-01180-7
33. Barzilai N, Huffman DM, Muzumdar RH, Bartke A. The critical role of metabolic pathways in aging. *Diabetes.* 2012;61(6):1315–1322. doi:10.2337/db11-1300
34. Sun M, Guo H, Wang Y, Ma D. Association of triglyceride glucose index with all-cause and cause-specific mortality among middle age and elderly US population. *BMC Geriatr.* 2022;22(1):461. doi:10.1186/s12877-022-03155-8
35. Han KY, Gu J, Wang Z, et al. Association between METS-IR and prehypertension or hypertension among normoglycemia subjects in Japan: A retrospective study. *Front Endocrinol (Lausanne).* 2022;13:851338. doi:10.3389/fendo.2022.851338
36. Guo W, Zhu W, Wu J, et al. Triglyceride glucose index is associated with arterial stiffness and 10-year cardiovascular disease risk in a Chinese population. *Front Cardiovasc Med.* 2021;8:585776. doi:10.3389/fcvm.2021.585776
37. Suba Z. Low estrogen exposure and/or defective estrogen signaling induces disturbances in glucose uptake and energy expenditure. *J Diabetes Metab.* 2013;4(5):1000272. doi:10.4172/2155-6156.1000272
38. Nakagomi A, Sunami Y, Kawasaki Y, Fujisawa T, Kobayashi Y. Sex difference in the association between surrogate markers of insulin resistance and arterial stiffness. *J Diabetes Complications.* 2020;34(6):107442. doi:10.1016/j.jdiacomp.2019.107442
39. Bukhari HM. Sociodemographic variables associated with the prevalence of insulin resistance using a non-invasive score system among adults in the Makkah region of Saudi Arabia. *Curr Res Nutr Food Sci.* 2023;11(2):685–695. doi:10.12944/CRNFSJ.11.2.19
40. Almubark RA, Althumairi NA, Alhamdan AA, et al. Socioeconomic and behavioral disparities among diabetics in Saudi Arabia: A nation-wide descriptive study. *Diabetes Metab Syndr Obes.* 2022;15:2693–2703. doi:10.2147/DMSO.S352769
41. Sacerdote C, Ricceri F, Rolandsson O, et al. Lower educational level is a predictor of incident type 2 diabetes in European countries: The EPIC-InterAct study. *Int J Epidemiol.* 2012;41(4):1162–1173. doi:10.1093/ije/dys091
42. Ferreira JRS, Zandonade E, Bezerra OMDPA, Salaroli LB. Insulin resistance by the triglyceride-glucose index in a rural Brazilian population. *Arch Endocrinol Metab.* 2022;66(6):848–855. doi:10.20945/2359-39970.0000509
43. Li X, Qin P, Cao L, et al. Dose–response association of the ZJU index and fatty liver disease risk: A large cohort in China. *J Gastroenterol Hepatol.* 2021;36(5):1326–1333. doi:10.1111/jgh.15286
44. Ebrahimi M, Seyedi SA, Nabipoorashrafi SA, et al. Lipid accumulation product (LAP) index for the diagnosis of nonalcoholic fatty liver disease (NAFLD): A systematic review and meta-analysis. *Lipids Health Dis.* 2023;22(1):41. doi:10.1186/s12944-023-01802-6
45. Bergman BC, Perreault L, Hunerdosse D, et al. Novel and reversible mechanisms of smoking-induced insulin resistance in humans. *Diabetes.* 2012;61(12):3156–3166. doi:10.2337/db12-0418
46. Bermudez V, Salazar J, Martínez MS, et al. Prevalence and associated factors of insulin resistance in adults from Maracaibo City, Venezuela. *Adv Prevent Med.* 2016;2016:9405105. doi:10.1155/2016/9405105
47. Bendsen NT, Christensen R, Bartels EM, et al. Is beer consumption related to measures of abdominal and general obesity? A systematic review and meta-analysis. *Nutr Rev.* 2013;71(2):67–87. doi:10.1111/j.1753-4887.2012.00548.x
48. Li Y, You A, Tomlinson B, et al. Insulin resistance surrogates predict hypertension plus hyperuricemia. *J Diabetes Invest.* 2021;12(11):2046–2053. doi:10.1111/jdi.13573
49. Shan S, Li S, Lu K, et al. Associations of the triglyceride and glucose index with hypertension stages, phenotypes, and their progressions among middle-aged and older Chinese. *Int J Public Health.* 2023;68:1605648. doi:10.3389/ijph.2023.1605648
50. Mei J, Li Y, Dong J, et al. Impacts of obesity on global subclinical left cardiac function represented by CMR-derived myocardial strain: TyG index may be a predictor. *Sci Rep.* 2023;13(1):16031. doi:10.1038/s41598-023-43343-z
51. Esler M. Sympathetic nervous system and insulin resistance: From obesity to diabetes. *Am J Hypertens.* 2001;14(11 Pt 2):304S–309S. doi:10.1016/S0895-7061(01)02236-1
52. McEniery CM, Wilkinson IB, Johansen NB, et al. Nondiabetic glucometabolic status and progression of aortic stiffness: The Whitehall II Study. *Diabetes Care.* 2017;40(4):599–606. doi:10.2337/dc16-1773
53. Daryabor G, Kabelitz D, Kalantar K. An update on immune dysregulation in obesity-related insulin resistance. *Scand J Immunol.* 2019;89(4):e12747. doi:10.1111/sji.12747
54. Ko J, Skudder-Hill L, Tarrant C, Kimita W, Bharmal SH, Petrov MS. Intra-pancreatic fat deposition as a modifier of the relationship between habitual dietary fat intake and insulin resistance. *Clin Nutr.* 2021;40(7):4730–4737. doi:10.1016/j.clnu.2021.06.017

The translation into Polish, cultural adaptation, and initial validation of the Action Research Arm Test in subacute stroke patients

Joanna Małecka^{1,A–F}, Magdalena Goliwąg^{2,B,F}, Katarzyna Adamczewska^{1,B,F}, Jacek Lewandowski^{2,E,F}, Dawid Łochyński^{1,A,C–F}

¹ Department of Neuromuscular Physiotherapy, Poznan University of Physical Education, Poland

² Department of Musculoskeletal Rehabilitation, Poznan University of Physical Education, Poland

A – research concept and design; B – collection and/or assembly of data; C – data analysis and interpretation; D – writing the article; E – critical revision of the article; F – final approval of the article

Advances in Clinical and Experimental Medicine, ISSN 1899–5276 (print), ISSN 2451–2680 (online)

Adv Clin Exp Med. 2025;34(7):1165–1173

Address for correspondence

Joanna Małecka

E-mail: malecka@awf.poznan.pl

Funding sources

None declared

Conflict of interest

None declared

Received on October 26, 2023

Reviewed on March 18, 2024

Accepted on July 29, 2024

Published online on December 4, 2024

Abstract

Background. In Poland, there are limited validated outcome measures to evaluate upper extremity function in stroke patients for clinical and research use. The Action Research Arm Test (ARAT) aims to assess functional performance of the upper extremities.

Objectives. To translate and culturally adapt the original version of ARAT into Polish, and to determine its reliability and validity.

Materials and methods. A Polish version of ARAT (ARAT-PL) was developed using a forward-backward translation. The study then examined 60 patients with subacute stroke. Internal consistency (α), test–retest and inter-rater reliability (intra-class correlation (ICC), κ), standard error of measurement (SEM), minimal detectable change (MDC), and floor and ceiling effects were determined. The construct validity was evaluated using the method of hypothesis testing based on the results of correlations (ρ) between subscale and total scores of the ARAT-PL and the upper and lower extremity section of the Fugl–Meyer Assessment (FMA-UE and FMA-LE).

Results. The internal consistency of the total scores and subscale was excellent ($\alpha = 0.97–0.99$). Test–retest and inter-rater reliability scores were almost perfect ($\kappa = 0.85–1.0$) and excellent for the total and subscale scores ($\text{ICC} = 0.99–1$). The SEM and MDC for the test–retest and inter-rater reliability were 0.479, 1.327 points and 0.335, 0.930 points, respectively. The ceiling effect amounted to 48%. The validity levels with respect to FMA-UE and FMA-LE were found to be high (ρ ranging from 0.70 to 0.83) and moderate (ρ ranging from 0.53 to 0.68), respectively.

Conclusions. A Polish version of ARAT is a reliable and valid tool for assessing upper extremity function in subacute stroke patients in Poland. However, it appears to have a ceiling effect that limits differentiation of patients with mild upper limb impairment.

Key words: stroke, outcome measure, ARAT, FMA, upper extremity function

Cite as

Małecka J, Goliwąg M, Adamczewska K, Lewandowski J, Łochyński D. The translation into Polish, cultural adaptation, and initial validation of the Action Research Arm Test in subacute stroke patients. *Adv Clin Exp Med.* 2025;34(7):1165–1173. doi:10.17219/acem/191775

DOI

10.17219/acem/191775

Copyright

Copyright by Author(s)

This is an article distributed under the terms of the Creative Commons Attribution 3.0 Unported (CC BY 3.0) (<https://creativecommons.org/licenses/by/3.0/>)

Background

Stroke is a leading cause of disability in modern societies.^{1,2} In a large number of patients, motor and functional deficits are observed after a stroke.³ Upper extremity dysfunction is present in approx. 30–66% of stroke survivors⁴; it manifests in limitations in reaching and grasping movements, resulting in serious deterioration in the ability to perform daily living activities.^{5,6}

There are various outcome measures to assess the level of upper limb functional capacity after stroke. Examples frequently seen in the literature and practice include the Fugl–Meyer Assessment for Upper Extremity (FMA-UE), the Jebsen Hand Function Test and the Chedoke Arm and Hand Activity Inventory.⁷ One of the commonly used upper extremity assessment measures for post-stroke patients is the Action Research Arm Test (ARAT).⁸ This test was described by Lyle in 1981,⁹ and was based on Carroll's Upper Extremity Function Test.^{10–12} It was designed for observation of the arm and hand during grasping, gripping, pinching and gross movements in people with cortical damage.¹³ Previous studies have shown good psychometric properties of this instrument in stroke patients.^{13–15} The ARAT has shown excellent internal consistency in stroke patients with mild-to-moderate hemiparesis ($\alpha = 0.98$).¹⁶ The test–retest and inter-rater reliability, as calculated using intraclass correlation (intra-class correlation (ICC): 0.92–0.99) for the total and all subscales' scores, was similarly excellent when tested in patients with subacute stroke.^{7,16–18} Studies examining the convergent validity of ARAT have reported moderate, good or excellent correlations between the absolute ($\rho = 0.77$ – 0.94) and subscale scores ($\rho = 0.67$ – 0.74) of ARAT and FMA.^{17–19} To date, the original version of the ARAT has been translated into Swedish,²⁰ Chinese²¹ and Spanish (in Chile).²² No studies have reported cultural adaptation of ARAT or assessed its reliability and validity on Polish stroke survivors; thus, there is a significant need to develop a Polish version of ARAT.

Objectives

The principal aim of the present study was to estimate the reliability and construct validity of a translated and culturally adapted Polish version of ARAT in the population of subacute patients with stroke. Construct validity was estimated by the correlation of total and subscale ARAT scores with scores for the translated upper and lower extremity sections of the FMA.²³

Materials and methods

Translation and cultural adaptation

Forward, backward and final translation

The ARAT was translated into Polish by following the international guidelines.^{24–27} Permission for the outcome measure translation was obtained from the author, Ronald Lyle (Wolters Kluwer Health rights). In the 1st and 2nd stages, the English version of ARAT was independently translated using a process that encompassed semantic, idiomatic, experimental, and conceptual meaning. The translation was performed by 2 bilingual Polish translators fluent in English (1 specialized in the physiotherapy field). The 2 Polish versions were compared; the differences between the translations were discussed and corrected, and the draft of the common version was jointly established.

In the 3rd stage, this Polish draft was back translated into English independently by 2 certified English translators. A common retranslated English version was then created. This was compared to the original English version by 2 native-speaking translators specialized in health sciences and rehabilitation. Where necessary, corrections were made to the retranslated version.

In the 4th stage, a panel of judges consisting of a neurologist, a psychologist, 2 neurological physiotherapists, 1 clinical neurophysiology and 1 orthopedic physiotherapist, and all the translators compared and discussed the differences between the translated and original versions of the ARAT. Based on the detected differences, the emerging Polish version of ARAT was corrected to obtain a satisfactory harmony between cultural language requirements and the original English instrument. Lastly, the linguistic consistency between the final Polish and original English versions was verified very carefully to ascertain the equivalence of concepts. The final version of ARAT-PL was therefore established (stages 5 and 6).

Study design, participants and initial evaluation

This was a cross-sectional study that lasted for 7 months. We recruited 60 stroke patients from the Bonifraterskie Medical Center hospital in Piaski, Poland. The inclusion criteria were: 1) a diagnosis of stroke, as indicated by computed tomography (CT) scans or magnetic resonance imaging (MRI), 2) hemiparesis, and 3) no additional orthopedic or neurological disabling deficits. The exclusion criteria were: 1) total hemiparesis in the upper extremity (i.e., score = 4 on the Modified Ashworth Scale), 2) serious visual and hearing disorders, 3) cognitive decline that limited administration of the tests, 4) disorders of speech and language, and 5) a native language other than Polish.

During the initial evaluation, we collected demographic data such as age, gender, weight, height, and upper limb lateralization. We also collected clinical data such as duration of illness, type of lesion, location of lesion, involved side, presence of comorbidities, and duration of rehabilitation in the hospital.

The study was approved by the Bioethical Committee of Poznan University of Medical Sciences (approval No. 187/19) and was carried out in accordance with the Declaration of Helsinki. Informed consent was obtained from all participants at the time of their enrolment in the study.

Procedure of assessment

The ARAT-PL and FMA were carried out by 2 experienced neurological physiotherapists trained in administration of each measure. Reproducibility, i.e., the degree to which the score is free from random error, was assessed with test–retest and inter-rater procedures.²⁸ To determine inter-rater reliability, 2 raters independently examined patients at the same time in a quiet hospital room.²⁹ Test–retest reliability was obtained by 1 observer examining the patients twice on the same day with a 2-h gap between assessments.²⁹ The results were collected for the total and subscales of ARAT and FMA.

Outcome measures

Action Research Arm Test

This clinical scale is an evaluative measure to assess dexterity and object-handling ability. It was initially designed for individuals who sustained stroke resulting in hemiplegia. The original ARAT consists of 4 subtests: Grasp, Grip, Pinch, and Gross Movement. Every item within the subtest is assessed on a 4-point ordinal scale and arranged with the most difficult task 1st and the easiest 2nd.¹⁷

Fugl–Meyer assessment

The FMA is a recommended clinical assessment of sensorimotor function of the upper and lower extremities; it has mostly been used after stroke.³⁰ The FMA has been translated into Polish but has not yet been cross-culturally adapted.²³ The present study administered only the motor domain of the (as yet unpublished) Polish version of FMA for the upper extremity (FMA-UE) and lower extremity (FMA-LE).²³ The maximum score for the total motor scale is 100 points (66 for FM-UE and 34 for FM-LE).^{18,31,32}

Statistical analyses

The statistical analysis was made using a software package in Statistica v. 13 (Tibco Software Inc Polska, Cracow, Poland) and R studio program (the psych package, v. 2.4.3).³³

Internal consistency

Internal consistency evaluates the homogeneity of the scale items.²⁸ This study used Cronbach's α to assess internal consistency for the subscales and total scale.^{34,35}

Reliability

The test–retest and inter-rater reliability of ARAT were determined using kappa coefficients, the ICC (ICC 2,k, absolute agreement, the command in RStudio: 1st line – choosing the psych package, 2nd line –library(psych) IC C(dane[,c(1,2)])\$results[5,]), and percentage of agreement (PA).^{8,36,37} Item reliability was established when more than 80% agreement was observed.⁸ The minimal detectable change and standard error of measurement were calculated for all scale items according to the following Equations 1,2:

$$SEM = SD\sqrt{1 - ICC} \quad (1)$$

$$MDC = 1.96 \times SEM \times \sqrt{2} \quad (2)$$

where ICC is the reliability of the test and SD is the standard deviation of all scores.

Validity

Construct validity was evaluated using hypotheses testing according to the guidelines of the Consensus-based Standards for the Selection of Health Measurement Instruments (COSMIN).²⁷ A total of 10 independent hypotheses were formed. For each of them, we defined the anticipated Spearman's rank correlation direction, correlation strength, and rationale; upon these, we based the hypothesis (Table 1,2).³⁸ We assessed the relationships of ARAT-PL scores with scores in FMA-UE (5 hypotheses) and FMA-LE (5 hypotheses) to determine the degree to which they were consistent with the formulated hypotheses. The construct validity rating for ARAT-PL was assessed according to the total number of confirmed hypotheses: 8–10 ($\geq 75\%$) indicated high construct validity, while 5–7 ($\geq 50\%$) indicated a moderate level.²⁷ The threshold values for the correlations determined in the present study (Table 1,2) were based on those indicated by Prinsen et al.²⁷

Spearman's rank correlation is computationally identical to Pearson's product-moment coefficient. Therefore, we computed the required sample size for Spearman's correlation using the software G*Power (v. 3.1.9.2; Kiel University, Germany)³⁹ for estimating sample size for Pearson's correlation (bivariate normal model). We assumed correlation p H1: 0.70 (we expected moderate correlation), alpha of 0.05, a power of 0.95, and correlation p H0: 0.0 (we expected low correlation) for a 1-tailed test (we expected correlation between both measures to be positive). The calculation estimated that at least 44 participants were necessary; our study had a sample of 60.

Table 1. The method of hypothesis testing used to assess construct validity of the ARAT-PL based on its associations with FMA-UE

Hypotheses tested	Rationale	Correlation expected	FMA-UE	
			correlation actual (p < 0.001)	confirmed?
1. There will be at least a moderate-strong positive correlation between the overall result of ARAT-PL and FMA-UE	ARAT-PL and FMA-UE measure similar constructs but asked differently (actual functional vs motor performance)	≥0.50	0.83	yes
2. There will be at least a moderate-strong positive correlation between the result of the ARAT-PL subtest Grasp and the total FMA-UE result	ARAT-PL and FMA-UE measure similar constructs but asked differently (actual grasp versus motor performance)	≥0.50	0.83	yes
3. There will be at least a moderate-strong positive correlation between the result of the ARAT-PL subtest Grip and the total result of FMA-UE	ARAT-PL and FMA-UE measure similar constructs but asked differently (actual grip vs motor performance)	≥0.50	0.80	yes
4. There will be at least a moderate-strong positive correlation between the result of the ARAT-PL subtest called Pinch and the total result of FMA-UE	ARAT-PL and FMA-UE measure similar constructs but asked differently (actual pinch grip vs motor performance)	≥0.50	0.82	yes
5. There will be at least a moderate-strong positive correlation between the result of the ARAT-PL subtest Gross Movement and the total result of FMA-UE	ARAT-PL and FMA-UE measure similar constructs but asked differently (actual gross movement vs motor performance)	≥0.50	0.71	yes

ARAT-PL – Polish version of the Action Research Arm Test; FMA-UE – Fugl–Meyer Assessment for Upper Extremity.

Table 2. The method of hypothesis testing used to assess construct validity of the ARAT-PL based on its associations with FMA-LE

Hypotheses tested	Rationale	Correlation expected	FMA-LE	
			correlation actual (p < 0.001)	confirmed?
6. There will be none-minimal positive correlation between the overall result of ARAT-PL and FMA-LE	ARAT-PL and FMA-LE measure unrelated constructs (actual functional vs lower limb motor performance)	≤0.30	0.59	no
7. There is no or low correlation between the result of the ARAT-PL subtest Grasp and the total result of the FMA-LE	ARAT-PL and FMA-LE measure unrelated constructs (grasp vs lower limb motor performance)	≤0.30	0.68	no
8. There is no or low correlation between the result of the ARAT-PL subtest Grip and the total FMA-LE result.	ARAT-PL and FMA-LE measure unrelated constructs (grip vs lower limb motor performance)	≤0.30	0.63	no
9. There is no or low correlation between the result of the ARAT-PL subtest Pinch and the FMA-LE total score.	ARAT-PL and FMA-LE measure unrelated constructs (pinch grip vs lower limb motor performance)	≤0.30	0.58	no
10. There is no or low correlation between the result of the ARAT-PL subtest Gross Movement and the total result of FMA-LE	ARAT-PL and FMA-LE measure unrelated constructs (gross movement vs lower limb motor performance)	≤0.30	0.53	no

ARAT-PL – the Polish version of the Action Research Arm Test; FMA-LE – Fugl–Meyer Assessment for Lower Extremity.

Floor and ceiling effects

Floor and ceiling effects were determined as the proportion of answers scoring beyond the lower (floor) and upper (ceiling) boundaries of the total ARAT score (0–57 points). The cutoff points for these boundaries were established at 5%, so that scores under 3 were considered as the floor and those above 54 as the ceiling. Floor and ceiling effects were established if more than 20% of patients fell outside either the set lower or upper boundaries.²¹ The level of significance selected throughout was $p < 0.05$.

Results

Clinical characteristics of the patients

A total of 60 subjects in the subacute stage of stroke participated in the examination, of whom 63.3% had left hemiplegia and 36.7% right hemiplegia. Of the patients, 31.6% were women and 68.4% were men. The mean age was 64 years (range: 31–85 years). The median length of time since stroke was 47 days (range: 22–138 days). Most of the patients were right-handed (93.3%); only 6.7% were ambidextrous.

Table 3. Changes introduced during the whole process of cultural adaptation

Forward translation		Backward translation		Final translation	
original words/ sentences	translated words/ sentences	original words/ sentences	translated words/ sentences	original words/ sentences	translated words/ sentences
Action Research Arm Test	Test assessing function of upper limb	Action Research Arm Test	Research Test of Upper Extremity Action	Research Test of Upper Extremity Action	Test of Upper Extremity Function
there are four subtests	consist of 4 subtests	ordered	arranged	rater	examiner
items in each are ordered	tasks are ordered	top	maximum	passess	execute correctly
zero	0	washer over bolt	bolt washer	no more need to be administered	the rest of the test is skipped
and again no more tests need to be performed in that subtest	and again there is no need to perform additional tasks in that subtest	1 st and 3 rd	index and ring	subject fails	subject does not complete the task
he	subject			no more test need to be performed	and the execution is skipped
wood	wooden			more	further
3 rd finger	ring finger			block, wood	wooden, block
2 nd finger	middle finger			pick up	lifting
1 st finger	index finger			pour water	decanting water
GM	gross movement			place hand	placing hand
grasp	static grip			hand to mouth	touching the mouth with the hand
grip	dynamic grip			pinch	pinch grip
pinch	pinch grip			numbers	addition of the word "points"
gross movement	total movement			grasp	
				static grip	precision grip
				dynamic grip	global movement

Translation and cultural adaptation

Multiple linguistic changes were required in the forward, backward, and final versions of the translation to obtain an ARAT-PL that was as consistent as possible with the original English version (Table 3).

Reliability

The ARAT-PL Grip, Grasp, Pinch, and Gross Movement Test subscale items exhibited almost perfect agreement: The calculated test–retest kappa values ranged from 0.95 to 1.00 (Table 4). The ICC coefficients for the subscales and total instrument score were in a range of 0.99–1.00, indicating excellent reliability (Table 4). The standard measurement error and minimal detectable change for the subscales ranged from 0 to 0.479 and 0 to 1.327 points, respectively; for the total ARAT-PL score calculated for the test–retest measurements (Table 5).

Inter-rater kappa values for the ARAT-PL subscale items ranged from 0.85 to 1.00 (Table 4); they exhibited almost perfect agreement. The ICC (2,k) coefficient values calculated for each subscale and the total score were above 0.99,

showing excellent reliability (Table 5). The intra-observer standard measurement error and minimal detectable change calculated for the subscales and total ARAT-PL score ranged from 0.112 to 0.335 and 0.310 to 0.930, respectively (Table 5).

Internal consistency

The total ARAT-PL score exhibited excellent internal consistency with a Cronbach's α value of 0.99. Similarly, the Cronbach's α values for the grasp, grip, pinch, and gross movement items amounted to 0.99, 0.98, 0.97, and 0.99, respectively. The Cronbach's α value for the FMA-UE was 0.93, also indicating excellent internal consistency.

Validity

Scatter plots of the correlations between the ARAT-PL and FMA scores are shown in Fig. 1. There were high correlations between ARAT-PL and FMA-UE absolute scores, and between all ARAT-PL subscale scores and FMA-UE absolute scores (Table 1). There were moderate correlations

Table 4. Kappa and percent agreement values for the test–retest and inter-rater reliability (n = 60)

Item		Test–retest		Inter-rater	
		κ	PA (%)	κ	PA (%)
Grasp	Block, wood, 10 cm cube	0.97	98.33	1.00	100
	Block, wood 2.5 cm cube	0.97	98.33	0.97	98.33
	Block, wood 5 cm cube	0.97	98.33	1.00	100
	Block, wood 7.5 cm cube	0.97	98.33	1.00	100
	Ball (cricket), 7.5 cm diameter	1.00	100	0.94	96.67
	Stone 10 × 2.5 × 1 cm	1.00	100	1.00	100
Grip	Pour water from glass to glass	1.00	100	1.00	100
	Tube 2.25 cm	0.97	98.33	0.94	96.67
	Tube 1 × 16 cm	0.97	98.33	0.97	98.33
	Washer (diameter: 3.5 cm) over bolt	1.00	100	1.00	100
Pinch	Ball bearing, 6 mm 3 rd finger and thumb	0.95	96.67	1.00	100
	Marble, 1.5 cm index finger and thumb	0.97	98.33	0.91	95.00
	Ball bearing 2 nd finger and thumb	1.00	100	0.95	96.67
	Ball bearing 1 st finger and thumb	0.91	95.00	0.97	98.33
	Marble 3 rd finger and thumb	1.00	100	1.00	100
	Marble 2 nd finger and thumb	0.97	98.33	1.00	100
Gross movement	Place hand behind head	1.00	100	0.96	98.33
	Place hand on top of head	1.00	100	1.00	100
	Hand to mouth	1.00	100	0.85	95.00

κ – kappa value; PA – percent agreement.

Table 5. Test–retest reliability (n = 60)

Subtest scores (points)	Lower 95% CI	ICC	95% CI	SEM	MDC
Test–retest reliability					
Grasp (0–18)	0.997	0.998	0.999	0.258	0.716
Grip (0–12)	0.999	0.999	0.999	0.129	0.358
Pinch (0–18)	0.997	0.999	0.999	0.214	0.593
Gross movement (0–9)	1.000	1.000	1.000	0.000	0.000
Total ARAT-PL (0–57)	0.999	0.999	0.996	0.479	1.327
Inter-rater reliability					
Grasp (0–18)	0.999	0.999	0.999	0.112	0.310
Grip (0–12)	0.998	0.999	0.999	0.144	0.400
Pinch (0–18)	0.999	0.999	0.999	0.129	0.358
Gross movement (0–9)	0.997	0.998	0.998	0.129	0.358
Total ARAT-PL (0–57)	0.999	0.999	0.999	0.335	0.930

95% CI – 95% confidence interval; ICC – intraclass correlation coefficient; SEM – standard measurement error; MDC – minimal detectable change; ARAT-PL – Polish version of the Action Research Arm Test.

between the ARAT-PL and FMA-LE absolute scores, and between all ARAT-PL subscales' scores and FMA-LE absolute scores (Table 2). Results for the hypotheses testing correlations are shown in Table 1 for the associations with FMA-UE and Table 2 for the associations with FMA-LE. Based on the absolute scoring method, ARAT-PL has 5 out of 10 hypotheses confirmed (50%), indicating moderate construct validity (Tables 1,2).

Floor and ceiling effects

The Polish version of ARAT had a significant ceiling effect, spanning 48% of tested patients, but no floor effect (12% of patients). It has been demonstrated that both FMA-UE and FMA-LE have significant ceiling effects (50% and 30% of patients, respectively) but no floor effect (0% of patients).

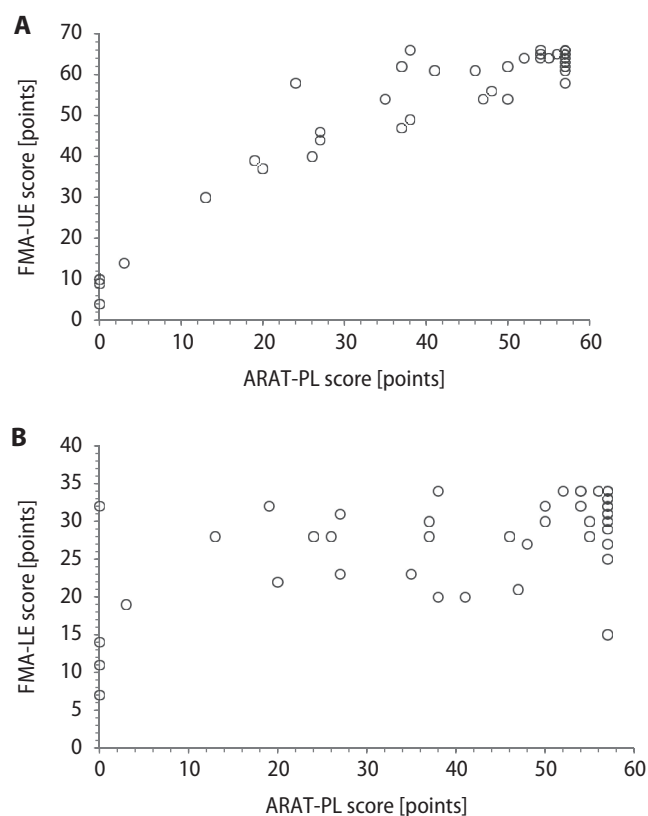


Fig. 1. The relationship between the scores of the ARAT-PL and FMA-UE (A) and the ARAT-PL and FMA-LE (B). See results in Table 1 and Table 2

ARAT-PL – the Polish version of the Action Research Arm Test;
FMA-UE – Fugl-Meyer Assessment for Upper Extremity;
FMA-LE – Fugl-Meyer Assessment for Lower Extremity.

Discussion

This is probably the first reported cross-cultural translation and adaptation based on rigorous methodology and strict regulation of this process. This study assessed the reliability and construct validity of a Polish version of ARAT. The hypotheses tested to evaluate construct validity showed that ARAT-PL had excellent reliability and moderate construct validity.

Therefore, this result provides an official, transculturally validated ARAT for wide and consistent clinical use across Poland, and for research across the world.

Reliability

The total scores and sub-scores of ARAT-PL showed excellent inter-rater and test–retest reliability. This agrees with the results of previous studies, which have reported ICC coefficients of 0.98 and 0.99 for inter-rater reliability^{13,40} and test–retest reliability²¹ in poststroke hemiparetic patients. Moreover, the agreement for individual ARAT-PL items assessed with Cohen's kappa coefficients was almost perfect, and the interobserver agreement measured via the percentage agreement was ≥ 90 . The latter result is even higher than reported in another study, which

found percentage agreement ≥ 70 .²⁰ Therefore, our study has shown that ARAT-PL has excellent reliability, comparable to the original scale.

Minimum detectable change and measurement error

The values for standard error of measurement and minimal detectable change were 0.34 and 0.93 for inter-rater, and 0.48 and 1.33 for test–retest measurements. Similar comparisons in past studies have shown higher values. One example produced standard error of measurement and minimal detectable change values for the test–retest assessment of post-stroke patients with ARAT of 1.3 and 3.5, respectively.⁴⁰ Another study reported minimal detectable change values of 13.1 and 3.5 for inter-rater and test–retest measurements performed with ARAT.¹³ The minimum detectable change captures the amount of change that must be observed in order to exceed measurement error, for assessments administered by the same or by different observers. The results suggest that ARAT-PL can produce very reliable data in subacute stroke patients, both across multiple sessions by the same experienced rater and for measurements performed by 2 different experienced raters.

Internal consistency

The Polish version of ARAT showed excellent internal consistency for both the total and subscale scores ($\alpha = 0.97$ – 0.99). These results are consistent with previous studies, which have reported excellent internal consistency for the original ARAT ($\alpha \geq 0.98$)^{39,16} and for the Chinese version ($\alpha = 0.98$)²¹ in subacute and chronic stroke patients. Our results show that the particular items of ARAT-PL have been well translated into Polish; this version is highly consistent with the original and other foreign adaptations.

Validity

This study found high correlation ($r = 0.71$ – 0.83) between the total and subtest scores of ARAT-PL and the total score of FMA-UE-PL in subacute post-stroke patients. These results agree with other studies, one of which indicated coefficients of 0.77 within 72 h of patient admission to the rehabilitation unit, and 0.87 in the 24 h before discharge.¹⁹ Another reported coefficients in the range of 0.71–0.74 for correlations between ARAT and FMA-UE in chronic patients with stroke.^{40,41} However, a further study found slightly higher correlation coefficients of 0.91 after 2 weeks and 0.94 8 weeks after stroke onset^{18,42} for the original ARAT and FMA-UE. Higher coefficient values of 0.90, 0.90, 0.82, and 0.92 have also been demonstrated for correlations between ARAT and FMA-UE performed 14, 30, 90, and 180 days after stroke, respectively.⁴⁰ However, the latter study had a smaller sample. Lastly, Wei et al.⁴³ found somewhat higher coefficient values of 0.93. However, they evaluated chronic stroke subjects before and after

upper-extremity rehabilitation robotic training. It seems that the strength of interdependence between ARAT and FMA-UE may be affected by many different factors, including 1) the size of the study sample, 2) the time of the administration of outcome measures after stroke, 3) the type of rehabilitation therapy to which studied subjects are subjected, and 4) translation-related differences between versions of the same instrument. Both ARAT and FMA-UE evaluate the degree of impairment of the upper limbs in patients with stroke. However, ARAT assesses the functioning of upper extremities using observational methods, while the FMA measures motor impairment. Therefore, collectively, these studies show that the ARAT score may effectively assess not only function, but also indirectly some motor impairment of the upper extremity.

Compared to the FMA, ARAT has a smart scoring system. Subjects with both severe and minor upper limb dysfunction may get minimum or maximum scores, and then no more tests need to be administered for them to receive a score for that subtest. This shortens the total time of evaluation. The advantage of ARAT is that it can very precisely evaluate hand movements and indicate the specific functional problem of the extremity, even if the patient seems to be in generally good functional shape. Our results show that ARAT is an appropriate tool for assessing people with moderate-to-severe stroke.

Floor and ceiling effects

We did observe a significant ceiling effect of ARAT-PL. The studied patients were in a range of 22–138 days after recovery from stroke. It was perhaps possible for many patients who had had minor strokes and longer histories of recovery, and had reached high functional status, to gain the highest scores in the ARAT-PL. Therefore, it seems that ARAT is a less useful outcome measure for people who substantially recover from stroke. For example, in cases of mild stroke we did not observe difficulties with completing the specific tasks; the only exception was the ability to pinch a marble with the 3rd finger and thumb. Therefore, a relatively large number of patients with mild stroke achieved maximum points. This may suggest that the scoring system of ARAT is not well designed for people with mild upper limb dysfunctions. In parallel, we observed a significant ceiling effect for FMA-UE; 50% of patients had total scores ≥ 64 . However, no floor effect was demonstrated. Hence, as with ARAT-PL, half the patients had near the maximal FMA-UE score. The FMA assesses some additional skills, such as movement coordination or reflex activity, and requires greater mobility skills than ARAT. Again, this shows that many of the studied patients had recovered well from stroke; for such patients, FMA-UE is not a challenging evaluation. The consistency between the results with ARAT and FMA-UE also suggests that recovery in movement coordination and muscle reflex activity is paralleled by upper extremity functional independence in subacute patients with stroke.^{17,44}

Limitations

The main limitations of the study were differences in rehabilitation protocol and in time of recovery after stroke; these might have affected the sample homogeneity. However, at the time of the study, we had limited access to a more homogenous group of stroke survivors. Future research with ARAT-PL and FMA-UE should separately analyze patients in the acute or chronic stage of stroke to improve the conditions of observational studies aimed at determining the interdependence of particular outcome measures. To show the construct validity of ARAT, we examined correlations with FMA-LE, finding a significant but lower correlation coefficient (0.59) as compared to the FMA-UE (0.83) for the total score relationship. This may falsely indicate that the level of upper extremity function was moderately related to the level of lower extremity function.

Conclusions

It can be concluded that ARAT-PL is a reliable and valid tool for assessing upper extremity function in subacute stroke survivors. Its only drawback is that it appears to have a ceiling effect, limiting the differentiation of patients with mild upper limb impairment after stroke. Despite this, our results support the clinical and research use of ARAT-PL in the Polish population of patients with stroke.

Data availability

The datasets generated and/or analyzed during the current study are available from the corresponding author on reasonable request.

Consent for publication

Not applicable.

ORCID iDs

Joanna Małecka  <https://orcid.org/0000-0002-3341-7385>
 Magdalena Goliwás  <https://orcid.org/0000-0002-3661-654X>
 Katarzyna Adamczewska  <https://orcid.org/0000-0002-8063-1253>
 Jacek Lewandowski  <https://orcid.org/0000-0002-3417-2084>
 Dawid Łochyński  <https://orcid.org/0000-0002-4274-0950>

References

1. Krakauer JW. Arm function after stroke: From physiology to recovery. *Semin Neurol.* 2005;25(4):384–395. doi:10.1055/s-2005-923533
2. Meng G, Meng X, Tan Y, et al. Short-term efficacy of hand-arm bimanual intensive training on upper arm function in acute stroke patients: A randomized controlled trial. *Front Neurol.* 2018;8:726. doi:10.3389/fneur.2017.00726
3. Verheyden G, Nieuwboer A, De Wit L, et al. Time course of trunk, arm, leg, and functional recovery after ischemic stroke. *Neurorehabil Neural Repair.* 2008;22(2):173–179. doi:10.1177/1545968307305456
4. Koh CL, Hsueh IP, Wang WC, et al. Validation of the action research arm test using item response theory in patients after stroke. *J Rehabil Med.* 2006;38(6):375–380. doi:10.1080/16501970600803252

5. Jonsdottir J, Thorsen R, Aprile I, et al. Arm rehabilitation in post stroke subjects: A randomized controlled trial on the efficacy of myoelectrically driven FES applied in a task-oriented approach. *PLoS One*. 2017;12(12):e0188642. doi:10.1371/journal.pone.0188642
6. Nakayama H, Stig Jørgensen H, Otto Raaschou H, Skyhøj Olsen T. Recovery of upper extremity function in stroke patients: The Copenhagen stroke study. *Arch Phys Med Rehabil*. 1994;75(4):394–398. doi:10.1016/0003-9993(94)90161-9
7. Hsueh IP, Hsieh CL. Responsiveness of two upper extremity function instruments for stroke inpatients receiving rehabilitation. *Clin Rehabil*. 2002;16(6):617–624. doi:10.1191/0269215502cr530oa
8. Barreca SR, Stratford PW, Lambert CL, Masters LM, Streiner DL. Test-retest reliability, validity, and sensitivity of the Chedoke Arm and Hand Activity Inventory: A new measure of upper-limb function for survivors of stroke. *Arch Phys Med Rehabil*. 2005;86(8):1616–1622. doi:10.1016/j.apmr.2005.03.017
9. Lyle RC. A performance test for assessment of upper limb function in physical rehabilitation treatment and research: *Int J Rehabil Res*. 1981;4(4):483–492. doi:10.1097/00004356-198112000-00001
10. Carroll D. A quantitative test of upper extremity function. *J Chronic Dis*. 1965;18(5):479–491. doi:10.1016/0021-9681(65)90030-5
11. McDonnell M. Action Research Arm Test. *Aust J Physiother*. 2008;54(3):220. doi:10.1016/S0004-9514(08)70034-5
12. Van Der Lee JH, De Groot V, Beckerman H, Wagenaar RC, Lankhorst GJ, Bouter LM. The intra- and interrater reliability of the action research arm test: A practical test of upper extremity function in patients with stroke. *Arch Phys Med Rehabil*. 2001;82(1):14–19. doi:10.1053/apmr.2001.18668
13. Hsieh CL, Hsueh IP, Chiang FM, Lin PH. Inter-rater reliability and validity of the Action Research arm test in stroke patients. *Age Ageing*. 1998;27(2):107–113. doi:10.1093/ageing/27.2.107
14. Lin JH, Hsu MJ, Sheu CF, et al. Psychometric comparisons of 4 measures for assessing upper-extremity function in people with stroke. *Phys Ther*. 2009;89(8):840–850. doi:10.2522/ptj.20080285
15. Chen HF, Lin KC, Chen CL. Rasch validation and predictive validity of the Action Research Arm Test in patients receiving stroke rehabilitation. *Arch Phys Med Rehabil*. 2012;93(6):1039–1045. doi:10.1016/j.apmr.2011.11.033
16. Van Wegen E, Nijland R, Verbunt J, Van Wijk R, Van Kordelaar J, Kwakkel G. A comparison of two validated tests for upper limb function after stroke: The Wolf Motor Function Test and the Action Research Arm Test. *J Rehabil Med*. 2010;42(7):694–696. doi:10.2340/16501977-0560
17. Yozbatiran N, Der-Yeghian L, Cramer SC. A standardized approach to performing the Action Research Arm Test. *Neurorehabil Neural Repair*. 2008;22(1):78–90. doi:10.1177/1545968307305353
18. Page SJ, Hade E, Persch A. Psychometrics of the Wrist Stability and Hand Mobility Subscales of the Fugl–Meyer Assessment in moderately impaired stroke. *Phys Ther*. 2015;95(1):103–108. doi:10.2522/ptj.20130235
19. Rabadi MH, Rabadi FM. Comparison of the Action Research Arm Test and the Fugl–Meyer Assessment as measures of upper-extremity motor weakness after stroke. *Arch Phys Med Rehabil*. 2006;87(7):962–966. doi:10.1016/j.apmr.2006.02.036
20. Nordin Å, Murphy M, Danielsson A. Intra-rater and inter-rater reliability at the item level of the Action Research Arm Test for patients with stroke. *J Rehabil Med*. 2014;46(8):738–745. doi:10.2340/16501977-1831
21. Zhao JL, Chen PM, Li WF, et al. Translation and initial validation of the Chinese version of the Action Research Arm Test in people with stroke. *Biomed Res Int*. 2019;2019:5416560. doi:10.1155/2019/5416560
22. Doussoulain SA, Rivas RS, Campos RV. Validation of “Action Research Arm Test” (ARAT) in Chilean patients with a paretic upper limb after a stroke [in Spanish]. *Rev Med Chile*. 2012;140:59–65.
23. Goliwas M, Małecka J, Lewandowski J, Kamińska E, Adamczewska K, Kocur P. Analysis of dependencies between Fugl–Meyer Assessment Scale test and Berg Balance Scale test as an assessment of the increased muscle tone in chronic-phase patients after a ischemic stroke. *Med Rehabil*. 2022;26(1):4–9. doi:10.5604/01.3001.0015.8241
24. Guillemin F, Bombardier C, Beaton D. Cross-cultural adaptation of health-related quality of life measures: Literature review and proposed guidelines. *J Clin Epidemiol*. 1993;46(12):1417–1432. doi:10.1016/0895-4356(93)90142-N
25. Beaton DE, Bombardier C, Guillemin F, Ferraz MB. Guidelines for the process of cross-cultural adaptation of self-report measures. *Spine (Phila Pa 1976)*. 2000;25(24):3186–3191. doi:10.1097/00007632-200012150-00014
26. Szczechowicz J, Lewandowski J, Sikorski J. Polish adaptation and validation of Burn Specific Health Scale – Brief. *Burns*. 2014;40(5):1013–1018. doi:10.1016/j.burns.2013.11.026
27. Prinsen CAC, Mokkink LB, Bouter LM, et al. COSMIN guideline for systematic reviews of patient-reported outcome measures. *Qual Life Res*. 2018;27(5):1147–1157. doi:10.1007/s11136-018-1798-3
28. Salter K, Jutai J, Teasell R, Foley N, Bitensky J, Bayley M. Issues for selection of outcome measures in stroke rehabilitation: ICF activity. *Disabil Rehabil*. 2005;27(6):315–340. doi:10.1080/09638280400008545
29. Mokkink LB, Terwee CB, Patrick DL, et al. The COSMIN study reached international consensus on taxonomy, terminology, and definitions of measurement properties for health-related patient-reported outcomes. *J Clin Epidemiol*. 2010;63(7):737–745. doi:10.1016/j.jclinepi.2010.02.006
30. Cecchi F, Carrabba C, Bertolucci F, et al. Transcultural translation and validation of Fugl–Meyer assessment to Italian. *Disabil Rehabil*. 2021;43(25):3717–3722. doi:10.1080/09638288.2020.1746844
31. Gladstone DJ, Danells CJ, Black SE. The Fugl–Meyer Assessment of motor recovery after stroke: A critical review of its measurement properties. *Neurorehabil Neural Repair*. 2002;16(3):232–240. doi:10.1177/154596802401105171
32. Rech KD, Salazar AP, Marchese RR, Schifino G, Cimolin V, Pagnussat AS. Fugl–Meyer Assessment scores are related with kinematic measures in people with chronic hemiparesis after stroke. *J Stroke Cerebrovasc Dis*. 2020;29(1):104463. doi:10.1016/j.jstrokecerebrovasdis.2019.104463
33. Revelle W. psych: Procedures for Psychological, Psychometric, and Personality Research. R package v. 2.1.3. Evanston, USA: Northwestern University; 2021. <https://cran.r-project.org/web/packages/psych/index.html>. Accessed August 15, 2023.
34. Andresen EM. Criteria for assessing the tools of disability outcomes research. *Arch Phys Med Rehabil*. 2000;81(12 Suppl 2):S15–S20. doi:10.1053/apmr.2000.20619
35. Nunnally JC, Bernstein IH. *Psychometric Theory*. 3rd ed. New York, USA: McGraw-Hill; 1994. ISBN:978-0-07-047849-7.
36. Koo TK, Li MY. A Guideline of selecting and reporting intraclass correlation coefficients for reliability research. *J Chiropract Med*. 2016;15(2):155–163. doi:10.1016/j.jcm.2016.02.012
37. McHugh ML. Interrater reliability: the kappa statistic. *Biochem Med (Zagreb)*. 2012;22(3):276–282. doi:10.11613/BM.2012.031
38. Hinkle DE, Wiersma W, Jurs SG. *Applied Statistics for the Behavioral Sciences*. 2nd ed. Boston, USA: Houghton Mifflin; 1988. ISBN:978-0-395-36911-1.
39. Faul F, Erdfelder E, Lang AG, Buchner A. G*Power 3: A flexible statistical power analysis program for the social, behavioral, and biomedical sciences. *Behav Res Methods*. 2007;39(2):175–191. doi:10.3758/BF03193146
40. Simpson LA, Eng JJ. Functional recovery following stroke: Capturing changes in upper-extremity function. *Neurorehabil Neural Repair*. 2013;27(3):240–250. doi:10.1177/1545968312461719
41. Hsieh YW, Wu CY, Lin KC, Chang YF, Chen CL, Liu JS. Responsiveness and validity of three outcome measures of motor function after stroke rehabilitation. *Stroke*. 2009;40(4):1386–1391. doi:10.1161/STROKEAHA.108.530584
42. De Weerd WJG. Measuring recovery of arm-hand function in stroke patients: A comparison of the Brunnstrom–Fugl–Meyer test and the Action Research Arm test. *Physiother Can*. 1985;37(2):65–70. doi:10.3138/ptc.37.2.065
43. Wei XJ, Tong KY, Hu XL. The responsiveness and correlation between Fugl–Meyer Assessment, Motor Status Scale, and the Action Research Arm Test in chronic stroke with upper-extremity rehabilitation robotic training. *Int J Rehabil Res*. 2011;34(4):349–356. doi:10.1097/MRR.0b013e32834d330a
44. See J, Dodakian L, Chou C, et al. A standardized approach to the Fugl–Meyer assessment and its implications for clinical trials. *Neurorehabil Neural Repair*. 2013;27(8):732–741. doi:10.1177/1545968313491000

Investigation of integron gene cassettes in trimethoprim-sulfamethoxazole-resistant *Acinetobacter baumannii* isolates

Cihat Öztürk^{1,A–F}, Rukiye Akyol^{2,B,C,E}, Sadık Küçükünay^{3,B,C,E}, Elif Sevim^{4,A,C,E,F}

¹ Department of Medical Microbiology, Faculty of Medicine, Kırşehir Ahi Evran University, Turkey

² Republic of Turkey Ministry of Health, Kırşehir Training and Research Hospital, Turkey

³ Department of Pharmacology, Faculty of Medicine, Kırşehir Ahi Evran University, Turkey

⁴ Department of Medical Biology, Faculty of Medicine, Kırşehir Ahi Evran University, Turkey

A – research concept and design; B – collection and/or assembly of data; C – data analysis and interpretation;

D – writing the article; E – critical revision of the article; F – final approval of the article

Advances in Clinical and Experimental Medicine, ISSN 1899–5276 (print), ISSN 2451–2680 (online)

Adv Clin Exp Med. 2025;34(7):1175–1181

Address for correspondence

Elif Sevim

E-mail: esevim@ahievran.edu.tr

Funding sources

None declared

Conflict of interest

None declared

Acknowledgements

The preliminary data of this article were presented as an oral abstract at the II International Gazi Health Sciences Congress.

Received on March 20, 2024

Reviewed on June 21, 2024

Accepted on July 10, 2024

Published online on December 13, 2024

Cite as

Öztürk C, Akyol R, Küçükünay S, Sevim E.

Investigation of integron gene cassettes in trimethoprim-sulfamethoxazole-resistant *Acinetobacter baumannii* isolates.

Adv Clin Exp Med. 2025;34(7):1175–1181.

doi:10.17219/acem/191058

DOI

10.17219/acem/191058

Copyright

Copyright by Author(s)

This is an article distributed under the terms of the

Creative Commons Attribution 3.0 Unported (CC BY 3.0)

(<https://creativecommons.org/licenses/by/3.0/>)

Abstract

Background. The spread of antibiotic-resistance genes among healthcare-associated infections (HAIs) poses serious problems in the treatment of these infections. Recently, these resistance genes have also been shown to be present in integrons.

Objectives. By focusing on integron-mediated mechanisms of antibiotic resistance, we sought to elucidate the genetic determinants underpinning the development of multidrug resistance in clinical isolates of *Acinetobacter baumannii*.

Materials and methods. In this study, 27 TMP-SXT-resistant *A. baumannii* isolates were obtained from various clinical samples. Class I and class II integrons were determined using polymerase chain reaction (PCR). Samples were sent for DNA sequence analysis of the integron to a private firm (BMLabosis, Ankara, Turkey). The similarities of the DNA sequences with the associated integron were determined using National Center for Biotechnology Information (NCBI) GenBank.

Results. While all isolates were resistant to TMT-SXT and gentamicin, amikacin and tobramycin resistance rates were detected as 70% and 26%, respectively. Class I and class II integrons were found in 1 strain and 2 isolates, respectively. It was also determined that the *dhfr12* gene and the *aadA2* gene were found in the class I integrons. It was determined that 2 isolates carrying class II integron had *dhfrA1* and *sat2* genes. Both class I and class II integrons were detected in 1 of these isolates.

Conclusions. Despite the low integron detection in the resistant isolates, with the detection of class I and class II integrons among *A. baumannii* isolates, it was determined that HAIs could spread very rapidly within the hospital and cause multidrug resistance. This study reveals the need for comprehensive surveillance and molecular characterization of integron-mediated resistance mechanisms to inform effective strategies to combat infections caused by multidrug-resistant (MDR) *A. baumannii*.

Key words: antibiotic resistance, *Acinetobacter baumannii*, integron gene cassettes

Background

Healthcare-associated infections (HAIs), commonly known as nosocomial infections, represent a significant burden on global public health, particularly due to the prevalence of antibiotic-resistant bacterial species as their primary causative agents. These infections have garnered attention as the leading cause of mortality and morbidity worldwide, a designation emphasized by authoritative bodies such as the Centers for Disease Control and Prevention (CDC) and the World Health Organization (WHO).¹ The pervasive presence of antibiotic-resistant pathogens in healthcare settings poses formidable challenges for clinicians, infection control practitioners and policymakers alike. With conventional treatment options increasingly compromised by the relentless evolution of resistance mechanisms, addressing the complex dynamics of HAIs and antibiotic resistance emerges as an urgent priority in safeguarding patient safety and optimizing healthcare outcomes.^{2,3} Healthcare-associated infections, also known as nosocomial infections, pose substantial medical and economic burdens not only in Turkey but globally.^{3,4} Furthermore, it was observed that bacterial co-infections were very common in people with an underlying viral infection; specifically during the coronavirus disease 2019 (COVID-19) pandemic, a global health threat commonly spread through respiratory droplets and aerosol transmission. Pneumonia and bloodstream infections (BSIs) were the most common causes of bacterial HAIs in COVID-19 patients.⁵ These infections contributed to prolonged hospital stays and led to severe complications in a significant proportion of hospitalized patients, ranging from 5% to 15%.^{3,4} Given the limited availability of effective antibiotic therapies for treating these infections, understanding the antibiotic resistance profiles and underlying resistance mechanisms of causative pathogens is crucial. Such knowledge is essential for informed antibiotic selection and plays a pivotal role in efforts aimed at reducing the rates of antibiotic resistance.³

In recent years, the incidence of infections caused by microorganism species, also known as ESKAPE pathogens (*Enterococcus faecium*, *Staphylococcus aureus*, *Klebsiella pneumoniae*, *Acinetobacter baumannii*, *Pseudomonas aeruginosa*, *Enterobacter* sp.), has not only increased but also due to multiple antibiotic resistance, these infections have increased. There are serious difficulties in the prevention, treatment and eradication.⁶ In 2018, *A. baumannii* was at the top of the list of “resistant bacteria that urgently require new antibiotic discovery” due to increasing resistance rates, published by the WHO.⁷ *Acinetobacter baumannii* is normally found in the soil and is a microorganism that can cause high levels of arsenic accumulation in the soil.⁸ However, this bacteria can cause, especially in intensive care units (ICUs), many different infections and severe clinical conditions such

as ventilator-associated pneumonia and catheter-associated bacteremia, urinary tract infections, soft tissue infections, septicemia, and meningitis, and it also causes failures in the control and treatment of infections, as well as a significant increase in healthcare costs.⁹ The antibiotic resistance profile in *A. baumannii* isolates may vary regionally and yearly, increasing antibiotic resistance and the occurrence of multiple antibiotic resistance infections cause clinicians to note serious difficulties in the management and treatment of patients.^{10,11} In recent years, Turkey and other countries have experienced a significant increase in the incidence of multidrug-resistant (MDR) *A. baumannii* isolates. Carbapenem-resistant *Acinetobacter* strains are generally MDR, and colistin or tigecycline are often used as a last resort in the treatment of *A. baumannii*. However, strains that are resistant even to these antibiotics have been reported.¹²

Carbapenems, aminoglycosides, sulbactam, colistin, and tigecycline are antimicrobial agents frequently used in the treatment of *Acinetobacter* infections that cause serious clinical conditions. While different groups of antibiotics can be used in the treatment of *A. baumannii* infections, treatment strategies aimed at eradicating the infection are mostly focused on broad-spectrum antibiotics.⁹ Trimethoprim-sulfamethoxazole (TMP-SXT) is recommended as the first choice, especially in the treatment of HAIs, due to its high potency against Gram-positive and Gram-negative bacteria; it can be used on a wide patient profile. However, in recent years, studies conducted in different geographical regions have begun to report the development of resistance against TMP-SXT.^{10,13} Previously, MDR *A. baumannii* infections could be treated with this antibiotic combination in sporadic cases, but now it is observed that resistance to this drug has become widespread in over 80% of isolates.¹⁴ Plasmids and integrons-induced changes in the dihydropteroate synthetase enzyme cause sulphonamide resistance in *A. baumannii*.¹⁵ If this resistance can be prevented or slowed down, effective treatment of healthcare-associated *A. baumannii* isolates can be achieved without the switch to last-resort antibiotics. Some researchers report that, due to resistance of *A. baumannii* to many antibiotics, studies aimed at elucidating its antibiotic resistance mechanisms should be continued in order to prevent becoming helpless in the face of infections.^{9,16}

In research concerning the acquired antibiotic resistance mechanisms of bacteria, a multitude of mobile genetic elements have been uncovered, including transposons, plasmids and integrons.¹⁷ Comparative sequence analyses of these elements have unveiled the presence of integrons, which represent a pivotal discovery in understanding the genetic basis of antibiotic resistance.^{18,19} Integrons are characterized as DNA elements harboring mobile gene cassettes along with a site-specific recombination system. These gene cassettes can encode various antibiotic resistance determinants, facilitating their dissemination among

bacterial populations through horizontal gene transfer mechanisms.²⁰ Integrons play a crucial role in the evolution and spread of antibiotic resistance genes, enabling bacteria to rapidly acquire and accumulate resistance traits, thereby posing significant challenges to clinical treatment strategies and public health efforts.²¹

Objectives

This investigation aimed to comprehensively examine the prevalence and distribution of class I and class II integron gene cassettes within TMP-SXT-resistant strains of *A. baumannii*. Also, by focusing on integron-mediated mechanisms of antibiotic resistance, particularly concerning TMP-SXT resistance, this research sought to elucidate the genetic determinants underpinning the development of multidrug resistance in clinical isolates of *A. baumannii*.

Materials and methods

A. baumannii isolates

This research was conducted in line with the recommendations of the Declaration of Helsinki. The Ethics Committee for Scientific Research in Health Sciences at Kırşehir Ahi Evran University (Kırşehir, Turkey) approved the study (approval No. 2024-04.17 issued on February 6, 2024). Twenty-seven *Acinetobacter baumannii* isolates resistant to TMP-SXT were obtained from various clinical samples used for routine diagnosis at the Kırşehir Training and Research Hospital in Turkey between September 2021 and November 2022. Identification and antibiotic susceptibilities of the isolates were performed using the Vitek-2 Automated System (BioMérieux SA, Craponne, France) at the the Kırşehir Training and Research Hospital. The phenotypic and demographic characteristics of *A. baumannii* isolates are provided in Table 1,2.

DNA extraction

Acinetobacter baumannii isolates in the Kırşehir Training and Research Hospital Medical Microbiology Laboratory Culture Collection were brought to the Medical Microbiology Laboratory of the Faculty of Medicine of Kırşehir Ahi Evran University via cold chain. Bacterial

Table 1. Susceptibility of *A. baumannii* isolates to various antibiotics

Antibiotics	Number of isolates R/S	Number of susceptible isolates n
Amikacin	19/8	8
TMP-SXT	27/0	0
Gentamicin	27/0	0
Tobramycin	7/20	20
Colistin	0/27	27
Tigecycline	0/27	27

n – number of *A. baumannii* isolate; R – resistant; S – susceptible.

Table 2. Distribution of *A. baumannii* isolates according to the sample type from which they were isolated

Sample type	n (%)
Urine	1 (3.7)
Wound culture	6 (22.2)
Sputum	6 (22.2)
Catheter culture	1 (3.7)
Blood culture	5 (18.6)
Other	8 (29.6)
Total	27 (100)

n – number of *A. baumannii* isolated; other – represents 1 of the wound, sputum and urine samples.

isolates were cultivated on blood agar under aseptic conditions and incubated at 37°C. DNA extraction from *A. baumannii* isolates was performed using the boiling method. A loopful from pure cultures was taken, dissolved in 300 µL of pure water, and incubated at 100°C for 10 min. Then, the samples were kept at room temperature and centrifuged at 12,000 g for 10 min, and the supernatant was used as template DNA.²²

Detection of class I and class II integron gene cassettes

In this study, the presence of class I and class II gene cassettes in *A. baumannii* isolates was determined with polymerase chain reaction (PCR). Specific primers used to amplify integron gene cassettes are shown in Table 3. Primers specific to integron gene cassettes were used in the PCR reaction. The PCR reaction was prepared by adding 1X PCR buffer without MgCl₂ (10 mM tris-HCl, pH 8.3 at 25°C, 50 mM KCl), 1.5 mM MgCl₂, 200 mM dNTP mix, 1.5 U

Table 3. Primers and polymerase chain reaction (PCR) conditions used in the study

Integron	Primer sequence (5'→3')	PCR conditions	Reference
Class I	F: GGCATCCAAGCAGCAAG	1 cycle 95°C, 3 min 36 cycle 95°C 45 s, 50°C 45 s, 72°C 5 min 1 cycle 72°C 10 dk	21
	R: AAGCAGACTTGACCTGA		
Class II	F: CCTTTTGTGCGCATATCCGTG		22
	R: TACCTGTTCTGCCGTATCT		

Taq DNA polymerase, and 10 pmol/ μ L of each primer in a final volume of 50 μ L. The final volume of the reaction was completed with sterile dH₂O.²³

Polymerase chain reaction conditions for the amplification of integron gene cassettes were as follows; first, the denaturation step at 95°C for 3 min, then 36 cycles of 45 s at 95°C, 45 s at 50°C, 5 min at 72°C, and a final extension was applied for 10 min at 72°C. Imaging of PCR products was done on 1% agarose gel electrophoresis containing ethidium bromide (EtBr) at 100 V for 1 h and observed under UV light. The size of the integron gene cassettes was determined by comparison with the DNA ladder. Samples were sent to BMLabosis (Ankara, Turkey) for DNA sequence analysis of integron gene cassettes.²³

Bioinformatics

All DNA sequences obtained from integron gene cassettes were processed using the BioEdit 7.09 program (Tom Hall, Ibis Biosciences, Carlsbad, USA). Similarities of the DNA sequences with their associated integron gene cassettes were determined using the National Center for Biotechnology Information (NCBI) GenBank Blast database.^{24,25} The obtained data were used to determine integron gene cassettes.

Genbank acceptance numbers

In this study, the GenBank acceptance numbers of the class I and class II integron sequences for the *A. baumannii* CO1 isolate were deposited in GenBank as OR417416 and OR417417, respectively. The GenBank accession number of the class II integron sequence for the *A. baumannii* CO2 isolate was deposited in GenBank as OR417418.

Results

In our comprehensive study, we investigated the antimicrobial resistance profiles of 27 *Acinetobacter baumannii* isolates, focusing on their susceptibility to a range of antibiotics commonly used in clinical practice. It was observed that all *A. baumannii* isolates exhibited resistance to TMP-SXT and gentamicin antibiotics, indicative of a concerning trend in multidrug resistance. Furthermore, a significant proportion of isolates demonstrated resistance to amikacin and tobramycin, with rates of 70% and 26%, respectively. Notably, none of the isolates exhibited resistance to colistin and tigecycline antibiotics, suggesting their continued

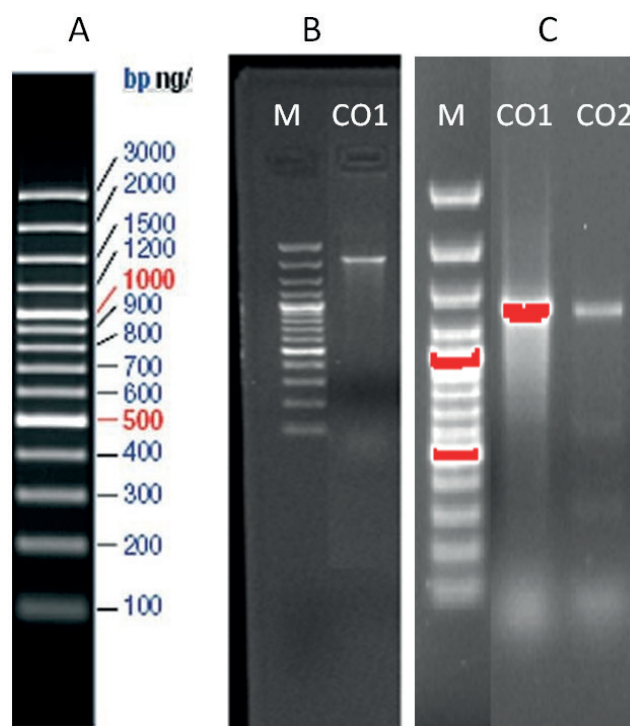


Fig. 1. Agarose gel electrophoresis image of class I and class II integron gene cassettes. A. DNA ladder (Thermo Scientific™ O'GeneRuler™ Ready-to-use 100 bp Plus DNA Ladder); B. Class I integron; C. Class II integron

efficacy as last-resort treatment options against *A. baumannii* infections (Table 1).

In addition to evaluating antimicrobial susceptibility, our study delved into the molecular mechanisms underlying antibiotic resistance, specifically focusing on the presence of integron gene cassettes. Through agarose gel electrophoresis and subsequent DNA sequencing, we detected the presence of class I and class II integrons in select TMP-SXT-resistant *A. baumannii* isolates. Specifically, 1 isolate (CO1) harbored a class I integron gene cassette, while both class I and class II integron gene cassettes were identified in 2 isolates (CO1 and CO2). The molecular characterization revealed that the class I integron gene cassette was approx. 2,000 base pairs in size, while the class II integron gene cassette measured approx. 1,271 base pairs (Fig. 1).

Further bioinformatic analysis, conducted through NCBI GenBank Blast, elucidated the genetic composition of the integron gene cassettes. Specifically, we identified the presence of the *dfrA12* gene, encoding the dihydrofolate reductase enzyme associated with TMP-SXT resistance, and the *aadA2* gene, encoding the aminoglycoside 3'-O-nucleotide transferase enzyme responsible for aminoglycoside resistance, within class I integrons (Table 4).

Table 4. Characteristics of integron gene cassettes in *Acinetobacter baumannii* isolates

Bacterial isolate	Integron	bp	Genes	Sample type	Antibiotic resistance status
CO1 isolate	class I	1818	<i>dfrA12, aadA</i>	sputum	TMP-SXT, gentamicin, amikasin, tobramycin
CO1 isolate	class II	1271	<i>dfrA1, sat2</i>		
CO2 isolate	class II	1272		blood	

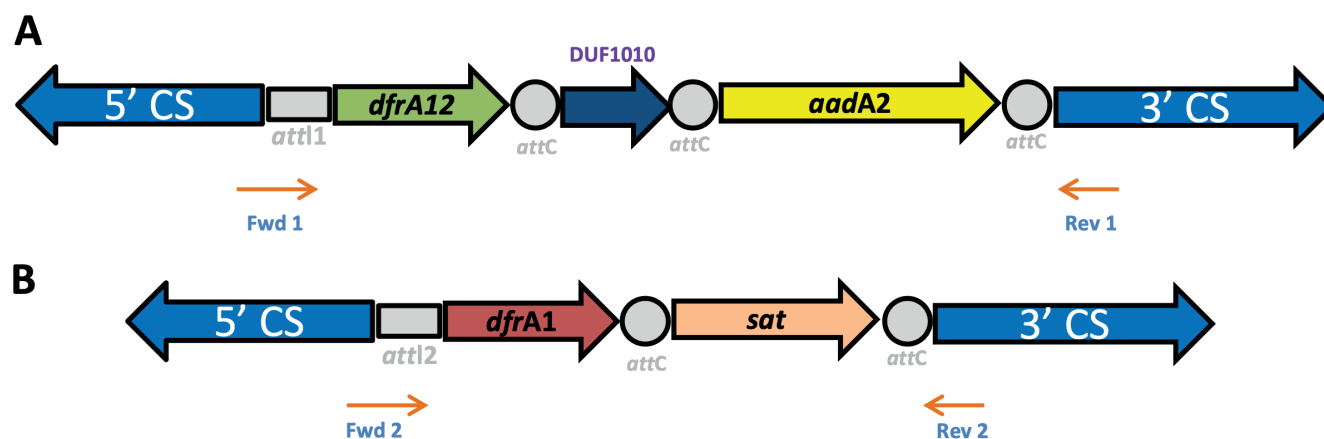


Fig. 2. Schematic representation of the gene cassette structure located in the class I integron and class II isolated from trimethoprim/sulfamethoxazole-resistant *Acinetobacter baumannii*. The horizontal arrows indicate the translation orientation of the genes. A. Schematic representation of the Class I integron gene cassette; B. Schematic representation of the Class II integron gene cassette

Notably, our study also unveiled the co-occurrence of both class I and class II integron gene cassettes within a single isolate, underscoring the complexity of antimicrobial resistance mechanisms in *A. baumannii* populations (Fig. 2).

Discussion

Due to the increasing multidrug resistance strains of *A. baumannii* in recent years, it has become more difficult to treat and control HAIs, and it is associated with increases in mortality.²⁶ Antibiotic resistance generally occurs horizontally through mobile elements such as transposons and plasmids. Integrons play an important role in the spread of antibiotic resistance among species due to their ability to integrate and carry extrachromosomal genetic elements such as plasmids or transposons. The emergence of integron gene cassettes in MDR *A. baumannii* isolates has led to the restriction of treatment alternatives against the agent and increased interest in searching for alternative treatments against the agent.²⁷

The escalating multidrug resistance observed in *A. baumannii* infections poses significant challenges in clinical management and infection control, causing increased mortality, morbidity and healthcare costs for hospitals.¹⁸ Horizontal transmission of antibiotic resistance genes, facilitated by mobile genetic elements such as transposons and plasmids, exacerbate this threat. Among these transmission mechanisms, integrons have emerged to play a pivotal role in mediating the dissemination of antibiotic resistance, owing to their capacity to capture and incorporate extrachromosomal genetic material, including plasmids and transposons. The emergence of integron gene cassettes within MDR *A. baumannii* strains has severely limited therapeutic options and underscored the urgent need for alternative treatment modalities.²⁷

In studies on the antibiotic resistance of *A. baumannii* isolates, the resistance status of TMP-SXT-resistant isolates to different antibiotics varies according to years and regions.^{10,26–28} In accordance with previous research findings, our study revealed that *A. baumannii* isolates exhibited resistance to TMP-SXT, as well as varying degrees of resistance to gentamicin (100%), amikacin (70%) and tobramycin (26%), while all isolates remained susceptible to colistin and tigecycline.

Integrons, especially in Gram-negative bacteria, possess the capability to transfer horizontally between bacteria via plasmids and transposons, facilitating both the dissemination of integrons between bacterial strains and the exchange of integron gene cassettes. This phenomenon contributes to intraclass variability in antibiotic resistance determinants within integrons and enables the rapid transmission of diverse antibiotic resistance traits among bacterial populations.²⁹ Our study data corroborate the presence of class I and class II integron gene cassettes encoding distinct antibiotic resistance determinants among *A. baumannii* isolates. By elucidating the genetic mechanisms underpinning antibiotic resistance, our findings underscore the importance of integrative approaches in combating MDR bacterial infections. Kostakoğlu et al.²⁵ reported that a class I integron gene cassette containing the *dfr* gene was detected in 45.4% of *A. baumannii* isolates resistant to TMP-SXT, while 6.4% of isolates sensitive to TMP-SXT also harbored this cassette. Similarly, in another study, it was found that 9.1% of *A. baumannii* isolates carried 2 different class I integron gene cassettes encoding *aacC1-aadA1* and *aac(3)-I* genes.²⁵ In contrast, Xu et al.²⁹ reported the presence of class I integrons in 13.51% of *A. baumannii* isolates but could not detect class I or class II integron gene cassettes. A multicenter study conducted across various regions in Turkey revealed that class I integrons were found in 6.4% of *A. baumannii* isolates, whereas class II integron gene cassettes were not detected. The class I integron identified in this study contained resistance genes such

as *aac(3)-I*, *aadA1* and *blaTEM-1*.³⁰ Conversely, in a study conducted in Iran, the rates of class I and class II integron gene cassettes in *A. baumannii* isolates were detected in 63.9% and 78.2%, respectively. Intriguingly, both class I and class II integron gene cassettes were identified in 49.6% of the isolates, although the specific antibiotic resistance genes within these cassettes were not elucidated.²⁷

In this research conducted in the Kırşehir province in Turkey, both class I and class II integrons were detected in *A. baumannii* isolates. In our study, contrary to previous findings, the simultaneous presence of *dfrA12* and *aadA* genes within class I integron gene cassettes indicates the existence of multiple subtypes of genes responsible for TMP-SXT and aminoglycoside resistance. This observation suggests a potential mechanism for the amplification of class I integrons contributing to multidrug resistance among *A. baumannii* isolates. Additionally, unlike previous studies, our research identified the co-occurrence of both class I and class II integrons within the same bacterial isolate. The presence of *dfrA12* and *aadA2* genes (GenBank accession No. OR417416) within the class I integron, along with *dfrA1*-Sat genes (GenBank accession No. OR417417) within the class II integron, underscores the likelihood of multiple integron gene cassettes harboring distinct genes in *A. baumannii* strains. This situation suggests the potential for rapid dissemination of multiple antibiotic resistance traits among the isolates. In addition to the aforementioned findings, another noteworthy observation was the presence of the *sat* gene alongside the *dfrA1* gene in an *A. baumannii* isolate carrying a class II integron. This observation implies that the dissemination of aminoglycoside resistance among TMP-SXT-resistant *A. baumannii* isolates might exhibit a heightened prevalence compared to other antibiotic resistance genes.

Limitations

The main limitation of this study was the sample size. It is essential to conduct integron gene cassette studies that examine antibiotic resistance on a population level, encompassing a diverse range of bacteria with varying resistance profiles. Such studies necessitate a coordinated national approach, and these limitations will be the primary focus of future research.

Conclusions

As a result of the analysis of the data we obtained in our research, it was revealed that colistin and tigecycline are still the most effective antibiotics in the treatment of infections caused by *A. baumannii*. Furthermore, this study reveals the need for comprehensive surveillance and molecular characterization of integron-mediated resistance mechanisms to inform effective strategies to combat infections caused by MDR *A. baumannii*.

Data availability


The datasets generated and/or analyzed during the current study are available from the corresponding author on reasonable request.


Consent for publication

Not applicable.

ORCID iDs

Cihat Öztürk  <https://orcid.org/0000-0003-2868-2317>

Rukiye Akyol  <https://orcid.org/0000-0002-6825-5638>

Sadık Küçükgünay  <https://orcid.org/0009-0005-7520-6788>

Elif Sevim  <https://orcid.org/0000-0002-6455-1333>

References

- Campos Monteiro R, Rodrigues Malta RC, Lacerda Rodrigues G, De Paiva Anciens Ramos GL, Dos Santos Nascimento J. *Acinetobacter baumannii*: A known pathogen, a new problem. *Germes*. 2023;13(4):381–384. doi:10.18683/germes.2023.1408
- Mankan T, Kaşıkçı MK. The knowledge level of nurses related to prevention of hospital infections [in Turkish]. *Ann Health Sci Res*. 2015; 4(1):11–16. <https://dergipark.org.tr/tr/download/article-file/2017049>. Accessed March 12, 2024.
- Yüreten Z. *Pseudomonas aeruginosa* ve *Acinetobacter baumannii* izolatlarında çeşitli antibiyotik duyarlılıkları ve pulse field gel electrophoresis (PFGE) yöntemiyle tiplendirilmesi (uzmanlık tezi). Kırıkkale, Turkey: Kırıkkale University; 2013. <https://acikerisim.kku.edu.tr/xmlui/bitstream/handle/20.500.12587/17330/352902.pdf?sequence=1&isAllowed=y>. Accessed August 21, 2024.
- Şenol A, Balin ŞÖ. Common infections in intensive care units, Gram-negative microorganisms, antibiotic resistance [in Turkish]. *KSÜ Tıp Fak Der*. 2021;16(1):35–39. <https://dergipark.org.tr/tr/download/article-file/922390>. Accessed March 12, 2024.
- Torge D, Bernardi S, Arcangeli M, Bianchi S. Histopathological features of SARS-CoV-2 in extrapulmonary organ infection: A systematic review of literature. *Pathogens*. 2022;11(8):867. doi:10.3390/pathogens11080867
- Lee CR, Lee JH, Park M, et al. Biology of *Acinetobacter baumannii*: Pathogenesis, antibiotic resistance mechanisms, and prospective treatment options. *Front Cell Infect Microbiol*. 2017;7:55. doi:10.3389/fcimb.2017.00055
- World Health Organization (WHO). WHO publishes list of bacteria for which new antibiotics are urgently needed. Geneva, Switzerland: World Health Organization (WHO); 2017. <https://www.who.int/news/item/27-02-2017-who-publishes-list-of-bacteria-for-which-new-antibiotics-are-urgently-needed>. Accessed August 21, 2024.
- Goswami R, Mukherjee S, Rana VS, et al. Isolation and characterization of arsenic-resistant bacteria from contaminated water-bodies in West Bengal, India. *Geomicrobiol J*. 2015;32(1):17–26. doi:10.1080/01490451.2014.920938
- Temel A, Eraz B. A global threat: *Acinetobacter baumannii* infections, current condition in antimicrobial resistance and alternative treatment approaches [in Turkish]. *Türk Hijyen ve Deneysel Biyoloji Dergisi*. 2019;77(3):367–378. <https://dergipark.org.tr/tr/download/article-file/1871752>. Accessed March 12, 2024.
- Duran H, Çeken N, Atik B. Resistance profile of *Acinetobacter baumannii* strains isolated from intensive care units: A five-years study [in Turkish]. *Mustafa Kemal Üniversitesi Tıp Dergisi*. 2021;12(44):199–204. <https://dergipark.org.tr/tr/download/article-file/1782138>. Accessed March 12, 2024.
- Marazzato M, Scribano D, Sarshar M, et al. Genetic diversity of antimicrobial resistance and key virulence features in two extensively drug-resistant *Acinetobacter baumannii* isolates. *Int J Environ Res Public Health*. 2022;19(5):2870. doi:10.3390/ijerph19052870
- Clark NM, Zhanel GG, Lynch JP. Emergence of antimicrobial resistance among *Acinetobacter* species: A global threat. *Curr Opin Crit Care*. 2016;22(5):491–499. doi:10.1097/MCC.0000000000000337

13. Özkaya E, Aydin F, Bayramoğlu G, Buruk CK, Sandalli C. Investigation of integrons, sul1-2 and dfr genes in trimethoprim-sulfamethoxazole-resistant *Stenotrophomonas maltophilia* strains isolated from clinical samples. *Mikrobiyol Bul.* 2014;48(2):201–212. doi:10.5578/mb.7262
14. Serapide F, Guastalegname M, Gulli SP, et al. Antibiotic treatment of carbapenem-resistant *Acinetobacter baumannii* infections in view of the newly developed β -lactams: A narrative review of the existing evidence. *Antibiotics (Basel).* 2024;13(6):506. doi:10.3390/antibiotics13060506
15. Leblebicioğlu H, Usluer G, Ulusoy S. *Antibiyotikler: Güncel Bilgiler Işığında*. Ankara, Turkey: Bilimsel Tıp; 2003. ISBN:978-975-6986-19-6.
16. Falagas ME, Vardakas KZ, Roussos NS. Trimethoprim/sulfamethoxazole for *Acinetobacter* spp.: A review of current microbiological and clinical evidence. *Int J Antimicrob Agents.* 2015;46(3):231–241. doi:10.1016/j.ijantimicag.2015.04.002
17. Naderi Z, Ghanbarpour R, Jajarmi M, et al. Antibiotic resistance profiling and phylotyping of human-diarrheagenic *Escherichia coli* pathotypes detected from diarrheic and non-diarrheic calves in Iran. *Mol Biol Rep.* 2024;51(1):494. doi:10.1007/s11033-024-09494-6
18. Köseoğlu Ö. Integrons [in Turkish]. *Mikrobiyol Bul.* 2004;38:305–312. https://www.mikrobiyolbul.org/managete/fu_folder/2004-03/2004-38-03-305-312.pdf. Accessed March 12, 2024.
19. Cambray G, Guerout AM, Mazel D. Integrons. *Annu Rev Genet.* 2010;44(1):141–166. doi:10.1146/annurev-genet-102209-163504
20. Gillings MR. Integrons: Past, present, and future. *Microbiol Mol Biol Rev.* 2014;78(2):257–277. doi:10.1128/MMBR.00056-13
21. Stokes HW, Hall RM. A novel family of potentially mobile DNA elements encoding site-specific gene-integration functions: Integrons. *Mol Microbiol.* 1989;3(12):1669–1683. doi:10.1111/j.1365-2958.1989.tb00153.x
22. Ausubel FM, Brent R, Kingston RE, et al., eds. *Short Protocols in Molecular Biology: A Compendium of Methods From Current Protocols in Molecular Biology*. 3rd ed. New York, USA: Wiley; 1997. ISBN:978-0-471-13781-8.
23. Altayb H, El Amin NM, Mukhtar MM, Ahmed Salih M, Siddig MSM. Molecular characterization and in silico analysis of a novel mutation in TEM-1 beta-lactamase gene among pathogenic *E. coli* infecting a Sudanese patient. *Am J Microbiol Res.* 2014;2(6):217–223. doi:10.12691/ajmr-2-6-8
24. Benson DA, Karsch-Mizrachi I, Clark K, Lipman DJ, Ostell J, Sayers EW. GenBank. *Nucl Acids Res.* 2012;40(Database issue):D48–D53. doi:10.1093/nar/gkr1202
25. Kostakoğlu U, Ertürk A, Yıldız İE, et al. Antibiotic resistance and integron gene cassettes in *Acinetobacter baumannii* isolates produced in lower respiratory tract samples taken from the intensive care unit. *KÜ Tıp Fak Derg.* 2020;22(3):450–460. doi:10.24938/kutfd.789547
26. Halaji M, Rezaei A, Zalipoor M, Faghri J. Investigation of class I, II, and III integrons among *Acinetobacter baumannii* isolates from hospitalized patients in Isfahan, Iran. *Oman Med J.* 2018;33(1):37–42. doi:10.5001/omj.2018.07
27. Mengeloğlu FZ, Çoçur Çiçek A, Koçoğlu E, Sandallı C, Budak EE, Özgümüş OB. Carriage of class 1 and 2 integrons in *Acinetobacter baumannii* and *Pseudomonas aeruginosa* isolated from clinical specimens and a novel gene cassette array: BlaOXA-11-cmlA7 [in Turkish]. *Mikrobiyol Bul.* 2014;41(8):48–58. PMID:24506715.
28. Sari B, Baran I, Alaçam S, Mumcuoğlu İ, Kurşun Ş, Aksu N. Investigation of oxacillinase genes in nosocomial multidrug-resistant *Acinetobacter baumannii* isolates by multiplex PCR and evaluation of their clonal relationship with Rep-PCR. *Mikrobiyol Bul.* 2015;49(2):249–258. doi:10.5578/mb.8884
29. Xu L, Deng S, Wen W, et al. Molecular typing, and integron and associated gene cassette analyses in *Acinetobacter baumannii* strains isolated from clinical samples. *Exp Ther Med.* 2020;20(3):1943–1952. doi:10.3892/etm.2020.8911
30. Çopur Çiçek A, Düzgün AÖ, Saral A, et al. Detection of class 1 integron in *Acinetobacter baumannii* isolates collected from nine hospitals in Turkey. *Asian Pac J Trop Biomed.* 2013;3(9):743–747. doi:10.1016/S2221-1691(13)60149-5

Esomeprazole inhibits liver inflammation and carcinogenesis by suppressing farnesoid X receptors and NF- κ B signaling

Chia-Chia Lu^{1,A,D}, Yi-Chin Yang^{2,B,C,D}, Yi-Wen Hung^{3,B,C,D}, Yen-Chun Peng^{4,5,6,A,B,D,F}

¹ Division of Gastroenterology, Department of Internal Medicine, Taichung Veterans General Hospital Chiayi Branch, Taiwan

² Center of Neural Science, Taichung Veterans General Hospital, Taiwan

³ Terry Fox Cancer Research Laboratory, Translational Medicine Research Center, China Medical University Hospital, Taichung, Taiwan

⁴ Division of Gastroenterology, Department of Internal Medicine, Taichung Veterans General Hospital, Taiwan

⁵ School of Medicine, National Yang Ming Chiao Tung University, Taipei, Taiwan

⁶ Department of Post-Baccalaureate Medicine, College of Medicine, National Chung Hsing University, Taichung, Taiwan

A – research concept and design; B – collection and/or assembly of data; C – data analysis and interpretation;

D – writing the article; E – critical revision of the article; F – final approval of the article

Advances in Clinical and Experimental Medicine, ISSN 1899–5276 (print), ISSN 2451–2680 (online)

Adv Clin Exp Med. 2025;34(7):1183–1189

Address for correspondence

Yen-Chun Peng

E-mail: pychunppp@gmail.com

Funding sources

This study was supported by grants from the Taichung Veterans General Hospital Chiayi branch RVHCY10909, RVHCY 111010 and RVHCY 112003, and combined research program from Taichung Veterans General Hospital (TCVGH-VHCY 1098607, TCVGH-VHVV1118601 and TCVGH-VHCY 1128607) Taichung, Taiwan, and China.

Conflict of interest

None declared

Acknowledgements

We would like to thank the Biostatistics Task Force of Taichung Veterans General Hospital, especially Ms. Chiann-Yi Hsu, for her and their support in the process of reviewing statistical analysis.

Received on August 18, 2023

Reviewed on April 7, 2024

Accepted on July 24, 2024

Published online on December 4, 2024

Cite as

Lu CC, Yang YC, Hung YW, Peng YC. Esomeprazole inhibits liver inflammation and carcinogenesis by suppressing farnesoid X receptors and NF- κ B signaling. *Adv Clin Exp Med.* 2025;34(7):1183–1189. doi:10.17219/acem/191596

DOI

10.17219/acem/191596

Copyright

Copyright by Author(s)

This is an article distributed under the terms of the Creative Commons Attribution 3.0 Unported (CC BY 3.0) (<https://creativecommons.org/licenses/by/3.0/>)

Abstract

Background. The activity of proton pump inhibitors (PPIs) hinders the function of proton pumps that generate stomach acid. Nuclear factor kappa B (NF- κ B) is a transcriptional factor engaged in inflammation, immunity and the formation of cancer. The farnesoid X receptor (FXR) is a nuclear receptor that governs the metabolism of bile acids and the metabolic functioning of the liver. The impact of PPIs on the signaling of FXRs and NF- κ B is not well understood.

Objectives. We aimed to study the effects of esomeprazole on FXRs and NF- κ B signaling in liver cells.

Materials and methods. For the liver cell model, we used the human liver cell line HepaG2. Cells were treated with lipopolysaccharides (LPS) and esomeprazole, and then we assessed the effects of esomeprazole on inflammatory and carcinogenic markers, NF- κ B and FXR. We applied the techniques of western blotting, reverse-transcription polymerase chain reaction (RT-PCR), confocal microscopic imaging, and electrophoretic mobility shift assay (EMSA).

Results. Lipopolysaccharides-induced FXRs and NF- κ B signaling upregulated the NF- κ B-associated cytokines interleukin 6 (IL-6), cyclooxygenase-2 (COX-2) and tumor necrosis factor alpha (TNF- α). Esomeprazole inhibited the upregulation of all these cytokines. Additionally, esomeprazole inhibited LPS-induced FXR expression and NF- κ B signaling in HepaG2 cells. The net effect on FXRs and NF- κ B signaling was the lower levels of the associated inflammatory and carcinogenic cytokines.

Conclusions. Our study provides insight into the potential therapeutic effects of esomeprazole on hepatic inflammation and carcinogenesis by inhibiting LPS-induced NF- κ B and FXR expression in HepG2 cells.

Key words: proton pump inhibitors, nuclear factor kappa B, farnesoid X receptor, lipopolysaccharides, HepaG2

Background

Proton pump inhibitors (PPIs) reduce the amount of acid produced in the stomach by inhibiting the action of proton pumps and are commonly used to treat conditions such as gastroesophageal reflux disease, peptic ulcer disease and Zollinger–Ellison syndrome.¹ The most commonly used PPIs include omeprazole, pantoprazole, lansoprazole, and esomeprazole. Clinically, PPIs have side effects such as headache, nausea, diarrhea, renal injury, and an increased risk of bone fractures,^{2,3} and the prolonged use of PPI is an important issue. The long-term use of PPIs has been suggested to increase the risk of liver carcinogenesis, including hepatocellular carcinoma (HCC) and cholangiocarcinoma.^{4–6} However, evidence is conflicting regarding the association between PPIs and HCC.^{7,8}

The mechanisms for which PPIs increase the risk of hepatic carcinogenesis are not fully understood, but is worth studying. Several mechanisms could be considered in PPI and hepatic carcinogenesis, including the altered gut microbiota, promoting the growth of harmful bacteria resulting in liver inflammation^{9–11} and hypergastrinemia. Gastrin is a hormone that possibly promotes liver cell proliferation, overgrowth and the development of tumors.¹² Conversely, several studies have suggested there is no association between PPI use and hypergastrinemia or carcinogenesis.^{13,14}

Nuclear factor kappa B (NF- κ B) signaling is a transcription factor involved in inflammation and carcinogenesis. Nuclear factor kappa B is activated by various stimuli, including inflammatory cytokines, oxidative stresses, and viral or bacterial infections.^{15,16} Activation of NF- κ B also affects hepatic cancer cells by regulating cell proliferation and apoptosis.^{17–19} Thus, NF- κ B signaling has been implicated in carcinogenesis,²⁰ and the sustained activation of NF- κ B in liver cells could contribute to hepatic carcinogenesis.²¹ The other nuclear receptor, farnesoid X receptor (FXR), is also expressed on hepatocytes and has bile acid metabolism and inflammation functions. The activation of FXR is recognized for its antitumor properties in the liver, like inhibition of liver tumor cell growth and proliferation, as well as induction of apoptosis in these cells.²²

The expression and interaction between FXR and NF- κ B in liver carcinogenesis is complex and not well understood. Farnesoid X receptor activation may inhibit NF- κ B signaling and reduce hepatobiliary inflammation, thereby preventing tumor development.²³

The effects of FXR and NF- κ B signaling vary depending on the specific cellular and molecular context. This variability highlights the existing knowledge gap in understanding the mechanisms underlying the effects of PPIs on liver carcinogenesis and the intricate interplay between FXR and NF- κ B. Further research in this area is essential to shed light on these complex interactions and their implications for liver health.

Objectives

This study aimed to investigate the effect of esomeprazole on hepatic carcinogenesis by examining the expression of NF- κ B and FXR.

Materials and methods

Cell culture

We cultured HepG2 cells, a human HCC cell line, in sterile flasks. The culture medium included Dulbecco's modified Eagle's medium (DMEM) supplemented with 10% fetal bovine serum (FBS), 1% L-glutamine and 1% penicillin-streptomycin. For sub-confluent cultures, HepG2 cells were seeded at a density of 2 to 4×10⁴ cells/cm², while for confluent cultures, we used a density of 8 to 10×10⁴ cells/cm². Cells were incubated at 37°C in a humidified incubator with 5% CO₂, with the culture medium replenished every 2–3 days, or as needed, to maintain optimal cell growth. After reaching 80–90% confluence, cells were passed to a new culture generation. First, cells were rinsed with phosphate-buffered saline (PBS) to remove serum and residual media. Then, trypsin-EDTA (ethylenediaminetetraacetic acid) was used to detach cells from the culture surface. Trypsin was neutralized with fresh media, and the cells were subsequently collected in pellets by centrifugation.

Real-time quantitative polymerase chain reaction

Total RNA was extracted from the cell cultures using the Trizol reagent. Genomic DNA was eliminated with DNase using the Turbo DNA-free kit (Applied Biosystems, Waltham, USA). Next, 1 µg of total RNA was reverse transcribed into Oligo (dT) using the Superscript III First-Strand Synthesis Super Mix (Invitrogen, Waltham, USA). Polymerase chain reaction (PCR) analysis was conducted using the Quant Studio 3 Real-Time PCR System (Thermo Fisher Scientific, Waltham, USA). Two microliters of cDNA were used as the template for PCR amplification, employing interleukin 6 (IL-6) primers (Supplementary Table 1).

Western blot analysis

Cells were first lysed in radioimmunoprecipitation assay (RIPA) buffer (R0278; MilliporeSigma, St. Louis, USA) supplemented with a protease inhibitor. Protein lysates were incubated on ice for 30 min with repeated vortexing every 5 min, and finally cleared by centrifugation at 6,000 g for 15 min at 4°C. Supernatants were then collected and stored at –80°C until further analysis. Protein concentrations in the extracts were determined using the BCA Protein Assay Kit (23225; Thermo Fisher Scientific). Aliquots of 30 µg of total protein extracted from cultured cells were

subjected to electrophoresis on a 10% sodium dodecyl-sulfate polyacrylamide gel electrophoresis (SDS-PAGE) at a constant voltage of 70 V for 30 min, followed by 110 V for 90 min in a running buffer (25 μ M Tris-HCl pH 8.3, 192 μ M glycine and 0.1% SDS).

Subsequently, proteins were transferred from the gel to a nitrocellulose membrane using a constant current of 350 mA for 90 min in a transfer buffer (25 μ M Tris-HCl pH 8.3, 150 μ M glycine and 5% v/v methanol). The nitrocellulose membrane was then blocked with 5% bovine serum albumin (BSA) in Tris-buffered saline (TBS; 20 μ M Tris pH 7.6, 137 μ M NaCl) for 1 h. Immunostaining was performed using a monoclonal FXR (NR1H4) antibody and Phospho-NF- κ B p65 (Ser536) antibody (both at 1/1,000 dilution; Cell Signaling Technology (CST), Danvers, USA), followed by incubation with a secondary polyclonal mouse anti-goat antibody conjugated to horseradish peroxidase (HRP) (diluted at 1/5,000; CST). Blots were developed using HRP and Trident Femto Western HRP Substrate (GTX14698; Gene Tex, Irvine, USA). Data acquisition was performed using a Geliance CCD camera (PerkinElmer, Waltham, USA). Image analysis was carried out using ImageJ software (National Institutes of Health (NIH), Bethesda, USA).

Confocal microscopy analysis

Laser confocal microscopy (Olympus FV1000; Olympus Corp., Tokyo, Japan) was employed to localize subcellular proteins, including NF- κ B. Immunofluorescence staining was performed to label samples with a fluorescently conjugated NF- κ B specific antibody. Subsequently, confocal microscopy was conducted using a confocal laser scanning microscope.

Sample preparations involved the following steps. First, cells were fixed and permeabilized, and the nonspecific binding sites were blocked using a blocking agent (e.g., BSA or serum). Next, samples were incubated with a primary antibody specific to NF- κ B while diluted in a blocking buffer. Afterward, samples were washed to remove any unbound primary antibodies. Samples were then incubated with a secondary antibody conjugated to a fluorescent dye, diluted in a blocking buffer, and washed again to eliminate any unbound secondary antibodies. Finally, samples were mounted on a microscope slide using a mounting medium, and images were taken with a confocal laser scanning microscope.

Electrophoretic mobility shift assay

HepG2 cells were first treated with esomeprazole and lipopolysaccharide (LPS), before being harvested to obtain nuclear extracts according to the standard procedures as described in the literature. To perform electrophoretic mobility shift assay (EMSA), we used a double-stranded DNA probe containing the consensus sequence for the NF- κ B binding site (5'-GGGACTTTCC-3'), which was labeled with biotin. The labeled DNA probe was incubated

with the nuclear extract in a binding buffer containing nonspecific competitor DNA (such as poly dI-dC) and a specific competitor DNA containing the NF- κ B binding site. The specific competitor DNA was obtained commercially or prepared by annealing oligonucleotides containing the NF- κ B binding site.

The binding reaction was conducted at room temperature for 30 min to allow the formation of NF- κ B-DNA complexes. Subsequently, the reaction mixture was loaded onto a non-denaturing polyacrylamide gel, which allowed electrophoresis to separate the NF- κ B-DNA complexes from the free DNA probes. After electrophoresis, gel visualization was achieved using autoradiography for the radioactive probes. As the NF- κ B DNA complex migrated more slowly than the free DNA probe, a shifted band appeared on the gel, indicating the presence of the complex.

Statistical analyses

Each group in this study was examined in each experiment. Results were presented as medians. The quantitative polymerase chain reaction (qPCR) results shown in the dot plots were obtained from 6 independent experiments ($n = 6$). All experiments were independently repeated 6 times. The Kruskal–Wallis test was conducted, and if differences were significant, the Dunn–Bonferroni test was applied. Differences were considered statistically significant at a p -value < 0.05 . For data analysis, we used IBM SPSS v. 22.0 (IBM Corp., Armonk, USA).

Results

Lipopolysaccharides increased the expression of NF- κ B signaling molecules in HepG2 cells

Lipopolysaccharides, a component of the outer membrane of Gram-negative bacteria, activates various signaling molecules in host cells, including the NF- κ B transcription factor. Such LPS activation plays a crucial role in regulating the expression of genes related to inflammation, immunity and cell survival. We found that LPS treatment increased NF- κ B expression and activated downstream targets by increasing the expression of inflammatory cytokines, such as IL-6, cyclooxygenase-2 (COX-2) and tumor necrosis factor alpha (TNF- α) (Fig. 1).

Lipopolysaccharides increased FXR expression in HepG2 cells

Lipopolysaccharides are known to increase FXR expression in various cells, including hepatocytes and macrophages. Activation of the FXR by LPS has been proposed to play a protective role in various diseases by regulating the expression of genes involved in inflammatory and

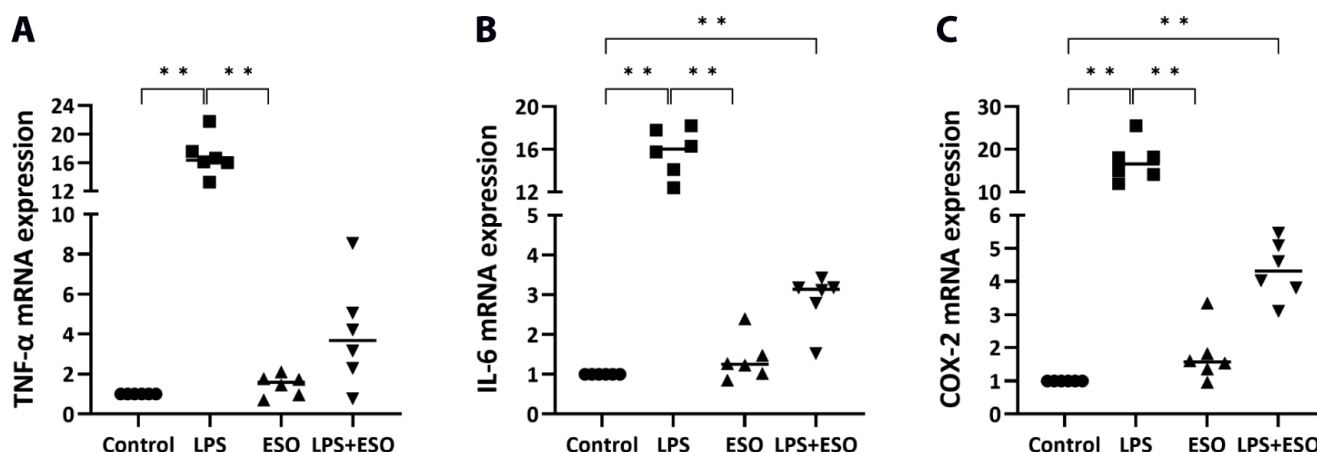


Fig. 1. Cytokine expression in HepG2 cells treated with LPS and ESO using real-time quantitative polymerase chain reaction (qPCR). The dot plot shows the level relative to the control group and illustrates the median. A. Lipopolysaccharides significantly upregulated the expression of TNF- α ; B. Lipopolysaccharides significantly upregulated the expression of IL-6; C. Lipopolysaccharides significantly upregulated the expression of COX-2. Esomeprazole could downregulate LPS-induced TNF- α , IL-6 and COX-2 expression. All 3 dot plots (A, B and C) were compared among 4 groups using the Kruskal–Wallis test. If the Kruskal–Wallis test showed a statistical difference among the 4 groups, post hoc comparisons between the groups were performed using Dunn–Bonferroni tests. The ** symbol on the chart indicates $p < 0.01$ according to the Dunn–Bonferroni tests. The median and the p-values from the Kruskal–Wallis test and the Dunn–Bonferroni tests can be found in Supplementary Table 2

TNF- α – tumor necrosis factor alpha; IL-6 – interleukin 6; COX-2 – cyclooxygenase-2; LPS – lipopolysaccharides; ESO – esomeprazole; LPS: 1 μ g/mL; ESO: 25 μ M; $n = 6$; ** $p < 0.01$.

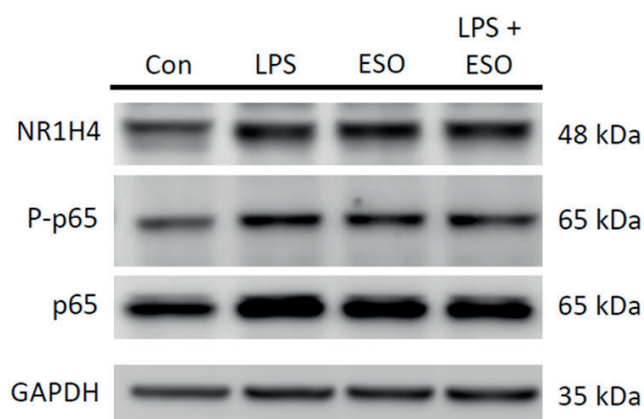


Fig. 2. Treatment with LPS for 12 h increased farnesoid X receptors (FXR) (NR1H4) expression in HepG2 cells. Expression of NF- κ B (p65), phospho-NF- κ B (p-p65) and FXR (NR1H4) in HepG2 cells treated with or without LPS and esomeprazole. Untreated control cells and cells treated with esomeprazole alone were also included. HepG2 cells were treated with LPS with or without esomeprazole for 12 h. Cell lysates were immunotransferred using anti-NF- κ B (p65), anti- κ B α and anti-phospho- κ antibodies. Immunotransference using an anti-GAPDH antibody was performed to confirm the equal sample load

Con – control untreated cells; LPS – lipopolysaccharides; NF- κ B – nuclear factor kappa B; ESO – esomeprazole; GAPDH – glyceraldehyde-3-phosphate dehydrogenase; LPS: 1 μ g/mL; ESO: 25 μ M.

immune responses. Figure 2 shows that LPS treatment for 12 h increased FXR expression in HepG2 cells. The confocal microscopic images in Fig. 3 demonstrate that esomeprazole inhibited LPS-induced NF- κ B expression. Based on these results, esomeprazole, in addition to treating acid-related disorders, likely exerts an anti-inflammatory effect by blocking the LPS activation of NF- κ B. Figure 4A illustrates that LPS treatment significantly upregulated the expression of FXR in HepG2 cells compared to the untreated

control group. This upregulation was significantly mitigated when the cells were co-treated with esomeprazole, indicating that esomeprazole effectively downregulated LPS-induced FXR expression (Supplementary Table 2).

Esomeprazole inhibited the expression of NF- κ B and FXR in HepG2 cells

Furthermore, as shown in Fig. 4B, LPS treatment resulted in a significant elevation in p-P65/P65 expression, highlighting an increase in NF- κ B activation. Co-treatment with esomeprazole led to a reduction in the LPS-induced p-P65 expression, although this reduction was borderline significant. The statistical significance of these findings was assessed using the Kruskal–Wallis test, which indicated significant differences among the treatment groups. Subsequent post hoc comparisons were conducted using Dunn–Bonferroni tests. Detailed p-values from both the Kruskal–Wallis and Dunn–Bonferroni tests are provided in Supplementary Table 2.

These results suggest that esomeprazole has a modulatory effect on LPS-induced changes in NF- κ B and FXR signaling pathways in HepG2 cells. Specifically, esomeprazole appears to counteract the pro-inflammatory effects induced by LPS, potentially through the regulation of the FXR and NF- κ B signaling.

Electrophoretic mobility shift assay showed esomeprazole inhibition of LPS-induced NF- κ B B expression

To investigate whether esomeprazole inhibits LPS-induced NF- κ B expression, we conducted an EMSA by incubating a radiolabeled DNA probe containing an NF- κ B

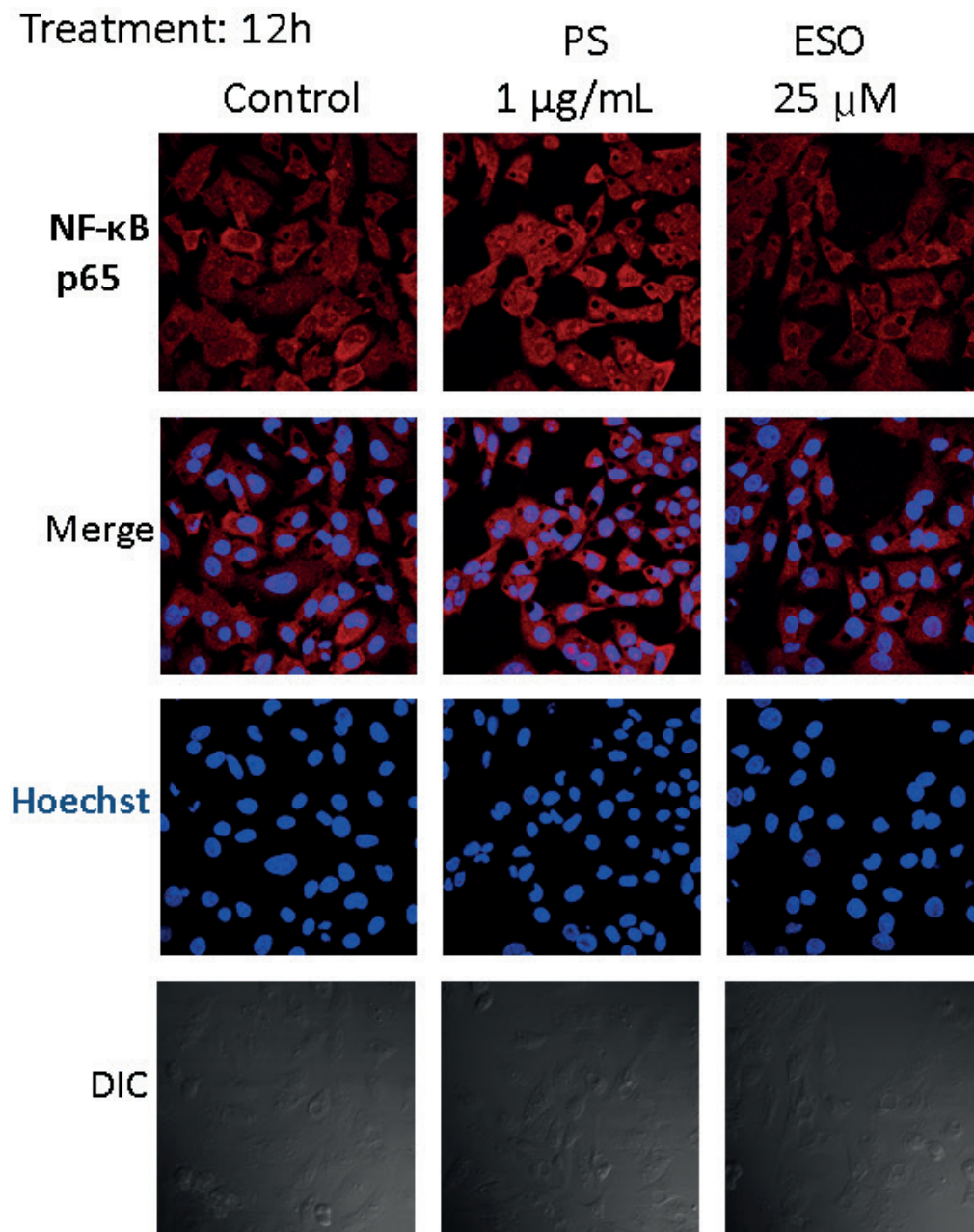


Fig. 3. Confocal microscopy images demonstrate that esomeprazole inhibits LPS-induced NF-κB expression. The expression of NF-κB (p65) and phospho-NF-κB (p65) in HepG2 cells was evaluated using confocal microscopy. The HepG2 cells were either untreated (control) or treated with LPS or esomeprazole for 12 h. The analysis also included merged images and control images (Hoechst and DIC)

Con – control untreated cells;
LPS – lipopolysaccharides;
ESO – esomeprazole;
NF-κB – nuclear factor kappa B;
DIC – differential interference;
LPS: 1 µg/mL; ESO: 25 µM.

binding site with nuclear extracts from LPS-treated cells, in the presence and absence of esomeprazole. If esomeprazole inhibits NF-κB expression in the presence of esomeprazole, EMSA should have revealed a diminished band pattern corresponding to the NF-κB-DNA complex. That was exactly what we observed (Fig. 5).

Discussion

Esomeprazole, a PPI, is widely used to reduce acid production in the stomach to treat acid-related disorders and has proven clinical outcomes. Thus, the long-term use of PPIs has been considered an important issue in medical care. Nuclear factor-kappa B is a transcription factor involved

in the regulation of inflammation and carcinogenesis. In the present study on HepaG2 cells, we found that esomeprazole inhibited LPS-induced FXR and NF-κB expression.

An interaction between FXRs and NF-κB has been observed in the liver. The FXR activation inhibits NF-κB activation, resulting in the downstream production of pro-inflammatory cytokines that contribute to liver injury and inflammation. On the other hand, NF-κB activation promotes liver inflammation and injury by promoting the production of pro-inflammatory cytokines, such as TNF-α and IL-6, leading to the progression of liver disease. Therefore, targeting FXRs and NF-κB is likely a complementary approach to treating liver diseases related to inflammation and injury. In our study, we found both FXRs and NF-κB are activated by esomeprazole in LPS-treated hepatocytes.

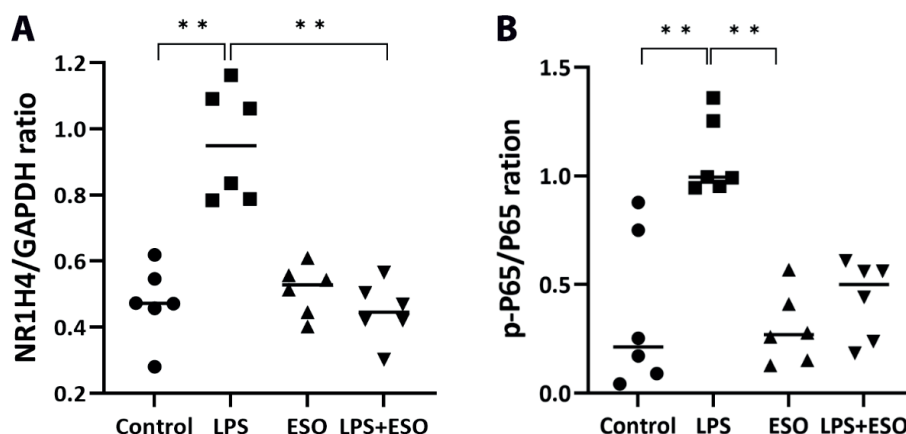


Fig. 4. Expression of NF- κ B (p65), phospho-NF- κ B (p-p65) and farnesoid X receptor (FXR) (NR1H4) in HepG2 cells treated with LPS and ESO as measured with western blotting. Dot plots indicate the levels relative to the control group and illustrate the median values. A. Lipopolysaccharides treatment significantly upregulated FXR expression. Co-treatment with ESO significantly downregulated LPS-induced FXR expression. B. Lipopolysaccharides treatment significantly upregulated the p-P65/P65 expression, while co-treatment with ESO showed a borderline significant downregulation of p-P65 expression. Statistical analysis was performed using the Kruskal–Wallis test to determine significance among groups. If a statistical difference was found, post hoc comparisons between groups were performed using Dunn–Bonferroni tests. The ** symbol on the chart indicates $p < 0.01$ according to the Dunn–Bonferroni tests. Detailed p-values from both the Kruskal–Wallis and Dunn–Bonferroni tests are provided in Supplementary Table 2

LPS – lipopolysaccharides; ESO – esomeprazole; NF- κ B – nuclear factor kappa B; GAPDH – glyceraldehyde-3-phosphate dehydrogenase; LPS: 1 μ g/mL; ESO: 25 μ M; n = 6; ** $p < 0.01$.

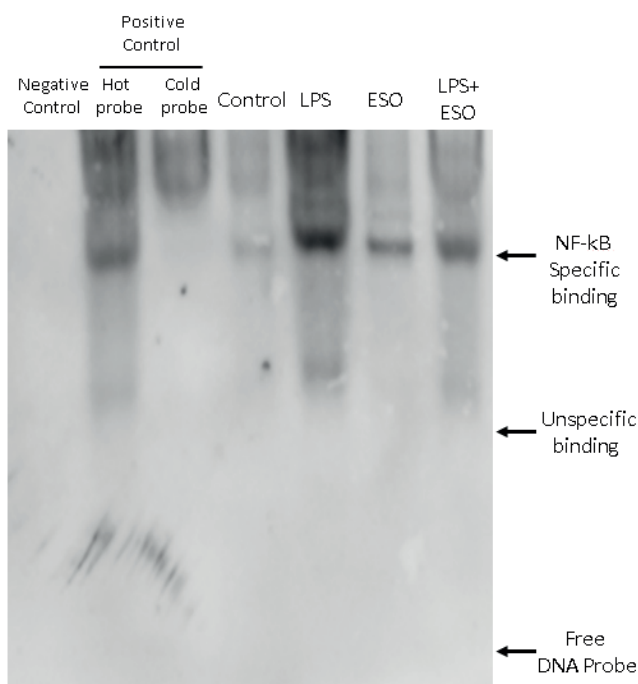


Fig. 5. Electrophoretic mobility shift assay (EMSA) revealed a diminished band pattern corresponding to the NF- κ B-DNA complex in the presence of esomeprazole. The expression of NF- κ B (p65) in HepG2 cells treated with or without LPS and esomeprazole was assessed using EMSA. Untreated control cells and cells treated with esomeprazole alone were also included. HepG2 cells were treated with LPS in the presence or absence of esomeprazole for 12 h. Cellular lysates were subjected to immunotransference using anti-NF- κ B and monitoring by free DNA probe

LPS – lipopolysaccharides; NF- κ B – nuclear factor kappa B; ESO – esomeprazole; LPS: 1 μ g/mL; ESO: 25 μ M.

The inflammatory as well as carcinogenesis effects were both inhibited by the PPI in HepG2 cells.

Proton pump inhibitors may play a protective role in inflammation and carcinogenesis. In studies of nerve cells,

PPIs exert mitochondrial apoptosis and attenuate NF- κ B signaling, suggesting its potential as an effective and safe anticancer treatment for gliomas.²⁴ An animal study found that PPIs inhibit the induction of several inflammatory mediators, including cytokines, chemokines and nitric oxide (NO), by suppressing NF- κ B, thereby preventing fulminant liver failure.²⁵

The PPI effect on the process of carcinogenesis may be paradoxical. Proton pump inhibitors paradoxically augment the anti-tumorigenic and gastrin in an APC^{Min/+} intestinal polyposis animal model.²⁶ Our study further demonstrated the potential inhibitory effect of esomeprazole on NF- κ B and its associated signaling pathways in hepatocytes.

The interaction between FXR and NF- κ B in the liver is complex and not fully understood. Wang et al. demonstrated that the FXR acts critically as a negative mediator of hepatic inflammation, contributing to hepatoprotection and suppressing hepatic carcinogenesis.²³ However, in our study, we found that both FXR and NF- κ B signaling were inhibited by esomeprazole in LPS-induced hepatic inflammation. The net effect of the inhibition of the FXR and NF- κ B is reduced levels of associated cytokines.

Limitations

The study primarily uses HepaG2 cells, which is a common cell line for liver-related research. However, the relevance of findings in cell lines to clinical outcomes in humans is often limited and may not fully represent the complexity of liver-related diseases. This article discusses the potential benefits of targeting FXRs and NF- κ B in liver diseases, but it may not fully capture the diverse nature of liver-related disorders, which can have multiple underlying causes and mechanisms.

Conclusions

Our study provides insight into the potential therapeutic effects of esomeprazole on hepatic inflammation and carcinogenesis by inhibiting LPS-induced NF- κ B and FXR expressions in HepG2 cells. However, more research is needed to fully understand its effects on gene expression and cellular pathways in various contexts, including in vivo and human studies.

Supplementary data

The Supplementary materials are available at <https://doi.org/10.5281/zenodo.12740310>. The package includes the following files:

Supplementary Table 1. Primers sequence used for RT-PCR.

Supplementary Table 2. HepG2 cells were treated with or without lipopolysaccharides or esomeprazole, and compared to untreated cells using qPCR.

Data availability


The datasets generated and/or analyzed during the current study are available from the corresponding author on reasonable request.


Consent for publication


Not applicable.

ORCID iDs

Chia-Chia Lu  <https://orcid.org/0009-0002-2509-2215>

Yi-Chin Yang  <https://orcid.org/0000-0002-9651-3761>

Yi-Wen Hung  <https://orcid.org/0000-0002-6154-8315>

Yen-Chun Peng  <https://orcid.org/0000-0002-8993-3039>

References

- Boparai V, Rajagopalan J, Triadafilopoulos G. Guide to the use of proton pump inhibitors in adult patients. *Drugs*. 2008;68(7):925–947. doi:10.2165/00003495-200868070-00004
- Schnoll-Sussman F, Niec R, Katz PO. Proton pump inhibitors. *Gastrointest Endosc Clin North Am*. 2020;30(2):239–251. doi:10.1016/j.giec.2019.12.005
- Schubert ML. Physiologic, pathophysiologic, and pharmacologic regulation of gastric acid secretion. *Curr Opin Gastroenterol*. 2017;33(6):430–438. doi:10.1097/MOG.0000000000000392
- Chang Y, Lin WY, Chang YC, et al. The association between baseline proton pump inhibitors, immune checkpoint inhibitors, and chemotherapy: A systematic review with network meta-analysis. *Cancers (Basel)*. 2022;15(1):284. doi:10.3390/cancers15010284
- Peng YC, Lin CL, Hsu WY, et al. Association between cholangiocarcinoma and proton pump inhibitors use: A nested case-control study. *Front Pharmacol*. 2018;9:718. doi:10.3389/fphar.2018.00718
- Song HJ, Jiang X, Henry L, Nguyen MH, Park H. Proton pump inhibitors and risk of liver cancer and mortality in patients with chronic liver disease: A systematic review and meta-analysis. *Eur J Clin Pharmacol*. 2020;76(6):851–866. doi:10.1007/s00228-020-02854-8
- Kao W, Su C, Chia-Hui Tan E, et al. Proton pump inhibitors and risk of hepatocellular carcinoma in patients with chronic hepatitis B or C. *Hepatology*. 2019;69(3):1151–1164. doi:10.1002/hep.30247
- Labenz C, Labenz J. Proton pump inhibitors in patients with liver cirrhosis: Evidence to improve their battered reputation. *Am J Gastroenterol*. 2021;116(11):2304. doi:10.14309/ajg.0000000000001394
- Cheung KS, Leung WK. Long-term use of proton-pump inhibitors and risk of gastric cancer: A review of the current evidence. *Ther Adv Gastroenterol*. 2019;12:175628481983451. doi:10.1177/1756284819834511
- Imhann F, Bonder MJ, Vich Vila A, et al. Proton pump inhibitors affect the gut microbiome. *Gut*. 2016;65(5):740–748. doi:10.1136/gutjnl-2015-310376
- Macke L, Schulz C, Koletzko L, Malfetherthner P. Systematic review: The effects of proton pump inhibitors on the microbiome of the digestive tract. Evidence from next-generation sequencing studies. *Aliment Pharmacol Ther*. 2020;51(5):505–526. doi:10.1111/apt.15604
- Hagiwara T, Mukaisho K, Nakayama T, Sugihara H, Hattori T. Long-term proton pump inhibitor administration worsens atrophic corpus gastritis and promotes adenocarcinoma development in Mongolian gerbils infected with *Helicobacter pylori*. *Gut*. 2011;60(5):624–630. doi:10.1136/gut.2010.207662
- Han YM, Park JM, Kangwan N, et al. Role of proton pump inhibitors in preventing hypergastrinemia-associated carcinogenesis and in antagonizing the trophic effect of gastrin. *J Physiol Pharmacol*. 2015;66(2):159–167. PMID:25903947.
- Tatsuguchi A, Hoshino S, Kawami N, et al. Influence of hypergastrinemia secondary to long-term proton pump inhibitor treatment on ECL cell tumorigenesis in human gastric mucosa. *Pathol Res Pract*. 2020;216(10):153113. doi:10.1016/j.prp.2020.153113
- Ghosh S, May MJ, Kopp EB. NF- κ B and REL proteins: Evolutionarily conserved mediators of immune responses. *Annu Rev Immunol*. 1998;16(1):225–260. doi:10.1146/annurev.immunol.16.1.225
- Richmond A. NF- κ B, chemokine gene transcription and tumour growth. *Nat Rev Immunol*. 2002;2(9):664–674. doi:10.1038/nri887
- Luedde T, Schwabe RF. NF- κ B in the liver: Linking injury, fibrosis and hepatocellular carcinoma. *Nat Rev Gastroenterol Hepatol*. 2011;8(2):108–118. doi:10.1038/nrgastro.2010.213
- Pan H, Fu X, Huang W. Molecular mechanisms of liver cancer. *Anticancer Agents Med Chem*. 2011;11(6):493–499. doi:10.2174/187152011796011073
- Yang Y, Kim S, Seki E. Inflammation and liver cancer: Molecular mechanisms and therapeutic targets. *Semin Liver Dis*. 2019;39(1):026–042. doi:10.1055/s-0038-1676806
- Karin M. Nuclear factor- κ B in cancer development and progression. *Nature*. 2006;441(7092):431–436. doi:10.1038/nature04870
- Lim KH, Choi HS, Park YK, et al. HBx-induced NF- κ B signaling in liver cells is potentially mediated by the ternary complex of HBx with p22-FLIP and NEMO. *PLoS One*. 2013;8(3):e57331. doi:10.1371/journal.pone.0057331
- Sun L, Cai J, Gonzalez FJ. The role of farnesoid X receptor in metabolic diseases, and gastrointestinal and liver cancer. *Nat Rev Gastroenterol Hepatol*. 2021;18(5):335–347. doi:10.1038/s41575-020-00404-2
- Wang YD, Chen WD, Wang M, Yu D, Forman BM, Huang W. Farnesoid X receptor antagonizes nuclear factor κ B in hepatic inflammatory response. *Hepatology*. 2008;48(5):1632–1643. doi:10.1002/hep.22519
- Geeviman K, Babu D, Prakash Babu P. Pantoprazole induces mitochondrial apoptosis and attenuates NF- κ B signaling in glioma cells. *Cell Mol Neurobiol*. 2018;38(8):1491–1504. doi:10.1007/s10571-018-0623-4
- Nakatake R, Hishikawa H, Kotsuka M, et al. The proton pump inhibitor lansoprazole has hepatoprotective effects in vitro and in vivo rat models of acute liver injury. *Dig Dis Sci*. 2019;64(10):2854–2866. doi:10.1007/s10620-019-05622-6
- Han YM, Baik Hahm K, Park JM, Hong SP, Kim EH. Paradoxically augmented anti-tumorigenic action of proton pump inhibitor and gastrin in APCMin/+ intestinal polyposis model1. *Neoplasia*. 2014;16(1):73–83. doi:10.1593/neo.131510

Unfolding memories: Crafting digital life storybooks for dementia care via telehealth

Ponnusamy Subramaniam^{1,A,C,E,F}, Preyaangka Thillainathan^{2,B-D}, Anthony Angwin^{3,A,C,E,F}, Shobha Sharma^{4,A,D-F}

¹ Clinical Psychology Program and Center for Healthy Ageing and Wellness (H-CARE), Faculty of Health Sciences, The National University of Malaysia, Kuala Lumpur, Malaysia

² Speech Sciences Program, Faculty of Health Sciences, The National University of Malaysia, Kuala Lumpur, Malaysia

³ Speech Pathology Program, School of Health and Rehabilitation Sciences, University of Queensland, Brisbane, Australia

⁴ Speech Sciences Program and Center for Healthy Ageing and Wellness (H-CARE), Faculty of Health Sciences, The National University of Malaysia, Kuala Lumpur, Malaysia

A – research concept and design; B – collection and/or assembly of data; C – data analysis and interpretation;

D – writing the article; E – critical revision of the article; F – final approval of the article

Advances in Clinical and Experimental Medicine, ISSN 1899–5276 (print), ISSN 2451–2680 (online)

Adv Clin Exp Med. 2025;34(7):1191–1200

Address for correspondence

Shobha Sharma

E-mail: shobha.sharma@ukm.edu.my

Funding sources

None declared

Conflict of interest

None declared

Received on January 7, 2024

Reviewed on October 2, 2024

Accepted on October 10, 2024

Published online on January 8, 2025

Abstract

Background. Dementia, a rapidly growing cognitive disorder, has a profound impact on the lives of individuals and their caregivers across the globe. Digital life storybooks have emerged as a promising non-pharmacological intervention to improve the wellbeing of people living with dementia (PLWD).

Objectives. This study aims to investigate the feasibility of developing and applying a digital life storybook for PLWD using telehealth, while evaluating its impact on communication skills, quality of life (QoL) and satisfaction levels.

Material and methods. A mixed-method study design will be employed, involving pairs of PLWD and their primary caregivers (dyads) recruited from a teaching hospital and a non-profit organization in Malaysia. The intervention involves the creation and use of a digital life storybook facilitated remotely via telehealth channels. Data will be collected at 6 points in time: prior to the commencement of development, prior to the submission of an application, on a biweekly basis, and at the conclusion of the assessment period. Quantitative measures will include the Holden Communication Scale, Quality of Life-Alzheimer's Disease Scale (QoL-AD) and Quality of the Caregiving Relationship (QCPR) questionnaire. Qualitative data will be gathered through validated open-ended questions.

Results. Implications of the study include facilitating future research, contributing to person-centered care practices, and providing caregivers with tools to better understand and connect with PLWD. The findings will contribute to the understanding of the mechanisms through which digital life storybooks can benefit PLWD and their caregivers.

Conclusions. The successful implementation of this protocol could have significant implications for dementia care in both formal and informal settings, and could ultimately improve the lives of those affected by dementia.

Key words: dementia, training, caregiver, telehealth, digital life storybook

Cite as

Subramaniam P, Thillainathan P, Angwin A, Sharma S. Unfolding memories: Crafting digital life storybooks for dementia care via telehealth. *Adv Clin Exp Med.* 2025;34(7):1191–1200. doi:10.17219/acem/194410

DOI

10.17219/acem/194410

Copyright

Copyright by Author(s)

This is an article distributed under the terms of the Creative Commons Attribution 3.0 Unported (CC BY 3.0) (<https://creativecommons.org/licenses/by/3.0/>)

Introduction

Dementia has emerged as one of the most rapidly growing disorders, contributing to significant disability among the elderly population worldwide.^{1–3} Recent estimates suggest that around 55 million people globally are affected by dementia, with this number expected to double every 20 years.^{4–6} This progressive condition can impact various cognitive functions, including memory, language, judgment, visuospatial abilities, personality, and communication,^{3,7,8} ultimately leading to dependence on caregivers.^{9,10}

Treatment of dementia has focused primarily on slowing the progression of symptoms through medication and therapy, as a definitive cure for dementia remains elusive.^{11–13} Non-pharmacological interventions aim to maintain or improve cognitive ability,^{14–16} communication and social interaction, and reduce behavioral symptoms in people living with dementia (PLWD), which can ultimately enhance their overall quality of life (QoL).^{17–20} Among these interventions, life storybooks have proven to be effective in the treatment of dementia, including improving mood, cognition, e.g., memory, maintaining identity, and overall wellbeing of PLWD.^{21–24}

A life storybook is a carefully crafted volume containing personalized photographs, familiar music and memorabilia, accompanied by concise text or captions that represent key events, important people and treasured memories from an individual's life story.^{25–28} Traditionally, the creation and development of life storybooks have relied on tangible prompts or memory cues to stimulate discussion and recollection of past activities and experiences, often taking the form of books, scrapbooks, photo albums, or memory books.^{28,29} However, technological advancements have facilitated the development of digital life storybooks specifically designed for PLWD.^{30–32} These interventions have taken various forms, such as interactive multimedia storytelling devices,³³ multimedia biographies,³⁴ reminiscence work using platforms like YouTube and the internet,³⁵ and the creation of personalized multimedia systems and digital life stories using life-logging entities.^{36–38} As emphasized by researchers,¹⁷ digital life storybooks offer the unique advantage of incorporating music, a powerful memory trigger, along with other auditory elements, such as narration.^{39–41} By combining video clips with photographs and presenting content in a cinematic format, digital life storybooks facilitate easy viewing for individuals with dementia, both independently and in the presence of others.^{42,43}

A recent systematic review compiled different studies addressing the effects of life storybooks on relatives and highlighted the crucial role of family members in curating the content of life storybooks for individuals with dementia.^{44–46} Involving family members in this process ensures the authenticity, accuracy and personal relevance of the life storybook, capturing the rich tapestry of the individual's life experiences.^{47,48} As primary caregivers and

close acquaintances, family members possess unique insights into the individual's life history, preferences and cherished memories, enabling them to create a narrative that deeply resonates with the PLWD.^{49,50} Moreover, this collaborative effort promotes a sense of connection and continuity for the individual, reinforcing their sense of identity and self-worth.^{51,52} The active engagement of family members in crafting life storybooks represents a meaningful therapeutic intervention that enhances QoL for individuals navigating the challenges of dementia.^{19,53}

However, the onset of the COVID-19 pandemic necessitated a shift in healthcare delivery, prioritizing safety and minimizing physical contact.^{54–57} In response to stringent pandemic restrictions, social distancing measures were widely adopted within healthcare settings.^{58,59} This imperative accelerated the rapid integration of telehealth solutions, enabling the provision of essential medical services while reducing the risk of viral transmission.^{54,60} By utilizing digital platforms and remote communication technologies, healthcare professionals were able to conduct consultations, monitor patient progress and provide timely medical advice, ensuring continuity of care in alignment with public health guidelines.^{61–63} This transformation in healthcare delivery not only highlights the adaptability of the medical field but also represents a significant advancement in leveraging technology to protect both patient and provider wellbeing during times of crisis.^{64–67}

The recent surge in interest in telehealth can be attributed to its multifaceted capabilities, which encompass a comprehensive range of clinical components. These include, but are not limited to, evaluation and assessment, ongoing monitoring, preventative measures, timely interventions, and expert consultations. In light of the increasing connectivity and digitalization of our world, telehealth has emerged as a comprehensive solution for the delivery of healthcare services.^{68,69} It has demonstrated the potential to benefit the older adult population by overcoming geographical distances and providing easier access to healthcare, saving time and reducing travel costs.^{70,71} Older adults receiving telehealth services have also reported high levels of satisfaction with the services provided, with minimal concerns.^{72–74} This adaptability underscores its potential to revolutionize healthcare delivery and improve accessibility, making it a crucial tool in modern healthcare systems.^{75,76}

A study by Laver et al.⁷⁷ emphasized the advantages of using telehealth for dementia care, replacing face-to-face home visit services with digital health technologies. The study concluded that the use of telehealth technologies to deliver non-pharmacological interventions for individuals with dementia and their caregivers may reduce the costs of delivering the intervention, increase accessibility and facilitate research translation.^{78,79} Findings from Cotelli et al.⁸⁰ indicated that cognitive interventions delivered via telehealth to individuals with mild cognitive impairment are comparable to the same services delivered

face-to-face.^{81–83} Furthermore, individuals with dementia and their caregivers have reported satisfaction with the use of telehealth for various outcomes, such as interaction with healthcare practitioners, addressing patient needs and its usefulness.^{70,84–86}

Telehealth used in dementia care services, especially for collaborative assessments, consultations and psychosocial interventions, has shown promising results in improving cognition, communication, overall QoL, reduced caregiver burden, and depression compared to those receiving the usual care.^{87–89} Despite numerous studies on various forms of digital life storybooks, research into the utilization of telehealth to train the development of material and use of digital life storybooks remains unpublished.^{31,90} The feasibility of using digital life storybooks to enhance communication is also still scarce.⁹¹ The effectiveness of digital life storybooks on communication, social interaction, relationships, and QoL of individuals with dementia through the training of digital life storybooks is yet to be explored.^{92,93}

Adapting healthcare interventions in culturally congruent ways appears to increase the acceptability of these practices.^{94,95} The benefits of using a life storybook for individuals with dementia, such as enhanced cognition, communication skills, reduced depression symptoms, and reduced caregiver burden, have been highlighted in previous studies.^{96,97} Conventionally, reminiscence therapy using digital life storybooks has been conducted face-to-face.^{17,28,98} Previous studies have shown that telehealth has shielded individuals with dementia and cognitive decline from unnecessary exposure while also allowing providers to connect their patients to much-needed community services.^{72,99–101} Thus, researchers need to study

the outcomes of the benefits, acceptability and satisfaction,¹⁰² to report the feasibility of developing a digital life storybook using a telehealth modality among individuals with dementia.^{103,104} More recently, in a single case study, Asano and Hird¹⁰⁵ compared the outcomes of a digital life story intervention with online family participation to those of face-to-face sessions conducted without family participation. The online intervention was delivered under the same conditions as face-to-face (twice a week, 30 min per session, for 4 weeks) using the same life storybook. The results demonstrated that both online cognitive stimulations involving family participation and in-person intervention led to improvements in depression, apathy, caregiver distress, and cognitive function scores as measured by the Mini-Mental State Examination (MMSE). This indicates that family members' remote participation could enhance the effectiveness of individualized cognitive stimulation, presenting a promising solution to accessibility challenges.

The current research, therefore, aimed to: 1) study the feasibility of developing a digital life storybook and its application for individuals with dementia via telehealth; 2) study the feasibility of applying a telehealth modality for the development of digital life storybooks for individuals with dementia; 3) compare the communication skills of individuals with dementia before and after using the digital life storybook via telehealth; 4) compare the QoL of individuals with dementia and their caregivers before and after using the digital life storybook via telehealth; and 5) evaluate the levels of satisfaction reported by individuals with dementia and their caregivers via telehealth. The conceptual framework of our research is presented in Fig. 1.

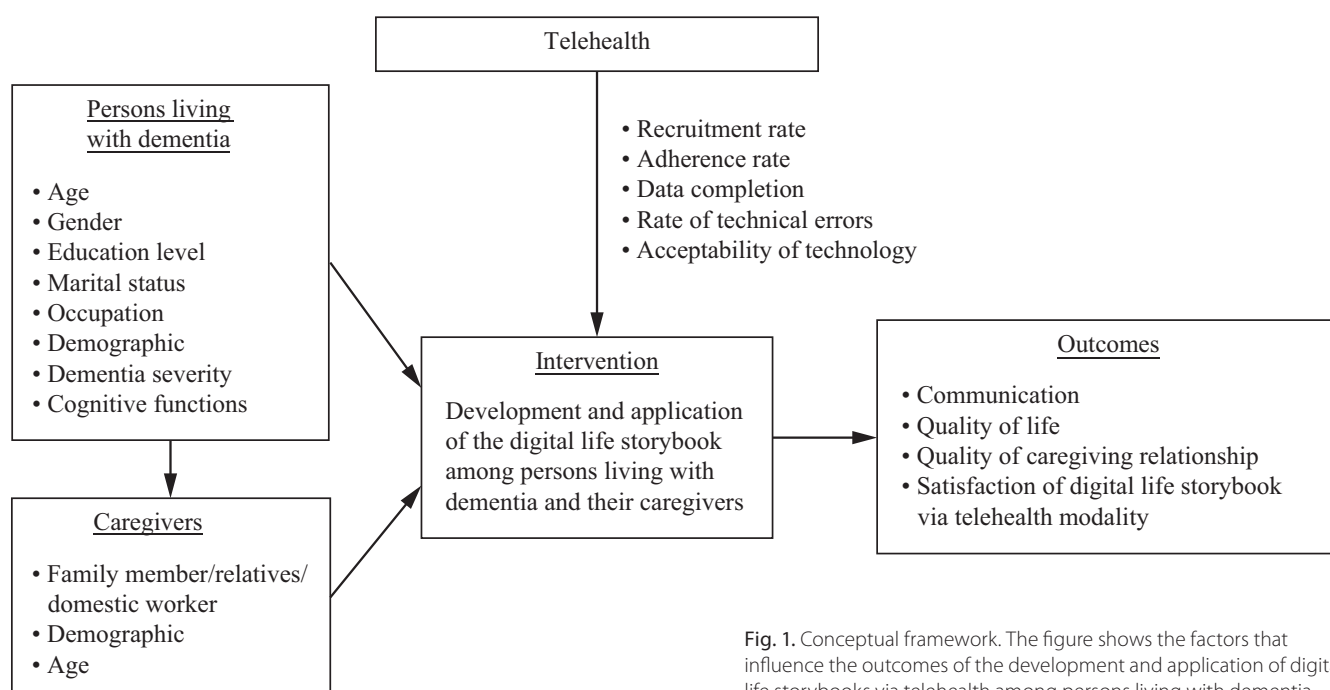


Fig. 1. Conceptual framework. The figure shows the factors that influence the outcomes of the development and application of digital life storybooks via telehealth among persons living with dementia

Materials and methods

This mixed-method study is designed to investigate the feasibility of developing and applying a digital life storybook for PLWD using telehealth methods. The study design is based on previous research that has demonstrated the effectiveness of life storybooks in improving the wellbeing of PLWD^{22–25} and the potential of telehealth in delivering non-pharmacological interventions for this population.^{72,75,85}

Study design and setting

The study involves the entire process of creating and using the digital life storybook, facilitated remotely via telehealth channels. A secure and interactive platform, a subscribed version of Zoom (Zoom Communications, San Jose, USA), will serve as the primary medium for all sessions due to its security features and varied interactive functionalities.¹¹⁰ Preparatory training sessions focusing on Zoom navigation and its diverse features will precede the commencement of the digital life storybook's creation and application for both the PLWD and their respective caregivers.

The digital life storybook's construction involves the use of video editing software such as Wondershare FilmoraX (Wondershare Technology Group, Shenzhen, China) or Windows Movie Maker (Microsoft Corp., Redmond, USA), undertaken by the researchers. This process entails compiling soft copies of photographs, images or videos displaying personal memorabilia, pertinent information, beloved songs, or music obtained from caregivers or family members. However, the responsibility of selecting relevant material and uploading chosen images, videos and songs onto a digital photo frame with audio-video capabilities lies with the caregiver or family, thereby maintaining the privacy of personal materials as the researchers refrain from direct involvement in this step.³⁴ Nonetheless, the researchers will guide the caregiver or family concerning image selection and crafting simple statements for each image. Tangible memorabilia will remain in the possession of PLWD or their families to complement the digital life storybook during subsequent reminiscence sessions.

A participatory design approach will be employed in the creation of the digital life storybook, emphasizing the active involvement of PLWD in the decision-making processes, design concepts, content creation, and direction of their life narratives.¹⁷ Collaboratively, researchers and caregivers will serve as co-editors, engaging in this process. However, it is essential to note that such involvement is voluntary rather than obligatory. The development of the digital life storybook will be done through 2 different approaches: first, full engagement with the PLWD, including a life review process, or alternatively, independent preparation by caregivers or family members and then presented to the PLWD as a "gift". Before the study commences, a comprehensive plan and design inclusive of a realistic timeline will be established. The structured process for constructing the digital

life storybook will draw upon Subramaniam et al.'s²⁹ research. Collaboration among PLWD, their caregivers, relatives, and researchers will entail compiling supplementary elements, including selecting and sourcing favored music, songs, video clips, and/or footage if available. The chronological organization of the digital life storybook will span from childhood to the present, segmented into distinct phases such as childhood, teenage years, career, mid-life, etc., based on available visual materials. This content will be enriched by background music, participants' preferred songs and a narrated storyline. Aligning with the individual's preferences, the chosen songs and music will accompany appropriate images whenever feasible. Additionally, expressions articulated by PLWD throughout the development process may be incorporated as quotations where fitting.

Narration will be provided by either the PLWD themselves or by caregivers/relatives. The spoken word will be reinforced by the text appearing on the screen or scrolling across the screen, in a clear font, allowing the PLWD sufficient time to read the words if they wish to do so. The language used for the narration will be preferred by the PLWD and not restricted.

Weekly online meetings between the researchers and the participant pairs (dyads) will be held to develop the digital life storybook, with each week focusing on 1 segment of the digital life storybook (e.g.: week 1: personal information; week 2: childhood; week 3: school; etc.). Each segment will be reviewed by the dyads (where possible) before moving on to the next segment of the digital life storybook. The dyads are allowed to amend each segment of the digital life storybook if they are not satisfied. The final product of the digital life storybook will be saved and uploaded to a digital photo book and mailed to the PLWD. Based on past research, it is expected that the digital life storybook will take approx. 7–10 weeks to develop and finalize.²⁹

Online training will be provided to the dyads on how to use the finalized digital life storybook. For purposes of this study, the dyads will be required to use the digital life storybook a minimum of 4 days a week, with each session lasting between 45 and 50 min, for 8 consecutive weeks.

Participants

Participants will be selected via purposive sampling techniques and recruited from the inpatient and outpatient case-loads of the geriatric medicine, family medicine and psychology clinics at a prominent teaching hospital in Malaysia and from a non-profit organization that supports people with Alzheimer's disease and their caregivers in Malaysia. The potential participants will be contacted via the phone to get their oral and written consent to be involved in this study.

To be included in the study, dyads will comprise people living with mild-to-moderate dementia and their primary caregivers (family/relatives) who would consent to participate in the research. Caregivers involved will have to be adult family members or relatives (aged 18 years and above)

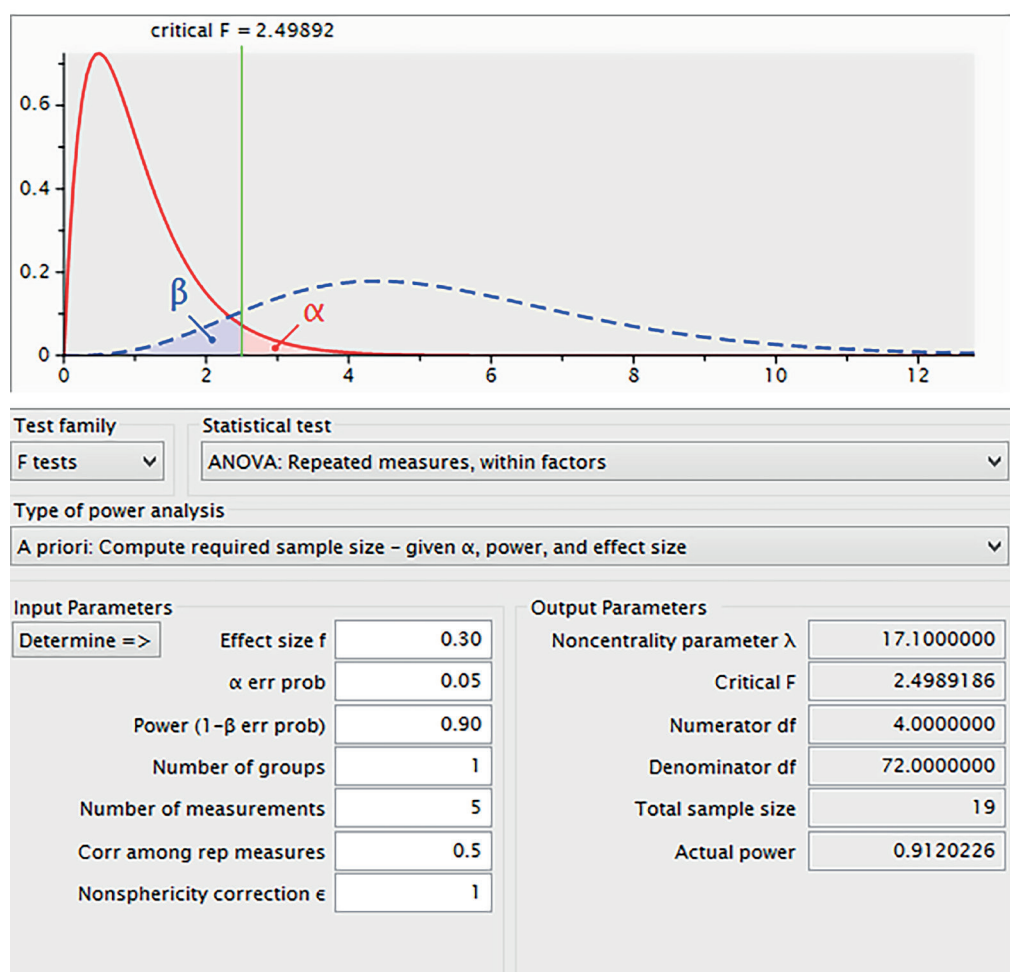


Fig. 2. Sample size calculation. The figure above shows the sample size calculation obtained using G*Power3 for this research

or their domestic helpers who can ensure access to maximal personalized information for the digital life storybook. The caregivers of PLWD should also have functional cognitive abilities and be able to independently perform functions of daily life. The dyads must be able to speak, read and write in a common language and must be able to commit to a period of 4–6 months for this study.

The dyads should have access to personal photographs/videos and/or memorabilia of PLWD and a personal computer, laptop, iPad or tablet with stable internet connections. However, they are not required to have any knowledge or skills associated with computers and technology and will not be required to control the digital life storybook system before this study.

Any PLWD with high medical dependency, moderate-to-severe (or greater) levels of cognitive impairment as indicated within their medical history, significant auditory or visual impairments, and major psychiatric or other mental health issues will be excluded from participating.

Sample size calculation

A priori power analysis was conducted using G*Power3,¹⁰⁶ for repeated measures analysis of variance (ANOVA) with a single group, a medium effect size ($d = 0.30$), and an α

of 0.05 as shown in Fig. 2. A dropout rate of 15% is anticipated, with a minimum of 22 participants needed to achieve a power of 0.90. Hence, this research will involve 22 dyads of participants who meet the inclusion criteria.

Data collection

The dyads will commence the study immediately upon consenting to participate. All questionnaires will be sent to the participants as editable PDF files or Google Forms (Google LLC, Mountain View, USA), to be completed online. Data will be collected at 6 points of time during the study period: pre-development, baseline (T0); pre-application (T1); follow-up assessment (T2, T3, T4) biweekly; and final assessment (T5) 2 weeks after T4. Progress will be monitored online using Zoom and all sessions will be video/audio recorded to allow for the monitoring of variations or changes in communication and didactic interactions. Records of the date, day and duration of digital life storybook usage will be charted in the record form provided to the participants. The main researcher will administer all the assessments during each point of time.

Information regarding the PLWD will be obtained from medical records and based on the formal diagnosis by the attending physician. Several screening tools will also

be used to select the potential participants based on the inclusion and exclusion criteria of this study to determine the severity of dementia, cognitive level and depression level respectively by the main researcher before the commencement of this study:

1) Clinical Dementia Rating (CDR).¹⁰⁷ The CDR is a clinician-rated dementia staging system with 5 levels – from no dementia to severe dementia. The CDR scores are healthy = 0; questionable dementia = 0.5; mild dementia = 1; moderate dementia = 2; severe dementia = 3.

2) MiniMental State Examination.¹⁰⁸ The MMSE is a 30-point test used to measure the cognitive status in adults which includes orientation, attention, memory, language, and visual-spatial skills.

3) Geriatric Depression Scale (GDS).¹⁰⁹ The GDS is a brief self-reported depression scale (yes/no) for older adults with a higher score indicating severe depression. In the GDS, a score of 0–9 is considered normal, 10–19 demonstrates mild depressive symptoms and 20–30 shows severe depression.

To evaluate the feasibility of the development and application of the digital life storybook via telehealth, recruitment rate, adherence and retention rate, data completion, rate of technical errors during videoconferencing, and acceptability of technology will be evaluated.¹¹⁰ The study will collect data to measure and compare the communication skills and QoL of people living with dementia, as well as the QoL of their caregivers throughout the study period.

The following measures will be used to monitor changes over time across the study duration:

1) Holden Communication Scale (HCS).¹¹¹ The HCS consists of 12 items assessing the conversation, awareness, knowledge and communication in both aspects of verbal and non-verbal communication. Each item contains 5 response options, ranging from 0 to 4, where higher scores indicate more difficulties in communication. The Cronbach's α of the HCS is 0.94 and test–retest reliability is $r = 0.71$. The Malay version of HCS will be translated and validated using content validity.

2) Quality of life-Alzheimer's Disease Scale (QOL-AD).¹¹² The QOL-AD is a 13-item questionnaire used to interview a PLWD to gather an indication of self-reported QoL via 4-point Likert scale items, with higher scores indicating higher QoL. Interrater reliability was excellent with all Cohen's κ values >0.70 . Internal consistency was excellent with a Cronbach's α coefficient of 0.82.

3) Quality of Carer–Patient Relationship Scale (QCPR).¹¹³ The QCPR is a 14-item questionnaire with 2 subscales, will be used to measure the quality of caregiving relationship between the PLWD and their caregiver/relatives. The questionnaire consists of 14 5-point Likert scale items, where a higher overall score on this scale indicates a higher relationship quality.

Qualitative measurements

To gather more in-depth information regarding the satisfactory levels of the development and application of the digital life storybook via telehealth and the perceived

value of the digital life storybook, a set of open-ended questions will be developed and validated. The caregiver and the PLWD will be asked the same questions separately in verbal interviews. The questions will cover feelings and thoughts about the content of the digital life storybook, the benefits of the digital life storybook, the repeat-watching experience, the ease of use of the telehealth modality, perceived strengths and challenges of the telehealth modality, and anything else they would like to share.

Data analysis

Quantitative data will be analyzed using the IBM SPSS software (IBM Corp., Armonk, USA). The demographic data of the dyads will be analyzed descriptively. The changes in communication skills of PLWD, QoL of PLWD and the quality of the caregiving relationship will be determined using a paired t-test at pre-development (baseline assessment) with post-development of the digital life storybook, and post-development with post application (final assessment) of the digital life storybook. A repeated-measures ANOVA will be employed to assess the changes from the post-development to the post-application of the digital life storybook. A value of $p < 0.05$ will be considered significant.

The qualitative data on the satisfaction levels of the development and application of the digital life storybook via telehealth and the perceived value of the digital life storybook will be analyzed thematically using the NVivo software (QSR International, Burlington, USA). The responses from the semi-structured interviews will be transcribed, and the coded data read and re-read and grouped according to emerging themes and reviewed. Each theme will be defined and named. The process will be counter-checked by members of the research team.

Discussion

The present study introduces an innovative online training protocol designed to empower caregivers in utilizing digital life storybooks for PLWD. This protocol adopts a participatory design approach in developing digital life storybooks via telehealth, aiming to explore their impact on communication skills and QoL for up to 2 months post-utilization. Additionally, it seeks to assess the satisfaction of both PLWD and their caregivers through qualitative interviews.

This approach builds upon the strengths of both telehealth and life storybooks, offering enhanced accessibility, flexibility and potential for personalized care. The protocol addresses key limitations of traditional training methods by enabling caregivers to access educational resources irrespective of geographical barriers and tailor their learning experience to their schedules.

Previous research has demonstrated that developing digital life storybooks via telehealth is as beneficial

as face-to-face sessions for PLWD and their caregivers.^{20,21} Similar findings were presented in the single case study by Asano and Hird¹⁰⁵ with online family participation. Telehealth-based development offers several advantages, including broader geographical reach, cost-effectiveness and time efficiency. Researchers showed that remotely delivered interventions involving caregivers of PLWD were both useful and effective.¹¹⁴ A systematic review¹¹⁵ of the use of technology in creating individualized, meaningful activities for PLWD also summarized that the use of technology in creating individualized, meaningful activities seems to be promising in terms of improving behavior and promoting relationships with others and that future studies should aim to build a more concrete evidence base by improving the methodological quality of research in the area. However, a standardized protocol for developing digital life storybooks via telehealth has been lacking.

This study introduces an online training program for creating digital life storybooks, building upon previous work in the field^{17,116} and aims to identify if online development/use of digital life storybooks through the proposed protocol will contribute to better use of technology for such services within PLWD and their caregivers. By providing a structured, accessible and user-friendly platform, this protocol has the potential to facilitate the effective implementation of digital life storybooks in various care settings.

Serving as a proof of concept, this study represents an initial step towards establishing the feasibility of developing life storybooks via telehealth. It lays the groundwork for gathering evidence to support this approach in future research and practice. The potential implications of this new protocol are far-reaching, providing a standardized framework for evaluating the impact of digital life storybooks on the wellbeing of PLWD and their caregivers. Moreover, widespread adoption of this protocol could contribute to a shift towards more person-centered care practices by equipping caregivers with tools to better understand and connect with the individuals they support.

From a theoretical perspective, this study contributes to our understanding of the mechanisms through which digital life storybooks can benefit individuals with dementia and their caregivers. It highlights the importance of capturing and honoring an individual's unique life experiences and the role that technology can play in facilitating this process. Future research could explore the potential for integrating online training programs with other therapeutic approaches, such as reminiscence therapy²⁹ or cognitive stimulation therapy.¹¹⁷

In terms of translational applications, the successful implementation of this protocol could have significant implications for dementia care delivery in both formal and informal care settings. The integration of these training programs into clinical practice may lead to more efficient and coordinated care delivery, fostering collaboration between formal and informal caregivers.

Limitations

It is important to acknowledge the limitations of this study, including technical challenges, access barriers, and the necessity for ongoing support and resources to ensure the successful integration of acquired knowledge into daily care routines. To address these limitations, the protocol incorporates user-friendly technology, simplified navigation and continuous reinforcement strategies.

Future studies should focus on addressing the identified limitations, such as technical barriers, personalization constraints and the practical application of acquired skills. Efforts should be made to develop user-friendly platforms, provide ongoing support and resources, and evaluate the efficacy of the intervention in diverse care settings. These endeavors will contribute to the refinement and broader applicability of digital life storybook interventions in dementia care.

Conclusions

This study introduces an innovative online training program for utilizing digital life storybooks in dementia care, offering a promising approach to enhance person-centered care and empower caregivers. The protocol demonstrates the potential for improving communication and relationship-building between caregivers and PLWD. Theoretically, this research advances our understanding of technology-mediated reminiscence by exploring how digital platforms can preserve and present autobiographical memories, contributing to the emerging field of digital gerontechnology. The implications are substantial, with the potential to revolutionize care delivery by enabling remote, personalized interventions. However, challenges remain, including the digital literacy of older caregivers and the technical infrastructure in nursing homes. Future research should address these limitations, perhaps by incorporating adaptive learning features to tailor the user interface to individual comfort levels with technology. Integration with complementary approaches, such as combining digital life storybooks with cognitive stimulation therapy, presents an exciting frontier for holistic dementia care. By refining this protocol through ongoing research and interdisciplinary collaboration, we can work towards a future where technology-enhanced, person-centered care becomes the standard, potentially reducing caregiver burden and improving QoL for PLWD. This study marks a significant step towards a future where technology-enhanced, person-centered care becomes the standard in dementia support and treatment.

ORCID iDs

Ponnusamy Subramaniam  <https://orcid.org/0000-0002-2361-4780>
Anthony Angwin  <https://orcid.org/0000-0003-4547-9433>
Shobha Sharma  <https://orcid.org/0000-0002-3396-7053>

References

- Prince M, Bryce R, Albanese E, Wimo A, Ribeiro W, Ferri CP. The global prevalence of dementia: A systematic review and metaanalysis. *Alzheimers Dement*. 2013;9(1):63. doi:10.1016/j.jalz.2012.11.007
- Livingston G, Sommerlad A, Orgeta V, et al. Dementia prevention, intervention, and care. *Lancet*. 2017;390(10113):2673–2734. doi:10.1016/S0140-6736(17)31363-6
- World Health Organization (WHO). Fact Sheets: Dementia. Geneva, Switzerland: World Health Organization (WHO); 2023. <https://www.who.int/news-room/fact-sheets/detail/dementia>. Accessed August 21, 2024.
- Wimo A, Guerchet M, Ali G, et al. The worldwide costs of dementia 2015 and comparisons with 2010. *Alzheimers Dement*. 2017;13(1):1–7. doi:10.1016/j.jalz.2016.07.150
- Nichols E, Szeoke CEI, Vollset SE, et al. Global, regional, and national burden of Alzheimer's disease and other dementias, 1990–2016: A systematic analysis for the Global Burden of Disease Study 2016. *Lancet Neurol*. 2019;18(1):88–106. doi:10.1016/S1474-4422(18)30403-4
- Alzheimer's Disease International (ADI). Dementia statistics. Lincolnshire, USA: Alzheimer's Disease International (ADI); 2023. <https://www.alzint.org/about/dementia-facts-figures/dementia-statistics/>. Accessed August 21, 2024.
- Gale SA, Acar D, Daffner KR. Dementia. *Am J Med*. 2018;131(10):1161–1169. doi:10.1016/j.amjmed.2018.01.022
- Arvanitakis Z, Shah RC, Bennett DA. Diagnosis and management of dementia: Review. *JAMA*. 2019;322(16):1589. doi:10.1001/jama.2019.4782
- Brodaty H, Donkin M. Family caregivers of people with dementia. *Dialogues Clin Neurosci*. 2009;11(2):217–228. doi:10.31887/DCNS.2009.11.2/hbrodaty
- Cheng ST. Dementia caregiver burden: A research update and critical analysis. *Curr Psychiatry Rep*. 2017;19(9):64. doi:10.1007/s11920-017-0818-2
- Rabinovici GD. Late-onset Alzheimer disease. *Continuum (Minneapolis)*. 2019;25(1):14–33. doi:10.1212/CON.0000000000000700
- Blackman C, Farber S, Feifer RA, Mor V, White EM. An illustration of SARS-CoV-2 dissemination within a skilled nursing facility using heat maps. *J Am Geriatr Soc*. 2020;68(10):2174–2178. doi:10.1111/jgs.16642
- Cummings JL, Tong G, Ballard C. Treatment combinations for Alzheimer's disease: Current and future pharmacotherapy options. *J Alzheimers Dis*. 2019;67(3):779–794. doi:10.3233/JAD-180766
- Olazarán J, Reisberg B, Clare L, et al. Nonpharmacological therapies in Alzheimer's disease: A systematic review of efficacy. *Dement Geriatr Cogn Disord*. 2010;30(2):161–178. doi:10.1159/000316119
- Clare L, Kudlicka A, Oyeboode JR, et al. Individual goal-oriented cognitive rehabilitation to improve everyday functioning for people with early-stage dementia: A multicentre randomised controlled trial (the GREAT trial). *Int J Geriatr Psychiatry*. 2019;34(5):709–721. doi:10.1002/gps.5076
- Shigihara Y, Hoshi H, Shinada K, Okada T, Kamada H. Non-pharmacological treatment changes brain activity in patients with dementia. *Sci Rep*. 2020;10(1):6744. doi:10.1038/s41598-020-63881-0
- Woods B, Subramaniam P. Digital life storybooks for people with dementia living in care homes: An evaluation. *Clin Interv Aging*. 2016;11:1263–1276. doi:10.2147/CIA.S111097
- Dyer SM, Harrison SL, Laver K, Whitehead C, Crotty M. An overview of systematic reviews of pharmacological and non-pharmacological interventions for the treatment of behavioral and psychological symptoms of dementia. *Int Psychogeriatr*. 2018;30(3):295–309. doi:10.1017/S1041610217002344
- Woods B, O'Philbin L, Farrell EM, Spector AE, Orrell M. Reminiscence therapy for dementia. *Cochrane Database Syst Rev*. 2018;3(3):CD001120. doi:10.1002/14651858.CD001120.pub3
- McDermott O, Charlesworth G, Hogervorst E, et al. Psychosocial interventions for people with dementia: A synthesis of systematic reviews. *Aging Ment Health*. 2019;23(4):393–403. doi:10.1080/13607863.2017.1423031
- Gridley K, Brooks J, Birks Y, Baxter K, Parker G. Improving care for people with dementia: Development and initial feasibility study for evaluation of life story work in dementia care. *Health Serv Deliv Res*. 2016;4(23):1–298. doi:10.3310/hsdr04230
- Gröndahl VA, Persenius M, Bååth C, Helgesen AK. The use of life stories and its influence on persons with dementia, their relatives and staff: A systematic mixed studies review. *BMC Nurs*. 2017;16(1):28. doi:10.1186/s12912-017-0223-5
- Elfrink TR, Zuidema SU, Kunz M, Westerhof GJ. Life story books for people with dementia: A systematic review. *Int Psychogeriatr*. 2018;30(12):1797–1811. doi:10.1017/S1041610218000376
- Doran C, Noonan M, Doody O. Life-story work in long-term care facilities for older people: An integrative review. *J Clin Nurs*. 2019;28(7–8):1070–1084. doi:10.1111/jocn.14718
- McIntosh L. Can the COVID-19 crisis strengthen our treatment escalation planning and resuscitation decision making? *Age Ageing*. 2020;49(4):525–525. doi:10.1093/ageing/afaa083
- Kindell J, Burrow S, Wilkinson R, David Keady J. Life story resources in dementia care: A review. *Qual Ageing Older Adults*. 2014;15(3):151–161. doi:10.1108/QAOA-02-2014-0003
- McKeown J, Ryan T, Ingleton C, Clarke A. 'You have to be mindful of whose story it is': The challenges of undertaking life story work with people with dementia and their family carers. *Dementia (London)*. 2015;14(2):238–256. doi:10.1177/1471301213495864
- Subramaniam P, Woods B. The impact of individual reminiscence therapy for people with dementia: Systematic review. *Exp Rev Neurother*. 2012;12(5):545–555. doi:10.1586/ern.12.35
- Subramaniam P, Woods B, Whitaker C. Life review and life story books for people with mild to moderate dementia: A randomised controlled trial. *Aging Ment Health*. 2014;18(3):363–375. doi:10.1080/13607863.2013.837144
- Massimi M, Berry E, Browne G, Smyth G, Watson P, Baecker RM. An exploratory case study of the impact of ambient biographical displays on identity in a patient with Alzheimer's disease. *Neuropsychol Rehabil*. 2008;18(5–6):742–765. doi:10.1080/09602010802130924
- Damianakis T, Tough A, Marziali E, Dawson DR. Therapy online: A web-based video support group for family caregivers of survivors with traumatic brain injury. *J Head Trauma Rehab*. 2016;31(4):E12–E20. doi:10.1097/HTR.0000000000000178
- Astell AJ, Smith SK, Potter S, Preston-Jones E. Computer interactive reminiscence and conversation aid groups: Delivering cognitive stimulation with technology. *Alzheimers Dement (N Y)*. 2018;4(1):481–487. doi:10.1016/j.trci.2018.08.003
- Astell AJ, Ellis MP, Bernardi L, et al. Using a touch screen computer to support relationships between people with dementia and caregivers. *Interacting with Computers*. 2010;22(4):267–275. doi:10.1016/j.intcom.2010.03.003
- Smith KL, Crete-Nishihata M, Damianakis T, Baecker RM, Marziali E. Multimedia biographies: A reminiscence and social stimulus tool for persons with cognitive impairment. *Journal of Technology in Human Services*. 2009;27(4):287–306. doi:10.1080/15228830903329831
- O'Rourke J, Tobin F, O'Callaghan S, Sowman R, Collins D. YouTube: A useful tool for reminiscence therapy in dementia? *Age Ageing*. 2011;40(6):742–744. doi:10.1093/ageing/afr100
- Kikhia B, Hallberg J, Bengtsson JE, Savenstedt S, Synnes K. Building digital life stories for memory support. *Int J Comput Healthcare*. 2010;1(2):161. doi:10.1504/IJCIH.2010.037460
- O'Donovan R, Kennedy N. "Four legs instead of two": Perspectives on a Nordic walking-based walking programme among people with arthritis. *Disabil Rehabil*. 2015;37(18):1635–1642. doi:10.3109/09638288.2014.972591
- Thoft DS, Møller AK, Møller AKK. Evaluating a digital life story app in a nursing home context: A qualitative study. *J Clin Nurs*. 2022;31(13–14):1884–1895. doi:10.1111/jocn.15714
- Sixsmith J, Sixsmith A, Callender M, Corr S. Wartime experiences and their implications for the everyday lives of older people. *Ageing Soc*. 2014;34(9):1457–1481. doi:10.1017/S0144686X13000214
- Cunningham S, Brill M, Whalley JH, et al. Assessing wellbeing in people living with dementia using reminiscence music with a mobile app (Memory Tracks): A mixed methods cohort study. *J Healthcare Eng*. 2019;2019:8924273. doi:10.1155/2019/8924273
- Moon S, Park K. The effect of digital reminiscence therapy on people with dementia: A pilot randomized controlled trial. *BMC Geriatr*. 2020;20(1):166. doi:10.1186/s12877-020-01563-2
- Ryan EB, Bannister KA, Anas AP. The dementia narrative: Writing to reclaim social identity. *J Aging Stud*. 2009;23(3):145–157. doi:10.1016/j.jaging.2007.12.018
- Thomas GEC, Crutch SJ, Camic PM. Measuring physiological responses to the arts in people with a dementia. *Int J Psychophysiol*. 2018;123:64–73. doi:10.1016/j.ijpsycho.2017.11.008

44. Fels DI, Astell AJ. Storytelling as a model of conversation for people with dementia and caregivers. *Am J Alzheimers Dis Other Dement.* 2011;26(7):535–541. doi:10.1177/1533317511429324
45. Coyle CE, Gleason SR, Mutchler JE. Spillover benefits and achieving sustainability of age-friendly communities. *Gerontologist.* 2022;62(1):29–35. doi:10.1093/geront/gnab060
46. Subramaniam P, Thillainathan P, Mat Ghani NA, Sharma S. Life Story Book to enhance communication in persons with dementia: A systematic review of reviews. *PLoS One.* 2023;18(10):e0291620. doi:10.1371/journal.pone.0291620
47. Arbel R, Heimler B, Amedi A. The sound of reading: Color-to-timbre substitution boosts reading performance via OVAL, a novel auditory orthography optimized for visual-to-auditory mapping. *PLoS One.* 2020;15(11):e0242619. doi:10.1371/journal.pone.0242619
48. Quinn C, Nelis SM, Martyr A, Morris RG, Victor C, Clare L. Caregiver influences on 'living well' for people with dementia: Findings from the IDEAL study. *Aging Ment Health.* 2020;24(9):1505–1513. doi:10.1080/13607863.2019.1602590
49. Stenhouse R, Tait J, Hardy P, Sumner T. Dangling conversations: Reflections on the process of creating digital stories during a workshop with people with early-stage dementia. *J Psychiatr Ment Health Nurs.* 2013;20(2):134–141. doi:10.1111/j.1365-2850.2012.01900.x
50. Hughes M, Hanna K, Wiles A, Taylor E, Giebel C. The experiences of caring for someone with dementia and a learning disability: A qualitative systematic review. *Dementia (London).* 2024;23(5):817–849. doi:10.1177/14713012231225797
51. Benbow SM, Kingston P. 'Talking about my experiences... at times disturbing yet positive': Producing narratives with people living with dementia. *Dementia (London).* 2016;15(5):1034–1052. doi:10.1177/1471301214551845
52. Kirk D, Kabdebo I, Whitehead L. Prevalence of distress, its associated factors and referral to support services in people with cancer. *J Clin Nurs.* 2021;30(19–20):2873–2885. doi:10.1111/jocn.15794
53. Hamel AV, Sims TL, Klassen D, Havey T, Gaugler JE. Memory matters: A mixed-methods feasibility study of a mobile aid to stimulate reminiscence in individuals with memory loss. *J Gerontol Nurs.* 2016;42(7):15–24. doi:10.3928/00989134-20160201-04
54. Doraiswamy S, Jithesh A, Mamtani R, Abraham A, Cheema S. Telehealth use in geriatrics care during the COVID-19 pandemic: A scoping review and evidence synthesis. *Int J Environ Res Public Health.* 2021;18(4):1755. doi:10.3390/ijerph18041755
55. Monaghesh E, Hajizadeh A. The role of telehealth during COVID-19 outbreak: A systematic review based on current evidence. *BMC Public Health.* 2020;20(1):1193. doi:10.1186/s12889-020-09301-4
56. Steinman MA, Perry L, Perissinotto CM. Meeting the care needs of older adults isolated at home during the COVID-19 pandemic. *JAMA Intern Med.* 2020;180(6):819. doi:10.1001/jamainternmed.2020.1661
57. Cheung G, Peri K. Challenges to dementia care during COVID-19: Innovations in remote delivery of group cognitive stimulation therapy. *Aging Ment Health.* 2021;25(6):977–979. doi:10.1080/13607863.2020.1789945
58. Capozzo R, Zoccollella S, Musio M, Barone R, Accogli M, Logroscino G. Telemedicine is a useful tool to deliver care to patients with amyotrophic lateral sclerosis during COVID-19 pandemic: Results from Southern Italy. *Amyotroph Lateral Scler Frontotemporal Degener.* 2020;21(7–8):542–548. doi:10.1080/21678421.2020.1773502
59. Chu IYH, Alam P, Larson HJ, Lin L. Social consequences of mass quarantine during epidemics: A systematic review with implications for the COVID-19 response. *J Travel Med.* 2020;27(7):taaa192. doi:10.1093/jtm/taaa192
60. Goodman-Casanova JM, Dura-Perez E, Guzman-Parra J, Cuesta-Vargas A, Mayoral-Cleries F. Telehealth home support during COVID-19 confinement for community-dwelling older adults with mild cognitive impairment or mild dementia: Survey study. *J Med Internet Res.* 2020;22(5):e19434. doi:10.2196/19434
61. Cuffaro L, Di Lorenzo F, Bonavita S, Tedeschi G, Leocani L, Lavorgna L. Dementia care and COVID-19 pandemic: A necessary digital revolution. *Neurol Sci.* 2020;41(8):1977–1979. doi:10.1007/s10072-020-04512-4
62. Edelman LS, McConnell ES, Kennerly SM, Alderden J, Horn SD, Yap TL. Mitigating the effects of a pandemic: Facilitating improved nursing home care delivery through technology. *JMIR Aging.* 2020;3(1):e20110. doi:10.2196/20110
63. Lam K, Lu AD, Shi Y, Covinsky KE. Assessing telemedicine unreadiness among older adults in the United States during the COVID-19 pandemic. *JAMA Intern Med.* 2020;180(10):1389. doi:10.1001/jamainternmed.2020.2671
64. Kichloo A, Albosta M, Dettloff K, et al. Telemedicine, the current COVID-19 pandemic and the future: A narrative review and perspectives moving forward in the USA. *Fam Med Com Health.* 2020;8(3):e000530. doi:10.1136/fmch-2020-000530
65. Perrin PB, Rybarczyk BD, Pierce BS, Jones HA, Shaffer C, Islam L. Rapid telepsychology deployment during the COVID-19 pandemic: A special issue commentary and lessons from primary care psychology training. *J Clin Psychol.* 2020;76(6):1173–1185. doi:10.1002/jclp.22969
66. Gogia SB, Maeder A, Mars M, Hartvigsen G, Basu A, Abbott P. Unintended consequences of tele health and their possible solutions: Contribution of the IMIA Working Group on Telehealth. *Yearb Med Inform.* 2016;25(1):41–46. doi:10.15265/IY-2016-012
67. Calton B, Abedini N, Fratkin M. Telemedicine in the time of coronavirus. *J Pain Symptom Manage.* 2020;60(1):e12–e14. doi:10.1016/j.jpainsymman.2020.03.019
68. Wootton R. The importance of telemedicine for developing countries. In: Wootton R, Patil NG, Patil NG, Scott RE, eds. *Telehealth in the Developing World.* 2nd ed. Boca Raton, USA: CRC Press; 2016:7–22. ISBN:978-1-85315-784-4.
69. Bajowala SS, Milosch J, Bansal C. Telemedicine pays: Billing and coding update. *Curr Allergy Asthma Rep.* 2020;20(10):60. doi:10.1007/s11882-020-00956-y
70. Costanzo MC, Arcidiacono C, Rodolico A, Panebianco M, Aguglia E, Signorelli MS. Diagnostic and interventional implications of telemedicine in Alzheimer's disease and mild cognitive impairment: A literature review. *Int J Geriatr Psychiatry.* 2020;35(1):12–28. doi:10.1002/gps.5219
71. Sekhon H, Sekhon K, Launay C, et al. Telemedicine and the rural dementia population: A systematic review. *Maturitas.* 2021;143:105–114. doi:10.1016/j.maturitas.2020.09.001
72. Sharma S, Ward EC, Burns C, Theodoros D, Russell T. Assessing dysphagia via telerehabilitation: Patient perceptions and satisfaction. *Int J Speech Lang Pathol.* 2013;15(2):176–183. doi:10.3109/17549507.2012.689333
73. Gately ME, Trudeau SA, Moo LR. In-home video telehealth for dementia management: Implications for rehabilitation. *Curr Geriatr Rep.* 2019;8(3):239–249. doi:10.1007/s13670-019-00297-3
74. Kruse C, Fohn J, Wilson N, Nunez Patlan E, Zipp S, Mileski M. Utilization barriers and medical outcomes commensurate with the use of telehealth among older adults: Systematic review. *JMIR Med Inform.* 2020;8(8):e20359. doi:10.2196/20359
75. Bashshur R, Doarn CR, Frenk JM, Kvedar JC, Woolliscroft JO. Telemedicine and the COVID-19 pandemic: Lessons for the future. *Telemed J E Health.* 2020;26(5):571–573. doi:10.1089/tmj.2020.29040.rb
76. Hollander JE, Carr BG. Virtually perfect? Telemedicine for Covid-19. *N Engl J Med.* 2020;382(18):1679–1681. doi:10.1056/NEJMp2003539
77. Laver KE, Crotty M, Low LF, et al. Rehabilitation for people with dementia: A multi-method study examining knowledge and attitudes. *BMC Geriatr.* 2020;20(1):531. doi:10.1186/s12877-020-01940-x
78. Kim H, Jho JH, Jang JW. The effect of telemedicine on cognitive decline in patients with dementia. *J Telemed Telecare.* 2017;23(1):149–154. doi:10.1177/1357633X15615049
79. Barton C, Morris R, Rothlind J, Yaffe K. Video-telemedicine in a memory disorders clinic: Evaluation and management of rural elders with cognitive impairment. *Telemed J E Health.* 2011;17(10):789–793. doi:10.1089/tmj.2011.0083
80. Cotelli M, Manenti R, Brambilla M, et al. Cognitive telerehabilitation in mild cognitive impairment, Alzheimer's disease and frontotemporal dementia: A systematic review. *J Telemed Telecare.* 2019;25(2):67–79. doi:10.1177/1357633X17740390
81. Broda A, Bieber A, Meyer G, et al; ActiCare Consortium. Perspectives of policy and political decision makers on access to formal dementia care: Expert interviews in eight European countries. *BMC Health Serv Res.* 2017;17(1):518. doi:10.1186/s12913-017-2456-0
82. Owens AP, Ballard C, Beigi M, et al. Implementing remote memory clinics to enhance clinical care during and after COVID-19. *Front Psychiatry.* 2020;11:579934. doi:10.3389/fpsy.2020.579934

83. Dequanter S, Gagnon MP, Ndiaye MA, et al. The effectiveness of e-health solutions for aging with cognitive impairment: A systematic review. *Gerontologist*. 2021;61(7):e373–e394. doi:10.1093/geront/gnaa065
84. Geddes MR, O'Connell ME, Fisk JD, et al. Remote cognitive and behavioral assessment: Report of the Alzheimer Society of Canada Task Force on dementia care best practices for COVID-19. *Alzheimers Dement*. 2020;12(1):e12111. doi:10.1002/dad2.12111
85. Isernia S, Cabinio M, Di Tella S, et al. Diagnostic validity of the smart aging serious game: An innovative tool for digital phenotyping of mild neurocognitive disorder. *J Alzheimers Dis*. 2021;83(4):1789–1801. doi:10.3233/JAD-210347
86. Saragih ID, Tonapa SI, Porta CM, Lee B. Effects of telehealth intervention for people with dementia and their carers: A systematic review and meta-analysis of randomized controlled studies. *J Nurs Scholarsh*. 2022;54(6):704–719. doi:10.1111/jnu.12797
87. Cheong CK, Lim KH, Jang JW, Jhoo JH. The effect of telemedicine on the duration of treatment in dementia patients. *J Telemed Telecare*. 2015;21(4):214–218. doi:10.1177/1357633X14566571
88. Lai FHY, Yan EWH, Yu KKY, Tsui WS, Chan DTH, Yee BK. The protective impact of telemedicine on persons with dementia and their caregivers during the COVID-19 pandemic. *Am J Geriatr Psychiatry*. 2020;28(11):1175–1184. doi:10.1016/j.jagp.2020.07.019
89. Toniolo S, Scarioni M, Di Lorenzo F, et al; Management Group of the EAN Dementia and Cognitive Disorders Scientific Panel. Dementia and COVID-19, a bidirectional liaison: Risk factors, biomarkers, and optimal health care. *J Alzheimers Dis*. 2021;82(3):883–898. doi:10.3233/JAD-210335
90. Loi SM, Cations M, Velakoulis D. Young-onset dementia diagnosis, management and care: A narrative review. *Med J Aust*. 2023;218(4):182–189. doi:10.5694/mja2.51849
91. Critten V, Kucirkova N. 'It brings it all back, all those good times; it makes me go close to tears': Creating digital personalised stories with people who have dementia. *Dementia (London)*. 2019;18(3):864–881. doi:10.1177/1471301217691162
92. Melunsky N, Crellin N, Dudzinski E, et al. The experience of family carers attending a joint reminiscence group with people with dementia: A thematic analysis. *Dementia (London)*. 2015;14(6):842–859. doi:10.1177/1471301213516332
93. Ballard C, Corbett A, Orrell M, et al. Impact of person-centred care training and person-centred activities on quality of life, agitation, and antipsychotic use in people with dementia living in nursing homes: A cluster-randomised controlled trial. *PLoS Med*. 2018;15(2):e1002500. doi:10.1371/journal.pmed.1002500
94. Jennings AA, Foley T, McHugh S, Browne JP, Bradley CP. 'Working away in that grey area...' A qualitative exploration of the challenges general practitioners experience when managing behavioural and psychological symptoms of dementia. *Age Ageing*. 2018;47(2):295–303. doi:10.1093/ageing/afx175
95. Scharlach AE. Aging in context: Individual and environmental pathways to aging-friendly communities. The 2015 Matthew A. Pollack Award Lecture. *Gerontologist*. 2017;57(4):606–618. doi:10.1093/geront/gnx017
96. Ahmad S, Jones D. Investigating the mining heritage significance for Kinta District, the industrial heritage legacy of Malaysia. *Procedia Soc Behav Sci*. 2013;105:445–457. doi:10.1016/j.sbspro.2013.11.047
97. Ingersoll-Dayton B, Spencer B, Kwak M, Scherrer K, Allen RS, Campbell R. The couples life story approach: A dyadic intervention for dementia. *J Gerontol Soc Work*. 2013;56(3):237–254. doi:10.1080/01634372.2012.758214
98. Elfrink TR, Ullrich C, Kunz M, Zuidema SU, Westerhof GJ. The Online Life Story Book: A randomized controlled trial on the effects of a digital reminiscence intervention for people with (very) mild dementia and their informal caregivers. *PLoS One*. 2021;16(9):e0256251. doi:10.1371/journal.pone.0256251
99. O'Connell ME, Crossley M, Cammer A, et al. Development and evaluation of a telehealth videoconferenced support group for rural spouses of individuals diagnosed with atypical early-onset dementias. *Dementia (London)*. 2014;13(3):382–395. doi:10.1177/147130121474143
100. Morcos R, Lazar I, Kucharik M, et al. The healthy, aging, and diseased kidney: Relationship with cardiovascular disease. *J Am Geriatr Soc*. 2021;69(2):539–546. doi:10.1111/jgs.16866
101. Shalaby R, Hrabok M, Spurvey P, et al. Recovery following peer and text messaging support after discharge from acute psychiatric care in Edmonton, Alberta: Controlled observational study. *JMIR Form Res*. 2021;5(9):e27137. doi:10.2196/27137
102. Rathnayake S, Moyle W, Jones C, Calleja P. mHealth applications as an educational and supportive resource for family carers of people with dementia: An integrative review. *Dementia (London)*. 2019;18(7–8):3091–3112. doi:10.1177/1471301218768903
103. Ploeg J, Ali MU, Markle-Reid M, et al. Caregiver-focused, web-based interventions: Systematic review and meta-analysis (part 2). *J Med Internet Res*. 2018;20(10):e11247. doi:10.2196/11247
104. O'Connor CM, Clemson L, Brodaty H, et al. The tailored activity program (TAP) to address behavioral disturbances in frontotemporal dementia: A feasibility and pilot study. *Disabil Rehabil*. 2019;41(3):299–310. doi:10.1080/09638288.2017.1387614
105. Asano T, Hird N. A pilot study of remote use of a life storybook intervention involving family members of persons with dementia. *Juniper Online J Case Studies*. 2023;14(1):555877. doi:10.19080/JOJCS.2023.14.555877
106. Faul F, Erdfelder E, Lang AG, Buchner A. G*Power 3: A flexible statistical power analysis program for the social, behavioral, and biomedical sciences. *Behav Res Methods*. 2007;39(2):175–191. doi:10.3758/BF03193146
107. Hughes CP, Berg L, Danziger W, Coben LA, Martin RL. A new clinical scale for the staging of dementia. *Br J Psychiatry*. 1982;140(6):566–572. doi:10.1192/bjp.140.6.566
108. Folstein MF, Folstein SE, McHugh PR. Mini-Mental State. *J Psychiatr Res*. 1975;12(3):189–198. doi:10.1016/0022-3956(75)90026-6
109. Yesavage JA, Brink TL, Rose TL, et al. Development and validation of a geriatric depression screening scale: A preliminary report. *J Psychiatr Res*. 1982;17(1):37–49. doi:10.1016/0022-3956(82)90033-4
110. Øra HP, Kirmess M, Brady MC, Sørli H, Becker F. Technical features, feasibility, and acceptability of augmented telerehabilitation in post-stroke aphasia: Experiences from a randomized controlled trial. *Front Neurol*. 2020;11:671. doi:10.3389/fneur.2020.00671
111. Strøm BS, Ytrehus S, Grov E. Sensory stimulation for persons with dementia: A review of the literature. *J Clin Nurs*. 2016;25(13–14):1805–1834. doi:10.1111/jocn.13169
112. Logsdon RG, Gibbons LE, McCurry SM, Teri L. Assessing quality of life in older adults with cognitive impairment. *Psychosom Med*. 2002;64(3):510–519. doi:10.1097/00006842-200205000-00016
113. Spruytte N, Van Audenhove C, Lammertyn F, Storms G. The quality of the caregiving relationship in informal care for older adults with dementia and chronic psychiatric patients. *Psychol Psychother*. 2002;75(3):295–311. doi:10.1348/147608302320365208
114. Gough N, Brkan L, Subramaniam P, et al. Feasibility of remotely supervised transcranial direct current stimulation and cognitive remediation: A systematic review. *PLoS One*. 2020;15(2):e0223029. doi:10.1371/journal.pone.0223029
115. Goodall G, Taraldsen K, Serrano JA. The use of technology in creating individualized, meaningful activities for people living with dementia: A systematic review. *Dementia (London)*. 2021;20(4):1442–1469. doi:10.1177/1471301220928168
116. Sweeney L, Wolverson E, Clarke C. Understanding the shared experiences of creating a digital life story with individuals with dementia and their spouse. *Dementia (London)*. 2021;20(5):1791–1813. doi:10.1177/1471301220970403
117. Toh HM, Ghazali SE, Subramaniam P. The acceptability and usefulness of cognitive stimulation therapy for older adults with dementia: A narrative review. *Int J Alzheimers Dis*. 2016;2016:5131570. doi:10.1155/2016/5131570

Microbial metabolomics in acute myeloid leukemia: From pathogenesis to treatment

Aneta Nowicka^{A–F}, Lidia Gil^{E,F}

Department of Hematology and Bone Marrow Transplantation, Poznan University of Medical Sciences, Poland

A – research concept and design; B – collection and/or assembly of data; C – data analysis and interpretation;

D – writing the article; E – critical revision of the article; F – final approval of the article

Advances in Clinical and Experimental Medicine, ISSN 1899–5276 (print), ISSN 2451–2680 (online)

Adv Clin Exp Med. 2025;34(7):1201–1212

Address for correspondence

Aneta Nowicka

E-mail: 69644@student.ump.edu.pl

Funding sources

None declared

Conflict of interest

None declared

Received on April 26, 2024

Reviewed on July 3, 2024

Accepted on July 24, 2024

Published online on October 21, 2024

Abstract

Acute myeloid leukemia (AML), the most common leukemia in adults, is a biologically heterogeneous disease arising from clonally proliferating hematopoietic stem cells. Increased appreciation of novel genetic methods has improved the understanding of AML biology. Recently, the emerging field of metabolomics has indicated qualitative and quantitative alterations in metabolic profiles in AML pathogenesis, progression and treatment. Multiple metabolic and molecular pathways regulate human metabolism and host–microbiome interactions may significantly affect this biochemical machinery. Microbiota have been found to play a significant role in hematopoietic function, metabolism and immunity, contributing to AML occurrence. A large number of studies have highlighted the importance of the composition and diversity of the gut microbiota (GM) in response to treatment and prognosis in AML. Moreover, strong evidence emphasizes the detrimental link between dysbiosis and infectious complications, a leading cause of morbidity and mortality for patients with AML. Several microbiota-related mechanisms have been linked to particular changes in host physiology so far, and microbial-derived metabolites belong to one of the most important. Circulating in the body, they modulate human conditions both locally and systemically. The extensive and diverse repertoire of bacterial metabolic functions plays a critical role in numerous processes, including leukemogenesis. Integrative analysis of microbiome and metabolome data is a promising avenue for better understanding the complex relationship between the microbiota, biochemical alterations and AML pathogenesis to effectively prevent, treat and mitigate its outcomes. This review concentrates on the pathologic roles and therapeutic implications of microbe-derived metabolites in AML settings.

Key words: microbiome, gut microbiota, short-chain fatty acids, microbial metabolites, AML treatment

Cite as

Nowicka A, Gil L. Microbial metabolomics in acute myeloid leukemia: From pathogenesis to treatment. *Adv Clin Exp Med.* 2025;34(7):1201–1212. doi:10.17219/acem/191559

DOI

10.17219/acem/191559

Copyright

Copyright by Author(s)

This is an article distributed under the terms of the Creative Commons Attribution 3.0 Unported (CC BY 3.0) (<https://creativecommons.org/licenses/by/3.0/>)

Introduction

Acute myeloid leukemia (AML) is one of the most heterogeneous hematological diseases arising from clonally proliferating hematopoietic stem cells. The development of novel genetic methods has improved our understanding of AML biology. Besides genetic and epigenetic alterations, an increasing amount of data has indicated that there is a relationship between the human microbiome and the pathogenesis of AML. A large number of studies have also highlighted the potential link between the composition of the gut microbiota (GM) and response to treatment, prognosis and infectious complications, a leading cause of morbidity and mortality for patients with AML. Recently, the emerging field of metabolomics has explained multiple metabolic and molecular pathways regulating human metabolism and host–microbiome interactions that may significantly contribute to AML outcomes. Circulating in the body, microbial-derived metabolites modulate human conditions, both locally and systemically. Integrative analysis of microbiome and metabolome data is a promising avenue for better understanding the complex relationship between the microbiota, biochemical alterations and the course of AML.

In this overview, we focused on microbial metabolite-mediated interactions between the host and the microbiota and the potential mechanisms by which these metabolites exert their impacts in the context of AML. To reveal the clinical and therapeutic significance of microbial metabolomics, we reviewed previous translational research in this setting. Our findings provide a strong foundation for diagnostic and therapeutic applications of its microbiota–host interaction. Targeting specific individual microbiome-related features, including a wide variety of small compounds, emerges as the next opportunity for interventions.

Acute myeloid leukemia

Acute myeloid leukemia is a clonal disorder characterized by the presence of immature blasts and arrested differentiation of malignant myeloid blasts in the bone marrow. Recent advancements in sequencing technology and the development of analytical tools have provided a comprehensive understanding of its biology, prognosis and treatment. Leukemogenesis is broadly dependent on genetic and epigenetic alterations that lead to dysregulated gene expression and function, but there are also hematopoietic and non-hematopoietic stromal components of the leukemic microenvironment that interact with pre-leukemic and leukemic clones to promote their survival, self-renewal and resistance to therapy. Recently, an increasing amount of data has indicated various previously unknown underlying mechanisms. Among them, exploration of the human microbiota and microbial metabolites holds immense potential to further

characterize AML biology. The relationship between the human microbiome and the pathogenesis of AML is not completely understood. Microbiota-induced dysregulated metabolic pathways may be implicated in leukemogenesis and the maintenance of leukemic blasts.

Identifying a whole spectrum of molecular events has led to the recent U.S. Food and Drug Administration (FDA) approval of several targeted therapies for improving the care of patients with AML. Currently, 60–70% of adult AML patients achieve complete remission after initial induction chemotherapy, and more than 25% of adults with AML are expected to survive 3 or more years and may be cured.¹ However, relapsed disease and treatment-related complications, mainly infections, are the most common causes of death. Following the concepts of personalized medicine, targeting the microbiota in a metabolite-dependent manner offers a novel adjuvant treatment approach that can improve treatment outcomes.

Microbiome

Microbiota is a diverse consortium of microorganisms that inhabit a defined environment. Along with its genomes, structural components, metabolites, and environmental factors, which are referred to as the microbiome, the microbial community residing in humans plays a critical role in host physiology.² The GM is considered the most significant microbiota in maintaining our health, but a variety of microorganisms are also localized in other regions, including the oral cavity, lungs, vagina, and skin. The microbial communities are in symbiosis with the host, contributing to the maintenance of tissue homeostasis, the integrity of mucosal epithelial barriers, immune system development, tolerance and response, protection of pathogen resistance, and modulation of inflammation. The human GM has crucial functions to digest foods and uptake nutrients.

Reduced diversity and altered composition of the microbiota, named dysbiosis, may directly cause disease or merely reflect disease-induced changes in the host immune and metabolic systems. Several established examples of changes in the GM have been associated with cardiovascular, neurological, metabolic, and inflammatory diseases, as well as all stages of cancer, including initiation, progression, treatment outcomes, and adverse reactions. In recent years, increasing evidence has confirmed the effect of the GM on pathological changes in hematological malignancies. Previous studies have revealed the remarkable reduction of GM diversity in AML patients, with significant differences in relative abundances of exact taxa in comparison to healthy controls.

The composition of the GM, as well as its dynamic changes, are individual for each person and are influenced by heredity, environment, lifestyle, and other factors. In the unique clinical scenario of AML patients, several factors, including prolonged hospitalization, multiple

Table 1. Examples of microbiota-derived metabolites and their functions in the host organism

Groups	Metabolites	Microbial agent	Functions	References
Short-chain fatty acids	acetate, propionate, butyrate, valerate, isobutyrate, isovalerate, 2-methylpropionate, hexanoate	Bacteroidetes (<i>Bacteroides</i> sp., <i>Prevotella</i>), Firmicutes (<i>Staphylococcus aureus</i> , <i>Coprococcus</i> , <i>Clostridium</i> , <i>Roseburia</i> , <i>Faecalibacterium</i> , <i>Eubacterium</i> , <i>Blautia</i>), Proteobacteria (<i>Campylobacter jejuni</i>), Actinobacteria (<i>Bifidobacterium</i> sp.), Verrucomicrobia (<i>Akkermansia muciniphila</i>)	host metabolic pathway regulation; inflammatory response regulation; local and systemic immunomodulation; maintenance of energy homeostasis; gut hormone production; microbiota composition regulation; defence against pathogens; maintenance of gut barrier integrity; intestinal permeability regulation; anticancer activity	3–9
Tryptophan and indole derivatives	indole, indole-3-propionic acid, 5-hydroxyl indole, indoxyl sulfate, N-acetyltryptophan, indoxyl sulfate, serotonin, melatonin, melatonin 6-sulfate	Firmicutes (<i>Lactobacillus</i> spp., <i>Clostridium</i>), Actinobacteria (<i>Bifidobacterium</i>), Bacteroidetes (<i>Bacteroides</i>), Proteobacteria (<i>Escherichia coli</i> , <i>Shigella</i>)	host metabolic pathway regulation; inflammatory response regulation; local and systemic immunomodulation; antioxidative functions; neuroprotection and cytoprotection; intestinal barrier regulation	10–12
Bile acid metabolites	cholic acid, deoxycholic acid, chenodeoxycholic acid, taurocholic acid, lithocholic acid, glycocholic acid, ursodeoxycholic acid	Actinobacteria (<i>Bifidobacterium</i>), Bacteroidetes (<i>Bacteroides</i>), Firmicutes (<i>Clostridium</i> , <i>Lactobacillus</i>), Proteobacteria (<i>Enterobacter</i>)	host metabolic pathway regulation; antimicrobial effects; intestinal barrier regulation	13,14
Choline metabolites	TMA, methylamine, dimethylglycine, dimethylamine	Firmicutes (<i>Faecalibacterium prausnitzii</i>), Proteobacteria, Actinobacteria (<i>Bifidobacterium</i>), Bacteroidetes (<i>Prevotella</i>), Fusobacteria (<i>Fusobacterium</i>)	pro-inflammatory response promotion; mitochondrial dysfunction exacerbation; cell membrane function regulations; neurotransmission; lipid metabolism and biosynthesis regulation	15
Vitamins	vitamin B2, vitamin B3, vitamin B5, vitamin B6, vitamin B9, vitamin B12, vitamin K	Actinobacteria (<i>Bifidobacterium</i>), Firmicutes (<i>S. aureus</i> , <i>Listeria. monocytogenes</i> , lactic acid bacteria, <i>Salmonella typhimurium</i>)	cellular metabolism regulation; immunomodulation; antimicrobial effects; DNA replication, methylation and repair	16

antibiotic administrations, gastrointestinal mucosal damage, and severe immune system and nutrition impairments, cause disruptions of the GM to a level rarely seen in other clinical conditions.

Recently, host–microbiome interactions via microbial metabolites have become a great area of interest in terms of the defining underlying mechanisms that connect the microbiota with particular changes in host physiology. The complete set of small molecules, including intermediate or end products of bacterial metabolism, termed the metabolome, is suspected to be a strong contributor to our health via constant inter-organ interactions. When the gut barrier is compromised, tissues and organs may be flooded with molecules from the diet and microbiota that negatively or positively impact the host immune system and metabolism. On the other hand, the feedback loop can modulate the micro-ecological balance.

Undigested foods reach the colon and serve as substrates for bacterial metabolism. Carbohydrates, proteins and fats, the major macronutrients, provide different microbiota-accessible nutrients to generate the synthesis of vitamins, short-chain fatty acids (SCFAs), essential amino acids, and secondary metabolites. Indigestible dietary carbohydrates select fiber-degrading, SCFA-producing bacteria, which are considered to be beneficial under normal conditions. Undigested proteins promote the growth of proteolytic bacteria connected with SCFAs, branched-chain fatty acids

and some toxic metabolites, including ammonia and hydrogen sulfide. Conjugated fatty acids are the main source of fat for bacterial metabolism. Overgrowth of acid-tolerant bacteria produces toxic compounds like hydrogen sulfide. Detailed and mechanistic knowledge about microbiome–host signaling pathways in AML is limited, even though progress has been made recently.

To date, most studies investigating a potential link between the fecal microbiome and AML have focused on microbiota-derived SCFAs, such as acetate, propionate and butyrate. In particular, a reduction in fecal SCFA concentrations has been observed, while investigation of SCFA levels in serum or plasma has led to more conflicting results. An increasing body of evidence now points to a potential role of different microbiome-derived components, such as lipopolysaccharides derived from bacterial cell walls, tryptophan-related metabolites, choline metabolites, secondary bile acids, and others, in the modulation of AML course (Table 1).^{3–16}

Metabolomics

Metabolomics is a branch of “omics” sciences that aims to identify small molecules in a given sample, such as body fluids or tissues, for in situ analysis of metabolic changes. When combined with genetic, protein expression and

analytical tools, this approach is a powerful tool for characterizing the enzymatic and metabolic activity of cellular pathways.¹⁷ The overarching goal of metabolomics is to assess these metabolites quantitatively and qualitatively for their diagnostic, therapeutic and prognostic potentials.

Due to the highly heterogeneous and dynamic nature of the metabolome, its characterization in the framework of different host–microbiome interactions is challenging. Bacterial metabolomes are thought to be composed of a few thousand metabolites, including more conserved products of core metabolism and energy production (nucleotides, amino acids, tricarboxylic acid cycle intermediates, glycolysis, and the pentose phosphate pathway) and arising from secondary metabolism.^{17,18} Currently, research uses an untargeted approach to identify all small molecules, which requires complex methodological and analyzing protocols. To capture metabolites of interest, targeted metabolomics offers more straightforward tools.¹⁹

The metabolome has been extensively investigated to identify characteristic signatures in many diseases. Specific metabolic profiles have also been associated with the different stages of AML patient management.^{20–22} Uncontrolled growth and proliferation of neoplastic cells result in a wide spectrum of metabolic disturbances reflected in leukemic cell metabolism directly (single cell metabolomics) but also in the bone microenvironment, blood and other biological specimens. In AML settings, there is a wealth of literature concerning metabolic alterations in the context of oncogenic mutations and epigenetic modifications.²³ However, the complexity of AML's issues, from diagnosis to completion, is influenced by more sophisticated interactions at different levels. The metabolic activities of the GM form an essential part of this machinery. Recent studies have focused mainly on fecal metabolites; therefore, a large-scale analysis of the relationship between microbes and the metabolic profiles of various tissues in an organism needs to be developed to provide consistent and comprehensive characterization of AML metabolic disturbances.

Does the microbiome drive AML?

Along with genetic and environmental factors, microorganisms have been reported as the next leading carcinogens, responsible for approx. 20% of human neoplasms.²⁴ The existence of selected microorganisms can modulate tumorigenesis via numerous mechanisms. At distant locations in the body, these effects are determined by the circulation of microbiota-dependent activated or suppressed immune cells, cytokines and metabolites. These last can play a critical role as cancer promoters or inhibitors. The oncogenic mechanisms of these complex connections have not yet been fully clarified.

Directly, microbiomes can produce toxic or carcinogenic compounds that modify cellular processes and initiate

signaling actions to control cell growth. Some products of bacterial metabolism, such as microbial catabolism of dietary proteins, polyamines, xenobiotics, or aromatic amino acids, can induce tumor expansion through oxidative stress and DNA instability.^{25–27} Indirectly, they are involved in the development and regulation of the immune system, a basic anti-tumor tool in the human body. There is evidence in favor of the role of the microbiota in the development and regulation of B lymphocytes, T helper lymphocytes and tolerogenic dendritic cells. Both commensal bacteria and their metabolites, such as butyric acid, are necessary for the development of regulatory T cells.^{28,29}

A growing body of research has applied metabolomics techniques to identify metabolites from different sample sources associated with AML pathogenesis. However, there is a lack of data on mechanistic insight into metabolite-induced changes in specific pathways. Among the most extensively studied, microbial-originated butyrate plays a multilevel role in AML pathogenesis and outcomes. Specifically, it activates suppressive regulatory T cells, reduces the proinflammatory pathway of NF- κ B, stimulates G-protein-coupled receptors 41 and 43, influences gene expression in cell growth and death at the epigenetic level, and aids in the barrier function of the epithelium, increasing the number of formations of tight junction proteins through the modulation of AMP-activated protein kinase.^{30–33} Propionate, another SCFA, can promote ferroptosis and apoptosis through mitophagy and ferroptosis mediated through acyl-CoA synthetase long-chain family member 4. This elicits anti-leukemia immunity in AML. Recent results showed that decreased levels of propionate in the feces of AML patients correlated with GM dysbiosis. Propionate suppressed AML progression both in vivo and in vitro. Acyl-CoA synthetase long-chain family member 4-induced ferroptosis increased the immunogenicity of AML cells, induced the release of damage-associated molecular patterns, and promoted dendritic cell maturation.³⁴

Currently, using a variety of statistical tools or advanced computational methods, studies are focused on the generation of paired metagenomic and metabolomic features from the AML cohort to determine potential diagnostic profiles correlated with leukemia onset, progression and relapse. In a comprehensive study, Wang et al. explained the role of microbiomes in AML progression in a metabolite-dependent manner. Antibiotic treatment-induced dysbiosis, a decrease in butyrate produced by the GM (especially *Faecalibacterium*), and the increased leakage of lipopolysaccharides through the damaged intestinal barrier into the blood accelerate AML progression.³⁵ As single-type samples may not fully reflect overall changes in organismal metabolism, Wu et al. investigated the differences in the metabolome of human blood and mice serum, liver and feces under conditions of AML. Significant differences in the serum and fecal metabolomes between the AML group and control group of mice successfully distinguished 2 different

profiles. Metabolic changes associated with AML primarily affect amino acid and glucose metabolism. Through cross-species validation, the study discovered the potential involvement of the carnosine–histidine metabolic pathway in the development and progression of AML. Analysis of the GM showed a significant negative correlation between the key metabolite carnosine and *Peptococcaceae* and *Campylobacteraceae*. Finally, a significant decrease in indole levels observed in mouse feces may contribute to the development of AML via weakened immune surveillance ability and exacerbation of intestinal inflammation.³⁶

Increasing attention to the pathogenic relationship between the microbiome and AML development in experimental and clinical studies has been drawn recently. However, considering the complexity of the connections between host metabolism, inflammation, immune responses, and hematopoiesis, many open questions remain to be explored.

Treatment and microbiome changes

The condition of AML patients is deeply complicated by the large number of factors influencing microbiome composition, which often makes it impossible to distinguish whether changes in microbiome composition are caused by a disease or causally involved in its pathogenesis.

Antibiotics

Emerging evidence suggests that antibiotic therapy leads to a reduction in microbiota diversity, promotion of antibiotic-resistant organisms, and disruption of the mucosal barrier function, consequently resulting in recurrent *Clostridioides difficile* or systemic infections, as well as alterations in its metabolic activity. Bacterial taxa responsible for essential metabolic functions, such as butyrate production, have been shown to decrease after just 7 days of broad-spectrum antibiotics. Beta-lactams and metronidazole, targeting obligate anaerobes in the gut, exacerbate this effect.³⁷

Nutrition

Nutrition is one of the most fundamental factors in maintaining a balanced human GM for patients undergoing leukemia therapy. In a mouse study, caloric restriction led to changes resembling those observed after cytotoxic therapy, including expansion of *Akkermansia* and *Bacteroides*, reduction of *Bacilli*, mucin glycan degradation with mucus layer thinning, decreased levels of acetate, propionate and butyrate, and elevated succinate concentrations.³⁸ In a small non-randomized study, in contrast to parenteral nutrition (PN), enteral nutrition (EN) was

found to expedite the recovery of microbiome diversity, composition and SCFA production post-transplant in pediatric patients.³⁹ Enteral nutrition exerts a trophic effect on the gut epithelium, providing essential nutrients for SCFA producers. Despite total PN being commonly utilized to enhance the nutritional status of graft-versus-host disease (GVHD) patients after allogeneic hematopoietic stem cell transplantation (allo-HSCT), EN is currently the preferred mode of nutritional support in cancer patients.⁴⁰ The adverse effects of parenteral feeding arise from impaired gut-associated lymphoid tissue function, including compromised adaptive immune cells, intestinal epithelium damage, alterations in metabolic product profiles, and changes in the intestinal microbiome. These factors collectively heighten susceptibility to infections.⁴¹ Conversely, EN-enhanced SCFA production shields against intestinal mucosal atrophy and bacterial translocation.^{42–44} A pilot study examining the effects of nutrition on post-allo-HSCT GM found that PN was less effective than EN in maintaining microbiota diversity and composition. Patients receiving EN showed higher levels of *Faecalibacterium* and *Ruminococcus E bromii*, while prolonged minimal oral intake reduced microbial diversity and decreased SCFA-associated taxa, such as *Faecalibacterium prausnitzii* and *Blautia*. These findings support the preference for EN over PN in allo-HSCT patient care.⁴⁵

Chemotherapy

An expanding body of research on acute leukemia patients has demonstrated a chemotherapy-induced adverse influence on intestinal barrier integrity, permeability and GM condition. Apart from notable differences in GM profiles, chemotherapy-treated patients exhibit diverse metabolite profiles. Reduced diversity and pathological composition of the GM translate directly to metabolic alterations that can potentially persist in survivors.^{46–51}

Rashidi et al. provided patient- and sample-level longitudinal GM and circulating microbiome data from AML patients hospitalized to receive induction chemotherapy. They showed a decrease in alpha diversity and a decline in citrulline (a marker of functional enterocyte mass) until approx. day 12, followed by a slow rise toward baseline. A significant association between 11 genera of the GM and 201 serum metabolites formed 2 distinct patterns. The 1st group of genera contained obligate anaerobic commensal genera in the Clostridia class. Metabolites were enriched in amino acid and xenobiotic pathways and included known microbial metabolites of dietary tryptophan and tyrosine, as well as butyrate/isobutyrate. Frequently pathogenic species, including *Enterococcus*, *Pseudomonas*, *Rothia*, and *Veillonella*, contributed to metabolites connected with the lipid pathway in the 2nd group.⁵² The profiles of the GM and metabolites in AML patients with and without chemotherapy and control individuals were

compared by Xu et al. Patients with AML presented an increased ratio of Firmicutes to Bacteroidetes. *Collinsella* and *Coriobacteriaceae* were significantly enriched in newly diagnosed AML patients, serving as AML biomarkers. Plenty of bacteria showed correlations with specific amino acid expressions. Among them, both *Collinsella* and *Coriobacteriaceae* were linked to fecal hydroxyprolyl-hydroxyproline, prolyl-tyrosine and tyrosyl-proline.⁵³ Hueso et al. linked induction chemotherapy (7+3 regimen) to intestinal barrier injury, reflected by a decrease in citrulline levels and significant loss of overall bacterial load and alpha and beta diversities, with a switch from anaerobic to aerotolerant bacteria. Gut impairment was associated with a reduction in fecal SCFAs, which mirrors its necessity in colonocyte support, crypt depth regulation, mucus secretion, tissue homeostasis maintenance, and intestinal repair.⁵⁴ Pötgens et al. recently investigated the links between GM changes and cachectic features in AML patients using a multi-omics approach, including fecal, blood and urine metabolome assessment. They observed that intensive treatment led to elevated systemic inflammation, muscle mass depletion, anorexia, and weight loss, along with transient impairment of gut barrier function and persistent alterations in GM composition marked by reduced diversity. At the end of the induction, *Lactobacillaceae* and *Campylobacter* levels increased, whereas 3 SCFA producers (*Intestinibacter bartlettii*, *Odoribacter splanchnicus* and *Gemmiger formicilis*) were reduced. Contrarily, *Enterococcus faecium* and *Staphylococcus* levels were increased at discharge. Metabolomics analyses indicated persistent reductions in urinary hippurate and fecal bacterial amino acid metabolites (2-methylbutyrate, isovalerate and phenylacetate).⁵⁵ New modalities, such as CPX-351, a liposomal cytarabine plus daunorubicin combination, approved for adults with newly diagnosed therapy-related AML or AML with myelodysplasia-related changes enhanced survival compared to the 7+3 regimen. In preclinical models, CPX-351 averted mucosal damage, dysbiosis and morbidity by activating the aryl hydrocarbon receptor–IL-22–IL-10 host pathway and generating immunomodulatory metabolites by anaerobes.⁵⁶

The bidirectional interplay between the microbiome and anticancer chemotherapy is significant. Gut microbiota and microbial metabolites influence both the effectiveness and adverse effects of chemotherapeutics, including immunotherapy. This relationship is further underscored by the concept of pharmacomicrobiomics, where microorganisms can also alter the biotransformation of drugs, affecting their bioavailability, bioactivity and toxicity through metabolites. Moreover, due to their anti-tumor activity, microbial-derived metabolites possess the property to exert the tumoricidal effect of conventional therapeutics. For example, sodium butyrate, a histone deacetylase inhibitor, enhances the efficacy of venetoclax against AML cells through an increase in apoptosis induction.⁵⁷

The combination of sodium butyrate with exogenous recombinant tumor necrosis factor-related apoptosis-inducing ligand (TRAIL) has demonstrated enhanced antiproliferative effects in leukemia cells harboring the t(8;21) translocation. TRAIL, a member of the tumor necrosis factor (TNF) cytokine family, functions in immune surveillance and selectively induces apoptosis in various cancer cells. Histone deacetylase inhibitors upregulate TRAIL receptor expression, increasing the susceptibility of target cells to TRAIL-induced apoptosis. In leukemia cells with the t(8;21) translocation, TRAIL expression is diminished, making the combination of sodium butyrate and recombinant TRAIL a promising therapeutic strategy for the clinical management of t(8;21) AML.⁵⁸

Neutropenic fever

Dysbiosis is intricately linked to infectious complications, which represent a prevalent cause of mortality among patients with hematologic malignancies. Neutropenic fever (NF) is a common clinical exacerbation, but its clear etiology usually cannot be found.

Recent evidence indicates a link between the microbiota and NF occurrence in AML patients. Rashidi et al. identified a shift in circulating metabolites after NF, of which 13 were associated with the GM. The level of metabolites contributing to intestinal epithelial health (citrulline) and bacterial metabolites of dietary tryptophan (indole) with known anti-inflammatory and gut-protective effects decreased after NF in parallel with an increase in mucolytic and a decrease in butyrogenic bacteria.⁵⁹ To better understand NF pathogenesis, the authors profiled the GM in 2 cohorts of patients with acute leukemia and showed that mucolytic species, *Akkermansia muciniphila*, expansion in the gut was associated with an increased risk for NF. Serum metabolites involved in the γ -glutamyl cycle, known oxidative stress mediators, correlated both with *A. muciniphila* and NF. Moreover, the level of gut microbial-derived indole compounds increased after *A. muciniphila* expansion and decreased before NF, suggesting their anti-inflammatory effects. This study suggests that NF relies on the pyrogenic and inflammatory effects of metabolites absorbed from the gut, and compromised mucolytic function of *A. muciniphila* is crucial in this process.⁶⁰ Similar studies on allo-HSCT patients with AML have yielded consistent evidence of the relationship between *A. muciniphila* and NF. In addition, irradiation, melphalan and caloric restriction increased the relative abundance of *A. muciniphila*. Moreover, caloric restriction of unirradiated mice reduced acetate, propionate and butyrate. Treatment with an antibiotic targeting *A. muciniphila* or propionate supplementation in mice preserved the mucus layer. These results suggest that there are comprehensive interactions between diet, metabolites, colonic mucus, and the microbiome in NF risk.³⁸

Microbiota-based approaches

Nutrition

Nutritional status significantly influences the outcomes of leukemia patients. Both malnutrition and obesity induce changes in the GM and alter the production of detrimental bacterial metabolites, which implies negative effects.^{61,62} Muscle mass serves as an independent factor in post-HSCT survival. The GM and its metabolites play a role in regulating metabolism, affecting skeletal muscle mass and function. A study implementing soy–whey blended protein in HSCT patients demonstrated improved muscle strength and area, along with increased GM alpha-diversity. Lack of response was associated with a reduction in butyrate-producing taxa, while taxa such as *Ruminococcus* and *Veillonella* showed positive correlations with muscle status. Furthermore, the group that responded positively to the intervention exhibited characteristics related to amino acid biosynthesis and the pentose phosphate pathway, both crucial for the anabolic processes involved in skeletal muscle regeneration.⁶³

Route of feeding

The documented role of EN in maintaining GM homeostasis resulted in its recommendation by main international guidelines. When comparing EN to total PN in 20 pediatric post-HSCT patients, the EN cohort exhibited rapid recovery of microbiome diversity, composition and SCFA production after transplantation. This was characterized by the restoration of *Faecalibacterium*, *Dorea*, *Blautia*, *Bacteroides*, *Parabacteroides*, and *Oscillospira*.³⁹

Diet

Disease-related alterations in eating habits and nutritional protocols among leukemia patients can lead to a depletion of dietary fiber, an essential nutrient for the GM. Significantly, Maia et al. conducted a study comparing the microbiological and nutritional composition of neutropenic and regular diets, revealing comparable microbial loads but decreased fiber and vitamin C content in the strict neutropenic diet.⁶⁴ Restriction of fruits and vegetables can disrupt the balance of the GM and increase the risk of bacterial overgrowth and translocation. Under conditions where dietary accessible substrates are limiting, host mucins serve as a source for microbial fermentation, promoting gut barrier injury. Given insufficient evidence supporting the beneficial effects of a low-bacterial diet on infection and mortality in neutropenic patients, a standardized approach focused on the safe handling of foods serves as a promising alternative to a restrictive diet.

Probiotics

Among cancer patients, the utilization of dietary and commercial probiotic supplements is becoming more common, but data are limited regarding the impact of probiotics on the microbiome in acute leukemia. In murine models of allo-HSCT, Sofi et al. demonstrated that administering a single strain of commensal bacteria, *Bacteroides fragilis*, led to increased GM diversity and an abundance of beneficial commensal bacteria, effectively alleviating the development of acute and chronic GVHD. The mechanism underlying this improvement was linked to elevated levels of SCFAs, interleukin 22 (IL-22) and regulatory T cells, which contributed to enhanced tight junction-related gut integrity and reduced production of inflammatory cytokines by pathogenic T cells.⁶⁵ Considering the limited efficacy of single selective probiotic supplementation in restoring AML-related dysbiosis, probiotic cocktails are being explored as alternative strategies. In one study, oral administration of a selected mixture of 17 butyrate-producing Clostridia strains to adult mice improved gut epithelial integrity, reduced GVHD severity and improved survival.⁶⁶

The recent live biotherapeutic products category of drug products relating to living organisms with notable effects on diseases has been designed by FDA to clarify pharmaceutical expectations.⁶⁷ *Clostridium butyricum* MIYAIRI 588 (CBM588), a spore-forming anaerobic bacterium, has been categorized as a live biotherapeutic product. In a prospective observational study, prophylactic CBM588 contributed to the preservation of intestinal microbiota diversity. Specifically, it significantly increased the abundance of *C. butyricum* while reducing cluster III microbiota early after HSCT.⁶⁸ An ongoing phase I clinical trial (NCT03922035) is evaluating the safety and tolerability of administering *C. butyricum* CBM 588 Probiotic Strain during HSCT (from day +1 to +28), with secondary outcomes including analysis of GM changes.

Prebiotics

Prebiotics, defined as “substrates selectively utilized by host microorganisms, conferring health benefits”, encompass fermentable, non-digestible carbohydrates metabolized by specific commensal bacteria in the colon.⁶⁹ Unlike probiotics, which contain live microbes, prebiotics are non-living nutrients present in both food and supplements. These include inulin, fructo-oligosaccharides, xylo-oligosaccharides, galacto-oligosaccharides, potato starch, conjugated linoleic acid, polyunsaturated fatty acids, human milk, phenolics, phytochemicals, and other readily fermentable dietary fibers. Administration of prebiotics significantly promotes beneficial groups of bacteria, especially SCFA producers, by providing them with essential substrates for microbial fermentation.^{70,71} Riwes et al. have successfully

demonstrated that prebiotic treatment with resistant starch in patients with allo-HSCT was feasible and promoted butyrogenic microbiota, increasing levels of intestinal butyrate in longitudinal observation.⁷² Future studies investigating prebiotic supplementation that include the measurement of circulating SCFA concentrations are warranted.

Postbiotics

Given the potential infection risk associated with probiotics and the requirement of a healthy gut microbial community for prebiotic digestion, postbiotics have emerged as a potentially safer and more efficient approach. Postbiotics encompass functional bioactive components derived from inactivated microbial cells or their constituents, often supplemented with metabolites.⁷³ In vitro and murine model studies have elucidated numerous beneficial effects of postbiotics, notably encompassing the preservation of the gastrointestinal tract barrier surface, the modulation of intestinal epithelial cell damage, and the regulation of innate and adaptive host immune responses.⁷⁴ Short-chain fatty acids, particularly butyrate, stand out as the most extensively researched postbiotics. In a leukemia setting, local delivery of exogenous butyrate has been shown to enhance the integrity of intestinal epithelial cell junctions, reduce apoptosis and alleviate GVHD in murine models, akin to the effects observed with 17 carefully selected strains of *Clostridia* known for their high butyrate production.⁷⁵ In addition to butyrate, propionate, another SCFA, has been found to protect intestinal epithelial cells and reduce acute GVHD severity, possibly through GPR43-mediated ERK phosphorylation and NLRP3 inflammasome activation.⁷⁶ Based on their unique characteristics and superior safety, postbiotics should be considered as a novel strategy for the improvement of outcomes of AML patients at all stages of therapy.

Fecal microbiota transplantation

The transfer of fecal material from healthy donors into the gastrointestinal tract of recipients, named fecal microbiota transplantation (FMT), imparts beneficial changes in both the microbial community and in metabolic profiles. Growing interest in the application of FMT in various clinical settings has led to its increasingly extensive use in the field of hematology with a great future. Fecal microbiota transplantation, being the ultimate probiotic, has provided clinical benefits to recipients of HSCT. The experience of recent years has shown a number of advantages of FMT in different indications, including restoration of dysbiotic microbiota, prevention of severe infections through eradication of antibiotic-resistant bacteria, treatment of GVHD, and prevention and treatment of *Clostridium difficile* infection.^{77–80} The risk of infection associated with the procedure remains the biggest concern of applying FMT to highly immunosuppressed

patients with hematologic conditions. Therefore, despite the currently encouraging results in terms of efficacy and safety, following the actual recommendations, FMT is indicated only for the 2nd recurrence of *C. difficile* infection.⁸¹ To avoid recipient exposure to potentially pathogenic foreign microorganisms, Taur et al. investigated the administration of autologous FMT, harvested before obtaining the restoration of microbiota diversity and composition to pre-transplant levels with *Lachnospiraceae*, *Ruminococcaceae* and *Bacteroidetes*, in a treatment arm only.⁸² Novel strategies for customizing the composition of FMT to specific recipients and developments in the fecal inoculum preparation processes may improve the safety and efficacy of the procedure. The infusion of selected bacteria via synthetic bacterial suspension, defined as “bacterial consortium”, with particular emphasis on SCFA producers, offers another potential solution.⁸³ Promising clinical outcomes encourage further evaluation of the use of FMT in AML settings with a special focus on its metabolic and immune effects.

Gut decontamination

Assuming that non-absorbable antibiotics can debulk intestinal bacteria and, therefore, decrease bacteremia and acute GVHD risk, some clinical centers practice gut decontamination (GD) in the peri-HSCT period. The rationale for this procedure is mainly based on promising results from murine, early single-arm, retrospective studies, while more recent research has presented varied results.^{84–87} In a prospective, randomized study, GD with vancomycin and polymyxin B did not affect Shannon diversity or clinical outcomes but decreased the prevalence or abundance of gut pathogens and bloodstream infections (BSIs).⁸⁸ By comparing 2 decontamination schedules, Weber et al. did not show a difference in rates of infectious complications between ciprofloxacin/metronidazole and rifaximin; however, rifaximin tended toward higher intestinal microbiota diversity along with enhancement of antibiotic-induced dysbiosis.⁸⁹ Due to the lack of evidence supporting a clear benefit of this procedure and a proven link between the use of some antibiotics and dysbiosis, current guidelines do not recommend GD as a standard practice; however, a precise understanding of the correlation between specific bacterial strains and AML patient outcomes may change our approach to this procedure. While broad-spectrum antibiotics that attack non-specifically may exacerbate gut dysbiosis, the use of antibiotics with a spectrum narrow enough to target a specific negative bacterial species and spare beneficial ones may induce favorable efficacy. Moreover, pretreatment profiling of the individual gut microbiome composition may help facilitate decisions regarding the proper choice of antibiotics. Future studies incorporating modern multi-omics approaches are needed to explore the specific impact of different antibiotics on the GM and clinical outcomes.

Discussion

Future directions

As the GM is a complex ecological system that requires community collaboration, the administration of a single microbial strain alone may be ineffective. Holistic reshaping of the composition of the keystone consortium of microbes could be a promising approach. Precise microbial engineering technologies, including various CRISPR/Cas systems, offer a comprehensive tool to produce higher yields of bioactive metabolites and improve safety. Accurate delivery of engineered bacteria to the target area is the main challenge, and the use of an encapsulation system is being investigated as one of the possible solutions.

Based on the current results of preclinical research on the role of microbial metabolites in AML, a novel concept of postbiotics represents a promising alternative or complementary option to improve therapeutic response, mitigate treatment-related toxicity, protect against infectious complications, and even prevent disease progression. Postbiotics refer to bioactive compounds, cell fractions or metabolic products of bacterial origin. In the absence of live microorganisms, postbiotics administration may eliminate the risks of potential infections, providing a safer solution compared to probiotics or FMT. The lack of standardization in terms of formulation, optimal dosage, duration, and route of administration poses challenges in determining the best clinical implementation. Therefore, prebiotics, probiotics and postbiotics are still only classified as health products rather than medicines, and regulatory rules limit their application in the medical field. The safety of these microbiome-based interventions is a critical consideration in immunocompromised patients and represents the main objective of ongoing trials. Furthermore, individual variability due to dynamic differences in the GM during treatment necessitates microbiome profiling in accordance with the assumptions of next-generation personalized medicine.

Considering the unique and multiple mechanisms of action of microbiota-derived metabolites, they provide an opportunity to overcome the limitations of current traditional medicines, including risks of adverse reactions, interactions, tolerance, and dependence, and they may reduce reliance on antibiotics, leading to lower healthcare costs. A better understanding of the complex interactions between the GM and host health will facilitate breakthroughs in innovative treatments that hold the potential to transform the coming face of medicine. Promising results from small preliminary studies highlight opportunities for future research.

Limitations

The lack of available or reliable prior research considering microbial metabolomics in the context of AML is the main limitation of this review. Despite significant


progress in understanding the role of microbial metabolites in many diseases, AML settings remain an open area for research. It is worth noting that in most of the above-discussed studies, patients with a diagnosis of AML represented only a small percentage of the total study group. Considering the unique metabolic profile of patients with leukemia, conditioned by the circumstances of the individual's health, the nature of the disease and the implications of treatment, current findings on the mechanistic role of microbial metabolites from different conditions cannot be directly applied to the context of AML. Future randomized clinical trials should be extended to include a larger sample and eliminate the influence of disturbing factors. Our paper does not provide a comprehensive discussion of mixed methods research, which involves combining different data collection methods in a single study. There are currently insufficient validated algorithms for use in clinical practice. In this case, various methods, including multi-omics-based strategies, should be applied more widely for a more effective understanding and investigation of microbiome-related changes in AML.

Conclusions

Metabolomics is becoming a dominant player in the functional assessment of AML issues, and it provides a novel perspective on our insight into its pathogenesis. Understanding the nature of the microbiome has direct translational importance, as microbial-derived products are both targets and modifiers of AML processes. In the future, microbial metabolic patterns may provide non-invasive biomarkers for early diagnosis, risk stratification, relapse prediction and detection, and even the identification of patients more likely to respond to treatment. Current personalized therapeutic approaches in AML are based on identifiable and targetable genomic lesions. Targeting specific individual microbiome-related features emerges as the next opportunity for therapeutic interventions. Ongoing efforts focusing on standardization in laboratory techniques and analysis are likely to result in the widespread adoption of metabolomics technology in clinical settings. Future efforts are needed to implement an integrative functional multi-omics approach in AML patient management. Despite treatment progress, addressing microbial metabolite challenges remains a crucial area for ongoing study and improvement.

ORCID iDs

Aneta Nowicka  <https://orcid.org/0009-0006-6955-5022>

Lidia Gil  <https://orcid.org/0000-0003-0700-3637>

References

1. National Institutes of Health (NIH). Cancer Stat Facts: Leukemia: Acute Myeloid Leukemia (AML). Bethesda, USA: National Institutes of Health (NIH);2024. <https://seer.cancer.gov/statfacts/html/amyl.html>. Accessed April 25, 2024.

2. Berg G, Rybakova D, Fischer D, et al. Microbiome definition re-visited: Old concepts and new challenges. *Microbiome*. 2020;8(1):103. doi:10.1186/s40168-020-00875-0
3. Vinelli V, Biscotti P, Martini D, et al. Effects of dietary fibers on short-chain fatty acids and gut microbiota composition in healthy adults: A systematic review. *Nutrients*. 2022;14(13):2559. doi:10.3390/nu14132559
4. Wu W, Sun M, Chen F, et al. Microbiota metabolite short-chain fatty acid acetate promotes intestinal IgA response to microbiota which is mediated by GPR43. *Mucosal Immunol*. 2017;10(4):946–956. doi:10.1038/mi.2016.114
5. Ciarlo E, Heinonen T, Herderschee J, et al. Impact of the microbial derived short chain fatty acid propionate on host susceptibility to bacterial and fungal infections in vivo. *Sci Rep*. 2016;6(1):37944. doi:10.1038/srep37944
6. Chang PV, Hao L, Offermanns S, Medzhitov R. The microbial metabolite butyrate regulates intestinal macrophage function via histone deacetylase inhibition. *Proc Natl Acad Sci U S A*. 2014;111(6):2247–2252. doi:10.1073/pnas.1322269111
7. Ranjbar R, Vahdani SN, Tavakoli S, Khodaie R, Behboudi H. Immunomodulatory roles of microbiota-derived short-chain fatty acids in bacterial infections. *Biomed Pharmacother*. 2021;141:111817. doi:10.1016/j.biopha.2021.111817
8. Li M, Van Esch BCAM, Wagenaar GTM, Garssen J, Folkerts G, Henricks PAJ. Pro- and anti-inflammatory effects of short chain fatty acids on immune and endothelial cells. *Eur J Pharmacol*. 2018;831:52–59. doi:10.1016/j.ejphar.2018.05.003
9. Tan J, McKenzie C, Potamitis M, Thorburn AN, Mackay CR, Macia L. The role of short-chain fatty acids in health and disease. *Adv Immunol*. 2014;121:91–119. doi:10.1016/B978-0-12-800100-4.00003-9
10. Venkatesh M, Mukherjee S, Wang H, et al. Symbiotic bacterial metabolites regulate gastrointestinal barrier function via the xenobiotic sensor PXR and toll-like receptor 4. *Immunity*. 2014;41(2):296–310. doi:10.1016/j.immuni.2014.06.014
11. Bansal T, Alaniz RC, Wood TK, Jayaraman A. The bacterial signal indole increases epithelial-cell tight-junction resistance and attenuates indicators of inflammation. *Proc Natl Acad Sci U S A*. 2010;107(1):228–233. doi:10.1073/pnas.0906112107
12. Zelante T, Iannitti RG, Cunha C, et al. Tryptophan catabolites from microbiota engage aryl hydrocarbon receptor and balance mucosal reactivity via interleukin-22. *Immunity*. 2013;39(2):372–385. doi:10.1016/j.immuni.2013.08.003
13. Ticho AL, Malhotra P, Dudeja PK, Gill RK, Alrefai WA. Bile acid receptors and gastrointestinal functions. *Liver Res*. 2019;3(1):31–39. doi:10.1016/j.livres.2019.01.001
14. Sarathy J, Detloff SJ, Ao M, et al. The Yin and Yang of bile acid action on tight junctions in a model colonic epithelium. *Physiol Rep*. 2017;5(10):e13294. doi:10.14814/phy2.13294
15. Yang S, Li X, Yang F, et al. Gut microbiota-dependent marker TMAO in promoting cardiovascular disease: Inflammation mechanism, clinical prognosis, and potential as a therapeutic target. *Front Pharmacol*. 2019;10:1360. doi:10.3389/fphar.2019.01360
16. Kaźmierczak-Siedlecka K, Marano L, Merola E, Roviello F, Połom K. Sodium butyrate in both prevention and supportive treatment of colorectal cancer. *Front Cell Infect Microbiol*. 2022;12:1023806. doi:10.3389/fcimb.2022.1023806
17. Wehrens R, Salek R, eds. *Metabolomics: Practical Guide to Design and Analysis*. Boca Raton, USA: Chapman and Hall/CRC; 2019. doi:10.1201/9781315370583
18. Jang C, Chen L, Rabinowitz JD. Metabolomics and isotope tracing. *Cell*. 2018;173(4):822–837. doi:10.1016/j.cell.2018.03.055
19. Roberts LD, Souza AL, Gerszten RE, Clish CB. Targeted metabolomics. *Curr Protoc Mol Biol*. 2012;98(1):Chapter 30:Unit 30.2.1–24. doi:10.1002/0471142727.mb3002s98
20. Wang Y, Zhang L, Chen WL, et al. Rapid diagnosis and prognosis of de novo acute myeloid leukemia by serum metabolomic analysis. *J Proteome Res*. 2013;12(10):4393–4401. doi:10.1021/pr400403p
21. Chen WL, Wang JH, Zhao AH, et al. A distinct glucose metabolism signature of acute myeloid leukemia with prognostic value. *Blood*. 2014;124(10):1645–1654. doi:10.1182/blood-2014-02-554204
22. Stockard B, Wu H, Guingab JD, et al. Metabolomics profiling reveals markers for chemosensitivity and clinical outcomes in pediatric AML patients. *Blood*. 2018;132(Suppl 1):1536–1536. doi:10.1182/blood-2018-99-116665
23. Stockard B, Garrett T, Guingab-Cagmat J, Meshinchi S, Lamba J. Distinct metabolic features differentiating FLT3-ITD AML from FLT3-WT childhood acute myeloid leukemia. *Sci Rep*. 2018;8(1):5534. doi:10.1038/s41598-018-23863-9
24. De Martel C, Ferlay J, Franceschi S, et al. Global burden of cancers attributable to infections in 2008: A review and synthetic analysis. *Lancet Oncol*. 2012;13(6):607–615. doi:10.1016/S1470-2045(12)70137-7
25. Loh YH, Jakszyn P, Luben RN, Mulligan AA, Mitrou PN, Khaw KT. N-nitroso compounds and cancer incidence: The European Prospective Investigation into Cancer and Nutrition (EPIC)–Norfolk Study. *Am J Clin Nutr*. 2011;93(5):1053–1061. doi:10.3945/ajcn.111.012377
26. Russell WR, Hoyles L, Flint HJ, Dumas ME. Colonic bacterial metabolites and human health. *Curr Opin Microbiol*. 2013;16(3):246–254. doi:10.1016/j.mib.2013.07.002
27. Pegg AE. Toxicity of polyamines and their metabolic products. *Chem Res Toxicol*. 2013;26(12):1782–1800. doi:10.1021/tx400316s
28. Furusawa Y, Obata Y, Fukuda S, et al. Commensal microbe-derived butyrate induces the differentiation of colonic regulatory T cells. *Nature*. 2013;504(7480):446–450. doi:10.1038/nature12721
29. Atarashi K, Tanoue T, Shima T, et al. Induction of colonic regulatory T cells by indigenous *Clostridium* species. *Science*. 2011;331(6015):337–341. doi:10.1126/science.1198469
30. Donohoe DR, Holley D, Collins LB, et al. A gnotobiotic mouse model demonstrates that dietary fiber protects against colorectal tumorigenesis in a microbiota- and butyrate-dependent manner. *Cancer Discov*. 2014;4(12):1387–1397. doi:10.1158/2159-8290.CD-14-0501
31. Vinolo MAR, Rodrigues HG, Nachbar RT, Curi R. Regulation of inflammation by short chain fatty acids. *Nutrients*. 2011;3(10):858–876. doi:10.3390/nu3100858
32. Louis P, Young P, Holtrop G, Flint HJ. Diversity of human colonic butyrate-producing bacteria revealed by analysis of the butyryl-CoA:acetate CoA-transferase gene. *Environ Microbiol*. 2010;12(2):304–314. doi:10.1111/j.1462-2920.2009.02066.x
33. Plöger S, Stumpff F, Penner GB, et al. Microbial butyrate and its role for barrier function in the gastrointestinal tract. *Ann N Y Acad Sci*. 2012;1258(1):52–59. doi:10.1111/j.1749-6632.2012.06553.x
34. Wei Y, Liu W, Wang R, et al. Propionate promotes ferroptosis and apoptosis through mitophagy and ACSL4-mediated ferroptosis elicits anti-leukemia immunity. *Free Radic Biol Med*. 2024;213:36–51. doi:10.1016/j.freeradbiomed.2024.01.005
35. Wang R, Yang X, Liu J, et al. Gut microbiota regulates acute myeloid leukaemia via alteration of intestinal barrier function mediated by butyrate. *Nat Commun*. 2022;13(1):2522. doi:10.1038/s41467-022-30240-8
36. Wu B, Xu Y, Tang M, et al. A metabolome and microbiome analysis of acute myeloid leukemia: Insights into the carnosine–histidine metabolic pathway. *Toxics*. 2023;12(1):14. doi:10.3390/toxics12010014
37. Haak BW, Littmann ER, Chaubard JL, et al. Impact of gut colonization with butyrate producing microbiota on respiratory viral infection following allo-HCT. *Blood*. 2018;131(26):2978–2986. doi:10.1182/blood-2018-01-828996
38. Schwabkey ZI, Wiesnoski DH, Chang CC, et al. Diet-derived metabolites and mucus link the gut microbiome to fever after cytotoxic cancer treatment. *Sci Transl Med*. 2022;14(671):eabo3445. doi:10.1126/scitranslmed.abo3445
39. D'Amico F, Biagi E, Rampelli S, et al. Enteral nutrition in pediatric patients undergoing hematopoietic SCT promotes the recovery of gut microbiome homeostasis. *Nutrients*. 2019;11(12):2958. doi:10.3390/nu11122958
40. Arends J, Bachmann P, Baracos V, et al. ESPEN guidelines on nutrition in cancer patients. *Clin Nutr*. 2017;36(1):11–48. doi:10.1016/j.clnu.2016.07.015
41. Pierre JF. Gastrointestinal immune and microbiome changes during parenteral nutrition. *Am J Physiol Gastrointest Liver Physiol*. 2017;312(3):G246–G256. doi:10.1152/ajpgi.00321.2016
42. Alpers DH. Enteral feeding and gut atrophy. *Curr Opin Clin Nutr Metab Care*. 2002;5(6):679–683. doi:10.1097/00075197-200211000-00011
43. MacFie J, Reddy BS, Gatt M, Jain PK, Sowdi R, Mitchell CJ. Bacterial translocation studied in 927 patients over 13 years. *Br J Surg*. 2005;93(1):87–93. doi:10.1002/bjs.5184

44. Ríos-Covián D, Ruas-Madiedo P, Margolles A, Gueimonde M, De Los Reyes-Gavilán CG, Salazar N. Intestinal short chain fatty acids and their link with diet and human health. *Front Microbiol.* 2016;7:185. doi:10.3389/fmicb.2016.00185
45. Andersen S, Staudacher H, Weber N, et al. Pilot study investigating the effect of enteral and parenteral nutrition on the gastrointestinal microbiome post-allogeneic transplantation. *Br J Haematol.* 2020;188(4):570–581. doi:10.1111/bjh.16218
46. Bai L, Zhou P, Li D, Ju X. Changes in the gastrointestinal microbiota of children with acute lymphoblastic leukaemia and its association with antibiotics in the short term. *J Med Microbiol.* 2017;66(9):1297–1307. doi:10.1099/jmm.0.000568
47. Rajagopala SV, Singh H, Yu Y, et al. Persistent gut microbial dysbiosis in children with acute lymphoblastic leukemia (ALL) during chemotherapy. *Microb Ecol.* 2020;79(4):1034–1043. doi:10.1007/s00248-019-01448-x
48. Bhuta R, DeNardo B, Wang J, et al. Durable changes in the gut microbiome in survivors of childhood acute lymphoblastic leukemia. *Pediatr Blood Cancer.* 2021;68(12):e29308. doi:10.1002/pbc.29308
49. Chua LL, Rajasuriar R, Azanan MS, et al. Reduced microbial diversity in adult survivors of childhood acute lymphoblastic leukemia and microbial associations with increased immune activation. *Microbiome.* 2017;5(1):35. doi:10.1186/s40168-017-0250-1
50. Chua LL, Rajasuriar R, Lim YAL, Woo YL, Loke P, Ariffin H. Temporal changes in gut microbiota profile in children with acute lymphoblastic leukemia prior to commencement, during, and post-cessation of chemotherapy. *BMC Cancer.* 2020;20(1):151. doi:10.1186/s12885-020-6654-5
51. De Pietri S, Ingham AC, Frandsen TL, et al. Gastrointestinal toxicity during induction treatment for childhood acute lymphoblastic leukemia: The impact of the gut microbiota. *Int J Cancer.* 2020;147(7):1953–1962. doi:10.1002/ijc.32942
52. Rashidi A, Ebadi M, Rehman TU, et al. Compilation of longitudinal gut microbiome, serum metabolome, and clinical data in acute myeloid leukemia. *Sci Data.* 2022;9(1):468. doi:10.1038/s41597-022-01600-2
53. Xu J, Kang Y, Zhong Y, et al. Alteration of gut microbiome and correlated amino acid metabolism are associated with acute myelocytic leukemia carcinogenesis. *Cancer Med.* 2023;12(15):16431–16443. doi:10.1002/cam4.6283
54. Hueso T, Ekpe K, Mayeur C, et al. Impact and consequences of intensive chemotherapy on intestinal barrier and microbiota in acute myeloid leukemia: The role of mucosal strengthening. *Gut Microbes.* 2020;12(1):1800897. doi:10.1080/19490976.2020.1800897
55. Pötgens SA, Lecop S, Havelange V, et al. Gut microbiota alterations induced by intensive chemotherapy in acute myeloid leukaemia patients are associated with gut barrier dysfunction and body weight loss. *Clin Nutr.* 2023;42(11):2214–2228. doi:10.1016/j.clnu.2023.09.021
56. Renga G, Nunzi E, Stincardini C, et al. CPX-351 exploits the gut microbiota to promote mucosal barrier function, colonization resistance, and immune homeostasis. *Blood.* 2024;143(16):1628–1645. doi:10.1182/blood.2023021380
57. Kawakatsu R, Tadayaki K, Yamasaki K, Yoshida T. Venetoclax efficacy on acute myeloid leukemia is enhanced by the combination with butyrate. *Sci Rep.* 2024;14(1):4975. doi:10.1038/s41598-024-55286-0
58. Yoshida T, Yamasaki K, Tadayaki K, et al. Tumor necrosis factor-related apoptosis-inducing ligand is a novel transcriptional target of runt-related transcription factor 1. *Int J Oncol.* 2021;60(1):6. doi:10.3892/ijo.2021.5296
59. Rashidi A, Ebadi M, Rehman TU, et al. Loss of microbiota-derived protective metabolites after neutropenic fever. *Sci Rep.* 2022;12(1):6244. doi:10.1038/s41598-022-10282-0
60. Rashidi A, Ebadi M, Rehman TU, et al. Altered microbiota-host metabolic cross talk preceding neutropenic fever in patients with acute leukemia. *Blood Adv.* 2021;5(20):3937–3950. doi:10.1182/bloodadvances.2021004973
61. Schaffrath J, Diederichs T, Unverzagt S, et al. Correlation of nutrition-associated parameters with non-relapse mortality in allogeneic hematopoietic stem cell transplantation. *Ann Hematol.* 2022;101(3):681–691. doi:10.1007/s00277-021-04736-0
62. Kerby EH, Li Y, Getz KD, et al. Nutritional risk factors predict severe acute graft-versus-host disease and early mortality in pediatric allogeneic hematopoietic stem cell transplantation. *Pediatr Blood Cancer.* 2018;65(2):e26853. doi:10.1002/pbc.26853
63. Ren G, Zhang J, Li M, et al. Gut microbiota composition influences outcomes of skeletal muscle nutritional intervention via blended protein supplementation in posttransplant patients with hematological malignancies. *Clin Nutr.* 2021;40(1):94–102. doi:10.1016/j.clnu.2020.04.030
64. Maia JE, Da Cruz LB, Gregorian LJ. Microbiological profile and nutritional quality of a regular diet compared to a neutropenic diet in a pediatric oncology unit. *Pediatr Blood Cancer.* 2018;65(3):e26828. doi:10.1002/pbc.26828
65. Sofi MH, Wu Y, Ticer T, et al. A single strain of *Bacteroides fragilis* protects gut integrity and reduces GVHD. *JCI Insight.* 2021;6(3):e136841. doi:10.1172/jci.insight.136841
66. Atarashi K, Tanoue T, Oshima K, et al. Treg induction by a rationally selected mixture of *Clostridia* strains from the human microbiota. *Nature.* 2013;500(7461):232–236. doi:10.1038/nature12331
67. Cordaillat-Simmons M, Rouanet A, Pot B. Live biotherapeutic products: the importance of a defined regulatory framework. *Exp Mol Med.* 2020;52(9):1397–1406. doi:10.1038/s12276-020-0437-6
68. Fukushima K, Kudo H, Oka K, et al. p1318: *Clostridium butyricum* miyairi 588 contributes to the maintenance of intestinal microbiota diversity early after hematopoietic cell transplantation. *Hemasphere.* 2023;7(Suppl 3):e200988b. doi:10.1097/01.HS9.0000972160.20098.8b
69. Gibson GR, Hutkins R, Sanders ME, et al. Expert consensus document: The International Scientific Association for Probiotics and Prebiotics (ISAPP) consensus statement on the definition and scope of prebiotics. *Nat Rev Gastroenterol Hepatol.* 2017;14(8):491–502. doi:10.1038/nrgastro.2017.75
70. Pichler MJ, Yamada C, Shuoker B, et al. Butyrate producing colonic *Clostridiales* metabolise human milk oligosaccharides and cross feed on mucin via conserved pathways. *Nat Commun.* 2020;11(1):3285. doi:10.1038/s41467-020-17075-x
71. Tandon D, Haque MM, Gote M, et al. A prospective randomized, double-blind, placebo-controlled, dose-response relationship study to investigate efficacy of fructo-oligosaccharides (FOS) on human gut microflora. *Sci Rep.* 2019;9(1):5473. doi:10.1038/s41598-019-41837-3
72. Riwe MM, Golob JL, Magenau J, et al. Feasibility of a dietary intervention to modify gut microbial metabolism in patients with hematopoietic stem cell transplantation. *Nat Med.* 2023;29(11):2805–2813. doi:10.1038/s41591-023-02587-y
73. Andermann TM, Rezvani A, Bhatt AS. Microbiota manipulation with prebiotics and probiotics in patients undergoing stem cell transplantation. *Curr Hematol Malig Rep.* 2016;11(1):19–28. doi:10.1007/s11899-016-0302-9
74. Salminen S, Collado MC, Endo A, et al. The International Scientific Association of Probiotics and Prebiotics (ISAPP) consensus statement on the definition and scope of postbiotics. *Nat Rev Gastroenterol Hepatol.* 2021;18(9):649–667. doi:10.1038/s41575-021-00440-6
75. Mathewson ND, Jenq R, Mathew AV, et al. Gut microbiome-derived metabolites modulate intestinal epithelial cell damage and mitigate graft-versus-host disease. *Nat Immunol.* 2016;17(5):505–513. doi:10.1038/ni.3400
76. Fujiwara H, Docampo MD, Riwe M, et al. Microbial metabolite sensor GPR43 controls severity of experimental GVHD. *Nat Commun.* 2018;9(1):3674. doi:10.1038/s41467-018-06048-w
77. DeFilipp Z, Peled JU, Li S, et al. Third-party fecal microbiota transplantation following allo-HCT reconstitutes microbiome diversity. *Blood Adv.* 2018;2(7):745–753. doi:10.1182/bloodadvances.2018017731
78. Battipaglia G, Malard F, Rubio MT, et al. Fecal microbiota transplantation before or after allogeneic hematopoietic transplantation in patients with hematologic malignancies carrying multidrug-resistance bacteria. *Haematologica.* 2019;104(8):1682–1688. doi:10.3324/haematol.2018.198549
79. Qi X, Li X, Zhao Y, et al. Treating steroid refractory intestinal acute graft-vs-host disease with fecal microbiota transplantation: A pilot study. *Front Immunol.* 2018;9:2195. doi:10.3389/fimmu.2018.02195
80. Webb BJ, Brunner A, Ford CD, Gazdik MA, Petersen FB, Hoda D. Fecal microbiota transplantation for recurrent *Clostridium difficile* infection in hematopoietic stem cell transplant recipients. *Transpl Infect Dis.* 2016;18(4):628–633. doi:10.1111/tid.12550
81. Van Prehn J, Reigadas E, Vogelzang EH, et al. European Society of Clinical Microbiology and Infectious Diseases: 2021 update on the treatment guidance document for *Clostridioides difficile* infection in adults. *Clin Microbiol Infect.* 2021;27(Suppl 2):S1–S21. doi:10.1016/j.cmi.2021.09.038

82. Taur Y, Coyte K, Schluter J, et al. Reconstitution of the gut microbiota of antibiotic-treated patients by autologous fecal microbiota transplant. *Sci Transl Med*. 2018;10(460):eaap9489. doi:10.1126/scitranslmed.aap9489
83. Quaranta G, Ianiro G, De Maio F, et al. "Bacterial consortium": A potential evolution of fecal microbiota transplantation for the treatment of *Clostridioides difficile* infection. *Biomed Res Int*. 2022;2022:5787373. doi:10.1155/2022/5787373
84. Bekkum DWV, Roodenburg J, Heidt PJ, Waaij DVD. Mitigation of secondary disease of allogeneic mouse radiation chimeras by modification of the intestinal microflora. *J Nat Cancer Inst*. 1974;52(2):401–404. doi:10.1093/jnci/52.2.401
85. Vossen JM, Guiot HFL, Lankester AC, et al. Complete suppression of the gut microbiome prevents acute graft-versus-host disease following allogeneic bone marrow transplantation. *PLoS One*. 2014;9(9):e105706. doi:10.1371/journal.pone.0105706
86. Beelen DW, Elmaagacli A, Müller KD, Hirche H, Schaefer UW. Influence of intestinal bacterial decontamination using metronidazole and ciprofloxacin or ciprofloxacin alone on the development of acute graft-versus-host disease after marrow transplantation in patients with hematologic malignancies: Final results and long-term follow-up of an open-label prospective randomized trial. *Blood*. 1999;93(10):3267–3275. doi:10.1182/blood.V93.10.3267.410k22_3267_3275
87. Gałązka P, Styczyński J, Czyżewski K, et al. Impact of decontamination therapy on gastrointestinal acute graft-versus-host disease after allogeneic hematopoietic cell transplantation in children. *Curr Res Transl Med*. 2021;69(3):103298. doi:10.1016/j.retram.2021.103298
88. Severyn CJ, Siranosian BA, Kong STJ, et al. Microbiota dynamics in a randomized trial of gut decontamination during allogeneic hematopoietic cell transplantation. *JCI Insight*. 2022;7(7):e154344. doi:10.1172/jci.insight.154344
89. Weber D, Oefner PJ, Dettmer K, et al. Rifaximin preserves intestinal microbiota balance in patients undergoing allogeneic stem cell transplantation. *Bone Marrow Transplant*. 2016;51(8):1087–1092. doi:10.1038/bmt.2016.66

Novel strategies of glutathione depletion in photodynamic and chemodynamic therapy: A review

Daniel Wolny^{1,A–F}, Mateusz Stojko^{2,B,D,F}, Alicja Zajdel^{1,A,E,F}

¹ Department of Biopharmacy, Faculty of Pharmaceutical Sciences, Medical University of Silesia, Sosnowiec, Poland

² Centre of Polymer and Carbon Materials, Polish Academy of Sciences, Zabrze, Poland

A – research concept and design; B – collection and/or assembly of data; C – data analysis and interpretation;

D – writing the article; E – critical revision of the article; F – final approval of the article

Advances in Clinical and Experimental Medicine, ISSN 1899–5276 (print), ISSN 2451–2680 (online)

Adv Clin Exp Med. 2025;34(7):1213–1221

Address for correspondence

Daniel Wolny

E-mail: dwolny@sum.edu.pl

Funding sources

The study was supported by the SUM grant: PCN-1-040/N/1/F.

Conflict of interest

None declared

Received on September 14, 2023

Reviewed on May 31, 2024

Accepted on July 9, 2024

Published online on September 20, 2024

Abstract

Cancer remains a health problem worldwide; therefore, developing new therapies to increase the effectiveness of anticancer treatments is necessary. Two such methods are photodynamic therapy (PDT) and chemodynamic therapy (CDT). The intensive growth and increased metabolism of tumors lead to elevated levels of reactive oxygen species (ROS) within cancer cells. These cells develop several antioxidant mechanisms to protect them from this oxidative stress. Antioxidants also make tumors more resistant to chemotherapy and radiation. Glutathione (GSH) is an important and the most abundant endogenous cellular antioxidant. Photodynamic therapy and CDT are new methods that are based on the production of ROS, therefore increasing oxidative stress in cancer cells. A significant problem with these therapies is the increased GSH levels, which is an adaptation of cancer cells to augmented metabolic processes. This paper presents various GSH depletion strategies that are used to improve PDT and CDT. While the main goal of GSH depletion in both PDT and CDT is to prevent its interaction with the ROS generated by these therapies, it should be remembered that the reduction of its level itself may initiate pathways leading to cancer cell death.

Key words: photodynamic therapy, chemodynamic therapy, glutathione depletion

Cite as

Wolny D, Stojko M, Zajdel A. Novel strategies of glutathione depletion in photodynamic and chemodynamic therapy:

A review. *Adv Clin Exp Med.* 2025;34(7):1213–1221.

doi:10.17219/acem/191025

DOI

10.17219/acem/191025

Copyright

Copyright by Author(s)

This is an article distributed under the terms of the Creative Commons Attribution 3.0 Unported (CC BY 3.0) (<https://creativecommons.org/licenses/by/3.0/>)

Introduction

The production of reactive oxygen species (ROS) is a natural consequence of oxygen metabolism and cellular biochemical reactions. As signaling molecules, ROS play an essential role in the activation of pathways that lead to cell proliferation and survival. However, in higher concentrations, they promote mutagenesis by damaging DNA, and in sufficiently high concentrations, they lead to oxidative stress, causing cell death. To prevent the adverse effects of high ROS levels, cells employ several antioxidant protective mechanisms to maintain cellular redox homeostasis and ensure normal functioning and survival.¹

Contrary to normal cells, cancer cells are characterized by significantly increased levels of ROS owing to their unrestrained growth and increased metabolism.² Moreover, higher levels of ROS increase the proliferation of cancer cells and tumor aggressiveness, promoting their ability to invade and metastasize.³ Increased ROS content forces cancer cells to intensify the antioxidant mechanisms that protect them from the negative effects of these oxidative stresses.² It has also been postulated that cancer cells maintain the concentration of ROS at a level that facilitates their progression.⁴ The increased amount of antioxidants and constantly elevated levels of ROS found in cancer cells make them resistant to chemotherapeutic agents and radiation. It has also been shown that cancer cells are highly dependent on their antioxidant systems to maintain an appropriate redox level and are, therefore, sensitive to external factors disrupting these systems.¹

Among the various endogenous cellular antioxidants, glutathione (GSH) is the most abundant. It is a major scavenger of ROS and plays an essential role in maintaining cell redox homeostasis. Although GSH plays an important role in the detoxification of carcinogens, its elevated concentration can be observed in many cancer types, which

increases the resistance of such cells to the toxic effects of many chemotherapeutic agents and radiation.¹

Due to the different amounts of ROS in cancer cells compared to normal cells, various tumor treatment strategies exacerbating oxidative stress have been developed.² Since GSH is a common cellular antioxidant whose main function is to remove free radicals and maintain cellular redox balance, it appears to be the optimal target for such anticancer therapies. There are many studies showing that GSH depletion increases oxidative stress, which leads to cancer cell death. Moreover, it has been shown that the reduction of GSH content in cancer cells makes them more susceptible to factors that increase ROS.¹

Objectives

Here, we describe GSH depletion strategies that could improve the effectiveness of 2 promising ROS-based treatments for cancer: photodynamic therapy (PDT) and chemodynamic (CDT) therapy.

Glutathione depletion strategies

Increased concentrations of GSH in tumor tissues compared to normal tissues have been observed in many neoplastic diseases.⁵ This increases the resistance of cancer cells to therapies based on potentiated oxidative stress.⁶ Depletion of GSH in cancer cells makes them more sensitive to therapeutic agents. Therefore, it should come as no surprise that various strategies are being developed to lower intracellular GSH levels to inhibit tumor growth and increase the effectiveness of therapy. These approaches include a reduction in the availability of substrates for GSH biosynthesis, inhibition of GSH synthesis, GSH conjugation, or increases in its oxidized form (GSSG), as well as promotion of GSH cellular efflux (Fig. 1).^{7–9}

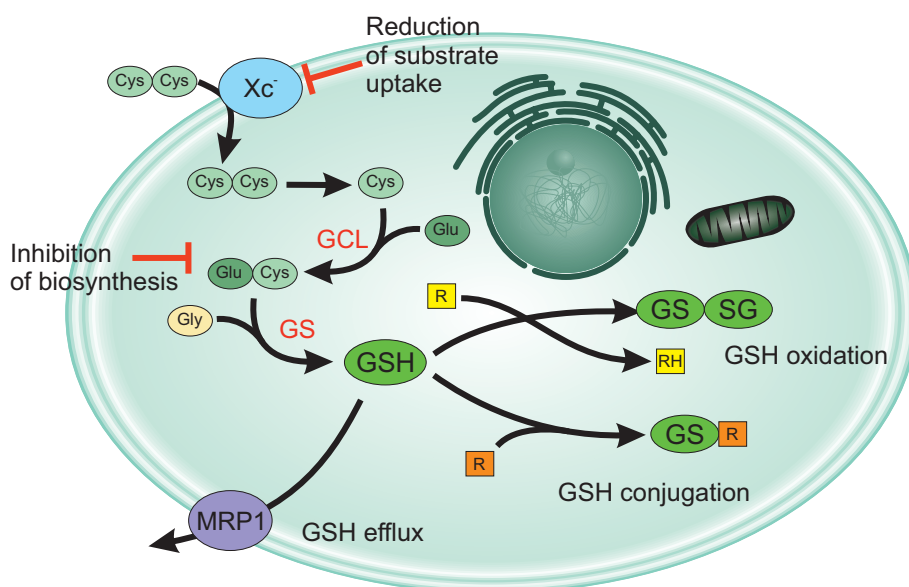


Fig. 1. Glutathione depletion strategies in cancer cells

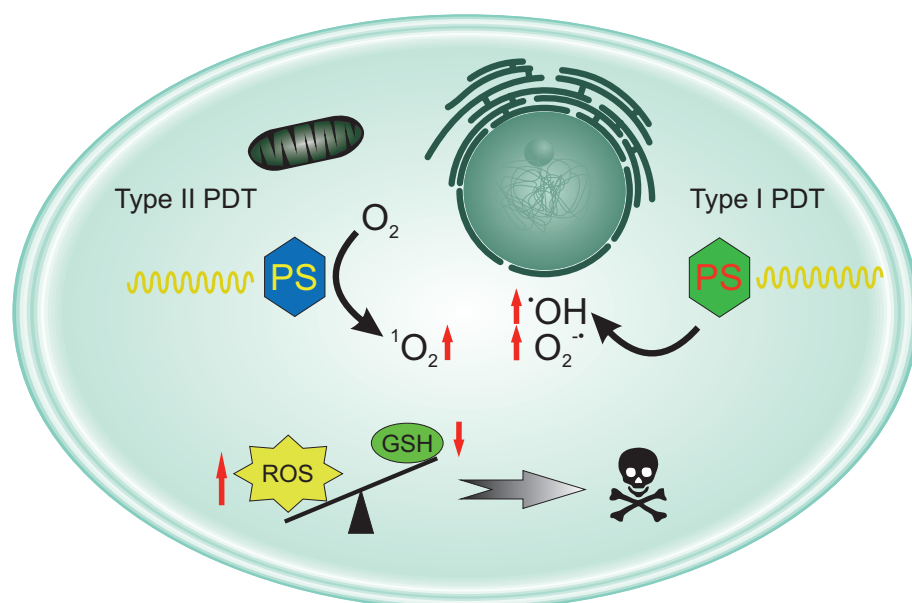


Fig. 2. The principles of photodynamic therapy

Glutathione depletion in photodynamic therapy

Photodynamic therapy (Fig. 2) is a new, developing anticancer therapy that is of great interest. The reasons for this are its undoubted advantages, such as low invasiveness, low toxicity, high effectiveness of therapy, and lack of drug resistance.^{10–14} Reactive oxygen species play a key role in PDT. They oxidize biological macromolecules, such as nucleic acids, proteins and lipids, altering cell signaling pathways and gene expression, as well as destroying membrane structures.¹⁵ This leads to apoptosis of cancer cells. Moreover, ROS within tumor tissues can also damage the microcirculation and cause immunogenic cell death.^{16–18} In this therapy, a photosensitizer (PS) is administered to the patient and activated with an appropriate wavelength of light. Photodynamic reactions can be classified into 2 types. In type I, light energy is transferred from excited molecules to biomolecules through a direct contact reaction. The radicalization mechanism involves the transfer of an electron or hydrogen, and the resulting radicals can initiate a radical chain reaction. This also produces superoxide radicals ($O_2^{\cdot-}$) and hydroxyl radicals ($\cdot OH$).¹⁹ Type II PDT is based on an indirect reaction, in which the excited PS reacts with molecular oxygen. As a result, singlet oxygen (1O_2) is generated, which is extremely electrophilic, causing damage to biomolecules and, consequently, destroying neoplastic cells.^{20,21} Most PDT in clinical applications are based on the second type of reaction.²²

Due to some limitations, PDT is not currently used as a first-line therapy in cancer treatment.^{23,24} To function effectively, it requires large amounts of oxygen in the tumor microenvironment (TME), which is unfortunately hypoxic.²⁵ In addition, cells trigger several defense mechanisms in response to PDT, e.g., cancer cells

increase the synthesis of various cytoprotective molecules. Redox-sensitive transcription factors are activated, which increases the amount of detoxification and antioxidant enzymes. Activation of anti-apoptotic pathways and over-expression of heat shock proteins prevent the formation of active apoptosomes.²⁶

New strategies to increase the effectiveness of PDT are constantly being developed. These include an increase in ROS production by reducing hypoxia in the TME,^{17,27} as well as reducing the efficiency of cancer cell antioxidant systems, with particular emphasis on GSH.^{19,28}

Hu et al. used docosahexaenoic acid (DHA) and 2,2-dimethoxy-2-phenylacetophenone (DMPA) placed in a ROS-sensitive dendrimer nanocarrier (RSV) to reduce intracellular GSH concentrations and increase the effectiveness of PDT.²⁹ Zinc phthalocyanate (ZnPc) was used as the PS. Irradiated by 665 nm light in the presence of endogenous H_2O_2 or ROS resulting from PDT, RSV is decomposed, and DHA and DMPA are released. Under light irradiation, DMPA becomes the initiator of the thiol-ene click reaction, which consists of GSH conjugation to double bonds within the DHA molecule. This directly reduces the cellular concentration of GSH. Moreover, Hu et al. showed that their therapeutic system significantly decreased intracellular concentrations of ATP, which is a cofactor for γ -glutamylcysteine synthetase, resulting in inhibition of GSH synthesis.

Cao et al. synthesized nanoparticles from an amphiphilic branched copolymer (PEG) with pendant vinyl groups containing chlorine e6 (Ce6) as a PS.³⁰ The vinyl groups form a hydrophobic core as the nanoparticle reacts with GSH in the thiol-ene click reaction, lowering its intracellular concentration while Ce6 is released.

Li et al. proposed the use of S-nitrosated human serum albumin (HSA-SNO) to lower GSH concentrations and increase the effectiveness of PDT therapy.³¹ HSA-SNO

binds GSH molecules, releasing nitric oxide (NO), which additionally occupies oxygen binding sites within the mitochondria, thus reducing cellular respiration of cancer cells and indirectly increasing the oxygen concentration needed for PDT.¹⁴

The use of 5-aminolevulinic acid (ALA) as a clinically approved PS has been attempted. Although it does not have the ability to photosensitize itself, it undergoes metabolism inside the cell, resulting in the formation of protoporphyrin IX (PpIX), which already possesses such properties.^{32,33} Compared to other PSs, ALA has low toxicity and is quickly removed from the body. However, at physiological pH, it is largely hydrophilic and, therefore, hardly penetrates biological barriers.^{34,35} The use of ester derivatives alleviates this drawback, but due to the presence of a nucleophilic amino group, these compounds are still not very stable under physiological conditions. Li et al. synthesized a number of ALA methyl ester derivatives in which the substituents were linked to the amino group via 2-hydroxyethyl disulfide.³⁶ After entering the cell, these derivatives react with GSH, which releases ALA and simultaneously lowers the intracellular GSH pool. Next, ALA was transformed into protoporphyrin IX.

An interesting solution was proposed by Meng et al., who created a metal-organic framework (MOF)-based nanocarrier using a disulfide-containing imidazole as an organic ligand and zinc (Zn^{2+}) as a coordination metal.³⁷ The nanocarrier was loaded with a PS (Ce6). To stabilize the MOF in an aqueous environment, its surface was covered with an amphiphilic polymer (pluronic F127). Glutathione depletion was accomplished through a disulfide-thiol exchange reaction and the decomposition of the MOF releases the PS. Meng et al. also demonstrated that the nanocarriers they used had a double therapeutic effect. The PS induces a typical PDT increase in ROS levels, leading to apoptosis. Glutathione depletion not only supports this process but also causes ferroptosis.³⁸

Ferroptosis is a cell death pathway that includes an iron-dependent Fenton reaction and lipid peroxidation.³⁹ This process is characterized by the accumulation of Lipids-OOH due to the disruption of their scavenging systems. The scavenging of toxic Lipids-OOH is carried out by their reduction to Lipids-OH by GSH peroxidase 4 (GPX4).⁴⁰ Glutathione is the reducing co-substrate of GPX4; therefore, GSH depletion or GSH synthesis disorders can trigger ferroptosis.⁴¹ There are many studies that have observed ferroptosis initiated by GSH depletion in both PDT and CDT.^{37,42–46}

Curcumin, isolated from *Curcuma longa*, is a natural chemopreventive drug for cancer.⁴⁷ Many studies have shown that this compound significantly decreases the level of hypoxia-inducible factor 1 α (HIF-1 α), which is overexpressed in several neoplastic diseases. Moreover, curcumin depletes GSH.^{48,49} Zhang et al. used a curcumin derivative (Cur-S-OA) to create a nanoparticle (ZnPc@Cur-S-OA), which decomposes in cancer cells in a ROS-responsive manner with the release of the PS (zinc phthalocyanate, ZnPc) and

free curcumin.⁵⁰ The curcumin derivative serves 2 distinct purposes. First, it acts as a PS stabilizer. Second, following nanoparticle decomposition, it acts as a chemotherapeutic agent, thereby improving PDT efficiency.

Liu et al. designed an oxidative stress amplifier (OSA), that is activated in cancer cells by its interaction with H_2O_2 .⁵¹ It is a micelle (DPL@CC) consisting of cinnamaldehyde (Cin), a GSH scavenger, and Ce6, a PS, coated with a ROS-reactive amphiphilic polymer (DPL). Cinnamaldehyde conjugates with GSH and blocks its thiol group, which is required to react with ROS. After OSA application, the level of GSH decreased to 18.9% compared to control cells.

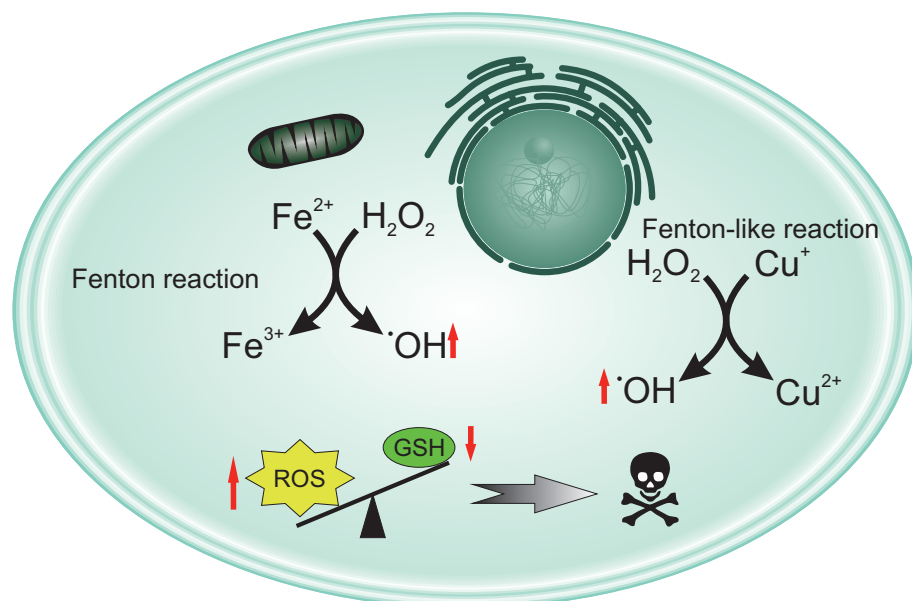
Cysteine is an essential substrate in GSH biosynthesis, and its deficiency significantly affects the formation rate and cellular concentration. Cystine, the oxidized form of cysteine, is present in the extracellular matrix (ECM) and is taken up by the cell through the X_c^- system. It is an anti-port glutamate/cystine transporter found in the cell membrane.⁵² The light chain of the X_c^- system (xCT) is overexpressed in many types of neoplastic diseases, which correlates with resistance to treatment and a poor prognosis in patients.^{53–56} A reduction in extracellular cystine uptake directly reduces the cellular concentration of GSH; thus, inhibiting the X_c^- system is another possible strategy for its depletion.⁵⁷ One of the compounds with the ability to inhibit the X_c^- system is erastin.³⁹ Zhul et al. designed a nanodrug containing erastin and Ce6 as the PS.⁴⁶ After entering cancer cells, erastin inhibited GSH biosynthesis, lowering the intracellular pool, enhancing Fe-induced lipid peroxidation, and inducing cell death via ferroptosis.^{39,58–62}

Wang et al. synthesized nanoparticles consisting of pyropheophorbide (PPa) as a PS and clopidogrel, which was responsible for increasing the effectiveness of PDT by GSH depletion.⁶³ Clopidogrel is a classic antiplatelet drug that is metabolized by cytochrome P450 (CYP2C19) to form a thiol metabolite.⁶⁴ This metabolite conjugates with GSH, lowering its intracellular pool and increasing the effectiveness of PDT. The disadvantage of this approach is that it is limited to cancer cells that overexpress CYP2C19.

Depletion of glutathione in chemodynamic therapy

Chemodynamic therapy (Fig. 3) is highly selective towards cancer cells with minimal side effects.⁶⁵ It is based on Fenton or Fenton-like reactions in which transition metal ions (e.g., Fe, Co, Ni, Cu, and Mn) react with hydrogen peroxide to form highly cytotoxic hydroxyl radicals ($Fe^{2+} + H_2O_2 \rightarrow Fe^{3+} + \cdot OH + OH^-$). This reaction is initiated in the TME, characterized by the overproduction of H_2O_2 , low catalase activity and a weakly acidic pH.^{66,67} Chemodynamic therapy is specific to cancer cells because the Fenton reaction is significantly limited in a weakly alkaline environment, and the limited amount of hydrogen peroxide is observed in normal cells.⁶⁸ The Fenton reaction

Fig. 3. Chemodynamic therapy basis



leads to oxidative stress, and the reactive hydroxyl radical reacts with proteins, lipids, and DNA, disrupting their function and leading to cancer cell death.⁶⁵

Compared to PDT, CDT is more selective and is initiated by internal factors; therefore, it does not require external energy in the form of light and does not depend on local oxygen concentrations.^{69,70} Nevertheless, some factors limit the effectiveness of CDT. The first is the limited amount of endogenous H_2O_2 in cancer cells and the low catalytic efficiency of chemodynamic agents.⁶⁵ Another limitation is the reaction environment. Most chemodynamic agents, such as iron-based nanomaterials, transition metal ions, and metal-organic frameworks, catalyze Fenton and Fenton-like reactions better in a more acidic environment (pH 3.0–5.0) than in the TME (pH 6.0–7.0).^{65,71} Finally, overexpression of GSH in the TME significantly reduces the production of hydroxyl radicals, reducing the effectiveness of CDT.⁶⁵ Therefore, researchers have focused on designing new nanomaterials that increase the efficiency of CDT by modifying the TME, by lowering its pH, increasing H_2O_2 concentrations, and depleting GSH.

Lin et al. created nanoparticles consisting of mesoporous silica coated with manganese dioxide (MnO_2).⁷² After internalization into cancer cells, the MnO_2 envelope undergoes a redox reaction with GSH, resulting in the formation of the oxidized form of GSH (GSSG) and Mn^{2+} ions. Manganese ions in the presence of carbonate ions (HCO_3^-) react with H_2O_2 , forming hydroxyl radicals through a Fenton-like reaction. Therefore, MnO_2 plays a dual role. Its reaction with GSH lowers the intracellular pool, resulting in increased susceptibility of cancer cells to oxidative stress. The same reaction leads to the formation of Mn ions, which are responsible for ROS generation. The use of a mesoporous silica core, on the other hand, ensures the controlled release of the drug. It should be noted that a similar strategy has been used by many researchers.⁷³

Compared with the classic Fenton reaction catalyzed by Fe^{2+} ions, a Fenton-like reaction is catalyzed by Cu^+ ions and can be carried out with greater efficiency in a weakly acidic environment. However, because of the low redox potential of $\text{Cu}^+/\text{Cu}^{2+}$, Cu^+ ions are easily oxidized to Cu^{2+} .^{74,75} Ma et al. proposed the use of copper-amino acid mercaptide nanoparticles (Cu-Cys NPs).⁷⁶ After endocytosis into cancer cells, these nanoparticles oxidize GSH and the copper is reduced to Cu^+ ions. These ions react with hydrogen peroxide to form hydroxyl radicals. The use of Cu^{2+} ions not only increases the efficiency of ROS production but is also an effective way to reduce the ratio of GSH to oxidized GSH (GSSG). The GSH depletion strategy using transition metal ions, which are reduced by GSH to substrates for the Fenton-like reaction, has been used in many studies.^{77–90}

Chen et al. designed nanoparticles containing Fe_3O_4 and β -lapachone (Lapa).⁹¹ The first of these compounds is the source of Fe^{2+} ions, which participate in the Fenton reactions. Lapa undergoes a transition from quinone to hydroquinone in the futile cycle catalyzed by NADPH:quinone oxidoreductase-1 (NQO1). The overexpression of NQO1 in cancer cells, which occurs at a ratio of 2–100 times, results in greater selectivity for these cells when Lapa is used.⁹² The futile cycle of Lapa not only generates H_2O_2 , increasing the efficiency of CDT, but also significantly reduces the cellular concentration of NADPH (60 mol/Lapa mol/5 min).⁹³ Since NADPH is a coenzyme of GSH reductase, reduction in its amount interferes with the function of this GSSG-reducing enzyme. This leads to increased oxidative stress in cancer cells.

Limitations

Article selection bias is a possible limitation of this study. Due to the abundance of works on this review topic, despite every effort, some works that should have been cited may

Table 1. Glutathione depletion strategies during PDT and CDT

Type of therapy	Mode of action	Agent	References
PDT	conjugation with GSH	docohexaenoic acid	29
		pendant vinyl groups	30
		S-nitrosated human serum albumin	31
		curcumin	50
		cinnamaldehyde	51
		thiol metabolite of clopidogrel	63
		phenethyl isothiocyanate	94
		mesoporous polydopamine	95
		quinone methide	96
	GSH oxidation	ALA derivative with disulfide bond	36,97
		disulfide-containing imidazole	37
		hemin	98,99
		Cu ²⁺	87,88,100,101
		Mn ⁴⁺	89,102,103
		Fe ³⁺	84
		NO	104
	inhibition of GSH biosynthesis	erastin	46
		buthionine sulfoximine	105
CDT	conjugation with GSH	2-nitroimidazole and 1H-imidazole-4-carbonitrile	106
	GSH oxidation	Cu ²⁺	76,80,81,90,107,108
		Mn ⁴⁺	72,86,109
		Fe ³⁺	82,110
		NO	111
	decrease of GSH reductase activity	β-lapachone	91
	inhibition of GSH biosynthesis	triptolide	112

PDT – photodynamic therapy; CDT – chemodynamic therapy; GSH – glutathione; ALA – 5-aminolevulinic acid; Cu²⁺ – cupric ion; Mn⁴⁺ – tetravalent manganese ion; Fe³⁺ – ferric ion; NO – nitric oxide.



have been omitted. In addition, many of the papers used the same GSH depletion strategies, so the authors decided not to cite some of them.

Conclusions

Cancer remains a global health problem despite the constant development of new medicines. Numerous studies focused on developing new therapeutic strategies to increase the effectiveness of anticancer treatment. Methods, such as PDT or CDT, are characterized by an increased specificity and selectivity for cancer cells and reduced side effects compared to traditional chemo- and radiotherapy. Despite the undoubted advantages of these oxidative stress-increasing therapies, they face certain problems in clinical applications. One of the most important obstacles is the adaptation of cancer cells to an increased concentration of ROS by increasing the production of GSH. This requires the development of effective strategies to reduce the concentration of this thiol compound in cancer

cells (Table 1). A simple and direct way to deplete GSH is to use compounds that react with GSH to form stable derivatives or transform it into an oxidized form (GSSG). This is also the most common strategy used by scientists to develop new PDTs and CDTs, as presented in this paper. Although the main goal of GSH depletion in both PDT and CDT is to prevent its interaction with ROS generated by these therapies, it should be remembered that reductions in GSH levels by itself may initiate pathways leading to cancer cell death.

ORCID iDs

Daniel Wolny  <https://orcid.org/0000-0002-1453-7779>
 Mateusz Stojko  <https://orcid.org/0000-0001-8868-9495>
 Alicja Zajdel  <https://orcid.org/0000-0003-3016-3444>

References

1. Lv H, Zhen C, Liu J, Yang P, Hu L, Shang P. Unraveling the potential role of glutathione in multiple forms of cell death in cancer therapy. *Oxid Med Cell Longev*. 2019;2019:3150145. doi:10.1155/2019/3150145
2. Gorrini C, Harris IS, Mak TW. Modulation of oxidative stress as an anti-cancer strategy. *Nat Rev Drug Discov*. 2013;12(12):931–947. doi:10.1038/nrd4002

3. Kumar B, Koul S, Khandrika L, Meacham RB, Koul HK. Oxidative stress is inherent in prostate cancer cells and is required for aggressive phenotype. *Cancer Res.* 2008;68(6):1777–1785. doi:10.1158/0008-5472.CAN-07-5259
4. Diehn M, Cho RW, Lobo NA, et al. Association of reactive oxygen species levels and radioresistance in cancer stem cells. *Nature.* 2009;458(7239):780–783. doi:10.1038/nature07733
5. Gamcsik MP, Kasibhatla MS, Teeter SD, Colvin OM. Glutathione levels in human tumors. *Biomarkers.* 2012;17(8):671–691. doi:10.3109/1354750X.2012.715672
6. Chen HHW, Kuo MT. Role of glutathione in the regulation of cisplatin resistance in cancer chemotherapy. *Met Based Drugs.* 2010;2010:430939. doi:10.1155/2010/430939
7. Barattin R, Perrotton T, Trompier D, et al. Iodination of verapamil for a stronger induction of death, through GSH efflux, of cancer cells overexpressing MRP1. *Bioorg Med Chem.* 2010;18(17):6265–6274. doi:10.1016/j.bmc.2010.07.031
8. Habermann KJ, Grünwald L, Van Wijk S, Fulda S. Targeting redox homeostasis in rhabdomyosarcoma cells: GSH-depleting agents enhance auranofin-induced cell death. *Cell Death Dis.* 2017;8(10):e3067. doi:10.1038/cddis.2017.412
9. Lo M, Wang Y, Gout PW. The x cystine/glutamate antiporter: A potential target for therapy of cancer and other diseases. *J Cell Physiol.* 2008;215(3):593–602. doi:10.1002/jcp.21366
10. Yun SH, Kwok SJJ. Light in diagnosis, therapy and surgery. *Nat Biomed Eng.* 2017;1(1):0008. doi:10.1038/s41551-016-0008
11. Dolmans DEJGJ, Fukumura D, Jain RK. Photodynamic therapy for cancer. *Nat Rev Cancer.* 2003;3(5):380–387. doi:10.1038/nrc1071
12. Lovell JF, Liu TWB, Chen J, Zheng G. Activatable photosensitizers for imaging and therapy. *Chem Rev.* 2010;110(5):2839–2857. doi:10.1021/cr900236h
13. Cheng L, Wang C, Feng L, Yang K, Liu Z. Functional nanomaterials for phototherapies of cancer. *Chem Rev.* 2014;114(21):10869–10939. doi:10.1021/cr400532z
14. Yu W, Liu T, Zhang M, et al. O₂ economizer for inhibiting cell respiration to combat the hypoxia obstacle in tumor treatments. *ACS Nano.* 2019;13(2):1784–1794. doi:10.1021/acsnano.8b07852
15. Dos Santos AF, De Almeida DRQ, Terra LF, Baptista MS, Labriola L. Photodynamic therapy in cancer treatment; An update review. *J Cancer Metast Treat.* 2019;5:25. doi:10.20517/2394-4722.2018.83
16. Hou Z, Zhang Y, Deng K, et al. UV-emitting upconversion-based TiO₂ photosensitizing nanoplateform: Near-infrared light mediated in vivo photodynamic therapy via mitochondria-involved apoptosis pathway. *ACS Nano.* 2015;9(3):2584–2599. doi:10.1021/nn506107c
17. Li X, Kwon N, Guo T, Liu Z, Yoon J. Innovative strategies for hypoxic-tumor photodynamic therapy. *Angew Chem Int Ed.* 2018;57(36):11522–11531. doi:10.1002/anie.201805138
18. Agostinis P, Berg K, Cengel KA, et al. Photodynamic therapy of cancer: An update. *CA Cancer J Clin.* 2011;61(4):250–281. doi:10.3322/caac.20114
19. Ming L, Cheng K, Chen Y, Yang R, Chen D. Enhancement of tumor lethality of ROS in photodynamic therapy. *Cancer Med.* 2021;10(1):257–268. doi:10.1002/cam4.3592
20. Liu Y, Liu Y, Bu W, et al. Hypoxia induced by upconversion-based photodynamic therapy: Towards highly effective synergistic bio-reductive therapy in tumors. *Angew Chem Int Ed.* 2015;54(28):8105–8109. doi:10.1002/anie.201500478
21. Van Straten D, Mashayekhi V, De Bruijn H, Oliveira S, Robinson D. Oncologic photodynamic therapy: Basic principles, current clinical status and future directions. *Cancers (Basel).* 2017;9(2):19. doi:10.3390/cancers9020019
22. Zhou Z, Song J, Nie L, Chen X. Reactive oxygen species generating systems meeting challenges of photodynamic cancer therapy. *Chem Soc Rev.* 2016;45(23):6597–6626. doi:10.1039/C6CS00271D
23. Moore CM, Pendse D, Emberton M. Photodynamic therapy for prostate cancer: A review of current status and future promise. *Nat Rev Urol.* 2009;6(1):18–30. doi:10.1038/ncpuro1274
24. Wilson WR, Hay MP. Targeting hypoxia in cancer therapy. *Nat Rev Cancer.* 2011;11(6):393–410. doi:10.1038/nrc3064
25. Feng L, Cheng L, Dong Z, et al. Theranostic liposomes with hypoxia-activated prodrug to effectively destruct hypoxic tumors post-photodynamic therapy. *ACS Nano.* 2017;11(1):927–937. doi:10.1021/acsnano.6b07525
26. Nowis D, Makowski M, Stokłosa T, Legat M, Issat T, Gołab J. Direct tumor damage mechanisms of photodynamic therapy. *Acta Biochim Pol.* 2005;52(2):339–352. PMID:15990919.
27. Larue, Myrzakhmetov, Ben-Mihoub, et al. Fighting hypoxia to improve PDT. *Pharmaceuticals (Basel).* 2019;12(4):163. doi:10.3390/ph12040163
28. Kimani SG, Phillips JB, Bruce JI, MacRobert AJ, Golding JP. Antioxidant inhibitors potentiate the cytotoxicity of photodynamic therapy. *Photochem Photobiol.* 2012;88(1):175–187. doi:10.1111/j.1751-1097.2011.01022.x
29. Hu J, Wang T, Zhou L, Wei S. A ROS responsive nanomedicine with enhanced photodynamic therapy via dual mechanisms: GSH depletion and biosynthesis inhibition. *J Photochem Photobiol B.* 2020;209:111955. doi:10.1016/j.jphotobiol.2020.111955
30. Cao H, Zhong S, Wang Q, Chen C, Tian J, Zhang W. Enhanced photodynamic therapy based on an amphiphilic branched copolymer with pendant vinyl groups for simultaneous GSH depletion and Ce6 release. *J Mater Chem B.* 2020;8(3):478–483. doi:10.1039/C9TB02120E
31. Li W, Yong J, Xu Y, et al. Glutathione depletion and dual-model oxygen balance disruption for photodynamic therapy enhancement. *Colloids Surf B Biointerfaces.* 2019;183:110453. doi:10.1016/j.colsurf.2019.110453
32. Xie J, Wang S, Li Z, et al. 5-aminolevulinic acid photodynamic therapy reduces HPV viral load via autophagy and apoptosis by modulating Ras/Raf/MEK/ERK and PI3K/AKT pathways in HeLa cells. *J Photochem Photobiol B.* 2019;194:46–55. doi:10.1016/j.jphotobiol.2019.03.012
33. Tewari KM, Eggleston IM. Chemical approaches for the enhancement of 5-aminolevulinic acid-based photodynamic therapy and photodiagnosis. *Photochem Photobiol Sci.* 2018;17(11):1553–1572. doi:10.1039/c8pp00362a
34. Kim, Johnson RP, Chung CW, Jeong YI, Kang DH, Suh H. Poly(L-histidine)-tagged 5-aminolevulinic acid prodrugs: New photosensitizing precursors of protoporphyrin IX for photodynamic colon cancer therapy. *Int J Nanomed.* 2012;7:2497–2512. doi:10.2147/IJN.S29582
35. Fotinos N, Campo MA, Popowycz F, Gurny R, Lange N. 5-aminolevulinic acid derivatives in photomedicine: Characteristics, application and perspectives. *Photochem Photobiol.* 2006;82(4):994–1015. doi:10.1562/2006-02-03-IR-794
36. Li K, Dong W, Miao Y, Liu Q, Qiu L, Lin J. Dual-targeted 5-aminolevulinic acid derivatives with glutathione depletion function for enhanced photodynamic therapy. *J Photochem Photobiol B.* 2021;215:112107. doi:10.1016/j.jphotobiol.2020.112107
37. Meng X, Deng J, Liu F, et al. Triggered all-active metal organic framework: Ferroptosis machinery contributes to the apoptotic photodynamic antitumor therapy. *Nano Lett.* 2019;19(11):7866–7876. doi:10.1021/acsnanolett.9b02904
38. Forcina GC, Dixon SJ. GPX4 at the crossroads of lipid homeostasis and ferroptosis. *Proteomics.* 2019;19(18):1800311. doi:10.1002/pmic.201800311
39. Dixon SJ, Lemberg KM, Lamprecht MR, et al. Ferroptosis: An iron-dependent form of nonapoptotic cell death. *Cell.* 2012;149(5):1060–1072. doi:10.1016/j.cell.2012.03.042
40. Wang Y, Liu T, Li X, Sheng H, Ma X, Hao L. Ferroptosis-inducing nanomedicine for cancer therapy. *Front Pharmacol.* 2021;12:735965. doi:10.3389/fphar.2021.735965
41. Niu B, Liao K, Zhou Y, et al. Application of glutathione depletion in cancer therapy: Enhanced ROS-based therapy, ferroptosis, and chemotherapy. *Biomaterials.* 2021;277:121110. doi:10.1016/j.biomaterials.2021.121110
42. Tang H, Chen D, Li C, et al. Dual GSH-exhausting sorafenib loaded manganese-silica nanodrugs for inducing the ferroptosis of hepatocellular carcinoma cells. *Int J Pharm.* 2019;572:118782. doi:10.1016/j.ijpharm.2019.118782
43. Wang S, Li F, Qiao R, et al. Arginine-rich manganese silicate nanobubbles as a ferroptosis-inducing agent for tumor-targeted theranostics. *ACS Nano.* 2018;12(12):12380–12392. doi:10.1021/acsnano.8b06399
44. Tang H, Li C, Zhang Y, et al. Targeted manganese doped silica nano GSH-cleaner for treatment of liver cancer by destroying the intracellular redox homeostasis. *Theranostics.* 2020;10(21):9865–9887. doi:10.7150/thno.46771
45. An P, Gao Z, Sun K, et al. Photothermal-enhanced inactivation of glutathione peroxidase for ferroptosis sensitized by an autophagy promoter. *ACS Appl Mater Interfaces.* 2019;11(46):42988–42997. doi:10.1021/acsnano.9b16124

46. Zhu T, Shi L, Yu C, et al. Ferroptosis promotes photodynamic therapy: Supramolecular photosensitizer-inducer nanodrug for enhanced cancer treatment. *Theranostics*. 2019;9(11):3293–3307. doi:10.7150/thno.32867
47. Imran M, Ullah A, Saeed F, Nadeem M, Arshad MU, Suleria HAR. Curcumin, anticancer, & antitumor perspectives: A comprehensive review. *Crit Rev Food Sci Nutr*. 2018;58(8):1271–1293. doi:10.1080/10408398.2016.1252711
48. Liao W, Xiang W, Wang FF, Wang R, Ding Y. Curcumin inhibited growth of human melanoma A375 cells via inciting oxidative stress. *Biomed Pharmacother*. 2017;95:1177–1186. doi:10.1016/j.biopha.2017.09.026
49. Bahrami A, Atkin SL, Majeed M, Sahebkar A. Effects of curcumin on hypoxia-inducible factor as a new therapeutic target. *Pharmacol Res*. 2018;137:159–169. doi:10.1016/j.phrs.2018.10.009
50. Zhang Z, Wang R, Huang X, et al. Self-delivered and self-monitored chemo-photodynamic nanoparticles with light-triggered synergistic antitumor therapies by downregulation of HIF-1 α and depletion of GSH. *ACS Appl Mater Interfaces*. 2020;12(5):5680–5694. doi:10.1021/acsami.9b23325
51. Liu Y, Zhou Z, Liu Y, et al. H₂O₂-activated oxidative stress amplifier capable of GSH scavenging for enhancing tumor photodynamic therapy. *Biomater Sci*. 2019;7(12):5359–5368. doi:10.1039/C9BM01354G
52. Lewerenz J, Hewett SJ, Huang Y, et al. The cystine/glutamate antiporter system x_c⁻ in health and disease: From molecular mechanisms to novel therapeutic opportunities. *Antioxid Redox Signal*. 2013;18(5):522–555. doi:10.1089/ars.2011.4391
53. Wada F, Koga H, Akiba J, et al. High expression of CD 44v9 and xCT in chemoresistant hepatocellular carcinoma: Potential targets by sulfasalazine. *Cancer Sci*. 2018;109(9):2801–2810. doi:10.1111/cas.13728
54. Toyoda M, Kaira K, Ohshima Y, et al. Prognostic significance of amino-acid transporter expression (LAT1, ASCT2, and xCT) in surgically resected tongue cancer. *Br J Cancer*. 2014;110(10):2506–2513. doi:10.1038/bjc.2014.178
55. Sugano K, Maeda K, Ohtani H, Nagahara H, Shibutani M, Hirakawa K. Expression of xCT as a predictor of disease recurrence in patients with colorectal cancer. *Anticancer Res*. 2015;35(2):677–682. PMID:25667445.
56. Okuno S, Sato H, Kuriyama-Matsumura K, et al. Role of cystine transport in intracellular glutathione level and cisplatin resistance in human ovarian cancer cell lines. *Br J Cancer*. 2003;88(6):951–956. doi:10.1038/sj.bjc.6600786
57. Savaskan NE, Hahnen E, Eyüpoglu IY. The x cystine/glutamate antiporter (xCT) as a potential target for therapy of cancer: Yet another cytotoxic anticancer approach? *J Cell Physiol*. 2009;220(2):531–532. doi:10.1002/jcp.21795
58. Dixon SJ, Patel DN, Welsch M, et al. Pharmacological inhibition of cystine–glutamate exchange induces endoplasmic reticulum stress and ferroptosis. *eLife*. 2014;3:e02523. doi:10.7554/eLife.02523
59. Xie Y, Hou W, Song X, et al. Ferroptosis: process and function. *Cell Death Differ*. 2016;23(3):369–379. doi:10.1038/cdd.2015.158
60. Yang WS, Stockwell BR. Ferroptosis: Death by lipid peroxidation. *Trends Cell Biol*. 2016;26(3):165–176. doi:10.1016/j.tcb.2015.10.014
61. Zheng DW, Lei Q, Zhu JY, et al. Switching apoptosis to ferroptosis: Metal–organic network for high-efficiency anticancer therapy. *Nano Lett*. 2017;17(1):284–291. doi:10.1021/acs.nanolett.6b04060
62. Bogdan AR, Miyazawa M, Hashimoto K, Tsuji Y. Regulators of iron homeostasis: New players in metabolism, cell death, and disease. *Trends Biochem Sci*. 2016;41(3):274–286. doi:10.1016/j.tibs.2015.11.012
63. Wang Q, Sun M, Li D, et al. Cytochrome P450 enzyme-mediated auto-enhanced photodynamic cancer therapy of co-nanoassembly between clopidogrel and photosensitizer. *Theranostics*. 2020;10(12):5550–5564. doi:10.7150/thno.42633
64. Kazui M, Nishiya Y, Ishizuka T, et al. Identification of the human cytochrome P450 enzymes involved in the two oxidative steps in the bio-activation of clopidogrel to its pharmacologically active metabolite. *Drug Metab Dispos*. 2010;38(1):92–99. doi:10.1124/dmd.109.029132
65. Wang X, Zhong X, Liu Z, Cheng L. Recent progress of chemodynamic therapy-induced combination cancer therapy. *Nano Today*. 2020;35:100946. doi:10.1016/j.nantod.2020.100946
66. Gatenby RA, Gillies RJ. Why do cancers have high aerobic glycolysis? *Nat Rev Cancer*. 2004;4(11):891–899. doi:10.1038/nrc1478
67. Nishikawa M, Tamada A, Kumai H, Yamashita F, Hashida M. Inhibition of experimental pulmonary metastasis by controlling biodistribution of catalase in mice. *Int J Cancer*. 2002;99(3):474–479. doi:10.1002/ijc.10387
68. Sztatowski TP, Nathan CF. Production of large amounts of hydrogen peroxide by human tumor cells. *Cancer Res*. 1991;51(3):794–798. PMID:1846317.
69. Tang Z, Liu Y, He M, Bu W. Chemodynamic therapy: Tumour microenvironment-mediated Fenton and Fenton-like reactions. *Angew Chem Int Ed*. 2019;58(4):946–956. doi:10.1002/anie.201805664
70. Zhang C, Bu W, Ni D, et al. Synthesis of iron nanometallic glasses and their application in cancer therapy by a localized Fenton reaction. *Angew Chem Int Ed*. 2016;55(6):2101–2106. doi:10.1002/anie.201510031
71. Fu S, Yang R, Zhang L, et al. Biomimetic CoO@AuPt nanozyme responsive to multiple tumor microenvironmental clues for augmenting chemodynamic therapy. *Biomaterials*. 2020;257:120279. doi:10.1016/j.biomaterials.2020.120279
72. Lin L, Song J, Song L, et al. Simultaneous Fenton-like ion delivery and glutathione depletion by MnO₂-based nanoagent to enhance chemodynamic therapy. *Angew Chem Int Ed*. 2018;57(18):4902–4906. doi:10.1002/anie.201712027
73. Yang G, Ji J, Liu Z. Multifunctional MnO₂ nanoparticles for tumor microenvironment modulation and cancer therapy. *WIREs Nanomed Nanobiotechnol*. 2021;13(6):e1720. doi:10.1002/wnan.1720
74. Anandan S, Miyauchi M. Photocatalytic activity of Cu₂-grafted metal-doped ZnO photocatalysts under visible-light irradiation. *Electrochemistry*. 2011;79(10):842–844. doi:10.5796/electrochemistry.79.842
75. Soltani T, Lee BK. Enhanced formation of sulfate radicals by metal-doped BiFeO₃ under visible light for improving photo-Fenton catalytic degradation of 2-chlorophenol. *Chem Eng J*. 2017;313:1258–1268. doi:10.1016/j.cej.2016.11.016
76. Ma B, Wang S, Liu F, et al. Self-assembled copper–amino acid nanoparticles for in situ glutathione and H₂O₂ sequentially triggered chemodynamic therapy. *J Am Chem Soc*. 2019;141(2):849–857. doi:10.1021/jacs.8b08714
77. Wang Z, Liu B, Sun Q, et al. Fusiform-like copper(II)-based metal–organic framework through relief hypoxia and GSH-depletion co-enhanced starvation and chemodynamic synergistic cancer therapy. *ACS Appl Mater Interfaces*. 2020;12(15):17254–17267. doi:10.1021/acsami.0c01539
78. Cao S, Li X, Gao Y, et al. A simultaneously GSH-depleted bimetallic Cu(II) complex for enhanced chemodynamic cancer therapy. *Dalton Trans*. 2020;49(34):11851–11858. doi:10.1039/D0DT01742F
79. Fu L, Wan Y, Qi C, et al. Nanocatalytic theranostics with glutathione depletion and enhanced reactive oxygen species generation for efficient cancer therapy. *Adv Mater*. 2021;33(7):2006892. doi:10.1002/adma.202006892
80. Hu C, Cai L, Liu S, Liu Y, Zhou Y, Pang M. Copper-doped nanoscale covalent organic polymer for augmented photo/chemodynamic synergistic therapy and immunotherapy. *Bioconjug Chem*. 2020;31(6):1661–1670. doi:10.1021/acs.bioconjchem.0c00209
81. Wu H, Chen F, Gu D, You C, Sun B. A pH-activated autocatalytic nanoreactor for self-boosting Fenton-like chemodynamic therapy. *Nanoscale*. 2020;12(33):17319–17331. doi:10.1039/D0NR03135F
82. Wu H, Gu D, Xia S, Chen F, You C, Sun B. One-for-all intelligent core–shell nanoparticles for tumor-specific photothermal–chemodynamic synergistic therapy. *Biomater Sci*. 2021;9(3):1020–1033. doi:10.1039/D0BM01734E
83. Tang W, Gao H, Ni D, et al. Bovine serum albumin-templated nano-platform for magnetic resonance imaging-guided chemodynamic therapy. *J Nanobiotechnol*. 2019;17(1):68. doi:10.1186/s12951-019-0501-3
84. Wang B, Dai Y, Kong Y, et al. Tumor microenvironment-responsive Fe(III)–porphyrin nanotheranostics for tumor imaging and targeted chemodynamic-photodynamic therapy. *ACS Appl Mater Interfaces*. 2020;12(48):53634–53645. doi:10.1021/acsami.0c14046
85. Gu D, An P, He X, et al. A novel versatile yolk-shell nanosystem based on NIR-elevated drug release and GSH depletion-enhanced Fenton-like reaction for synergistic cancer therapy. *Colloids Surf B Biointerfaces*. 2020;189:110810. doi:10.1016/j.colsurfb.2020.110810
86. He H, Yang Q, Li H, et al. Hollow mesoporous MnO₂-carbon nanodot-based nanopatform for GSH depletion enhanced chemodynamic therapy, chemotherapy, and normal/cancer cell differentiation. *Microchim Acta*. 2021;188(4):141. doi:10.1007/s00604-021-04801-5

87. Chen M, Zhao S, Zhu J, et al. Open-source and reduced-expenditure nanosystem with ROS self-amplification and glutathione depletion for simultaneous augmented chemodynamic/photodynamic therapy. *ACS Appl Mater Interfaces*. 2022;14(18):20682–20692. doi:10.1021/acsami.2c01782
88. Li Y, He G, Fu LH, et al. A microneedle patch with self-oxygenation and glutathione depletion for repeatable photodynamic therapy. *ACS Nano*. 2022;16(10):17298–17312. doi:10.1021/acsnano.2c08098
89. Lu J, Mao Y, Feng S, et al. Biomimetic smart mesoporous carbon nanozyme as a dual-GSH depletion agent and O₂ generator for enhanced photodynamic therapy. *Acta Biomater*. 2022;148:310–322. doi:10.1016/j.actbio.2022.06.001
90. Shen WY, Jia CP, Liao LY, et al. Copper(II) complex enhanced chemodynamic therapy through GSH depletion and autophagy flow blockade. *Dalton Trans*. 2023;52(11):3287–3294. doi:10.1039/D2DT04108A
91. Chen Q, Zhou J, Chen Z, Luo Q, Xu J, Song G. Tumor-specific expansion of oxidative stress by glutathione depletion and use of a Fenton nano-agent for enhanced chemodynamic therapy. *ACS Appl Mater Interfaces*. 2019;11(34):30551–30565. doi:10.1021/acsami.9b09323
92. Ma X, Huang X, Moore Z, et al. Esterase-activatable β -lapachone pro-drug micelles for NQO1-targeted lung cancer therapy. *J Control Release*. 2015;200:201–211. doi:10.1016/j.jconrel.2014.12.027
93. Li LS, Bey EA, Dong Y, et al. Modulating endogenous NQO1 levels identifies key regulatory mechanisms of action of β -lapachone for pancreatic cancer therapy. *Clin Cancer Res*. 2011;17(2):275–285. doi:10.1158/1078-0432.CCR-10-1983
94. Hu H, Chen J, Yang H, et al. Potentiating photodynamic therapy of ICG-loaded nanoparticles by depleting GSH with PEITC. *Nanoscale*. 2019;11(13):6384–6393. doi:10.1039/C9NR01306G
95. Hu H, Liu X, Hong J, et al. Mesoporous polydopamine-based multifunctional nanoparticles for enhanced cancer phototherapy. *J Colloid Interface Sci*. 2022;612:246–260. doi:10.1016/j.jcis.2021.12.172
96. Jung E, Kwon S, Song N, et al. Tumor-targeted redox-regulating and antiangiogenic phototherapeutics nanoassemblies for self-boosting phototherapy. *Biomaterials*. 2023;298:122127. doi:10.1016/j.biomaterials.2023.122127
97. Li K, Dong W, Qiu L, et al. A new GSH-responsive prodrug of 5-aminolevulinic acid for photodiagnosis and photodynamic therapy of tumors. *Eur J Med Chem*. 2019;181:111582. doi:10.1016/j.ejmech.2019.111582
98. Chen J, Chen F, Zhang L, et al. Self-assembling porphyrins as a single therapeutic agent for synergistic cancer therapy: A one stone three birds strategy. *ACS Appl Mater Interfaces*. 2021;13(24):27856–27867. doi:10.1021/acsami.1c04868
99. Xiao X, Chen M, Zhang Y, et al. Hemin-incorporating DNA nanozyme enabling catalytic oxygenation and GSH depletion for enhanced photodynamic therapy and synergistic tumor ferroptosis. *J Nanobiotechnol*. 2022;20(1):410. doi:10.1186/s12951-022-01617-0
100. Wang Y, Wu W, Liu J, et al. Cancer-cell-activated photodynamic therapy assisted by Cu(II)-based metal–organic framework. *ACS Nano*. 2019;13(6):6879–6890. doi:10.1021/acsnano.9b01665
101. Xie Z, Liang S, Cai X, et al. O₂-Cu/ZIF-8@Ce6/ZIF-8@F127 composite as a tumor microenvironment-responsive nanoplat-form with enhanced photo-/chemodynamic antitumor efficacy. *ACS Appl Mater Interfaces*. 2019;11(35):31671–31680. doi:10.1021/acsami.9b10685
102. Fan H, Yan G, Zhao Z, et al. A smart photosensitizer–manganese dioxide nanosystem for enhanced photodynamic therapy by reducing glutathione levels in cancer cells. *Angew Chem Int Ed*. 2016;55(18):5477–5482. doi:10.1002/anie.201510748
103. Zhu J, Xiao T, Zhang J, et al. Surface-charge-switchable nanoclusters for magnetic resonance imaging-guided and glutathione depletion-enhanced photodynamic therapy. *ACS Nano*. 2020;14(9):11225–11237. doi:10.1021/acsnano.0c03080
104. Deng Y, Jia F, Chen S, et al. Nitric oxide as an all-rounder for enhanced photodynamic therapy: Hypoxia relief, glutathione depletion and reactive nitrogen species generation. *Biomaterials*. 2018;187:55–65. doi:10.1016/j.biomaterials.2018.09.043
105. Lee HM, Kim DH, Lee HL, Cha B, Kang DH, Jeong YI. Synergistic effect of buthionine sulfoximine on the chlorin e6-based photodynamic treatment of cancer cells. *Arch Pharm Res*. 2019;42(11):990–999. doi:10.1007/s12272-019-01179-0
106. Li Y, Zhao P, Gong T, et al. Redox dyshomeostasis strategy for hypoxic tumor therapy based on DNAzyme-loaded electrophilic ZIFs. *Angew Chem Int Ed*. 2020;59(50):22537–22543. doi:10.1002/anie.202003653
107. Zhang WX, Hao YN, Gao YR, Shu Y, Wang JH. Mutual benefit between Cu(II) and polydopamine for improving photothermal–chemodynamic therapy. *ACS Appl Mater Interfaces*. 2021;13(32):38127–38137. doi:10.1021/acsami.1c12199
108. Jia S, Ke S, Tu L, et al. Glutathione/pH-responsive copper-based nanoplat-form for amplified chemodynamic therapy through synergistic cycling regeneration of reactive oxygen species and dual glutathione depletion. *J Colloid Interface Sci*. 2023;652:329–340. doi:10.1016/j.jcis.2023.08.043
109. Xu X, Zhang R, Yang X, et al. A honeycomb-like bismuth/manganese oxide nanoparticle with mutual reinforcement of internal and external response for triple-negative breast cancer targeted therapy. *Adv Healthc Mater*. 2021;10(18):2100518. doi:10.1002/adhm.202100518
110. Yang X, Wang L, Guo S, et al. Self-cycling free radical generator from LDH-based nanohybrids for ferroptosis-enhanced chemodynamic therapy. *Adv Healthc Mater*. 2021;10(18):2100539. doi:10.1002/adhm.202100539
111. Yu W, Jia F, Fu J, et al. Enhanced transcutaneous chemodynamic therapy for melanoma treatment through cascaded Fenton-like reactions and nitric oxide delivery. *ACS Nano*. 2023;17(16):15713–15723. doi:10.1021/acsnano.3c02964
112. Huang Y, Wu S, Zhang L, Deng Q, Ren J, Qu X. A metabolic multistage glutathione depletion used for tumor-specific chemodynamic therapy. *ACS Nano*. 2022;16(3):4228–4238. doi:10.1021/acsnano.1c10231

Acute kidney injury during transplantation and the role of inflammasomes: A brief review

Klaudia Szymanek^{1,B,D}, Karolina Tądel^{2,E}, Iwona Bil-Lula^{2,A,B,D–F}

¹ Students' Scientific Association at Division of Clinical Chemistry and Laboratory Hematology, Department of Medical Laboratory Diagnostics, Faculty of Pharmacy, Wrocław Medical University, Poland

² Division of Clinical Chemistry and Laboratory Hematology, Department of Medical Laboratory Diagnostics, Faculty of Pharmacy, Wrocław Medical University, Poland

A – research concept and design; B – collection and/or assembly of data; C – data analysis and interpretation;

D – writing the article; E – critical revision of the article; F – final approval of the article

Advances in Clinical and Experimental Medicine, ISSN 1899–5276 (print), ISSN 2451–2680 (online)

Adv Clin Exp Med. 2025;34(7):1223–1236

Address for correspondence

Iwona Bil-Lula

E-mail: iwona.bil-lula@umw.edu.pl

Funding sources

None declared

Conflict of interest

None declared

Received on September 28, 2023

Reviewed on April 29, 2024

Accepted on July 1, 2024

Published online on November 6, 2024

Abstract

The increasing demand for an effective therapeutic modality in the form of organ transplantation leads to the need to improve the long-term outcomes of the process. Ischemia/reperfusion injuries (IRI) are an integral part of the kidney transplantation process, contributing to inflammation, oxidative stress and activation of the immune system. Inflammasomes, as a component of the immune response, in the form of inflammatory mediators during infection or tissue damage, initiate cell death called pyroptosis. In this context, we have defined the process of inflammasome activation in response to IRI, which is a potential cause of early kidney rejection due to increased susceptibility of the kidneys to ischemia. This review focuses on analyzing the modulation of inflammasome activity in kidney transplants and the activation of the NLRP3 inflammasome as a crucial element of kidney injury during the transplantation procedure, which could be a potential target for future preventive/therapeutic strategies.

Key words: organ transplantation, ischemia/reperfusion injury, inflammatory process, inflammasome, NLRP3

Cite as

Szymanek K, Tądel K, Bil-Lula I. Acute kidney injury during transplantation and the role of inflammasomes: A brief review. *Adv Clin Exp Med.* 2025;34(7):1223–1236. doi:10.17219/acem/190676

DOI

10.17219/acem/190676

Copyright

Copyright by Author(s)

This is an article distributed under the terms of the Creative Commons Attribution 3.0 Unported (CC BY 3.0) (<https://creativecommons.org/licenses/by/3.0/>)

Introduction

Organ transplants, including kidney transplants, are one of the greatest achievements of modern medicine.¹ The etymology of the term “transplantation” comes from the Latin word *transplantare*, meaning “to graft” or “transfer”. The mentioned concept is defined as “the transplantation of an entire organ or only a specific part, designated tissue, or cells from one body to another or within the same body”.² This dictionary definition is consistent with the one proposed by the World Health Organization (WHO), which adds the therapeutic function of restoring organ function.³ Understanding the concept of transplantation according to both mentioned sources is also accepted in the literature.^{4,5}

The 1st successful kidney transplant was performed in 1954 on identical twins. Currently, there is an increased demand for kidney transplants among patients, resulting in a higher number of transplants performed in Poland and worldwide.¹ According to the latest data from Poltransplant, 2,058 people were enrolled for a transplant procedure in 2021, of whom 749 underwent the procedure.⁶

Types of kidney transplants

The literature divides kidney transplants into 3 main groups: autologous, xenogeneic and allogeneic. Autologous transplantation, also known as autograft, involves the removal of a kidney and its re-implantation.^{4,7} Xenogeneic transplantation is performed between 2 different species. Challenges in xenotransplantation arise from the differences between the 2 species, which are related to the distinct structures of coagulation proteins, the occurrence of inflammatory reactions in the recipient's body and the risk of virus transmission. The utilization of this type of transplantation requires further research before becoming an alternative to kidney allograft.⁸

Allogeneic transplantation is antagonistic to xenogeneic transplantation. This is the most widespread and involves transplantation between a donor and recipient of the same species.⁴

Another criterion for classification is the origin of the organ. Transplantology allows for the transplantation of a kidney from either a living or deceased donor.⁹ Kidneys from living donors can come from related individuals and anonymous individuals. An anonymous donor can donate their organ to a specified recipient or the first recipient on the waiting list for transplantation.¹⁰

A crossmatch transplant is used in cases of immunological mismatch between the donor and recipient. This method involves the exchange of organs between 2 pairs. A specific variation of crossmatch transplant is a chain transplant, which involves more than 2 pairs in the transplant process.^{10,11}

Kidney transplantation as a therapeutic method

Currently, the number of patients suffering from severe kidney diseases is continuously increasing. Lifestyle diseases such as type 2 diabetes (T2D), hypertension and obesity are predisposing factors for the development of chronic kidney disease (CKD). The diagnosis is established based on an estimated glomerular filtration rate (eGFR) value below 60 mL/min/1.73 m², abnormalities detected in urine tests, as well as kidney structure abnormalities observed through imaging and/or histopathological examinations, that persist for more than 3 months.¹² The progressive course of the disease may be associated with a steady decline in glomerular filtration efficiency. Estimated glomerular filtration rate values below 15 mL/min/1.73 m² qualify for the diagnosis of end-stage renal disease (ESRD). This stage, with a range of complications such as metabolic disorders, water-electrolyte disturbances, as well as cardiovascular (CV) disorders, requires renal replacement therapy (RRT). Despite the use of modern hemodialysis techniques, mortality among such patients ranges from 20% to 50% within 24 months.¹³ A significantly longer survival and improved quality of life compared to dialysis therapy are achieved by transplanting a failing organ. The greatest benefits are observed in patients with diabetes, especially young ones. Patients aged 20–39 years and treated with dialysis have an average life expectancy of 8 years, compared to 25 years after transplantation.^{14,15} Preemptive organ transplantation significantly extends the survival time of patients and transplant efficacy while reducing the risks of adverse side effects of dialysis. It also allows avoiding the need to create an arteriovenous fistula (AVF) for hemodialysis or implanting a catheter for peritoneal dialysis.¹⁶

The conditions for achieving the expected results of RRT are the appropriate qualification of the patient for transplantation, done through health assessment and the identification of contraindications.¹⁷

An essential clinical aspect in achieving therapeutic benefits from a transplant is immunologic compatibility. Antibodies directed against human leukocyte antigen (HLA) and red blood cells antigens (ABO) incompatibilities between the donor and recipient initiate rejection of the graft in approx. 30% of cases. For many years, ABO incompatibility was an absolute contraindication for transplantation. The reaction of iso-agglutinins with ABO blood group antigens induces complement system activation.¹⁸ The 2nd important element in donor-recipient selection based on immunological factors is minimal HLA mismatch, absence of panel reactive antibodies (PRA) and negative results in the donor lymphocyte crossmatch with the recipient's serum. These methods provide an opportunity to detect donor-specific antibodies (DSA), allowing for risk stratification of graft rejection.¹⁹ Removal of circulating antibodies or a reduction in their production are known

as desensitization processes, making transplantation acceptable despite partial compatibility. This effect is mainly achieved through plasmapheresis or immunoadsorption (IA). An alternative for immunologically incompatible pairs is the possibility of undergoing crossmatch/chain transplant, as described above.^{18,19}

Appropriate immunosuppression is a key element in maintaining the function of the transplanted organ while preventing rejection. Currently, a treatment regimen combining several medications is used, achieving an appropriate level of immunosuppression while reducing the risk of drug toxicities.²⁰

Transplantation efficacy and complications

In recent years, the effectiveness of transplantation, particularly proper graft function, has improved. However, improvements in long-term outcomes remain a challenge in the field of transplantology.²¹ In Poland, according to data from Poltransplant, the 5-year patient survival rate (2001–2015) was 88%, while the 10-year survival rate was 74%.⁶ The most common factors that negatively affect allografts in the 1st year after transplantation include CV failure, infections and acute rejection (AR). After the 1st year, chronic rejection contributes to the loss of proper kidney function.²² Episodes of organ rejection can be caused by cell-mediated responses involving T lymphocytes or the presence of antibodies, such as ABMR.²³ Delayed graft function (DGF), which lacks a precise definition, is associated with acute kidney injury (AKI) requiring dialysis therapy.²⁴ The incidence of DGF after deceased-donor kidney transplants ranges from 5% to 50%, with an increasing trend.²⁵ Chronic kidney transplant rejection (CKTR) is described by progressive deterioration of graft function, usually emerging 1 year after transplant, along with hypertension and proteinuria. Chronic kidney transplant rejection typically occurs in patients with insufficient immunosuppression; however, the main cause remains the sustained allogeneic immune response.²⁶

Technological advancements and the development of surgical techniques have significantly reduced adverse effects associated with the operation. These mainly involve vascular complications and urological complications.^{27,28}

Acute kidney injuries in the transplant process

The transplanted organ is predisposed to multiple injuries related to the body's immune response, toxicity resulting from pharmacotherapy or ischemia/reperfusion (I/R) injuries (IRI),²⁹ which will be further discussed in the context of this study, given the subject of the research conducted.

Ischemia/reperfusion injuries are defined as a series of cellular processes consisting of 2 distinct stages: ischemia – following the cessation of blood flow to the organ – and the action of restoring the flow of blood to the organ, otherwise known as reperfusion. Paradoxically, reperfusion exacerbates the injury by activating various biochemical mechanisms. These processes lead to endothelial cell damage, contributing, among other things, to the generation of reactive oxygen species (ROS) and activation of neutrophils and platelets, which are significant clinical problems during myocardial infarction (MI), ischemic stroke and AKI.^{30,31} There is a higher frequency of IRI in donors after cardiac death (DCDs) and expanded criteria donors (ECDs), which correlates with a longer warm ischemia time (WIT).³² Modern transplantology defines WIT as the period counted from the time the organ is dissected free from the donor until it is cooled (WIT I). Subsequently, there is a cold ischemia time (CIT) during kidney preservation in a hypothermic preservation solution, followed by the 2nd episode of warm ischemia during organ implantation in the recipient (WIT II).^{33,34} A prolonged CIT contributes to DGF and potentially shortens the long-term survival of the graft. The DCDs are particularly susceptible to the negative consequences of CIT; hence, this period should be minimized.³⁵

Mechanism of injury

Ischemia/reperfusion injuries are associated with vascular dysfunction, leading to increased vascular permeability and recruitment of inflammatory cells, contributing to multiple injuries.³⁶ Insufficient exposure of cells to oxygen initiates a metabolic shift to anaerobic metabolism, accompanied by tissue acidosis. The resulting acidosis, associated with lactate-dependent adenosine triphosphate (ATP) production, is due to the accumulation of lactic acid that is not removed by the circulation. The change in the direction of ATP synthase, with a noticeable increased hydrolysis, results in a decrease in intracellular ATP levels and the accumulation of ATP metabolites, such as hypoxanthine. These processes lead to negative consequences, including destabilization of lysosomal membranes, leakage of lysosomal enzymes, and subsequent cell structure breakdown.^{31,37} To compensate for the disturbed acid-base and water-mineral balances, the activity of the Na⁺-K⁺-ATPase ion pump is inhibited, with a simultaneous increase in the role of the Na⁺/H⁺ exchanger, contributing to an intracellular increase in sodium ions and water, leading to osmotic swelling. Dysfunction of the Na⁺/Ca²⁺ pump leads to increased Ca²⁺ levels, resulting in the activation of calcium-dependent proteases, such as calpains, upon reperfusion. The resulting calcium overload initiates the synthesis of ROS (Fig. 1).^{37,38} During reperfusion, the mitochondrial burst of ROS is responsible for adverse protein carbonylation and lipid peroxidation.

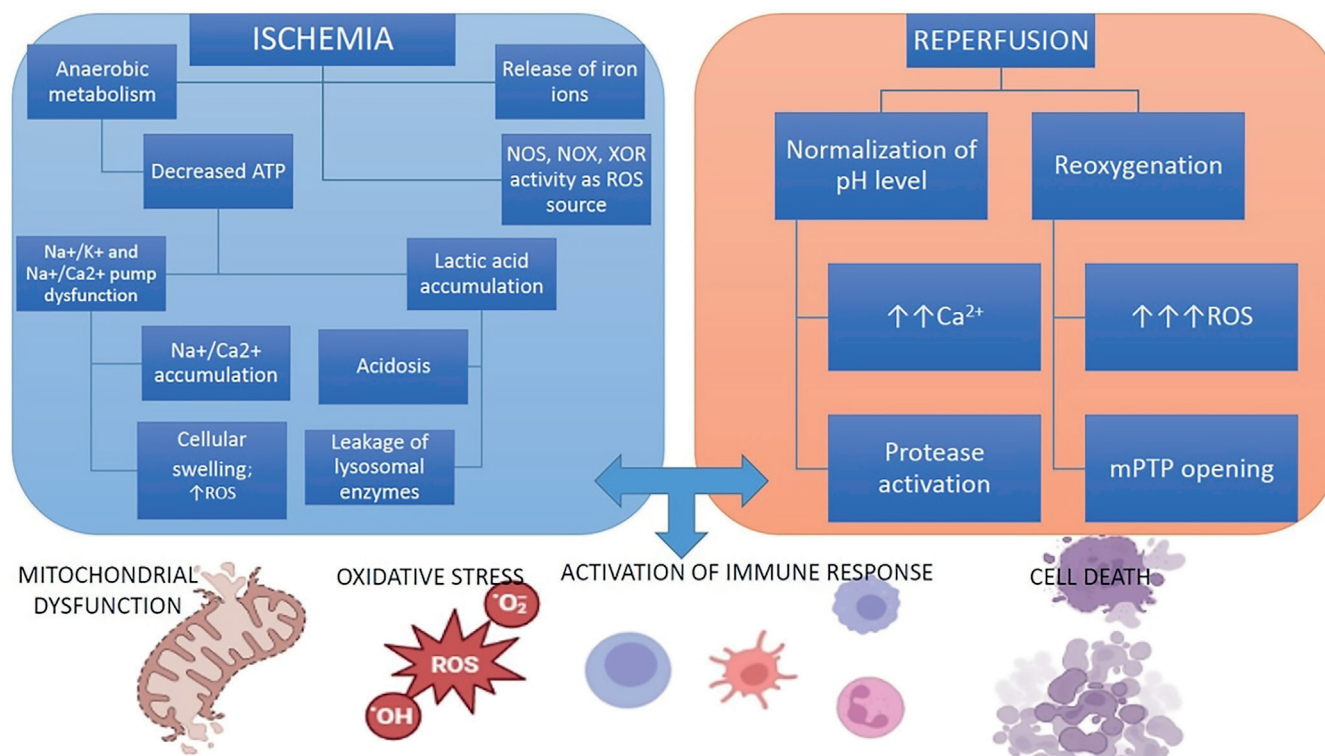


Fig. 1. Simplified diagram of the effect of ischemia/reperfusion on the cell

ROS – reactive oxygen species; NOS – nitric oxide synthase; NOX – NADPH oxidases; XOR – xanthine oxidoreductase; mPTP – mitochondrial mega-channel PTP.³⁹

Simultaneously, an inflammatory response is initiated, activating cell adhesion receptors. Neutrophils migrate through the endothelial wall into the tissue parenchyma, releasing cytotoxic mediators such as tumor necrosis factor (TNF) and interleukins (ILs), and directly or indirectly leading to the production of highly reactive species such as superoxide anion ($O_2^{\cdot-}$), hydrogen peroxide (H_2O_2) and peroxynitrite ($ONOO^-$). Normalization of pH affects calpain activation along with the sustained high calcium levels, contributing to the opening of the mitochondrial permeability transition pore (mPTP) and the release of cytochrome C enzymes, inducing cell death through apoptosis and necrosis.^{39,40}

Mitochondria play a significant role in the cascade of kidney injuries and other organ injuries resulting from I/R. During ischemia, ATP hydrolysis leads to an increase in free inorganic phosphate, which increases membrane permeability. After 60 min of WIT, the electron transport system complexes show reduced activity, resulting in the reduction of iron-sulfur proteins associated with complex I (NADH dehydrogenase) or complex II (succinate dehydrogenase) of the electron transport chain, leading to the release of iron ions (Fe^{2+}), reduction of hydrogen peroxide (H_2O_2) and ROS generation.⁴¹ Further conformational changes in the complexes during acute ischemia lead to their inhibition and arrest of electron flow. During reperfusion, the availability of oxygen and energetic substrates fuels oxidative metabolism, leading to a significant increase in electron leakage through the mitochondria compared to normal function levels.^{42,43} Matrix

metalloproteinases (MMPs) demonstrate a significant impact on kidney injury during transplantation by degrading extracellular matrix (ECM) components, responsible for disrupting the integrity of tissues and facilitating inflammatory cell infiltration. This enzymatic activity intensifies tissue damage and promotes fibrosis, complicating the recovery process post-transplant.⁴⁴ Dendritic cells (DCs) act as a link between innate and adaptive immune responses, directly through antigen presentation to B and T cells or indirectly through cytokine signaling. In the context of kidney transplantation, $CD4^+$ T lymphocytes play a crucial role in the pathophysiology. Normally, T cell activation occurs through antigen binding, but the effects of ROS and cytokines on this process were also demonstrated. The required antigen presentation by DCs or B cells was targeted in therapy, where the blockade of the costimulatory system inhibited T cell activation and alleviated IRI in animal models.⁴⁵

Cellular damage as a result of I/R triggers various types of cell death, including apoptosis, necrosis and autophagy. Renal I/R initiate apoptosis in proximal tubular cells.⁴⁶ Caspases, which are serine proteases, act as the main regulators and molecular effectors activated by pro-apoptotic stimuli (dependent on either the intrinsic mitochondrial pathway or death receptors), leading to the initiation of events that result in the release of mitochondrial cytochrome c into the cytosol, chromosomal DNA fragmentation, and morphological changes that are typical of apoptosis.⁴⁷ Autophagy is a process involving self-degradation and the rebuilding of damaged organelles

and proteins, protecting the cell from apoptosis after AKI and supporting regeneration. Autophagy, involving intracellular lysosomal degradation, is a series of catabolic processes, starting with a small membrane phagophore in the cytoplasm, then elongating to become, at the final stage, a double-membrane structure called an autophagosome, which fuses with lysosomes to form an autophagolysosome. Activated mammalian target of rapamycin (mTOR) signaling leads to the degradation of intracellular components, transporting them back to the cytoplasm for the reuse of macromolecules. Prolonged autophagy activation, however, can have adverse effects after an ischemic incident, triggering pathways leading to kidney cell death and exacerbating kidney injury (KI).⁴⁸ The use of murine models with deficiencies of autophagy-related (ATG) proteins that play a crucial role in autophagosome formation to study the effect of autophagy in I/R helped more definitively demonstrate the protective function of this process in the preservation of tubular integrity.⁴⁹

Markers of kidney injury during transplantation

There is a continuous need to define new markers used in routine monitoring of patients to serve as warning signals at different time points during transplantation.⁵⁰ Currently, the gold standard for assessing kidney function is eGFR, which is calculated based on serum creatinine levels. However, due to the influence of various additional factors, such as diet, muscle mass, metabolism, and sex, serum creatinine measurements have limited utility. In addition, creatinine levels will increase in 50% of renal failure and AKI and may not reflect renal tubular damage.⁵¹ Cystatin C is another commonly used functional biomarker of glomerular filtration, with increased sensitivity in detecting early renal dysfunction (within 24 h) compared to serum creatinine.⁵² The most promising new biomarkers, as reflected in the literature, with the clinical application are neutrophil gelatinase-associated lipocalin (NGAL) and kidney injury molecule-1 (KIM-1).⁵⁰

Neutrophil gelatinase-associated lipocalin is a protein produced by cells of the gastrointestinal, respiratory and immune systems, hepatocytes, and also by renal distal tubular epithelial cells. Toxic KI and I/R lead to the increased urinary excretion of NGAL, making it one of the earliest markers of KI. During acute tubular injury, NGAL also plays a protective role by enhancing autophagy in distal tubular cells, inhibiting apoptosis and inducing regeneration. Recently, attention has been drawn to the use of NGAL as a marker for CKD, including diabetic nephropathy, as well as a marker for CV risk. In kidney transplantation, NGAL, measured in the early post-transplant period, is considered a predictor of DGF.^{53,54} Studies revealed lower urine NGAL (uNGAL) levels in kidney transplant recipients in the early days after transplantation, which,

in combination with other parameters, serves as a helpful marker in the early assessment of kidney function.^{55,56} Moreover, both uNGAL levels and serum NGAL levels were found to be useful in determining and predicting early-stage KI.^{57,58} The lack of standardization of the measurements, the excretion of a large amount of urine and its dilution, as well as the induction of NGAL by some drugs such as cephalosporins, cisplatin and bisphosphonates limit its clinical application.^{53,59}

The 2nd widely documented marker is KIM-1, a transmembrane type I glycoprotein, a sensitive and reproducible biomarker of AKI with nephrotoxic and ischemic origins. It is expressed on the surface of the renal proximal tubular epithelial cells (PTECs). Its extracellular domain is cleaved by metalloproteinases and secreted into the urine in response to hypoxia or damage to the renal tubules.⁵⁹ The use of KIM-1 levels is currently being investigated for monitoring kidney transplant recipients, contributing to the early detection of organ rejection.^{59,60}

Interleukin 18, a pro-inflammatory cytokine, is activated by caspase-1. In healthy individuals, serum and urine levels remain generally low; however, these levels significantly increase in damaged kidney tissues. Interleukin-18 is often measured as a mediator and biomarker of ischemic tissue damage causing AKI.⁵¹

YKL-40 is a glycoprotein that plays an important role in tissue damage, inflammation, tissue remodeling, and protection against apoptosis. According to studies, YKL-40 influences organ repair mechanisms after ischemic injury in mice, making it a potentially useful marker for injury in transplants and as a prognostic marker for assessing the suitability of donor kidneys for transplantation.^{61,62}

Fatty acid-binding protein (FABP) is a cytoplasmic protein involved in fatty acid metabolism, contributing to the reduction of oxidative stress during I/R. Its highest expression is found in the distal tubular cells, making it a major marker of injury in the transplanted organ. Its levels in perfusion solutions were found to correlate with high vascular resistance and early graft dysfunction; however, their sensitivity and specificity are insufficient to make decisions about graft rejection.⁶³

In several experimental and clinical models, the utility of urine biomarkers such as uNGAL, urinary KIM-1 (uKIM-1), urinary IL-18 (uIL-18), and urinary FABP (uFABP) was identified in AKI and/or IRI.⁶⁴

A promising kidney-related biomarker is the Klotho protein. It exhibits diverse physiological actions, such as reducing oxidative stress and inhibiting the apoptosis and fibrotic processes. During I/R, Klotho is an early biomarker of AKI and shows decreased levels in urine and blood, preceding the rise in creatinine levels. Furthermore, in studies on its expression, Klotho correlated with eGFR 1 week after transplantation. Albuminuria, certain medications and local or systemic inflammation can reduce its expression. However, the standardization of soluble Klotho measurement methods remains an unresolved issue, necessitating

further research on the potential use of Klotho as a marker for AKI.^{65,66}

A major challenge still lies in implementing discovered biomarkers into clinical practice due to the lack of standardized guidelines for method validation and the complexity and multifactorial nature of injuries. Larger, multicenter validation studies are necessary before new solutions can be widely used in practice.⁶⁷

Methods of injury prevention

Reducing the effect of IRI during the transplantation process involves several approaches: proper preparation of the donor and recipient, minimizing CIT and optimizing perfusion of the transplanted organ. Recommended supplementation for the recipient includes Thymoglobulin (Sanofi, Paris, France), whose short-term effectiveness in preventing the risk of AR is widely documented in the literature.^{31,68}

Protein Klotho and its role in reducing the expression of MMPs provide an alternative for kidney protection during transplantation. Matrix metalloproteinases, as proteolytic enzymes, can degrade extracellular proteins and play a crucial role in the remodeling of the ECM.⁶⁹ Therefore, the use of MMP inhibitors may demonstrate a protective effect on kidney grafts, making it a subject for further research.^{70,71} Klotho can protect against both AKI and CKD through gene therapy or administration of its soluble form, reducing unfavorable treatment outcomes regardless of the etiology, as shown in preclinical studies. Research findings support the protective protein concept; however, its clinical application in humans remains uncertain and clinical efficacy needs confirmation.⁶⁵

Innovative techniques continue to be a challenge and a focus for researchers in the field of graft protection. In one of the latest studies, an electric field was used to activate Na⁺/K⁺ pumps, thus maintaining optimal ATP levels. In murine AKI models during WIT and CIT, this technique reduced KI, suggesting its potential usefulness in minimizing allograft dysfunction.⁷²

Inflammasome

In response to molecular patterns, a protein complex called the inflammasome coordinates the body's immune response to engage protective mechanisms against infectious agents and initiates them during physiological disturbances. Inflammasome activation is part of the innate immune process, leading to the secretion of pro-inflammatory cytokines such as IL-1 β and IL-18, thus participating in the inflammatory process.⁷³ Mature IL-1 β is a potent mediator in various immune reactions, recruiting and shaping immune system cells to the site of infection, while IL-18 is responsible for producing interferon gamma

(IFN- γ) and enhancing the cytolytic activity of NK cells and T lymphocytes. Active caspase, which is a product of inflammasome assembly, contributes to the secretion of interleukins and cell death, known as pyroptosis, exerting a significant effect on the defense against bacteria and viruses.⁷⁴

Various stimuli, including pathogen-associated molecular patterns (PAMPs) and damage-associated molecular patterns (DAMPs), activate inflammasome formation processes through pattern recognition receptors (PRRs), which are regarded as sensors. In most cases, each inflammasome contains an adaptor protein called an apoptosis-associated speck-like protein containing a CARD (ASC) and a procaspase enzyme that acts as an effector. Currently, 5 main representatives of PRRs have been identified: NLRP1, NOD-like receptor family pyrin domain-containing 3 (NLRP3), NLRC4 (belonging to the nucleotide oligomerization domain (NOD)-like receptor family – NLR), pyrin, and absent in melanoma 2 (AIM2), which serve as the basis for inflammasome assembly.^{75,76} Inflammasomes represented by these 5 sensors, known as canonical inflammasomes, can directly activate caspase-1 and are found in many tissues. Their presence is increased in bone marrow, lymphoid tissues and immune cells such as neutrophils, monocytes and macrophages. Furthermore, NLRP3 inflammasomes are activated in endothelial, epithelial and mesenchymal cells. Non-canonical inflammasomes participate in the activation of caspase-4/5 (in humans) and -11 (in mice) in response to lipopolysaccharides (LPSs) of Gram-negative bacteria. Recently, several new intracellular complexes have been discovered: NLRP6, NLRP7, NLRP12, and interferon gamma-inducible protein 16 (IFI16), whose activation mechanisms require further research.^{77,78}

Structurally, members of the NLR family consist of an N-terminal pyrin domain – PYD (for NLRPs) or a caspase recruitment domain – CARD (for NLRCs), a central nucleotide-binding oligomerization domain called NACHT, and C-terminal leucine-rich-repeats (LRRs). The NLR activation triggers a rapid oligomerization process, leading to the recruitment and binding of inactive pro-caspase-1, directly (NLRC4) or via the adaptor protein ASC, which is typical of NLRP3.⁷⁹ Different inflammasomes may exhibit differences in overall structure. Unlike NLRP3 and AIM2, NLRC4 representatives may contain only a CARD domain, not requiring the ASC domain for procaspase recruitment. On the other hand, AIM2 belongs to the AIM2-like receptor family (ALR) possessing 2 main components – HIN200 and PYD.⁸⁰

A peptidoglycan fragment derived from both Gram-positive and Gram-negative bacteria directly binds to human NLRP1, causing its structural change. It plays a significant role in human keratinocytes, where UVB radiation induces activation, contributing to skin inflammation and increasing susceptibility to cancer development.⁸¹ The NLRC4 inflammasome responds to bacterial infections, during which, after ligand binding by the NAIP part, it initiates

the assembly of the NAIP/NLRC4 inflammasome. Due to its ability to recognize host DNA, AIM2 is crucial for protecting the body against DNA viruses, other pathogens and the abnormal accumulation of self-DNA in the cytosol. Its involvement in the pathogenesis of systemic lupus erythematosus (SLE) and tumors was also found.^{82,83}

The NLRP3 inflammasome is the most widely described in the literature and serves as a key focus of research. It consists of 3 essential components typical of the NLR group: NLRP3 receptor, ASC adaptor and pro-caspase-1. The receptor has a NACHT domain (named after NAIP, CIITA, HET-E, and TEP-1 components) that is capable of oligomerization and functions as an ATPase; a PYD domain that enables interaction with ASC (forming protein-protein interactions); and leucine-rich repeat domains (LRRs) at the C-terminal end, recognizing microbial signals and microbial ligands (Fig. 2). In the ASC protein, there is also a distinguishable part responsible for the binding of procaspase – the CARD domain.^{84,85} The molecular signal associated with danger is received by the LRR domain, leading to the oligomerization of NLRP3 monomers through their NACHT domains. This is followed by interaction between the NLRP3 PYD and ASC domains, resulting in the assembly of many ASC filaments into a single aggregate of macromolecules, forming a “speck” within the activated cell. Finally, pro-caspase-1 is recruited to the complex through interactions between the CARD domains (CARD–CARD interactions), facilitated by ASC. Full-length pro-caspase-1 has an N-terminal CARD, a central large catalytic domain (p20) and a C-terminal small catalytic subunit domain (p10). This unit is subsequently cleaved at the p20–p10 junction, and further processed between the CARD and p20, ultimately releasing the active form, the p20–p10 heterotetramer, from the inflammasome.^{84,86,87} NEK7, a serine/threonine kinase, is often cited as a key NLRP3-specific component required for activation. However, recent research shows that in various cell systems, the polymerization of the ASC domain is independent of NEK7.^{88,89}

Activation of the NLRP3 inflammasome is crucial for host defenses against pathogen invasion and maintaining homeostasis. However, excessive response additionally

contributes to the progression of various inflammatory diseases, such as arthritis, atherosclerosis, T2D, and cancers. Many studies imply that neuroinflammatory and neurodegenerative diseases, such as Alzheimer’s disease and Parkinson’s disease, are also linked to the NLRP3 inflammasome. Dysregulation of the activation of this multidimensional complex can also lead to several autoimmune diseases, including multiple sclerosis; thus, activation must be tightly regulated, and the molecular mechanisms of this process and their connection to disease pathogenesis are becoming an increasingly popular subject for researchers.⁹⁰

Inflammasome activation

Inflammasome activation, with particular emphasis on NLRP3, in response to the release of molecules (from infected cells and damaged tissues), through PRR, is tightly regulated in resting cells. Canonical activation follows a standard 2-step model in which 2 signals are required for optimal activation of the NLRP3 inflammasome. Cytokine receptors, toll-like receptors (TLRs) and tumor necrosis factor receptors (TNFR) are stimulated by molecules such as IL-1 β , LPS and TNF. This leads to the initiation of a cell pathway involving nuclear factor kappa B (NF- κ B), triggering the transcription of NLRP3 components.⁹¹ This stage, referred to as the priming or initiating signal, is 1 of 2 necessary factors for initiating the complex process of inflammasome activation and assembly. Some studies indicate that the transcription process is unnecessary during priming, as evidenced by time observations between NLRP3 inflammasome activation and the increase in its expression. Furthermore, while TLR-related signaling is essential for rapid NLRP3 activation, current attention is primarily focused on the dependence of this receptor on the MyD88 adaptor protein and IL-1 receptor-associated kinases, IRAK-1 and IRAK-4.⁷⁷ Increasing evidence implies that the initiating signal, additionally serving as an inducer of posttranslational modifications (PTMs), enables NLRP3 activation.⁹¹

However, to initiate functional inflammasome assembly, a 2nd stimulus is required, such as ATP, ROS, viral proteins,

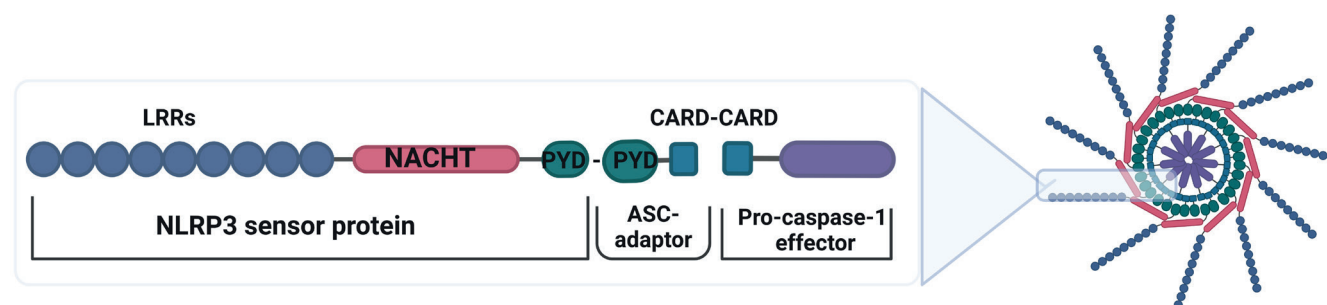


Fig. 2. The general structure of the NLRP3 inflammasome.

NLRP3 – NOD-like receptor 3, containing the pyrin domain; ASC – adaptor protein; LRRs – leucine-rich repeats; NACHT – oligomerization domain (components: NAIP, CIITA, HET-E, and TEP1); PYD – pyrin domain; CARD – caspase activation and recruitment domain.

toxins, or uric acid released by neighboring necrotic cells or damaged tissues.⁹¹

An essential element in the activation pathways is ion flow within the cell, particularly involving potassium, calcium, sodium, and chloride ions. A decrease in intracellular potassium concentration occurs, in part, through the P2X7R receptor and TWEAK2 in response to the accumulated extracellular reservoir of ATP, indirectly triggering inflammasome activation. Nigericin, a commonly used NLRP3 inflammasome agonist, correlates with potassium efflux.⁹² Consequently, high cytoplasmic K⁺ levels inhibit inflammasomes. However, it has not been determined how K⁺ efflux is detected by NLRP3 and enables the assembly and activation of the inflammasome. The role of potassium ion flow from the cytosol to the extracellular compartment seems to be associated with other types of triggers, such as lysosomal destabilization and the action of its enzymes. Despite its significant role in NLRP3 activation, the exact nature underlying potassium flow remains to be fully understood.⁹³

Signaling associated with calcium flow is often emphasized as critical for the activation of the NLRP3 inflammasome. It is hypothesized that calcium influx into mitochondria enhances mitochondrial stress and intensifies its activation. However, contrary to earlier data, recent systematic studies have revealed that calcium flux does not occur in response to most NLRP3 activators. Moreover, it is neither necessary nor sufficient for its activation; thus, the interconnections in the cell pathway remain a subject of ongoing research. The flow of chloride ions and the associated intracellular channel proteins, such as chloride intracellular channel 1 (CLIC1) and 4 (CLIC4), are required for NLRP3 activation.^{94,95}

The release of both mitochondrial DNA (mtDNA) and mitochondrial ROS (mtROS) from damaged mitochondria is a process also associated with the NLRP3 activation pathway. Reactive oxygen species generation, especially from mitochondria, was one of the first identified factors that could contribute to inflammasome activation. However, recent studies imply that mtROS might be released by NLRP3 activators but is not the cause of its activation. In another study concerning mitochondria, it was found that mtDNA must first be oxidized (ox-mtDNA) to activate NLRP3. Furthermore, many scientific reports suggest a hypothesis that preventing the removal of damaged mitochondria initiates NLRP3 activity, implying that these organelles play an important role in the activation pathway.^{95,96} Cardiolipin is a highly negatively charged lipid located on the inner side of the mitochondrial membrane. In response to cellular stress, its externalization occurs, which is necessary for autophagy and cell death. It was found that mitochondrial dysfunction allows direct interaction between cardiolipin and NLRP3 through the LRR domain, activating the inflammasome. In another study, the effect of LPS on the binding of cardiolipin with caspase-1 was identified, leading to inflammasome activation.^{84,97} Adenosine triphosphate is a central product of the mitochondria and

a known activator of NLRP3 through the involvement of the P2X7R receptor. Adenosine triphosphate can also enhance the inflammasome-induced production of IL-1 β and IL-18 in innate immune cells.⁹⁸ It should be noted that NLRP3 has a motif that binds and hydrolyzes ATP in the NACHT domain, called Walker B, which is required for inflammasome activity. Recent studies have identified that MCC950 – a common inhibitor – binds to this motif, preventing NLRP3 from attaining an active conformation.⁹³

NLRP3 activation in response to lysosome destabilization correlates with lysosomal membrane permeabilization (LMP) and the release of lysosomal hydrolases, such as cathepsins, into the cytosol. Lysosomal membrane permeabilization is induced by a wide range of pro-inflammatory stimuli, e.g., monosodium urate (MSU) and crystalline cholesterol. This leads to a potassium efflux, consequently increasing mtROS and cardiolipin externalization.⁸⁴

As mentioned at the beginning of the chapter, post-translational processes of NLRP3 are likely to play an important role in its assembly. Ubiquitination contributes to inflammasome activation through deubiquitinating enzymes (DUBs). Phosphorylation events, in turn, control the assembly and activation of inflammasomes.⁹⁹

During activation, as a result of the previously described structural changes in NLRP3, activated caspase-1 transforms pro-IL-1 β and pro-IL-18 into their mature forms. Another critical and direct substrate of caspase-1 is gasdermin D (GSDMD) – the principal executor of pyroptosis. Caspase-1 processes cytosolic GSDMD to release its N-terminal domain with a high affinity for the cell membrane, where it inserts and forms pore-like structures on the membrane. This particular structure allows the release of IL-1 β and IL-18 into the extracellular space (Fig. 3). Besides releasing pro-inflammatory cytokines and other contents, the pores in the membrane lead to pathological ion flows, ultimately resulting in cell death, known as pyroptosis.¹⁰⁰ Pyroptosis is characterized by nuclear shrinkage and nuclear DNA fragmentation. The genetic material damage during pyroptosis is limited, and the overall nuclear structure remains intact. Inflammatory mediators that are released during the process recruit and activate immune cells, enhancing the body's immune response. Unbalanced activation of this form of cell death can lead to an inflammatory response that disrupts host homeostasis.¹⁰¹

The apoptotic effectors BAX and BAK induce NLRP3 inflammasome activation and IL-1 β secretion. It is worth noting that a large number of cell death effectors, such as caspase-8, MLKL and GPX4, directly or indirectly regulate NLRP3 inflammasome activation in response to various PAMPs and DAMPs.¹⁰² NLRP3 activation may affect the induction of autophagy, and, on the other hand, autophagy may modulate the inflammasome, reducing its activity. According to researchers, this bidirectional regulation ensures a balance between the required host defenses and the prevention of excessive inflammation.¹⁰²

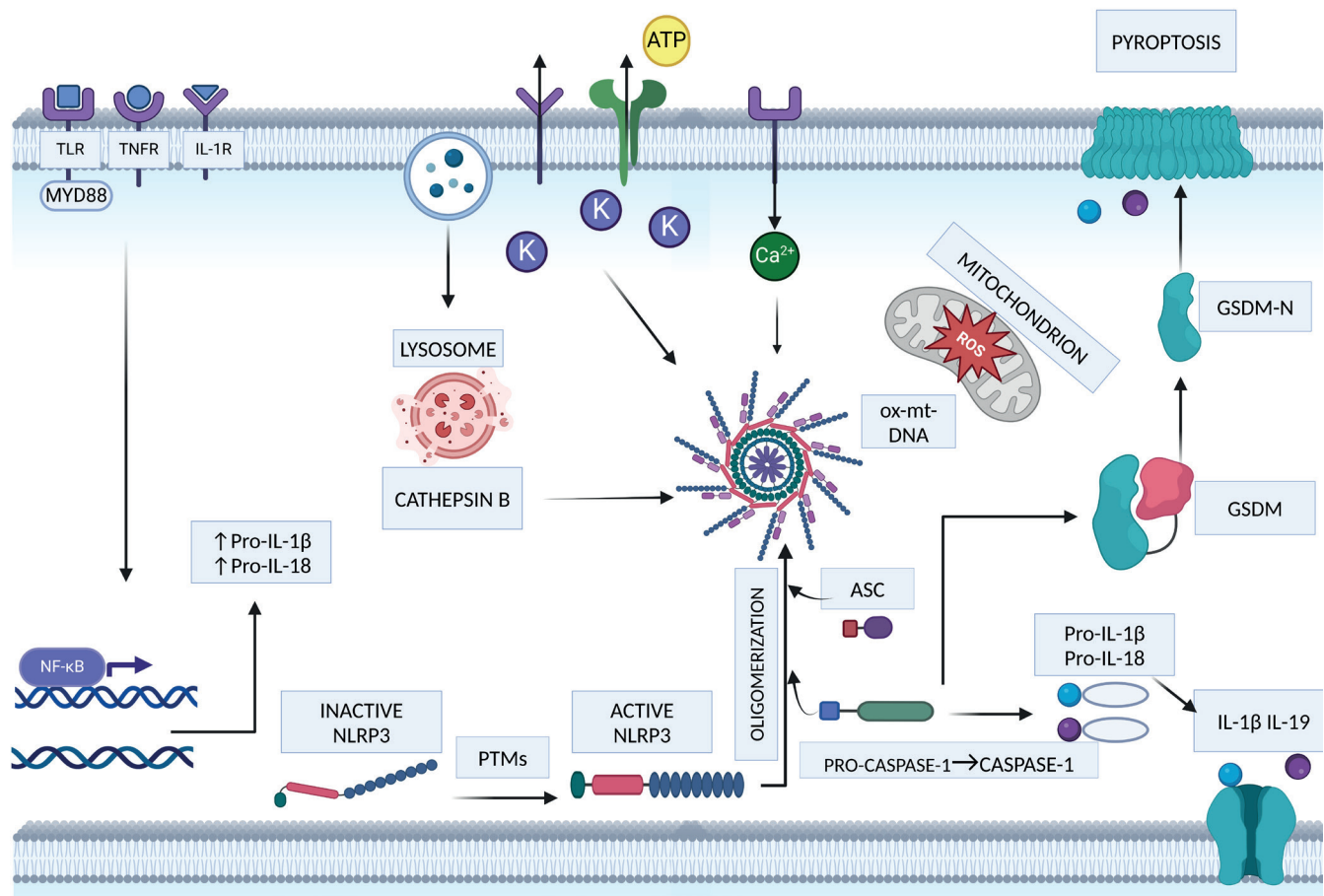


Fig. 3. Simplified scheme of NLRP3 inflammasome activation

NF-κB – nuclear factor κB; TLR – toll-like receptor; TNFR – tumor necrosis factor receptor; IL-1R – interleukin 1 receptor; GSDM – gasdermin D; GSDM-N – N-terminal fragment of gasdermin D; PTMs – posttranslational modifications; ROS – reactive oxygen species; ox-mtDNA – oxidized mitochondrial DNA.⁷⁶

There are also inhibitory factors related to these protein complexes. An example is the cytokine IFN-γ, which affects the immunopathologic response by regulating nitric oxide production and inhibiting NLRP3 inflammasome formation through its nitrosylation. Moreover, carbon monoxide (CO) acts as an inhibitor of caspase-1 activation and the secretion of IL-1β and IL-18.¹⁰³

The cytosolic response pathway to LPS, involving caspase-4/5 in humans and caspase-11 in mice, was termed non-canonical due to the signal received by TLR4-TRIF. Lipopolysaccharides from Gram-negative bacteria, which is delivered into the cytosol via outer membrane vesicles (OMVs), are taken up by cells, with the simultaneous initiation of interferon type I, which affects caspase-11 expression and generates specific guanylate-binding proteins (GBPs) and immunity-related GTPase family member b10 proteins (IRGB10) that directly target the cell membrane of the engulfed bacteria in a GBP-dependent manner, disrupting the microorganism's structural integrity and releasing LPS and lipid A into the cytoplasm. Part of the lipid A molecule directly interacts with the proper caspase-4/5/11 recruitment domain, leading to their

oligomerization and activation. The subsequent steps of the process resemble the canonical pathway.⁹⁰

Alternative NLRP3 inflammasome activation requires only 1 signal. Toll-like receptors ligands are sufficient to initiate NLRP3 inflammasome activation in human monocytes. The main differences between alternative and classical inflammasome activation (canonical and non-canonical) involve a lack of dependence on the flow of potassium and pyroptosis.⁸⁰

Functions of the inflammasome in the body

The inflammasome plays a crucial role in regulating the inflammatory state and protecting the body. The NLRP3 inflammasome can be activated by bacterial and viral components, as well as intracellular signals such as mitochondrial damage, protein aggregates or abnormal ion levels. Cell death following inflammasome activation, known as pyroptosis, also serves as an important protective mechanism against bacterial infections. It inhibits

pathogen replication within cells, promotes the phagocytosis of remaining bacteria, and induces the release of pro-inflammatory proteins involved in the pathogenesis of various chronic inflammatory diseases.¹⁰⁴ The NLRP3 inflammasome is activated in the presence of bacterial infections, including *Staphylococcus aureus*, group B *Streptococcus*, *Listeria monocytogenes*, and *Neisseria gonorrhoeae*. Meanwhile, the AIM2 inflammasome plays a critical role in alerting the innate immune system during invasion by certain extracellular and intracellular bacteria, as exemplified by *Streptococcus pneumoniae*.^{83,105} Viral nucleic acids are typically detected by AIM2 (ALR) inflammasomes; however, several viruses and their components, including the influenza virus, poliovirus and enterovirus, are sufficient to stimulate the NLRP3 inflammasome. Consequently, NLRP3 inflammasome activation inhibits virus replication, reducing mortality in murine models.¹⁰⁶

Dysregulation of NLRP3 inflammasome complex formation may promote chronic inflammation by increasing IL-1 β release. However, improper activation of the complex may also lead to severe pathological damage.¹⁰⁴ The response to DAMPs in the absence of a microbial factor is termed sterile inflammation, occurring in conditions such as atherosclerosis, T2D, neurodegenerative disorders, and cancer.⁷⁸

The inflammasome coordinates the body's immune response to engage protective mechanisms during disturbances in physiological processes. There is evidence linking the NLRP3 inflammasome to organ injury, neurologic diseases and CV diseases.^{104–106} Increased NLRP3 expression was documented in atherosclerotic plaques, correlating with the severity of coronary artery disease (CAD). Inflammasome activation in endothelial cells is associated with impaired coronary flow, while IL-1 β and IL-18 may lead to improper vasodilation. Activation of the NLRP3 inflammasome was identified as a potent mediator of the inflammatory response, releasing pro-inflammatory mediators IL-1 β and IL-18 that enhance lipid deposition and foam cell accumulation, ultimately contributing to the progression of atherosclerosis.^{107,108} Furthermore, there was NLRP3 inflammasome activation in cardiomyocytes during acute myocardial infarction (AMI). This results in inflammation and cell death in the form of pyroptosis. In neutrophils, interleukins promote the release of ROS and enzymes, causing damage to cardiomyocytes.¹⁰⁹

Chronic inflammation is a significant aspect of the pathogenesis of T2D. Activation of the NLRP3 inflammasome occurs in response to glucose, free fatty acids and mtROS.¹¹⁰ The production of IL-1 β also plays a crucial role, leading to the induction of insulin resistance and impaired pancreatic β -cell function.¹¹¹

In many studies investigating inflammasome activation during cerebral I/R events in rodents, there was an increased expression of inflammasome components such as NLRP3, caspase-1, IL-1 β , and IL-18 already in the initial hours, which is consistent with the hyperacute and

acute phases of strokes in humans.^{112–114} Therefore, there were harmful inflammatory effects of complex activation. The use of an inflammasome inhibitor reduces the expression of inflammatory mediators. Franke et al. induced ischemic strokes in mice through a 60-min middle cerebral artery occlusion followed by 3-h, 7-h and 23-h reperfusion periods. Besides confirming the effectiveness of the inhibitor, they observed reduced infiltration of immune system cells in the ischemic hemisphere, along with preserved blood–brain barrier (BBB) integrity.¹¹³ Furthermore, in a more recent study, it was proved that the addition of the MCC950 inhibitor resulted in a reduction in brain injury caused by oxidative stress in rats.¹¹⁴

Inflammasome in the kidney transplant process

Improving the effectiveness of RRT in the form of transplantation involves, among other things, reducing IRI, which is also the underlying pathophysiology of dysfunction in many organs. Increased production of ROS, cell damage and cell death can mobilize DAMPs that are necessary for initiating the inflammasome activation pathway, thus leading to an intensified cascade of the inflammatory process.¹¹²

Ischemia/reperfusion is a potential cause of early kidney rejection due to increased susceptibility of the kidneys to ischemia. A complex sequence of biochemical events resulting in renal cell death due to reduced oxygen levels and subsequent reperfusion determines the severity of the damage and initiation of the inflammatory response, leading to renal dysfunction.^{31–45} Currently, there are few scientific studies related to NLRP3 inflammasome activation during the kidney transplant process. In 1 publication, there was a decline in transplant efficacy due to the intensified effects of WIT, which was associated with increased NLRP3 expression resulting from prolonged organ storage in hypothermia.¹¹⁵

Tissue ischemia, which is a main cause of AKI, serves as a potential source of ligands for NLRP3 activation. Inflammasome-related studies were conducted on both murine and human renal tissues subjected to I/R, where effectors in the form of caspase-1, IL-1 β and IL-18 were also measured. High levels of NLRP3 and its effectors in human and murine renal tubular epithelial (RTE) cells indicate a crucial role in initiating inflammatory responses during tissue damage. Lack of NLRP3 provides protection against renal cell death during IRI and loss of kidney function; however, silencing the ASC domain alone or effectors (caspase-1, IL-1 β and IL-18) did not yield such positive effects.^{116,117} Confirmation of these observations was obtained in another study, where various renal tubular cell lines, primary mouse renal tubular cells lacking NLRP3 (knockout, KO) and a unilateral ureteral obstruction (UUO) model were used in vitro. Cellular hypoxia induced a significant increase in NLRP3 regardless


of ASC, caspase-1 and IL-1 β . During oxygen deprivation, NLRP3 in renal tubular cells was relocated from the cytosol to the mitochondria and was bound to mitochondrial antiviral signaling protein (MAVS). Deletion of NLRP3 or MAVS weakened mtROS production and depolarization of mitochondrial membrane potentials under hypoxic conditions. In response to unilateral ureteral obstruction, mice with silenced NLRP3 exhibited less fibrosis and apoptosis compared to wild-type mice.¹¹⁸ Findings from a more recent study on the acute and chronic phases of ischemic AKI indicated persistent overexpression of NLRP3, which is associated with abnormal renal tubular repair and correlated with infiltrating macrophages and fibrosis. The hypothesis was raised that elevated NLRP3 levels after AKI could serve as a new biomarker for chronic kidney lesions, predicting the transition from AKI to CKD, and a marker for monitoring long-term effects, similar to KIM-1 and NGAL. However, this requires confirmation in further clinical studies.¹¹⁹ One promising therapeutic strategy for renal IRI is to prevent NLRP3 activation through the use of inhibitors. An example is a study using H₂S, which acts to inhibit cell pyroptosis via the NLRP3/caspase-1 pathway and reduce I/R-induced AKI. The exact mechanism of action remains subject to further research.¹²⁰ An alternative approach involves using endothelial progenitor cells (EPCs), which play an important role in maintaining vascular integrity and endothelial repair. The EPCs were cultured from human peripheral blood and administered to mice 5 min before reperfusion. This resulted in a reduction in NLRP3 expression levels and cleaved caspase-1 compared to the control group. Inflammasome-induced inflammation is a potential target of EPCs to treat I/R-induced AKI and prevent progression to CKD.^{121,122}

Conclusions

Kidney transplants are one of the greatest achievements of modern medicine, since the number of patients suffering from severe kidney diseases is continuously increasing. However, improvements in long-term outcomes remain a challenge in the field of transplantology. The transplanted organ is predisposed to multiple injuries related to the body's immune response, toxicity resulting from pharmacotherapy, and IRI. This review proved that the activation of NLRP3 inflammasomes is a crucial element of kidney injury during transplant procedures. We have described the pathways of inflammasome activation indicating the NLRP3 inflammasome as a potential target for future preventive/therapeutic strategies.

ORCID iDs

Karolina Tądel  <https://orcid.org/0000-0002-0978-8274>

Iwona Bil-Lula  <https://orcid.org/0000-0002-2769-0166>

References

1. Sher NM, Nazli R, Zafar H, Fatima S. Effects of lipid based Multiple Micronutrients Supplement on the birth outcome of underweight pre-eclamptic women: A randomized clinical trial. *Pak J Med Sci*. 2021; 38(1):219–226. doi:10.12669/pjms.38.1.4396
2. Transplantacja. In: *Encyklopedia PWN*. Warsaw, Poland: Wydawnictwa Naukowe PWN; 2022. <https://encyklopedia.pwn.pl/haslo/transplantacja;3988774.html>. Accessed November 10, 2022.
3. World Health Organization (WHO). Global Glossary of Terms and Definitions on Donation and Transplantation. Geneva, Switzerland: World Health Organization (WHO); 2009. <https://iris.who.int/bitstream/handle/10665/341813/WHO-HTP-EHT-CPR-2009.01-eng.pdf?sequence=1>. Accessed November 21, 2022.
4. Kimszal E. Zespół transplantacyjny – rola pielęgniarki anestezjologicznej. *Piel Pol*. 2020;76(2):122–126. doi:10.20883/pielpol.2020.14
5. Darlington D, Anitha FS, Joseph C. Study of knowledge, attitude, and practice of organ donation among medical students in a tertiary care centre in south India. *Cureus*. 2019;11(6):e4896. doi:10.7759/cureus.4896
6. Czerwiński R, Malanowski P, Grzywacz. Poltransplant Biuletyn Informacyjny. Centrum Organizacyjno-Koordinacyjne ds. Transplantacji Poltransplant. 2022. https://files.poltransplant.org.pl/Biuletyn_2022_.www.pdf. Accessed November 11, 2022.
7. Azhar B, Patel S, Chadha P, Hakim N. Indications for renal auto-transplant: An overview. *Exp Clin Transplant*. 2015;13(2):109–114. PMID:25871361.
8. Surna S, Adamczak M. Ksenotransplantacja nerki. *Forum Nefrol*. 2019; 12(2):114–124. https://journals.viamedica.pl/forum_nefrologiczne/article/view/65101/48813. Accessed November 21, 2023.
9. Voora S, Adey DB. Management of kidney transplant recipients by general nephrologists: Core Curriculum 2019. *Am J Kidney Dis*. 2019;73(6):866–879. doi:10.1053/j.ajkd.2019.01.031
10. Rao PS, Ojo A. The alphabet soup of kidney transplantation: SCD, DCD, ECD. Fundamentals for the practicing nephrologist. *Clin J Am Soc Nephrol*. 2009;4(11):1827–1831. doi:10.2215/CJN.02270409
11. Davis CL, Delmonico FL. Living-donor kidney transplantation: A review of the current practices for the live donor. *J Am Soc Nephrol*. 2005; 16(7):2098–2110. doi:10.1681/ASN.2004100824
12. Kanda H, Hirasaki Y, Iida T, et al. Perioperative management of patients with end-stage renal disease. *J Cardiothorac Vasc Anesth*. 2017;31(6):2251–2267. doi:10.1053/j.jvca.2017.04.019
13. Gusev E, Solomatina L, Zhuravleva Y, Sarapultsev A. The pathogenesis of end-stage renal disease from the standpoint of the theory of general pathological processes of inflammation. *Int J Mol Sci*. 2021; 22(21):11453. doi:10.3390/ijms222111453
14. Woderska-Jasińska A, Hermanowicz M, Włodarczyk Z. Transplantacja nerki jako metoda leczenia nerkozastępczego pacjenta z przewlekłą chorobą nerek. *Innow Piel*. 2021;6(1):73–83. doi:10.21784/lwP.2021.006
15. Augustine J. Kidney transplant: New opportunities and challenges. *Cleve Clin J Med*. 2018;85(2):138–144. doi:10.3949/ccjm.85gr.18001
16. Abramowicz D, Hazzan M, Maggiore U, et al. Does pre-emptive transplantation versus post start of dialysis transplantation with a kidney from a living donor improve outcomes after transplantation? A systematic literature review and position statement by the Descartes Working Group and ERBP. *Nephrol Dial Transplant*. 2016;31(5): 691–697. doi:10.1093/ndt/gfv378
17. Chadban SJ, Ahn C, Axelrod DA, et al. KDIGO Clinical Practice Guideline on the Evaluation and Management of Candidates for Kidney Transplantation. *Transplantation*. 2020;104(4 Suppl 1):S11–S103. doi:10.1097/TP.0000000000003136
18. Salvadori M, Tsalouchos A. Current protocols and outcomes of ABO-incompatible kidney transplantation. *World J Transplant*. 2020;10(7): 191–205. doi:10.5500/wjt.v10.i7.191
19. Park Y, Ko EJ, Chung BH, Yang CW. Kidney transplantation in highly sensitized recipients. *Kidney Res Clin Pract*. 2021;40(3):355–370. doi:10.23876/j.krccp.21.012
20. Lim MA, Kohli J, Bloom RD. Immunosuppression for kidney transplantation: Where are we now and where are we going? *Transplant Rev (Orlando)*. 2017;31(1):10–17. doi:10.1016/j.trre.2016.10.006

21. Montenegro MI, Perkins JD, Kling CE, Sibulesky L, Dick AA, Reyes JD. Machine perfusion decreases delayed graft function in donor grafts with high kidney donor profile index. *Exp Clin Transplant*. 2021;19(1): 8–13. doi:10.6002/ect.2019.0139
22. Hariharan S, Israni AK, Danovitch G. Long-term survival after kidney transplantation. *N Engl J Med*. 2021;385(8):729–743. doi:10.1056/NEJMra2014530
23. Senev A, Coemans M, Lerut E, et al. Eplet mismatch load and de novo occurrence of donor-specific anti-HLA antibodies, rejection, and graft failure after kidney transplantation: An observational cohort study. *J Am Soc Nephrol*. 2020;31(9):2193–2204. doi:10.1681/ASN.2020010019
24. Mannon RB. Delayed graft function: The AKI of kidney transplantation. *Nephron*. 2018;140(2):94–98. doi:10.1159/000491558
25. Morath C, Döhler B, Kälble F, et al. Pre-transplant HLA antibodies and delayed graft function in the current era of kidney transplantation. *Front Immunol*. 2020;11:1886. doi:10.3389/fimmu.2020.01886
26. Lai X, Zheng X, Mathew JM, Gallon L, Leventhal JR, Zhang ZJ. Tackling chronic kidney transplant rejection: Challenges and promises. *Front Immunol*. 2021;12:661643. doi:10.3389/fimmu.2021.661643
27. Salamin P, Deslarzes-Dubuis C, Longchamp A, et al. Predictive factors of surgical complications in the first year following kidney transplantation. *Ann Vasc Surg*. 2022;83:142–151. doi:10.1016/j.avsg.2021.08.031
28. Dos Santos Mantovani M, Coelho De Carvalho N, Archangelo TE, et al. Frailty predicts surgical complications after kidney transplantation: A propensity score matched study. *PLoS One*. 2020;15(2):e0229531. doi:10.1371/journal.pone.0229531
29. Cooper JE, Wiseman AC. Acute kidney injury in kidney transplantation. *Curr Opin Nephrol Hypertens*. 2013;22(6):698–703. doi:10.1097/MNH.0b013e328328365b388
30. Panah F, Ghorbanihaghjo A, Argani H, Asadi Zarmehri M, Nazari Soltan Ahmad S. Ischemic acute kidney injury and Klotho in renal transplantation. *Clin Biochem*. 2018;55:3–8. doi:10.1016/j.clinbiochem.2018.03.022
31. Salvadori M, Rosso G, Bertoni E. Update on ischemia-reperfusion injury in kidney transplantation: Pathogenesis and treatment. *World J Transplant*. 2015;5(2):52. doi:10.5500/wjt.v5.i2.52
32. Saat TC, Van Den Akker EK, IJzermans JNM, Dor FJMF, De Bruin RWF. Improving the outcome of kidney transplantation by ameliorating renal ischemia reperfusion injury: Lost in translation? *J Transl Med*. 2016;14(1):20. doi:10.1186/s12967-016-0767-2
33. Marzouk K, Lawen J, Alwayn I, Kiberd BA. The impact of vascular anastomosis time on early kidney transplant outcomes. *Transplant Res*. 2013;2(1):8. doi:10.1186/2047-1440-2-8
34. Khan TFT, Ahmad N, Serageldien AS, Fourtounas K. Implantation warm ischemia time in kidney transplant recipients: Defining its limits and impact on early graft function. *Ann Transplant*. 2019;24:432–438. doi:10.12659/AOT.916012
35. Summers DM, Watson CJE, Pettigrew GJ, et al. Kidney donation after circulatory death (DCD): State of the art. *Kidney Int*. 2015;88(2):241–249. doi:10.1038/ki.2015.88
36. Philipponnet C, Aniot J, Garrouste C, Kemeny JL, Heng AE. Ischemia reperfusion injury in kidney transplantation: A case report. *Medicine (Baltimore)*. 2018;97(52):e13650. doi:10.1097/MD.00000000000013650
37. Chatauret N, Badet L, Barrou B, Hauet T. Ischemia–reperfusion: From cell biology to acute kidney injury. *Prog Urol*. 2014;24(24 Suppl 1): S4–S12. doi:10.1016/S1166-7087(14)70057-0
38. Bellini MI, Tortorici F, Amabile MI, D'Andrea V. Assessing kidney graft viability and its cells metabolism during machine perfusion. *Int J Mol Sci*. 2021;22(3):1121. doi:10.3390/ijms22031121
39. Nieuwenhuijs-Moeke GJ, Pischke SE, Berger SP, et al. Ischemia and reperfusion injury in kidney transplantation: Relevant mechanisms in injury and repair. *J Clin Med*. 2020;9(1):253. doi:10.3390/jcm9010253
40. Soares ROS, Losada DM, Jordani MC, Évora P, Castro-e-Silva O. Ischemia/reperfusion injury revisited: An overview of the latest pharmacological strategies. *Int J Mol Sci*. 2019;20(20):5034. doi:10.3390/ijms20205034
41. Jassem W, Fuggle SV, Rela M, Koo DDH, Heaton ND. The role of mitochondria in ischemia/reperfusion injury. *Transplantation*. 2002;73(4): 493–499. doi:10.1097/00007890-200202270-00001
42. Webster KA. Mitochondrial membrane permeabilization and cell death during myocardial infarction: Roles of calcium and reactive oxygen species. *Future Cardiol*. 2012;8(6):863–884. doi:10.2217/fca.12.58
43. Bi J, Zhang J, Ren Y, et al. Irsin alleviates liver ischemia-reperfusion injury by inhibiting excessive mitochondrial fission, promoting mitochondrial biogenesis and decreasing oxidative stress. *Redox Biol*. 2019;20:296–306. doi:10.1016/j.redox.2018.10.019
44. Wang X, Khalil RA. Matrix metalloproteinases, vascular remodeling, and vascular disease. *Adv Pharmacol*. 2018;81:241–330. doi:10.1016/b.s.apha.2017.08.002
45. Tejchman K, Kotfis K, Sierńko J. Biomarkers and mechanisms of oxidative stress: Last 20 years of research with an emphasis on kidney damage and renal transplantation. *Int J Mol Sci*. 2021;22(15):8010. doi:10.3390/ijms22158010
46. Priante G, Giancesello L, Ceol M, Del Prete D, Anglani F. Cell death in the kidney. *Int J Mol Sci*. 2019;20(14):3598. doi:10.3390/ijms20143598
47. Castaneda MP, Swiatecka-Urban A, Mitsnefes MM, et al. Activation of mitochondrial apoptotic pathways in human renal allografts after ischemia/reperfusion injury. *Transplantation*. 2003;76(1):50–54. doi:10.1097/01.TP.0000069835.95442.9F
48. Lin TA, Wu VCC, Wang CY. Autophagy in chronic kidney diseases. *Cells*. 2019;8(1):61. doi:10.3390/cells8010061
49. Pallet N, Livingston M, Dong Z. Emerging functions of autophagy in kidney transplantation. *Am J Transplant*. 2014;14(1):13–20. doi:10.1111/ajt.12533
50. Halawa A. The early diagnosis of acute renal graft dysfunction: A challenge we face. The role of novel biomarkers. *Ann Transplant*. 2011;16(1):90–98.
51. Malyszko J, Lukaszuk E, Glowinska I, Durluk M. Biomarkers of delayed graft function as a form of acute kidney injury in kidney transplantation. *Sci Rep*. 2015;5(1):11684. doi:10.1038/srep11684
52. Rimes-Stigare C, Ravn B, Awad A, et al. Creatinine- and cystatin C-based incidence of chronic kidney disease and acute kidney disease in AKI survivors. *Crit Care Res Pract*. 2018;2018:7698090. doi:10.1155/2018/7698090
53. Kielar M, Dumnicka P, Gala-Błądzińska A, et al. Urinary NGAL measured after the first year post kidney transplantation predicts changes in glomerular filtration over one-year follow-up. *J Clin Med*. 2020; 10(1):43. doi:10.3390/jcm10010043
54. Ozbilgin S, Ozkardesler S, Akan M, et al. Renal ischemia/reperfusion injury in diabetic rats: The role of local ischemic preconditioning. *Biomed Res Int*. 2016;2016:8580475. doi:10.1155/2016/8580475
55. Kanter J, Beltran S, Molina D, et al. Urinary neutrophil gelatinase-associated lipocalin after kidney transplantation: Is it a good biomarker to assess delayed graft function? *Transplant Proc*. 2013;45(4): 1368–1370. doi:10.1016/j.transproceed.2013.01.019
56. Capelli I, Baraldi O, Comai G, et al. Urinary neutrophil gelatinase-associated lipocalin is a biomarker of delayed graft function after kidney transplantation. *Transplant Res Risk Manag*. 2017;9:15–21. doi:10.2147/TRRM.S122090
57. Lacquaniti A, Caccamo C, Salis P, et al. Delayed graft function and chronic allograft nephropathy: Diagnostic and prognostic role of neutrophil gelatinase-associated lipocalin. *Biomarkers*. 2016;21(4): 371–378. doi:10.3109/1354750X.2016.1141991
58. Rostami Z, Nikpoor M, Einollahi B. Urinary neutrophil gelatinase associated lipocalin (NGAL) for early diagnosis of acute kidney injury in renal transplant recipients. *Nephro Urol Mon*. 2013;5(2):745–752. doi:10.5812/numonthly.9385
59. Rogulska K, Wojciechowska-Kosko I, Dołęgowska B, et al. The most promising biomarkers of allogeneic kidney transplant rejection. *J Immunol Res*. 2022;2022:6572338. doi:10.1155/2022/6572338
60. Shahbaz SK, Pourrezagholi F, Barabadi M, et al. High expression of TIM-3 and KIM-1 in blood and urine of renal allograft rejection patients. *Transplant Immunol*. 2017;43–44:11–20. doi:10.1016/j.trim.2017.07.002
61. Aldea PL, Rachisan AL, Stanciu BI, et al. The perspectives of biomarkers in predicting the survival of the renal graft. *Front Pediatr*. 2022;10:869628. doi:10.3389/fped.2022.869628
62. Puthumana J, Hall IE, Reese PP, et al. YKL-40 associates with renal recovery in deceased donor kidney transplantation. *J Am Soc Nephrol*. 2017;28(2):661–670. doi:10.1681/ASN.2016010091
63. Moser MAJ, Sawicka K, Arcand S, et al. Proteomic analysis of perfusate from machine cold perfusion of transplant kidneys: Insights into protection from injury. *Ann Transplant*. 2017;22:730–739. doi:10.12659/AOT.905347

64. Salvadori M, Tsalouchos A. Biomarkers in renal transplantation: An updated review. *World J Transplant.* 2017;7(3):161. doi:10.5500/wjt.v7.i3.161
65. Donate-Correa J, Matos-Perdomo E, González-Luis A, et al. The value of Klotho in kidney transplantation. *Transplantation.* 2023;107(3):616–627. doi:10.1097/TP.0000000000004331
66. Thongprayoon C, Neyra JA, Hansrivijit P, et al. Serum Klotho in living kidney donors and kidney transplant recipients: A meta-analysis. *J Clin Med.* 2020;9(6):1834. doi:10.3390/jcm9061834
67. Warmużńska N, Łuczykowski K, Bojko B. A review of current and emerging trends in donor graft-quality assessment techniques. *J Clin Med.* 2022;11(3):487. doi:10.3390/jcm11030487
68. Chen G, Gu J, Qiu J, et al. Efficacy and safety of thymoglobulin and basiliximab in kidney transplant patients at high risk for acute rejection and delayed graft function. *Exp Clin Transplant.* 2013;11(4):310–314. doi:10.6002/ect.2012.0103
69. Nagase H, Visse R, Murphy G. Structure and function of matrix metalloproteinases and TIMPs. *Cardiovasc Res.* 2006;69(3):562–573. doi:10.1016/j.cardiores.2005.12.002
70. Hałucha K, Banaszkiewicz M, Rak-Pasikowska A, Bil-Lula I. MMP-2 inhibition prevents platelet activation in ischemia/reoxygenation conditions. *Adv Clin Exp Med.* 2022;31(12):1375–1384. doi:10.17219/acem/152286
71. Krzywonos-Zawadzka A, Franczak A, Moser MAJ, Olejnik A, Sawicki G, Bil-Lula I. Pharmacological protection of kidney grafts from cold perfusion-induced injury. *Biomed Res Int.* 2019;2019:9617087. doi:10.1155/2019/9617087
72. Chen W, Wang L, Liang P, et al. Reducing ischemic kidney injury through application of a synchronization modulation electric field to maintain Na⁺/K⁺-ATPase functions. *Sci Transl Med.* 2022;14(635):eabj4906. doi:10.1126/scitranslmed.abj4906
73. Man SM, Kanneganti T. Regulation of inflammasome activation. *Immunol Rev.* 2015;265(1):6–21. doi:10.1111/imr.12296
74. He Y, Hara H, Núñez G. Mechanism and regulation of NLRP3 inflammasome activation. *Trends Biochem Sci.* 2016;41(12):1012–1021. doi:10.1016/j.tibs.2016.09.002
75. Rathinam VAK, Fitzgerald KA. Inflammasome complexes: Emerging mechanisms and effector functions. *Cell.* 2016;165(4):792–800. doi:10.1016/j.cell.2016.03.046
76. Kelley N, Jeltama D, Duan Y, He Y. The NLRP3 inflammasome: An overview of mechanisms of activation and regulation. *Int J Mol Sci.* 2019;20(13):3328. doi:10.3390/ijms20133328
77. Chen C, Xu P. Activation and pharmacological regulation of inflammasomes. *Biomolecules.* 2022;12(7):1005. doi:10.3390/biom12071005
78. Li Y, Huang H, Liu B, et al. Inflammasomes as therapeutic targets in human diseases. *Sig Transduct Target Ther.* 2021;6(1):247. doi:10.1038/s41392-021-00650-z
79. Alatschan A, Benkő S. Nuclear receptors as multiple regulators of NLRP3 inflammasome function. *Front Immunol.* 2021;12:630569. doi:10.3389/fimmu.2021.630569
80. Yang Y, Wang H, Kouadir M, Song H, Shi F. Recent advances in the mechanisms of NLRP3 inflammasome activation and its inhibitors. *Cell Death Dis.* 2019;10(2):128. doi:10.1038/s41419-019-1413-8
81. Fenini G, Karakaya T, Hennig P, Di Filippo M, Beer HD. The NLRP1 inflammasome in human skin and beyond. *Int J Mol Sci.* 2020;21(13):4788. doi:10.3390/ijms21134788
82. Vance RE. The NAIP/NLRC4 inflammasomes. *Curr Opin Immunol.* 2015;32:84–89. doi:10.1016/j.coi.2015.01.010
83. Kumari P, Russo AJ, Shivcharan S, Rathinam VA. AIM2 in health and disease: Inflammasome and beyond. *Immunol Rev.* 2020;297(1):83–95. doi:10.1111/imr.12903
84. Swanson KV, Deng M, Ting JPY. The NLRP3 inflammasome: Molecular activation and regulation to therapeutics. *Nat Rev Immunol.* 2019;19(8):477–489. doi:10.1038/s41577-019-0165-0
85. Ohto U, Kamitsukasa Y, Ishida H, et al. Structural basis for the oligomerization-mediated regulation of NLRP3 inflammasome activation. *Proc Natl Acad Sci U S A.* 2022;119(11):e2121353119. doi:10.1073/pnas.2121353119
86. Zahid A, Li B, Kombe AJK, Jin T, Tao J. Pharmacological inhibitors of the NLRP3 inflammasome. *Front Immunol.* 2019;10:2538. doi:10.3389/fimmu.2019.02538
87. Biasizzo M, Kopitar-Jerala N. Interplay between NLRP3 inflammasome and autophagy. *Front Immunol.* 2020;11:591803. doi:10.3389/fimmu.2020.591803
88. Sharif H, Wang L, Wang WL, et al. Structural mechanism for NEK7-licensed activation of NLRP3 inflammasome. *Nature.* 2019;570(7761):338–343. doi:10.1038/s41586-019-1295-z
89. Machtens DA, Bresch IP, Eberhage J, Reubold TF, Eschenburg S. The inflammasome activity of NLRP3 is independent of NEK7 in HEK293 cells co-expressing ASC. *Int J Mol Sci.* 2022;23(18):10269. doi:10.3390/ijms231810269
90. Huang Y, Xu W, Zhou R. NLRP3 inflammasome activation and cell death. *Cell Mol Immunol.* 2021;18(9):2114–2127. doi:10.1038/s41423-021-00740-6
91. Ding Y, Ding X, Zhang H, Li S, Yang P, Tan Q. Relevance of NLRP3 inflammasome-related pathways in the pathology of diabetic wound healing and possible therapeutic targets. *Oxid Med Cell Longev.* 2022;2022:9687925. doi:10.1155/2022/9687925
92. Di A, Xiong S, Ye Z, et al. The TWIK2 potassium efflux channel in macrophages mediates NLRP3 inflammasome-induced inflammation. *Immunity.* 2018;49(1):56–65.e4. doi:10.1016/j.immuni.2018.04.032
93. Moretti J, Blander JM. Increasing complexity of NLRP3 inflammasome regulation. *J Leukoc Biol.* 2021;109(3):561–571. doi:10.1002/JLB.3MR0520-104RR
94. Katsnelson MA, Rucker LG, Russo HM, Dubyak GR. K⁺ efflux agonists induce NLRP3 inflammasome activation independently of Ca²⁺ signaling. *J Immunol.* 2015;194(8):3937–3952. doi:10.4049/jimmunol.1402658
95. Akbal A, Dernst A, Lovotti M, Mangan MSJ, McManus RM, Latz E. How location and cellular signaling combine to activate the NLRP3 inflammasome. *Cell Mol Immunol.* 2022;19(11):1201–1214. doi:10.1038/s41423-022-00922-w
96. Zhou R, Yazdi AS, Menu P, Tschopp J. A role for mitochondria in NLRP3 inflammasome activation. *Nature.* 2011;469(7329):221–225. doi:10.1038/nature09663
97. Elliott EL, Miller AN, Banoth B, et al. Cutting edge: Mitochondrial assembly of the NLRP3 inflammasome complex is initiated at priming. *J Immunol.* 2018;200(9):3047–3052. doi:10.4049/jimmunol.1701723
98. Tiwari-Heckler S, Robson SC, Longhi MS. Mitochondria drive immune responses in critical disease. *Cells.* 2022;11(24):4113. doi:10.3390/cells11244113
99. Shim DW, Lee KH. Posttranslational regulation of the NLR family pyrin domain-containing 3 inflammasome. *Front Immunol.* 2018;9:1054. doi:10.3389/fimmu.2018.01054
100. Santa Cruz Garcia AB, Schnur KP, Malik AB, Mo GCH. Gasdermin D pores are dynamically regulated by local phosphoinositide circuitry. *Nat Commun.* 2022;13(1):52. doi:10.1038/s41467-021-27692-9
101. Zhang J, Wirtz S. Does pyroptosis play a role in inflammasome-related disorders? *Int J Mol Sci.* 2022;23(18):10453. doi:10.3390/ijms231810453
102. Lv S, Liu H, Wang H. The interplay between autophagy and NLRP3 inflammasome in ischemia/reperfusion injury. *Int J Mol Sci.* 2021;22(16):8773. doi:10.3390/ijms22168773
103. Kim JK, Jin HS, Suh H, Jo E. Negative regulators and their mechanisms in NLRP3 inflammasome activation and signaling. *Immunol Cell Biol.* 2017;95(7):584–592. doi:10.1038/icb.2017.23
104. Fusco R, Siracusa R, Genovese T, Cuzzocrea S, Di Paola R. Focus on the role of NLRP3 inflammasome in diseases. *Int J Mol Sci.* 2020;21(12):4223. doi:10.3390/ijms21124223
105. Jo EK, Kim JK, Shin DM, Sasakawa C. Molecular mechanisms regulating NLRP3 inflammasome activation. *Cell Mol Immunol.* 2016;13(2):148–159. doi:10.1038/cmi.2015.95
106. Zhao C, Zhao W. NLRP3 inflammasome: A key player in antiviral responses. *Front Immunol.* 2020;11:211. doi:10.3389/fimmu.2020.00211
107. Abbate A, Toldo S, Marchetti C, Kron J, Van Tassell BW, Dinarello CA. Interleukin-1 and the inflammasome as therapeutic targets in cardiovascular disease. *Circ Res.* 2020;126(9):1260–1280. doi:10.1161/CIRCRESAHA.120.315937
108. Burger F, Baptista D, Roth A, et al. NLRP3 inflammasome activation controls vascular smooth muscle cells phenotypic switch in atherosclerosis. *Int J Mol Sci.* 2021;23(1):340. doi:10.3390/ijms23010340

109. Buckley LF, Libby P. Inhibiting NLRP3 inflammasome activity in acute myocardial infarction: A review of pharmacologic agents and clinical outcomes. *J Cardiovasc Pharmacol*. 2019;74(4):297–305. doi:10.1097/FJC.0000000000000701
110. Zhang H, Fu Q, Liu J, et al. Risk factors and outcomes of prolonged recovery from delayed graft function after deceased kidney transplantation. *Ren Fail*. 2020;42(1):792–798. doi:10.1080/0886022X.2020.1803084
111. Ambati J, Magagnoli J, Leung H, et al. Repurposing anti-inflammasome NRTIs for improving insulin sensitivity and reducing type 2 diabetes development. *Nat Commun*. 2020;11(1):4737. doi:10.1038/s41467-020-18528-z
112. Mohamadi Y, Mousavi M, Khanbabaie H, et al. The role of inflammasome complex in ischemia-reperfusion injury. *J Cell Biochem*. 2023;124(6):755–764. doi:10.1002/jcb.27368
113. Franke M, Bieber M, Kraft P, Weber ANR, Stoll G, Schuhmann MK. The NLRP3 inflammasome drives inflammation in ischemia/reperfusion injury after transient middle cerebral artery occlusion in mice. *Brain Behav Immun*. 2021;92:221–231. doi:10.1016/j.bbi.2020.12.009
114. Joaquim LS, Danielski LG, Bonfante S, et al. NLRP3 inflammasome activation increases brain oxidative stress after transient global cerebral ischemia in rats. *Int J Neurosci*. 2023;133(4):375–388. doi:10.1080/00207454.2021.1922402
115. Wang XW, Guo RD, Ma JG, Wang YW, Zou XF. Effects of prolonged cold ischemia on the DCD kidney function and Inflammasome expression in rat kidney transplants. *Transplant Immunol*. 2022;74:101511. doi:10.1016/j.trim.2021.101511
116. Iyer SS, Pulsikens WP, Sadler JJ, et al. Necrotic cells trigger a sterile inflammatory response through the Nlrp3 inflammasome. *Proc Natl Acad Sci U S A*. 2009;106(48):20388–20393. doi:10.1073/pnas.0908698106
117. Shigeoka AA, Mueller JL, Kambo A, et al. An inflammasome-independent role for epithelial-expressed Nlrp3 in renal ischemia-reperfusion injury. *J Immunol*. 2010;185(10):6277–6285. doi:10.4049/jimmunol.1002330
118. Kim SM, Kim YG, Kim DJ, et al. Inflammasome-independent role of NLRP3 mediates mitochondrial regulation in renal injury. *Front Immunol*. 2018;9:2563. doi:10.3389/fimmu.2018.02563
119. Zheng Z, Xu K, Li C, et al. NLRP3 associated with chronic kidney disease progression after ischemia/reperfusion-induced acute kidney injury. *Cell Death Discov*. 2021;7(1):324. doi:10.1038/s41420-021-00719-2
120. Ni J, Jiang L, Shen G, et al. Hydrogen sulfide reduces pyroptosis and alleviates ischemia-reperfusion-induced acute kidney injury by inhibiting NLRP3 inflammasome. *Life Sci*. 2021;284:119466. doi:10.1016/j.lfs.2021.119466
121. Jang HN, Kim JH, Jung MH, et al. Human endothelial progenitor cells protect the kidney against ischemia-reperfusion injury via the NLRP3 inflammasome in mice. *Int J Mol Sci*. 2022;23(3):1546. doi:10.3390/ijms23031546
122. Komada T, Muruve DA. The role of inflammasomes in kidney disease. *Nat Rev Nephrol*. 2019;15(8):501–520. doi:10.1038/s41581-019-0158-z